Limonoid biosynthesis in *Azadirachta indica*: Characterization of pathway genes and analysis of labeled metabolites through stable isotope feeding

Thesis Submitted to **AcSIR** For the Award of
the Degree of
DOCTOR OF PHILOSOPHY
In Biological Sciences

By
T. Aarthy
10BB12A26068

Under the guidance of
Dr. H.V.Thulasiram
CSIR-National Chemical laboratory
Pune – 411008, India
March 2019

Everyone can rise above their circumstances and achieve success if they are dedicated and passionate about what they do.

-Nelson Mandela

CERTIFICATE

This is to certify that the work incorporated in this Ph.D. thesis entitled "**Limonoid biosynthesis in *Azadirachta indica*: Characterization of pathway genes and analysis of labeled metabolites through stable isotope feeding**" submitted by **Ms. T. Aarthy** to Academy of Scientific and Innovative Research (AcSIR) in fulfillment of the requirements for the award of the Degree of **Doctor of Philosophy** in **Biological Sciences**, embodies original research work under my supervision/guidance. I further certify that this work has not been submitted to any other University or Institution in part or full for the award of any degree or diploma. Research material obtained from other sources has been duly acknowledged in the thesis. Any text, illustration, table etc., used in the thesis from other sources, have been duly cited and acknowledged.

It is also certified that this work done by the student, under my supervision, is plagiarism free.

T. Aarthy

(STUDENT)

Thulasiram. H.V.
19/03/2019

(SUPERVISOR)
Dr. H. V. Thulasiram
Principal Scientist
Division of Organic Chemistry
Pune – 411008, India

DECLARATION

I, Ms. **T. Aarthy**, hereby declare that the work incorporated in the thesis entitled "**Limonoid biosynthesis in *Azadirachta indica*: Characterization of pathway genes and analysis of labeled metabolites through stable isotope feeding**" submitted by me to the Academy of Scientific and Industrial Research (AcSIR), for the degree of **Doctor of Philosophy** in **Biological Sciences** has been carried out by me at CSIR-National Chemical Laboratory under the guidance of **Dr. H. V. Thulasiram**. This work is original and has not been submitted to any other university or institution for the award of any degree or diploma. Such material, as has been obtained from other sources, has been duly acknowledged.

T. A
19/3/2019

T. Aarthy
Research Fellow,
Division of Organic Chemistry,
CSIR-National Chemical Laboratory.
Pune-411008.

Dedicated to My Beloved Grandparents...

ACKNOWLEDGMENT

Feeling gratitude and not expressing it is like wrapping a present and not giving it.

- William Arthur Ward

I would take this opportunity to express my gratitude to everyone who accompanied, helped and supported me during the journey of the PhD programme.

First of all, I thank my research supervisor Dr. H. V. Thulasiram, for his constant guidance and support. I am indebted to him for introducing me to this interesting area of research. I will always cherish his valuable suggestions, which have greatly helped in developing skills and multitasking.

I am grateful to Director, CSIR-National Chemical Laboratory, Pune and Head, Division of Organic Chemistry, for infrastructure and support to complete my research work. I sincerely acknowledge the Department of Biotechnology (DBT), New Delhi for providing Junior and Senior Research Fellowships, which supported me for my research at NCL for five years.

I thank my doctoral advisory committee Chairman, Dr. Vidya Gupta, members Dr. Mahesh J. Kulkarni and Dr. Jomon Joseph for their readily suggestions, critical evaluation and reviewing of my work reports and presentations from time to time during my Ph.D.

I am grateful for the help of Dr. B. Santhakumari, Dr. Anjan Banerjee, Dr. S. Dhanasekaran, Dr. Subash chandrabose, Dr. Muthu Krishnan and Dr. Neelima Iyer during my work at NCL.

I am thankful for the timely help from Prasad, Fayaj, Sudha, which has eased my research work. I acknowledge the cheerful environment and help rendered by my labmates, Pankaj, Swati, Saikat, Prabhakar, Harshal, Dipesh, Devdutt, Krithika, Avinash, Fayaj, Shrikant, Ashish, Prasad, Sharanbasappa, Sonia, Priyadarshini, Nilofer, Ajay, Pruthviraj, Yugendra, Balaji, Radha, Uttara, Rani, Vijayashree, Ramesha, Shiva, Jennifer, Nilesh, Kuhoo, Anirban, Manoj, Ashish, Jagadeesha, Manu, Supriya, Nagesh, Varsha, Sudha, Pooja, Aaditi, Shruti, Nivedita, Chaya, Chitra, Jeevitha, Sandip, Bhagyashree, Smita, Shaila, Sneha, Nikita, Chetan, Preeti. I am happy to extend my thanks to collaborators and friends Pushpa, Bhavani, Harpreet, Arati, Soujanya, Sweta, Amar, Mahesh.

I sincerely thank friends from NCL, Swamy, Shrikant, Amrita, Swapnil, Bharat, Deepika, Bhusan, Pranali, Harshavardhan, Pankaj, HariKrishna, Jagadeesh, and IISER,

Bhavani, Nevedha, Boominathan, Suraj, Maduri, Harpreet, Vyankatesh, Amit, Kirti, Ravi, Ameya, Krithika.

I am thankful to NCL friends and collegues Rajambal, Senthil, Sandeep, Sudha, Vinodh, Poulomi, Nimisha, Rupa, Suman, Sana, Vidya, Subhadarshinee, Harshitha, Rajeshwari, Prachi, Swetha, Reema, Rohini, Anurag, Rohil, Rahul, Meenakshi, Aswathy, Suwarna, Bhagyashree, Abha who eased the stay and work at NCL.

Friends play a major role in life by giving encouragement and happiness; I thank my college friends, Nevedha, Agatha Shiny, Geetha, Karuna, Anbu, Raji, Swathyshree, Mariayammal.

I am very happy to express my heartfelt gratitude to my family members even though, it is not enough of words for the love and affection that they showered on me. First and foremost I extend my gratitude and respect to my beloved grandparents, late Mr. M. Muthumanickam and Mrs. M. Santhadevi for their endless love, inspiration and encouragement without which I couldnot imagine how the life would have been. I thank my parents, in particular my Mom Mrs. T. Ayizhai, who ever struggled for my well being and also for her support during my Ph.D. enduring my absence since a long period. I recognize the kindness and appreciation of my dear aunty Ms. M. Athirai and I am indebted to her. I always thank Vijay for his moral support during my hardships, and reassurance during tough times. I thank all my relatives who stood together during ups and downs in course of time.

Last but foremost, I thank Almighty for blessing me with strength and good health to move ahead with enthusiasm after gaining new experience through crossing the obstacles in all the circumstances in life.

T. Aarthy

CONTENTS

List of Tables

List of figures

ABBREVIATIONS

ATP:	Adenosine Triphosphate
ABC:	ATP- Binding Cassette
AGC:	Automated Gain Control
BAP:	Benzyl Amino Purine
bHLH:	Basic helix–loop–helix
BLAST:	Basic Local Alignment Search Tool
bp:	base pair
BSA:	Bovine Serum Albumin
bZIP:	Basic Leucine Zipper
CCC:	Counter-current chromatography
cDNA:	Complementary deoxyribo nucleic acid
CFP/YFP:	Cyan/yellow fluorescent protein
CIP:	Calf intestinal phosphatase
CRISPR:	Clustered regulatory inter spaced short palindromic repeats
CYP:	Cytochrome P450
CPR:	Cytochrome P450 reductase
CPW media:	Cell protoplast washing media
CHO:	Chinese hamster ovary
Co-IP:	Co-immunoprecipitation
2,4-D:	2,4 -dicholoroacetic acid
DEPC:	Diethyl pyrocarbonate
DHAP:	Dihydroxy acetone Phosphate
DMAPP:	Dimethylallyl pyrophosphate
DNA:	Deoxy ribonucleic acid
DNase:	Deoxyribonuclease
DTT:	Dithiothritol
DXS:	Deoxyxylulose-phosphate synthase
EC_{50}:	Half maximal effective concentration
ELF4A:	Elongation Factor 4A
eSEM:	environmental Scanning Electron Microscopy
ESI:	Electro Spray Ionisation
EST:	Expressed Sequence Tags
EIC:	Extracted Ion Chromatogram
FPP:	Farnesyl pyrophosphate
FRET:	Fo¨rster resonance energy transfer
FRET:	Fluorescence resonance energy transfer
FCS:	Fluorescence correlation spectroscopy
GC–MS:	Gas chromatography–Mass Spectrometry
GFP:	Green fluorescent protein
GPP:	Geranyl pyrophosphate
GAP:	Glyceraldehyde 3-phosphate
GGPP:	Geranylgeranyl pyrophosphate
Glc:	Glucose
HESI:	Heated Electrospray Ionisation
HMG-CoA:	3-hydroxy-3-methyl-glutaryl-coenzyme A
HMGR:	3-hydroxy-3-methyl-glutaryl-coenzyme A reductase

HPLC:	High Performance Liquid Chromatography
HPA:	Human pancreatic amylase
HRMS:	High Resolution Mass Spectrometry
HSP:	Heat shock protein
IPP:	Isopentenyl diphosphate
IPTG:	Isopropyl β-D-1-thiogalactopyranoside
IGR:	Insect growth regulation
IDI:	Isopentenyl diphosphate isomerase
Kbp:	Kilo basepair
KDa:	Kilo Dalton
LDH:	Lactate dehydrogenase
LAESI:	Laser Ablation Electrospray Ionization
LC–MS:	Liquid chromatography–Mass Spectrometry
MATE transporter:	Multidrug And Toxic compound Extrusion transporter
MEP:	2-C-methylerythritol 4-phosphate
MIF:	Migration inhibitory factor
mM:	milli molar
MPLC:	Medium-pressure liquid chromatography
mRNA:	messenger ribonucleic acid
MS Imaging:	MSI
MVA:	Mevalonate
MS:	Murashige and Skoog
m/z:	mass/charge
NAA:	Naphthalene acetic acid
NADPH:	Nicotinamide adenine dinucleotide phosphate reduced
NAF:	Non-aqueous fractionation
NCE:	Normalized Collision Energy
NEB:	New England Biolabs
Ni-NTA:	Nickel-nitrilotriacetic acid
NMR:	Nuclear magnetic resonance
NPF:	NITRATE TRANSPORTER 1/PEPTIDE TRANSPORTER (NRT1/PTR) Family
NTC:	No template control
Nt-JAT1:	*Nicotiana tabacum*- jasmonate-inducible alkaloid transporter1
OD:	Optical Density
ORF:	Open reading frame
PAGE:	Polyacrylamide Gel Electrophoresis
pI:	Isoelectric point
PBP:	Periplasmic Binding Protein
PCR:	Polymerase Chain Reaction
PMSF:	Phenyl methyl sulphonyl fluoride
PTTH:	Prothoracicotropic hormone
qPCR:	quantitative Polymerase Chain Reaction
QTOF:	Quadrupole Time of Flight
RBL:	Rice Bran Lipase
RNA:	Ribonucleic acid
rRNA:	Ribosomal Ribonucleic acid
RT:	Retention Time

SDS:	Sodium dodecyl sulphate
TCA:	Tricarboxylic acid
TAG:	Triglycerides
TPS:	Terpene synthase
TPP:	Thiamine pyrophosphate
TAP:	Tandem affinity purification
TBY-2:	Tobacco Bright yellow-2
TIC:	Total Ion Chromatogram
UPLC:	Ultra Pressure Liquid Chromatography
VOC:	Volatile Organic Compound

ABSTRACT

Introduction

Due to their immobile nature, plants have evolved and adapted to different environmental stresses by effective synthesis, storage and emission of secondary metabolites in the necessary time and space. These secondary metabolites or natural products are of immense fortitude to mankind due to its different kind of ameliorating property on human health ailments. Neem tree, one of the Indian medicinal plant well-known and being used for its healing property from ancient past is of profound interest and hence, the study of its biosynthetic pathway, understanding its localization, regulation etc., will pave the way to design an efficient way of treating human diseases as a natural means of medicament. The thesis entitled, "**Limonoid biosynthesis in *Azadirachta indica*: Characterization of pathway genes and analysis of labeled metabolites through stable isotope feeding**" is concerned with the study of biosynthesis of limonoids and other secondary metabolites and their localization in neem.

CHAPTER 1

Introduction and objective of the thesis

Neem tree is known for its bountiful and diverse natural products conferring numerous medicinal and agricultural uses for mankind[1]. Among these plenty of natural products, most of them belong to triterpenoid (limonoids)[2]. More than 150 limonoids have been isolated and characterized from neem so far and each of them has been studied for its biological activities[3]. Azadirachtin, one of the highly complex limonoid had been studied widely for its excellent anti-feedant, insecticidal property, with no proven harmful effects on vertebrates and are found to be an unsurpassable natural product identified hitherto for its efficiency. The successful chemical synthesis of this complex molecule was accomplished after 22 years of efforts by Ley *et al.*[4, 5]. Azadirachtin and other bioactive limonoids are highest in the fruits of neem tree. There is an indispensable requisite for metabolic engineering of this pathway in heterologous system. Therefore, the study of azadirachtin biosynthetic pathway is highly essential to harness the biosynthetic capacity of the tree for its medicinal properties. Following are the main goals of the thesis,

- To identify and characterize the organelles/ intra-cellular compartments involved in the storage of limonoids in different tissues.
- To trace the flow of carbon in limonoid skeleton through stable isotope feeding experiments.
- To study the expression level of the genes involved in isoprene biosynthetic pathway and to characterize the putative candidate genes associated with limonoid biosynthesis.

CHAPTER 2

Development of *in vitro* cultures of neem, limonoid profiling and study of organelles and cells involved in limonoid storage

In our laboratory, we have identified previously, the tissue and developmental stage specific differential distribution and abundance of ring intact (basic) and C-seco limonoids in different neem tissues[6]. This incredible and impressive abundance of limonoids in fruit and leaf tissues actuated us to look for the specialized cells involved in accumulating limonoids and also the development of neem plantlets, *in vitro* callus from kernel and callus derived suspension system to study limonoid biosynthesis. C-seco limonoid group exists as major limonoid synthesized in the *in vitro* plantlets and also callus and suspension cells. In the present study, histochemical analysis of different tissues has been carried out to study the limonoid localization in cellular and subcellular compartments. It suggested that laticifers are rich in basic limonoids and oil bodies are found to be the major source of C-seco-limonoids in pericarp and kernel of neem fruit respectively, whereas limonoids exist in abundance in idioblast vacuoles in pericarp and leaf tissues. Average number of idioblasts per mm^2 of tissue was comparatively high in pericarp to that of leaf, which matched with the abundance of limonoids in these tissues respectively (Figure 1).

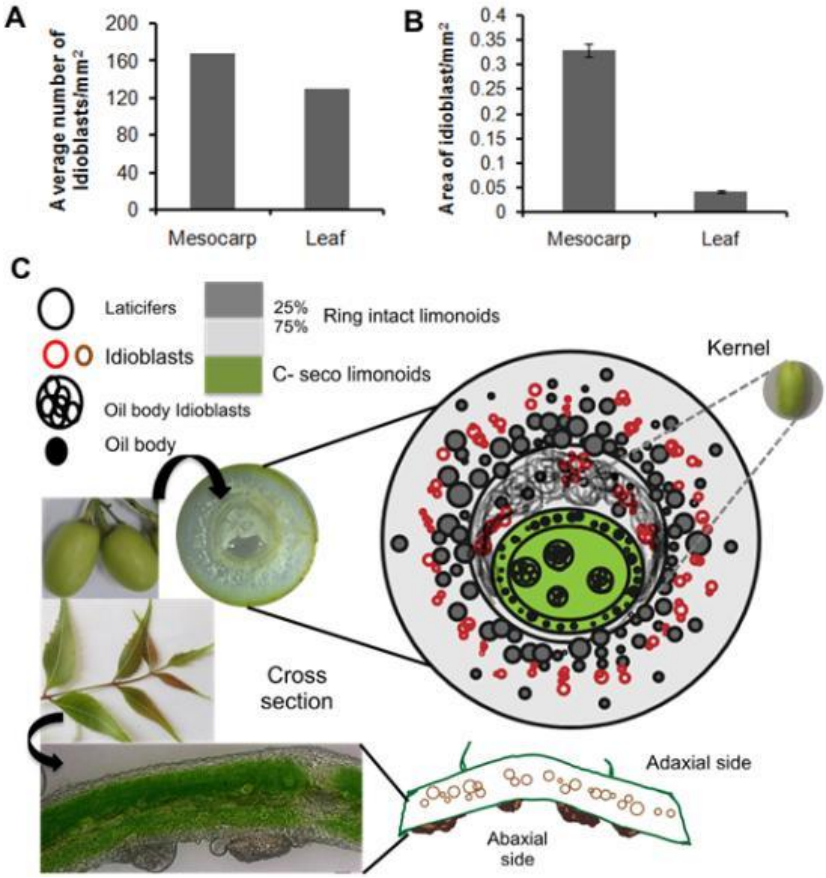

Figure 1. (A) Number of idioblasts in different tissues and (B) their area contribution (C) Model showing cellular and subcellular compartmentalization of limonoids in neem fruit and leaf

CHAPTER 3

Ex vivo tracer study of limonoid biosynthesis in *Azadirachta indica*

Neem tree serves as a cornucopia for triterpenoids called limonoids that are of profound interest to humans due to their diverse biological activities. A well-known potent anti-feedant, highly complex molecule, azadirachtin and many other biologically active limonoids are distributed in different tissues of neem[7]. The biosynthetic machinery that plant cell employs for the production remains unexplored for this wonder tree. Herein, we report the tracing of limonoid biosynthetic pathway through feeding experiments using ^{13}C labeled isotopologues of glucose in neem cell suspension. In order to identify the signature fragment of azadirachtin A generated through ESI-MS, fragments generated from MS/MS of azadirachtin derivatives such as azadirachtin B, H, 3-deacetylazadirachtin A, epi-azadirachtin D, vepaol were studied comparatively at different normalized collision energies. The plausible fragmentation pathway for azadirachtin A has been proposed showing the structure-fragment relationship. This helped in tandem mass spectrometry (MS/MS) analyses of labeled limonoid

extract,which lead to the identification of signature isoprenoid units involved in azadirachtin and other limonoid biosynthesis (Figure 2). Therefore, the isoprene units contributed for limonoid skeleton biosynthesis are found to be formed through mevalonate (MVA) pathway (Figure 3).

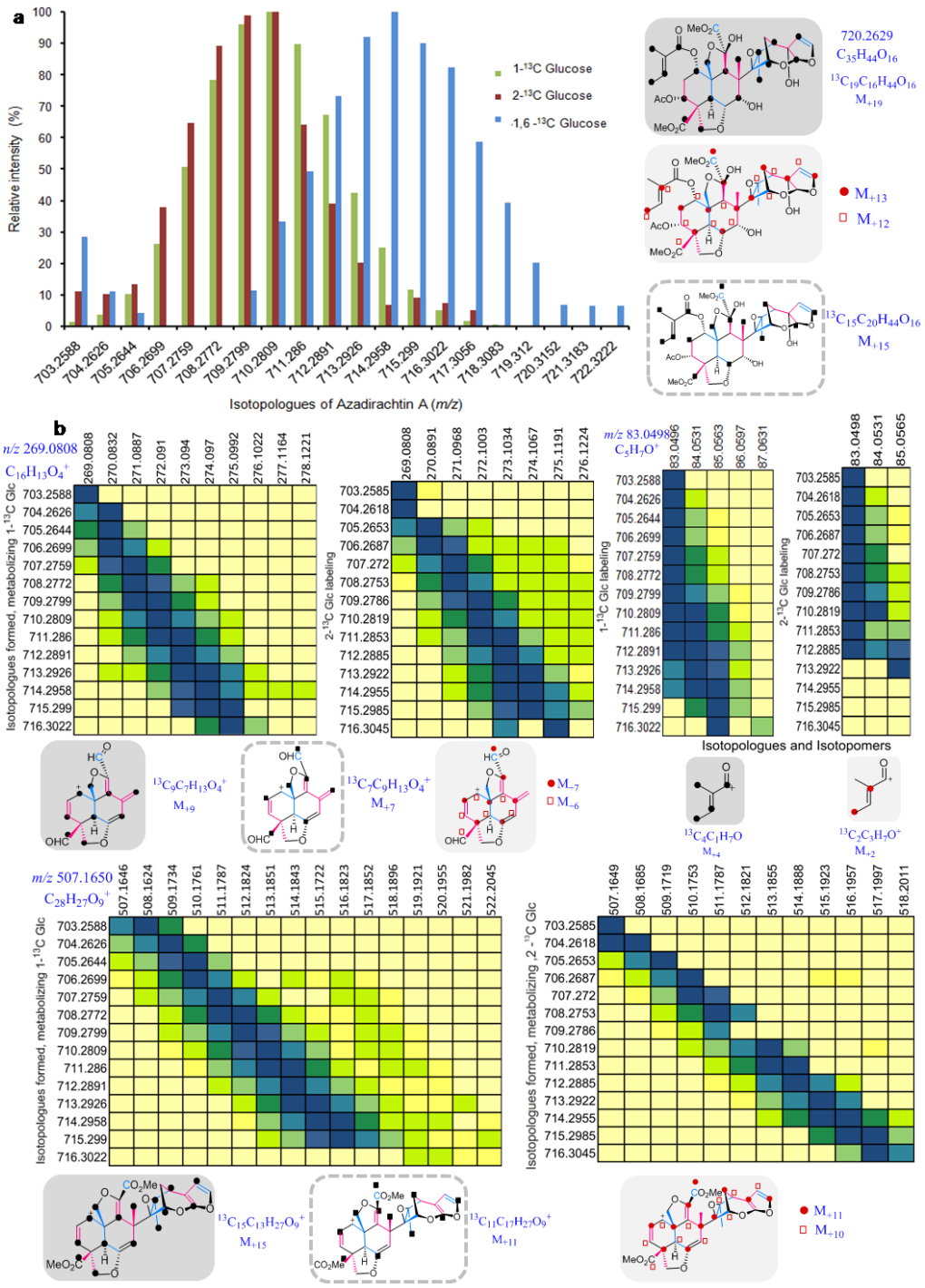

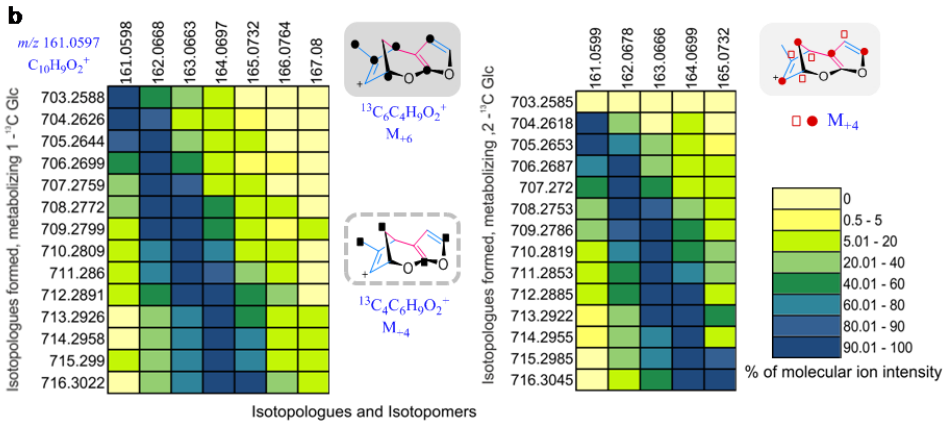

Figure 2. Distribution of azadirachtin A isotopologues and isotopomers obtained from ESI-MS and MS/MS analysis. (a) Comparison of relative intensity of isotopologues of protonated ion adduct $[M\text{-}H_2O+H]^+$ of azadirachtin A obtained from independent labeling experiments with [1-^{13}C], [2-^{13}C], [1,6-^{13}C] Glc. (b) Heatmap of isotopologue of azadirachtin A in the masss pectra vs. relative intensity of each of the isotopologues for individual fragments (*m/z* 83.0498, 161.0597, 269.0808, 507.1650 derived from different part of the skeleton are represented) obtained when subjected to tandem MS at collision energy of 20%. The structure of the molecule and its fragments are given in grey boxes for the molecule denoting its ^{13}C pattern of formation through MVA pathway and dashed line boxes for its formation through MEP pathway. The black dots and squares represent the position of ^{13}C carbón incorporated from [1-^{13}C]Glc / [1,6-^{13}C] Glc whereas the red dots corresponding to those from [2-^{13}C] Glc.

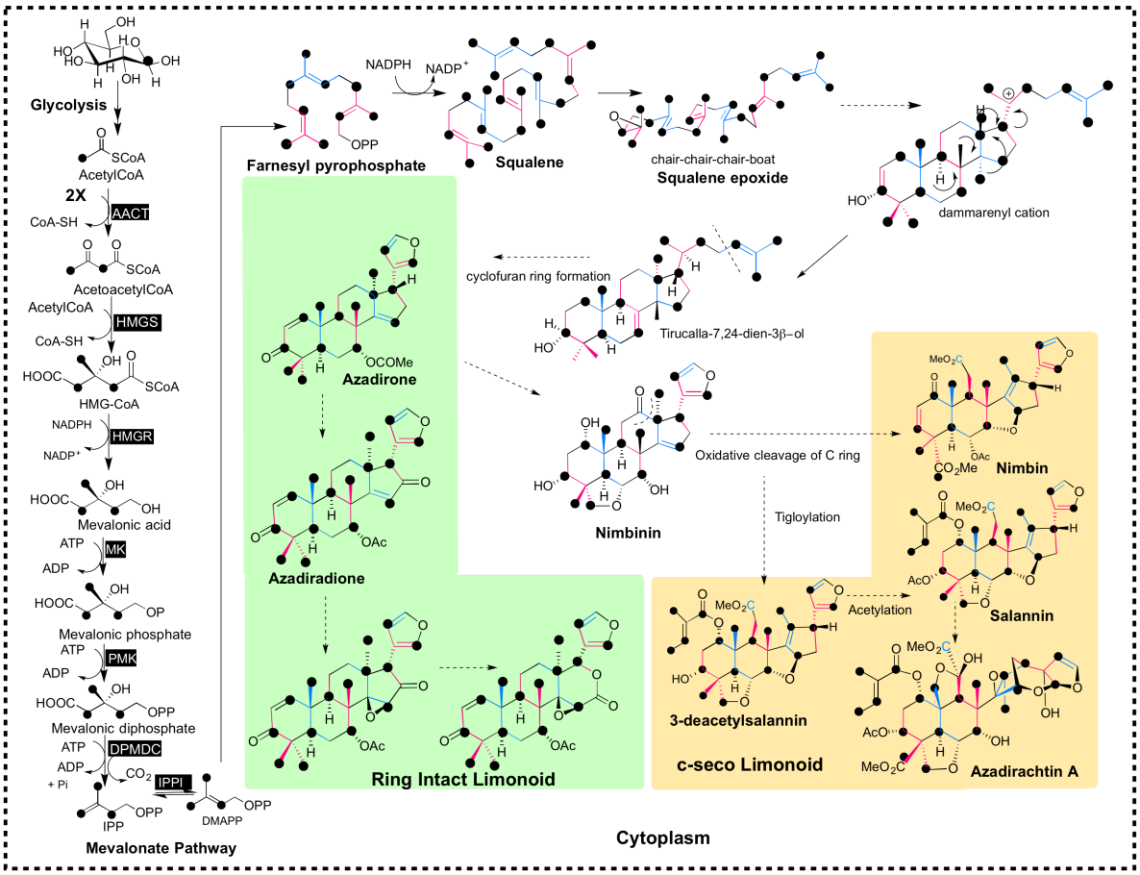

Figure 3. Simplified scheme showing limonoid biosynthesis in neem being contributed by isoprene units formed through MVA pathways evident from the labeling experiment with ^{13}C glucose. C-seco and ring intact limonoid are represented in yellow and green boxes respectively. (Alternate isoprene units of the limonoid skeleton are shown in pink and blue, dotted arrow shown here are the uncharacterized steps in the pathway).

CHAPTER 4

Study of the role of MVA and MEP pathway in limonoid biosynthesis and characterization of pathway genes

To study the role of MVA and MEP pathway towards limonoid biosynthesis, chemical inhibition of the pathways along with concomitant ^{13}C Glc labeling was carried out. Treatment of cell suspension with mevinolin, a specific inhibitor for MVA pathway, resulted in drastic decrease in limonoid levels whereas their biosynthesis was unaffected with fosmidomycin mediated plastidial methylerythritol 4-phosphate (MEP) pathway inhibition (Figure 4). This was also conspicuous, as the expression level of genes encoding for the rate-limiting enzyme of MVA pathway, 3-hydroxy-3-methyl-glutaryl-coenzyme A reductase (HMGR) was comparatively higher to that of deoxyxylulose-phosphate synthase (DXS) of MEP pathway in different tissues and also in the *in vitro* grown cells as evident from real-time PCR analysis (Figure 5).

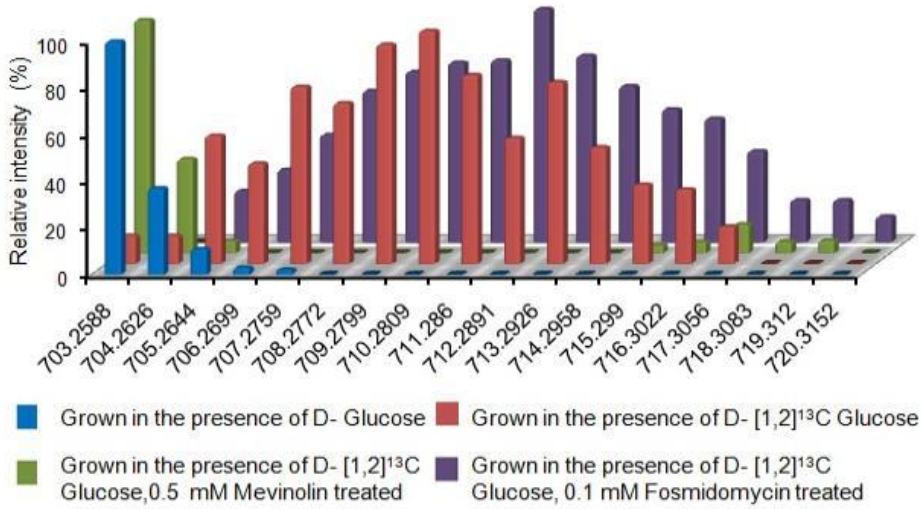

Figure 4. Chemically inhibited MVA and MEP pathway cells grown in the presence of [1,2-^{13}C] Glc to monitor the formation of isotopologues. Fosmidomycin treatment didn't interfere with (limonoid) azadirachtin A biosynthesis as evidenced from the labeling experiment carried out during the pharmocological inhibition of the cells with mevinolin and fosmidomycin.

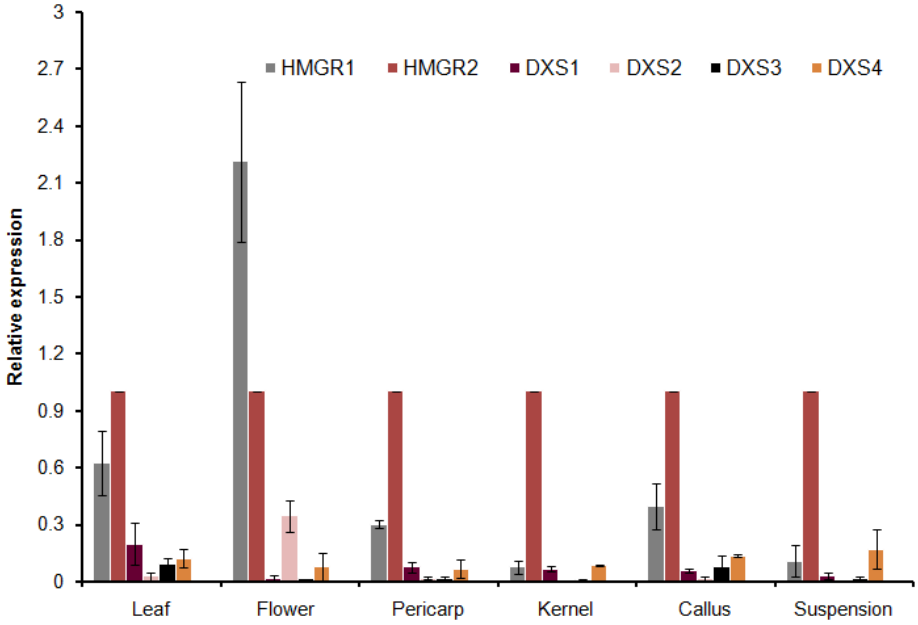

Figure 5. Expression profile of HMGR and DXS genes in various tissues relative to the expression of HMGR2.

This chapter also deals with the cloning of putative acyltransferase genes in neem. Neem limonoids being triterpenoids are biosynthesized from the triterpene intermediate squalene, which en route to 2,3 oxidosqualene leading to cyclized triterpene intermediate which further modifies to form protolimonoids. Limonoids further undergoes numerous functionalizations such as redox reactions, hydroxylation, acetylation, tigloylation etc. to form several limonoids in multistep pathway, which are yet to be elucidated. In order to understand limonoid diversity in neem, putative acyltransferase ORFs were selected from neem transcriptome for cloning. The selected acyltransferases matched with BAHD family of plant acetyltransferases, which transfers group from CoA to natural products. The two full-length ORFs were cloned into bacterial and yeast vector systems and characterization of the expressed protein to understand its function with limonoids and/ other terpene or non-terpene alcohols as substrates.

References

1. K. K. Singh, Suman Phogat, R.S. Dhillon, Alka Tomar, *Neem, a Treatise*, I.K. International Publishing House, 2009.
2. E. D. Morgan, *Bioorg. Med. Chem.*, 2009, **17**, 4096-4105.
3. A. Roy and S. Saraf, *Biol. Pharm. Bull.*, 2006, **29**, 191-201.
4. G. E. Veitch, E. Beckmann, B. J. Burke, A. Boyer, S. L. Maslen and S. V. Ley, *Angew. Chem. Int. Ed.*, 2007, **119**, 7773-7776.
5. K. Sanderson, *Nature*, 2007, **448**, 630-631.
6. A. Pandreka, D. S. Dandekar, S. Haldar, V. Uttara, S. G. Vijayshree, F. A. Mulani, T. Aarthy and H. V. Thulasiram, *BMC Plant Biol.*, 2015, **15**, 1-14.
7. G. Brahmachari, *Chembiochem*, 2004, **5**, 409-421.

Chapter 1

Introduction

1.1. Introduction

In living system, chemical reactions occur through careful regulation of integrated network of enzymes existing in the form of metabolic pathways. The processes involved in the synthesis and transformation of crucially important molecules of life such as carbohydrates, proteins, fats and nucleic acids are the primary metabolic processes and the molecules formed are termed as primary metabolites[1]. In contrast, other groups of metabolites are restricted to a specific organism or group of organism or produced under specific conditions, specific location or time, and such compounds are called as secondary metabolites[1]. They are broadly classified into three major groups as terpenoids, alkaloids and phenylpropanoids[1,2].

These secondary metabolites play a vital role in the protection of the organism such as deterrence or avoidance of the predators through toxic compounds, production of volatiles and coloring agents serving to attract or interact with other organisms[3]. Plants due to its sessile nature need to survive extraordinary stresses which can be carried out using ideal mechanism mediated through secondary metabolites[1,3]. Hence, they produce diverse number of natural products in order to survive in case of biotic and abiotic stresses occurring from the environment[2]. These molecules may directly be involved in defense or in the chemical signaling to activate different pathways to positively or negatively interact with the organism in the environment. Such metabolites formed as a result of secondary metabolism also serves as pharmacologically active natural products. Thus, the natural products produced by microorganisms, plants and marine species have been successfully employed as a drug candidate for treating human ailments. These natural products serve as lead molecules for drug discovery. To exemplify, aspirin and taxol derived from willow and yew tree serves as a medication for fever and cancer chemotherapy respectively, and are of great pharmacological significance for mankind. The scientific plant secondary metabolite research can be dated to 1805, marked by the isolation of morphine from poppy (then called as *Principium somniferum*) by a German pharmacist, Wilhelm Sertürner[4]. Since that time, research in this field has been developed in three aspects as

1. Mechanical insights into biosynthetic pathway.

2. Functional role of them as a communication, protection, attraction and defense responses to the producer with other organisms.

3. The third aspect as the evolutionary connection between gene diversity and plasticity of secondary metabolites playing an ecological role in dynamic interactions of plant with its varying environment[4,5,6,7].

Knowledge on mechanistic aspects of metabolites advented with radioactively-labeled nuclides in early 1950s followed by the emergence of stable nuclides as tracers[4,5,6,7,8]. Ecological aspect has been realised post-1950s based on understanding such as gene duplication, one of the major driving forces for gene diversification resulting in metabolite diversity[4,5,9,10].

Hence, depending on the significance of natural product for mankind, the secondary metabolite biosynthetic pathway has been intensively studied in plants. An example of plant with numerous bioactive molecules studied for its various pharmocological activities is the medicinal tree *Azadirachta indica*.

1.2. Neem tree – *Azadirachta indica*

In 1830, French botanist, Antoine Laurent de Jussieu identified *Melia Azadirachta*, which he renamed later as *Azadirachta indica* A. Juss. The Latinized form of the name is derived from Persian as *Azadi*- free, *diracht*- tree, which means, the tree free from insect and diseases[11]. Neem tree, gained honour as a wonder tree, native to Indian sub-continent is one of the highest source of secondary metabolites. It has been used traditionally since ancient times in Ayurveda, Siddha and Unani medicine for the treatment of myriads of human ailments and is slowly drawing the attention of scientific community because of its immense, inexpensive and multifaceted medicinal potential[11,12]. Every part of the tree has been studied by various research groups all over the world for its chemical composition and has been completely characterized. The major metabolic diversity of neem has been attributed to limonoids, exclusively found in Meliaceae family of trees belongs to the terpenoid class of metabolites[13]. Apart from these triterpenes, various other terpenes such as monoterpenes, sesquiterpenes and diterpenes are found to be present in neem[14]. Other class of secondary metabolites such as phenolics, flavonoids, chalcones and coumarins has also been characterized from neem[14,15]. Such a diverse secondary metabolite biosynthesis has evolved in the plant for its defense from the environmental and biotic factors, and this has been a boon to mankind as it serves as medicinal natural products for treatment of various ailments.

Apart from these diverse natural products, it is a rich source of fatty acids and aliphatic hydrocarbons. Fatty acids of neem comprise triglycerides (TAG) of oleic, palmitic, stearic acids. Plenty of knowledge has been accumulated over the years about the plethora of medicinal properties of this tree [16,15,17].

Figure 1.1. A healthy neem tree in the CSIR-NCL campus used in this study.

The tree has been placed in the following systematic position.

Kingdom:	Plantae
(unranked):	Angiosperms
(unranked):	Eudicots
(unranked):	Rosids
Order:	Sapindales
Family:	Meliaceae
Genus:	*Azadirachta*
Species:	*A. indica*

1.3. Ethnobotany and ethnomedicine of neem

Neem has been used in the folkloric and traditional system of medicine in different parts of south-Asian continent[11]. Neem seed has become integral part of farming in Indian agricultural system due to its insect derogating property[18]. Leaves and twigs are used as manure and mulched in the agricultural fields. Fresh and young twigs are used by people to keep the teeth clean, neem leaves or oil is burned to keep away the mosquitoes, leaves soaked water, is used for treating skin ailments and chicken pox etc.[19]. Therefore, neem twigs and leaves are used to treat dental and gastrointestinal disorders, malaria fevers, skin diseases in folklore medicine in India[20,18,12]. Whereas in Bali (Indonesia), the neem leaves are used as a diuretic and to treat diabetes, headache, heartburn, and also for stimulating appetite[12]. The plethora of medicinal properties of the tree is attributed to several class of bioactive natural products, the predominant ones are the triterpenes called limonoids[13].

1.4. Limonoids

Limonoids are present and widely distributed in the families of Meliaceae, Rutaceae and in few species of Simaroubaceae[13]. The term limonoid was coined after limonin from citrus, the first isolated bitter tasting principle[21]. Limonoids from neem are termed as meliacins[21]. Based on their chemical, they are termed as tetranortriterpenoids. They all possess 4,4,8-trimethyl-17-furanylsteroid skeleton or a metabolite derived from the skeleton. They are of moderate polarity, insoluble in water but soluble in organic solvents. Limonoids are bioactive molecules that have undergone complex functionization in the skeletal structure composed of steroid skeleton consisting of A, B, C and D rings[13]. The C ring is cleaved and opened to give a group of limonoids called C-seco limonoids and the ones without such modification are termed as ring intact (basic) limonoids. Based on the modification in the ring, limonoids are further classified into six different groups such as promeliacins, amoorstatins and vepinins, vilasinins, azadirones, gedunins, and c-seco meliacins such as nimbins, salannins, azadirachtins[14,21,16, 2,4].

Protolimonoids or protomeliacins contain C-8 side chain at C-17 position and are the precursor for all the limonoids[14]. Azadirone group of limonoids are predicted to be the next intermediate after protolimonoids and first tetranortriterpenoids formed from protolimonoids[14]. Vepinins are molecules, which has an oxygen bridge between C-7 and

C-15 positions whereas, vilasinins possess ester linkage between C-6 and C-28 positions[14]. Amoorstatin is the only group of limonoid which possess oxygen bridge between C-9 and C-29 position, however it neither has any ether linkage between C-6 and C-28, C-7 and C-15 nor C-14 and C-15 like that of other groups of limonoids[14]. Gedunin possess epoxy lactone in the D ring due to insertion of oxygen between C-16 and C-17[14]. C-seco limonoids are characterized by opening of C ring and ether bridge formation at C-7α and 15β positions as found in nimbolide, nimbin, salannin and its derivatives[14] (Figure 1.2).

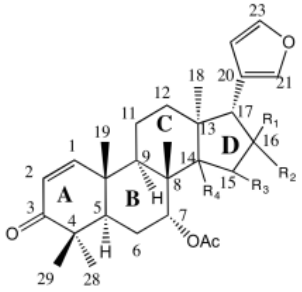

Protolimonoids and Apo-protolimonoids		
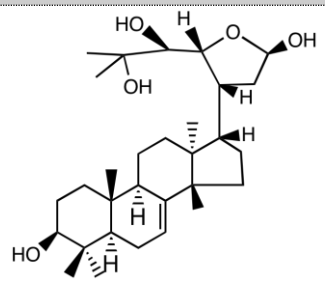 **Meliantriol**	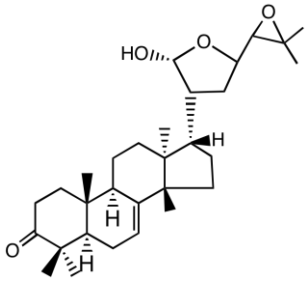 **Melianone**	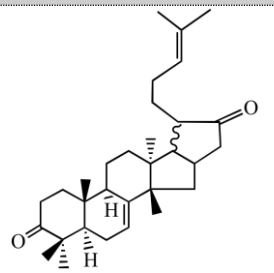 **Kulactone**
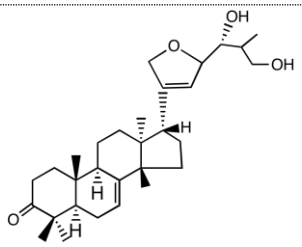 **Nimbocinone**	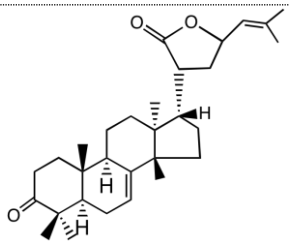 **Nimolinone**	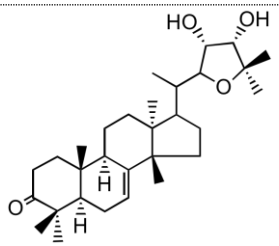 **Odoratone**
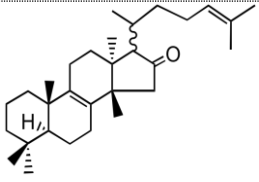 **Limocinone**	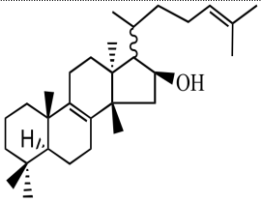 **Limocinol**	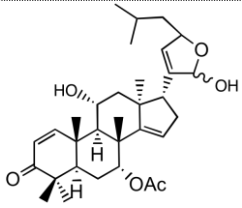 **Azadirachtol**

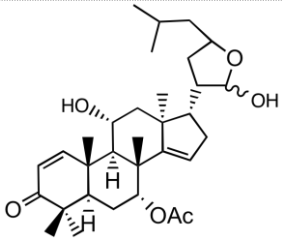 **Azadirachnol**	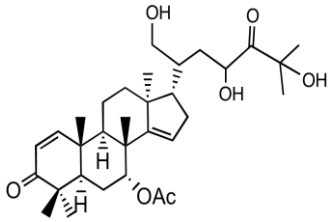 **Azadirol**	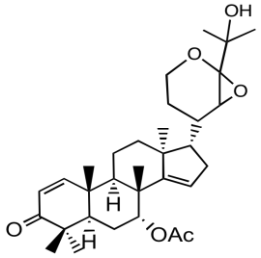 **Diepoxyazadirol**
Azadirone		
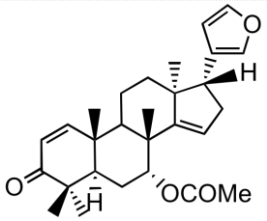 **Azadirone**	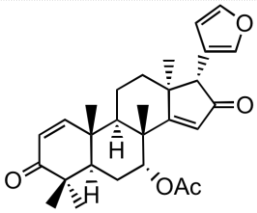 **Azadiradione**	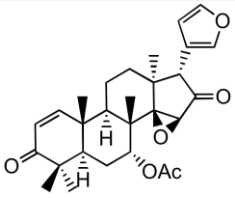 **Epoxyazadiradione**
Vilasinin		
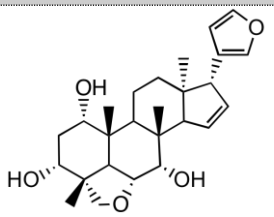 **Vilasinin**	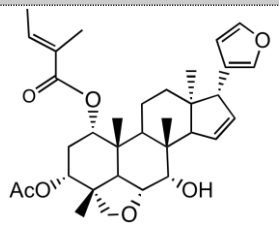 **1-O-seneccioyl-3-O-acetylvilasinin**	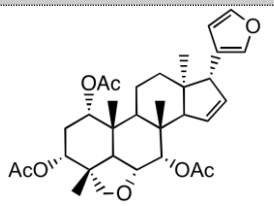 **Vilasinintriacetate**
Amoorstatins and Vepinin		
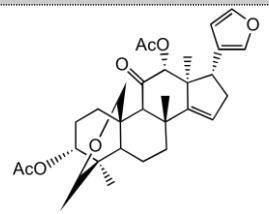 **Azadirachtanin**		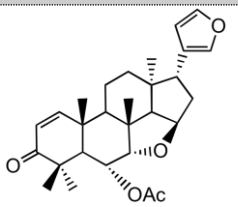 **Vepinin**
Gedunin		
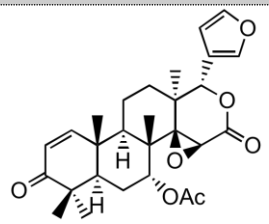 **Gedunin**	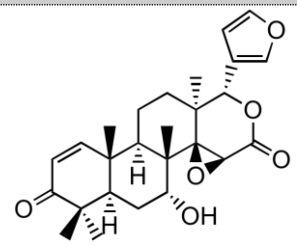 **7α-Deacetylgedunin**	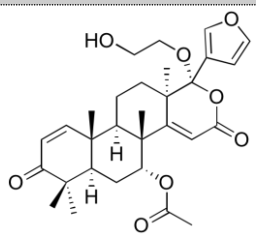 **Mahmoodin**

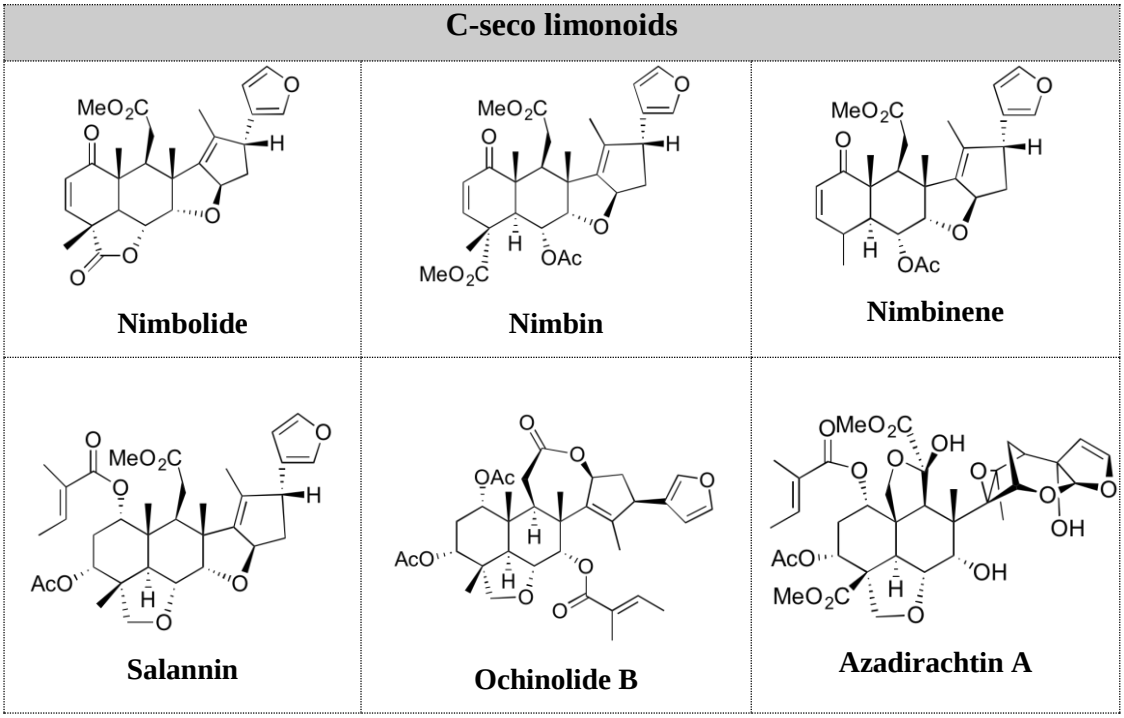

Figure 1.2. Skeletal diversity of neem limonoids. Chemical structures of limonoids identified in this study classified according to ring modification, as ring intact and ring C- seco limonoids.

1.5. Isolation of neem limonoids

Neem limonoid isolation has been successfully employed for more than six decades, indeed, with greatly evolving separation technologies thereby expediting and simplifying the purification of individual limonoids. Siddiqui was a pioneer in the field of limonoid isolation from neem tree[22]. The first limonoid isolated by him was nimbin in the year 1942[14] and followed by many other limonoids[14,15,23–26]. Most fascinating limonoid, azadirachtin A possessing potent anti-feedant and exhibiting growth regulatory activity against insects was first isolated by Morgan in 1968[27]. Before the isolation of azadirachtin A, in the year of 1959, the extra-ordinary anti-insecticidal property of neem tree was already recognized by Heinrich Schmutterer, when he observed that the desert locust, *Schistocerca gregaria* didn't affect the neem tree during the invasion of other plants in Sudan[27].

Since limonoids are present as complex mixture, they cannot be isolated and quantified directly from the crude extract, but requires fractionation in case of isolation from larger quantity sample. Flash chromatography is a rapid technique employed for the separation of limonoids in fractions from the complex mixture of neem metabolite extract which contains tremendous amounts of green pigments[28–30]. Biotage™ flash

chromatography developed has been an improved and quicker method when compared to the usage of gravity column chromatography[29]. Supercritical fluid chromatography has also been successfully employed for the analysis of limonoids in the smaller scale[2931]. Counter-current chromatography (CCC), a liquid-liquid partition method has been successfully used for the separation of different limonoids in fractions prior to HPLC, as it helps in avoiding irreversible contamination of solid support matrix due to pigments, unlike other techniques[32]. Combined used of preparative layer chromatography, open-column reversed phase chromatography and HPLC were instrumental in the isolation and purification of azadirachtins and other major limonoids to its highest purity for different studies[30,33–36,37–40,41,31,42]. The pure azadirachtin congeners were isolated efficiently using reverse phase medium-pressure liquid chromatography (MPLC). Saikat *et al* has developed a MPLC based separation method for expedient isolation of various limonoids in fractions from crude extract of neem in large scale[43,44]. Liquid Chromatography Electrospray Ionization Tandem Mass Spectrometry and atmospheric pressure chemical ionization provided the rapid, sensitive and accurate quantification of limonoids[45,46]. More than 150 limonoids have been isolated and characterized from neem so far and fascinating biological activity of some of them has been extensively studied[13,21].

1.6. Bioactivity of neem limonoids

The bioactive potential of neem limonoids has been realized in the fields of agriculture and human welfare.

1.6.1. Neem limonoids in Agriculture

Azadirachtin A, an effective insect growth deterrent, is found to be the best potential natural insecticide candidate identified so far from the plant sources[22]. It also possesses remarkable non-toxicity to vertebrates[22,47]. Unlike other insecticide, which exerts its effect on the nervous system of insects, azadirachtin was known to act on the endocrine system[48], thereby affecting the feeding behavior, development, reproduction and metabolism in insects. Its effect on ecdysteroid and juvenile hormone titers of insect is through blockage of morphogenetic peptide hormone release (e.g. PTTH; allatotropins)[47]. Hence, the physiology of the insect is affected resulting in overall reduction in fitness of the insect[47]. EC_{50} vary from10^{-10} to 10^{-9} M and 10^{-5} to 10^{-3} M for

insect and mammalian cell lines respectively, and hence toxicity of it is 100 times less on mammals[22]. Thus, azadirachtin act as an ecdysis inhibitor, growth inhibition occurs through hormonal imbalance, and acts as an anti-feedant by the stimulation of specific deterrent chemoreceptors, interfering with other chemoreceptors on the mouthparts[48]. It also interferes with the pupation and adult eclosion rates[49]. Azadirachtin A was found to possess acaricidal activity as evidence from the activity against the camel tick, *Hyalomma dromedarii*[50]. Azadirachtin A, B and H were found to possess nematicidal activity as shown from the study of their activity against the reniform nematode *Rotylenchulus reniformis* at EC_{50} of 119.1 ppm, 96.6 ppm and 141.2 ppm respectively[24,51]. Apart from the potent insecticidal limonoid azadirachtin A, limonoids such as salannin, 7-deacetylgedunin, gedunin, 17-hydroxyazadiradione, and 6-deacetylnimbin are also found to affect the gut enzyme activity and glycolytic enzyme lactate dehydrogenase (LDH) on rice leaf folder larvae thereby providing a evidence that gut physiology of larvae and [52] are disturbed by the uptake of limonoids[53]. 6β-hydroxygedunin inhibited 50% of the growth of *Helicoverpa armigera* and *Spodoptera litura* with higher efficacy in comparison to gedunin, salannin, azadiradione, nimbocinol and nimbinene[54–56].

Margosan-O® a commercial product made of neem extract concentrate was approved by USA Environmental Protection Agency for use as a natural pesticide which was followed by the availability of several neem-based products from different countries[57]. The commercial product Margosan-O®, contains the potent anti-feedant azadirachtin and it fulfills all the criteria of effective insect anti-feedant which includes the need for selective toxicity, activity at low concentration, economic viability, stability, and compatibility with existing plant protection methods[58]. Neem oil, a major component extracted form neem kernel is found to increase the efficacy of neem based insecticides[59]. It also helps in the reduction of virus transmission by aphid, when compared to oil-free extracts[49,60–65]. Neem oil is also found to be potential pesticide for termite control[66] and has strong acaricidal activity[67,50,68,69,70,71,72,73,74]. Formulations of neem oil was also found to be a effective fungicide as seen from the studies on the pathogenic fungus *Macrophomina phaseolina* and *Sclerotium rolfsii*[75]. The oil also showed activity against the larvae of malarial vector mosquitoes[76,73,77]. Toxicity of neem oil has been very well documented for various agricultural pests across its all

developmental stages from nymph, larvae to adult insects[72,78,79,80,81,82,83,84,85,86,87,88,89,90,65,91,92].

1.6.2. Neem limonoids in Pharmaceutical and human welfare

Different parts of neem tree have been employed for the treatment of human ailments from time immemorial in traditional system of medicine in India. Neem extracts from various parts of the tree have been proved to have the following properties such as anti-malarial, anti-microbial, anti-inflammatory, anti-pyretic, anti-mitotic, anti-tubercular, anti-viral, anti-fertility, anti-diabetic, anti-gastric ulcer, anti-arthritic, anti-carcinogenic etc. through various *in vitro* and *in vivo* studies[21]. But, few studies projects the role of individual limonoids which confer the therapeutic value for respective extracts, its mechanism of action, its effect on other pathways in the cell, dosage level etc. Neem bark extract showed activity against Herpes simplex virus type-1, the causative agent for various skin lesions to encephalitis. A ring intact limonoid, mahmoodin showed significant anti-bacterial activity against various Gram-positive and Gram-negative organisms[25]. The anti-angiogenic potential of ethanol extract of neem leaves over human umbilical vein endothelial cells has been evaluated by Mahapatra *et al.* and the study showed that limonoids such as nimbolide and 2,3-dehydrosalannol effects it through inhibition of vascular endothelial growth factor[52].

Nimbolide, a limonoid from leaf and flower, arrested the growth of murine neuroblastomas cells[93] and human carcinoma cells (HT-29), through the upregulation of p21, which is the downstream effector of p53, a gene that encodes anti-cancer protein[19]. A recent study provided mechanistic insights into therapeutic potential of nimbolide, as it promotes apoptosis and attenuates cell proliferation in carcinomas[94]. Anti-proliferative, apoptosis inducing effect and mechanism of action of nimbolide has been elucidated and described by Singh *et al*. in prostate cancer cell lines[95]. Another individual group has studied its therapeutic potential for pancreatic cancer as it regulates apoptosis and autophagy in pancreatic cancer cells[96]. Neem limonoids induces intrinsic p53-independent apoptotic cell death in multiple cancer cell types[97]. The manifestation of anti-cancer activity by gedunin was found through inhibition of heat shock protein (hsp90) in breast cancer cell lines[98]. In addition to the apoptotic potential of gedunin, it is effective in causing erythrosis, the suicidal death of erythrocyte which is characterized by cell shrinkage[99]. Gedunin's antimalarial activity was studied to be efficient against

Plasmodium falciparum when compared to the anti-malarial drug chloroquine itself as per a study made by MacKinnon *et al*[100]. *In vitro* anti-plasmodial activity was exhibited by the limonoids, neemfruitin A and B isolated from neem fruit, in addition gedunin and azadirone, the limonoids already known for this activity[101]. Protective effect of salannin on gastric lesions and spermicidal effect of salannin, nimbin and nimbidin has been identified. Nimbidin, a mixture of tetranortriterpenes such as nimbin, nimbinin, nimbidinin, nimbolide and nimbidic acid also possesses potent anti-inflammatory, anti-arthritic and anti-ulcer activities as evidenced by the study which showed the inhibition of some of the functions of macrophages and neutrophils relevant to the inflammatory response by the action of nimbidin *in vitro* and *in vivo* in rats[102]. Macrophage migration inhibitory factor (MIF) responsible for proinflammatory reactions in many infectious and non-infectious diseases is inhibited by epoxyazadiradione, the mechanism of action of it is through inhibition of tautomerase activity of MIF[103]. Azadiradione and gedunin could bind and inactivate Human pancreatic α-amylase (HPA) inhibitors thereby rendering it to be used for the further studies towards the development of anti-diabetic drug[104]. Azadirachtin A, apart from its agronomical potential was found to have an osteogenic activity as it stimulated osteoblast differentiation and mineralization of bones in an *in vivo* study carried out in pups[105].

Azadirachtin possess inhibitory action against Rice Bran Lipase (RBL) which can be used for the increased shelf life of food, as lipase activity yields high levels of free fatty acids in the oil, which becomes unsuitable for processing to edible oil[106].

1.7. Neem limonoid - Terpenoids

Limonoids belong to the terpenoid class, one of the largest classes of natural products. The term ‘terpene’ is derived from the Greek name for terebinth tree, *Pistachia terebinthus*, the source of turpentine[107] and the resin of it containing terpenes is used by people all over the Middle East for treatment of various diseases. Terpenoid (Isoprenoids) constitute diverse organic compounds, which plays major biological role in all the three domains of life (bacteria, archaea and eukaryotes). More than ten thousands of the discovered terpenoids, are produced by plants[108]. Such a huge structural diversity of enormous number of isoprenoids is contributed by C_5 carbon skeletons of isoprene units, the number of repetitions of this unit, cyclization, rearrangement and various further chemical modifications[109]. Almost all the metabolic processes involved

in the cell require isoprenoids, and isoprenoids exists as either containing only of isoprene units or a part of molecule composed of isoprene unit. They are again classified into primary and secondary metabolites based on their functional significance in the cell[109]. As primary metabolites, sterols give structural integrity to the cell membrane in most eukaryotes and it is replaced by hopanoids in prokaryotes[109,110]. In vertebrates, sterols act as precursors for steroid hormones and bile acids. Further, plant growth regulators such as abscissic acid, gibberellic acids and brassinosteroids mediate many physiological responses by inducing diversity of responses in plants; photosynthetic pigments such as carotenoids, chlorophylls are involved in carbon fixation in all the phototrophs[111]. Long acyclic isoprenic chains in the quinones such as plastoquinone-9, plastoquinone K1, ubiquinone, menaquinone, tocopherol, dolichols are produced as primary metabolites through 'Isoprenoid pathway'[109,110]. Ubiquinones and menaquinones are electron carriers and the major components of the aerobic and anaerobic respiratory chains, respectively[109]. Dolichols are long-chain, membrane-bound isoprenoids, which are required for cell wall peptidoglycan synthesis[109]. Prenylated proteins are involved in the regulation and sub-cellular molecule trafficking. Plants produce myriads of secondary metabolites that mediate important interactions between plants and their environment[109]. And most of them are defense compounds and they are of boon to mankind as it finds application in medicine and agriculture. They are conveniently classified into monoterpenes, sesquiterpenes, diterpenes, sesterpenes, triterpenes, tetraterpenes, and polyterpenes based on the number of basic isoprene unit it contains[109].

1.8. Chemistry of limonoids

The major group of isoprenoids present in neem is triterpenoids, which can be classified as proto-limonoids, mononortriperpenoids, di-, tri-, tetra-, penta-, hexa- and nona-nortriperpenoids depending on the number of carbon units removed from the proto-limonoids during its formation[14,21]. Limonoids fall in the category of tetranortriperpenoids, which is formed by the excision of terminal four carbon units during its formation from the proto-limonoids[112].

Protolimonoids are suggested to be initial step or immediate limonoid intermediates formed in the biosynthetic pathway[14]. They have an intact C-8 side chain present on the C-17 of the D ring. Further modification occurs in the side chain for the

formation of furan ring, attached to C-17 of D ring. The protolimonoids so far identified and isolated from neem include meliantriol, melianone, nimolinone, nimbocinone, limocinol, limocinone, kulactone, odoratone[14]. Some of the *in vitro* experiments suggested that protolimonoid structures such as euphane, tricallane or butyrospermol (Δ^7 isomer of euphol) might act as biosynthetic precursors for limonoids[14]. Azadirachtol, azadirachnol, azadirol and diepoxyazadirol are some of the *apo*-protolimonoids isolated and characterized from neem[14]. *Apo*-protolimonoids are rearranged from protolimonoids by the introduction of oxygen at C-7 with concomitant migration of the C-14 methyl group to C-8[14]. It is suggested from the previous studies and prediction that apo-rearrangement of butyrospermol may lead to the formation of other limonoids in the proceeding steps[14,112].

Of the limonoids, isolated and characterized from neem, azadirachtin represents one of the highly complex limonoid in neem[112]. The molecule of azadirachtin has three carbocyclic and five heterocyclic rings and contains 16 stereogenic centres, of which, 7 are fully substituted[113]. It has a plethora of oxygen functionality, comprising enol, ether, acetal, hemi-acetal and tetra-substituted oxirane, as well as a variety of carboxylic esters[113]. Different structural analogues of azadirachtin has been reported such as A, B, C, D, E, F, H, I, K, M, N, vepaol, 3-deacetylazadirachtin[113,14]. The dihydrofuran acetal moiety of azadirachtin is said to be mainly responsible for its anti-feedant activity, while the decalin fragment is known to be responsible for the observed insect growth regulation (IGR) and development effects[113,114].

1.9. Chemical synthesis of limonoids

The formidable challenge that makes chemical synthesis of limonoids a difficult task are the chemical complexity due to multitude of stereogenic centres, high density of oxygen atoms, its instability at acidic and alkaline pH, high temperature, light etc. Limonoids such as azadiradione, azadirachtins have been chemically synthesized so far in the laboratories[115,116,117,27]. As the potential of neem tree to relieve global problem such as environmental stress is realized, Ley *et al*. at Imperial College, London and later at Cambridge University took efforts for the total synthesis this complex insecticidal molecule, azadirachtin A and could succeed in 2008, after three decades of constitutive success and failure stories[118,117,116]. Seventy one steps are involved in the total synthesis of azadirachtin which gave a final yield of 0.00015%[116,117] and stereoselective

azadiradione synthesis was accomplished in twenty steps starting from *trans, trans* farnesol as a starting material[115]. These synthetic limonoids synthesis requiring quite a lot number of steps makes it unlikely to be possible to make on any scale. In order to obtain these bioactive metabolites through biosynthetic means, understanding of its biosynthetic pathway is highly essential.

1.10. Biosynthesis of limonoids in *Azadirachta indica*

Besides the remarkable knowledge on the potential bioactivity of neem limonoids, very little is known about their biosynthetic pathway (Figure 1.3). Limonoid biosynthetic pathway deviates from the steroid biosynthesis[119] at the formation of triterpene skeleton, through cyclization of 2,3(*S*)-oxidosqualene catalyzed by triterpene synthase. Oxidosqualene is formed by epoxidation of squalene (30C), which is formed through non-head-to-tail, 1'-1 condensation of two units of farnesyl pyrophosphate (FPP)[120] catalyzed by squalene synthase. FPP is formed through the most common chain elongation reaction by the coupling of isopentenyl pyrophosphate (IPP) with its allylic pyrophosphate, dimethyl allyl pyrophosphate (DMAPP) or with geranyl pyrophosphate (GPP)[121,122–124,125,126]. In higher plants, biosynthesis of isoprenoid precursor, IPP and its isomer, DMAPP occurs through either of the two biosynthetic pathways: mevalonate pathway (MVA) or the methyl-erythritol phosphate pathway (MEP) or through combination of both the isoprene pathways[127,122,121,125, 127, 132].

The pathway uses key enzymes such as oxidosqualene cyclases, which construct the basic triterpenoid skeletons, cytochrome P450 monooxygenases, which mediate oxidations and acetyltransferases, which performs acetylation of some of the functional groups.

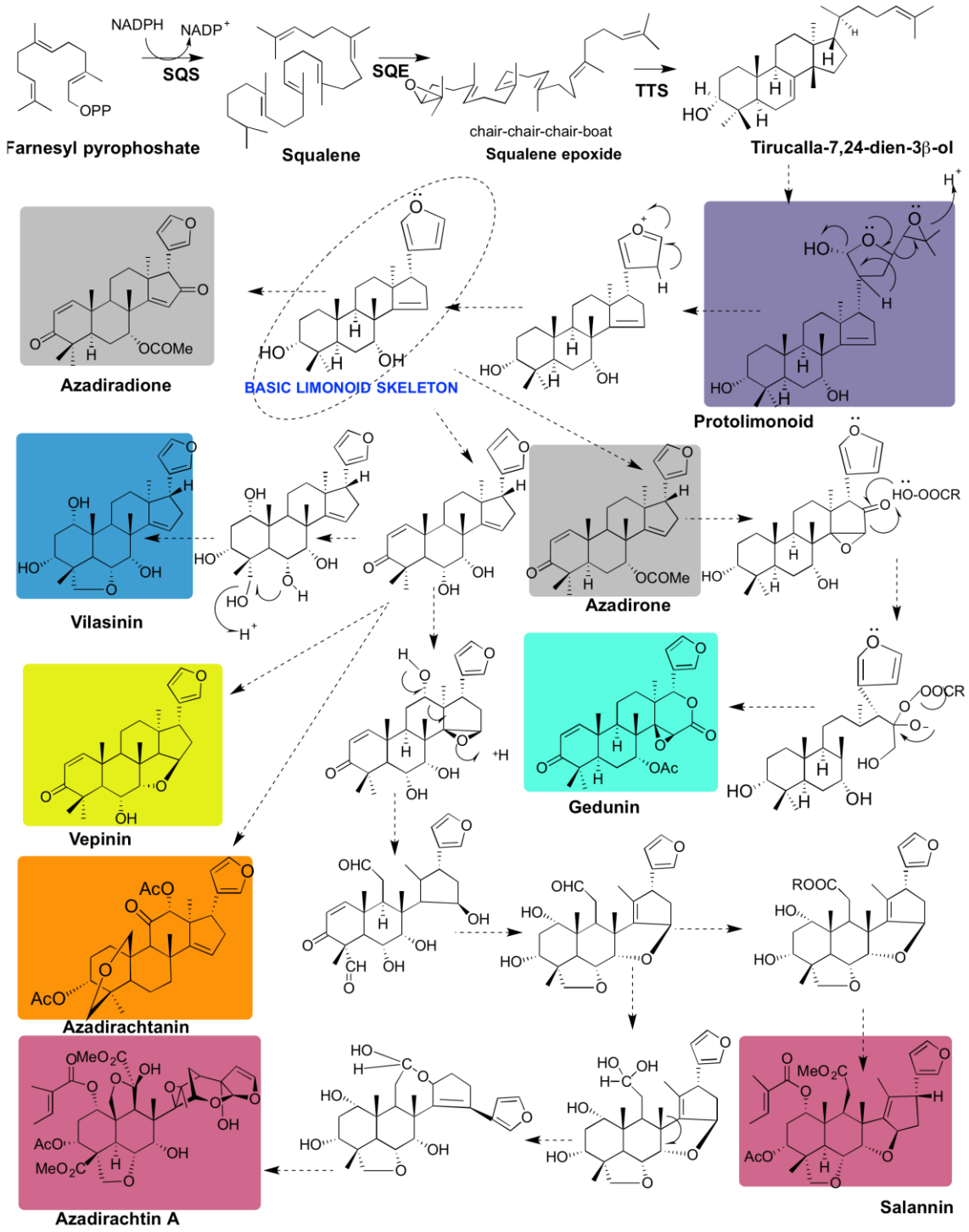

Figure 1.3. Proposed scheme and mechanisms for the formation of different limonoid skeletons.

1.11. Isoprenoid biosynthesis

The first recognition of isoprene as a repetitive motif in natural products was provided by Wallach (1887)[128]. He isolated isoprene from the pyrolysis products of turpentine oil[107], which is mainly composed of monoterpenes such as α-pinene, β-pinene and lower proportions of carene, camphene, dipentene, and terpinolene. He found that

head-to-tail condensation of branched C5 units was the origin for all terpenoids[128]. This simple rule did not fit with many isoprenoid structures found later. An extended biogenetic isoprene rule was proposed by Ruzicka who studied the structures of various isoprenoids[129] and validated its consistency with known structures.

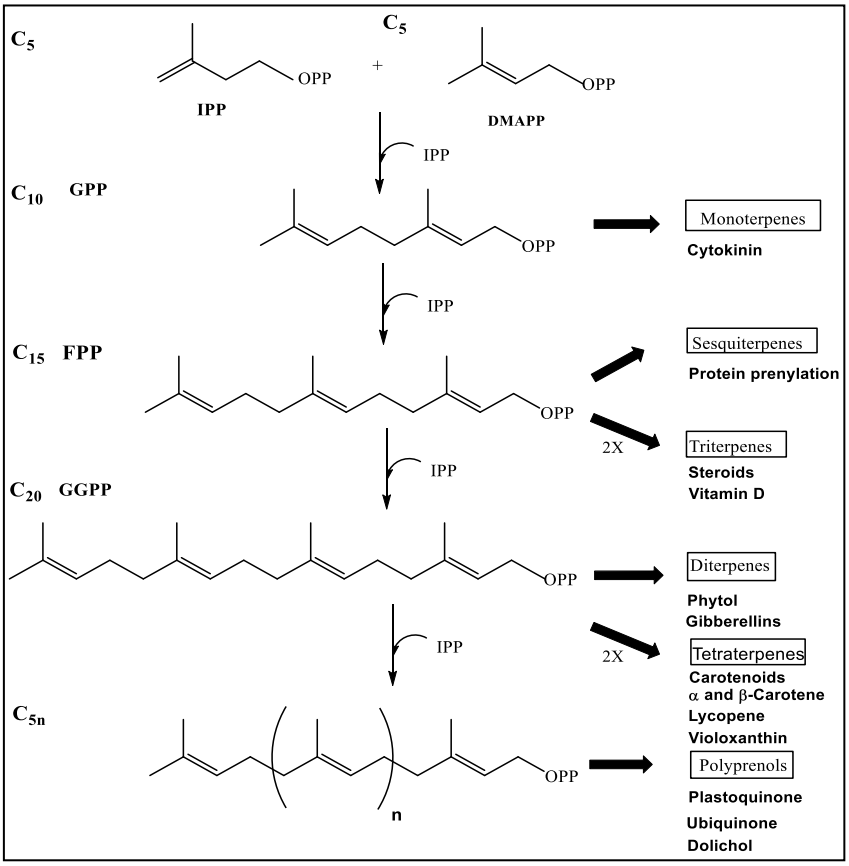

Figure 1.4. Biosynthesis of isoprenoids of various classes from C_5 isoprene unit

Isoprenoids (terpenoids) are biosynthesized through condensation reaction of the C_5 isoprene units, isopentenyl pyrophosphate (IPP) and its isomer dimethylallyl pyrophosphate (DMAPP). The biosynthetic scheme of different classes of isoprenoids is outlined in Figure 1.4 and has been reviewed by McGarvey and Bouvier[128,130]. Dual pathway for isoprenoid precursor biosynthesis namely, classical mevalonate pathway (MVA) and methyl-erythritol phosphate pathway (MEP) has been identified in different living systems[109]. Mevalonate pathway is distributed in eukaryotes such as fungi, plants, animals, whereas MEP pathway occurs in bacteria, archaea, plants and some actinomycetes, which are discussed in detail below.

1.11.1 Mevalonate pathway for Isoprenoid biosynthesis

MVA pathway was established in 1958 by Bloch and Linen, when the biosynthetic pathway of cholesterol in liver tissues and ergosterol in yeast were studied by feeding experiments with isotopically labeled precursors which brought out the phenomenon to existence that basic C_5 carbon skeleton of isoprene unit, IPP, is biosynthesized from the acetyl-CoA as precursor[131,132,133]. Mevalonate pathway begins with the condensation reaction of three acetyl-CoA units yielding 3-hydroxy-3-methylglutaryl-CoA, which is reduced by NADPH forming the precursor mevalonic acid (MVA) constituting the first committed intermediate of this pathway[134].

Two groups initiated the study of contribution of acetate for the biosynthesis of steroids independently. Cholesterol biosynthesis was studied in liver by Little *et al*.[135] in 1950 and the ergosterol biosynthesis was studied by using mutant strain of *Neurospora crassa* incapable of forming acetate from carbon source which was supplied with exogenous acetate labeled with ^{14}C in the methyl group and ^{13}C in the carboxyl group[136]. Bonner and Arreguin during the study of rubber biosynthesis speculated that three acetate molecules combined to make the isoprene subunit and proposed a scheme[133] starting from acetate. This was later confirmed from the identification of β-hydroxy-β-methylglutarate in *Crotalaria sp.* for the first time from the degradation studies performed with dicrotaline[137]. β-hydroxy-β-methylglutarate which was structurally related to be the condensation product of acetate was not showing any activity, which was later, found that the actual intermediate was in the form of coenzyme-A derivative. No role other than that of isoprenoid precursor is known for mevalonate. Reduction of HMG-CoA occurs by HMG-CoA reductase (HMGR), which was considered to be the rate-limiting step in this pathway[132]. Further, isopentenyl pyrophosphate (IPP) is formed from mevalonic acid by decarboxylation and phosphorylation by the consumption of 3 ATP molecules[131]. This pathway was believed to be the only source of isoprene biosynthesis in all living organisms ubiquitously until the discovery of non-mevalonate pathway[121]. Study of this pathway has significance in the field of medicine. Some of metabolites produced by some microbes and synthetic drug mimic the structure of MVA pathway intermediates, which can be used to slow down the synthesis of isoprene units through this pathway[132]. For example, a statin drug, mevinolin, the inhibitor of this pathway has been used as a cholesterol lowering agent in humans[132].

1.11.2 Methyl-erythritol Phosphate pathway

Non-mevalonate pathway for isoprenoid biosynthesis was first discovered by Gtrard Flesch and Michel Rohmer (1988)[138,139]. This pathway is present in bacterial and in plastids of the prototrophic organisms[123]. The enzymes of this alternate ‘‘non-mevalonate’’ pathway (also called Rohmer pathway) are unique and do not use any of the enzymes of mevalonate pathway[140]. The pathway comprises 8 steps[141] and the first dedicated step is the synthesis of 1-Deoxy-D-xylulose 5-phosphate (DOXP) from pyruvate and glyceraldehyde-3-phosphate (GAP), which is catalyzed by thiamine pyrophosphate (TPP) dependent DOXP synthase (DXS) through transketolase-like decarboxylation reaction. In the second step, 2-C-methyl-D-erythritol-4-phosphate (MEP) is formed from DOXP through intramolecular rearrangement and reduction step catalyzed by enzyme DOXP reductoisomerase (DXR) in the presence of NADPH[124]. The next step of the pathway is the conversion of MEP to 4-(diphosphocytidyl)-2-C-methyl-D-erythritol (CDP-ME) in a cytidine triphosphate (CTP)-dependent reaction catalysed by CDP-ME synthase. Further step in pathway is the phosphorylation of 2-hydroxy group of CDP-ME converting into 4-(diphosphocitidyl)-2-C-methyl-D-erythritol-2-phosphate (CDP-ME2P) by an enzyme termed as CDP-ME kinase. The next step in this pathway is the transformation of CDP-ME2P into a cyclic intermediate 2-C-methyl-D-erythritol-2,4 cyclodiphosphate (MECP), catalyzed by MECP synthase[124,142]. ME cyclodiphosphate was then converted into 1-hydroxy-2-methyl-2-(E)-butenyl-4-diphosphate under the catalysis of 1-hydroxy-2-methyl-2-(E)-butenyl-4-diphosphate synthase[124,142]. The final enzyme 1-hydroxy-2-methyl-2-(E)-butenyl-4-diphosphate reductase converts the above substrate into isopentenyl pyrophosphate (IPP) and dimethylallyl pyrophosphate (DMAPP) by intramolecular skeletal rearrangement[143]. The pathway was has been extensively studied by Rohmer, Lichtenthaler and many other research group[124,142,109,144,132,145,146,147,148,149,139,150,145,141,151,111] and it is summarized in Figure 1.5. Study of the enzyme structures and function of this pathway has furthered the advancement in drug discovery for parasite and microbial diseases[140,141,146,147]. As these organisms possess only MEP pathway for the biosynthesis of isoprene units, drugs which blocks this pathway of parasites and bacteria affecting human will not have side effects on humans, mammals possess only MVA pathway for isoprenoid biosynthesis. For example, fosmidomycin, natural antibiotic from *Streptomyces lavendulae*[152] an inhibitor of DXP reductoisomerase completey inhibited bacterial (*E. coli*) growth at 6.25

μg/mL[132,139]. Drugs inhibiting this pathway has been effective against malarial parasite *Plasmodium falciparum* [132,140,141]. Another drug ketoclomazone, is a derivative of a soil-applied herbicide, clomazone, also known as dimethazone exhibited antibacterial activity against the pathogenic bacterium, *Haemophilus influenzae*, with an MIC value of 12.5 μg/mL[153]. Further, the metabolites involved in photosynthesis such as chlorophyll, carotenoids, tocopherols, phytols are biosynthesed through this pathway and flux through this pathway is accelerated in the presence of light, which shows that circadian clock and feedback control exists for the diurnal control of the MEP pathway[140,138,139,144,145,146]. Thus, plant serves as excellent model system for identification of potential drugs.

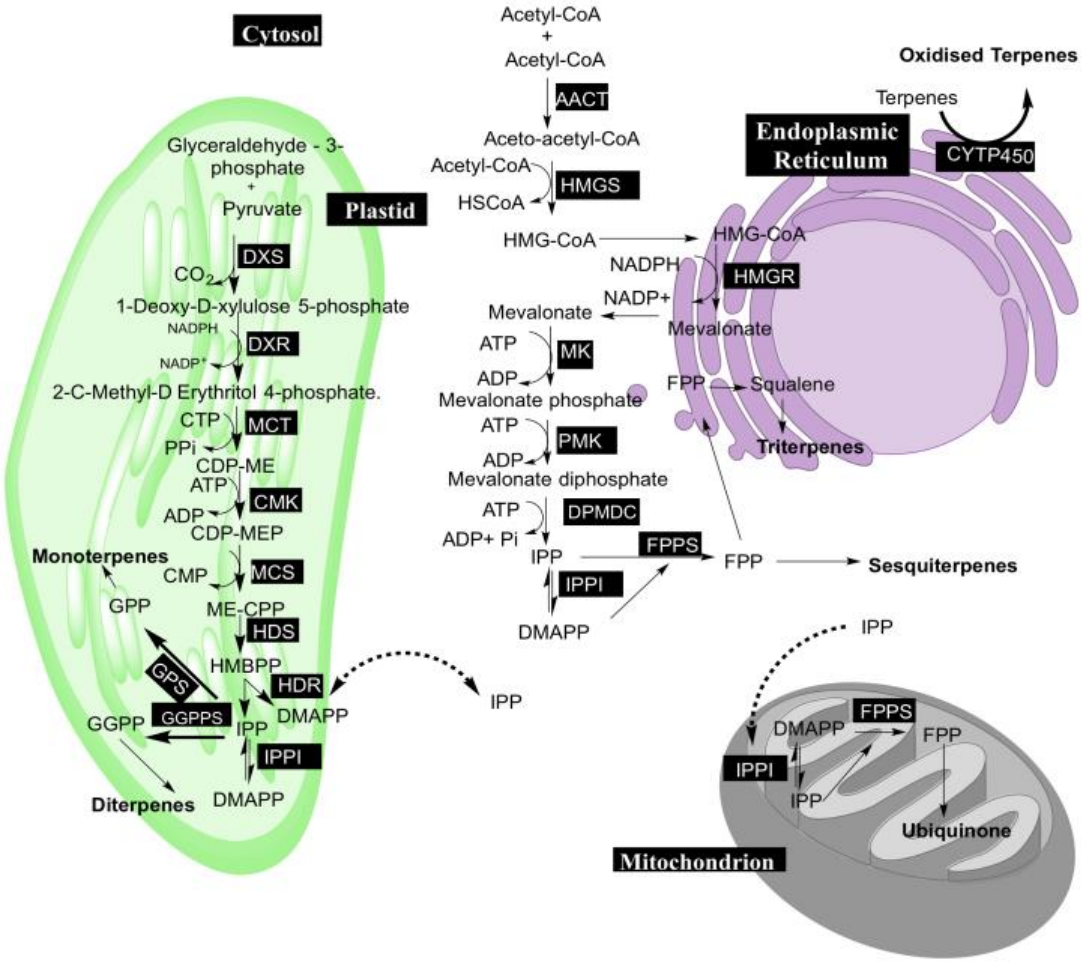

Figure 1.5. Compartmentation and localization of different isoprenoids in a plant cell. *Enzyme abbreviations.* AACT, acetoacetyl-CoA thiolase; HMGS, 3-hydroxy-3-methylglutaryl-CoA synthase; HMGR, 3-hydroxy-3-methylglutaryl-CoA reductase; MK, mevalonate kinase; PMK, 5-phosphomevalonate kinase; DPMDC, 5-diphosphomevalonate decarboxylase; IPPI,

IPP-DMAPP isomerase; DXS, 1-deoxy-D-xylulose-5-phosphate synthase; DXR, 1-deoxy-D-xylulose-5-phosphate reducto-isomerase; MCT, 2-C-methyl-D-erythritol-4-phosphate cytidyltransferase; CMK, 4-(cytidine 5-diphospho)-2-C-methyl-D-erythritol kinase; MCS, 2-C-methyl-D-erythritol-2,4-cyclodiphosphate synthase; HDS, 1-hydroxy-2-methyl-2-(*E*)-butenyl-4-diphosphate synthase; HDR, 1-hydroxy-2-methyl-2-(*E*)-butenyl-4-diphosphate reductase, FPPS, Farnesyl pyrophosphate synthase; GPS, geranyl pyrophosphate synthase; GGPPS, geranylgeranyl pyrophosphate synthase.

1.12. Localization of isoprenoid biosynthesis in plant cells

In plant systems, these two parallel pathways involved in the biosynthesis of differential isoprenoid end products occur in different cellular compartments[124]. Classical MVA pathway is localized in the cytosol of the plant cell, whereas MEP pathway occurs in the plastids (Figure 1.5). In plants, monoterpenes, diterpenes, tetraterpenes and terpenoids involved in photosynthetic machinery (carotenoids, phytol, prenyl chain of plastoquinone) are synthesized through the plastidic MEP pathway, whereas sesquiterpenes, triterpenes, sterols and prenyl chain of ubiquinone through the cytosolic MVA pathway[122]. However, in addition to this general rule, few pieces of research have found that FPP synthase is also found to be present in the plastids in rice, wheat and tobacco [154]. Surprisingly, in tomato, sesquiterpenes (+)-α-santalene, (+)-endo-β-bergamotene, and (-)-endo-a-bergamotene are found to be formed in the plastids through novel pathway from Z,Z -farnesyl pyrophosphate catalyzed by plastidial zFPS[155,156]. The labeling experiments with ^{13}C-labeled mevalonate and ^{2}H-labeled 1-deoxy-D-xylulose have confirmed that the biosynthesis of IPP occurs at two sites[127]. Isoprenoid biosynthesis occurs in three subcellular locations in plant cells. The plant MVA pathway is again localized in three cellular compartments: cytosol, Endoplasmic reticulum, and peroxisome. Most of the mevalonate pathway enzymes are localized in peroxisomes, which has been identified in plants and mammalian cells through GFP tagging of the genes of this pathway whereas HMG-CoA reductase (HMGR) is partly localized to endoplasmic reticulum[157].

Plant sterols such as sitosterol, stigmasterol, campesterol were shown to be biosynthesized through MVA pathway in *Lemna gibba* and in *Daucus carota* by Lichtenthaler[123]. The prenyl chain of ubiquinones are derived from the isoprene units formed from MVA pathway[158], synthesis of which is localized to mitochondria. Biosynthesis of diterpenes such as Ginkgolide A, is compartmentalized to plastids[139]. The biosynthetic origin of monoterpenes of *Pelargonium graveolens, Thymus vulgaris*,

Mentha pulegium was reported to be through MEP pathway[159]. Exclusive operation of MEP pathway for the biosynthesis of the diterpenes marrubiin[160], salvinorin A[161], andrographolide[162] and plaunotol[163] from *Marrubium* v*ulgare*, *Salvia divinorum*, *Andrographis paniculata* and *Croton stellatopilosus*, respectively, and hemiterpene 2-methyl-3-buten-2-ol[164] from *Pinus ponderosa* were evidenced by different research groups. Contribution of both the pathways for the formation of different plant metabolites are summarized (Table 1.1).

1.13. Cross-talk between the cytosolic and the plastidial pathway

Besides this division of labor for terpenoid biosynthesis in higher plants, cross-talk between these two pathways due to traversing of isoprene units (IPP and DMAPP) across the thylakoid membranes are reported in several studies[108]. The term, 'cross-talk' was used for the first time by Hemmerlin[165] for this cooperation between both isoprenoid pathways. Labeling studies with stable isotope labeled glucose and inhibitor studies with pathway-specific inhibitors have clearly demonstrated an exchange of isoprene intermediates between compartments of the two pathways[165,166,167,168,169]. But, the exchange of isoprene units occur either unidirectionally or bidirectionally or at only under certain physiological conditions which all differ in each plant species. In *Arabidopsis thaliana* seedlings, soon after inhibition of either one of the pathway there is an exchange of isoprene units between plastid and cytosol complementing each other for the biosynthesis of metabolites in these compartments respectively[168]. In another independent study in *Arabidopsis thaliana* seedlings, it was found that there was minor contribution of MVA pathway for Gibberellin biosynthesis, when the MEP pathway was blocked and when MVA pathway was blocked, sterol biosynthesis was supported by MEP pathway[166]. In tobacco Bright Yellow-2 (TBY-2) cells, the growth inhibition due to perturbation by pathway specific inhibitors was complemented by the isoprene units synthesized from the other pathway, which showed that there was an exchange of isoprenes between the compartments under the conditions of physiological stress by inhibitors[165]. Substrate transport assays conducted in intact chloroplasts of *Brassica juncea*, *Brassica oleracea*, *Spinacea oleracea* recorded that plastid membranes possessed a unidirectional proton symport system for the export from plastids, of specific isoprenoid intermediates, isopentenyl pyrophosphate and geranyl pyrophosphate with high efficiency and with low transport rates for farnesyl pyrophosphate and

dimethylallyl pyrophosphate involved in the metabolic cross talk between cytosolic and plastidial pathways[170]. The sesquiterpene lactone, artemisinin from the plant *Artemisia annua* has also been shown to be synthesized from both pools of isoprene precursors[171]. Respective contributions of two pathways toward formation of dolichols in *Coluria geoides* hairy root culture studied by feeding labeled glucose showed through NMR and mass spectrometric analysis that both pathways contribute for the isoprene units incorporated into polyisoprenoid chains, but in a differential way which was further confirmed by pathway-specific precursors [5-^{2}H]-mevalonate or [5,5-$^{2}H_2$]-deoxyxylulose, both of which were incorporated into dolichols and by inhibition of dolichols synthesis by inhibitors of the respective pathways mevinolin and fosmidomycin. Initial 13 isoprene units incorporated was found to be synthesized in plastid, which was supplied from both the pathways and the later part of polyisoprenoid chain was made of isoprene units solely from MVA pathway which culminated in the conclusion that there is a unidirectional flow of isoprene units from cytosol to plastid, but not in reverse[169]. The transport direction is of *vice versa* to the former studies reported independently by Bick *et al*.[170], Dudareva *et al*[172] and by Hampel *et al*.[173] for the biosynthesis of sesquiterpene, β-caryophyllene.

Labeling studies revealed that there is a differential contribution of isoprene units from the two pathways in the biosynthesis of metabolites. When studying the ^{13}C-labeling of the diterpene ginkgolide from ^{13}C-glucose, three isoprenoid units were found to be labeled *via* MVA pathway and the fourth isoprenoid unit *via* DOXP/MEP pathway[139]. In Chamomile, sesquiterpenes bisabolol oxide A and chamazulene, when analysed, showed that two of the isoprene building blocks were predominantly formed *via* the new triose:pyruvate pathway whereas, the third unit was of mixed origin, being derived from both the mevalonic acid pathway and the triose:pyruvate pathway[174]. This biosynthetic inequality was also observed in *Torreya nucifera* cell culture for the biosynthesis of the diterpene, Hinokiol, which is biosynthesized through the MVA as well as MEP route. The terminal IPP showed preferential labeling through MEP pathway and unfavourable labeling through MVA pathway[175]. β-Sitosterol and stigmasterol from *Croton sublyratus* callus cultures were reported to be biosynthesized from isoprene units equally contributed by both the mevalonate pathway and the DOXP pathway[176]. Apart from the exchange of isoprene units, geranyl pyrophosphate (GPP) is also found to cross the plastidial membrane act as substrate for enzymes in cytoplasm[177,178]. Expression in tomato fruit

cytosol, *Ocimum basilicum* α–zingiberene synthase (ZIS) possessing both mono- and sesquiterpene synthase activity along with plastidial expression of heterogenous GPPS-SSU resulted in increased production of monoterpene products compared to expression of ZIS alone[177]. But no such cross over of FPP and GGPP has been observed so far[156].

Organism	**Isoprenoid**	**Pathway**	**References**
Eubacteria			
Rhodopseudomonas palustris	Hopanoids	MEP	[138]
Rhodopseudomonas acidophila	Hopanoids	MEP	[138]
Methylobacterium organophilum	Hopanoids	MEP	[138]
Zymomonas mobilis	Hopanoids	MEP	[179]
Methylobacterium fujisawaense	Hopanoids	MEP	[179]
Alicyclobacillus acidoterrestris	Hopanoids	MEP	[179]
Escherichia coli	Ubiquinone	MEP	[179]
Citrobacter freundii	Ubiquinone Q-8	MEP	[180]
Salmonella typhimurium	Ubiquinone Q-8	MEP	[180]
Erwinia carotovora	Ubiquinone Q-8	MEP	[180]
Pseudomonas aeruginosa	Ubiquinone Q-8/9	MEP	[180]
Pseudomonas fluorescens	Ubiquinone Q-8/9	MEP	[180]
Burkholderia caryophylli	Ubiquinone Q-8	MEP	[180]
Burkholderia gladioli	Ubiquinone Q-8	MEP	[180]
Ralstonia pickettii	Ubiquinone Q-8	MEP	[180]
Acinetobacter calcoaceticus	Ubiquinone Q-9	MEP	[180]
Mycobacterium phlei	Dihydromenaquinone MK-9	MVA	[180]
Mycobacterium smegmatis	Dihydromenaquinone MK-9	MVA	[180]
Myxococcus fulvus	Menaquinone MK-8	MVA	[180]
Chloroflexus aurantiacus	Verrucosan-2β-ol	MVA	[181]
Streptomyces sp. JP95	Geosmin	MEP	[182]
Actinomycetes			
Streptomyces aeriouvifer	Menaquinone and naphterin	MVA and MEP	[183]
Actinoplanes sp.	Terpenoids, Menaquinone	MVA and MEP	[184]

Archea			
Streptomyces UC5319	Pentalenolactone	MVA	[185]
Caldariella acidophila	Phytanyl chain	MVA	[186]
Halobacterium cutirubrum	Glycerol	MVA	[187]
Halobacterium halobium	Glycerol	MVA	[188]
Haloarcula japonica	Phytanyl chain	MVA	[189]
Green algae			
Scenedesmus obliquus	All isoprenoids	MEP	[190]
Chlamydomonas reinhardtii	All isoprenoids	MEP	[191]
Chlorella fusca	All isoprenoids	MEP	[191]
Euglena gracilis	Phytol, Ergosterol	MVA	[191]
Cynobacteria			
Synechocystis	Phytol, β-carotene	MEP	[191]
Bryophtes			
Ricciocarposnatans, Conocephalum conicum	Cubebanol, Ricciocarpin A, Stigmasterol	MVA	[192]
	Phytol	MEP	[193]
Fossombronia pusilla	Geosmin	MVA	[182]
Fossombronia alaskana	Neo-epi-verrucosane	MEP	[194]
Higher plants			
Nicotiana tobaccum	Ubiquinone	MVA	[158]
Ginkgo biloba	Ginkgolide A	MEP	[139]
Taxus chinensis	Taxol	MEP	[195]
Marrubium vulgare	Marrubiin	MEP	[160]
Lemna gibba	Sitosterol, stigmasterol,	MVA	[122]
	Phytol, β-Carotene, Lutein, Plastoquinone-9	MEP	[123]
Daucus carota	Sitosterol, Stigmasterol	MVA	[122]
	Phytol	MEP	[122]
	Terpinolene	MEP	[173]
	Caryophyllene	MEP and MVA	[173]
Pelargonium graveolens	Geraniol	MEP	[159]
Thymus vulgaris	Thymol	MEP	[159]

Mentha pulegium	Pulegone	MEP	[159]
Croton sublyratus	β-sitosterol, stigmasterol	MEP and MVA	[176]
Croton stellatopilosus	β-sitosterol, stigmasterol	MVA	[196]
	Plaunotol	MEP	[163]
Hordeum vulgare	Sitosterol, stigmasterol	MVA	[122]
	Phytol	MEP	[122]
Pinus ponderosa	2-methyl-3-buten-2-ol	MEP	[164]
Populus nigra	Hemiterpene	MEP	[127]
Chelidonium majus	Hemiterpene	MEP	[127]
Salix viminalis	Hemiterpene	MEP	[127]
Matricaria recutita	Chamomile	MEP and MVA	[174]
Marrubium vulgare	Marrubiin	MEP	[160]
Salvia divinorum	Salvinorin A	MEP	[161]
Ophiorrhiza pumila	Camptothecin	MEP	[197]
Cyperus iria	Juvenile Hormone III	MVA	[198]
Andrographis paniculata	Andrographolide	MEP	[162]
Artemisia annua	Artemisinin	MEP and MVA	[171]
Arabidopsis thaliana	Gibberellins	MEP	[168]
Vitis vinifera	Linalool, Geraniol	MEP	[199]
Torreya nucifera	Hinokiol	MEP and MVA	[175]
Coluria geoides	Dolichols	MEP and MVA	[169]
Catharanthus roseus	β-carotene, lutein, phytol	MEP	[143]
Antirrhinum majus	Ocimene, myrcene, linalool, nerolidiol	MEP	[172]
Eucalyptus globulus	Cineol	MEP	[200]
Fungi and yeast			
Aschersonia aleyrodis	Ergosterol, dihydro-ubiquinone, β-carotene, hopanoids	MVA	[201]

Rhodotorula glutinis	Ergosterol, ubiquinone	MVA	[201]

Table 1.1. Contribution of two pathways (MVA and MEP) to the synthesis of different isoprenoids in different domains of life.

1.14. Tissue specific metabolic compartmentation of limonoids

Tissue-specific metabolic profiling showed that limonoids were found to be present in different degrees of abundance in various tissues of neem[120]. Fruit tissue was found to be the highest source of limonoids followed by leaves. Fruit pericarp was found to possess the highest quantity of limonoids among all tissues followed by kernel, the richest source of azadirachtin A and other C-seco limonoids (Figure 1.6). Fruit pericarp contains upto 9 mg/g tissue, azadiradione in the 2nd and 3rd developmental stages and 6 mg/g azadirachtin A in kernel at 5th developmental stage.

The limonoid profile of each of the tissues was unique in the terms of the abundance and distribution of different limonoids. Nimocinol, a ring intact limonoid is the most abundant limonoid (upto 2.5 mg/g) in the leaves of neem tree. Ring intact limonoids such as azadirone and epoxyazadiradione were the dominant limonoid in flowers comparatively. C-seco limonoid, salannin was identified to be higher in the stem tissue comparatively[120].

Though the tissue-specific profile of limonoids is known, their synthesis, localization and transport of limonoids remain uninvestigated in neem. Synthesis and localization of metabolites in specific compartments in cells and tissues of plant is controlled by several factors.

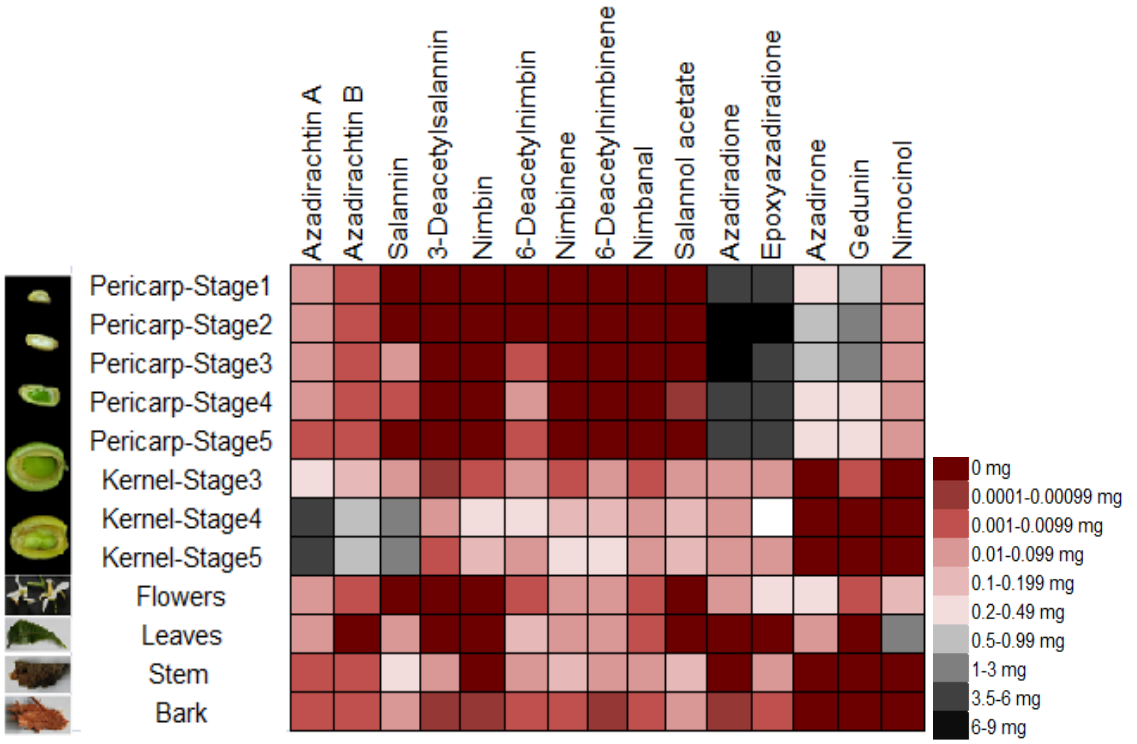

Figure 1.6. Distribution of limonoids across different tissues[120]**.** Kernel is formed only in last three developmental stages of the fruit, pericarp from all the five developmental stages of the fruit. **Legend-** Amount of limonoids (mg/g of tissue).

1.15. Factors playing role for subcellular-localization in plants

Compartmentation is an efficient way to separate and organize various cellular processes in a cell and is achieved by several factors as follows.

1.15.2 Substrate availability

The isoprene precursors, IPP and DMAPP are biosynthesized parallel through two pathways, MVA and MEP in cytosol and plastids respectively in plants. The flux of both the pathways is independently regulated and hence the substrate pool availability in these subcellular compartments varies to a larger extent, which in turn is reflected in the yield of the terpene products generated by different terpene synthases that uses isoprene units as precursors[202].

1.15.2 Enzyme targeting

Some plant proteins are being targeted to multiple compartments, even though a single gene encodes them[202]. This phenomenon of dual targeting occurs due to alternate

splicing of gene resulting in two protein variants that are targeted to two different organelles or locations[202]. This can occur even due to tandem of targeting signals in the preprotein which are recognized by the protein import machineries of both organelles[202]. Thus, the expression levels of the transcripts encoding for these protein variants (isoforms) occurring in different tissues determine the flux towards the end product biosynthesis[202]. For example, in *C. roseus,* isopentenyl diphosphate isomerases (IDI), catalyzing the interconversion of two isoprene universal C5 units are transcribed as short and long mRNAs. The protein encoded by long mRNAs are transported into mitochondria and/or chloroplasts whereas the 'short' proteins, lacking the targeting signal, are localized in peroxisomes[203]. Apart from this type of regulation, secondary metabolite biosynthesis can occur in specific compartment or cell type by expression of the mRNA encoding for the biosynthetic enzymes only in that cell type. To exemplify, toxin, thapsigargin biosynthesis occurs in secretory ducts and the transcripts encoding for the enzymes are found to be localized in the epithelial cells surrounding the ducts[204].

1.15.3 Transporters involving in transfer of metabolites

Most of the metabolites are not membrane permeable and transport of the metabolites is facilitated by intracellular transporters, which helps in partitioning the intermediates of a metabolic pathway across cellular compartments[205,206,202]. In plants, MATE (Multidrug And Toxic compound Extrusion) transporter, ABC (ATP- Binding Cassette) transporter and NPF (NITRATE TRANSPORTER 1/PEPTIDE TRANSPORTER (NRT1/PTR) Family) transporters[207,208] plays a major role for transportation of metabolites across membranes. MATE transporter uses H^+/Na^+ gradient across membrane to drive toxic compounds out of the cytoplasm. One of the transporters of MATE family, in *Nicotiana tabacum,* called jasmonate-inducible alkaloid transporter1 (Nt-JAT1) localized in the leaf cell tonoplast plays an important role in the efflux of nicotine into the vacuoles of the leaves, especially after its xylem mediated translocation from root, its site of biosynthesis, to leaves[209]. Among ABC transporters, most of them have been found to localize in the vacuolar membrane and supposedly are involved in the sequestration of secondary metabolites. It is involved in the transport of metal ions, primary and secondary metabolites that is energized by ATP[210]. NPF transporters are involved in transport of several type of hormones and metabolites such as Auxin, ABA, and glucosinolates[207]. For example, in *Catharanthus roseus*, the

transporters such as CrNPF2.4, CrNPF2.5 and CrNPF2.6 are capable of transporting iridoid glucoside intermediates across different cell types thereby aiding pathway orchestration[211]. Additionally, another transporter CrNPF2.9, in epidermal cells is involved in intracellular movement of metabolites. This transporter exports strictosidine, the central intermediate of this pathway, into the cytosol, once it is biosynthesized from its imported precurcors, secologanin and tryptamine in the vacuole[212]. Thus at cellular level, substrate channeling to enzymes is accomplished by sub-cellular or sub-structural compartmentation. At molecular level, increase in substrate availability to enzymes is facilitated by the formation of multi-enzyme complexes (metabolon formation)[213].

1.16. Metabolic channeling in biosynthesis of metabolites

In addition to cellular and sub-cellular compartmentation existing for the natural product biosynthesis, sequential enzymes in a pathway are organized in close proximity, called metabolons which helps in efficient channeling of the intermediates, thereby preventing undesirable metabolic cross-talk, leakage of potentially toxic intermediates[213,214,215]. Metabolic channeling expedites the transit of metabolic intermediate from active site of one enzyme to that of the next and helps in rescuing the dilution of intermediates into bulk phase of the cell[213].

The metabolon formation can also be in the form of transient structures occurring through the dynamic process of assembly and disassembly, which help plants to change the profile rapidly to encounter the biotic and abiotic stress[215]. Metabolons can be studied by Fluorescence correlation spectroscopy (FCS), Co-immunoprecipitation (Co-IP), Tandem affinity purification (TAP) method, Yeast-2-hybrid methods, Fluorescence resonance energy transfer (FRET) etc.[216]. Well studied metabolon formation in primary metabolic pathways have been documented for glycolysis, calvin cycle, tricarboxylic acid cycle, fatty acid oxidation etc, whereas in secondary metabolic pathways, cyanogenic glucoside dhurrin biosynthetic pathway metabolon in sorghum has been archived[214–216].

1.17. Technologies to study metabolite compartmentation

Study of metabolite compartmentation involves advanced and specific metabolomics tools probing organelle or specific cell of interest, which varies according to the aim of the investigation[217,218,219–222,223]. Some of the strategies to elucidate these factors include stable isotope labeling, non-invasive analysis of metabolites using FRET sensors, single-cell metabolomics, non-aqueous fractionation (NAF) and traditional methods such as immunohistochemical analysis, organelle or protoplast preparations are coupled with different microscopic techniques and non-targeted or unbiased metabolic analysis respectively (Figure 1.7)[202,224]. Non-targeted analysis can be performed by metabolic fingerprinting, where no chromatographic separation is performed before MS analysis or through metabolic profiling which requires chromatographic separation prior to mass spectrometric analysis[225,226]. Commonly used hardware platforms for metabolic profiling in plant biology includes GC-MS, LC-MS and NMR[227–233,234,235,236]. Protoplast isolation followed by fractionation of it into different populations can help in profile different cells separately. Further cellular organelles can be release from protoplast and fractionated to study its metabolite content[226]. Non-aqueous fractionation allows the identification of compartment specific metabolites by generation of gradient by application of a mixture of two non-aqueous organic solvents followed by separation of individual gradients and its metabolites which can be interpreted by computational analysis[237]. In this technique, the metabolism of the sample is arrested by snap-freezing followed by homogenization and freeze drying of it before introducing into the organic solvent system[226]. Live single-cell mass spectrometry helps in identification of metabolites to macromolecules and thereby, it aids in understanding the behavior of individual cells. The mass spectrometric detection was accomplished from a live single cell or even an organelle by drawing out the cell contents by a metal-coated microcapillary (nanospray tip) under video-microscopy and directly feeding into a mass spectrometer via a nano-electrospray ionization plume[238]. The technical advances in metabolomics have taken new dimensions such as, spatially resolved metabolomics and mass spectrometry imaging[226,222]. Laser assisted micro-dissection helps in the isolation of desired tissue or cell type from heterologous population followed by profiling of it for genes, proteins or metabolites[239–241]. Metabolite imaging can be performed using Laser Ablation Electrospray Ionization (LAESI)-mass spectrometry, which maps the ions and can dissect the region specific localization of metabolites in contrasting plant organs[242,243]. MS Imaging (MSI) technique requires matrix application over the tissue

followed by MS imaging measurement, which uses laser irradiation to desorbing the analyte molecules from tissue and to ionize the molecules, it uses probe beam such as solvent stream or ion beam or laser. The ions are identified in the mass analyzers and MSI data acquired are interpreted in the form of ion map which has greatly helped in cell specific localization of *Catharanthus* terpene indole alkaloid intermediates in different cell types[244]. Furthermore, FRET based fluorescent nanosensors offers the advantage of monitoring dynamic changes in the concentration of specific or wide range of solute which in turn will help in revealing the transport of metabolites across the cells[245]. For example, in a separate study, maltose-binding protein as a prototype, nanosensors were constructed which uses PBP (Periplasmic Binding Protein) fusion with green fluorescent proteins and binding of the substrate to this chimeric protein causes changes in the PBP which increases fluorescence resonance energy transfer (FRET) between two coupled green fluorescent proteins[246,244]. This helps in imaging the changes in concentration of specific metabolite over time by non-invasive means[246,247].

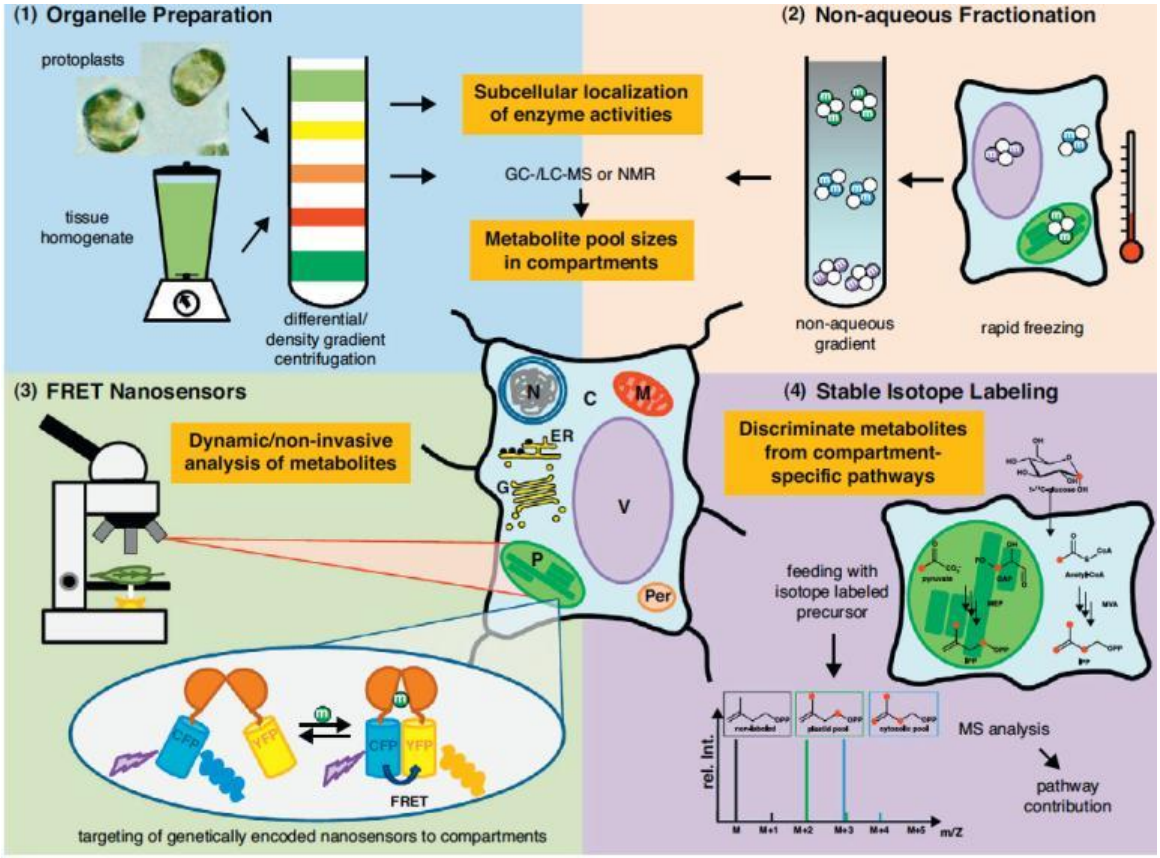

Figure 1.7. Technologies for metabolic profiling at the subcellular compartment level. (**Adapted from Heinig *et al*[202].**) Simplified scheme of a plant cell showing major compartments involved in metabolism including plastid (P), mitochondria (M), peroxisome (Per), vacuole (V), ER, golgi (G), nucleus (N), and cytosol (C). (1) preparation of organelles from homogenized tissue or protoplasts with subsequent metabolic profiling; (2) non-aqueous fractionation (3) Fo¨rster resonance energy transfer nano sensors are genetically encoded and can be targeted to multiple compartments thus allowing a dynamic and noninvasive analysis of single metabolites in living plant cells; (4) stable isotope labeling combined with MS analysis. Abbreviations: m: metabolite.

1.18. Metabolic engineering

Metabolic engineering is considered as a simplest form of synthetic biology, which deals with the construction of new biological components such as enzymes, genetic circuits or redesign of the existing biological systems for the production of secondary metabolites (Figure 1.8) [248,249]. Synthetic biology approach can be in either of the two forms, top-down and/or bottom-up approaches. In top-down approach, exogenous genes are introduced into a tractable host system, which leads to reprogramming of its native metabolic network[250]. Bottom-up approach, involves *de novo* construction of synthetic genomes or other components behaving similar to the living systems[250]. In this cell free approach, cell's growth, regulatory network, transportation and other factors do not limit the production of metabolites[250].

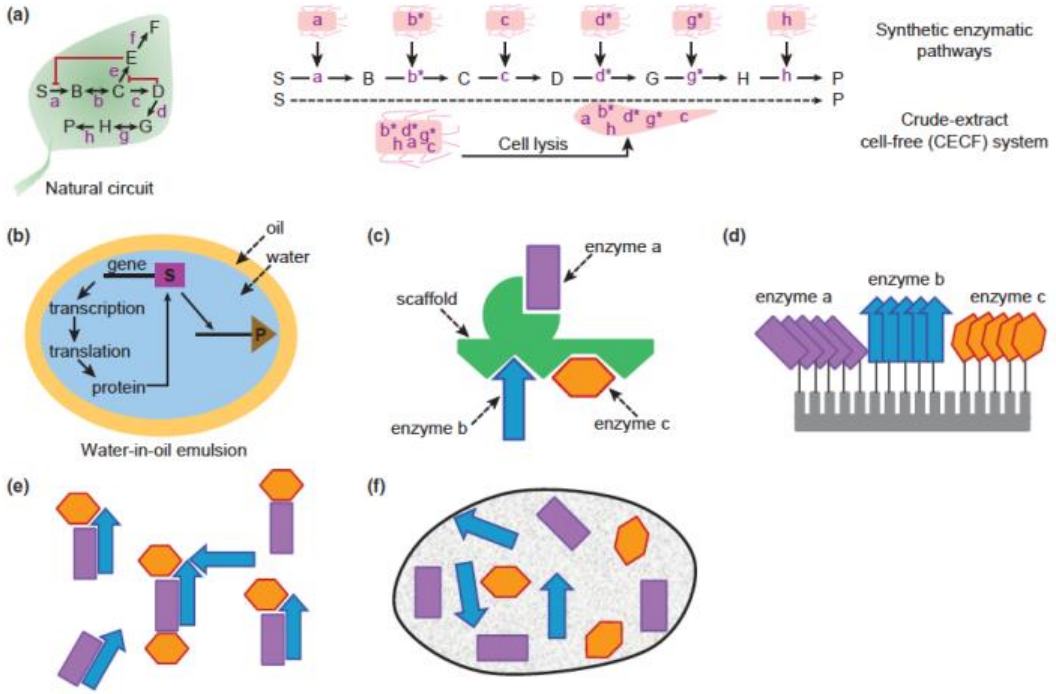

Figure 1.8. *in vitro* synthetic biology platforms (**Adapted from Tessa Moses *et al.***[250]) (a) Synthetic enzymatic pathways in which purified enzymes are combined with reaction components in an aqueous environment to convert a substrate to a product through a series of reactions, (b) *In vitro* compartmentalization using water-in-oil emulsions. (c–f) Metabolic channeling brings enzymes in close proximity with their substrate (c) protein scaffolding, (d) tethering enzymes to a surface, (e) covalently linking related enzymes into aggregates and (f) foam dispersion techniques in which the enzymes are encapsulated using surfactants. a, b, c, d, e, f, g, h, native enzymes; b*,d*,g*, synthetically modified enzymes; B, C, D, E, F, G, H intermediates; P, product; S, substrate.

Metabolic engineering of terpenes have attained considerable progress by reconstructing metabolic pathway of plants in tractable heterologous systems or "platform cell factories" such as *E.coli*[251], *Aspergillus niger*, *Bacillus subtilis*, *Corynebacterium glutamicum*, Chinese hamster ovary (CHO) cells and *Saccharomyces cerevisiae*[252]. Reconstruction of the pathway into host can be actuated by utilizing the conceptual modular structure of biosynthesis of terpenes[253]. First module (M1) involves the biosynthesis of prenyl pyrophosphate substrates, dimethylallyl pyrophosphate (DMAPP; C5), geranyl pyrophosphate (GPP; C10), farnesyl pyrophosphate (FPP; C15), and geranylgeranyl pyrophosphate (GGPP; C20) from IPP (C5). The second module (M2) is assigned to cyclization of prenyl pyrophosphate by terpene synthase (TPS),

which generates basic terpene skeleton. This module is again subdivided into two sub-modules M2a and M2b, which encompasses class II and class I TPS respectively. TPS of both the classes differ in their mechanism of initiation of carbocationic cyclization and rearrangement reactions. In third module (M3), these basic structures are functionalized by modifying enzymes such as cytochrome P450s, Fe(II)-dependent dioxygenases, acetyltransferases, methyltransferases, reductases, glycosyltransferases, etc.[253] (Figure 1.9).

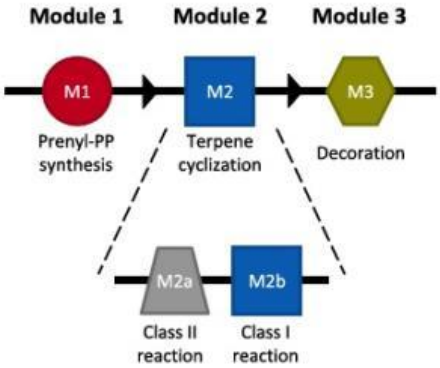

Figure 1.9. Conceptual modular structure of terpene biosynthesis (**Adapted from C. Ignea *et al.*** [253]).

Plug-and-play construction methods involve combining different module-specific parts individually and also together in the heterologous system as gene clusters help in accomplishing the following

1. Combinatorial biosynthesis of natural products
2. To produce different scaffolds of pathway intermediates utilizing the substrate promiscuity of TPS
3. Combinatorial biosynthesis to generate novel compounds
4. Single-deletion and multiple-deletion constructs can be assembled in the plug-and-play scaffold to elucidate and characterize the steps of unknown biosynthetic pathway.
5. Cryptic pathway can be activated by inserting different promoters to enhance the expression of each of the genes in the cassette[254,255].

Many of the medicinally important natural products and carotenoids[256] has been engineered into heterologous system using this plug-and-play strategy. Advancements for gene editing such as clustered regulatory inter spaced short palindromic repeats (CRISPR)-cas9 has helped in one step metabolic pathway integration into tractable hosts

at any of the desired location in the chromosome[257]. Thus metabolic engineering aims not only at increasing the productivity of bioactive natural products (Figure 1.11), but also serves as a bottom-up approach for discovery of novel natural product and its biosynthetic pathway whereas, in top-down approach, biological samples from diverse environments are extracted for metabolites, screened for bioactivity and the active molecules are structurally elucidated[258]. One of the first examples of the medicinal natural product successfully been biosynthesized in *Saccharomyces* is an anti-malarial sesquiterpene lactone artemisinin and is economical when compared to extraction from natural sources. Metabolic engineering of 15 enzymes in yeast including selected genes of MVA pathway along with amorphadiene synthase, CYP71AV1, and AaCPR yielded upto 25g/L of artemisinic acid[259]. Whereas, introduction of all the genes of MVA pathway along with the above mentioned genes gave production of >40 g/L of the intermediate amorphadiene under the fermentation condition of restricted ethanol feed with lower oxygen uptake rate[260]. Semi-synthetic formation of artemisinin from artemisinic acid gave 55% yield[261]. Higher the number of ring systems and chiral centres it possess, more complex the metabolite is. For example, artemisinin contains 4 rings and 7 chiral centres whereas, single ring containing salicylic acid from willow bark was synthesized chemically in 2 steps achieving 90% yield[262]. Morphine from Opium poppy has 5 ring system and 5 chiral centres and was biosynthetically produced upto 2.4 mg/L by engineering of 25 enzymes into yeast. Taxadiene, one of the intermediate in formation of taxol, an anti-cancer agent from Pacific Yew tree is biosynthesized through metabolic engineering of 6 enzymes in *E.coli (*dxs, idi, ispD, and ispF genes the MEP pathway bottlenecks in the upstream module and GGPP synthase taxadiene synthase in downstream module as synthetic operons) which yields up to 1g/L[263]. In addition to this strategy, targeting the biosynthetic pathway gene into specific sub-cellular compartments such as yeast mitochondria has considerable improvement in the yield. For example, in yeast 8-and 20-fold improvement was achieved in production of valencene and amorphadiene by co-engineering the truncated and deregulated HMG1, mitochondrion-targeted heterologous FDP synthase and a mitochondrion-targeted valencene synthase, or amorphadiene synthase[264]. These enhancements are achieved by directing the flux through MVA pathway by deregulation through overexpressing the truncated HMG1 or a mutated form of HMG2, mutated version of the sterol transcription factor UPC2[265], since HMGR is subjected to regulation on multiple levels.

Other strategies for engineering in *Saccharomyces* can be through replacing endogenous promoters of competing pathway branches with repressible promoters. As a eukaryote, *Saccharomyces* possesses an endoplasmic reticulum (ER) that allows the heterologous expression of membrane-localized cytochrome P450 enzymes. Hence, the overexpression of heterologous protein in ER has been enhanced in a separate strategy to increase the capacity of a yeast triterpene production platform by transforming the subcellular morphology of ER, using the following gene knock-out targets[266].

- E3 ligase-encoding HRD1 of the HMGCoA reductase degradation (HRD) pathway, which is involved in ER-associated degradation (ERAD) of HMGR, the MVA pathway gatekeeper.
- PEP4-encoded proteinase A which is responsible for the maturation of various vacuolar peptidases as it has effect on the stability of heterologous proteins.
- PAH1, which encodes phosphatidic acid phosphatase that generates neutral triglycerides from phosphatidic acid in yeast and dysfunction of which results in drastic proliferation of outer nuclear membrane and the ER[266].

Similiarly, in plants, the redirection of terpene precursor to specific compartment such as cytosol and plastid by using separate gene constructs for patchoulol synthase (PTS) and amorphadiene synthase along with its substrate (farnesyl pyrophosphate) provider FPP synthase (FPS) targeted to the compartments helps in 1000 fold increase of the product[267].

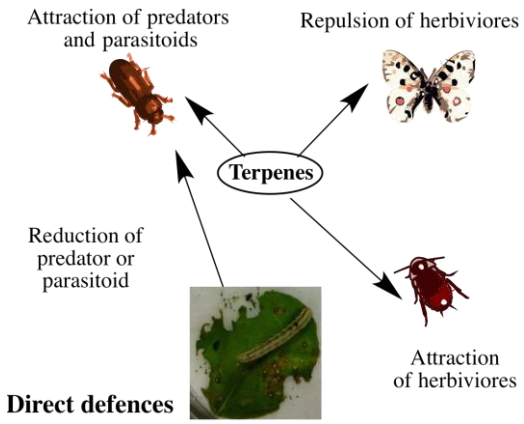

Figure 1.10. Direct and indirect defenses in plants

Apart from the production of pharmaceutically important natural products through metabolic engineering in heterologous system, overexpression or altering the genes in native host helps in improving the immunity and defense of plant and microbes against

diverse biotic stress factors in the environment. Induced indirect defense of plant includes tritrophic interaction, as in order to defend themselves against feeding herbivores, plant emit volatiles that attracts the enemies of herbivores such as predators and parasitoids (Figure 1.10)[268]. For example, introduction of new gene targeted into mitochondria involved in the biosynthesis of sesquiterpene volatiles that are not present in the volatile blend of *Arabidopsis* help in the attraction of carnivorous predatory mites which prey on the herbivores and hence are known to aid in the fitness of the plant[269]. These studies not only help for improving the fitness traits of the plant but also to understand the role of each volatiles terpenes released by plants[270]. Overexpression of transcriptional factors involved in the biosynthetic pathway of interest can also ease the improvement in production of the secondary metabolite in the native plants. Basic helix–loop–helix (bHLH) and Basic Leucine Zipper (bZIP) transcription factors are involved in many of the regulatory processes of eukaryotes whereas WRKY and AP2/ERF are involved in the regulation mechanism for the defense responses in plants[271]. Overexpression of one of these factors has helped in increasing the productivity of artimisinin in *A. annua* and indole alkaloids in *Catharanthus*[271].

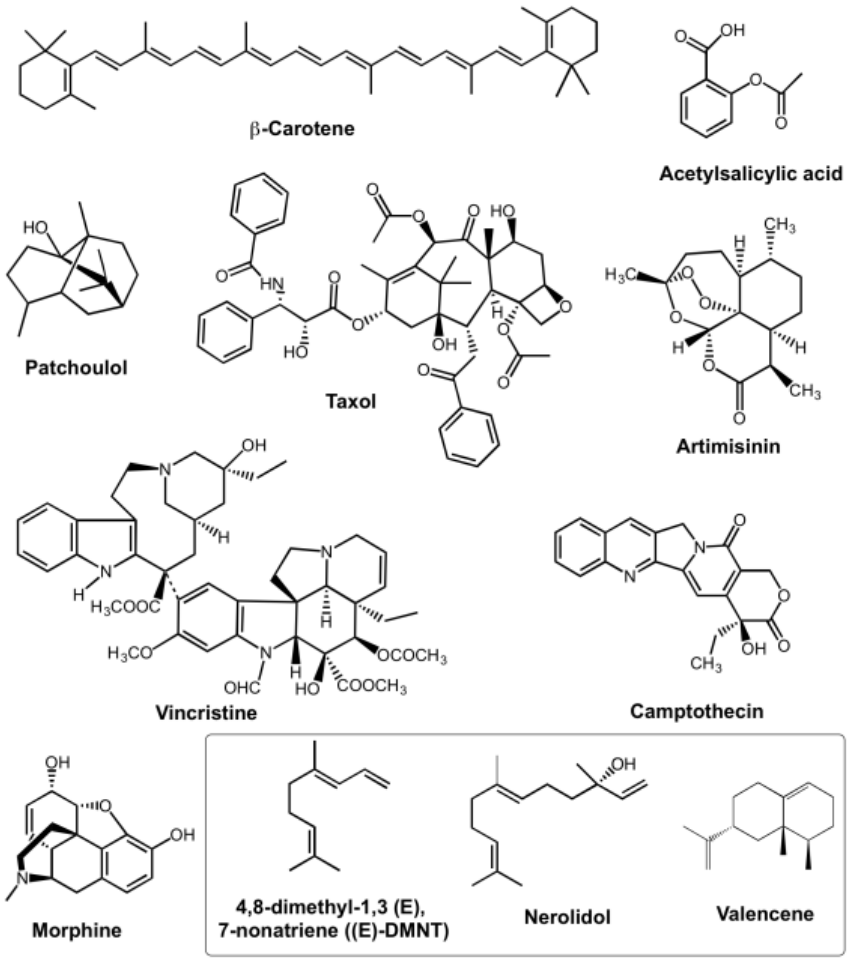

Figure 1.11. Medicinal natural products from plants in which biosynthetic pathway has been completely or partially engineered into heterologous system or semi-synthesis or total synthesis has been attempted to increase the productivity. In box- Volatile Organic Compounds (VOCs) engineered into non-host plant to study indirect plant defense.

In order to optimize the biosynthetic potential of these secondary metabolites for mankind by engineering in the native host, one must understand where their metabolism is coordinated within the cell and tissue. As biochemical steps of a single pathway occur at different subcellular locations, determination of factors such as substrate availability, enzyme localization, transport of intermediates act as an important constraint in metabolic engineering[272,202]. In particular, plants have complicated intracellular organization with metabolite flow between compartments which are highly regulated and orchestrated between different metabolic pathways[224]. Targeting the enzymes to non-native compartments helps in increasing the production as if there is less competition for pathway intermediates and normal regulatory mechanisms that control

the flux of carbon down any particular biosynthetic pathway[224]. For example, essential-oil producing plants involved in accumulation of monoterpenes have highly specialized anatomical structures that are involved the biosynthesis and storage. Engineering of monoterpene biosynthetic pathway into plants which does not produce monoterpenes will be challenging due to non-availability of specialized secretory strictures[273]. Hence, limited knowledge on the subcellular compartmentation such as localization of enzymes, substrates, localization and transport of products serves as a bottleneck in metabolic engineering. Unraveling the metabolon formation, subcellular localization of enzymes and intermediates, substrate availability will strengthen the productivity and yield of natural products harnessed through metabolic engineering. In precis, the synthetic biology and different approaches of genomics have paid impetus to decipher the indigenous medicinal value to the modern world[274].

1.19. Main objectives of the Thesis

Azadirachta indica, one of the medicinal tree producing diverse triterpenoids is well known for its insecticidal, anti-feedant limonoid azadirachtin A. The genes involved in the biosynthetic steps of the upstream pathway have been already studied, but the gene / enzyme characterization is still lacking for many biosynthetic steps in the downstream pathway. Exception from the structure, synthesis, the biological activity of different limonoids, its quantitative occurrence in different tissues, upstream few steps of the pathway other information on limonoid biosynthesis and localization has not been elucidated in this tree. Therefore, the main objectives of this thesis are

1. To identify and characterize the organelles/ intra-cellular compartments involved in the storage of limonoids in different tissues.
2. To trace the flow of carbon in limonoid skeleton through stable isotope feeding experiments.
3. To study the expression level of the genes involved in isoprene biosynthetic pathway and to characterize the putative candidate genes associated with limonoid biosynthesis.

In order to achieve the above goals, histochemical studies have been carried out for different tissues of neem and the intra-cellular organelles have been isolated for micro-metabolic profiling to identify limonoids in the intracellular organelle level. To

trace the flow of carbon through feeding experiment, *in vitro* plantlets, callus and cell suspension cultures were established as a system, and limonoid-producing ability of it has been studied. To further corroborate the participative role of MVA and MEP pathway genes with respective to limonoid synthesis, inhibitor studies and expression studies have been carried out followed by the characterization of the putative acetyl transferases involved in functionalization of limonoids in the downstream steps of limonoid biosynthesis. Thus the present studies will pave way for future thrusts such as characterization of further downstream steps of limonoid biosynthesis, regulation of the pathway, location of biosynthesis of intermediates of each step of the pathway, its intra- and intercellular transportation mechanism etc. Interrogation into above perspectives will help in overexpression of the pathway in native host or metabolic engineering into heterologous system.

1.20 References

1 R. M. Goodman, *Encyclopedia of Plant and Crop Science (Print)*, Taylor & Francis, Newyork, 2004.
2 E. Lewinsohn and M. Gijzen, *Plant Sci.*, 2009, **176**, 161–169.
3 R. A. Dixon, *Nature*, 2001, **411**, 843.
4 T. Hartmann, *Phytochemistry*, 2007, **68**, 2831–2846.
5 E. Pichersky and D. R. Gang, *Trends Plant Sci.*, 2000, **5**, 439–445.
6 M. Wink, *Phytochemistry*, 2003, **64**, 3–19.
7 H. Massalha, E. Korenblum, D. Tholl and A. Aharoni, *Plant J.*, 2017, **90**, 788–807.
8 T. Hartmann, *Entomol. Exp Appl.*, 1996, **80**, 177–188.
9 K. Saito, *Curr. Opin. Plant Biol.*, 2013, **16**, 373–380.
10 B. Moore, R. L. Andrew, C. Kulheim and W. J. Foley, *New Phytol.*, 2013, **201**, 733–750.
11 V. S. Kumar and V. Navaratnam, *Asian Pac. J. Trop. Biomed.*, 2013, **3**, 505–514.
12 R. Subapriya and S. Nagini, *Curr. Med. Chem. Anti-Cancer Agents*, 2005, **5**, 149–156.
13 A. Roy and S. Saraf, *Biol. Pharm. Bull.*, 2006, **29**, 191–201.
14 K. K. Singh Suman Phogat, R.S. Dhillon, Alka Tomar, *Neem, a Treatise*, I.K. International Publishing House, 2009.
15 S. Siddiqui, B. S. Siddiqui, S. Faizi and T. Mahmood, *J. Nat. Prod.*, 1988, **51**, 30–43.
16 S. Momchilova, D. Antonova, I. Marekov, L. Kuleva, B. Nikolova-Damyanova and G. Jham, *J. Liq. Chromatogr. Relat. Technol.*, 2007, **30**, 11–25.
17 B. S. Siddiqui, S. T. Ali, M. T. Rajput, T. Gulzar, M. Rasheed and R. Mehmood, *Nat. Prod. Res.*, 2009, **23**, 271–283.
18 G. Brahmachari, *Chembiochem*, 2004, **5**, 409–421.
19 R. Paul, M. Prasad and N. K. Sah, *Cancer Biol. Ther.*, 2011, **12**, 467–476.
20 T. Lakshmi, V. Krishnan, R. Rajendran and N. Madhusudhanan, *Pharmacogn. Rev.*, 2015, **9**, 41–44.
21 Q. G. Tan and X. D. Luo, *Chem Rev.*, 2011, **112**, 2591.
22 E. D. Morgan, *Bioorg. Med. Chem.*, 2009, **17**, 4096–4105.
23 B. S. Siddiqui, F. Afshan and S. Faizi, *Tetrahedron*, 2001, **57**, 10281–10286.
24 M. A. Siddiqui and M. M. Alam, in *Neem and Environment, Vols 1 and 2*, 1996, pp. 669–678.
25 S. Siddiqui, S. Faizi, B. S. Siddiqui and Ghiasuddin, *J Nat Prod*, 1992, **55**, 303–310.

26 S. Siddiqui, T. Mahmood, B. S. Siddiqui and S. Faizi, *J. Nat. Prod.*, 1986, **49**, 1068–1073.
27 S. V Ley, A. A. Denholm and A. Wood, *Nat. Prod. Rep.*, 1993, **10**, 109–157.
28 A. P. Jarvis and E. D. Morgan, *Phytochem. Anal.*, 2000, **11**, 184–189.
29 A. P. Jarvis, E. D. Morgan and C. Edwards, *Phytochem. Anal.*, 1999, **10**, 39–43.
30 R. B. Yamasaki, J. A. Klocke, S. M. Lee, G. A. Stone and M. V Darlington, *J. Chromatogr.*, 1986, **356**, 220–226.
31 S. Johnson and E. D. Morgan, *J. Chromatogr. A*, 1997, **761**, 53–63.
32 J. C. T. Silva, G. N. Jham, R. D. L. Oliveira and L. Brown, *J. Chromatogr. A*, 2007, **1151**, 203–210.
33 D. R. Schroeder and K. Nakanishi, *J. Nat. Prod.*, 1987, **50**, 241–244.
34 C. J. Hull, W. R. Dutton and B. S. Switzer, *J. Chromatogr.*, 1993, **633**, 300–304.
35 T. R. Govindachari, G. Sandhya and S. P. Ganeshraj, *J. Chromatogr.*, 1990, **513**, 389–391.
36 T. R. Govindachari, G. Gopalakrishnan and G. Suresh, *J. Liq. Chromatogr. R. T.*, 1997, **20**, 1633–1636.
37 T. R. Govindachari, G. Gopalakrishnan and G. Suresh, *J. Liq. Chromatogr. Relat. Technol.*, 1996, **19**, 1729–1733.
38 T. R. Govindachari, G. Gopalakrishnan, R. Malathi and N. D. P. Singh, *Nat. Prod. Lett.*, 1999, **13**, 157–162.
39 T. R. Govindachari, G. Gopalakrishnan and G. Suresh, *Fitoterapia*, 1999, **70**, 558–560.
40 T. R. Govindachari, G. Suresh and G. Gopalakrishnan, *J. Liq. Chromatogr.*, 1995, **18**, 3465–3471.
41 P. T. Deota, P. R. Upadhyay, K. B. Patel, K. J. Mehta, B. V Kamath and M. H. Mehta, *J. Liq. Chromatogr. Relat. Technol.*, 2000, **23**, 2225–2235.
42 S. Johnson and E. D. Morgan, *Phytochem. Anal.*, 1997, **8**, 228–232.
43 S. Haldar, F. A. Mulani, T. Aarthy, D. S. Dandekar and H. V Thulasiram, *J. Chromatogr. A*, 2014, **1366**, 1–14.
44 S. Haldar, P. B. Phapale, S. P. Kolet and H. V Thulasiram, *Anal. Methods*, 2013, **5**, 5386–5391.
45 O. Schaaf, A. P. Jarvis, S. A. van der Esch, G. Giagnacovo and N. J. Oldham, *J. Chromatogr. A*, 2000, **886**, 89–97.
46 G. Sarais, P. Caboni, E. Sarritzu, M. Russo and P. Cabras, *J. Agric. Food Chem.*, 2008, **56**, 2939–2943.
47 A. J. Mordue and A. Blackwell, *J. Insect Physiol.*, 1993, **39**, 903–924.
48 K. P. Sieber and H. Rembold, *J. Insect Physiol.*, 1983, **29**, 523–527.
49 D. T. Lowery and M. B. Isman, in *Neem and Environment, Vols 1 and 2*, 1996, pp. 253–264.
50 D. H. Al-Rajhy, A. M. Alahmed, H. I. Hussein and S. M. Kheir, *Pest Manag. Sci.*, 2003, **59**, 1250–1254.
51 V. Sharma, S. Walia, J. Kumar, M. G. Nair and B. S. Parmar, *J. Agric. Food Chem.*, 2003, **51**, 3966–3972.
52 S. Mahapatra, C. Y. F. Young, M. Kohli, R. J. Karnes, E. W. Klee, M. W. Holmes, D. J. Tindall and K. V Donkena, *Evid. Based Complement. Altern. Med.*, 2012, 14.
53 S. S. Nathan, K. Kalaivani, K. Murugan and P. G. Chung, *Pestic. Biochem. Physiol.*, 2005, **81**, 113–122.
54 O. Koul, J. S. Multani, G. Singh, W. M. Daniewski and S. Berlozecki, *J. Agric. Food Chem.*, 2003, **51**, 2937–2942.
55 O. Koul, G. Singh, R. Singh, J. Singh, W. M. Daniewski and S. Berlozecki, *J. Biosci.*, 2004, **29**, 409–416.
56 O. Koul, J. S. Multani, S. Goomber, W. M. Daniewski and S. Berlozecki, *Aust. J. Entomol.*, 2004, **43**, 189–195.
57 NationalResearchCouncil, *Neem: A Tree for Solving Global Problems*, National

Academy Press, Washington, DC, 1992.
58 I. M. Scott and N. K. Kaushik, *Arch. Environ.Contam. Toxicol.*, 1998, **35**, 426–431.
59 J. D. Stark and J. F. Walter, *J. Agric. Food Chem.*, 1995, **43**, 507–512.
60 D. T. Lowery, S. Bellerose, M. J. Smirle, C. Vincent and J. G. Pilon, *Entomol. Exp. Appl.*, 1996, **79**, 203–209.
61 D. T. Lowery, K. C. Eastwell and M. J. Smirle, *Ann. Appl. Biol.*, 1997, **130**, 217–225.
62 D. T. Lowery and M. B. Isman, *Entomol. Exp. Appl.*, 1994, **72**, 77–84.
63 D. T. Lowery and M. B. Isman, *J. Chem. Ecol.*, 1993, **19**, 1761–1773.
64 D. T. Lowery and M. B. Isman, in *Bioregulators for Crop Protection and Pest Control*, 1994, vol. 557, pp. 78–91.
65 D. T. Lowery and M. B. Isman, *J. Econ. Entomol.*, 1996, **89**, 602–607.
66 M. Ishida, M. Serit, K. Nakata, L. R. Juneja, M. Kim and S. Takahashi, *Biosci. Biotechnol. Biochem*, 1992, **56**, 1835–1838.
67 S. Abdel-Shafy and A. A. Zayed, *Vet. Parasitol.*, 2002, **106**, 89–96.
68 S. S. Garboui, T. G. T. Jaenson and K. Palsson, *Exp. Appl. Acarol.*, 2006, **40**, 271–277.
69 Y. H. Du, J. L. Li, R. Y. Jia, Z. Q. Yin, X. T. Li, C. Lv, G. Ye, L. Zhang and Y. Q. Zhang, *Vet. Parasitol.*, 2009, **163**, 175–178.
70 Y. H. Du, R. Y. Jia, Z. Q. Yin, Z. H. Pu, J. Chen, F. Yang, Y. Q. Zhang and Y. Lu, *Vet. Parasitol.*, 2008, **157**, 144–148.
71 S. M. F. Broglio-Micheletti, N. Valente, L. A. de Souza, D. O. P. Lopes and J. M. dos Santos, *Rev. Bras. Parasitol. Vet.*, 2010, **19**, 44–48.
72 Y. X. Deng, D. X. Shi, Z. Q. Yin, J. H. Guo, R. Y. Jia, J. Xu, X. Song, C. Lv, Q. J. Fan, X. X. Liang, F. Shi, G. Ye and W. Zhang, *Exp. Parasitol.*, 2012, **130**, 475–477.
73 C. H. Anjali, Y. Sharma, A. Mukherjee and N. Chandrasekaran, *Pest Manag. Sci.*, 2012, **68**, 158–163.
74 J. Xu, Q. J. Fan, Z. Q. Yin, X. T. Li, Y. H. Du, R. Y. Jia, K. Y. Wang, C. Lv, G. Ye, Y. Geng, G. Su, L. Zhao, T. X. Hu, F. Shi, L. Zhang, C. L. Wu, C. Tao, Y. X. Zhang and D. X. Shi, *Vet. Parasitol.*, 2010, **169**, 399–403.
75 A. Rani, S. Jain and P. Dureja, *J.Pest Sci.*, 2009, **34**, 253–258.
76 F. O. Okumu, B. G. J. Knols and U. Fillinger, *Malar. J.*, , DOI:6310.1186/1475-2875-6-63.
77 V. K. Dua, A. C. Pandey, K. Raghavendra, A. Gupta, T. Sharma and A. P. Dash, *Malar. J.*, , DOI:12410.1186/1475-2875-8-124.
78 G. P. Das, *Indian J. Agr. Sci.*, 1986, **56**, 743–744.
79 R. K. Akhauri, M. M. Sinha and R. P. Yadav, in *Neem and Environment, Vols 1 and 2*, 1996, pp. 559–563.
80 C. Adarkwah, D. Obeng-Ofori, C. Buttner, C. Reichmuth and M. Scholler, *J.Pest Sci.*, 2010, **83**, 471–479.
81 H. Aliakbarpour, M. R. C. Salmah and O. Dzolkhifli, *J.Pest Sci.*, 2011, **84**, 503–512.
82 J. I. Fernandes, F. D. Ribeiro, T. R. Correia, K. Coumendouros, G. G. Verocai, P. I. Fazio, D. D. da Silva and F. B. Scott, *Rev. Bras. Med. Vet.*, 2010, **32**, 25–30.
83 J. M. de Araujo, E. J. Marques and J. V de Oliveira, *Neotrop. Entomol.*, 2009, **38**, 520–525.
84 Y. K. Mathur and S. Nigam, in *Neem and Environment, Vols 1 and 2*, 1996, pp. 335–342.
85 A. Mochizuki, *Appl. Entomol. Zool.*, 1993, **28**, 254–256.
86 N. S. Sabhanayakam, K. Ramalingam, S. Selvi and B. Krishnakumari, in *Neem and Environment, Vols 1 and 2*, 1996, pp. 315–319.
87 P. I. Gandhi, K. Gunasekaran and T. Sa, *J.Pest Sci.*, 2006, **79**, 103–111.
88 M. K. Choudhury, *Indian J. Pharm. Sci.*, 2009, **71**, 562–563.
89 P. V Pinheiro, E. D. Quintela, J. P. de Oliveira and J. C. Seraphin, *Pesq. Agropec. Bras.*, 2009, **44**, 354–360.
90 T. D. Yadav, in *Neem and Environment, Vols 1 and 2*, 1996, pp. 343–348.
91 D. T. Lowery and M. J. Smirle, *Entomol Exp Appl.*, 2000, **95**, 201–207.

92 M. Baumgart, in *Neem and Environment, Vols 1 and 2*, 1996, pp. 405–412.
93 E. Cohen, G. B. Quistad, P. R. Jefferies and J. E. Casida, *Pest. Sci.*, 1996, **48**, 135–140.
94 J. Sophia, T. K. K. Kishore, J. Kowshik, R. Mishra and S. Nagini, *Sci. Rep.*, 2016, **6**, 1–13.
95 P. R. Singh, R. Arunkumar, V. Sivakamasundari, G. Sharmila, P. Elumalai, E. Suganthapriya, A. B. Mercy, K. Senthilkumar and J. Arunakaran, *Cell Biochem. Funct.*, 2014, **32**, 217–228.
96 R. Subramani, E. Gonzalez, A. Arumugam, S. Nandy, V. Gonzalez, J. Medel, F. Camacho, A. Ortega, S. Bonkoungou, M. Narayan, A. K. Dwivedi and R. Lakshmanaswamy, *Sci. Rep.*, 2016, **6**, 1–12.
97 P. Srivastava, N. Yadav, R. Lella, A. Schneider, A. Jones, T. Marlowe, G. Lovett, K. O'Loughlin, H. Minderman, R. Gogada and D. Chandra, *Carcinogenesis*, 2012, **33**, 2199–2207.
98 G. E. L. Brandt, M. D. Schmidt, T. E. Prisinzano and B. S. J. Blagg, *J. Med. chem.*, 2008, **51**, 6495–6502.
99 A. Lupescu, R. Bissinger, J. Warsi, K. Jilani and F. Lang, *Cell. Physiol. Biochem.*, 2014, **33**, 1838–1848.
100 S. MacKinnon, T. Durst, J. T. Arnason, C. Angerhofer, J. Pezzuto, P. E. SanchezVindas, L. J. Poveda and M. Gbeassor, *J. Nat. Prod.*, 1997, **60**, 336–341.
101 G. Chianese, S. R. Yerbanga, L. Lucantoni, A. Habluetzel, N. Basilica, D. Taramelli, E. Fattorusso and O. Taglialatela-Scafati, *J. Nat. Prod.*, 2010, **73**, 1448–1452.
102 G. Kaur, M. S. Alam and M. Athar, *Phytother. Res.*, 2004, **18**, 419–424.
103 A. Alam, S. Haldar, H. V Thulasiram, R. Kumar, M. Goyal, M. S. Iqbal, C. Pal, S. Dey, S. Bindu, S. Sarkar, U. Pal, N. C. Maiti and U. Bandyopadhyay, *J. Biol. Chem.*, 2012, **287**, 24844–24861.
104 S. Ponnusamy, S. Haldar, F. Mulani, S. Zinjarde, H. Thulasiram and A. RaviKumar, *PLoS One*, 2015, **10**, 1–19.
105 P. Kushwaha, V. Khedgikar, S. Haldar, J. Gautam, F. A. Mulani, H. V Thulasiram and R. Trivedi, *Bioorg. Med. Chem. Lett.*, 2016, **26**, 3719–3724.
106 Gangadhara, P. R. Kumar and V. Prakash, *J. Sci. Food Agric.*, 2009, **89**, 1642–1647.
107 J. Bohlmann and C. I. Keeling, *Plant J.*, 2008, **54**, 656–669.
108 W. Eisenreich, F. Rohdich and A. Bacher, *Trends Plant Sci.*, 2001, **6**, 78–84.
109 J. Chappell, *Annu. Rev. Plant Physiol. Plant Mol. Biol.*, 1995, **46**, 521–547.
110 H. K. Lichtenthaler, *Photosynth. Res.*, 2007, **92**, 163–179.
111 P. Pulido, C. Perello and M. Rodriguez-Concepcion, *Mol. Plant*, 2012, **5**, 964–967.
112 P. M. Dewick, in *Medicinal Natural Products*, John Wiley & Sons, Ltd, 2001, pp. 167–289.
113 S. Srivastava and A. K. Srivastava, in *Bioactive Molecules and Medicinal Plants*, eds. K. G. Ramawat and J. M. Merillon, Springer Berlin Heidelberg, Berlin, Heidelberg, 2008, pp. 233–254.
114 A. J. Nisbet, *An. Soc. Entomol. Bras.*, 2000, **29**, 615–632.
115 E. J. Corey and R. W. Hahl, *Tetrahedron Lett.*, 1989, **30**, 3023–3026.
116 G. E. Veitch, E. Beckmann, B. J. Burke, A. Boyer, S. L. Maslen and S. V. Ley, *Angew. Chem. Int. Ed.* , 2007, **119**, 7773–7776.
117 G. E. Veitch, A. Boyer and S. V Ley, *Angew. Chem. Int. Ed.*, 2008, **47**, 9402–9429.
118 K. Sanderson, *Nature*, 2007, **448**, 630–631.
119 P. Benveniste, *Ann. Rev. Plant Physiol.*, 1986, **37**, 275–308.
120 A. Pandreka, D. S. Dandekar, S. Haldar, V. Uttara, S. G. Vijayshree, F. A. Mulani, T. Aarthy and H. V Thulasiram, *BMC Plant Biol.*, 2015, **15**, 1–14.
121 T. J. Bach, *Lipids*, 1995, **30**, 191–202.
122 H. K. Lichtenthaler, M. Rohmer and J. Schwender, *Physiol. Plant.*, 1997, **101**, 643–652.
123 H. K. Lichtenthaler, J. Schwender, A. Disch and M. Rohmer, *FEBS Lett*, 1997, **400**, 271–274.

124 H. K. Lichtenthaler, *Annu. Rev. Plant Physiol. Plant Mol. Biol.*, 1999, **50**, 47–65.
125 H. V Thulasiram, H. K. Erickson and C. D. Poulter, *Science (80-.).*, 2007, **316**, 73–76.
126 H. V Thulasiram and C. D. Poulter, *J. Am. Chem. Soc.*, 2006, **128**, 15819–15823.
127 J. Schwender, J. Zeidler, R. Groner, C. Muller, M. Focke, S. Braun, F. W. Lichtenthaler and H. K. Lichtenthaler, *FEBS Lett.*, 1997, **414**, 129–134.
128 D. J. McGarvey and R. Croteau, *Plant Cell*, 1995, **7**, 1015–1026.
129 L. Ruzicka, *Experientia*, 1953, **9**, 357–367.
130 F. Bouvier, A. Rahier and B. Camara, *Prog. Lipid Res.*, 2005, **44**, 357–429.
131 K. Bloch, S. Chaykin, A. H. Phillips and A. Dewaard, *J. Biol. Chem.*, 1959, **234**, 2595–2604.
132 T. Kuzuyama, *Biosci. Biotechnol. Biochem.*, 2002, **66**, 1619–1627.
133 R. Zetterstrom, *Acta Paediatr.*, 2009, **98**, 1223–1227.
134 T. W. Goodwin, *Annu. Rev. Plant Physiol.*, 1979, **30**, 369–404.
135 H. N. Little and K. Bloch, *J. Biol. Chem.*, 1950, **183**, 33–46.
136 R. C. Ottke, E. L. Tatum, I. Zabin and K. Bloch, *J. Biol. Chem.*, 1951, **189**, 429–433.
137 R. Adams and B. L. Vanduuren, *J. Am. Chem. Soc.*, 1953, **75**, 2377–2379.
138 G. Flesch and M. Rohmer, *Eur. J. Biochem.*, 1988, **175**, 405–411.
139 M. Rohmer, *Lipids*, 2008, **43**, 1095–1107.
140 N. Dellas, S. T. Thomas, G. Manning and J. P. Noel, *Elife*, , DOI:10.7554/eLife.00672.
141 W. Eisenreich, A. Bacher, D. Arigoni and F. Rohdich, *Cell. Mol. Life Sci.*, 2004, **61**, 1401–1426.
142 H. K. Lichtenthaler, *Fett-Lipid*, 1998, **100**, 128–138.
143 D. Arigoni, S. Sagner, C. Latzel, W. Eisenreich, A. Bacher and M. H. Zenk, *Proc. Natl. Acad. Sci. U. S. A.*, 1997, **94**, 10600–10605.
144 M. Wanke, K. Skorupinska-Tudek and E. Swiezewska, *Acta Biochim. Pol.*, 2001, **48**, 663–672.
145 V. S. Dubey, R. Bhalla and R. Luthra, *J. Biosci.*, 2003, **28**, 637–646.
146 W. Eisenreich, M. Schwarz, A. Cartayrade, D. Arigoni, M. H. Zenk and A. Bacher, *Chem. Biol.*, 1998, **5**, R221–R233.
147 M. Rohmer, *Pure Appl. Chem.*, 1999, **71**, 2279–2284.
148 M. Rohmer, *Nat. Prod. Rep.*, 1999, **16**, 565–574.
149 M. Rohmer, *Pure Appl. Chem.*, 2007, **79**, 739–751.
150 M. Rodriguez-Concepcion and A. Boronat, *Plant Physiol.*, 2002, **130**, 1079–1089.
151 W. N. Hunter, *J. Biol. Chem.*, 2007, **282**, 21573–21577.
152 N. Singh, G. Cheve, M. Avery and C. McCurdy, *Curr. Pharm. Des.*, 2007, **13**, 1161–1177.
153 Y. Matsue, H. Mizuno, T. Tomita, T. Asami, M. Nishiyama and T. Kuzuyama, *J. Antibiot. (Tokyo).*, 2010, **63**, 583–588.
154 K. Sanmiya, O. Ueno, M. Matsuoka and N. Yamamoto, *Plant Cell Physiol.*, 2018, **40**, 348–354.
155 N. Leonhardt, M. Causse, S. Thoraval and C. Escoffier, *Plant Cell*, 2009, **21**, 301–317.
156 C. E. Vickers, M. Bongers, Q. Liu, T. Delatte and H. Bouwmeester, *Plant, Cell Environ.*, 2014, **37**, 1753–1775.
157 M. Sapir-Mir, A. Mett, E. Belausov, S. Tal-Meshulam, A. Frydman, D. Gidoni and Y. Eyal, *Plant Physiol.*, 2008, **148**, 1219–1228.
158 A. Disch, A. Hemmerlin, T. J. Bach and M. Rohmer, *Biochem. J.*, 1998, **331**, 615–621.
159 W. Eisenreich, S. Sagner, M. H. Zenk and A. Bacher, *Tetrahedron Lett.*, 1997, **38**, 3889–3892.
160 W. Knoss, B. Reuter and J. Zapp, *Biochem. J.*, 1997, **326**, 449–454.
161 L. Kutrzeba, F. E. Dayan, J. Howell, J. Feng, J. L. Giner and J. K. Zjawlony, *Phytochemistry*, 2007, **68**, 1872–1881.
162 N. Srivastava and A. Akhila, *Phytochemistry*, 2010, **71**, 1298–1304.
163 J. Wungsintaweekul and W. De-Eknamkul, *Tetrahedron Lett.*, 2005, **46**, 2125–2128.

164 J. Zeidler and H. K. Lichtenthaler, *Planta*, 2001, **213**, 323–326.
165 A. Hemmerlin, J. F. Hoeffler, O. Meyer, D. Tritsch, I. A. Kagan, C. Grosdemange-Billiard, M. Rohmer and T. J. Bach, *J. Biol. Chem.*, 2003, **278**, 26666–26676.
166 H. Kasahara, A. Hanada, T. Kuzuyama, M. Takagi, Y. Kamiya and S. Yamaguchi, *J. Biol. Chem.*, 2002, **277**, 45188–45194.
167 J. Schwender, C. Gemunden and H. K. Lichtenthaler, *Planta*, 2001, **212**, 416–423.
168 O. Laule, A. Furholz, H. S. Chang, T. Zhu, X. Wang, P. B. Heifetz, W. Gruissem and B. M. Lange, *Proc. Natl. Acad. Sci. U S A*, 2003, **100**, 6866–6871.
169 K. Skorupinska-Tudek, J. Poznanski, J. Wojcik, T. Bienkowski, I. Szostkiewicz, M. Zelman-Femiak, A. Bajda, T. Chojnacki, O. Olszowska, J. Grunler, O. Meyer, M. Rohmer, W. Danikiewicz and E. Swiezewska, *J. Biol. Chem.*, 2008, **283**, 21024–21035.
170 J. A. Bick and B. M. Lange, *Arch. Biochem. Biophys.*, 2003, **415**, 146–154.
171 M. J. Towler and P. J. Weathers, *Plant Cell Rep.*, 2007, **26**, 2129–2136.
172 N. Dudareva, S. Andersson, I. Orlova, N. Gatto, M. Reichelt, D. Rhodes, W. Boland and J. Gershenzon, *Proc. Natl. Acad. Sci. U S A*, 2005, **102**, 933–938.
173 D. Hampel, A. Mosandl and M. Wust, *Phytochemistry*, 2005, **66**, 305–311.
174 K. P. Adam and J. Zapp, *Phytochemistry*, 1998, **48**, 953–959.
175 J. W. Yang and Y. Orihara, *Tetrahedron*, 2002, **58**, 1265–1270.
176 W. De-Eknamkul and B. Potduang, *Phytochemistry*, 2003, **62**, 389–398.
177 M. Gutensohn, I. Orlova, T. T. H. Nguyen, R. Davidovich-rikanati, M. G. Ferruzzi, Y. Sitrit, E. Lewinsohn, E. Pichersky and N. Dudareva, *Plant J.*, 2013, 351–363.
178 R. Davidovich-Rikanati, E. Lewinsohn, E. Bar, Y. Iijima, E. Pichersky and Y. Sitrit, *Plant J.*, 2008, **56**, 228–238.
179 M. Rohmer, M. Knani, P. Simonin, B. Sutter and H. Sahm, *Biochem. J.*, 1993, **295**, 517–524.
180 S. R. Putra, A. Disch, J. M. Bravo and M. Rohmer, *Fems Microbiol. Lett.*, 1998, **164**, 169–175.
181 C. Rieder, G. Strauss, G. Fuchs, D. Arigoni, A. Bacher and W. Eisenreich, *J. Biol. Chem.*, 1998, **273**, 18099–18108.
182 D. Spiteller, A. Jux, J. Piel and W. Boland, *Phytochemistry*, 2002, **61**, 827–834.
183 H. Seto, H. Watanabe and K. Furihata, *Tetrahedron Lett.*, 1996, **37**, 7979–7982.
184 H. Seto, N. Orihara and K. Furihata, *Tetrahedron Lett.*, 1998, **39**, 9497–9500.
185 D. E. Cane, T. Rossi, A. M. Tillman and J. P. Pachlatko, *J. Am. Chem. Soc.*, 1981, **103**, 1838–1843.
186 M. Derosa, A. Gambacorta and B. Nicolaus, *Phytochemistry*, 1980, **19**, 791–793.
187 N. Moldoveanu and M. Kates, *Biochim. Biophys. Acta*, 1988, **960**, 164–182.
188 K. Kakinuma, M. Yamagishi, Y. Fujimoto, N. Ikekawa and T. Oshima, *J. Am. Chem. Soc.*, 1988, **110**, 4861–4863.
189 T. Eguchi, M. Morita and K. Kakinuma, *J. Am. Chem. Soc.*, 1998, **120**, 5427–5433.
190 J. Schwender, M. Seemann, H. K. Lichtenthaler and M. Rohmer, *Biochem. J.*, 1996, **316**, 73–80.
191 A. Disch, J. Schwender, C. Muller, H. K. Lichtenthaler and M. Rohmer, *Biochem. J.*, 1998, **333**, 381–388.
192 K. P. Adam, R. Thiel, J. Zapp and H. Becker, *Arch. Biochem. Biophys.*, 1998, **354**, 181–187.
193 R. Thiel and K. P. Adam, *Phytochemistry*, 2002, **59**, 269–274.
194 W. Eisenreich, C. Rieder, C. Grammes, G. Hessler, K. P. Adam, H. Becker, D. Arigoni and A. Bacher, *J. Biol. Chem.*, 1999, **274**, 36312–36320.
195 W. Eisenreich, B. Menhard, P. J. Hylands, M. H. Zenk and A. Bacher, *Proc. Natl. Acad. Sci. U S A*, 1996, **93**, 6431–6436.
196 D. Kongduang, J. Wungsintaweekul and W. De-Eknamkul, *Tetrahedron Lett.*, 2008, **49**, 4067–4072.
197 Y. Yamazaki, M. Kitajima, M. Arita, H. Takayama, H. Sudo, M. Yamazaki, N. Aimi and

K. Saito, *Plant Physiol.*, 2004, **134**, 161–170.
198 J. C. Bede, P. E. A. Teal, W. G. Goodman and S. S. Tobe, *Plant Physiol.*, 2001, **127**, 584–593.
199 F. Luan and M. Wust, *Phytochemistry*, 2002, **60**, 451–459.
200 C. Rieder, B. Jaun and D. Arigoni, *Helv. Chim. Acta*, 2000, **83**, 2504–2513.
201 A. Disch and M. Rohmer, *Fems Microbiol. Lett.*, 1998, **168**, 201–208.
202 U. Heinig, M. Gutensohn, N. Dudareva and A. Aharoni, *Curr. Opin. Biotechnol.*, 2013, **24**, 239–246.
203 C. V Guirimand G, Guihur A, Phillips M, Oudin A, Glévarec G, Melin C, Papon N, Clastre M, St-Pierre B, Rodríguez-Concepción M, Burlat V, *Plant Mol. Biol.*, 2012, **79**, 443–459.
204 T. B. Andersen, K. A. Martinez-Swatson, S. A. Rasmussen, B. A. Boughton, K. Jorgensen, J. Andersen-Ranberg, N. Nyberg, S. B. Christensen and H. T. Simonsen, *Plant Physiol.*, 2017, **174**, 56–72.
205 K. Yazaki, *Curr. Opin. Plant Biol.*, 2005, **8**, 301–307.
206 N. Linka and A. P. M. Weber, *Mol. Plant*, 2010, **3**, 21–53.
207 S. Leran, K. Varala, J. C. Boyer, M. Chiurazzi, N. Crawford, F. Daniel-Vedele, L. David, R. Dickstein, E. Fernandez, B. Forde, W. Gassmann, D. Geiger, A. Gojon, J. M. Gong, B. A. Halkier, J. M. Harris, R. Hedrich, A. M. Limami, D. Rentsch, M. Seo, Y. F. Tsay, M. Y. Zhang, G. Coruzzi and B. Lacombe, *Trends Plant Sci.*, 2014, **19**, 5–9.
208 Y. F. Tsay, C. C. Chiu, C. B. Tsai, C. H. Ho and P. K. Hsu, *Febs Lett.*, 2007, **581**, 2290–2300.
209 M. Morita, N. Shitan, K. Sawada, M. C. E. Van Montagu, D. Inze, H. Rischer, A. Goossens, K. M. Oksman-Caldentey, Y. Moriyama and K. Yazaki, *Proc. Natl. Acad. Sci. U. S. A.*, 2009, **106**, 2447–2452.
210 J. Zhao and R. A. Dixon, *Trends Plant Sci.*, 2009, **15**, 72–80.
211 B. Larsen, V. L. Fuller, J. Pollier, A. Van Moerkercke, F. Schweizer, R. Payne, M. Colinas, S. E. O'Connor, A. Goossens and B. A. Halkier, *Plant Cell Physiol.*, 2017, **58**, 1507–1518.
212 R. M. E. Payne, D. Y. Xu, E. Foureau, M. Carqueijeiro, A. Oudin, T. D. de Bernonville, V. Novak, M. Burow, C. E. Olsen, D. M. Jones, E. C. Tatsis, A. Pendle, B. A. Halkier, F. Geu-Flores, V. Courdavault, H. H. Nour-Eldin and S. E. O'Connor, *Nat. Plants*, , DOI:1620810.1038/nplants.2016.208.
213 K. Jorgensen, A. V Rasmussen, M. Morant, A. H. Nielsen, N. Bjarnholt, M. Zagrobelny, S. Bak and B. L. Moller, *Curr. Opin. Plant Biol.*, 2005, **8**, 280–291.
214 T. Laursen, J. Borch, C. Knudsen, K. Bavishi, F. Torta, H. J. Martens, D. Silvestro, N. S. Hatzakis, M. R. Wenk, T. R. Dafforn, C. E. Olsen, M. S. Motawia, B. Hamberger, B. L. Moller and J. E. Bassard, *Science (80-.).*, 2016, **354**, 890–893.
215 T. Laursen, B. L. Moller and J. E. Bassard, *Trends Plant Sci.*, 2015, **20**, 20–32.
216 J.-E. Bassard and B. A. Halkier, *Phytochem. Rev.*, , DOI:10.1007/s11101-017-9509-1.
217 J. W. Allwood and R. Goodacre, *Phytochem. Anal.*, 2009, **21**, 33–47.
218 H. F. Wu, J. Guo, S. L. Chen, X. Liu, Y. Zhou, X. P. Zhang and X. D. Xu, *J. Pharm. Biomed. Anal.*, 2013, **72**, 267–291.
219 M. Hur, A. A. Campbell, M. Almeida-de-Macedo, L. Li, N. Ransom, A. Jose, M. Crispin, B. J. Nikolau and E. S. Wurtele, *Nat. Prod. Rep.*, 2013, **30**, 1569.
220 O. Potterat and M. Hamburger, *Nat. Prod. Rep.*, 2013, **30**, 546–564.
221 H. F. Wu, J. Guo, S. L. Chen, X. Liu, Y. Zhou, X. P. Zhang and X. D. Xu, *J. Pharm. Biomed. Anal.*, 2012, **72**, 267–291.
222 L. W. Sumner, Z. Lei, B. J. Nikolau and K. Saito, *Nat. Prod. Rep.*, 2015, **32**, 212–229.
223 K. J. Dietz, *J. Exp.Bot.*, 2017, **68**, 5695–5698.
224 S. Q. Wu and J. Chappell, *Curr. Opin. Biotechnol.*, 2008, **19**, 145–152.
225 M. A. Farag, A. Porzel and L. A. Wessjohann, *Phytochemistry*, 2012, **76**, 60–72.
226 S. Kueger, D. Steinhauser, L. Willmitzer and P. Giavalisco, *Plant J.*, 2012, **70**, 39–50.

227 R. N. Trethewey, A. J. Krotzky and L. Willmitzer, *Curr.Opin. Plant Biol.*, 1999, **2**, 83–85.
228 J. Kopka, A. Fernie, W. Weckwerth, Y. Gibon and M. Stitt, *Genome Biol.*, 2004, **5**, 9.
229 P. Krishnan, N. J. Kruger and R. G. Ratcliffe, *J. Exp.Bot.*, 2005, **56**, 255–265.
230 R. G. Ratcliffe and Y. Shachar-Hill, *Biol. Rev.*, 2005, **80**, 27–43.
231 A. Bouslimani, L. M. Sanchez, N. Garg and P. C. Dorrestein, *Nat. Prod. Rep.*, 2014, **31**, 718–729.
232 A. K. Jarmusch and R. G. Cooks, *Nat. Prod. Rep.*, 2013, **31**, 730–738.
233 J. L. Wolfender, G. Marti, A. Thomas and S. Bertrand, *J.Chromatogr. A*, 2015, **1382**, 136–164.
234 J. Lisec, N. Schauer, J. Kopka, L. Willmitzer and A. R. Fernie, *Nat. Protoc.*, 2006, **10**, 1457.
235 J. M. Halket, D. Waterman, A. M. Przyborowska, R. K. P. Patel, P. D. Fraser and P. M. Bramley, *J. Exp.Bot.*, 2005, **56**, 219–243.
236 A. K. Jarmusch and R. G. Cooks, *Nat. Prod. Rep.*, 2014, **31**, 730–738.
237 S. Klie, S. Krueger, L. Krall, P. Giavalisco, U. I. Flugge, L. Willmitzer and D. Steinhauser, *Front Plant Sci.*, 2011, **2**, 27.
238 T. Fujii, S. Matsuda, M. L. Tejedor, T. Esaki, I. Sakane, H. Mizuno, N. Tsuyama and T. Masujima, *Nat. Prot.*, 2015, **10**, 1445–1456.
239 L. Yi, Z. T. Liang, Y. Peng, X. Yao, H. B. Chen and Z. Z. Zhao, *J. Chromatogr. A*, 2012, **1248**, 93–103.
240 J. J. Fang, A. Ramsay, S. Renouard, C. Hano, F. Lamblin, B. Chabbert, F. Mesnard and B. Schneider, *Front Plant Sci.*, 2016, **7**, 14.
241 V. Gautam and A. K. Sarkar, *Mol. Biotechnol.*, 2015, **57**, 299–308.
242 D. W. Etalo, R. C. H. De Vos, M. Joosten and R. D. Hall, *Plant Physiol.*, 2015, **169**, 1424–1435.
243 Y. J. Lee, D. C. Perdian, Z. H. Song, E. S. Yeung and B. J. Nikolau, *Plant J.*, 2012, **70**, 81–95.
244 K. Yamamoto, K. Takahashi, H. Mizuno, A. Anegawa, K. Ishizaki, H. Fukaki, M. Ohnishi, M. Yamazaki, T. Masujima and T. Mimura, *Proc. Natl. Acad. Sci. U S A*, 2016, **113**, 3891–3896.
245 M. Stitt and A. R. Fernie, *Curr. Opin. Biotechnol.*, 2003, **14**, 136–144.
246 M. Fehr, W. B. Frommer and S. Lalonde, *Proc. Natl. Acad. Sci. U. S. A.*, 2002, **99**, 9846–9851.
247 I. L. Medintz, *Trends Biotechnol.*, 2006, **24**, 539–542.
248 C. Khosla and J. D. Keasling, *Nat. Rev. Drug Discov.*, 2003, **2**, 1019–1025.
249 P. J. Facchini, J. Bohlmann, P. S. Covello, V. De Luca, R. Mahadevan, J. E. Page, D. K. Ro, C. W. Sensen, R. Storms and V. J. J. Martin, *Trends Biotechnol.*, 2012, **30**, 127–131.
250 T. Moses, J. Pollier, J. M. Thevelein and A. Goossens, *New Phytol.*, 2013, **200**, 27–43.
251 Y. Katsuyama, N. Funa, I. Miyahisa and S. Horinouchi, *Chem.Biol.*, 2007, **14**, 613–621.
252 J. Nielsen and J. D. Keasling, *Cell*, 2016, **164**, 1185–1197.
253 C. Ignea, E. Ioannou, P. Georgantea, S. Loupassaki, F. A. Trikka, A. K. Kanellis, A. M. Makris, V. Roussis and S. C. Kampranis, *Metab. Eng.*, 2015, **28**, 91–103.
254 H. J. Frasch, M. H. Medema, E. Takano and R. Breitling, *Curr. Opin. Biotechnol.*, 2013, **24**, 1144–1150.
255 Y. Z. Luo, B. Enghiad and H. M. Zhao, *Nat. Prod. Rep.*, 2016, **33**, 174–182.
256 C. Q. Zhang, X. X. Chen, N. D. Lindley and H. P. Too, *Biotechnol. Bioeng.*, 2017, **115**, 174–183.
257 M. C. Bassalo, A. D. Garst, A. L. Halweg-Edwards, W. C. Grau, D. W. Domaille, V. K. Mutalik, A. P. Arkin and R. T. Gill, *ACS Synth. Biol.*, 2016, **5**, 561–568.
258 Y. Z. Luo, R. E. Cobb and H. M. Zhao, *Curr. Opin. Biotechnol.*, 2014, **30**, 230–237.
259 D. K. Ro, E. M. Paradise, M. Ouellet, K. J. Fisher, K. L. Newman, J. M. Ndungu, K. A. Ho, R. A. Eachus, T. S. Ham, J. Kirby, M. C. Y. Chang, S. T. Withers, Y. Shiba, R.

Sarpong and J. D. Keasling, *Nature*, 2006, **440**, 940–943.
260 P. J. Westfall, D. J. Pitera, J. R. Lenihan, D. Eng, F. X. Woolard, R. Regentin, T. Horning, H. Tsuruta, D. J. Melis, A. Owens, S. Fickes, D. Diola, K. R. Benjamin, J. D. Keasling, M. D. Leavell, D. J. McPhee, N. S. Renninger, J. D. Newman and C. J. Paddon, *Proc. Natl. Acad. Sci. U. S. A.*, 2012, **109**, 111–118.
261 C. J. Paddon, P. J. Westfall, D. J. Pitera, K. Benjamin, K. Fisher, D. McPhee, M. D. Leavell, A. Tai, A. Main, D. Eng, D. R. Polichuk, K. H. Teoh, D. W. Reed, T. Treynor, J. Lenihan, M. Fleck, S. Bajad, G. Dang, D. Dengrove, D. Diola, G. Dorin, K. W. Ellens, S. Fickes, J. Galazzo, S. P. Gaucher, T. Geistlinger, R. Henry, M. Hepp, T. Horning, T. Iqbal, H. Jiang, L. Kizer, B. Lieu, D. Melis, N. Moss, R. Regentin, S. Secrest, H. Tsuruta, R. Vazquez, L. F. Westblade, L. Xu, M. Yu, Y. Zhang, L. Zhao, J. Lievense, P. S. Covello, J. D. Keasling, K. K. Reiling, N. S. Renninger and J. D. Newman, *Nature*, 2013, **496**, 528–+.
262 C. Owen, N. J. Patron, A. Huang and A. Osbourn, *Curr. Opin. Chem. Biol.*, 2017, **40**, 24–30.
263 P. K. Ajikumar, W.-H. Xiao, K. E. J. Tyo, Y. Wang, F. Simeon, E. Leonard, O. Mucha, T. H. Phon, B. Pfeifer and G. Stephanopoulos, *Science (80-.).*, 2010, **330**, 70–74.
264 M. Farhi, E. Marhevka, T. Masci, E. Marcos, Y. Eyal, M. Ovadis, H. Abeliovich and A. Vainstein, *Metab. Eng.*, 2011, **13**, 474–481.
265 P. Broun, *Curr. Opin. Plant Biol.*, 2004, **7**, 202–209.
266 P. Arendt, K. Miettinen, J. Pollier, R. De Rycke, N. Callewaert and A. Goossens, *Metab. Eng.*, 2017, **40**, 165–175.
267 S. Q. Wu, M. Schalk, A. Clark, R. B. Miles, R. Coates and J. Chappell, *Nat. Biotechnol.*, 2006, **24**, 1441–1447.
268 J. Degenhardt, J. Gershenzon, I. T. Baldwin and A. Kessler, *Curr. Opin. Biotechnol.*, 2003, **14**, 169–176.
269 I. F. Kappers, A. Aharoni, T. van Herpen, L. L. P. Luckerhoff, M. Dicke and H. J. Bouwmeester, *Science*, 2005, **309**, 2070–2072.
270 A. Aharoni, M. A. Jongsma and H. J. Bouwmeester, *Trends Plant Sci.*, 2005, **10**, 594–602.
271 X. Lu, K. X. Tang and P. Li, *Front Plant Sci.*, , DOI:164710.3389/fpls.2016.01647.
272 R. Kunze, W. B. Frommer and U. I. Flugge, *Metab. Eng.*, 2002, **4**, 57–66.
273 S. S. Mahmoud and R. B. Croteau, *Trends Plant Sci.*, 2002, **7**, 366–373.
274 F. S. Li and J. K. Weng, *Nat. Plants*, 2017, 3, 1-7 (article No.17109).

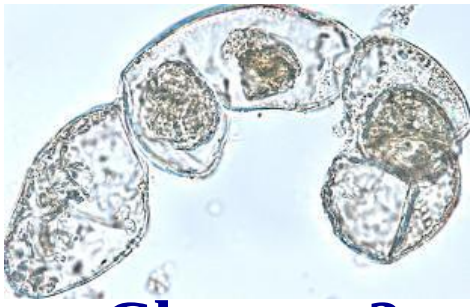

Chapter 2

Development of *in vitro* cultures of neem, limonoid profiling and study of organelles and cells involved in metabolite storage

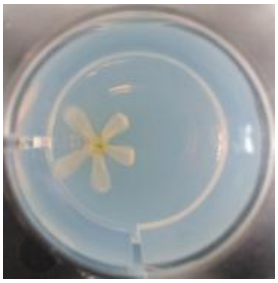

Tissue sectioning

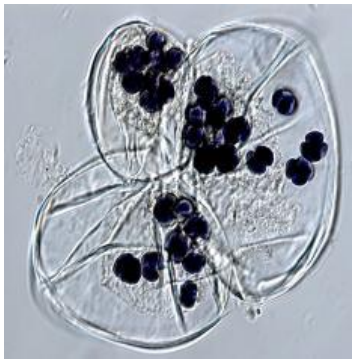

Chapter 2: Section A
Establishment of neem cell culture, limonoid profiling and quantification

2A.1. Introduction

Various parts of neem tree serves mankind since time immemorial with its bountiful medicinal properties, of these the neem seed has been used widely as a natural insecticide in agricultural practice[1, 2]. The most active and characteristic compound of neem tree, azadirachtin A is found in most of the tissues of neem, however its occurrence is rich in the seed kernel[3, 4]. Azadirachtin A, an effective insect growth deterrent, is found to be the best potential natural insecticide candidate identified so far from the plant sources, also possesses remarkable non-toxicity to vertebrates[3]. Characterization of this highly oxygenated, complex molecule was startling in such a way that it paid impetus for the perseverance of the researchers from both biological and chemical fields. In particular, following the determination of correct structure of azadirachtin in 1985[5], Ley and co-workers achieved the total synthesis of this molecule after two decades of efforts[6, 7]. Seventy one steps are involved in the total synthesis, but the final yield was only 0.00015%[6, 7], which warrants the alternative ways such as biosynthesis through tissue culture means, for the production of azadirachtin. Considering the efficient activity of biopesticide, azadirachtin A, several studies have been reported for the optimization of increasing its productivity and also the biomass of neem in cell culture and also as plants[8-22]. Secondary metabolite biosynthetic potential of plants varies genetically and environmentally according to geographical location and hence is the metabolite production of the *in vitro* cells derived from the explant[23]. Besides these variation, cell and tissue developed *in vitro* undergoes somoclonal variation and also variation in the secondary metabolite production over time. Taken together these factors, new cell lines need to be established from the plant tissue before the initiation of experiment to establish its physiological, genetic and other characteristics. Various studies performed with neem tissue culture are callus culture[10], suspension culture[8-10], hairy root culture[11, 16], somatic embryogenesis[24-27], androgenesis[13] for the propagation of whole plant *in vitro* [12, 28-30] aiming at increasing the population of neem tree. Somatic embryogenesis, i.e., the formation of embryo from the somatic cells of the explant has been reported to induce in the presence of different concentrations of the hormone thidiazuron (TDZ)[27]. Hence, this serves as an effective method for mass propagation of elite neem plants followed by hardening them in green house conditions[27]. Anther culture developed in neem helped in the production of haploid

plants thereby avoiding the heterozygous nature of the plants formed from seeds due to cross pollination (Figure 2A.1)[13]. Cell suspension culture and hairy root culture has been developed and used extensively for the large-scale production of azadirachtin A[11, 31, 32]. Different media composition was found to have effect on the azadirachtin production from various explants obtained from different geographical conditions[11, 20]. Hence, it is necessary to establish the suitable media and hormonal composition for the new explants, for the appropriate development of cell and organs. Moreover, also, other pharmacologically active limonoid levels were not improved so far through tissue culture as evident from the literature. The present work was carried out with the objective of developing neem plantlets, callus and cell suspension *in vitro* in order to profile them for the diversity of limonoids and thereby to study limonoid biosynthesis.

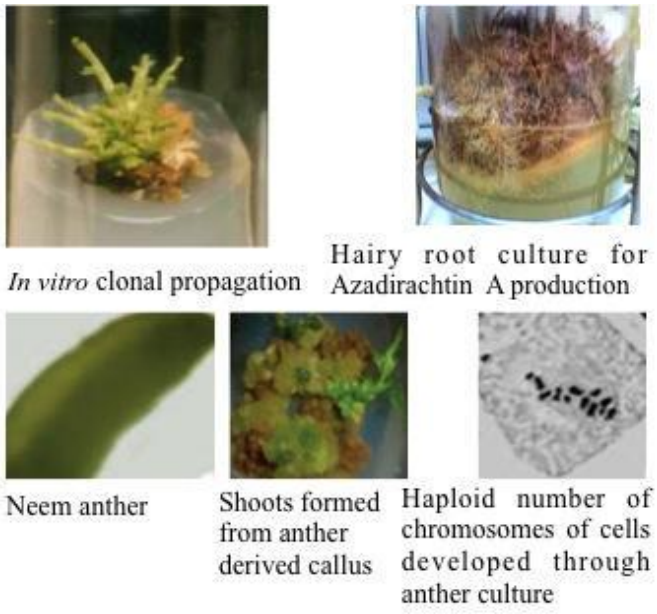

Figure 2A.1. Various neem plant tissue cultures carried out for the improved production of azadirachtin A [8, 13, 26, 28-30]

2A.2. Results and discussion

2A.2.1. Optimization of growth regulator composition for callus

Following surface sterilization of neem fruits, the kernel was excised and inoculated over MS media supplemented with 2 mg/L 2,4- D, 1 mg/L BAP for auxin and cytokinin respectively and also over media containing 2 mg/L NAA, 0.2 mg/L BAP (Figure 2A.2). Even though the explants grown over the hormone combination 2 mg/L 2,4- D, 1 mg/L BAP showed callusing, it turned brown and fragile over time (Figure

2A.3C). The intact cotyledons showed sprouting in 2-3 weeks interval whereas the others showed callusing from the cut ends over the hormone combination 2 mg/L NAA, 0.2 mg/L BAP (Figure 2A.3A, Figure 2A.3B). Henceforth, cotyledons with the incised ends were inoculated over MS media containing 2 mg/L NAA, 0.2 mg/L BAP.

Figure 2A.2. (A) Surface sterilized neem fruits **(B), (C)** Kernel excised from the sterilized fruit and inoculated over MS media of different growth regulators composition

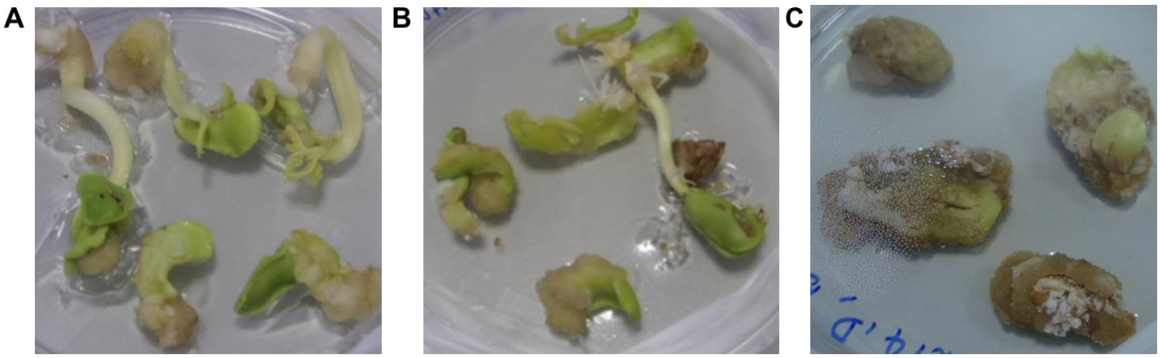

Figure 2A.3. The explant over 2-3 weeks of incubation (A) (B) Kernel explant inoculated over media with NAA and BAP. **(C)** Kernel explant inoculated over media with 2,4-D and BAP.

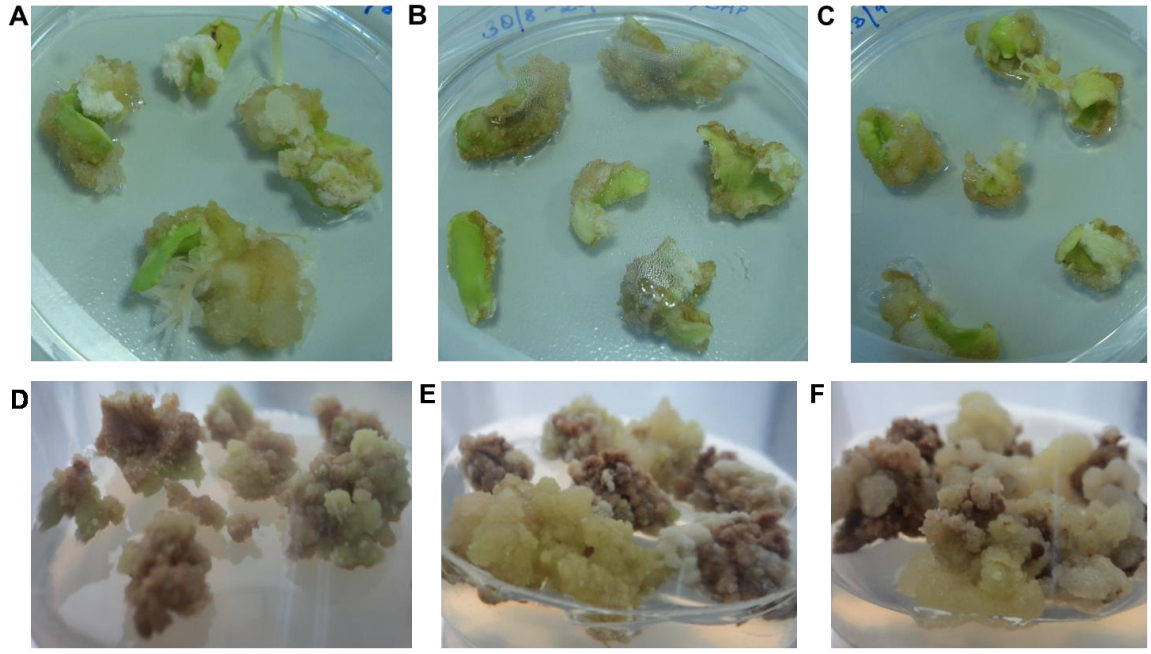

Figure 2A.4. Different stages of explant and callus (A) The explant over 4 weeks of incubation over media with NAA and BAP showing callusing **(B)** The callus developed from explant was excised after 4 weeks and re-incubated in the media of same composition **(C)** Re-incubated explant showing callusing again **(D) (E) (F)** Excised callus sub-cultured every 4 weeks and maintained in regular intervals showing difference in morphology.

Every three weeks, the newly formed callus was excised, both the parental and callus tissue were sub-cultured into media of same composition. Different calli showed different morphology, colour ranged from yellowish green, green, brown and friability, moisture content etc. (Figure 2A.4). Tight, compact callus showed better properties as it was immune to infestation when compared to loose callus with high water content. Callus was profiled for its limonoid content.

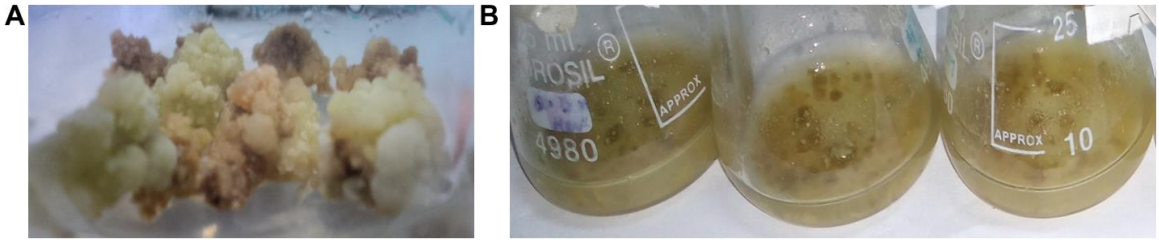

Figure 2A.5. (A) Friable callus was used for development of cell suspension culture **(B)** suspension culture developed from the friable callus.

2A.2.2. Metabolic profiling of neem callus

Limonoid profiling of callus at different subculturing stage and of different morphology was carried out using UPLC-ESI (+)-HRMS based targeted profiling by comparison with 15 limonoid standards isolated and characterized from neem (Figure 2A6).

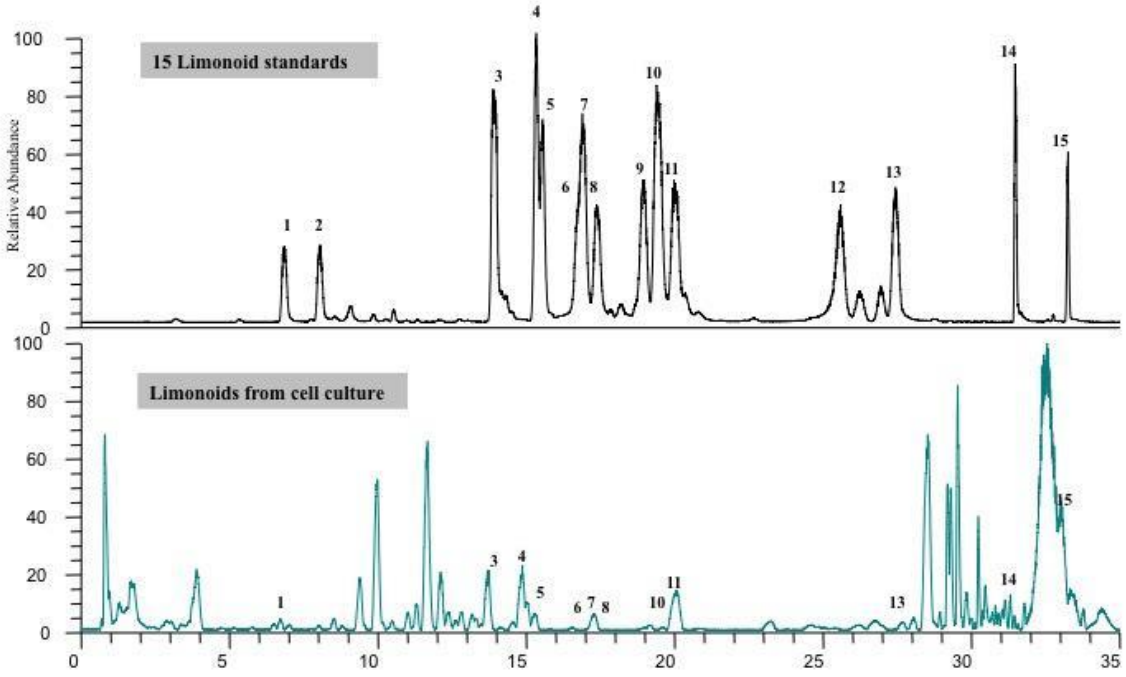

Figure 2A.6. Metabolic profiling of callus cells by comparison with 15 authentic limonoid standards isolated and characterized from neem. 1-Azadirachtin A, 2- Azadirachtin B, 3- 6-deacetylnimbin, 4- Azadiradione, 5- 6-deacetylnimbinene, 6- Nimbanal, 7- Nimbin, 8- 3-deacetylsalannin, 9- Gedunin, 10- Nimbinene, 11- Salannin, 12- Epoxyazadiradione, 13- Salannolacetate, 14- Azadirone, 15- Nimocinol.

2A.2.3. Establishment of cell suspension and neem plantelets

The callus cultures which showed limonoid formation in every sub-cultures were selected and cut finely, inoculated into liquid MS media of same hormonal composition (2 mg/L NAA, 0.2 mg/L BAP) (Figure 2A.5).

2A.2.4. Metabolic profiling of neem plantlets and cell suspension

Neem plantlets and a stable cell suspension were established from the callus culture obtained from kernel, in order to profile and quantify the individual limonoids formed and therefore to perform feeding experiments for tracing the limonoid biosynthetic pathway. Neem seedling was developed from the cotyledon in four weeks

of inoculation. Limonoid profiling was carried out using UPLC-ESI (+)-HRMS based targeted profiling from individual parts of the seedling such as leaf, root, stem and withered cotyledon. Azadirachtin A was found to be the major limonoid identified in the different part of seedling followed by azadirachtin B (Figure 2A.7). Azadirachtin A present in the stem of the plant was 123 μg/g, 100 μg/g of root, 81 μg/g of leaf and 7 μg/g of withered cotyledons respectively.

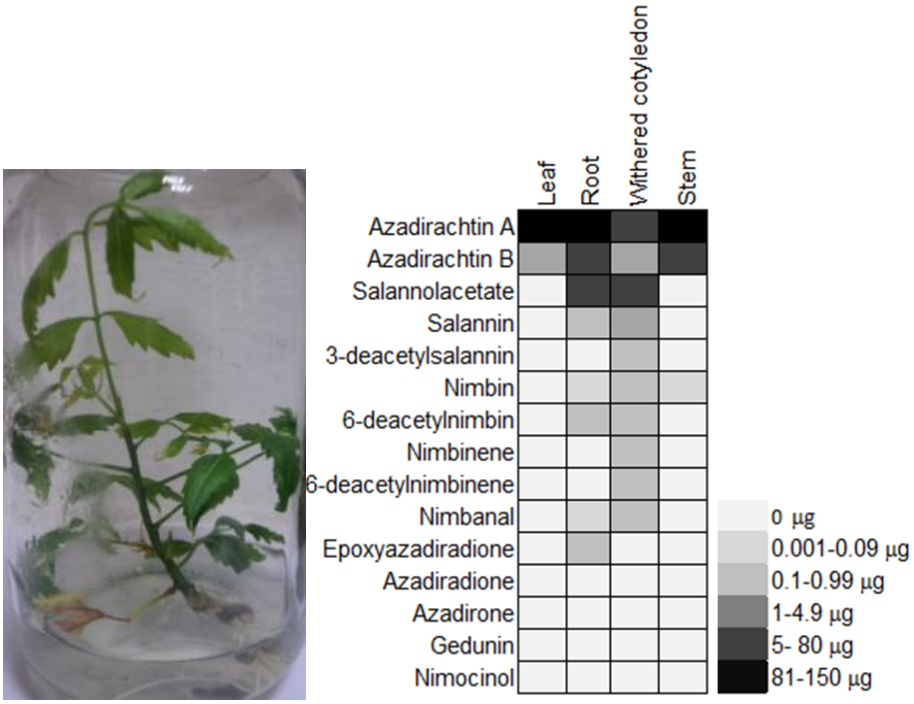

Figure 2A.7. Targeted limonoid profile (*Right*) of *in vitro* grown neem seedling emerged from cotyledons (*Left*).

The studies indicated that both ring intact (basic) and C-seco limonoids were identified in the newly formed callus however, in subsequent subcultures, the levels of ring intact limonoids decreased gradually. At the end of three subcultures, the basic limonoids were not detected. C-seco limonoids such as azadirachtin A, salannin, salannolacetate, 3-deacetylsalannin, nimbin, 6-deacetylnimbin, nimbinene, 6-deacetylnimbinene, nimbanal were found in callus and suspension culture of neem cells as identified (Figure 2A.8) and quantified based on extracted ion chromatogram. Callus inoculum of 0.2 g, was dispersed in 5 mL of liquid MS media to initiate cell suspension culture, which showed a typical growth curve (Figure 2A.9B). A lag phase of 5 days was observed from the day of inoculation, followed by exponential phase for the next 5 days.

Following the exponential phase, linear growth phase was observed for 9 days and the stationary phase started from day 20. Nine limonoids identified in the suspension culture were quantified over the time course of cellular growth (Figure 2A.9A). Limonoid accumulation in cells was recorded highest in the stationary phase of growth. Among the nine C-seco limonoids identified, level of 6-deacetylnimbin and 6-deacetylnimbinene were higher (17 µg/g and 8 µg/g of cells respectively) among the tetranor- and pentanor-triterpenoid group of limonoids, respectively in the cell suspension culture. In the media, the limonoids were identified in traces (Figure 2A.9). The traces of limonoids identified in the media may be from the ruptured cells formed during the generation of suspension from callus. These results show that limonoids are synthesized and stored inside the suspension cells.

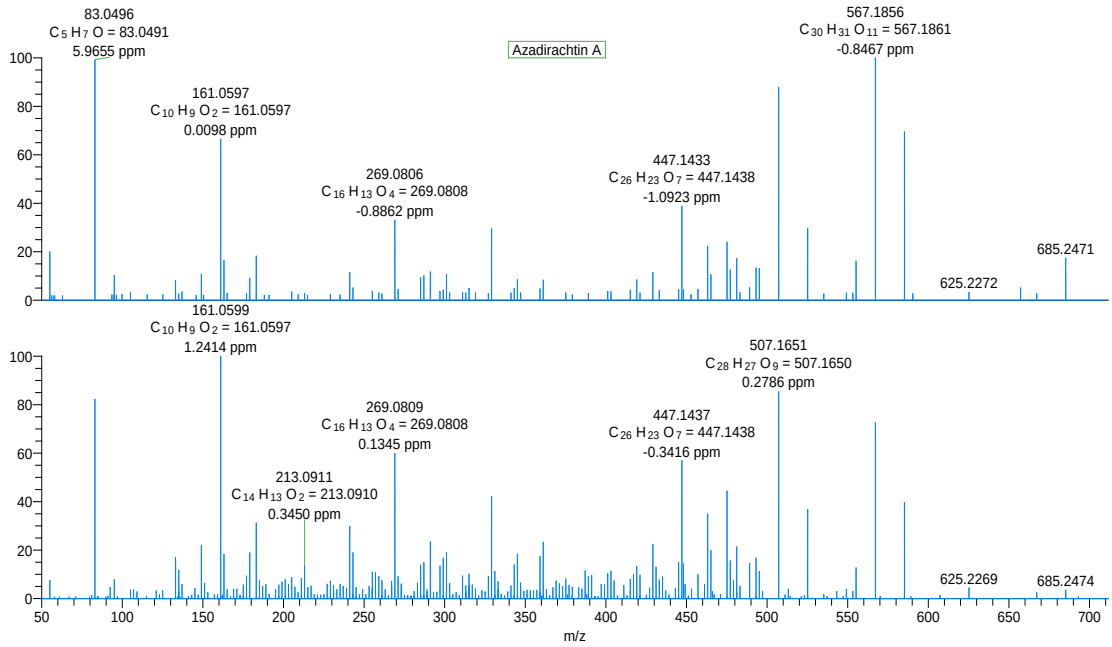

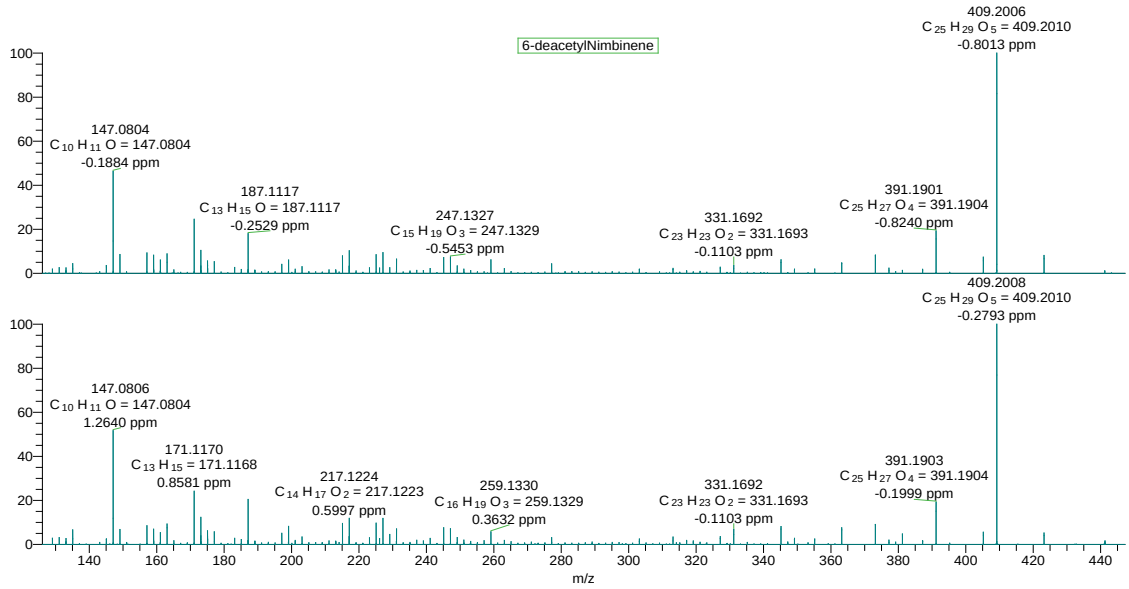
6-deacetylNimbinene
409.2006
C 25 H 29 O 5 = 409.2010
-0.8013 ppm
147.0804
C 10 H 11 O = 147.0804
-0.1884 ppm
187.1117
C 13 H 15 O = 187.1117
-0.2529 ppm
247.1327
C 15 H 19 O 3 = 247.1329
-0.5453 ppm
331.1692
C 23 H 23 O 2 = 331.1693
-0.1103 ppm
391.1901
C 25 H 27 O 4 = 391.1904
-0.8240 ppm
409.2008
C 25 H 29 O 5 = 409.2010
-0.2793 ppm
147.0806
C 10 H 11 O = 147.0804
1.2640 ppm
171.1170
C 13 H 15 = 171.1168
0.8581 ppm
217.1224
C 14 H 17 O 2 = 217.1223
0.5997 ppm
259.1330
C 16 H 19 O 3 = 259.1329
0.3632 ppm
331.1692
C 23 H 23 O 2 = 331.1693
-0.1103 ppm
391.1903
C 25 H 27 O 4 = 391.1904
-0.1999 ppm
m/z

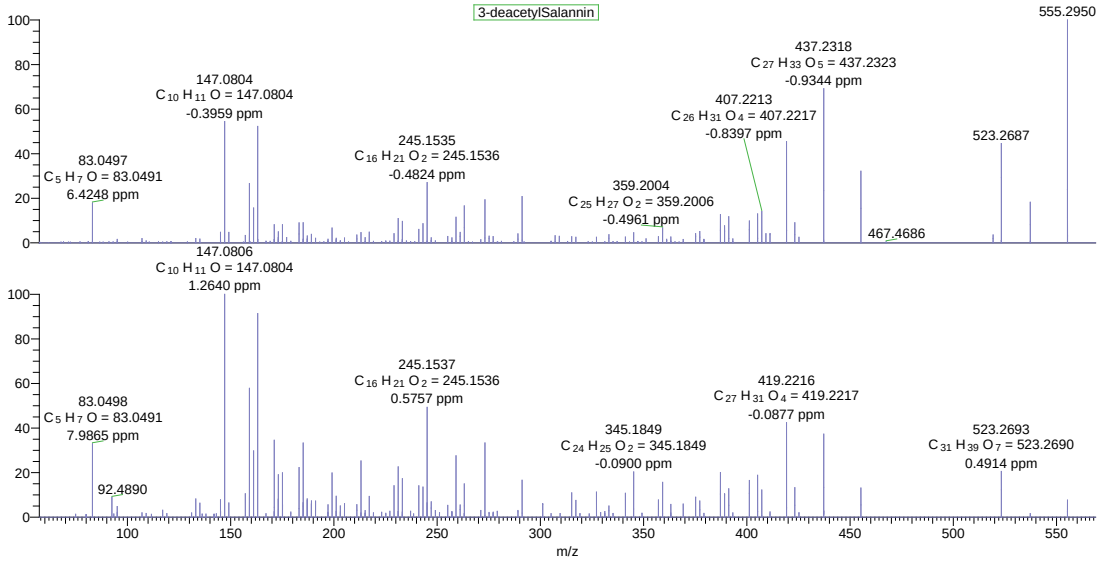
3-deacetylSalannin
555.2950
437.2318
C 27 H 33 O 5 = 437.2323
-0.9344 ppm
147.0804
C 10 H 11 O = 147.0804
-0.3959 ppm
407.2213
C 26 H 31 O 4 = 407.2217
-0.8397 ppm
245.1535
C 16 H 21 O 2 = 245.1536
-0.4824 ppm
523.2687
83.0497
C 5 H 7 O = 83.0491
6.4248 ppm
359.2004
C 25 H 27 O 2 = 359.2006
-0.4961 ppm
467.4686
147.0806
C 10 H 11 O = 147.0804
1.2640 ppm
245.1537
C 16 H 21 O 2 = 245.1536
0.5757 ppm
419.2216
C 27 H 31 O 4 = 419.2217
-0.0877 ppm
83.0498
C 5 H 7 O = 83.0491
7.9865 ppm
345.1849
C 24 H 25 O 2 = 345.1849
-0.0900 ppm
523.2693
C 31 H 39 O 7 = 523.2690
0.4914 ppm
92.4890
m/z

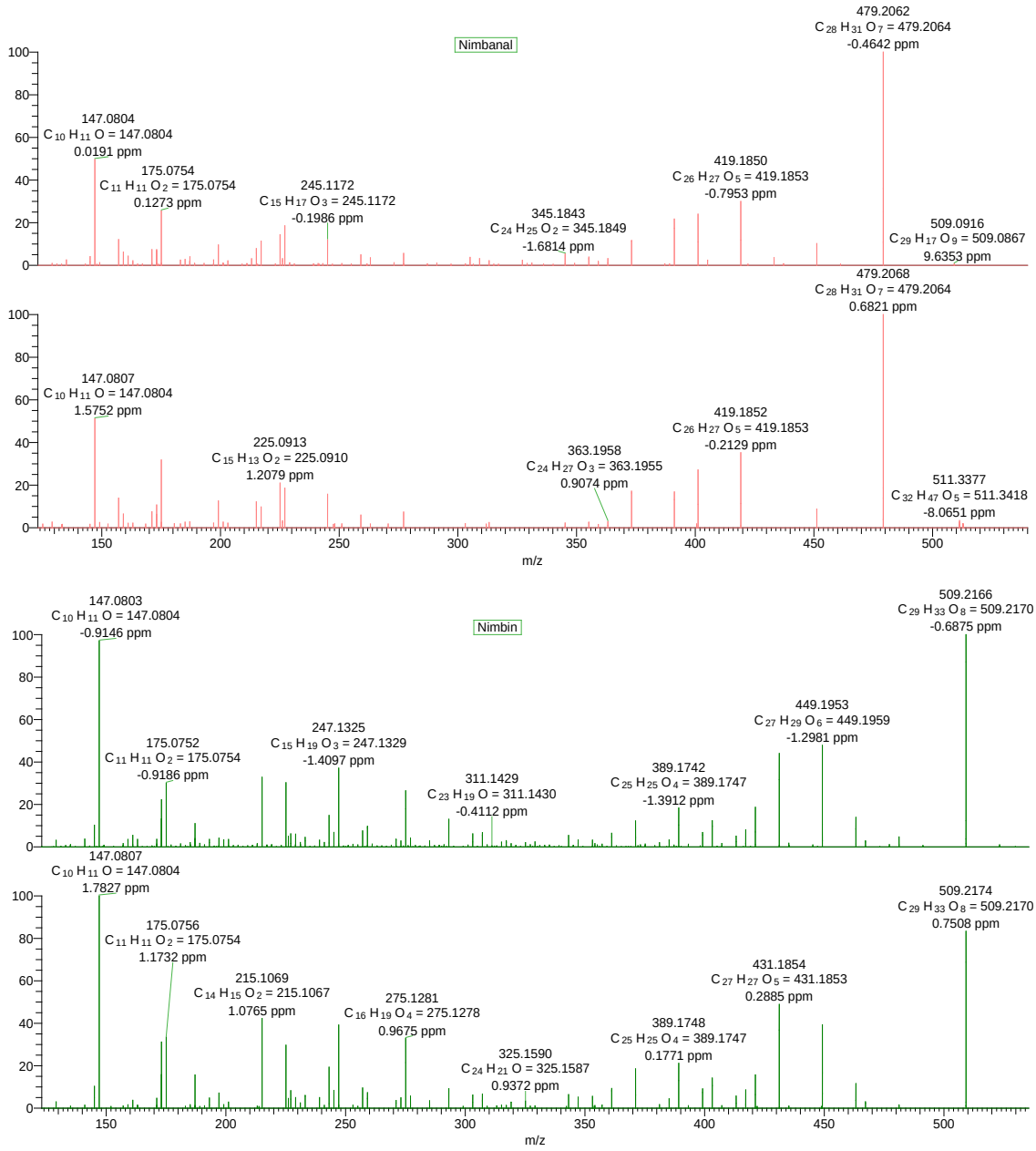
Nimbanal
479.2062
C 28 H 31 O 7 = 479.2064
-0.4642 ppm
147.0804
C 10 H 11 O = 147.0804
0.0191 ppm
175.0754
C 11 H 11 O 2 = 175.0754
0.1273 ppm
245.1172
C 15 H 17 O 3 = 245.1172
-0.1986 ppm
345.1843
C 24 H 25 O 2 = 345.1849
-1.6814 ppm
419.1850
C 26 H 27 O 5 = 419.1853
-0.7953 ppm
509.0916
C 29 H 17 O 9 = 509.0867
9.6353 ppm
479.2068
C 28 H 31 O 7 = 479.2064
0.6821 ppm
147.0807
C 10 H 11 O = 147.0804
1.5752 ppm
225.0913
C 15 H 13 O 2 = 225.0910
1.2079 ppm
363.1958
C 24 H 27 O 3 = 363.1955
0.9074 ppm
419.1852
C 26 H 27 O 5 = 419.1853
-0.2129 ppm
511.3377
C 32 H 47 O 5 = 511.3418
-8.0651 ppm
m/z

Nimbin
147.0803
C 10 H 11 O = 147.0804
-0.9146 ppm
175.0752
C 11 H 11 O 2 = 175.0754
-0.9186 ppm
247.1325
C 15 H 19 O 3 = 247.1329
-1.4097 ppm
311.1429
C 23 H 19 O = 311.1430
-0.4112 ppm
389.1742
C 25 H 25 O 4 = 389.1747
-1.3912 ppm
449.1953
C 27 H 29 O 6 = 449.1959
-1.2981 ppm
509.2166
C 29 H 33 O 8 = 509.2170
-0.6875 ppm
147.0807
C 10 H 11 O = 147.0804
1.7827 ppm
175.0756
C 11 H 11 O 2 = 175.0754
1.1732 ppm
215.1069
C 14 H 15 O 2 = 215.1067
1.0765 ppm
275.1281
C 16 H 19 O 4 = 275.1278
0.9675 ppm
325.1590
C 24 H 21 O = 325.1587
0.9372 ppm
389.1748
C 25 H 25 O 4 = 389.1747
0.1771 ppm
431.1854
C 27 H 27 O 5 = 431.1853
0.2885 ppm
509.2174
C 29 H 33 O 8 = 509.2170
0.7508 ppm
m/z

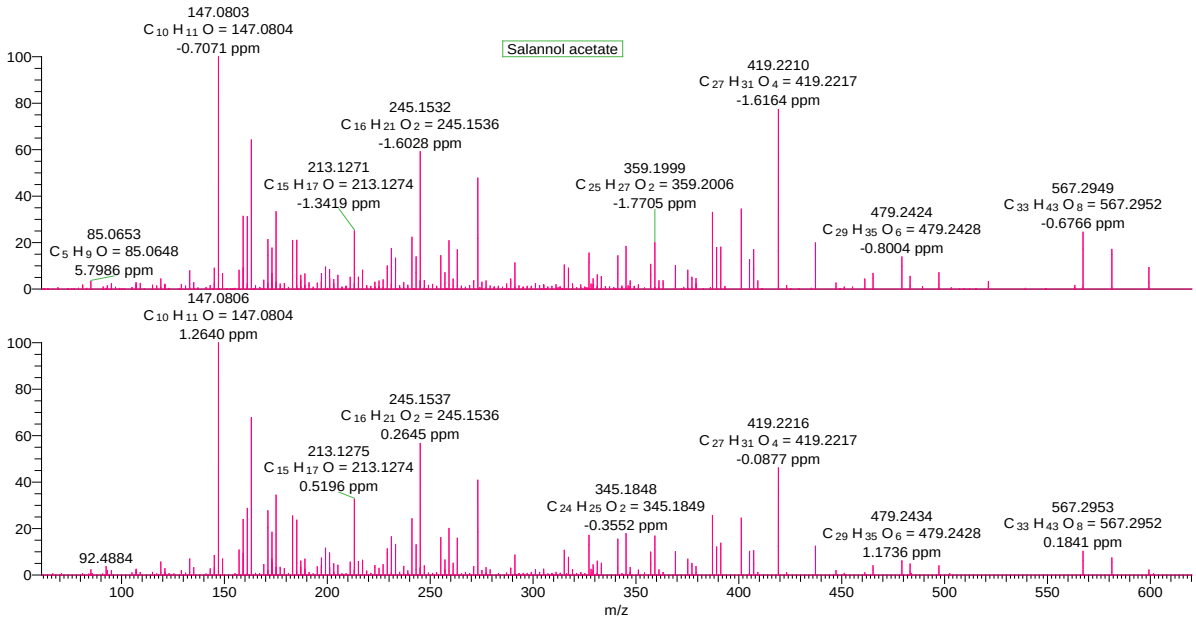
Salannol acetate
147.0803
C10 H11 O = 147.0804
-0.7071 ppm
85.0653
C5 H9 O = 85.0648
5.7986 ppm
213.1271
C15 H17 O = 213.1274
-1.3419 ppm
245.1532
C16 H21 O2 = 245.1536
-1.6028 ppm
359.1999
C25 H27 O2 = 359.2006
-1.7705 ppm
419.2210
C27 H31 O4 = 419.2217
-1.6164 ppm
479.2424
C29 H35 O6 = 479.2428
-0.8004 ppm
567.2949
C33 H43 O8 = 567.2952
-0.6766 ppm
147.0806
C10 H11 O = 147.0804
1.2640 ppm
92.4884
213.1275
C15 H17 O = 213.1274
0.5196 ppm
245.1537
C16 H21 O2 = 245.1536
0.2645 ppm
345.1848
C24 H25 O2 = 345.1849
-0.3552 ppm
419.2216
C27 H31 O4 = 419.2217
-0.0877 ppm
479.2434
C29 H35 O6 = 479.2428
1.1736 ppm
567.2953
C33 H43 O8 = 567.2952
0.1841 ppm
m/z

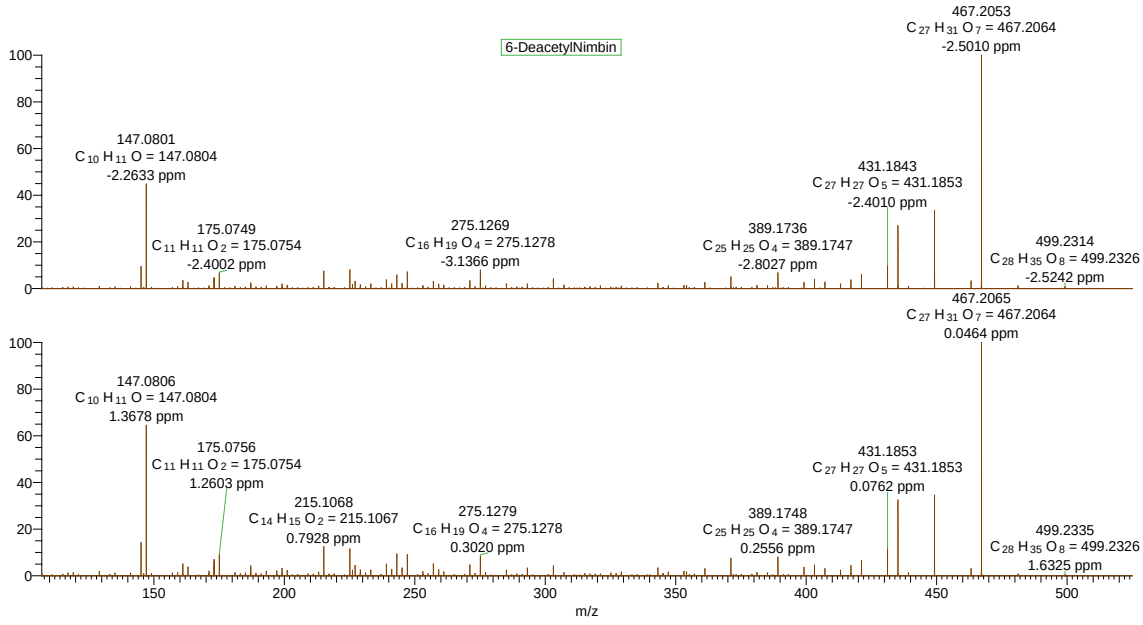
6-DeacetylNimbin
147.0801
C10 H11 O = 147.0804
-2.2633 ppm
175.0749
C11 H11 O2 = 175.0754
-2.4002 ppm
275.1269
C16 H19 O4 = 275.1278
-3.1366 ppm
389.1736
C25 H25 O4 = 389.1747
-2.8027 ppm
431.1843
C27 H27 O5 = 431.1853
-2.4010 ppm
467.2053
C27 H31 O7 = 467.2064
-2.5010 ppm
499.2314
C28 H35 O8 = 499.2326
-2.5242 ppm
147.0806
C10 H11 O = 147.0804
1.3678 ppm
175.0756
C11 H11 O2 = 175.0754
1.2603 ppm
215.1068
C14 H15 O2 = 215.1067
0.7928 ppm
275.1279
C16 H19 O4 = 275.1278
0.3020 ppm
389.1748
C25 H25 O4 = 389.1747
0.2556 ppm
431.1853
C27 H27 O5 = 431.1853
0.0762 ppm
467.2065
C27 H31 O7 = 467.2064
0.0464 ppm
499.2335
C28 H35 O8 = 499.2326
1.6325 ppm
m/z

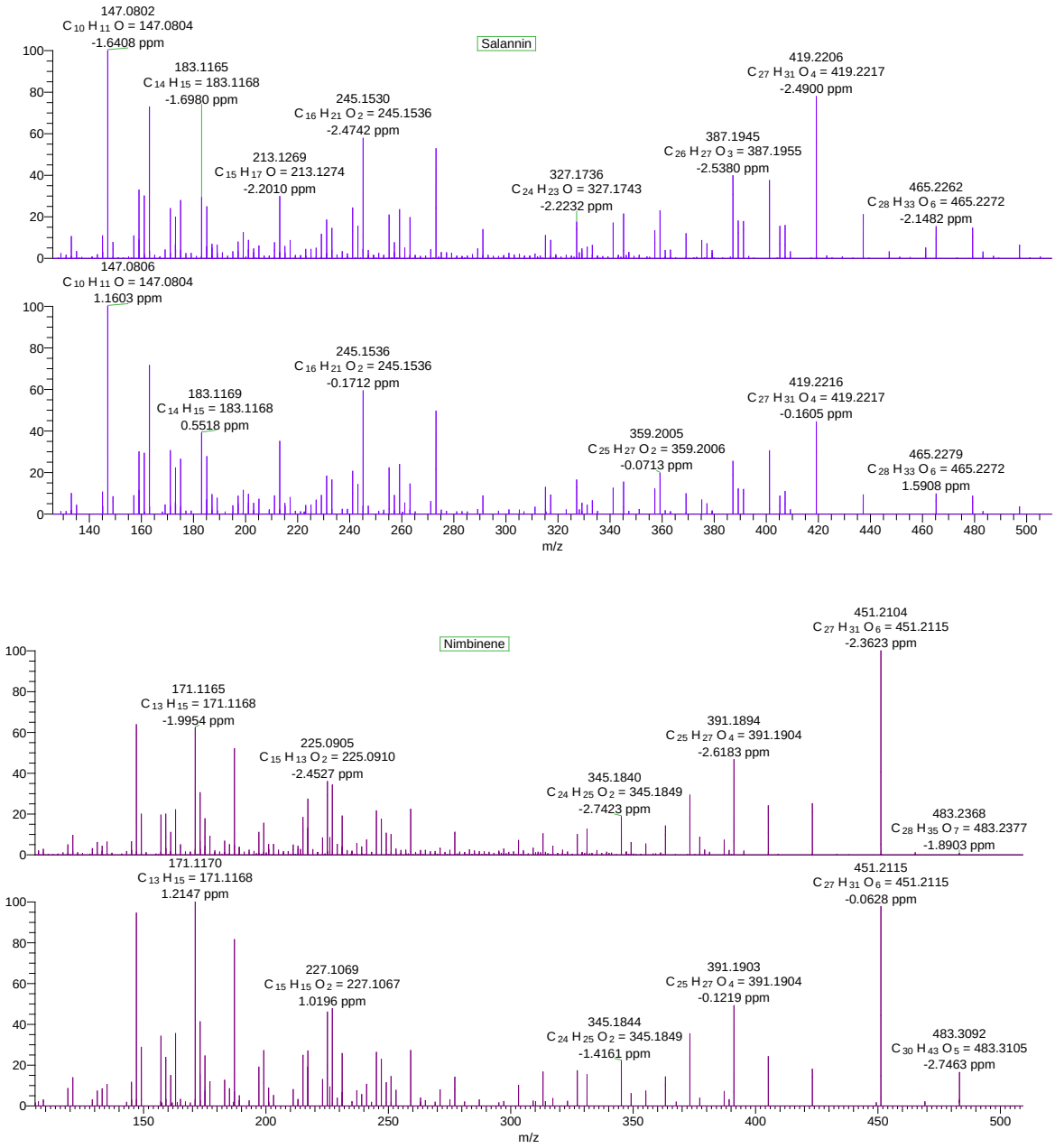

Figure 2A.8. Overlay of MS/MS spectra of 9 limonoids standards (bottom) and the limonoids biosynthesized from cell culture (top).

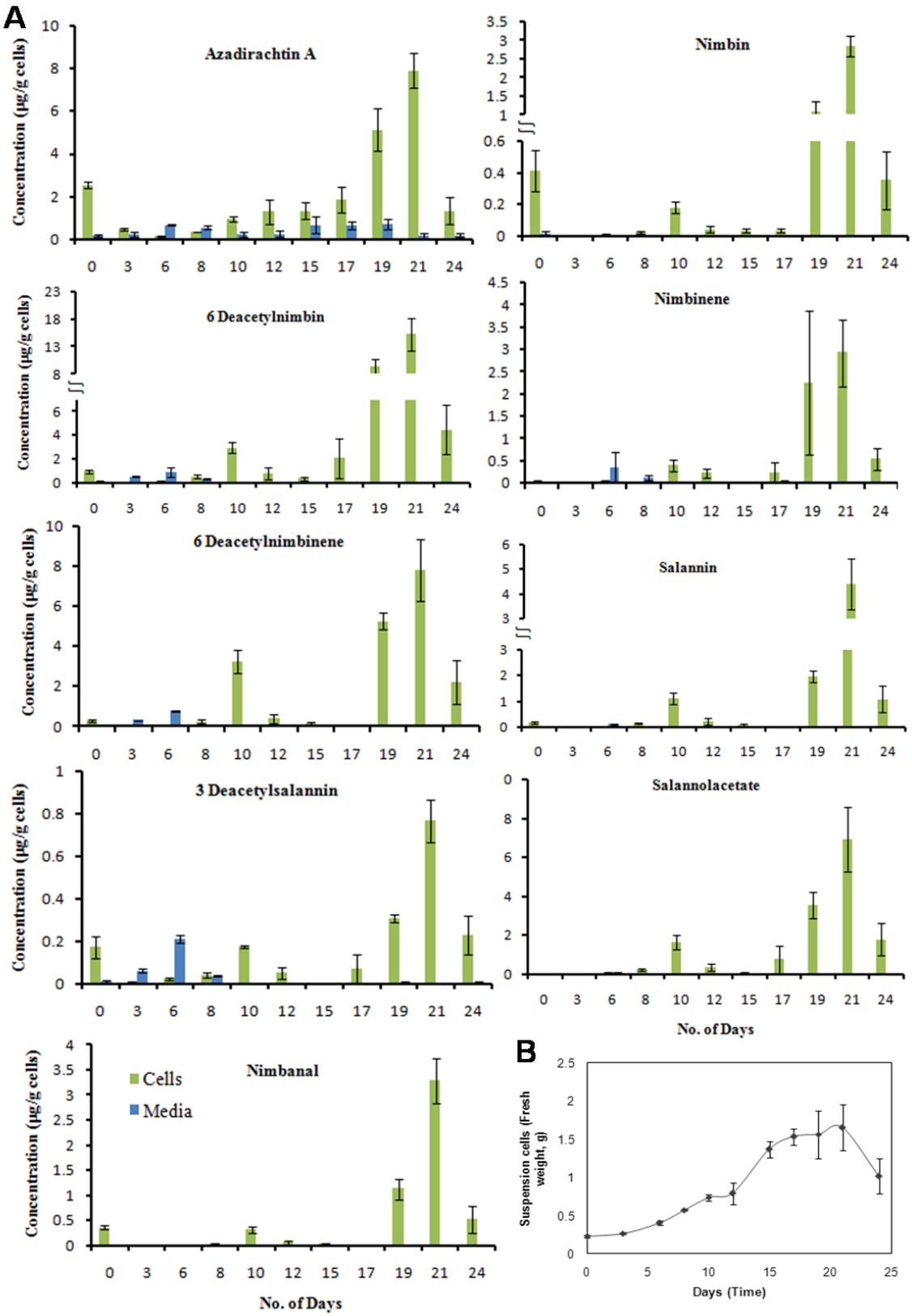

Figure 2A.9. Growth of suspension cells and time course study of limonoid biosynthesis. (A) limonoid content during the course of cellular growth. **(B)** Growth curve obtained with cell suspension.

The azadirachtin production from cell culture developed from different plant parts has been studied, aiming to maximize its productivity[8, 22]. Our study gives insights into specific limonoid profile during growth and development of neem plant. The neem cotyledons inoculated over media has grown into a seedling, the withered cotyledon has lost its limonoid content and limonoids might have been distributed into the growing plant part during its development. This has been hypothesized based on the quantitative comparison of individual limonoid content of the different plant parts and found that azadirachtin A was highest in stem, followed by root and leaf during plant development. Limonoid profiling studies of *in vitro* plant and neem sapling leaves demonstrated the high level occurrence of C-seco limonoids, specifically azadirachtin A in similitude to the pattern of kernel tissue (Figure 2A.7), whereas the leaves of wild grown neem tree were known to contain ring intact limonoid, nimocinol as a major compound[4]. This growth specific differential limonoid profile can be explained in terms of chemical defense theory[33]. The high levels of potent insect deterrent azadirachtin A can protect the young leaf, as soft tissues are more susceptible to herbivory. Whereas azadirachtin A content was less (700 fold less than nimocinol) in mature leaf. Similar observation on defense mechanism has been reported in tea leaves, where caffeine is found to accumulate in young leaves and its biosynthesis has been halted as the leaf ages and get cellulose and lignin deposits for its protection from predators[34].

Our present study indicates that undifferentiated, suspension cells and callus derived from kernel contain C-seco limonoids. C-seco limonoids are continued to be biosynthesized in subsequent subculturing (Figure 2A.8, 2A.9), and on the other hand shows the absence of ring intact limonoids. This follows the trend of limonoid content as that of its parent tissue, the fruit kernel however the occurrence of individual C-seco limonoids varies. Azadirachtin A was found to be the abundant C-seco limonoids in kernel whereas kernel derived cell lines contain 6-deacetylnimbin and 6-deacetylnimbinene in high levels (Figure. 2A.9).

2A.3. Conclusion

Callus and suspension culture were established from neem kernel inoculated in MS media with 2 mg/L NAA and 0.2 mg/L BAP. *in vitro* plantlets were obtained from cotyledons after 30 days of inoculation. Time course study for limonoid biosynthesis

showed that its accumulation was recorded high on the day 21 of the growth phase. 6-deacetylnimbin was the highly biosynthesized limonoid identified in the cell culture. 6-deacetylnimbin, azadirachtin A and salannolacetate are the major limonoids among the 9 limonoids identified in cell suspension. In the *in vitro* plantlets, azadirachtin A, B and salannolacetate were the major limonoids produced.

2A.4. Materials and methods

2A.4.1. Plant materials

For the initiation of cell culture, fruits in third to fourth developmental stages were collected from CSIR-NCL campus. Neem fruits at different developmental stages were collected during the month of April-June.

2A.4.2. Surface sterilization of neem fruits

Hard green neem (*Azadirachta indica*) fruits obtained from NCL campus was surface sterilized by rinsing in deionised water followed by incubation in 1% Bavistin supplemented with few drops of Tween-20 for two hours under shaking. It was then rinsed thrice in deionised water followed by washing in 70% ethanol for 30 sec. Then 1% sodium hypochlorite solution was used for surface sterilization for 7 min. The fruits were then rinsed thoroughly in sterile, deionised water several times.

2A.4.3. Development of callus from neem kernel

For formation of callus, kernels separated from hard seed coat or testa were aseptically transferred and inoculated over MS (Murashige and Skoog) basal media supplemented with 3% sucrose, 2 mg/l NAA and 0.2 mg/l BA at pH 5.8 and solidified with 0.25 % Phytagel^{TM} in 66 mm × 59 mm magenta culture vessel. It was then incubated under the conditions of 600 lumens of light during 12 hours day/night cycle at 25 °C.

2A.4.4. Generation of cell suspension from callus

Azadirachta indica suspension cell cultures were initiated from cultured callus and maintained in liquid MS (Murashige and Skoog) basal media of same composition mentioned earlier and grown with rotatory gyration at 125 rpm at 25 °C in dark.

2A.4.5. Growth conditions for neem plantlets

Hard green neem (*Azadirachta indica)* fruits were surface sterilized and the cotyledons (kernel) were obtained from the fruit as mentioned earlier. The cotyledons were inoculated over MS (Murashige and Skoog) basal media with 0.25% Phytagel™ (Sigma) and incubated at 25 °C in a growth chamber (Percival Scientific) with a cycle of 16-h light/8-h darkness.

2A.4.6. Harvesting cells and Extraction of limonoids

The suspension culture cells were collected from media by centrifugation at 2500 × *g* for 10 min at 25 °C. The cells were homogenized in ice-cold methanol. The supernatant was collected after centrifugation at 2500 × *g* for 10 min at 25 °C. The cells were again resuspended in twice the volume of methanol and extracted twice again. The methanol extract was pooled together and evaporated to dryness. The residue was partitioned between water and ethylacetate thrice. The ethylacetate pool was then evaporated to dryness under reduced pressure and constituted with LC-MS grade methanol to the volume of 1 mL. To quantify limonoids in the media, it was partitioned with ethylacetate and extracted, as mentioned above.

2A.4.7. Limonoid profiling in callus and cell culture

Targeted metabolic profiling of callus at different subculturing stage of callus and cell suspension was carried out with LC-ESI-MS as described below by comparison with the 19 limonoid standards isolated and characterized from neem fruit and oil[35, 36]. The identified limonoids were subjected to tandem MS to confirm their identity based on the presence or absence of the signature fragments as established in our previous study[35, 36].

2A.4.8. LC-ESI-Mass Spectrometry conditions

Analysis of neem limonoids was performed with Thermo Scientific QExactive™ hybrid quadrupole-Orbitrap mass spectrometer associated with Accela 1250 pump and Accela open AS. The conditions of HESI source include capillary temperature of 320 °C, Heater temperature at 350 °C, s-lens RF level of 50, Spray voltage of 3.6 kV, spray current of 0.9 μA with sheath gas flow rate of 41, Auxiliary gas flow rate of 9 and sweep

gas flow rate of 3. Standards, as well as the extracted samples, were analyzed in positive ionization mode, in full MS-scan with scan range of 100 to 1000 *m/z*. Following were the properties of the scan performed- resolution 70,000, AGC target 1e6, Maximum IT 200 ms. Waters Acquity UPLC BEH C_{18} column (particle size 1.7 μm, 2.1 X 100 mm) was used as the stationary phase while the solvent system of methanol and water containing 0.1% formic acid served as the mobile phase. The gradient started with 40% methanol (5 min isocratic), it was then increased to 50% (5 min isocratic), followed by 60% methanol for the next 15 minutes and over the next 4 minutes it was isocratic with 65% methanol. It was then increased to 90% methanol for 4 minutes. For the last 2 minutes, it was isocratic with 40% methanol. Constant flow rate of 0.3 mL min^{-1} was maintained throughout the run time of 35 min. The chromatograms and mass spectral data were processed by Xcalibur qual browser (version 2.3; Thermo Scientific).

2A.4.9. Time course of cellular growth and limonoid formation

0.2 g of callus tissue was inoculated in liquid MS to generate suspension and the cells were harvested at 12 different time points. Fresh weight of cells at different time points were estimated and limonoids were extracted from cell mass at each time point. Based on the calibration curve of authentic standards, 9 limonoids were quantified by considering the peak area of extracted ion chromatogram (EIC) corresponding to the combined protonated and sodiated molecular ions[4]. From the *in vitro* plantlets, leaf, stem, root and withered cotyledon were collected and quantification of limonoids was performed as mentioned above.

Chapter 2: Section B

Study of localization of neem metabolites in different tissues

2B.1. Introduction

In the process of co-evolutionary arms race between plants and the biotic or abiotic environment it interacts, each plant species have carved a niche for itself by evolving specialized metabolism due to its specific ecological challenge and is therefore unique to each plant species and is not shared by other plant family[37]. Myriads of plant specialized metabolites in aggregate has evolved in plants as an arsenal of defense because of adaptive selection of the new response of other organisms results in further selection in plants for higher fitness. These evolution occurs not only with the synthesis of new metabolite but also with the specialized cell types specifically enriched with specialized molecular machinery for the synthesis, transportation and storage of these metabolites [38].

Anatomical clues in plants that have sequestered lots of active compounds are

- Glandular trichomes,
- Laticifers and idioblasts
- Secretory cavities
- Resin canals
- Floral & extrafloral nectaries.

Plants are capable of producing remarkable variety of metabolites in terms of chemical complexity and diversity that shows differential spatial distribution in tissues[39, 40]. For immense biosynthesis of specialized metabolites and their sequestration, plants have evolved specialized anatomical appendages and cell types such as trichomes, idioblast cells, laticifers, resin cells, secretory cells, gland or cavities[41-43]. These structures help plants for the efficient utilization of secondary metabolites for defense or pollinator attraction and also to protect the adverse and detrimental effect for the producing plant[44-51]. Site of synthesis and localization of a different class of secondary metabolites in plants varies and shows a higher extent of compartmentation. Glandular trichomes have been known remarkably for the synthesis of a different class of terpenes, essential oils and other secondary metabolites in plants[42,52-54]. For example, sesquiterpene lactones uvedalin and enhydrin have been found to be localized into glandular trichomes in leaf[55]. Essential oils in Eucalyptus are stored in sub-dermal secretary cavities[56]. Similiarly, secretory cells present in the trichomes of peppermint were found to synthesis and store monoterpenes[57]. This metabolite production capacity

of trichomes is not only attributed to high expression level of the pathway genes but also due to the photosynthetic efficiency for generating energy, carbon and reducing power etc which acts as substrate and cofactors for enzymes respectively.[58]. The intracellular site of synthesis, translocation, localization of terpene indole alkaloids and tropane alkaloids in *Catharanthus* and opium poppy respectively in different cell types such as laticifers and idioblasts has been significantly revealed[59-64].

Apart from the specialized cells, vacuoles and vesicles are important intracellular organelles, which are known to accumulate secondary metabolites thereby aiding in prevention of self-toxicity for the host cells[65]. Synthesis of a complex secondary metabolite requires multiple organelles such as chloroplast, cytosol, endoplasmic reticulum, vesicles, vacuoles and nucleus. In addition to the specific localization of alkaloids in vacuoles of *Catharanthus*[66], alkaloids are also found to exist as a complex with tannins showing vacuolar compartmentation[67]. Another notable intracellular compartment existing in plants is oil body, found predominantly in seed but it also occur in other parts[41]. Oil body also called as oleosomes, is a sphere of triacylglycerol bounded by a phospholipids monolayer with basic proteins oleosins embedded in it, conferring stability[41, 68, 69]. It serves as food reserves for germination and post-germinative growth of the seedlings by resisting the physical stresses caused during germination and desiccation [41]. Oil bodies of few plants and liverworts are also found to biosynthesize and accumulate terpenoids as evidenced from the localization of enzymes and metabolites in it[70-72]. The secretory structures are considered as natural cell factories and are becoming important targets for metabolic engineering[73].

For example, the study of *Catharanthus roseus* terpene indole alkaloid biosynthesis showed that five intracellular compartments such as chloroplast, vacuole, nucleus, endoplasmic reticulum and cytosol, four different cell types such as epidermis, internal phloem-associated parenchyma, laticifers and idioblasts are involved at various steps. Such studies have also implicated many issues namely, localization and expression of pathway enzymes, mechanisms of intra- and intercellular trafficking of intermediates, cloning and functional characterization of genes coding for pathway enzymes, mechanism of regulation of pathway by transcription factors, control of relative diversion of metabolite flux at crucial branch points and ultimately, improving metabolic engineering approaches[43,57, 74, 75]. Thus, these sub-cellular compartments serve

as an efficient storage site for the biosynthesis and storage of secondary metabolite which helps in defense of the plants from various biotic and abiotic factors.

In our laboratory, we have identified previously, the tissue and developmental stages specific differential distribution and abundance of ring intact (basic) and C-seco limonoids in different neem tissues[4]. This incredible and impressive abundance of limonoids in fruit and leaf tissues actuated us to look for the specialized cells involved in accumulating limonoids and other metabolites. Numerous resin glands on the surface of neem leaves, secreting resin, accumulates flavonoids, and have been identified already[76, 77]. Here, in our present investigation, we discuss about the cellular and sub-cellular structures involved in the storage of limonoids, flavonoids, sesquiterpenes and hydrocarbons in neem.

Purpose of the present study is to provide new elements on morphology, localization of limonoids and other metabolites in each of the specialized structures and also to elucidate the role of them in interaction with biotic factors such as insects. As a first step to determine the structures involved in the biosynthesis and storage of limonoids, we studied the histology and histochemistry of fruit, leaf and flower. Idioblasts, the specialized cells involved in localization of secondary metabolites were evident from its natural pigmentation. Further, the lipophilic components of the cells were unveiled through histochemical analysis. Moreover, the protoplast, cell homogenate and organelle purifications were carried out followed by targeted and untargeted metabolic profiling of the isolated cells and organelles using HRMS as a strategy to elucidate the localization of limonoids and other metabolites in their respective cells and intracellular compartments. Thus the presence of morphological elements such as trichomes, laticifers, pollen, idioblasts, vacuoles, vesicles, oil bodies, cytoplasmic droplets meant for different functions were deciphered through our study. Furthermore, the herbivory deterrence of the latex has been confirmed based on the studies on insect, *Helicoverpa armigera*. Though the anti-feedant, insect growth regulatory, anti-insecticidal properties of several limonoids have been investigated through several studies[78-85], and on different insects, the effect of neem fruit latex, the cytosol of laticifer cells have not been examined so far. Hence, effect of neem latex on insect feeding and survival is examined through this study.

2B.2. Results and discussion

2B.2.1. Identification of limonoids in neem fruit latex

One of the distinctive ways of defense for plants against predators is mediated through endogenous fluid, latex stored in the highly specialized laticifer cells, which is known to harbor bioactive secondary metabolites[86] and has been found to be present in plant parts such as stem, fruits, leaves etc. in different plant system[86]. Neem is very well known for its effective and diverse biological activities. Despite the wide knowledge on the chemistry and medicinal property of neem, localization of these medicinally active metabolites in specialized cells and structures of the plant has not been examined heretofore. Although, several biologically active limonoids have been isolated from various neem tissues, no information is available on the limonoid content of milky latex of neem fruit. In order to identify the limonoid content of neem latex, the crude extract was subjected to Thin Layer Chromatography (TLC) analysis (Figure 2B.1). Neem limonoids such as azadiradione, epoxyazadiradione, azadirone and other triterpenes such as α–amyrin, β–amyrin, lupeol and Euphorbia *tirucalli* isolates tirucallol and euphol were used as standards. From the TLC analysis, azadiradione, epoxyazadiradione and azadirone were found to be the major limonoids. UPLC-ESI (+)-MS/MS characterization was further done to identify the limonoids present in trace amounts (as mentioned in materials and methods)[4]. Analysis of total ion chromatogram (TIC) and mass spectra indicated the presence of over thirty limonoids (Appendix Figure 2B.1, Table 2B.1). Seventeen of them were identified based on the comparison of retention time and *m/z* value respectively, with that of authentic standards isolated and characterized from neem[35, 36] (Table 2B.1). The limonoids were then confirmed for its identity by subjecting it to MS/MS of different normalized collision energies (NCEs) and *m/z* values of signature fragments engendered were matched with already available *m/z* signatures generated from authentic limonoid standards[35, 36]. For the identification of limonoids for which standard was not available, elemental composition was generated in Xcalibur qual browser for the individual *m/z* values and molecular formula was assigned putatively. These limonoids were further confirmed by comparing signature MS/MS fragments obtained at standardized NCE of 20% and 25% for C-seco limonoids and ring intact limonoids, respectively (Appendix Figure 2B.1, Table 2B.1). Further, relative abundance of individual limonoids in latex was calculated (Figure 2B.3) based on the

peak area obtained from the extracted ion chromatogram generated from the *m/z* for the corresponding limonoids. Absolute quantification was carried out for the fifteen limonoids with authentic standards based on the standard curve drawn for each of them by considering both protonated molecule as well as sodium adduct ions[4] (Table 2B.1). The basic limonoid, azadiradione was found to be the major constituent in the latex, followed by epoxyazadiradone and gedunin whereas complex, highly modified C-seco limonoids such as nimbin, salannin, azadirachtin and its derivatives were identified in traces (Figure 2B.3, Table 2B.1). The concentration of azadiradione and epoxyazadiradione present in the latex was found to be 3.2 and 2.4 mg mL^{-1}, respectively. Thus, limonoid profile of latex suggests that ring intact (basic) limonoids such as azadiradione and epoxyazadiradione represents the metabolic fingerprint of neem fruit laticifer cells. Neem latex profile reveals high abundance of ring intact limonoids, azadiradione and epoxyazadiradione, which underpins our hypothesis that it, is one of the intermediate in limonoid biosynthetic pathway. The early step intermediate, azadiradione accumulates in higher amount and azadirachtin, a complex, final step limonoid is being present in trace amount in the latex obtained from neem fruit stage 3. This is in contrast to the composition of latex from laticifer of poppy (*Papaver somniferum*) and *Catharanthus roseus* that were found to accumulate the final step metabolite and late step intermediate, morphine[63] and demetoxyvindoline respectively, the products of alkaloid biosynthetic pathway in latex[62, 86].

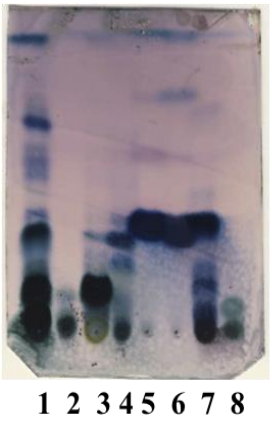

1. Neem latex extract
2. Azadiradione
3. Epoxyazadiradione
4. Azadirone
5. Lupeol
6. α +β amyrin
7. Tirucalli extract
8. Neem latex extract

Figure 2B.1. TLC profile of neem latex limonoid

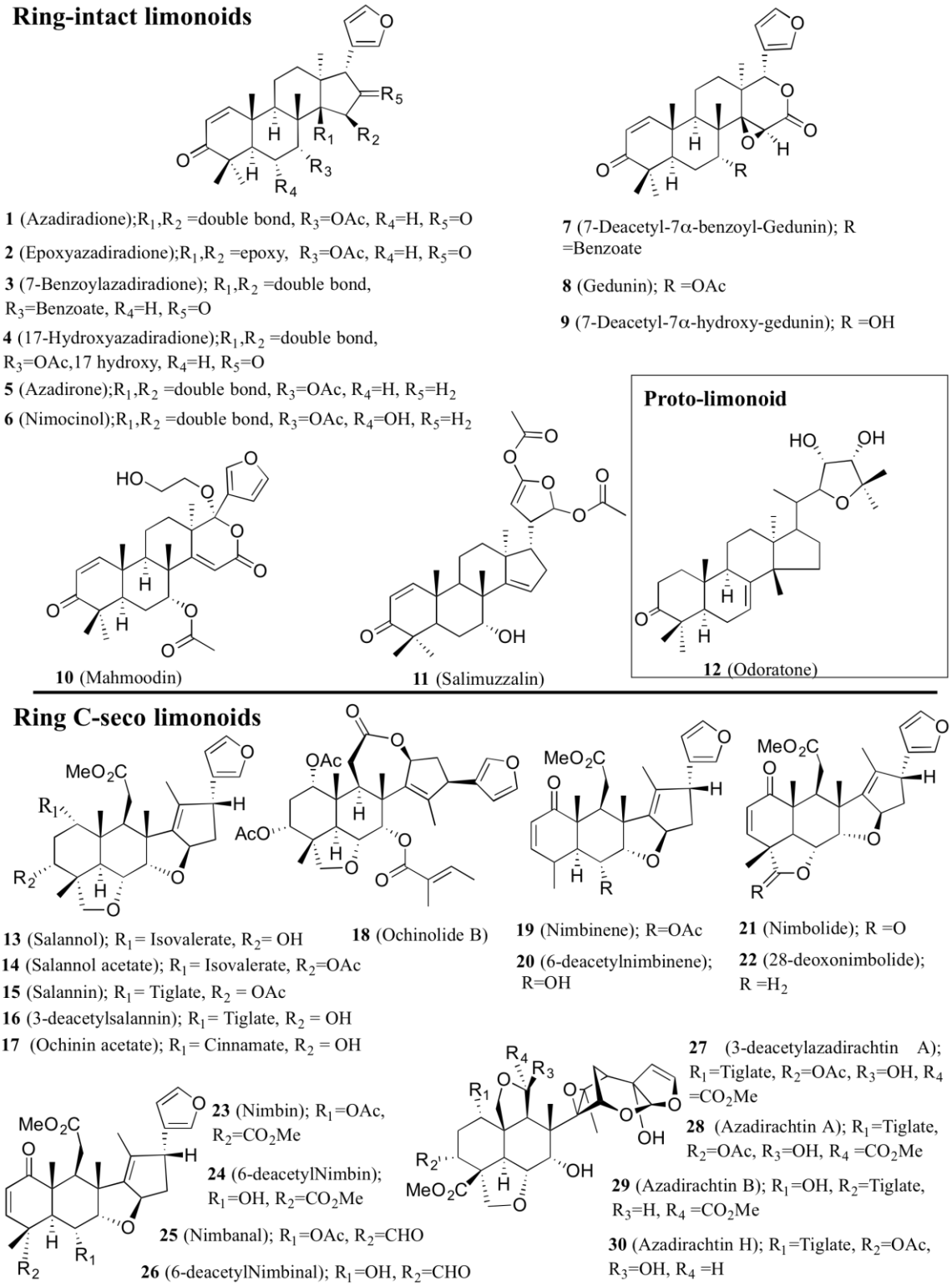

Figure 2B.2. Skeletal diversity of neem limonoids. Chemical structures of limonoids identified in latex, classified according to ring modification, as ring intact and ring C- seco limonoids.

S.No.	Limonoids	R_t (min)	Concentration (mg/mL)	Extracted ions (*m/z*)		Formula	Molecular Ion (*m/z*)	NCE %
1.	Azadirachtin A	7.4	0.0070	703	743	$C_{35}H_{44}O_{16}$	$[M+H-H_2O]^+$, $[M+Na]^+$	20
2.	Azadirachtin B	8.6	0.0050	645	685	$C_{33}H_{42}O_{14}$	$[M+H-H_2O]^+$, $[M+Na]^+$	20
3.	6-deacetylnimbin	14.7	0.3370	499	521	$C_{28}H_{34}O_8$	$[M+H]^+$, $[M+Na]^+$	20
4.	Azadiradione	16.3	3.2300	451	473	$C_{28}H_{34}O_5$	$[M+H]^+$, $[M+Na]^+$	25
5.	6-deacetylnimbinene	16.5	0.1610	441	463	$C_{26}H_{32}O_6$	$[M+H]^+$, $[M+Na]^+$	20
6.	Nimbanal	17.8	0.5290	511	533	$C_{29}H_{34}O_8$	$[M+H]^+$, $[M+Na]^+$	20
7.	Nimbin	18.0	0.5280	541	563	$C_{30}H_{36}O_9$	$[M+H]^+$, $[M+Na]^+$	20
8.	3-deacetylsalannin	18.5	0.0677	555	577	$C_{32}H_{42}O_8$	$[M+H]^+$, $[M+Na]^+$	20
9.	Gedunin	20.4	0.5650	483	505	$C_{28}H_{34}O_7$	$[M+H]^+$, $[M+Na]^+$	25
10.	Nimbinene	20.7	0.0340	483	505	$C_{28}H_{34}O_7$	$[M+H]^+$, $[M+Na]^+$	20
11.	Salannin	21.3	0.0222	597	619	$C_{34}H_{44}O_9$	$[M+H]^+$, $[M+Na]^+$	20
12.	Epoxyazadiradione	27.4	2.4800	467	489	$C_{28}H_{34}O_6$	$[M+H]^+$, $[M+Na]^+$	25
13.	Salannolacetate	28.4	0.0145	599	621	$C_{34}H_{46}O_9$	$[M+H]^+$, $[M+Na]^+$	20
14.	Nimocinol	29.9	0.0414	453	475	$C_{28}H_{36}O_5$	$[M+H]^+$, $[M+Na]^+$	25
15.	Azadirone	31.7	0.119	437	459	$C_{28}H_{36}O_4$	$[M+H]^+$, $[M+Na]^+$	25
16.	Azadirachtin H	3.57	-	645	685	$C_{33}H_{43}O_{14}$	$[M+H-H_2O]^+$, $[M+Na]^+$	20
17.	Mahmoodin	10.03	-	527	549	$C_{30}H_{38}O_8$	$[M+H]^+$, $[M+Na]^+$	20
18.	6-deacetylnimbinal	12.93	-	469	491	$C_{27}H_{32}O_7$	$[M+H]^+$, $[M+Na]^+$	20
19.	Ochinolide B	13.37	-	625	647	$C_{35}H_{44}O_{10}$	$[M+H]^+$, $[M+Na]^+$	20
20.	28-deoxonimbolide	14.44	-	453	475	$C_{27}H_{32}O_6$	$[M+H]^+$, $[M+Na]^+$	20
21.	7-deacetyl-7α-hydroxygedunin	19.59	-	441	463	$C_{26}H_{32}O_6$	$[M+H]^+$, $[M+Na]^+$	25
22.	7-deacetyl-7α-benzoylgedunin	27.12	-	545	567	$C_{33}H_{36}O_7$	$[M+H]^+$, $[M+Na]^+$	20
23.	Salannol	24.64	-	557	579	$C_{32}H_{44}O_8$	$[M+H]^+$, $[M+Na]^+$	20

24.	Odoratone	30.68	-	473	495	$C_{30}H_{48}O_4$	$[M+H]^+$, $[M+Na]^+$	25
25.	Ochininacetate	22.22	-	603	625	$C_{36}H_{42}O_8$	$[M+H]^+$, $[M+Na]^+$	20
26.	7-benzoylazadiradione	24.7	-	513	535	$C_{33}H_{36}O_5$	$[M+H]^+$, $[M+Na]^+$	25
27.	Hydroxyazadiradione	12.49	-	467	489	$C_{28}H_{34}O_6$	$[M+H]^+$, $[M+Na]^+$	25
28.	Nimbolide	12.14	-	467	489	$C_{27}H_{30}O_7$	$[M+H]^+$, $[M+Na]^+$	20
29.	3-deacetylazadirachtin A	4.9	-	661	701	$C_{33}H_{42}O_{15}$	$[M+H-H_2O]^+$, $[M+Na]^+$	20
30.	Salimuzzalin	28.9	-	513	535	$C_{30}H_{40}O_7$	$[M+H]^+$, $[M+Na]^+$	25

Table 2B.1. Limonoids identified in the neem latex based on the comparison of retention time with the standards and also from the presence of signature fragments unique for the specific class of limonoids obtained from tandem MS analysis ('-' denotes that absolute quantification has not been carried out).

2B.2.2. Ultrastructure and histochemistry of latex

Since, latex was found to be a rich source of limonoids, we were curious to look for its morphology and ultrastructure. Preliminary investigation of the latex under light microscope showed the presence of abundant spherical vesicles (Figure 2B.3B, 2B.3D). The vesicular nature of the spherical bodies was further confirmed using environmental Scanning Electron Microscopy (eSEM) and size of them were 6 - 15 μm in diameter having smooth surface morphology (Figure 2B.3C). It also manifested the presence of particles, named as type I and II for easier understanding. Type I particles ranged from 1 - 3 μm diameter and type II particles were abundant in number and are less than 1 μm in size (Figure 2B.3C, 2B.3G). To further identify the nature of vesicles, histochemical analysis was performed in which we stained the diluted latex with different dyes. The optical light microscopic examination of cytoplasmic vesicles treated with the dye, Oil Red O stained them red showing their lipophilic nature (Figure 2B.3E), which was further confirmed, more specifically, by confocal microscopy of the vesicles stained with Nile Red. The Nile Red stained vesicles, fluoresce magenta at 648 to 698 nm emission (Figure 2B.3F), indicating the presence of polar lipids in the vesicle membrane but not the neutral lipids as it seldom generated green fluorescence at 525 to 567 nm

emission collected. However, chemical composition of them is still undiscovered as separation of these components is challenging.

The multitude of cytoplasmic vesicles present in the neem fruit latex are relatively largest when compared to the ones identified so far in the latex of other plant systems such as *C. roseus*[87] and opium poppy[88]. Role of these cytoplasmic vesicles towards limonoid biosynthesis has not yet been elucidated and needs to be studied further. Apart from these vesicles, the most prominent component of the latex is the particles, which in para rubber tree (*Hevea brasiliensis*) and *Euphorbia* species latex were found to play essential role in accompanying the secondary metabolites[89, 90].

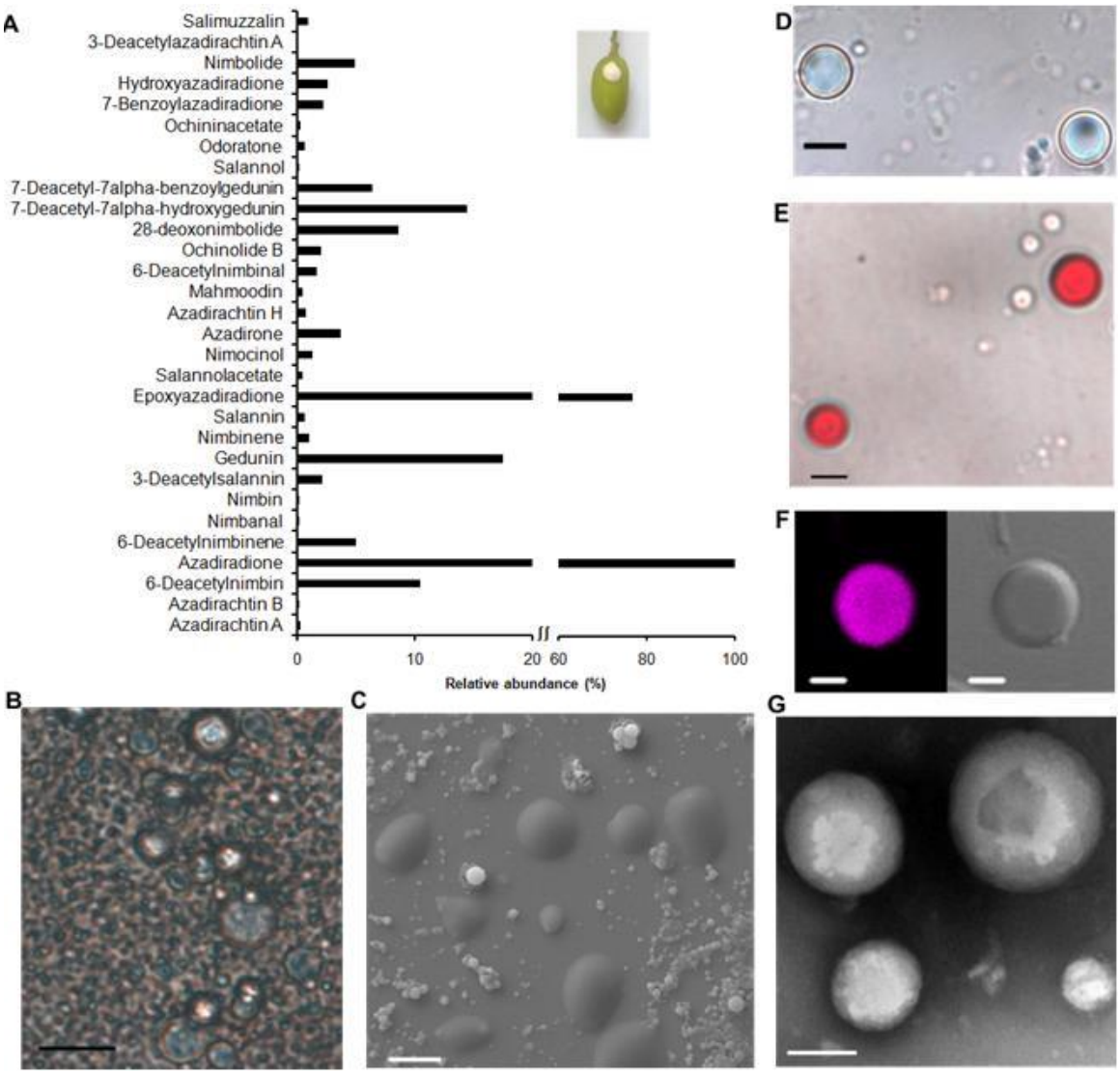

Figure 2B.3. Bright field, fluorescence micrograph of cytoplasmic vesicles and ultrastructure of components present in neem fruit latex. (A) Relative distribution of neem

limonoids obtained from fruit latex. **(B)** undiluted latex, Bar = 10 μm. **(C)** eSEM image in 3500 X magnification showing cytoplasmic vesicles and other particles present in diluted latex, Bar = 10 μm. **(D)** 250 X diluted latex, Bar = 5 μm. **(E)** diluted latex stained with the dye Oil Red O, Bar = 5 μm. **(F)** confocal microscopy image of Nile Red stained latex vesicle, Bar = 2 μm. **(G)** transmission electron micrograph of diluted latex showing type II particle , Bar = 0.2 μm

2B.2.3. The cellular and sub-cellular compartmentation of limonoids in fruit pericarp

The specialized cells also called idioblasts, involved in the sequestration of limonoids remain rarely investigated in neem[91]. To understand about the structure and organization of specialized cells in the fruit pericarp, we examined the sections of fruit, generated using vibratome by light microscopy. The transverse section of the third developmental stage fruit gave rise to sections of small kernel surrounded by pericarp (Kernel at the centre has been separated, Figure 2B.4A). The optical light microscopic examination of pericarp revealed the presence of laticifer cells, the site of localization of white latex in the fruit (Figure 2B.4B and 2B.4A). The length of the laticifer cells was found along the longitudinal axis of pericarp. Epicarp of the fruit was deprived of laticifers and they were intense in the mesocarp and endocarp regions (Figure 2B.4A). In addition to laticifers, the longitudinal (Figure 2B.4G) section of pericarp (Figure 2B.4B, 2B.4D and 2B.4E), showed the presence of idioblast cells, which were naturally colored, dark reddish brown in hue and were concentrated near the laticifer cells. It varied in size from 20 - 70 μm in diameter. Fused tricarpels of the fruit, as evidenced from the cross section of third developmental stage of fruit (Figure 2B.4A) also showed the presence of idioblast cells (Figure 2B.4D and 2B.4E).

Further, to study the limonoid profile of pericarp cells devoid of latex, of pericarp tissue was treated with cell wall digestive enzymes, which yielded dissociated cells (Figure 2B.4C). These cells exhibited the presence of prominent vacuoles. Limonoid profiling of this dissociated pericarp cells showed that azadiradione and epoxyazadiradione are the major constituents, in this tissue (Figure 2B.4I). Abundant idioblast vacuoles from the pericarp tissue of the fruit were obtained which was characterized for its morphology using light microscopy (Figure 2B.4F). The pericarp idioblast vacuoles characterized by eSEM showed hemispherical morphology, ranging from 3 - 7 μm diameter (Figure 2B.4J). Azadiradione and epoxyazadiradione obtained

from the idioblast vacuoles were found to be 5.8 and 2.5 mg/g of tissue, respectively. Remarkably, limonoid levels of the pericarp idioblast vacuoles along with the amount from latex were in agreement with the limonoid content of the pericarp tissue (Figure 2B.4H). The individual limonoid profile of latex, and pericarp cells showed a limonoid distribution pattern that is paradigm of the pericarp limonoid profile[4] and from this study, we could infer that azadiradione and epoxyazadiradione present in fruit are the most abundant limonoids in the neem tree.

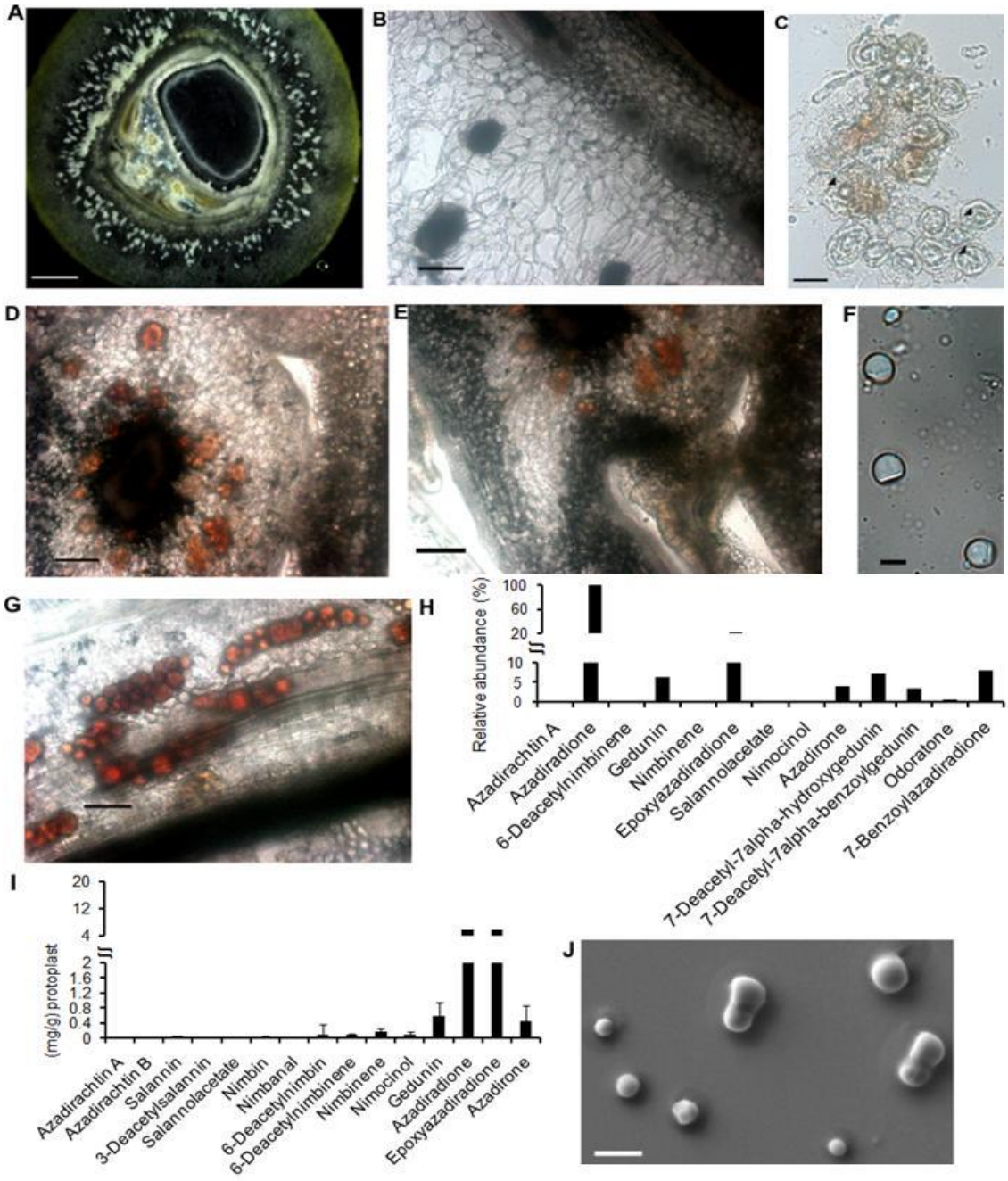

Figure 2B.4. Distribution of idioblast cells and laticifers in fruit pericarp. (A) tissue section of 30 μm thickness of young fruit, Bar = 1 mm **(B)** transverse section of pericarp focusing endocarp, Bar = 100 μm. **(C)** dissociated pericarp cells, arrows pointing to the vacuoles Bar = 20 μm. **(D)(E)** transverse section of pericarp showing one of the carpel of tricarpellate gynoecium, Bar= 100 μm. **(F)** micrograph of idioblast vacuoles isolated from pericarp, Bar = 5 μm. **(G)** longitudinal section of pericarp, Bar = 100 μm. **(H)** limonoid profile of vacuoles **(I)** limonoid profile of pericarp cells devoid of latex. **(J)** electron micrograph of idioblast vacuoles of pericarp, Bar = 10 μm.

2B.2.4. The evidence for intracellular localization of limonoids in kernel

In order to identify the compartmentation existing for localization of limonoids in kernel, histochemical studies of kernel was carried out. The kernel section (30 micron thickness obtained) was stained with toluidine blue evidenced the presence of idioblasts cells in the kernel section as idioblasts took magenta coloration, differentiating them from the other cells (Figure 2B.5E). Nile red stained kernel section showed the presence of oil bodies of variable size range present in the different cells (Figure 2B.5I). Light microscopic examination of the epidermal region of kernel section demonstrated the presence of single prominent oil body in each cell, which ranged in size from 3 - 15 μm (Stained with Nile Red dye for discrimination, Figure 2B.5A). Epi-fluorescent microscopic observation showed red and green fluorescence from the oil bodies present in epidermis (Figure 2B.5K).

In order to understand the limonoid content of different cell types, protoplast preparation from different tissues were carried out. Kernel protoplast generated two types of population, the larger size ones (population I) being more than 100 μm in diameter harboring numerous oil bodies found as floating layer (Figure 2B.5B) and the smaller size protoplast (population II) pelleted at the bottom, less than or equal to 50 μm diameter, with the oil bodies being present in it (Figure 2B.5D). However, size of the protoplasts formed was found to be larger in the kernel of the fully matured fruit (Figure 2B.5C). The floating protoplast population was exhibiting green pigmentation whereas the pelleted population was of white coloration. The protoplast population I is enriched with high level of azadirachtin A and other limonoids being present in a meager amount, whereas population II demonstrated a modest amount of limonoids when compared to population I (Figure 2B.5F).

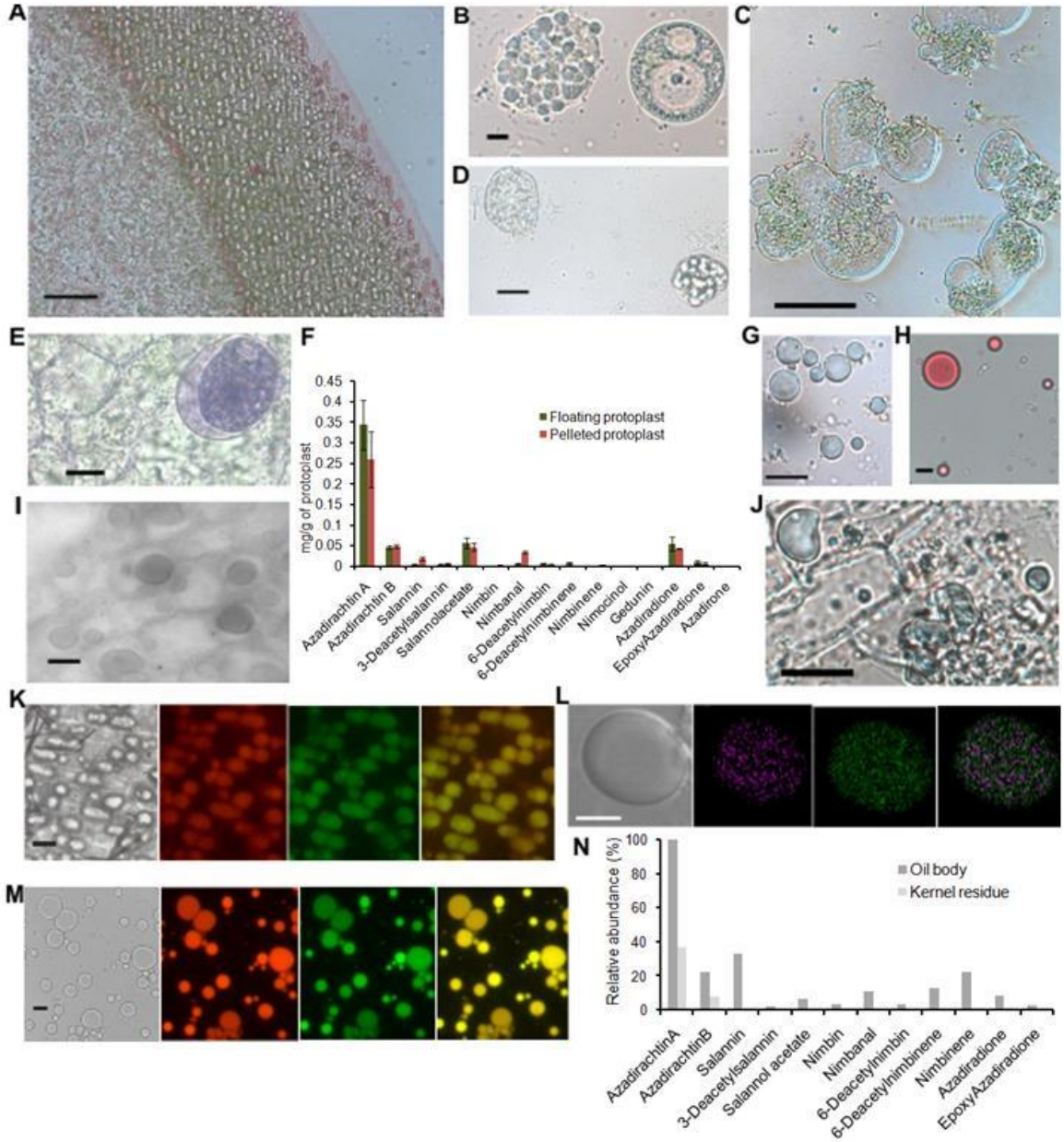

Figure 2B.5. Intracellular compartmentation in fruit kernel (A) kernel stained with Nile Red dye for discrimination of oil bodies in the epidermis, Bar = 50 μm. **(B)** floating protoplast population of kernel, Bar = 10 μm**. (C)** floating protoplast obtained from 4th developmental stage kernel Bar = 20 μm. **(D)** pelleted protoplast population of kernel, Bar = 20μm. **(E)** kernel stained with toluidine blue distinguishing the idioblast cell, Bar = 10 μm. (F) limonoid profile of kernel protoplast population. **(G)** micrograph of kernel oil bodies, Bar= 10 μm. **(H)** isolated oil bodies stained with the dye Oil Red O, Bar =10 μm. **(I)** light micrograph of kernel section stained with Nile Red, Bar = 20 μm. **(J)** Kernel residues showing vacuoles, Bar = 10 μm. **(K)** Epi-fluorescent micrograph of Nile Red stained kernel epidermis showing oil bodies, Bar = 10 μm **(L)** confocal microscopy image of the isolated oil bodies from kernel, Bar = 5 μm. **(M)** Epi-fluorescent micrograph of the isolated oil bodies from kernel, Bar = 10 μm. **(N)** limonoid profile of kernel oil bodies.

To explore the chemical composition of oil bodies, isolation of it was carried using differential centrifugation, which is obtained as floating layer. When the oil bodies were isolated completely from the kernel (Figure 2B.5G), the kernel residue revealed the presence of vacuoles (Figure 2B.5J). Discrimination of vacuoles from the oil bodies was based upon non-uptake of lipophilic dyes and also, it had a distinct shape unlike that of oil bodies, which possessed vesicular nature. The lipophilic nature of the isolated oil bodies was evidenced again from its uptake of Oil Red O dye (Figure 2B.5H). Confocal microscopic studies of the isolated oil bodies stained with Nile Red dye, confirmed the presence of both polar and neutral lipids in it based on its magenta and green fluorescence, respectively obtained at two different emissions wavelengths as described earlier (Figure 2B.5L). Nile Red stained oil bodies in epi-fluorescence microscopy, showed both red and green fluorescence but the intensity were comparatively high in the small sized oil bodies less than 10 μm diameter (Figure 2B.5M). Comparison of total limonoid content of oil bodies and kernel residue harboring vacuoles depicted that oil bodies act as a major contributor of kernel limonoids (Figure 2B.5N) and the limonoids found in the kernel residue may be possibly contributed from the vacuoles (Figure 2B.5J). The oil body idioblast in kernel tissue harboring C-seco limonoids has been characterized from our studies.

Thus, the oil bodies present exclusively in kernel, represent vital feature for compartmentation in neem, which were more prominent in the epidermal cells and smaller in the cells of other regions of kernel tissue, and limonoids were accumulated in them predominantly. Oil bodies are suggested to be formed by budding out of cytoplasm oriented hemimembrane of endoplasmic reticulum membrane following the incorporation of neutral lipids such as triglycerides[92]. The contribution of oil bodies towards the storage of the invaluable insecticidal limonoid, azadirachtin A is revealed through the study of limonoid profile of isolated oil bodies and the oil body harboring floating protoplast population. Moreover, the morphology of oil bodies differed from that of the vesicles present in the latex. The oil bodies coalesce often and forms a floating layer in high-density solutions whereas, such density mediated separation was not observed with the cytoplasmic vesicles of the latex. Oil bodies acting as a site for intracellular accumulation of limonoids enables the plant cell for the compartmentation

of the water insoluble limonoid containing lipophilic domain from rest of the cytosol. This kind of co-occurrence of terpenoids in oil bodies has been reported previously in *Coleus forskohlii* root cork cells for the diterpenoid, forskolin[93]. Comparably, the metabolism of isoprenoids have been reported in the *Marchantia polymorpha* thalli oil bodies[70], whereas *Arabidopsis* leaf oil bodies produce a phytoalexin under a pathological condition and an enzyme involved in sterol biosynthesis was also found to be localized in the lipid particles[72, 94]. Oil cells in lemon grass leaves is also found to accumulate higher amounts of monoterpenes, citral[95] and similiarly cinnamaldehyde in oil cells of *C. cassia*[96]. These oil cells are lignified to protect the surrounding cells from the toxic effect of metabolite. To our knowledge, this study gives first evidence for the kernel oil bodies acting as the subcellular factories for the triterpenoids. Based on the limonoid profile of oil bodies and kernel residue containing vacuole, we hypothesize that, azadirachtin, the final product of limonoid biosynthetic pathway may be biosynthesized in the oil bodies and are transported to vacuoles through membrane fusion for sequestration in vacuoles, as proved for berberine synthesis for alkaloid compartmentation in *Berberis* species, according to a previous study where vesicles are considered to fuse with the vacuoles to release its contents[97, 98].

2B.2.5. Morphological characterization of suspension cells

Since each tissue was found to be specialized with cellular or sub-cellular compartments for limonoid localization, we studied undifferentiated suspension cells. These cells were derived from callus formed from the kernel tissue. For microscopic studies, suspension cells were generated from callus of different sub-culturing stages. Cells showed the presence of numerous granules in the cytoplasm when obtained from the initial sub-culturing stage (stage three) of callus (Figure 2B.6A). The number of granules in the cell was dwindling in the subsequent subculturing and at the end of two years of maintenance, (22 subcultures) most of the cells were either devoid of granules, or with few small granules (Figure 2B.6C). The morphology of the cell was recorded through eSEM (Figure 2B.6B). To study further, composition of the suspension cells, histochemical staining studies were carried out. Upon lugol's iodine staining, violet coloration was observed on these granules, which shows that they may play a role in starch storage (Figure 2B.6D). The investigation of suspension cells with lipophilic

stains such as Oil Red O and Nile Red showed absence of staining, which in fact suggests the absence of lipophilic oil bodies as that of kernel, the parent tissue.

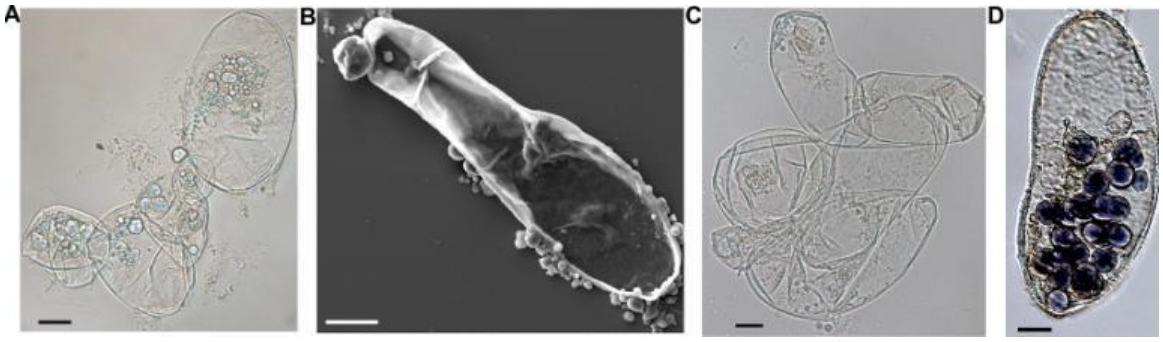

Figure 2B.6. Morphological characterization of *in vitro* cultured, undifferentiated cells (A) Cells of suspension derived from callus of third subculturing stage, Bar = 20 μm. **(C)** cells of suspension derived from callus maintained for one and a half years, Bar = 20 μm. **(B)** Scanning electron micrograph of a cell from suspension culture derived from callus of third subculturing stage, Bar = 20 μm. **(D)** same suspension cells stained with lugol's Iodine, Bar = 10 μm.

2B.2.6. Anatomical features of leaves associated with specialized cells and organelles

The cross section of neem leaf evinced the presence of distinct cells (idioblasts) interspersed among the mesophyll cells in the leaf blade, characterized by brownish yellow color (Figure 2B.7A). The size of the leaf idioblasts ranged from 18- 22 μm in diameter. Furthermore, in order to evidence idioblasts and the intracellular organelles in the leaf, the tissue was subjected to homogenization (Figure 2B.7C) and protoplast isolation separately which when examined through light microscopy, evidenced the individual idioblasts filled with numerous idioblast vacuoles (Figure 2B.7B). To further study the subcellular compartments involved in the intracellular localization of limonoids, the organelles were isolated from the tissue and limonoids were characterized from it. We carried out protoplast isolation from leaves of the *in vitro* grown neem plants, which manifested the aggregation of white particles at the top of the green protoplast pellet that was found to be idioblast vacuoles as evidenced through light micrograph (Figure 2B.7D). The white particles were characterized using eSEM that ranged in size from 0.5 – 3 μm diameter (Figure 2B.7F). Limonoid profile of these

idioblast vacuoles signified the presence of limonoids with the typical pattern of limonoid present in the *in vitro* leaf tissue (Figure 2B.7E).

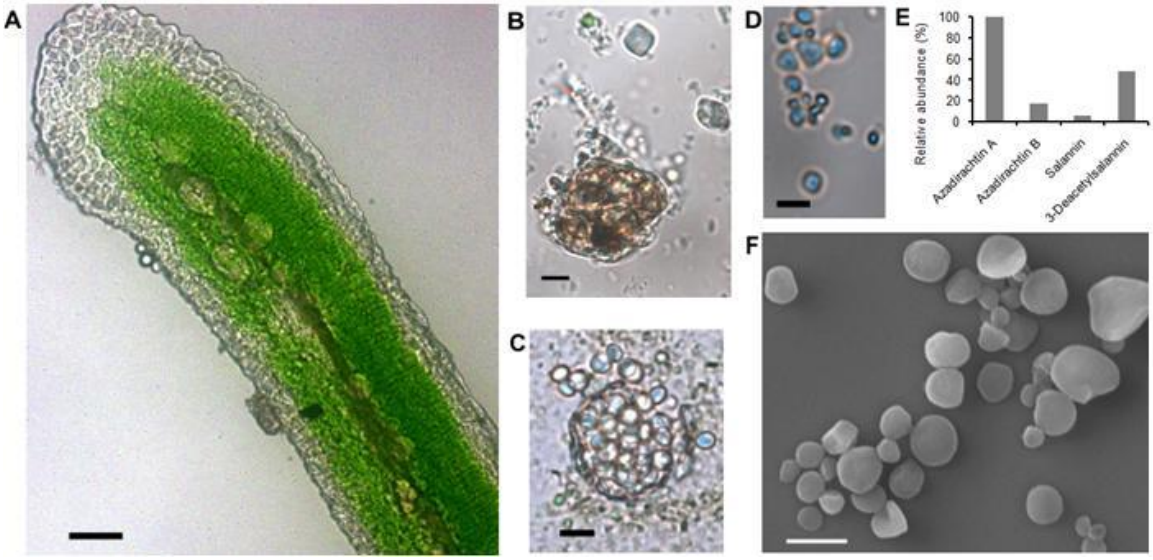

Figure 2B.7. Limonoid compartmentation in leaf tissue (A) transverse section of leaf, Bar = 50 µm. **(B)** leaf idioblast cell, Bar = 5 µm. **(C)** leaf idioblast protoplast, Bar = 10 µm. **(D)** micrograph of leaf idioblast vacuoles, Bar = 5 µm. **(E)** limonoid profile of leaf idioblast vacuoles. **(F)** electron micrograph of idioblast vacuoles obtained from leaves of in vitro grown neem seedling, Bar = 3 µm.

Neem idioblast cells of fruit pericarp and leaf showed red to brown coloration and interestingly, they seldom possess the fluorescent property as that of phenolics containing idioblasts of *Egeria densa*[99], indole alkaloid idioblast cells of *C. roseus*[61] and *Camptotheca acuminate*[100]. Neem idioblasts of pericarp and leaf possess numerous small vacuoles rather than a large central vacuole typical to other parenchymal cells and these vacuoles facilitate the accumulation of specific limonoids, characteristic of the individual tissues. Quantitative comparison of azadiradione and epoxyazadiradione in vacuoles and latex of pericarp suggested that vacuoles serve as a major site for limonoid accumulation over latex, in the fruit pericarp. Idioblast vacuoles isolated from the different tissues revealed limonoid profile corresponding the respective tissues (Figures 2B.4, 2B.5, 2B.7). Similar type of secondary metabolite idioblasts containing multitude of vacuoles has been observed in *Ruta graveolens* root and suspension culture, which are considered to be involved in storage of alkaloid, acridone[101]. Apart from the idioblast

vacuoles, central vacuole of barley was found to accumulate flavonoids whereas in the mesophyll vacuoles of *C. roseus*, presence of phenolics and indole alkaloids has been identified[102-104].

2B.2.7. Morphology, anatomy and physiology of neem flower

Sectioning of floral petal was performed using vibratome to study the distribution of specialized cells involved in the storage of secondary metabolites. The sections of floral petals studied through light microscopy and scanning electron microscopy showed that, the petals possess non-glandular trichomes (Figure 2B.8A and 2B.8B). They were prevalent as either long or short hairs (Figure 2B.8A and 2B.8B). The long hairs reached up to 100 - 150 μm, whereas the length of short hairs was of 40 - 50 μm. Both the trichomes are unicellular and short hairs were abundant in numbers when compared to the long ones. The long non-glandular trichomes were found to be distributed across all floral parts.

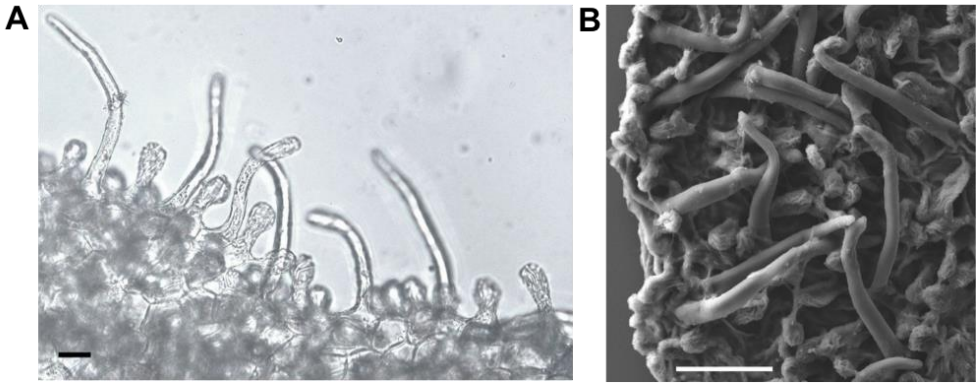

Figure 2B.8. Section of floral petal (A) Light micrograph showing two types of non-glandular trichomes on the surface, Bar = 20 μm, **(B)** eSEM image of trichomes on floral surface, Bar = 50 μm

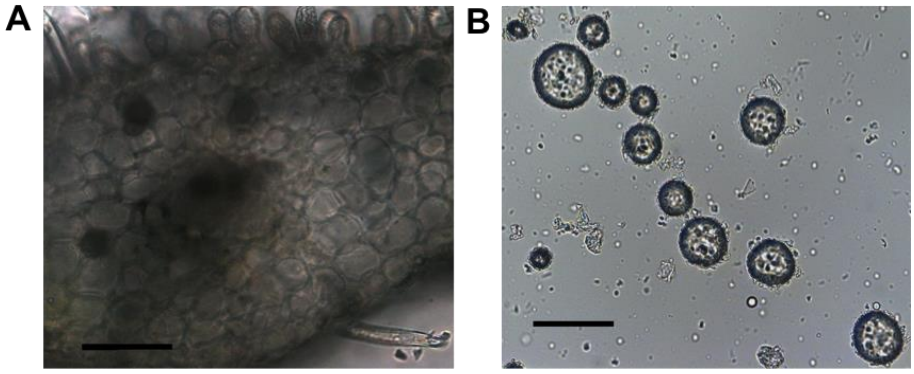

Figure 2B.9. Secretory vesicles of flower (A) Section of floral petal showing secretory vesicles, Bar = 50 µm. **(B)** secretory vesicles from flower, Bar = 50 µm

The cross section of the floral parts (Figure 2B.9A) showed brown colored secretory vesicles of varying sizes from 20 - 50 µm in diameter present in some of the cells. On density based centrifugal separation, these vesicles were obtained as a floating layer (Figure 2B.9B). These vesicles exhibited auto-fluorescence in red, green and blue channels and the merge of images obtained from 3 channels with the bright field shows bluish auto-fluorescence (Figure 2B.10B).

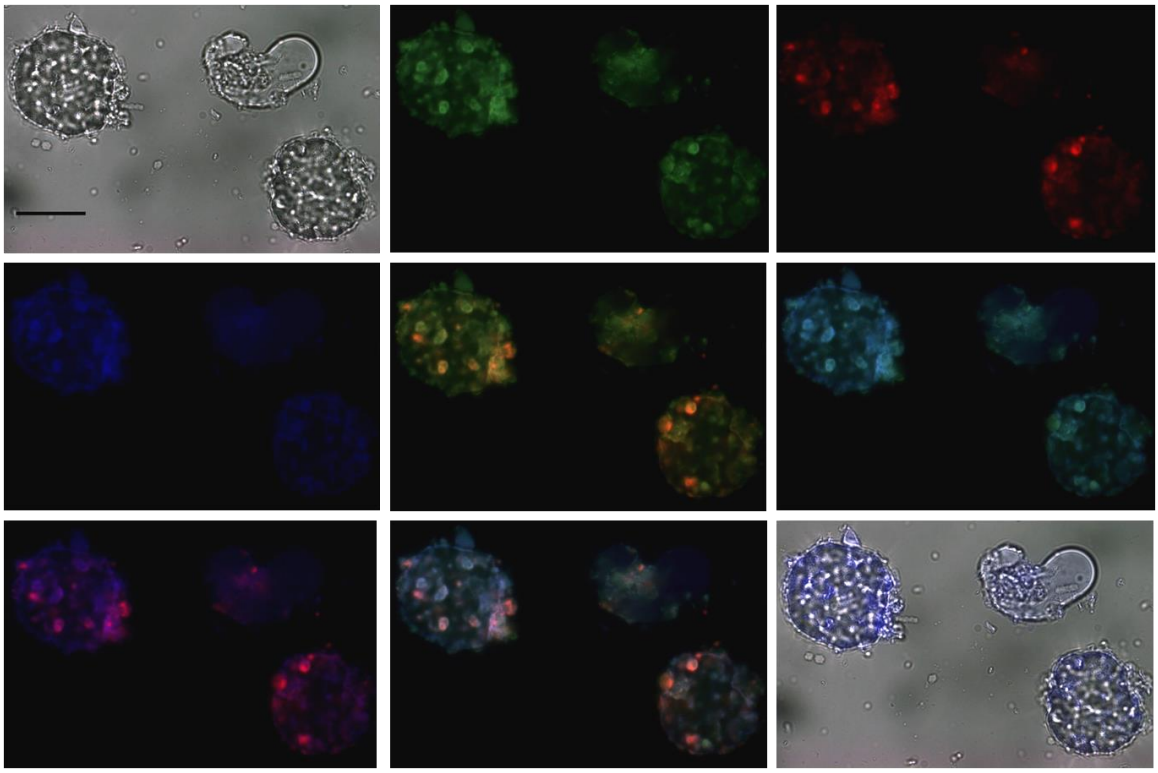

Figure 2B.10. Isolated secretory vesicles in epi-fluorescent microscopy, **1st**, Bright-field image. **2nd**, Green channel revealing autofluorescence. **3rd**, Red channel revealing autofluorescence. **4th**, Blue channel revealing autofluorescence. **5th**, Merge of the green and red channel. **6th**, Merge of the green and blue channel. **7th**, Merge of red and green channel. **8th**, Merge of all 3-channel images. **9th**, Merge of all 3-channel images with corresponding bright-field image. Bar = 50 µm

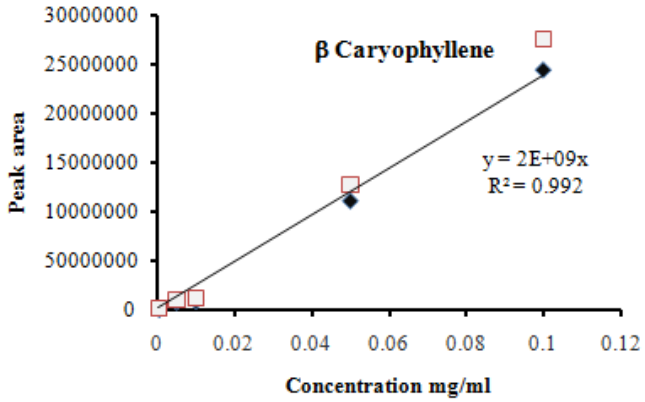

Figure 2B.11. Standard graph of β-caryophyllene constructed from the peak area of different standard concentrations in GC-QTOF analysis

Metabolic profiling of the isolated vesicles evidenced β–caryophyllene as the major sesquiterpene followed by γ elemene and humulene (Figure 2B.12). β–caryophyllene was quantified absolutely based on the standard curve made from different concentrations (Figure 2B.11). β–caryophyllene amounted to 0.01 mg/g of flower tissue and same quantity was found too in the isolated secretory vesicle (Figure 2B.12). Other sesquiterpenes identified in the flower are enumerated in Table 2B.2. LC-ESI-MS analysis showed that two monoacylglycerides such as palmitoyl and stearoyl glycerol were predominant in these vesicles (Appendix Figure 2B.5.3).

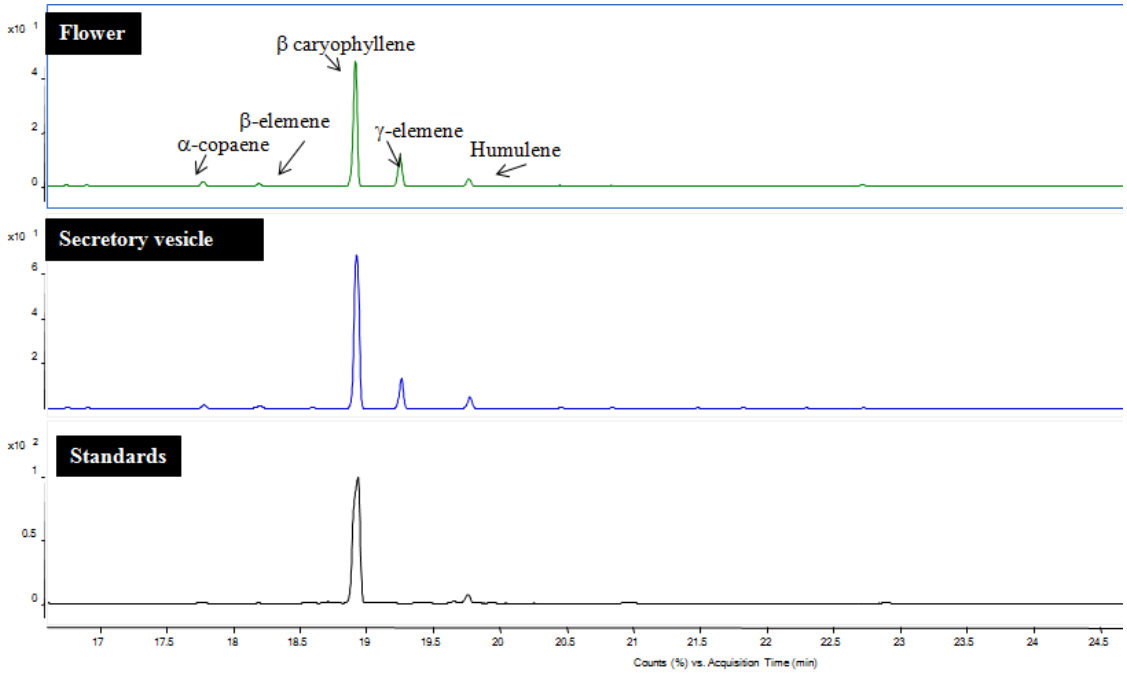

Figure 2B.12. Comparison of chromatogram of extracts from whole flower and isolated secretory vesicles with β caryophyllene and humulene standards.

Cross-section of floral parts also evidenced the presence of cytoplasmic accumulations of 0.5 – 2 μm size (Figure 2B.13A). These were isolated from the supernatant (Figure 2B.13B) and were found to contain long chain hydrocarbons (Figure 2B.13C).

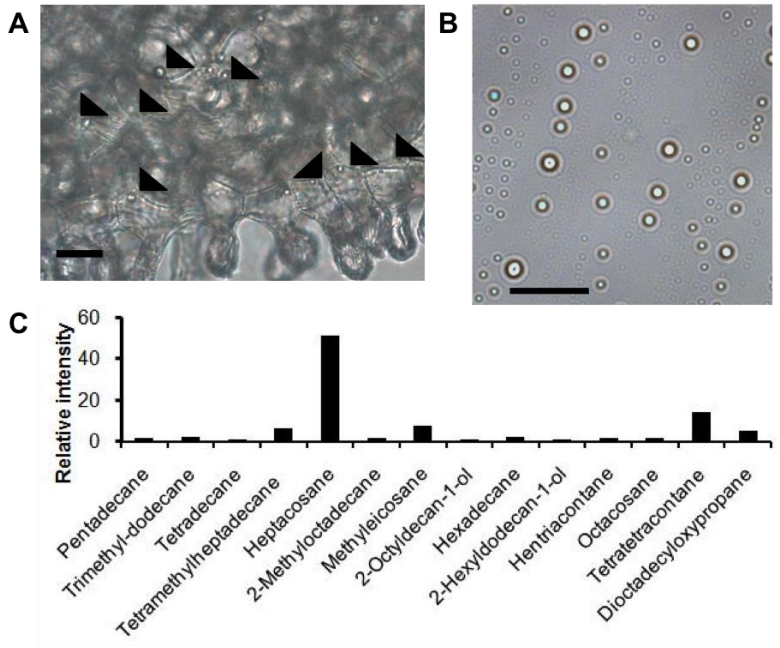

Figure 2B.13. Flower hydrocarbons (A) Section of floral petal showing cytoplasmic accumulations (marked with arrows), Bar = 20 μm **(B)** Isolated cytoplasmic accumulation bodies Bar = 10 μm **(C)** Relative intensity of hydrocarbons from flower.

Cross-section of anther showed pollen grains in the locule (Figure 2B.14A) and pollen exhibited green and blue autofluorescence evidenced through epi-fluorescence microscopy (Figure 2B.14B). Flavonoids emit in the blue region[105] and also, pollen grains are enriched in flavonoids (Figure 2B.15) and total flavanoids in flower was confirmed based on protonated, sodium adducts and based on MS/MS signature fragments (Figure 2B.5.4, Table 2B.3, Table 2B.4). Quantification of flavonoids in flower showed that glucosides were more abundant flavonoids followed by prenylated flavonoids and flavonol aglycones were relatively very low (Figure 2B.15). The autofluorescence exhibited by pollen grains of neem, was comparable to that of *Zea mays*[106] and can be found to be obtained due to the abundant occurrence of flavonoids in

pollen[107, 108] and comparably, flavonoids were found to occur in tapetosomes in *Brassica*[109]. Flavonoids are found to act as antioxidant and act as effective UV-B absorbers thereby helping the plants to cope up with environmental stresses[110]. It impies that flavonoids which act as protectant for plant, confers pharmocological and anti-oxidant properties for mankind.

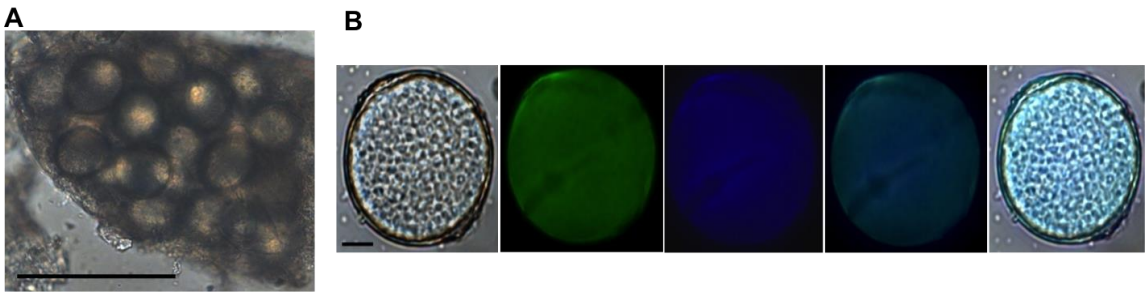

Figure 2B.14. Neem pollen micrograph (A) Hand section of anther showing pollen grains Bar = 100 μm **(B)** Pollen grain in epi-fluorescent microscopy, **1st**, Bright-field image of pollen. **2nd**, Green channel revealing autofluorescence. **3rd**, Blue channel revealing autofluorescence. **4th**, Merge of the green and blue channel. **5th**, Merge of all 2-channel images with corresponding bright-field image. Bar = 10 μm

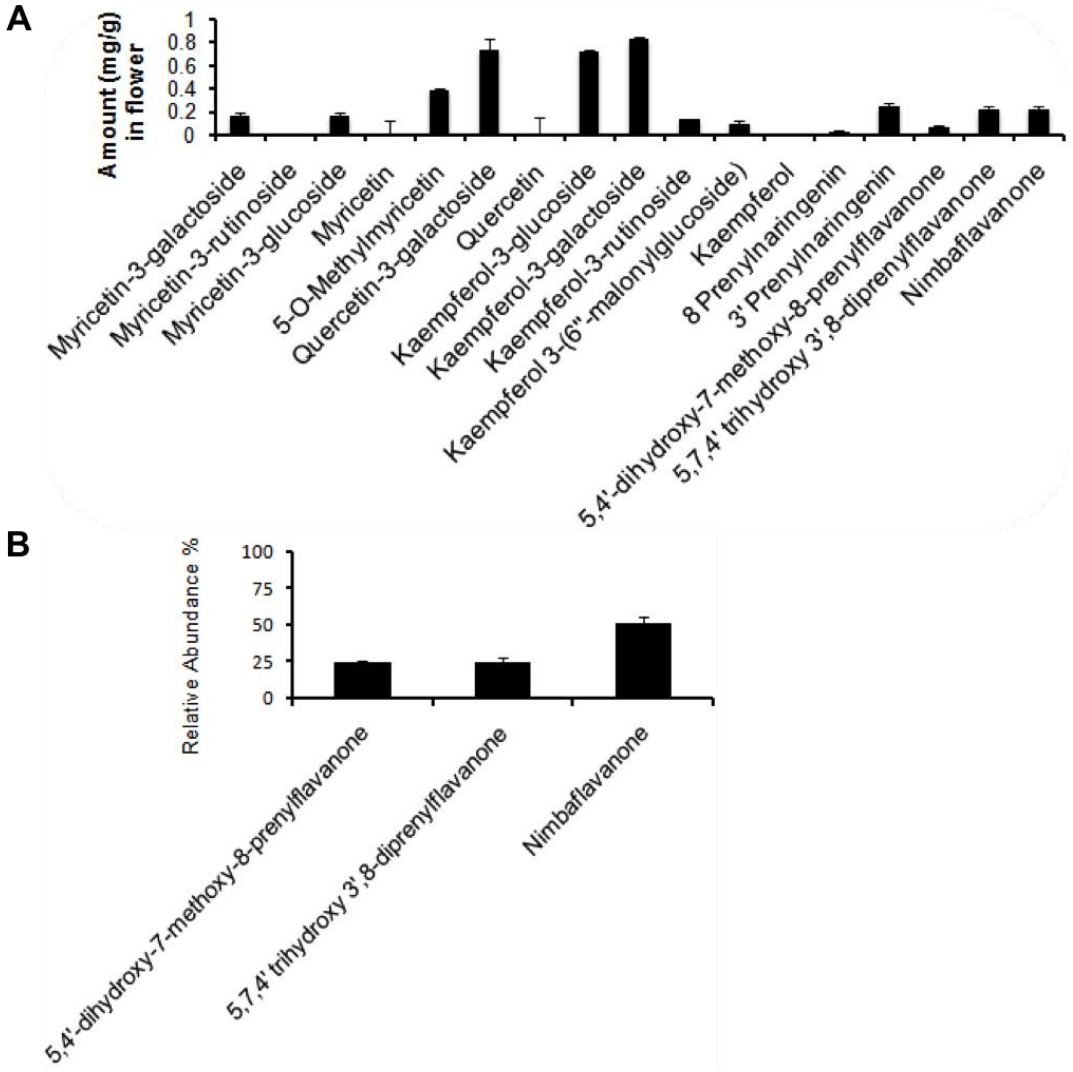

Figure 2B.15. (A) Quantification of flavonols from flower **(B)** pollen flavonols from LC-HRMS obtained from analysis

S.No.	Terpenes	Retention time	Relative Intensity
1.	Elixene	16.6	2.04
2.	α-copaene	17.8	3.12
3.	β-elemene	18.3	2.15
4.	β-caryophyllene	18.9	63.89
5.	γ-Elemene	19.2	15.87
6.	Humulene	19.7	4.60
7.	Aromadendrene	19.9	0.50
8.	β-cubebene	20.4	0.78
9.	γ-Himachalene	20.8	0.91
10.	α–Farnesene	21.1	0.62
11.	δ–Cadinene	21.3	0.18

12.	β-Cadinene	21.4	0.66
13.	Elemol	21.5	0.05
14.	Geranyl-α-terpinene	21.8	0.30
15.	Sesquiterpene hydrocarbon ($C_{15}H_{24}$)	22.1	0.37
16.	Gurjenene	22.3	0.63
17.	γ-Murrolene	22.7	1.51
18.	Himachalene	22.8	0.62
19.	Sesquiterpene hydrocarbon ($C_{15}H_{24}$)	23.7	0.13
20.	Farnesol	25.9	1.07

Table 2B.2. List of sesquiterpenes identified in the flower and its relative intensity of distribution.

S. No.	**Flavanols**	**R_t (min)**	**Extracted ions (*m/z*)**		**Formula**	**Molecular ions(*m/z*)**
1.	Myrcetin-3-galactoside	2.5	481.0976	503.0796	$C_{21}H_{20}O_{13}$	$[M+H]^+$, $[M+Na]^+$
2.	Myrcetin-3-rutinoside	2.5	627.1555	649.1375	$C_{27}H_{30}O_{17}$	$[M+H]^+$, $[M+Na]^+$
3.	Myrcetin-3-glucoside	3	481.0976	503.0796	$C_{21}H_{20}O_{13}$	$[M+H]^+$, $[M+Na]^+$
4.	Quercetin-3-galactoside (Hyperin)	4.2	465.1027	487.0847	$C_{21}H_{20}O_{12}$	$[M+H]^+$, $[M+Na]^+$
5.	Myricetin	5.1	319.0445	341.0264	$C_{15}H_{10}O_8$	$[M+H]^+$,
6.	Kaempferol-3-glucoside (Astralagin)	5.6	449.1078	471.0897	$C_{21}H_{20}O_{11}$	$[M+H]^+$, $[M+Na]^+$
7.	Kaempferol-3-galactoside	5.4	449.1078	471.0897	$C_{21}H_{20}O_{11}$	$[M+H]^+$, $[M+Na]^+$
8.	Kaempferol-3-rutinoside (Nicotiflorin)	5.4	595.1657	617.1476	$C_{27}H_{30}O_{13}$	$[M+H]^+$, $[M+Na]^+$
9.	Kaempferol 3-(6"-malonylglucoside)	6.3	535.1082	557.0901	$C_{24}H_{22}O_{14}$	$[M+H]^+$, $[M+Na]^+$
10.	Quercetin	6.7	303.0499	325.0319	$C_{15}H_{10}O_7$	$[M+H]^+$, $[M+Na]^+$
11.	5-O-Methylmyricetin	8.1	333.0604	355.0421	$C_{16}H_{12}O_8$	$[M+H]^+$, $[M+Na]^+$
12.	Kaempferol	11	287.055	309.0369	$C_{15}H_{10}O_6$	$[M+H]^+$, $[M+Na]^+$
13.	8 Prenylnaringenin	20.1	341.1383	363.1202	$C_{20}H_{20}O_5$	$[M+H]^+$, $[M+Na]^+$
14.	3' Prenylnaringenin	25.3	341.1383	363.1202	$C_{20}H_{20}O_5$	$[M+H]^+$, $[M+Na]^+$

15.	5,4'-dihydroxy-7-methoxy-8-	30.9	355.154	377.1359	$C_{21}H_{22}O_5$	$[M+H]^+$, $[M+Na]^+$
16.	5,7,4' trihydroxy 3',8-diprenyl flavanone	31.6	409.2009	431.1829	$C_{25}H_{28}O_5$	$[M+H]^+$, $[M+Na]^+$
17.	Nimbaflavanone	34.2	423.2166	445.1985	$C_{26}H_{30}O_5$	$[M+H]^+$, $[M+Na]^+$

Table 2B.3. List of flavonoids identified in the flower based on protonated and sodium molecular ions

	Flavonols	**Precursor ions**	**Product ions**
1	Myrcetin-3-galactoside	481.0976, $C_{21}H_{21}O_{13}$	85.0291 ($C_4H_5O_2$, 8.9), 127.0394 ($C_6H_7O_3$, 2.2), 165.0188 ($C_8H_5O_4$, 0.4), 217.0477 ($C_{12}H_9O_4$, 0.1), 245.0447 ($C_{13}H_9O_5$, 0.4), 273.0390 ($C_{14}H_9O_7$, 0.6), 301.0345 ($C_{15}H_9O_7$, 0.3), 319.0452($C_{15}H_{11}O_8$, 100)
2	Myrcetin-3-rutinoside	627.1555, $C_{27}H_{31}O_{17}$	85.0291($C_4H_5O_2$, 13.1), 129.0551 ($C_6H_9O_3$, 2.1), 319.0452($C_{15}H_{11}O_8$, 100),
3	Myrcetin-3-glucoside	481.0976, $C_{21}H_{21}O_{13}$	85.0291 ($C_4H_5O_2$, 8.9), 97.0290 ($C_5H_5O_2$, 2.8), 127.0393 ($C_6H_7O_3$, 2.1), 145.0499 ($C_6H_9O_4$, 1), 165.0185 ($C_8H_5O_4$, 0.3), 195.0277 ($C_9H_7O_5$), 245.0448 ($C_{13}H_9O_5$, 0.2), 273.0400 ($C_{14}H_9O_6$, 0.5), 319.0451 ($C_{15}H_{11}O_8$, 100)
4	Quercetin-3-galactoside (Hyperin)	465.1027, $C_{21}H_{21}O_{12}$	85.0290 ($C_4H_5O_2$, 8.9), 97.0289 ($C_5H_5O_2$, 3), 127.0392 ($C_6H_7O_3$, 2.2), 165.0185 ($C_8H_5O_4$, 0.2), 217.0477 ($C_{12}H_9O_4$, 0.2), 257.0455 ($C_{14}H_9O_5$, 0.2), 303.0500 ($C_{15}H_{11}O_7$, 100),
5	Myricetin	319.0445, $C_{15}H_{11}O_8$	121.0137 ($C_3H_5O_5$, 1.1), 153.0186 ($C_7H_5O_4$, 3.1), 165.0183 ($C_8H_5O_4$, 1.6), 273.0388 ($C_{14}H_9O_6$, 5.6), 319.0452 ($C_{15}H_{11}O_8$, 100)
6	Kaempferol-3-glucoside (Astralagin)	449.1075, $C_{21}H_{21}O_{11}$	85.0290 ($C_4H_5O_2$, 9.4), 127.0393 ($C_6H_7O_3$, 2.3), 153.0183 ($C_7H_5O_4$, 0.1), 165.0180 ($C_8H_5O_4$, 0.1), 213.0912 ($C_{13}H_9O_3$, 0.1), 270.0500 ($C_{15}H_{10}O_5$, 0.1), 287.0551 ($C_{15}H_{11}O_6$, 100),
7	Kaempferol-3-galactoside	449.1075, $C_{21}H_{21}O_{11}$	85.0290 ($C_4H_5O_2$, 9.4), 127.0393 ($C_6H_7O_3$, 2.3), 153.0183 ($C_7H_5O_4$, 0.1), 165.0180 ($C_8H_5O_4$, 0.1), 213.0912 ($C_{13}H_9O_3$, 0.1), 287.0551 ($C_{15}H_{11}O_6$, 100)
8	Kaempferol-3-rutinoside (Nicotiflorin)	595.1657, $C_{27}H_{31}O_{13}$	85.0290 ($C_4H_5O_2$, 14.2), 97.0290 ($C_5H_5O_2$,1.2), 129.0549 ($C_6H_9O_3$, 2.9), 145.0497 ($C_6H_9O_4$, 0.9), 287.0552 ($C_{15}H_{11}O_6$, 100)
9	Kaempferol 3-(6"-malonylglucoside)	535.1082, $C_{24}H_{23}O_{14}$	69.0342 (C_4H_5O, 3.9), 81.0341 (C_5H_5O,4.1), 85.0290 ($C_4H_5O_2$,9.9), 105.0187 ($C_3H_5O_4$, 3.6), 109.0289 ($C_6H_5O_2$, 7.5), 127.0393 ($C_6H_7O_3$, 10.4), 145.0497 ($C_6H_9O_4$, 2), 159.0290 ($C_6H_7O_5$, 5.9), 171.0288 ($C_7H_7O_5$, 0.4), 231.0500 ($C_9H_{11}O_7$, 0.6), 287.0562 ($C_{15}H_{11}O_6$, 100)

10	Quercetin	303.0499, $C_{15}H_{11}O_7$	165.0185 ($C_8H_5O_4$, 0.6), 229.0502 ($C_{13}H_9O_4$, 1.1), 257.0455 ($C_{14}H_9O_5$, 0.2), 285.0757 ($C_{15}H_9O_6$, 1), 303.0501 ($C_{15}H_{11}O_7$,100)
11	5-O-Methylmyricetin	333.0604, $C_{16}H_{13}O_8$	137.0236 ($C_7H_5O_3$, 0.2), 153.0184 ($C_7H_5O_4$, 1.2), 165.0182 ($C_8H_5O_4$, 0.4), 179.0345 ($C_9H_7O_4$, 0.4), 219.0289 ($C_{11}H_7O_5$, 0.6), 245.0452 ($C_{13}H_9O_5$, 0.4), 273.0394 ($C_{14}H_9O_6$, 1.5), 290.0418 ($C_{14}H_{10}O_7$, 1.3), 301.0348 ($C_{15}H_9O_7$, 2), 318.0374 ($C_{15}H_{10}O_8$, 61.3), 333.0608 ($C_{16}H_{13}O_8$, 100)
12	Kaempferol	287.0550, $C_{15}H_{11}O_6$	68.9977 (C_3HO_2, 0.9), 121.0283 ($C_7H_5O_2$, 1.1), 153.0180 ($C_7H_5O_4$, 1.6), 165.0182 ($C_8H_5O_4$, 1.1), 183.0287 ($C_8H_7O_5$, 0.5), 213.0546 ($C_{13}H_9O_3$, 0.6), 231.0651 ($C_{13}H_{11}O_4$, 0.5), 241.0492 ($C_{14}H_9O_4$, 0.6), 258.0515 ($C_7H_5O_4$, 0.6), 269.0439 ($C_{15}H_9O_5$, 0.2), 287.0551 ($C_{15}H_{11}O_6$,100)
13	8 Prenylnaringenin	341.1383, $C_{20}H_{21}O_5$	107.0497 (C_7H_7O, 1.84), 121.0651 (C_8H_9O, 3.6), 141.0186 ($C_6H_5O_4$, 1), 147.0443 ($C_9H_7O_2$, 3.7),165.0184 ($C_8H_5O_4$, 37.7), 179.0344 ($C_9H_7O_4$, 2), 183.0290 ($C_8H_7O_5$, 100), 191.0341 ($C_{10}H_7O_2$, 4.9), 221.0811 ($C_{12}H_{13}O_4$, 3.7), 285.0759 ($C_{16}H_{13}O_5$, 49.2), 341.1386 ($C_{20}H_{21}O_5$, 10)
14	3' Prenylnaringenin	341.1383, $C_{20}H_{21}O_5$	69.0706 (C_5H_9 , 10.8), 133.065 (C_9H_9O, 4.4), 147.0442 ($C_9H_7O_2$, 5), 153.0183 ($C_7H_5O_4$, 100), 171.0289 ($C_7H_7O_5$, 21.6), 173.0599 ($C_{11}H_9O_2$, 21.6), 215.0708 ($C_{13}H_{11}O_3$,11.7), 221.0598 ($C_{15}H_9O_2$, 10.7), 249.0547 ($C_{16}H_9O_3$, 3.8), 267.0652 ($C_{16}H_{11}O_4$, 78.1), 273.0758 ($C_{15}H_{13}O_5$, 8.7), 285.0758 ($C_{16}H_{13}O_5$, 18.1), 299.0916 ($C_{17}H_{15}O_5$, 2), 341.1385 ($C_{20}H_{21}O_5$, 13.2)
15	5,4'-dihydroxy-7-methoxy-8-prenylflavanone	355.1540, $C_{21}H_{23}O_5$	121.0651 (C_8H_9O, 4.6), 135.0807 ($C_9H_{11}O$, 8.7), 161.0599 ($C_{10}H_9O_2$, 2.6), 165.0184 ($C_8H_5O_4$, 57.4), 183.0290 ($C_8H_7O_5$, 100), 191.0340 ($C_{10}H_7O_4$, 7.4), 221.0809 ($C_{12}H_{13}O_4$, 3.5), 299.0916 ($C_{17}H_{15}O_5$, 35.5), 355.1544 ($C_{21}H_{23}O_5$, 3.2)
16	5,7,4' trihydroxy3',8-diprenyl flavanone	409.2009, $C_{25}H_{29}O_5$	153.0183 ($C_7H_5O_4$, 8.2), 165.0184 ($C_8H_5O_4$, 51.7), 183.0289 ($C_8H_7O_5$, 100), 189.1275 ($C_{13}H_{17}O$, 14.3), 193.0497 ($C_{10}H_9O_4$, 12.7), 213.0912 ($C_{17}H_{13}O_5$, 7.2), 221.0809 ($C_{12}H_{13}O_4$, 5.6), 267.0652 ($C_{16}H_{11}O_4$, 4.7), 279.0652 ($C_{17}H_{11}O_4$, 3.9), 297.0759 ($C_{17}H_{13}O_5$, 5.3), 335.1278 ($C_{21}H_{19}O_4$, 10.6), 353.1385 ($C_{21}H_{21}O_5$, 22.6)
17	5,7, dihydroxy-4' methoxy-8, 3' bis (3-methylbut-2-enyl) flavan-4-one (Nimbaflavanone)	423.2166, $C_{26}H_{31}O_5$	121.0651 (C_8H_9O, 1.5), 147.0807 ($C_6H_5O_4$, 5.5), 165.0184 ($C_8H_5O_4$, 31.6), 183.0290 ($C_8H_7O_5$, 100), 193.0498 (28.3), 203.1432 ($C_{14}H_{19}O$, 13.2), 209.0963 ($C_{15}H_{13}O$, 4.4), 219.0654 ($C_{12}H_{11}O_4$,10.1), 227.1068 ($C_{15}H_{15}O_2$, 11.2), 311.0917 ($C_{18}H_{15}O_5$, 4), 367.1543 ($C_{22}H_{23}O_5$, 12.5)

Table 2B.4. Precursor fragments of flavonoids and its intensity obtained upon fragmentation at 30% NCE

Neem floral tissues contained only non-glandular trichomes, which in general are known to protect the surface of the plant parts from predators by acting as a physical barrier[111]. Glandular trichomes are considered as a factory for biosynthesis of terpenes and these were not found in neem, instead the sesquiterpenes were identified to be localized in the secretory vesicles distributed across cells in all the parts of flower. These sesquiterpenes are presumed to be emitted through granulocrine secretion. Whereas, in *Marchantia thalli,* sesquiterpene lactones have been found to be localized in oil bodies [71]. The predominance of β-caryophyllene and elemene in flower suggests that they serves to attract pollinators[112] and also for the defense against pathogens as evidenced in *Arabidopsis*[113]. Moreover, sesquiterpene volatiles have been found to be biosynthesized in the anther and pollens in grapevine flowers[114]. From this study, it is known that storage of sesquiterpenes in secretory vesicles helps in secretion of them in appropriate conditions. Thus, these studies give the physiological importance of the metabolite localization in these tissues for specific functions in the tree.

2B.2.8. Comparison of idioblasts of fruit pericarp and leaves

Comparison of size, number and area occupied by idioblasts in different tissues of neem was compared with that of limonoid content of the respective tissues. Idioblasts in pericarp were concentrated adjacent to laticifers, which are abundant in the mesocarp, and were considered for enumeration of number of idioblasts. Number of idioblasts in the mesocarp of pericarp was 168/mm^2, whereas it was 130/mm^2 in the leaf (Figure 2B.16A). The area occupied by the idioblasts in each tissue was calculated (Figure 2B.16B) and found that idioblasts in mesocarp occupy maximum area of 0.32 mm^2/mm^2 and in leaf; the area was found to be 0.04 mm^2/mm^2. This data correlates with the limonoid content of these tissues as the pericarp was found to contribute for the maximum limonoid content followed by leaf[4]. The overview of different type of compartmentation existing in fruit and leaf tissues has been depicted in Figure 2B.16C, emphasizing the localization of different class of limonoids in those compartments of fruit.

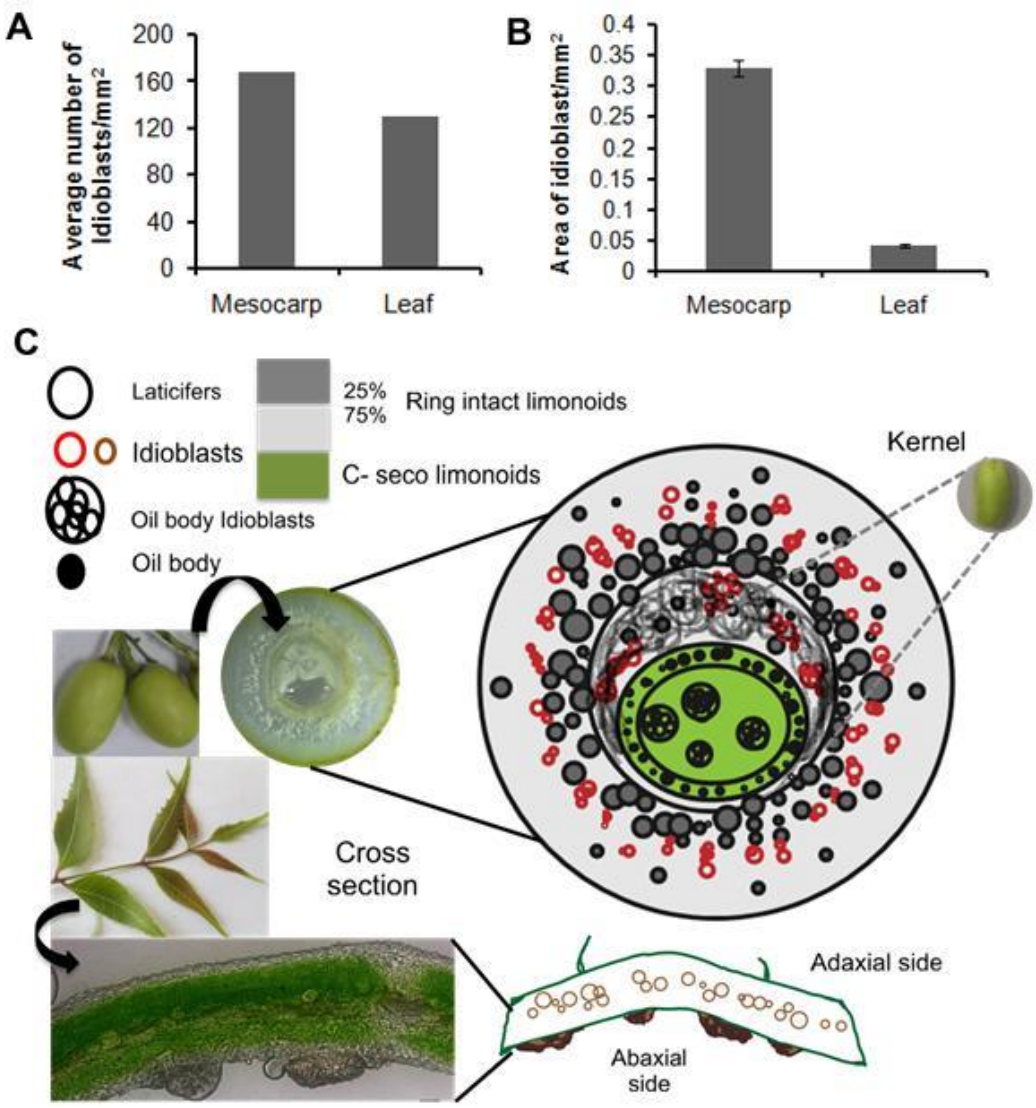

Figure 2B.16. (A) Number of idioblasts in different tissues and **(B)** their area contribution **(C)** Model showing cellular and subcellular compartmentalization of limonoids in neem fruit and leaf

2B.2.9. Feeding deterrence of neem fruit latex for insects

Laticifers are distributed across plant kingdom in order to impart defense response against insects and animals by exuding the cytoplasmic latex that are enriched with specialized metabolites[86]. To understand further, the defensive action of the neem fruit latex, we performed no choice assay, dual choice assay and multiple choice assay with *Helicoverpa armigera.* In no choice assay, larvae of third instar were presented with a leaf disc treated with latex of 1µL, 5µL, 10 µL, 20 µL. The larvae didn't feed on the leaf disc treated with latex of 5 µL and the volume above (Figure 2B.17). When it is force

fed with the latex treated leaf discs over the above mentioned amount of latex, it died. This shows that latex of 0.56 μL/cm^2 and above has feeding inhibition, physiological effects and mortality effects on insects.

In dual choice assay, *Helicoverpa armigera* was allowed into the plate containing the combination of latex treated and untreated leaf discs (Figure 2B.18). We found that, the larvae fed upon control leaf discs but did not consume the leaf discs which are treated with 0.56 μL latex /cm^2 and the above concentrations. However, larvae fed upon leaf discs treated at 0.112 μL latex/cm^2 but their body weight is reduced compared to that of the control larvae. Dual choice feeding assay was also performed with two latex treated and two control leaves containing plate in which two 3rd instar larve were allowed (Figure 2B.19). The dual choice assay confirms the herbivory deterrence of the latex, which may be due to the contribution of the potentiation effect of all ring intact limonoids[115] and traces of ring C-seco limonoids, in particular azadirachtin and its natural derivatives.

In multiple choice assay, 1 μg azadirachtin A (318 ng/cm^2), a potent insecticide was painted over the leaf disc along with 1, 5, 10, 20 μL latex treated and control leaf discs. The larvae preferred the control and 1 μL latex treated leaf discs to the above concentrations. When the larvae fed the azadirachtin treated leaf disc, it didn't feed further due to its anti-feedant effect.

Previous studies shows that EC_{50} of azadirachtin was 0.26 ppm, very effective and potent against *H. armigera*, when compared to other limonoids such as 6β-hydroxygedunin, gedunin, salannin and nimbinene whose EC_{50} values are 24.2, 50.8, 74.5 and 391.4 ppm respectively[85]. In our present study, it is well obvious that efficacy of different azadirachtin molecules, combined with the potentiation effect of different non-azadirachtin limonoids in latex gives evidence for the actual inhibitory effect of the neem fruit latex. The diverse limonoids present in the latex differ in their structure, hence their mode of actions such as feeding deterrence, physiological toxicity, growth inhibition, anti-feedant action etc. in combination are evidenced from the herbivory detterance through choice assays with neem latex.

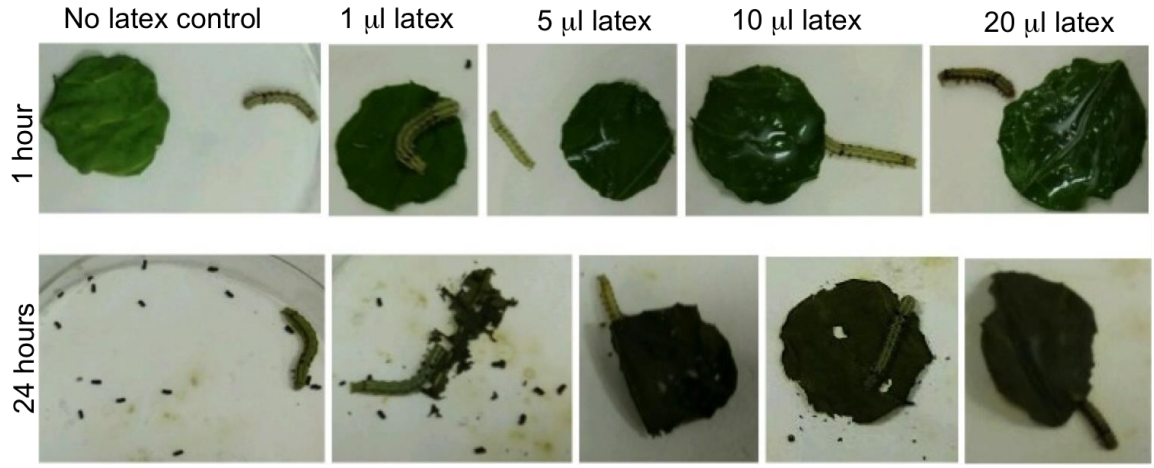

Figure 2B.17. No choice feeding assay with *Helicoverpa armigera.* 1st control leaf disc; **In other plates** leaf disc was treated with neem fruit latex of different volume.

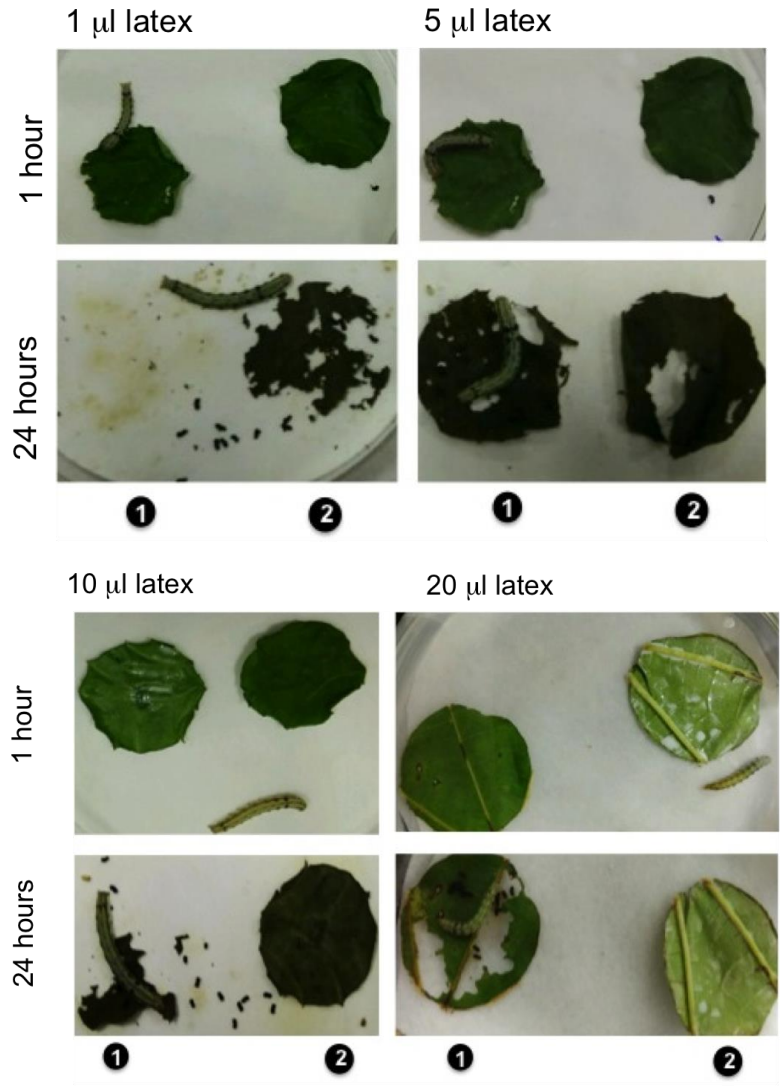

Figure 2B.18. Dual choice feeding assay with *Helicoverpa armigera.* 1, control leaf disc; **2,** leaf disc treated with neem fruit latex of different volume (A) For 12 hours; (B) 24 hours.

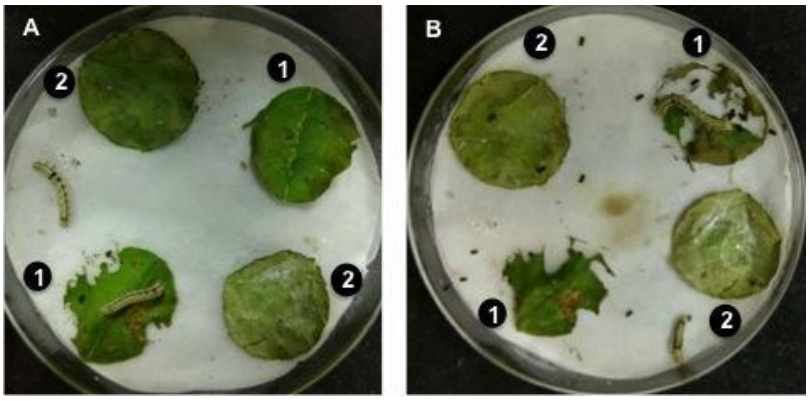

Figure 2B.19. Dual choice feeding assay with 2 *Helicoverpa armigera* /plate. 1, control leaf disc; **2,** leaf disc treated with neem fruit latex of 2.24 µL /cm^2 (A) For 12 hours; (B) 24 hours.

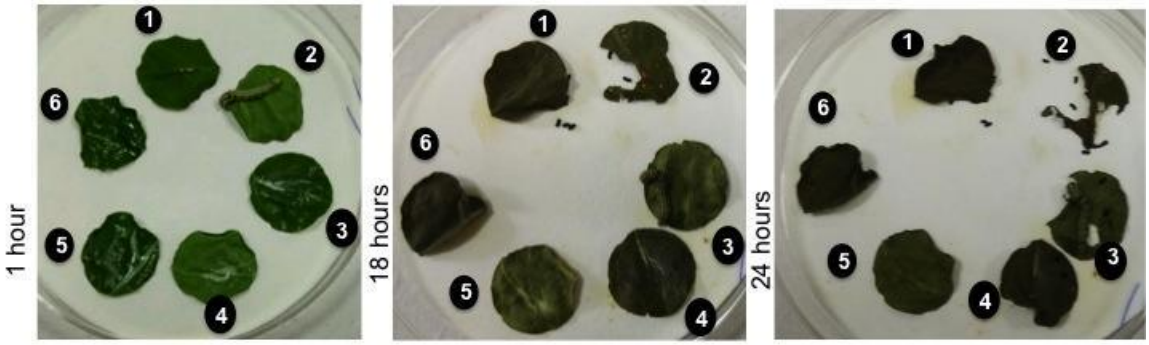

Figure 2B.20. Multiple Choice feed assay **1,** control; **2,** 1 µL latex; **3,** 5 µL latex; **4,** 10 µL latex; **5,** 20 µL latex; **6,** 1 µg azadirachtin A

2B.3. Conclusion

Though, the localization of each step of limonoid biosynthetic pathway remains unclear, and can be understood only after the characterization of enzymes involved in different steps of the pathway, localization of different limonoids and other metabolites in specific intracellular compartments such as oil bodies, idioblast vacuoles, secretory vesicles and latex, the cytosol of laticifers is presented through our studies. Our present investigation will help to study the future prospect of identification of limonoid biosynthetic pathway steps in the individual organelles and latex, their biosynthesis, translocation, the underlying regulatory interplay involved etc. It also provides valuable insights into the exemplary compartmentation existing for efficient triterpenoid

accumulation in *A. indica*, notably mediated by specialized cell types and organelles. Interrogation into the above perspectives will give an understanding to efficiently engineer a heterologous system through synthetic biology approach for the production of C-seco limonoids and intermediates.

2B.4. Materials and methods

2B.4.1. Plant materials

Neem leaves, flowers, and fruits were collected from a tree in CSIR-NCL campus during the month of March-August. Latex was collected from the fresh fruits in its second to third stage of development for various experiments. For the initiation of cell culture, fruits in third to fourth developmental stages were collected.

2B.4.2. Extraction of limonoids from neem fruit latex

Fresh, unripe neem fruits were lanced with a surgical blade at the bottom in the pericarp region to collect the milky latex. The latex was dissolved in water and extracted thrice with equal volume of n-hexane. The hexane extract was concentrated under reduced pressure to dryness. The extracted latex was again re-extracted with equal volume of ethylacetate thrice and the pooled ethylacetate extract was concentrated under reduced pressure, reconstituted in LCMS grade methanol and analyzed using thin layer chromatography (TLC). TLC was performed on pre-coated Merck silica gel plates (TLC Silica gel 60 F254) using the solvent system ethylacetate: hexane (10:90) and the spots were visualized under UV lamp and developed using charring reagent (92% ethanol, 3.2% anisaldehyde, 2.8% H_2SO_4 and 2% AcOH). To further identify the limonoids in traces, the diluted extract was injected in LC-ESI-MS as described below.

2B.4.3. Tissue sectioning and microscopy

Neem kernel, pericarp, leaf and flower were embedded in 4% agarose and subjected to slicing, using vibrating blade microtome (Leica) of speed and amplitude set at 30 mm/s and 20 mm respectively until a section of 20-30 micron thickness was obtained. Cross section of pericarp was visualized under stereomicroscope (Leica) to study the distribution of laticifers. The kernel sections were stained with Toluidine Blue for the identification of idioblast cells and Nile Red for discriminating the lipophilic

nature of the organelle. It was then visualized with Axio Observer.Z1 (Carl Zeiss) under bright field and epi-fluorescence microscopy under red, green and blue filters. Neem fruit latex was diluted 250 fold and visualized under ×63 objective and it was further stained with Toluidine Blue, Oil Red O, Lugol's iodine and Nile Red (Sigma Aldrich). Nile Red stained latex were imaged in Axioobserver^{TM} LSM 710 Carl Zeiss laser scanning confocal microscope with a ×63 Plan-Apochromat 1.4 NA oil immersion objectives respectively. The sample was excited with the 514-nm line from the argon laser, and the emitted light was collected at two different ranges from 648 to 698 nm and 525 to 567 nm[93].

2B.4.4. Environmental Mode Scanning Electron Microscopy and Transmission Electron Microscopy of latex

For scanning electron microscopy, neem latex was collected in 0.1 M phosphate buffer, pH 7.4 with 0.4 M mannitol and 6% glutaraldehyde. Diluted, fixed and dried sample was then subjected to eSEM, FEI Quanta 200 3D. The scale bar for all the eSEM images was made using ImageJ software. Fixed and diluted latex was placed on copper grids (400 mesh, Carbon type B) for transmission electron microscopy. For contrasting the grids, uranyl acetate was used. Electron micrographs were obtained at 120 kV with Tecnai-T20.

2B.4.5. Isolation of neem protoplasts from different tissues and limonoid profiling

Neem protoplasts were prepared from different tissue like fruit pericarp, kernel and leaves by modifying the method as described previously[116]. In brief, the neem tissues were cut into small pieces of 2 mm size in the presence of cell protoplast washing media (CPW) of following composition, 0.75 M mannitol, 10 mM $CaCl_2$, 10 mM MES at pH 5.8, 0.1% BSA and incubated in dark for 2 hrs for plasmolysis. In case of pericarp tissue, the latex was exuded from the fruit and the pericarp tissue was washed with CPW buffer to remove remnants of latex, henceforth the pericarp laticifers were devoid of latex. The plasmolysed tissues were transferred to CPW containing enzyme mixture of cellulase 1.5%, pectinase 2%, and hemicellulase 1% (Sigma Aldrich) and incubated in dark for 16 hours with intermittent shaking every hour. After enzyme digestion, the mixture was vigorously shaken for few seconds and filtered through muslin cloth to

remove pieces of tissue and the protoplast pelleted at 100 g and washed thrice with CPW containing 0.55 M mannitol. The protoplast pellet was resuspended in the following buffer, MES pH 5.8, 10 mM $CaCl_2$, and 0.1% BSA and 0.6 M sucrose. The resuspended protoplasts were visualized through optical microscope. Extraction of limonoids from different tissue protoplasts was carried out using dichloromethane thrice and the extract was concentrated under reduced pressure, later reconstituted with LC-MS grade methanol for ESI-LC-MS. In case of *in vitro* leaves, the tissue was subjected to enzyme treatment for 5 hours.

2B.4.6. Isolation of oil bodies from kernel and vacuoles from fruit, leaves and limonoid profiling

Oil bodies were isolated from neem kernel from the modification in protocol as reported earlier[93]. Neem kernels were homogenized in the presence of CPW solution (5 mL/100mg) and subjected to sonication for 2 min. The homogenized cells were centrifuged at 1000 × *g* for 10 min. The floating layer obtained was visualized in microscope. For histochemical analysis, the kernel was fixed in the same solution mentioned above in the presence of 6% glutaraldehyde and subjected to homogenization and centrifugation as described above. The oil body layer obtained was stained with Nile Red stain and imaged using confocal microscope at ×100 oil immersion objective of confocal microscope as described earlier. To remove the oil bodies from the cells completely, the above-described process was repeated several times, by centrifugation at 10000 × *g*. Complete extraction of oil bodies from kernel resulted in the observation of vacuoles in the kernel tissue. The oil bodies and kernel residues were subjected to extraction for limonoids as described above. The pericarp tissue was pulverized in the presence of CPW solution and the solution obtained was fixed in the presence of glutaraldehyde as described above and the fixed solution was filtered through filter paper of 10 μm pore size to remove the debris. The filtrate was visualized for the vacuoles with light and electron microscopy. For the isolation of vacuoles from leaves, the leaves from *in vitro* grown plants was subjected to protoplast isolation as described above, whereas the incubation time with enzyme mixture was increased to nine hours. The idioblast vacuoles were released from the protoplasts and the vacuoles formed as a

white layer in the protoplast pellet. The white layer was subjected to filtration and fixation as stated above, to study the morphology of vacuoles through eSEM.

2B.4.7. Isolation of vesicles, pollen and cytoplasmic droplets from flower

The flower tissue was subjected to homogenization into fine powder under liquid N_2. The homogenized powder was constituted in CPW buffer (5mL/g) and mixed evenly[93]. The homogenate was centrifuged at 3500 ×*g* and the floating layer was collected in a separate tube, which contained secretory vesicles and pollen grains. The pollen grains settled down at the bottom of the tube in few hours. The floating layer and settled pollen grains were subjected to filtration through filter paper of pore size 10 micron and the filtrate contained the cytoplasmic droplets. The three fractions were extracted with n-hexane followed by ethylacetate thrice and the pooled extracts were concentrated to dryness under reduced pressure. The pooled extract of vesicular fraction was passed through glass wool to remove the remnants of fused vesicle residues. The extracts were re-dissolved in methanol and n-hexane for analysis in LC-ESI-MS and GC-QTOF respectively as per the conditions described below.

2B.4.8. LC-ESI-Mass Spectrometry conditions

Analysis of neem limonoids was performed through target and untargeted profiling, with Thermo Scientific QExactive™ hybrid quadrupole-Orbitrap mass spectrometer associated with Accela 1250 pump and Accela open AS. The conditions of HESI source include capillary temperature of 320 °C, Heater temperature at 350 °C, s-lens RF level of 50, spray voltage of 3.6 kV, spray current of 0.9 μA with sheath gas flow rate of 41, Auxiliary gas flow rate of 9 and sweep gas flow rate of 3. Standards as well as the extracted samples were analyzed in positive ionization mode, in full MS-scan with scan range of 80 to 1000 *m/z*. Following were the properties of the scan performed-resolution 70,000, AGC target 1e6, Maximum IT 200 ms. Waters Acquity UPLC BEH C_{18} column (particle size 1.7 μm, 2.1 X 100 mm) was used as the stationary phase while the solvent system of methanol and water containing 0.1% formic acid served as the mobile phase. The gradient started with 40% methanol (5 min isocratic), it was then increased to 50% (5 min isocratic), followed by 60% methanol for the next 15 minutes and over the next 4 minutes it was isocratic with 65% methanol. It was then increased to

90% methanol for 4 minutes. For the last 2 minutes, it was isocratic with 40% methanol. Constant flow rate of 0.3 mL min^{-1} was maintained throughout the run time of 35 min. The chromatogram and mass spectral data were processed by Xcalibur qual browser (version 2.3; Thermo Scientific). 15 limonoids were confirmed based on the authentic standards isolated, purified and characterized from neem[4]. Further, MS/MS for all the identified limonoids through was performed in PRM mode, with protonated adduct as precursors in inclusion list. 20% NCE was employed for C-seco limonoids and 25% for ring intact limonoids at MS resolution of 35000, whereas for confirmation of flavonoids 30% NCE was used at a resolution of 17500. Quantification of flavonoids was carried out relative to the known concentration of authentic standard Kaempferol (Sigma Aldrich).

2B.4.9. GC-MS analysis

The extract was reconstituted in n-Hexane and it was analyzed by a 7890B Gas Chromatograph coupled to an Accurate-Mass Q-TOF GC/MS 7200 (Agilent Technologies). Separation was performed by using 30 m × 250 μm × 0.25 μm HP-5 capillary column with helium as a carrier gas at a flow rate of 1 $mLmin^{-1}$. The extract of 1 μL was injected in splitless mode. The temperature program was set at 60 °C for 2 min, followed by a temperature gradient from 60 °C to 250 °C at a ramping rate of 5 °C/min, and held at 250 °C for 14min. Sesquiterpenes and hydrocarbons were identified by matching the acquired mass spectra with the reference library (National Institute of Standards and Technology) using Agilent MassHunter Qualitative analysis tool (B.06.00). Standard curve for β caryophyllene (Sigma-Aldrich) was made for quantification of it in the whole flower and also in the isolated secretory vesicles. Standard curve was made with β caryophyllene of different concentrations such as 0.1 mg/ml, 0.05 mg/mL, 0.01 mg/mL, 0.005 mg/mL, 0.001 mg/mL.

2B.4.10. Feeding assay with neem fruit latex

Feeding-choice assay was performed with third instar larvae of *Helicoverpa armigera*. The larvae were reared on an artificial diet in the laboratory and they were starved for 4 h before each assay. Freshly collected leaves of *Ricinus communis* were cut into 2.8 cm diameter discs using cork borer and were used as feed for the larvae. Neem

fruit latex (0.112, 0.56, 1.12 and 2.24 μL /cm^2 painted on both adaxial and abaxial side of leaf disc). In no choice assay, over a petridish containing moistened filter paper, a treated leaf disc was placed. In dual choice feeding assay, both latex treated and untreated (control) leaf discs were placed in a plate. In another dual choice assay, the treated and untreated leaf discs were placed at alternating positions, with 2 larvae each left at the center. In multiple choice assays, total of 6 leaf discs were placed each of 2 cm in diameter, the control and azadirachtin treated leaves discs were presented along with four latex treated leaf discs. The experiment was performed in duplicates and the feeding preference of the larvae for the treated and untreated leaf discs were monitored for 24 hours.

2B.5. Appendix

Azadirachtin H

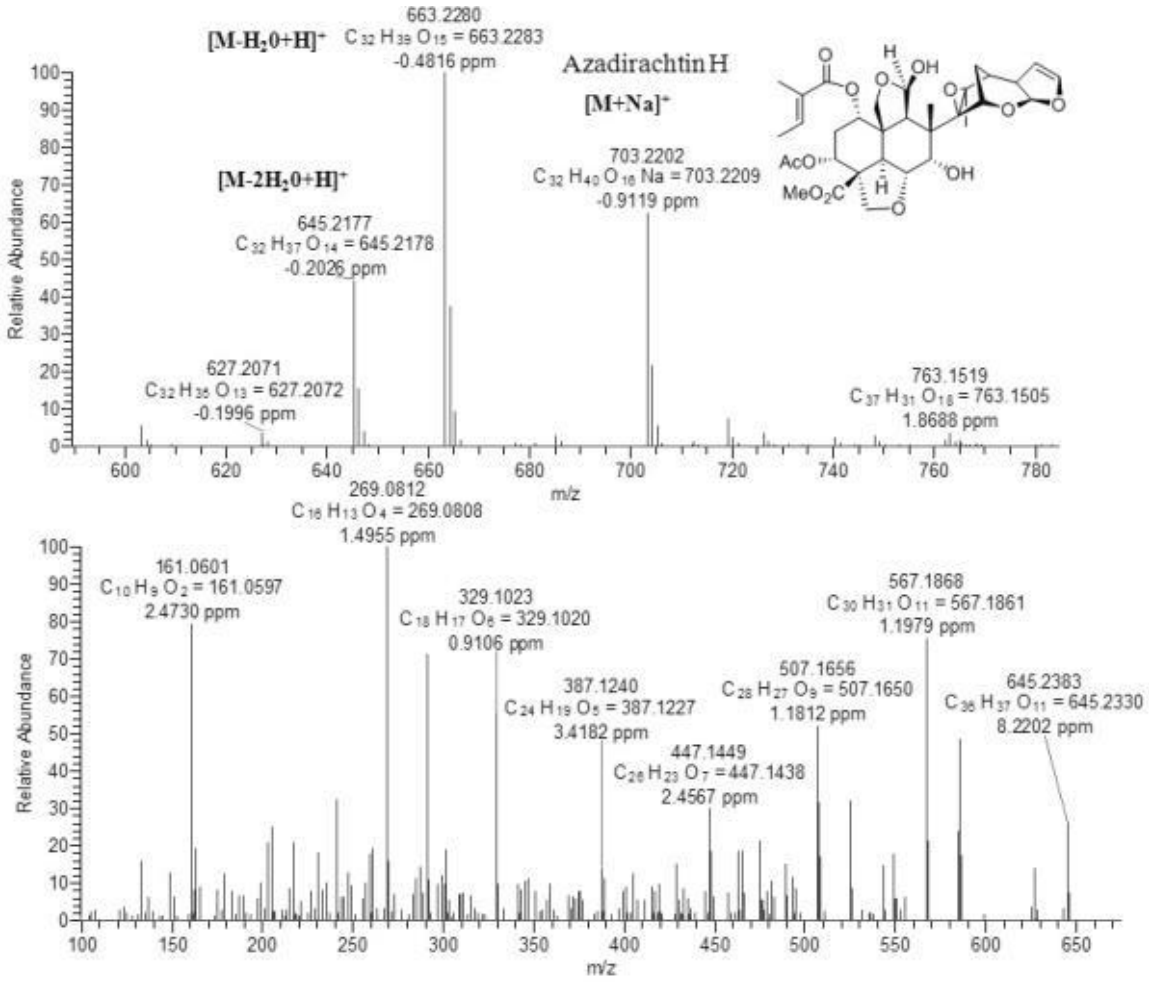

Mahmoodin

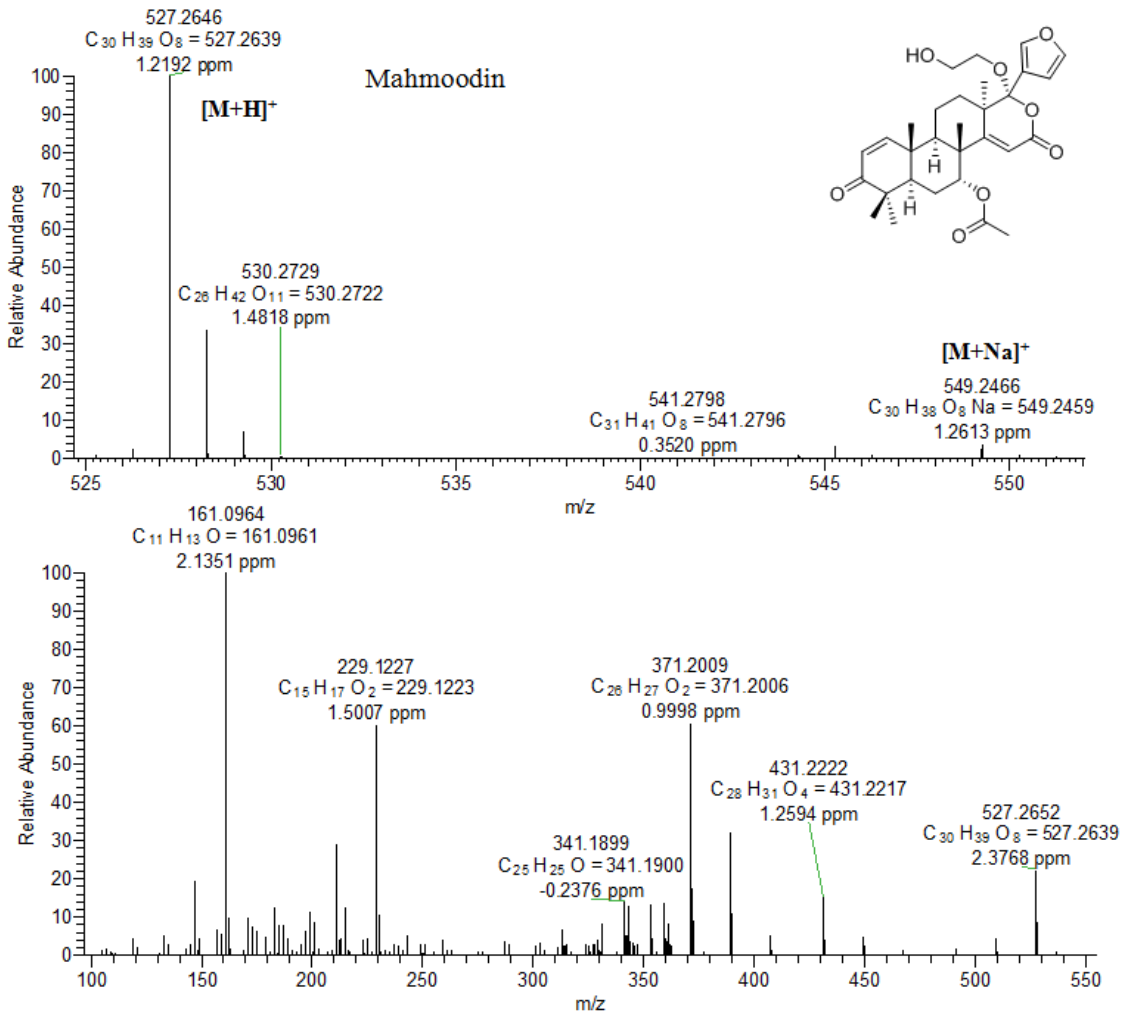
Mahmoodin
527.2646
C30 H39 O8 = 527.2639
1.2192 ppm
[M+H]+
530.2729
C26 H42 O11 = 530.2722
1.4818 ppm
541.2798
C31 H41 O8 = 541.2796
0.3520 ppm
[M+Na]+
549.2466
C30 H38 O8 Na = 549.2459
1.2613 ppm
Relative Abundance
m/z
161.0964
C11 H13 O = 161.0961
2.1351 ppm
229.1227
C15 H17 O2 = 229.1223
1.5007 ppm
371.2009
C26 H27 O2 = 371.2006
0.9998 ppm
431.2222
C28 H31 O4 = 431.2217
1.2594 ppm
341.1899
C25 H25 O = 341.1900
-0.2376 ppm
527.2652
C30 H39 O8 = 527.2639
2.3768 ppm
Relative Abundance
m/z

6-deacetylnimbinal

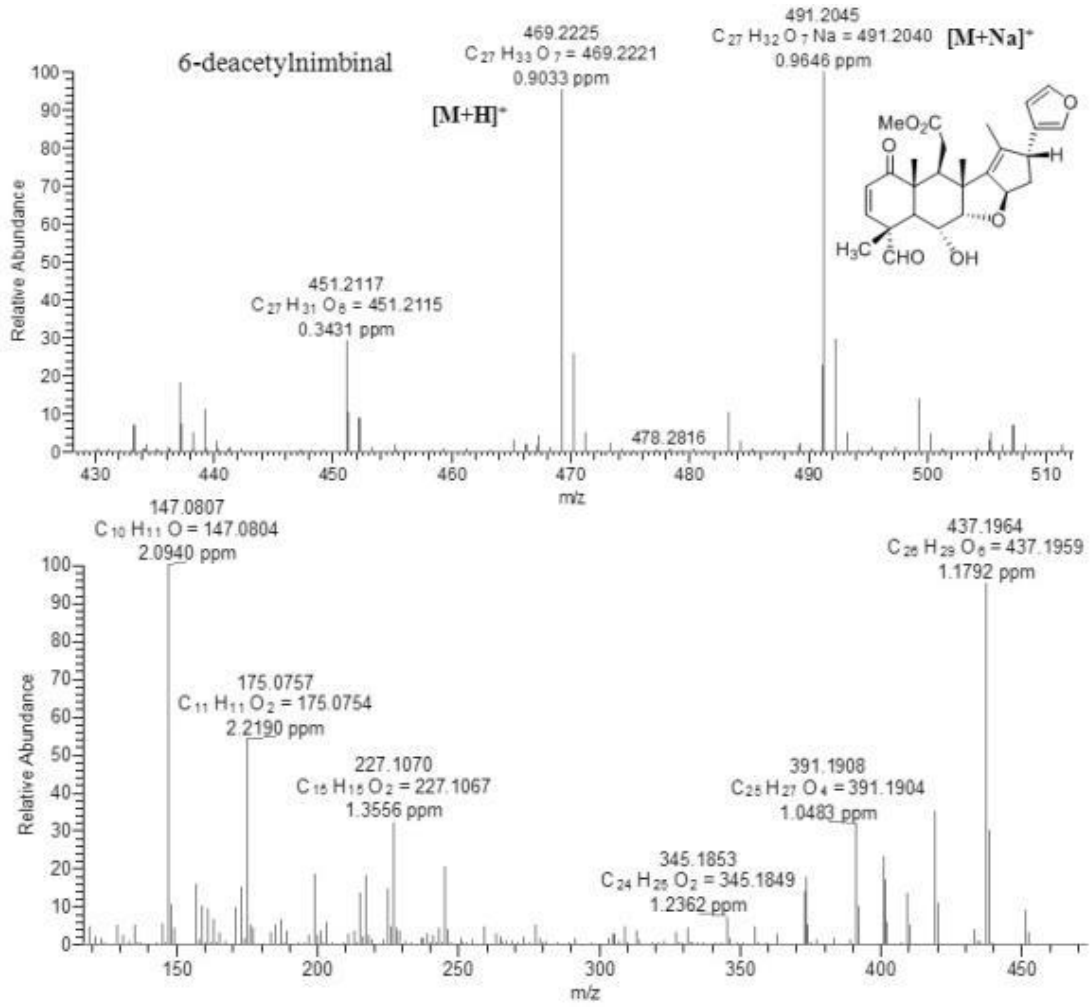

Ochinolide B

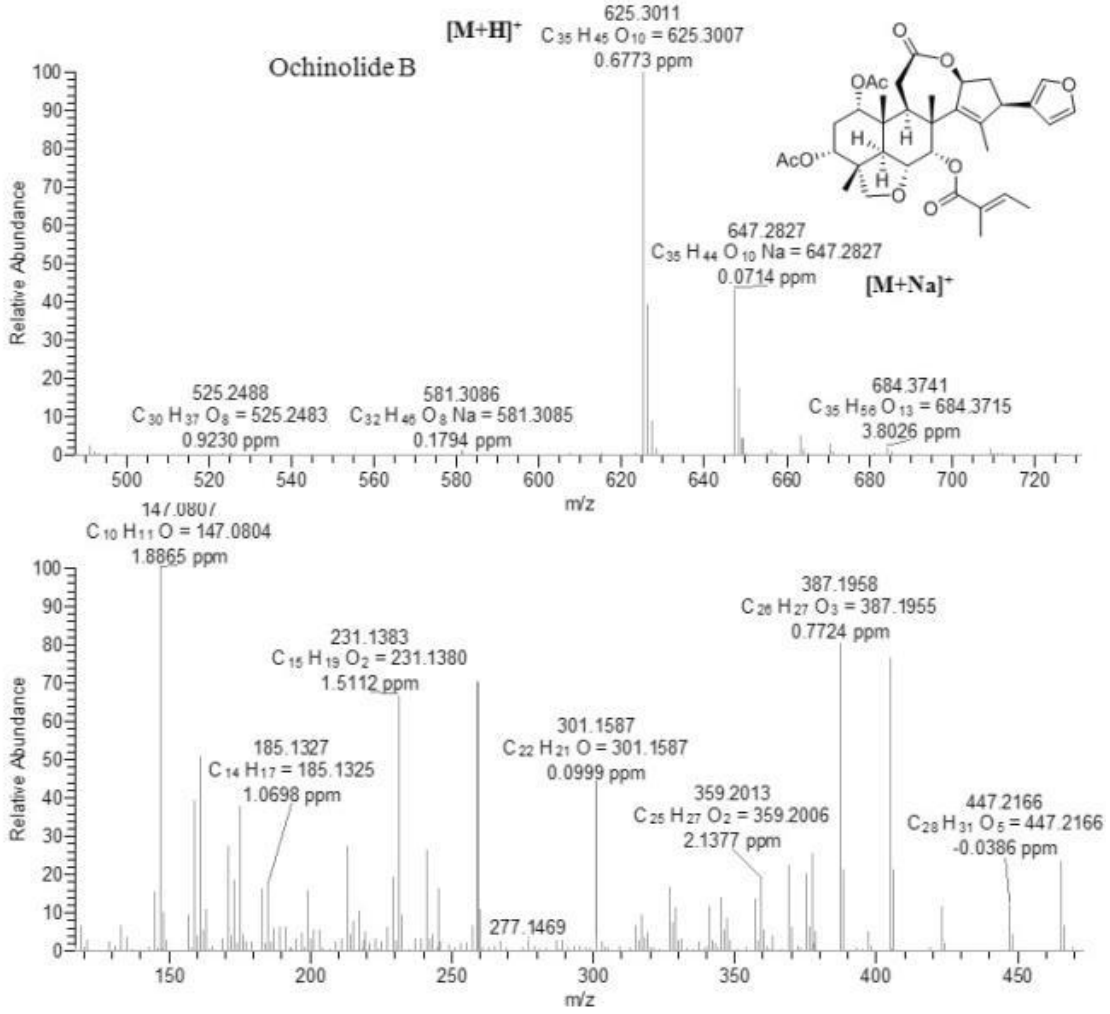

28-deoxonimbolide

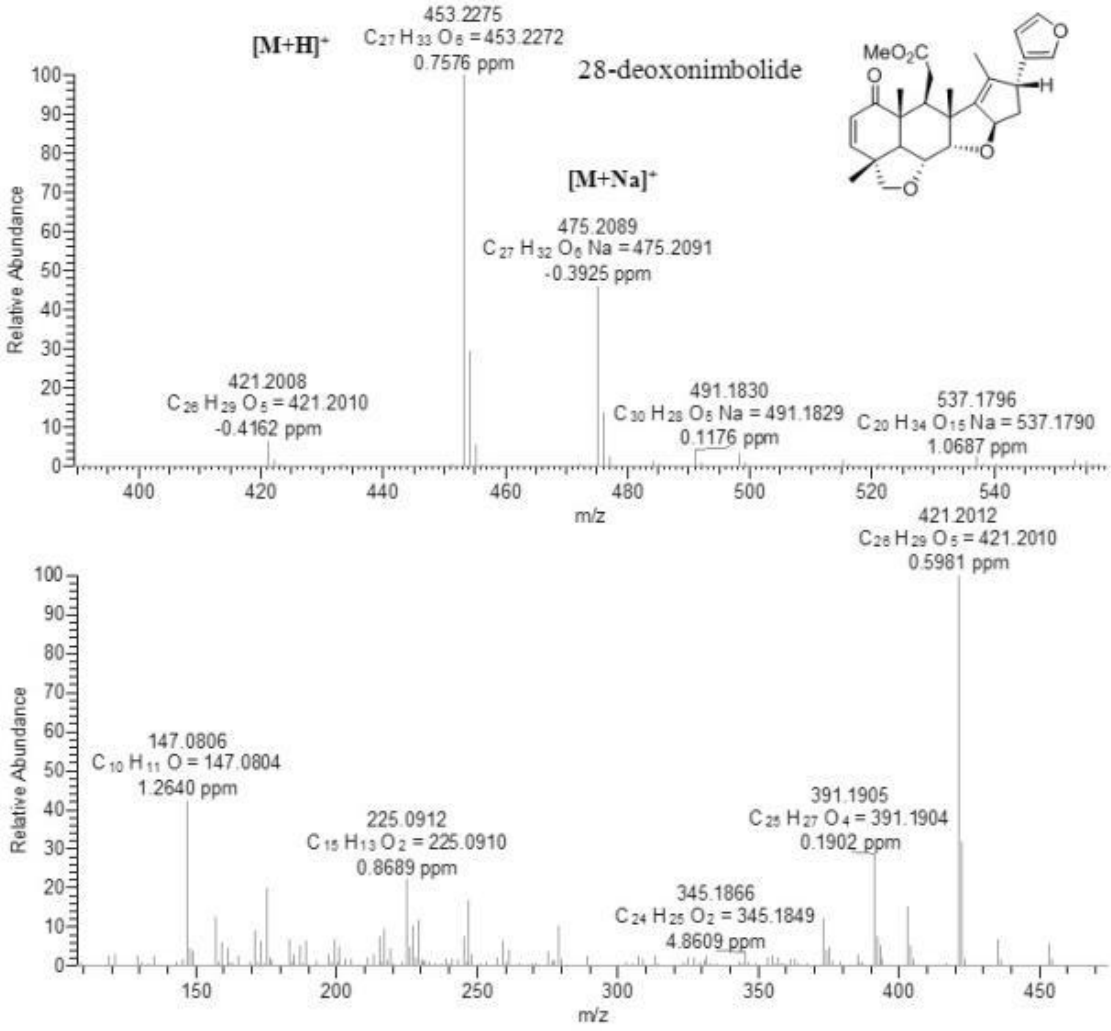

7-deacetyl-7-α-hydroxygedunin

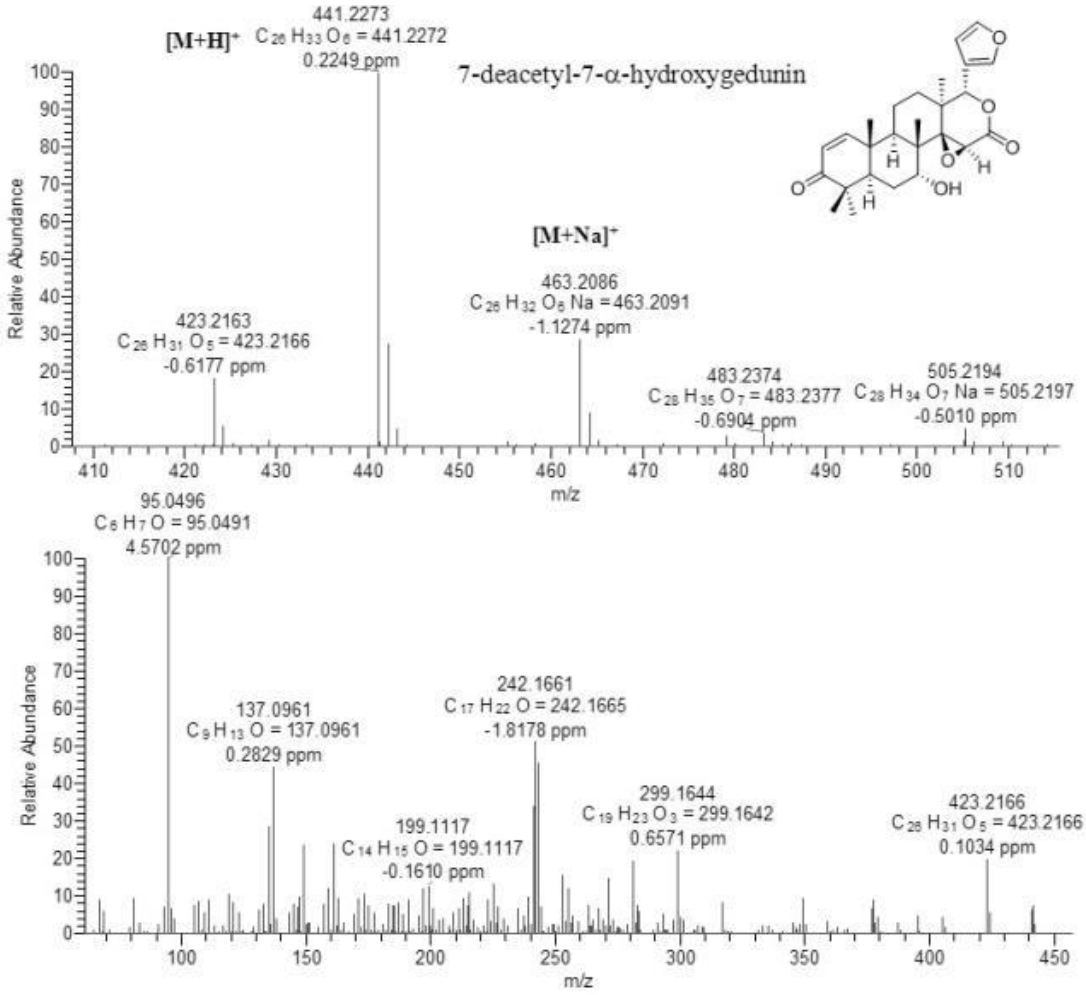

7-deacetyl-7-α-benzoylgedunin

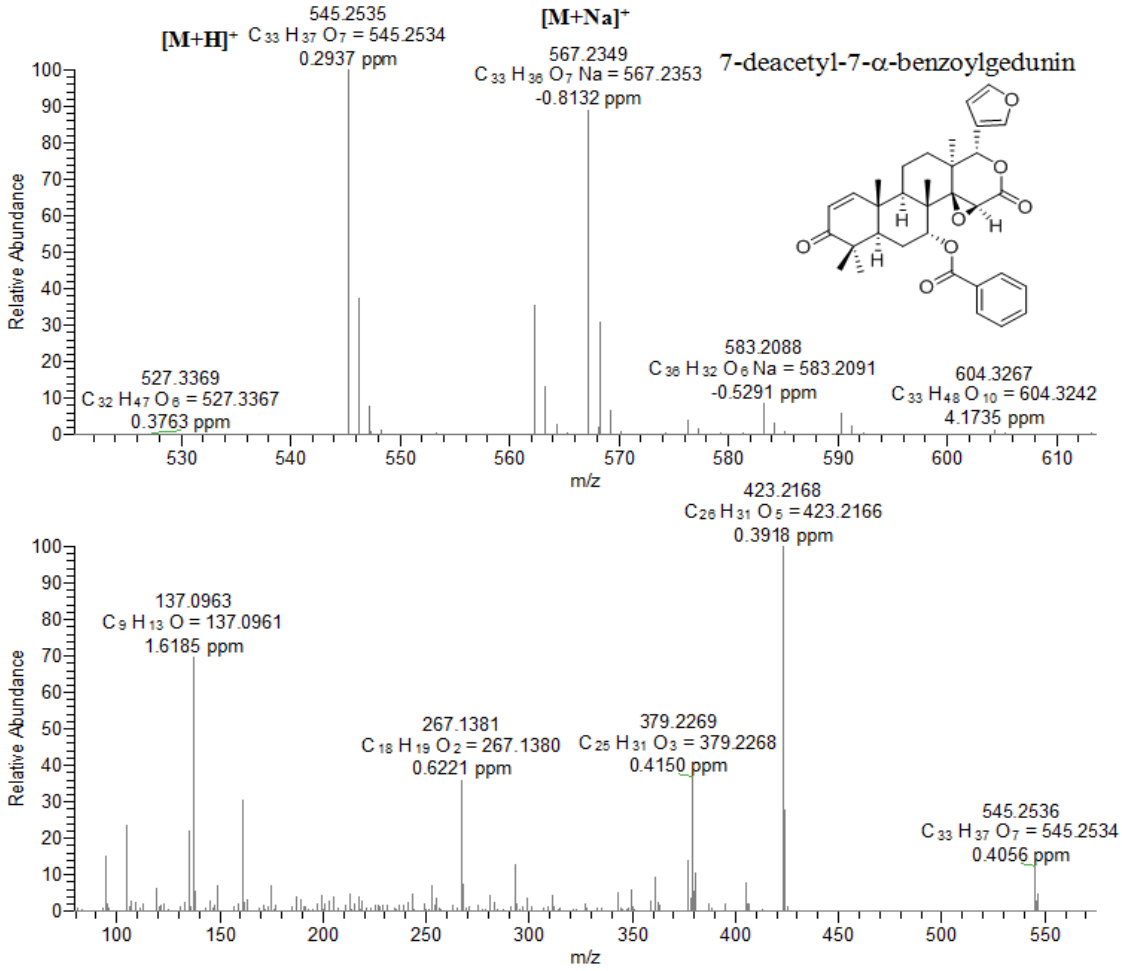

Salannol

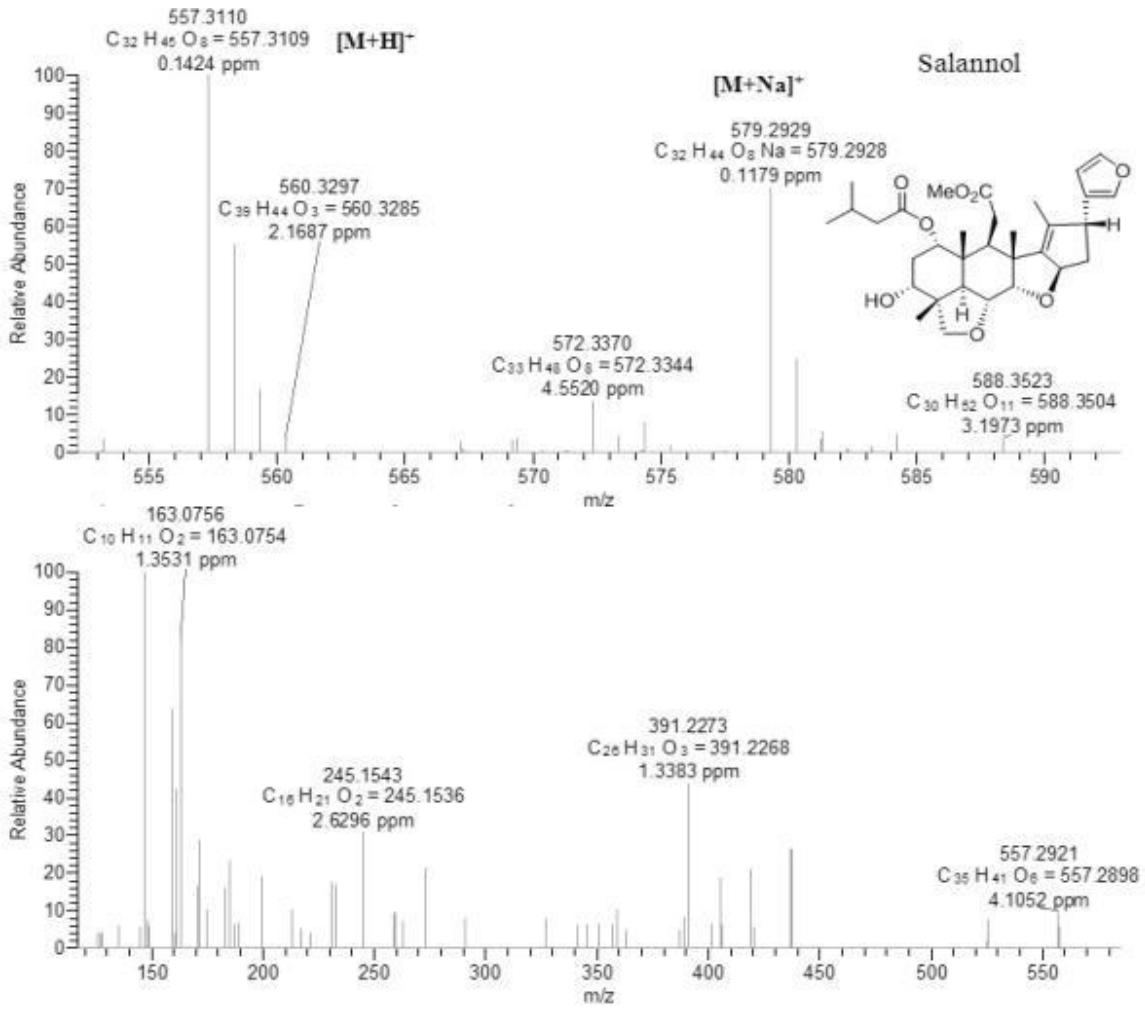
557.3110
C32 H45 O8 = 557.3109
0.1424 ppm
[M+H]+
Salannol
[M+Na]+
579.2929
C32 H44 O8 Na = 579.2928
0.1179 ppm
560.3297
C39 H44 O3 = 560.3285
2.1687 ppm
572.3370
C33 H48 O8 = 572.3344
4.5520 ppm
588.3523
C30 H52 O11 = 588.3504
3.1973 ppm
Relative Abundance
m/z
163.0756
C10 H11 O2 = 163.0754
1.3531 ppm
391.2273
C26 H31 O3 = 391.2268
1.3383 ppm
245.1543
C16 H21 O2 = 245.1536
2.6296 ppm
557.2921
C35 H41 O6 = 557.2898
4.1052 ppm
Relative Abundance
m/z

Odoratone

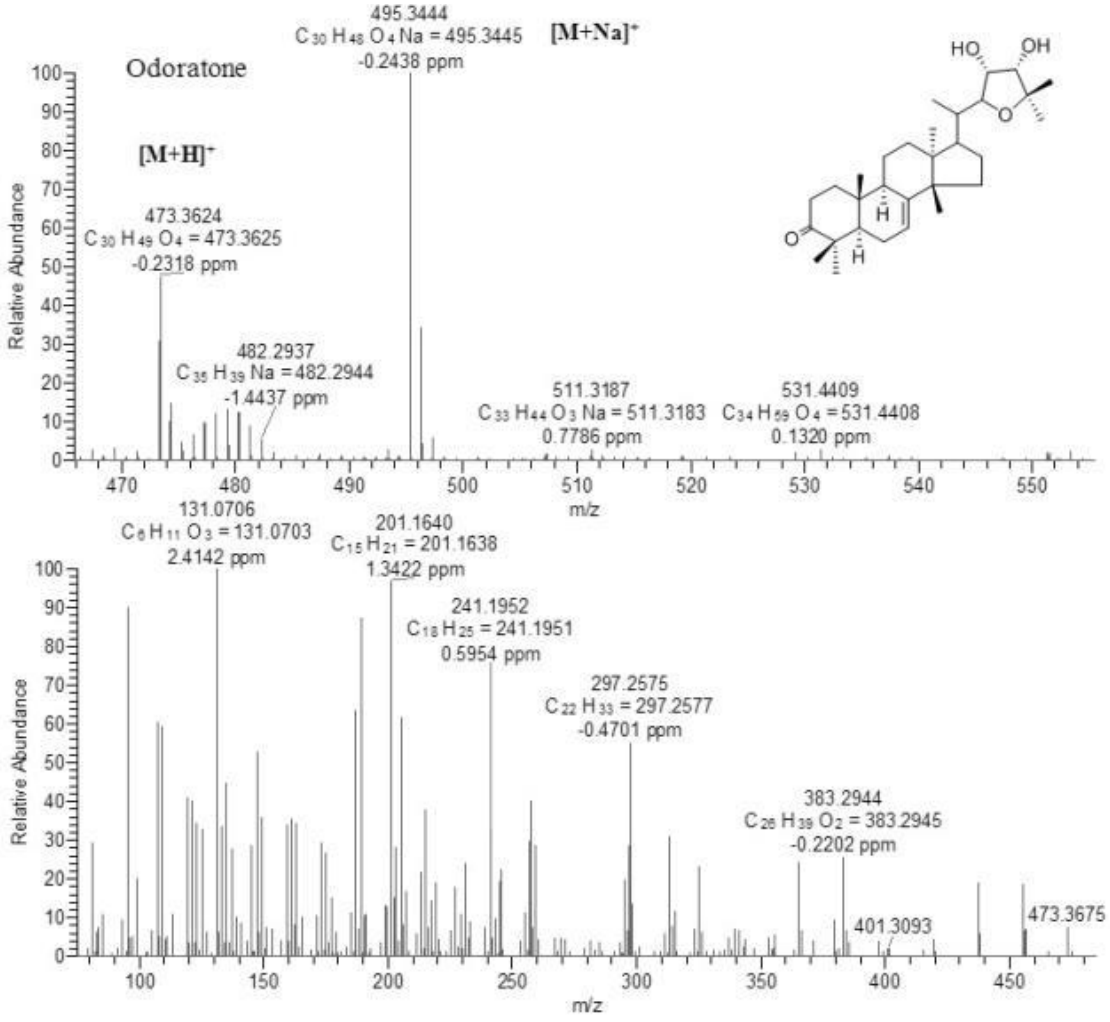
Odoratone
[M+H]+
495.3444
C30 H48 O4 Na = 495.3445
-0.2438 ppm
[M+Na]+
473.3624
C30 H49 O4 = 473.3625
-0.2318 ppm
482.2937
C35 H39 Na = 482.2944
-1.4437 ppm
511.3187
C33 H44 O3 Na = 511.3183
0.7786 ppm
531.4409
C34 H59 O4 = 531.4408
0.1320 ppm
Relative Abundance
m/z
HO
OH
O
H
H
131.0706
C8 H11 O3 = 131.0703
2.4142 ppm
201.1640
C15 H21 = 201.1638
1.3422 ppm
241.1952
C18 H25 = 241.1951
0.5954 ppm
297.2575
C22 H33 = 297.2577
-0.4701 ppm
383.2944
C26 H39 O2 = 383.2945
-0.2202 ppm
401.3093
473.3675
Relative Abundance
m/z

Ochinin acetate

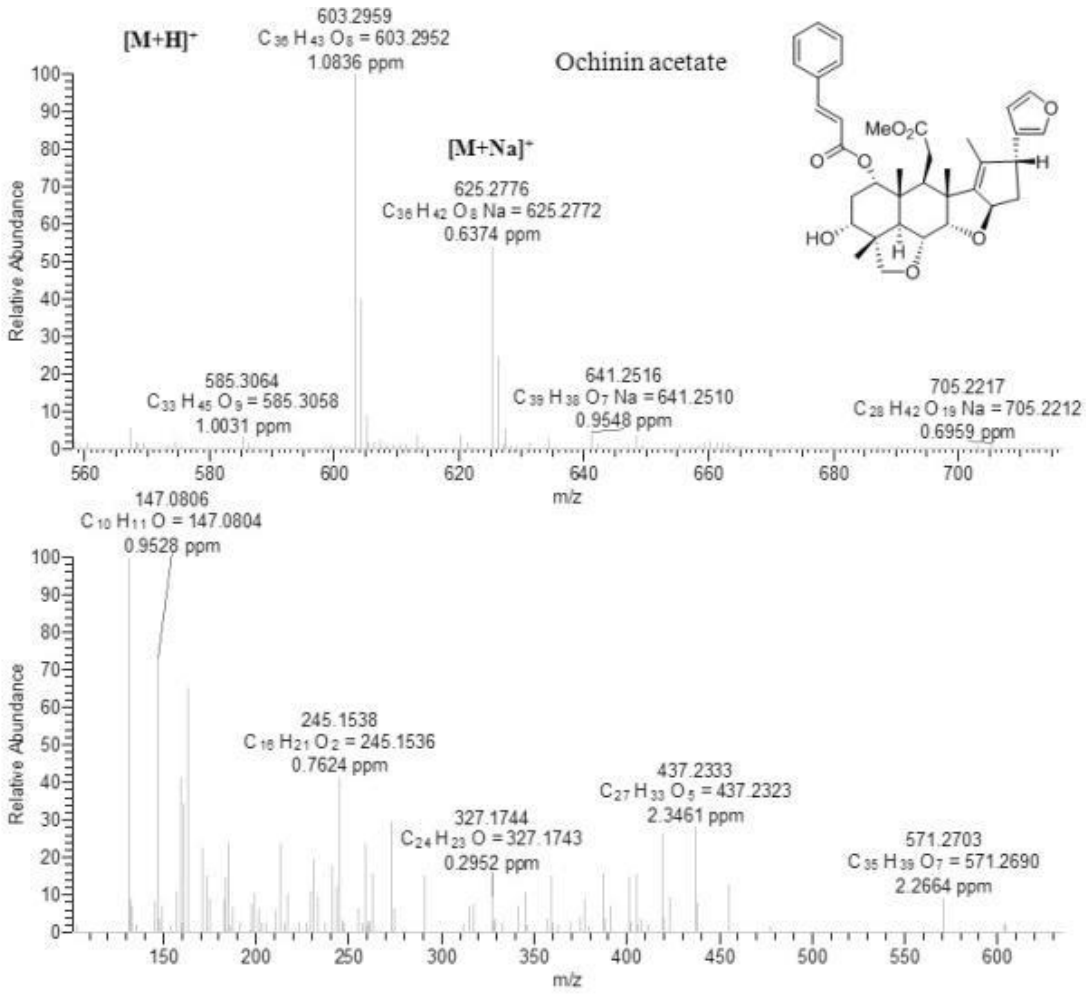

7-benzoylazadiradione

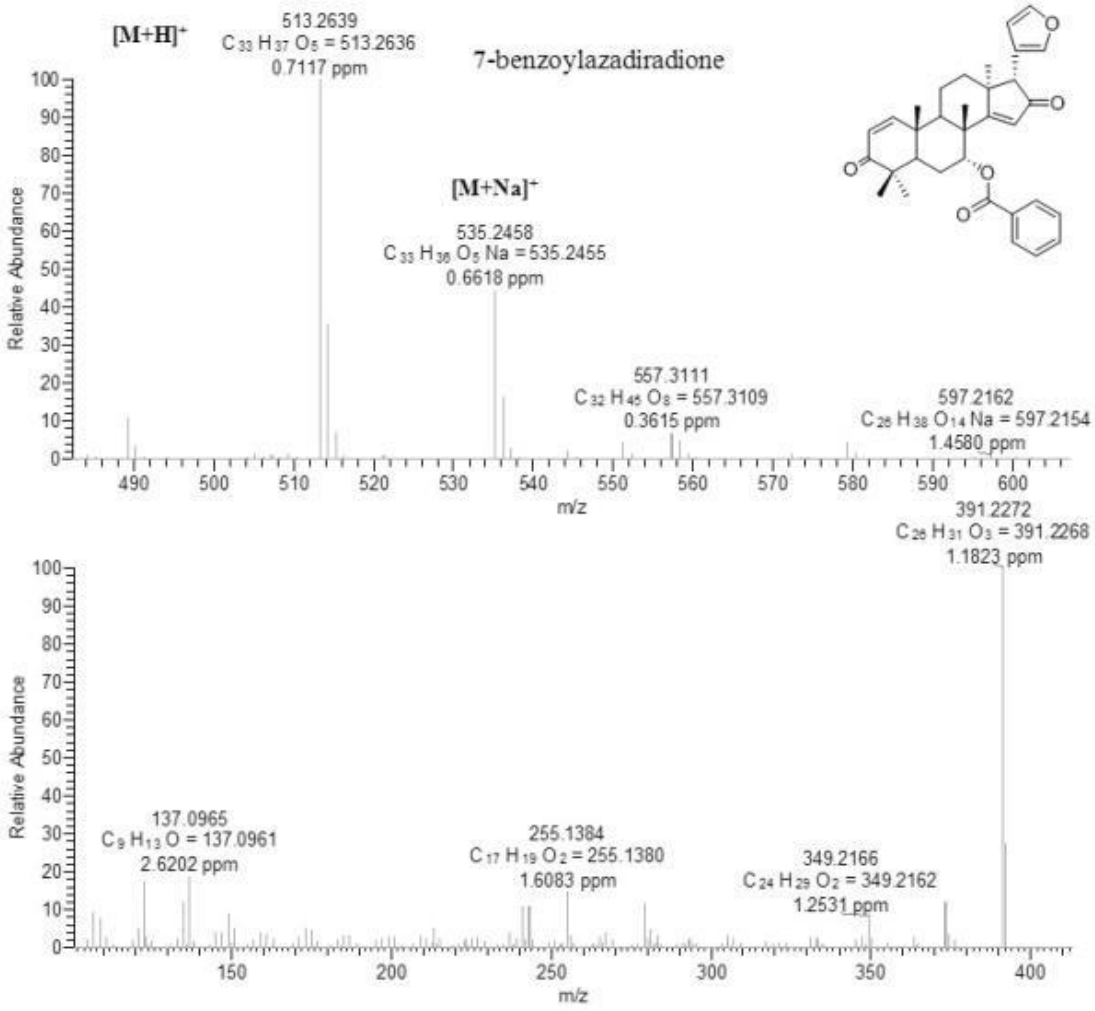

17-hydroxyazadiradione

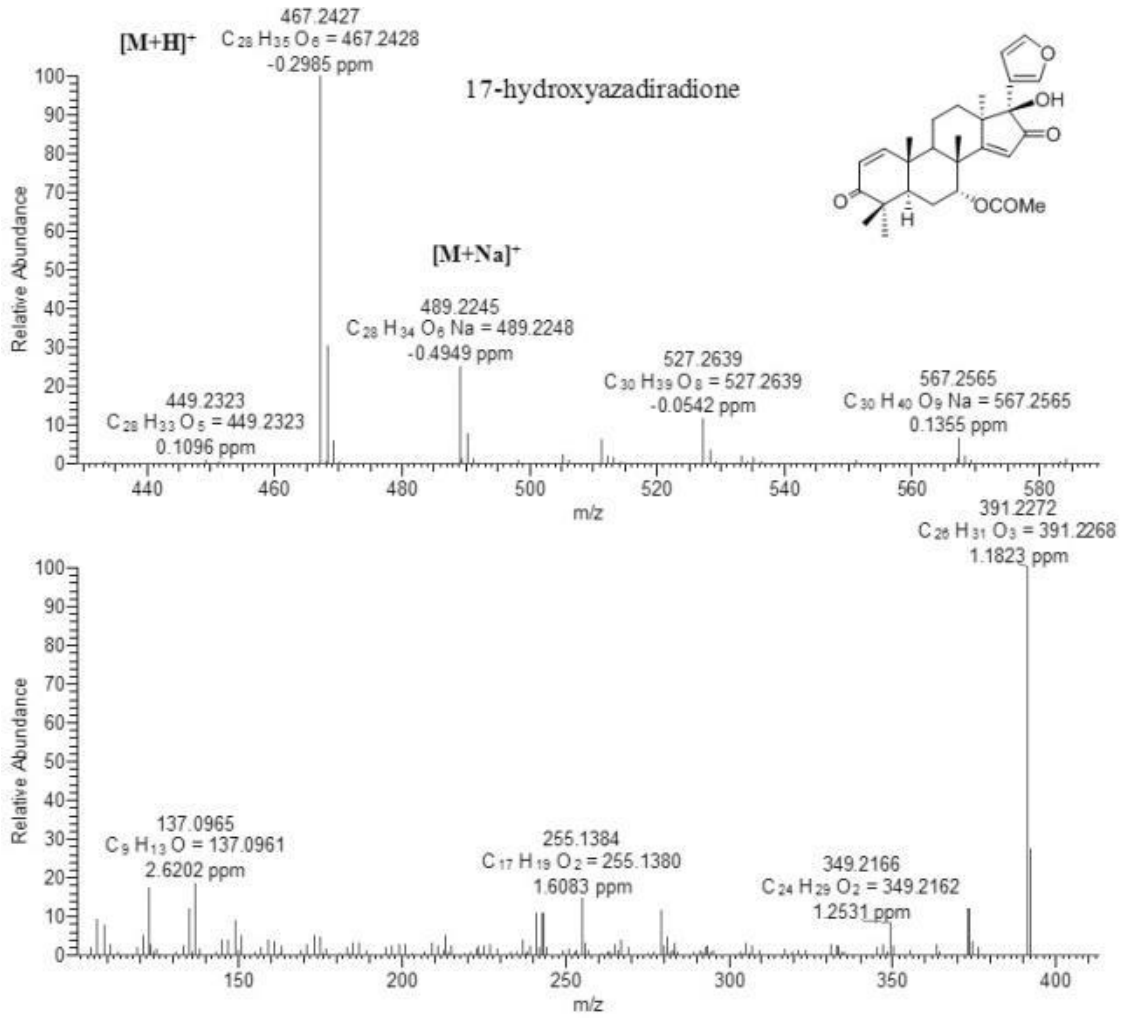

Nimbolide

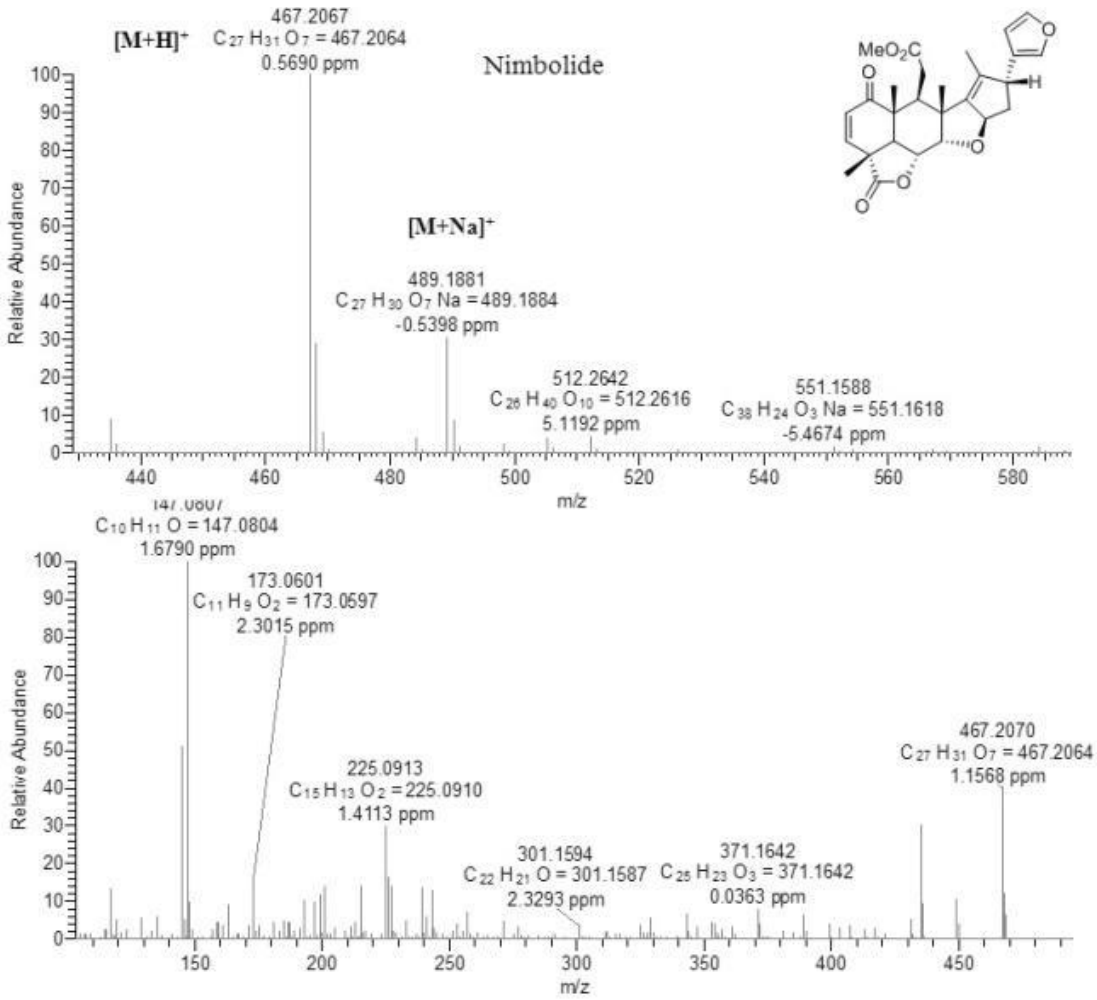
[M+H]+
467.2067
C27 H31 O7 = 467.2064
0.5690 ppm
Nimbolide
MeO2C
[M+Na]+
489.1881
C27 H30 O7 Na = 489.1884
-0.5398 ppm
512.2642
C26 H40 O10 = 512.2616
5.1192 ppm
551.1588
C38 H24 O3 Na = 551.1618
-5.4674 ppm
Relative Abundance
m/z
C10 H11 O = 147.0804
1.6790 ppm
173.0601
C11 H9 O2 = 173.0597
2.3015 ppm
225.0913
C15 H13 O2 = 225.0910
1.4113 ppm
301.1594
C22 H21 O = 301.1587
2.3293 ppm
371.1642
C25 H23 O3 = 371.1642
0.0363 ppm
467.2070
C27 H31 O7 = 467.2064
1.1568 ppm

3-deacetylazadirachtin A

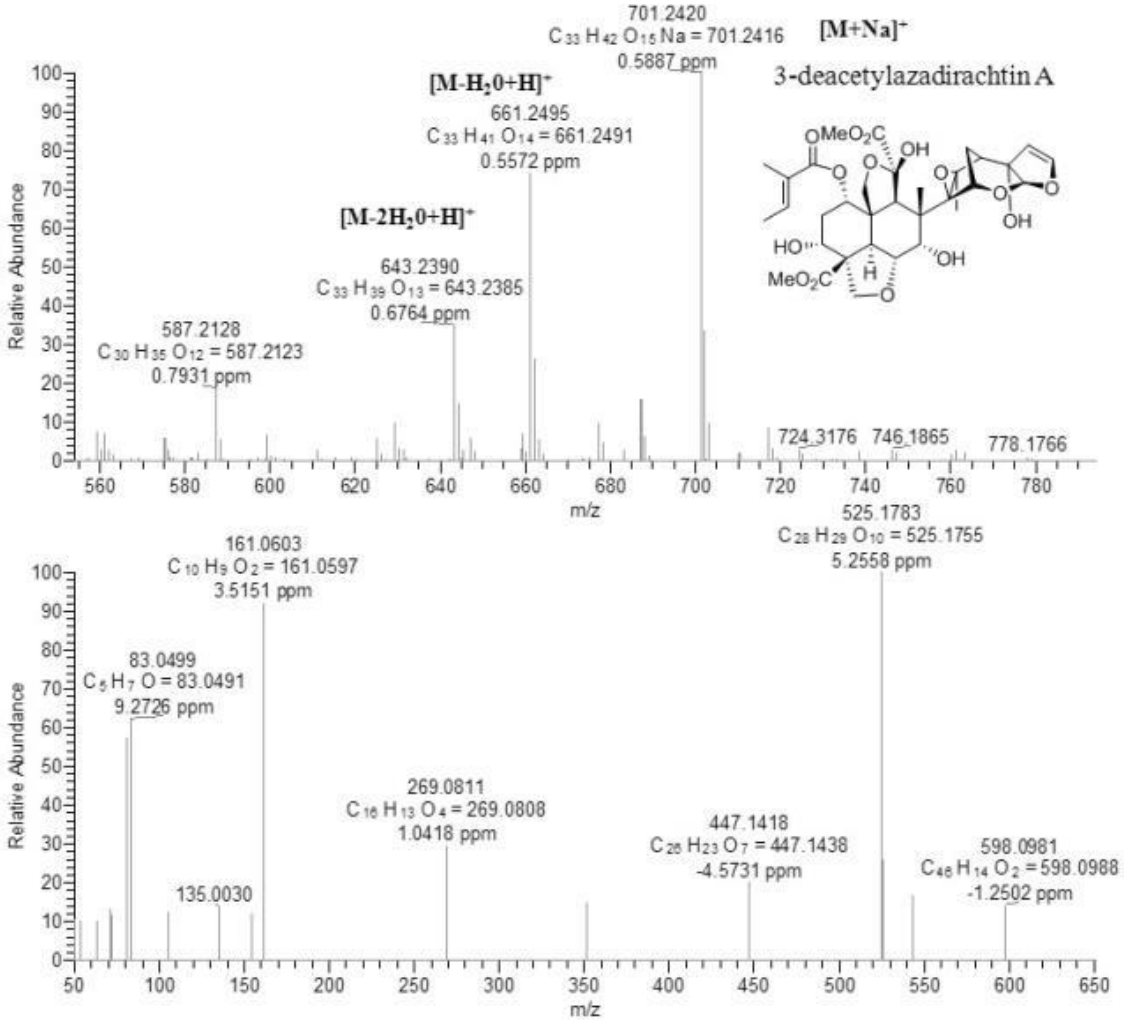

Salimuzzalin

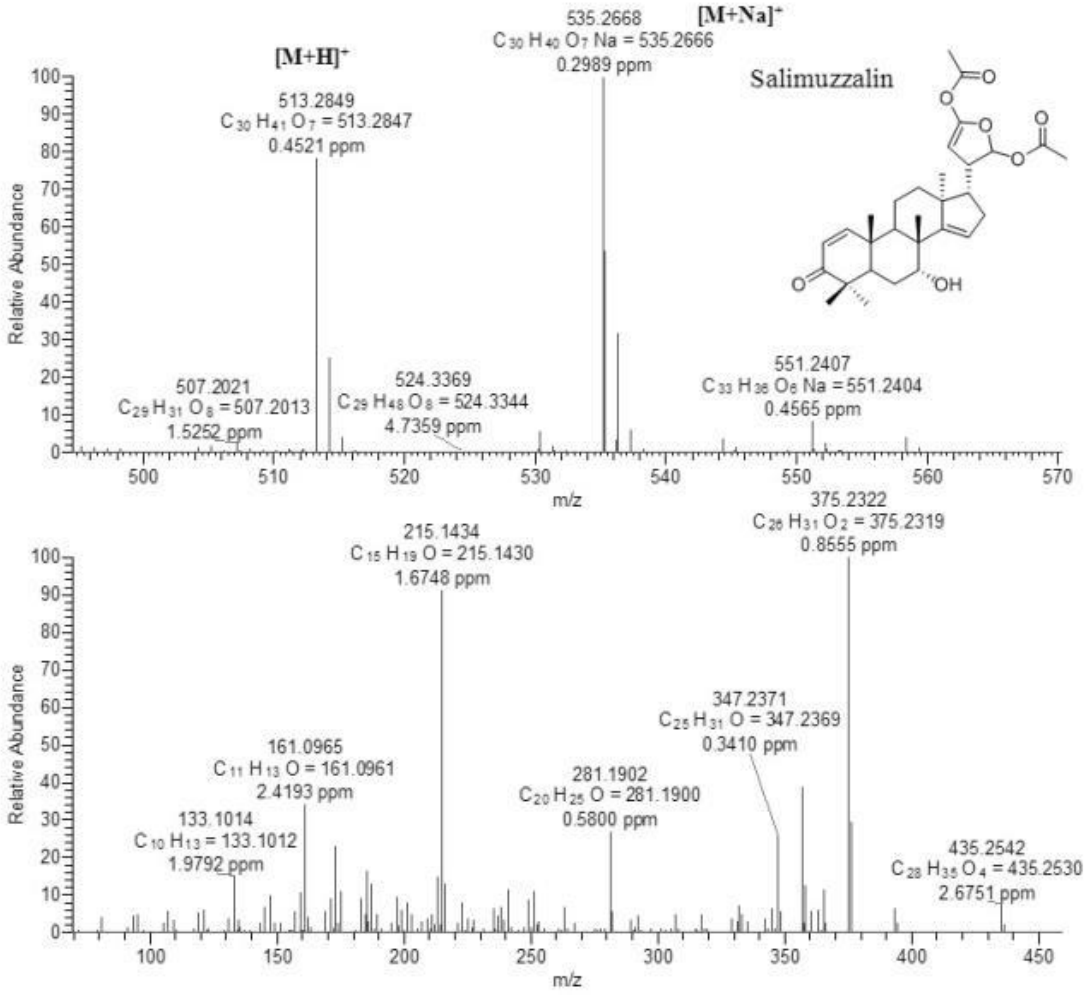

Figure 2B.5.1. Mass spectra and the corresponding MS/MS fragmentation pattern for the 15 identified limonoids from neem latex.

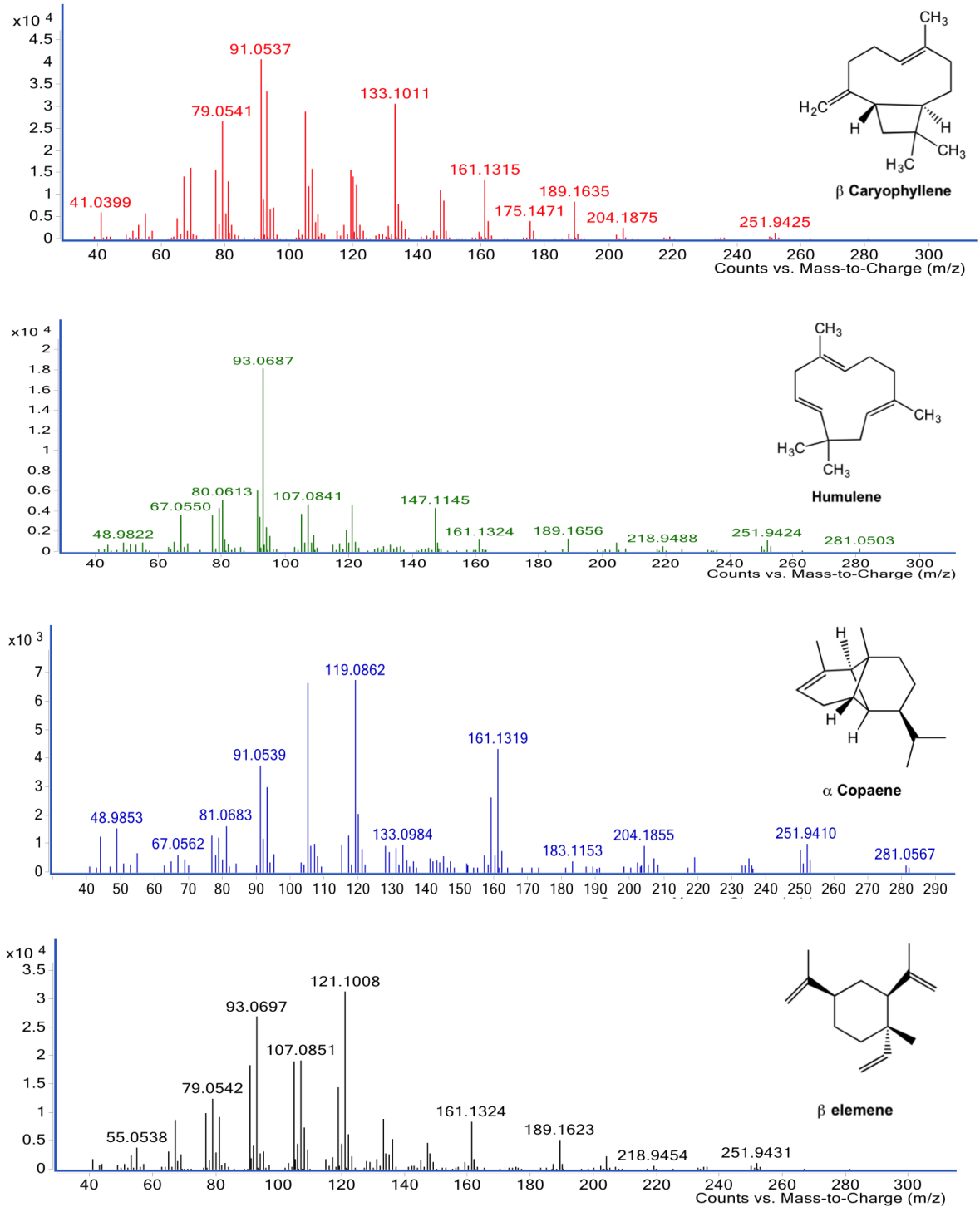

Figure 2B.5.2. Mass spectra of the major sesquiterpenes from the whole flower and the secretory vesicles isolated from neem flowers

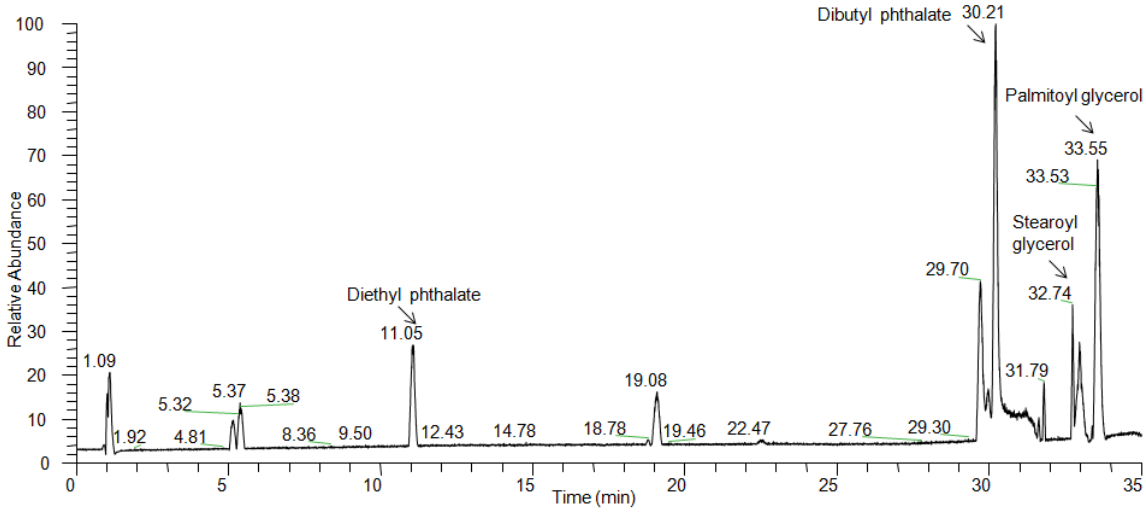

Figure 2B.5.3. Chromatogram showing secretory vesicle isolates analyzed in LC-HRMS showing triacylglycerol and phthalates.

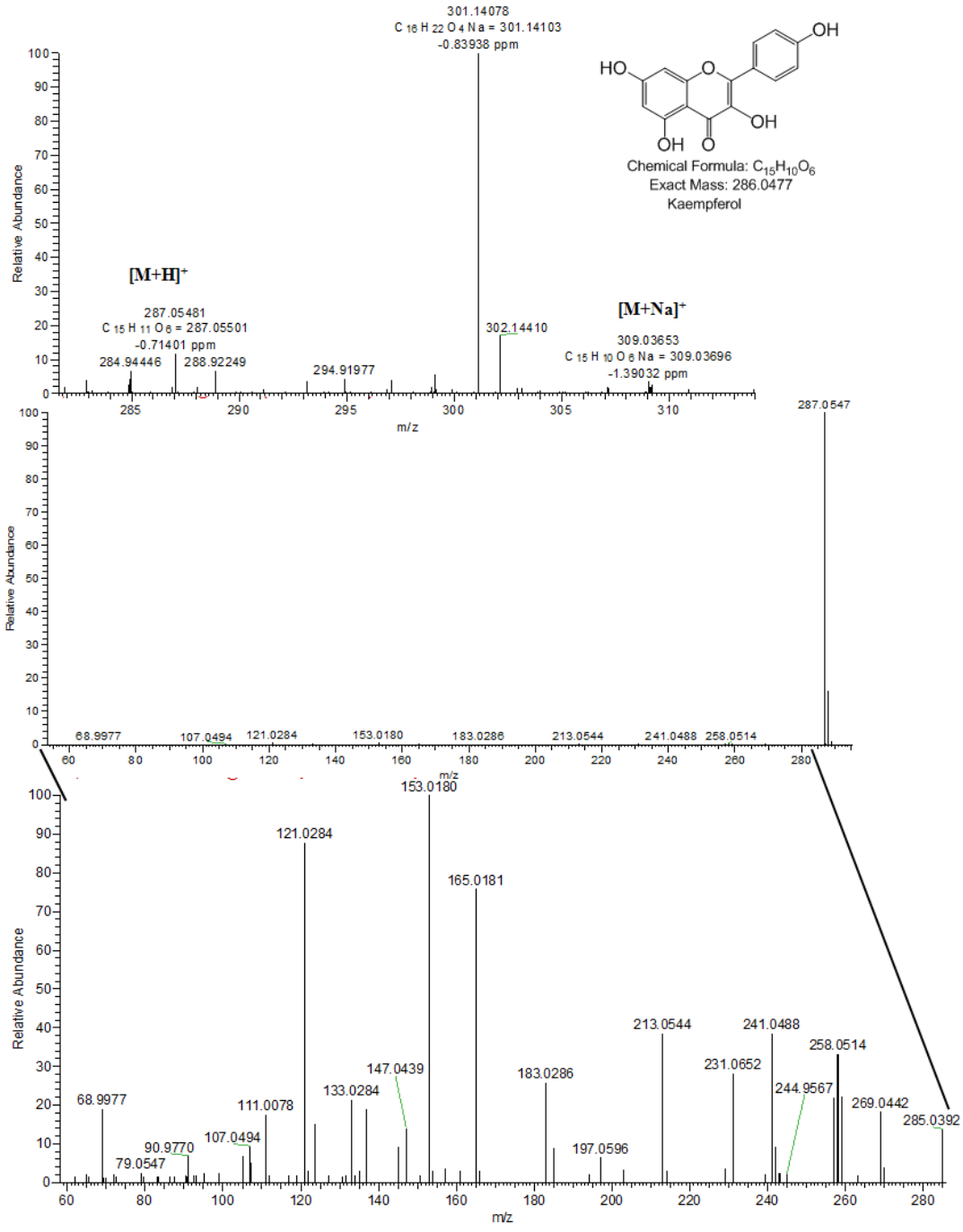
301.14078
C 16 H 22 O 4 Na = 301.14103
-0.83938 ppm
Chemical Formula: C15H10O6
Exact Mass: 286.0477
Kaempferol
[M+H]+
287.05481
C 15 H 11 O 6 = 287.05501
-0.71401 ppm
284.94446
288.92249
294.91977
302.14410
[M+Na]+
309.03653
C 15 H 10 O 6 Na = 309.03696
-1.39032 ppm
Relative Abundance
m/z
287.0547
68.9977
107.0494
121.0284
153.0180
183.0286
213.0544
241.0488
258.0514
153.0180
121.0284
165.0181
213.0544
241.0488
258.0514
147.0439
183.0286
231.0652
133.0284
244.9567
269.0442
68.9977
111.0078
285.0392
107.0494
90.9770
197.0596
79.0547

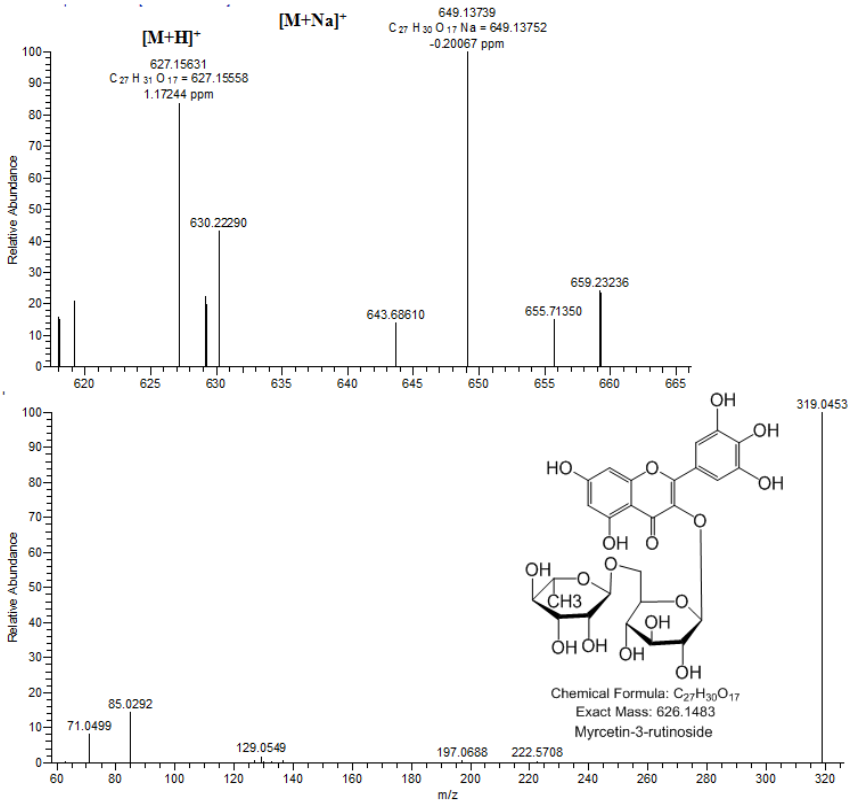
[M+H]+
627.15631
C 27 H 31 O 17 = 627.15558
1.17244 ppm
[M+Na]+
649.13739
C 27 H 30 O 17 Na = 649.13752
-0.20067 ppm
630.22290
643.68610
655.71350
659.23236
Relative Abundance
m/z
319.0453
85.0292
71.0499
129.0549
197.0688
222.5708
Chemical Formula: C27H30O17
Exact Mass: 626.1483
Myrcetin-3-rutinoside

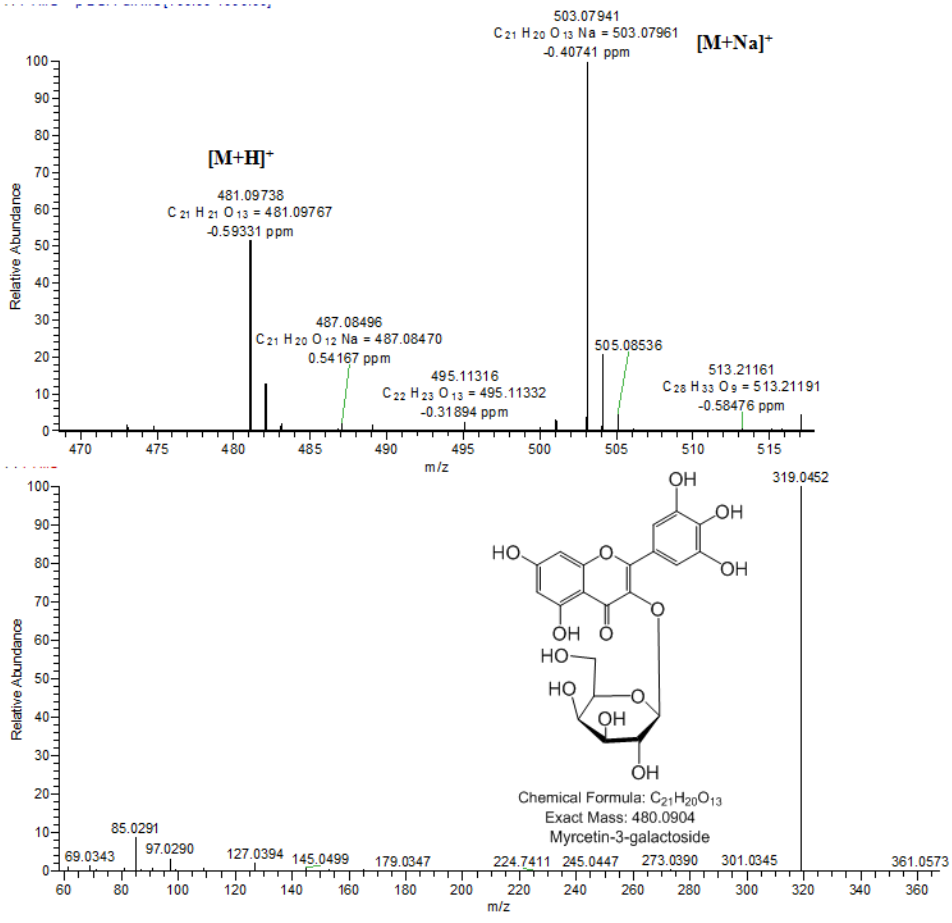
503.07941
C 21 H 20 O 13 Na = 503.07961
-0.40741 ppm
[M+Na]+
[M+H]+
481.09738
C 21 H 21 O 13 = 481.09767
-0.59331 ppm
487.08496
C 21 H 20 O 12 Na = 487.08470
0.54167 ppm
495.11316
C 22 H 23 O 13 = 495.11332
-0.31894 ppm
505.08536
513.21161
C 28 H 33 O 9 = 513.21191
-0.58476 ppm
Relative Abundance
m/z
319.0452
85.0291
69.0343
97.0290
127.0394
145.0499
179.0347
224.7411
245.0447
273.0390
301.0345
361.0573
Chemical Formula: C21H20O13
Exact Mass: 480.0904
Myrcetin-3-galactoside

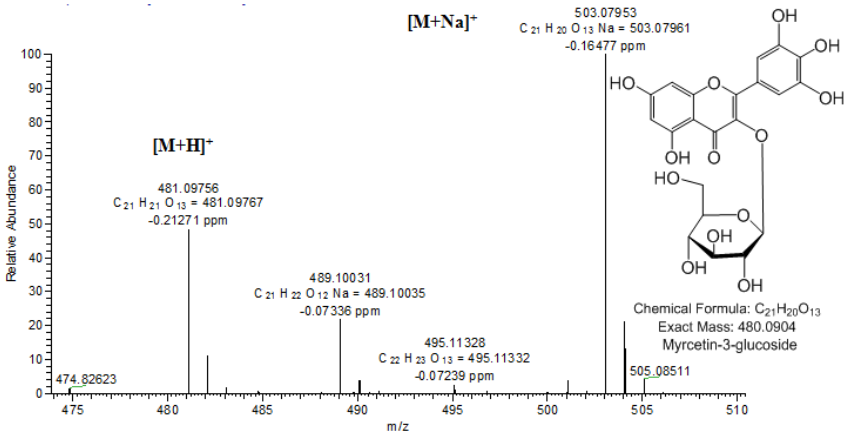
[M+Na]+
503.07953
C 21 H 20 O 13 Na = 503.07961
-0.16477 ppm
[M+H]+
481.09756
C 21 H 21 O 13 = 481.09767
-0.21271 ppm
489.10031
C 21 H 22 O 12 Na = 489.10035
-0.07336 ppm
495.11328
C 22 H 23 O 13 = 495.11332
-0.07239 ppm
474.82623
505.08511
Relative Abundance
m/z
Chemical Formula: C21H20O13
Exact Mass: 480.0904
Myrcetin-3-glucoside

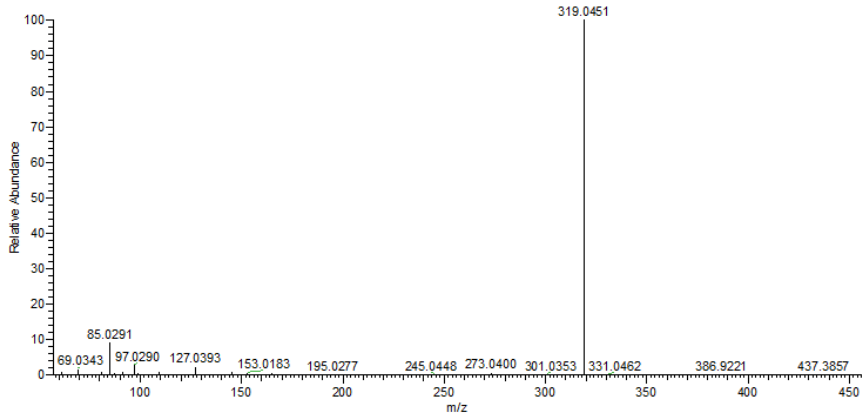
319.0451
85.0291
69.0343
97.0290
127.0393
153.0183
195.0277
245.0448
273.0400
301.0353
331.0462
386.9221
437.3857
Relative Abundance
m/z

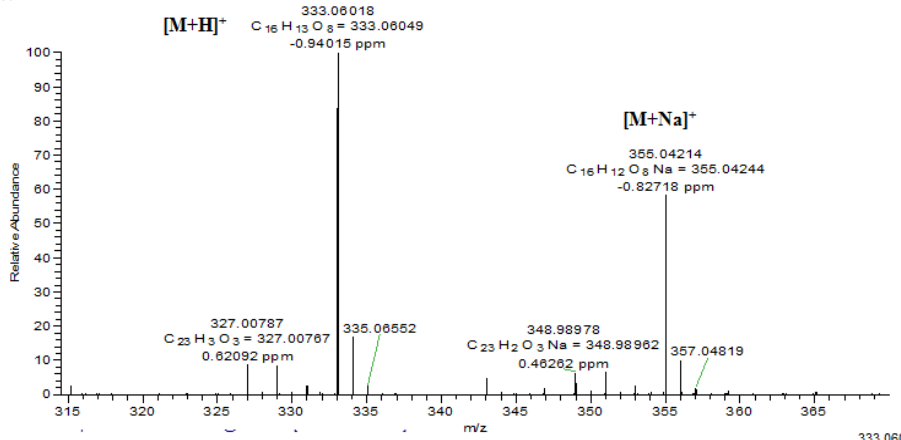
[M+H]+
333.06018
C 16 H 13 O 8 = 333.06049
-0.94015 ppm
[M+Na]+
355.04214
C 16 H 12 O 8 Na = 355.04244
-0.82718 ppm
327.00787
C 23 H 3 O 3 = 327.00767
0.62092 ppm
335.06552
348.98978
C 23 H 2 O 3 Na = 348.98962
0.46262 ppm
357.04819
Relative Abundance
m/z

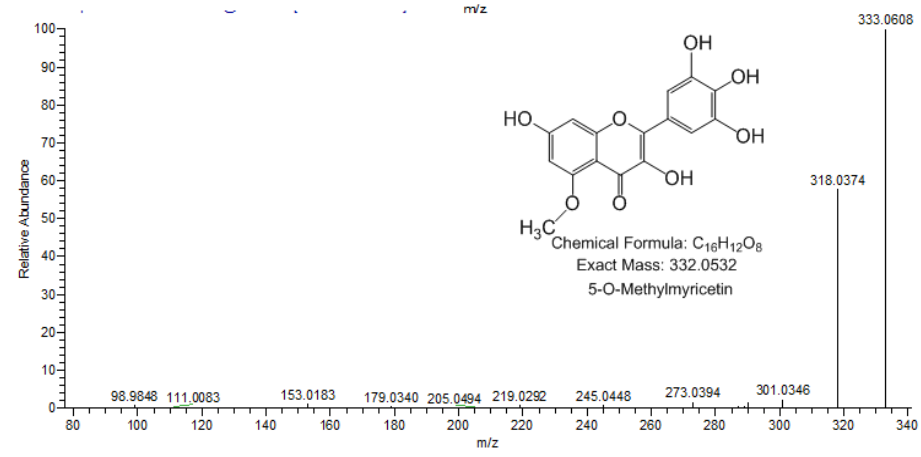
333.0608
318.0374
98.9848
111.0083
153.0183
179.0340
205.0494
219.0292
245.0448
273.0394
301.0346
Relative Abundance
m/z
Chemical Formula: C16H12O8
Exact Mass: 332.0532
5-O-Methylmyricetin

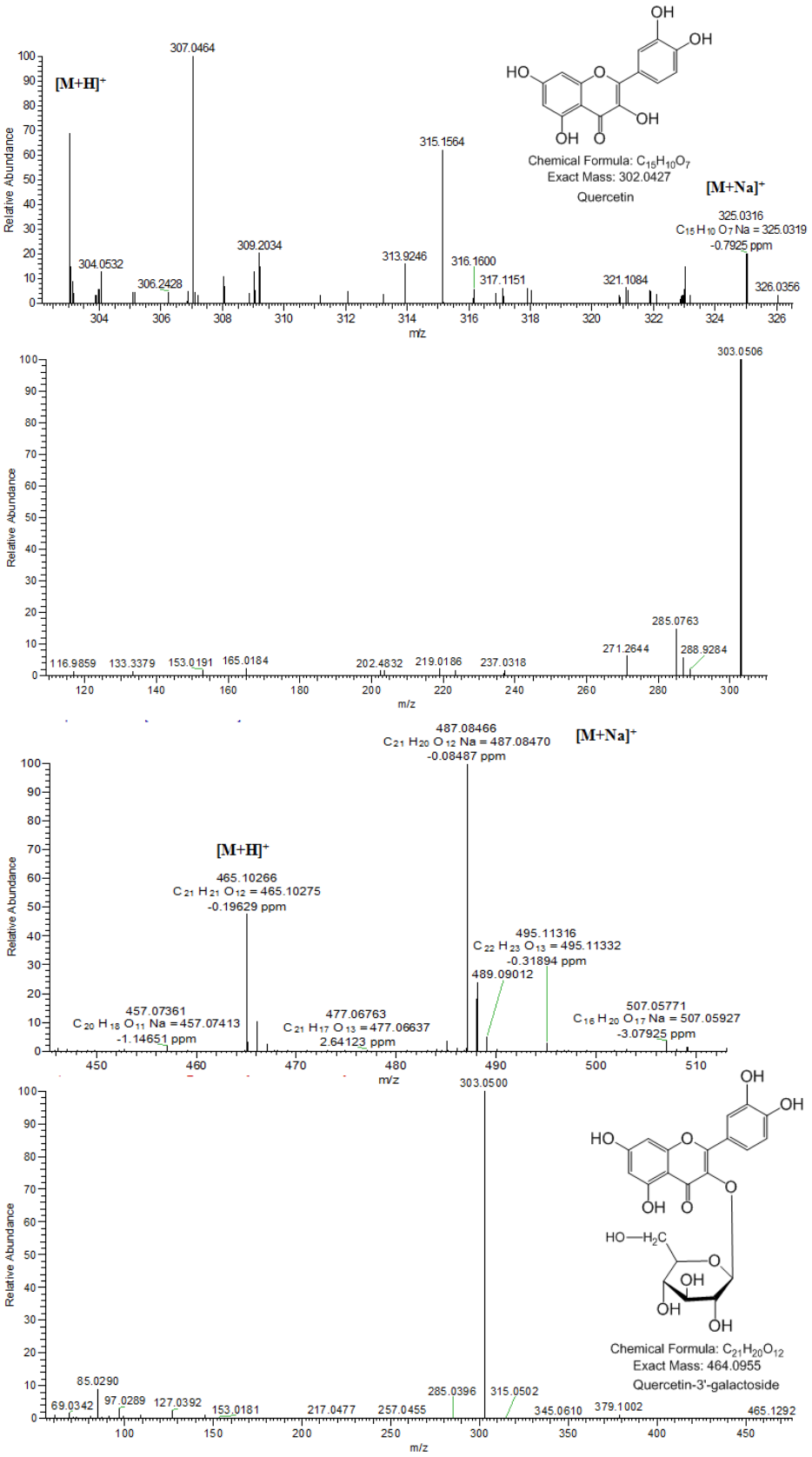
[M+H]+
307.0464
315.1564
309.2034
313.9246
316.1600
304.0532
306.2428
317.1151
321.1084
326.0356
[M+Na]+
325.0316
C15 H10 O7 Na = 325.0319
-0.7925 ppm
Chemical Formula: C15H10O7
Exact Mass: 302.0427
Quercetin
Relative Abundance
m/z
303.0506
285.0763
271.2644
288.9284
116.9859
133.3379
153.0191
165.0184
202.4832
219.0186
237.0318
487.08466
C21 H20 O12 Na = 487.08470
-0.08487 ppm
[M+Na]+
[M+H]+
465.10266
C21 H21 O12 = 465.10275
-0.19629 ppm
495.11316
C22 H23 O13 = 495.11332
-0.31894 ppm
489.09012
457.07361
C20 H18 O11 Na = 457.07413
-1.14651 ppm
477.06763
C21 H17 O13 = 477.06637
2.64123 ppm
507.05771
C16 H20 O17 Na = 507.05927
-3.07925 ppm
303.0500
85.0290
69.0342
97.0289
127.0392
153.0181
217.0477
257.0455
285.0396
315.0502
345.0610
379.1002
465.1292
Chemical Formula: C21H20O12
Exact Mass: 464.0955
Quercetin-3'-galactoside

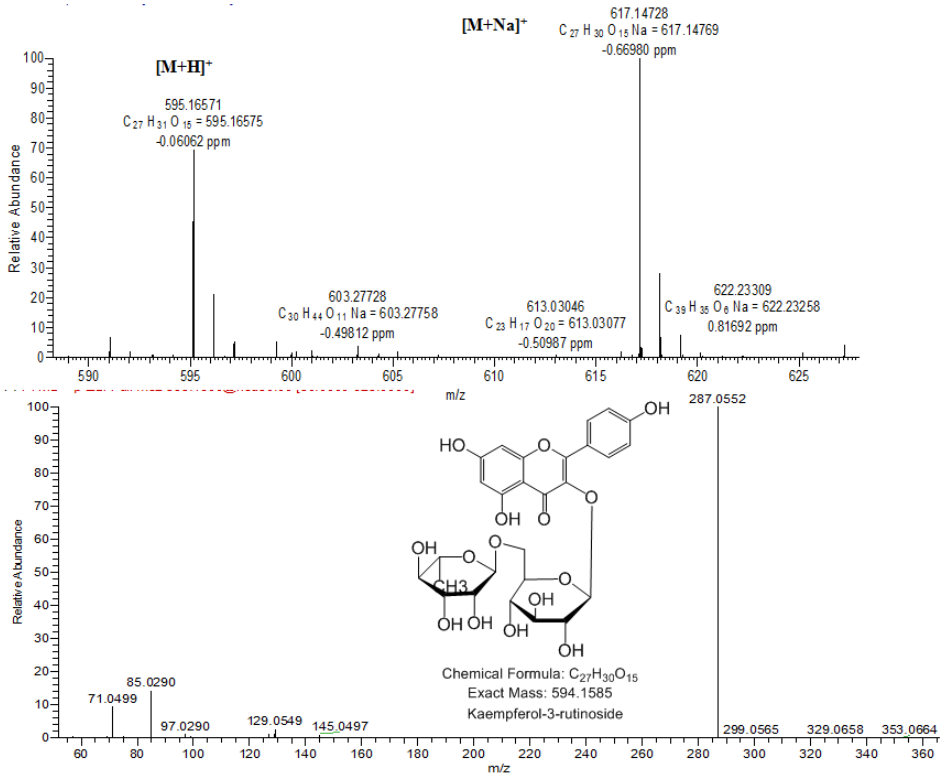
[M+Na]+
617.14728
C 27 H 30 O 15 Na = 617.14769
-0.66980 ppm
[M+H]+
595.16571
C 27 H 31 O 15 = 595.16575
-0.06062 ppm
603.27728
C 30 H 44 O 11 Na = 603.27758
-0.49812 ppm
613.03046
C 23 H 17 O 20 = 613.03077
-0.50987 ppm
622.23309
C 39 H 35 O 6 Na = 622.23258
0.81692 ppm
Relative Abundance
m/z
287.0552
85.0290
71.0499
97.0290
129.0549
145.0497
299.0565
329.0658
353.0664
Chemical Formula: C27H30O15
Exact Mass: 594.1585
Kaempferol-3-rutinoside

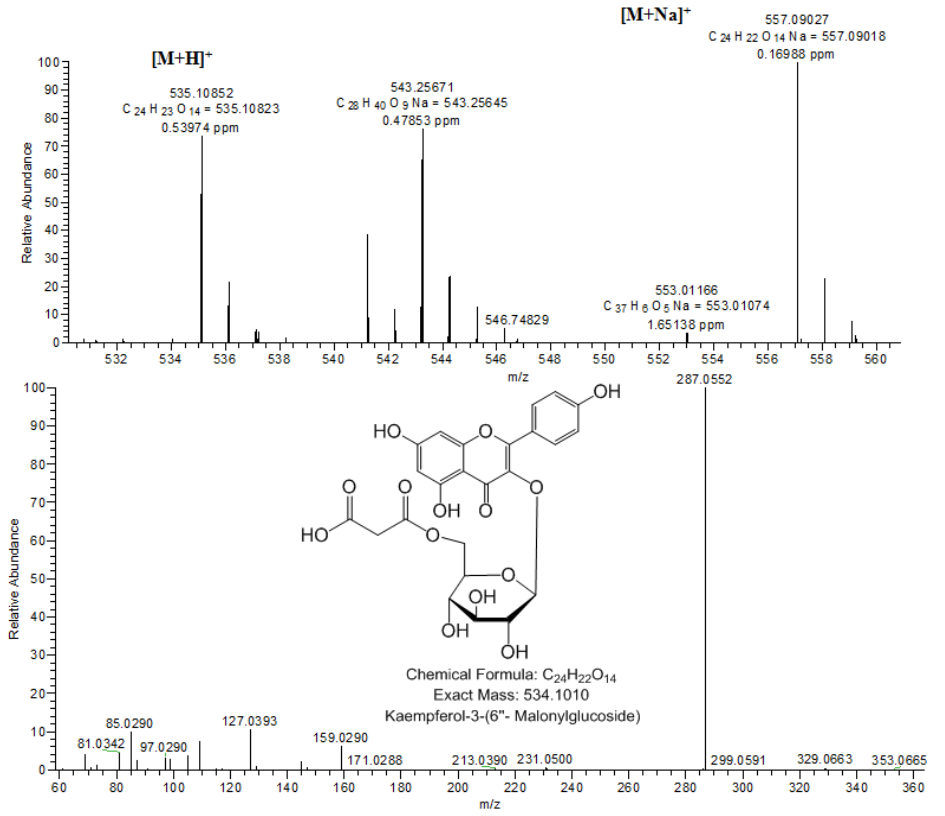
[M+Na]+
557.09027
C 24 H 22 O 14 Na = 557.09018
0.16988 ppm
[M+H]+
535.10852
C 24 H 23 O 14 = 535.10823
0.53974 ppm
543.25671
C 28 H 40 O 9 Na = 543.25645
0.47853 ppm
546.74829
553.01166
C 37 H 6 O 5 Na = 553.01074
1.65138 ppm
Relative Abundance
m/z
287.0552
85.0290
81.0342
97.0290
127.0393
159.0290
171.0288
213.0390
231.0500
299.0591
329.0663
353.0665
Chemical Formula: C24H22O14
Exact Mass: 534.1010
Kaempferol-3-(6"- Malonylglucoside)

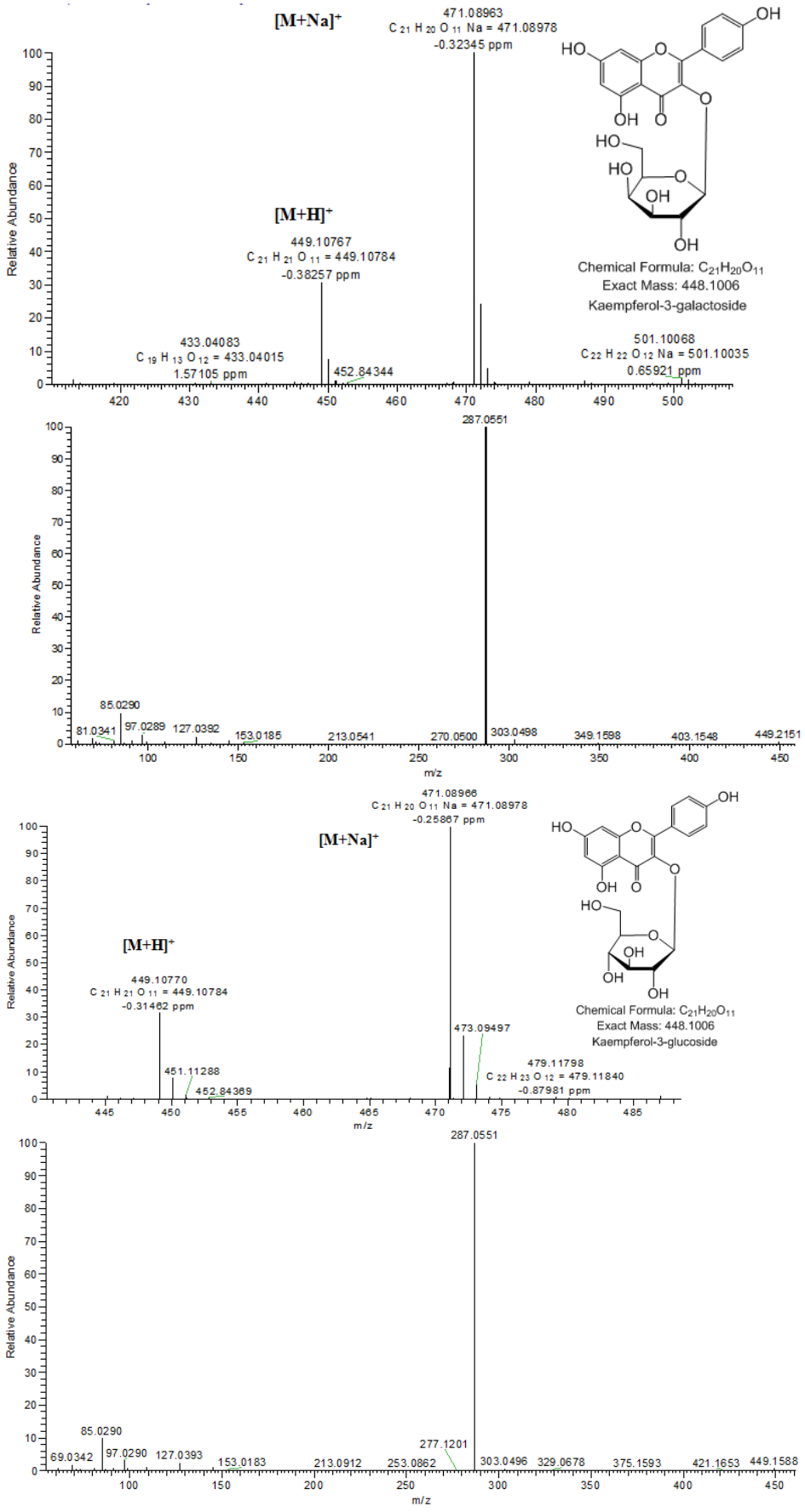
[M+Na]+
471.08963
C 21 H 20 O 11 Na = 471.08978
-0.32345 ppm
[M+H]+
449.10767
C 21 H 21 O 11 = 449.10784
-0.38257 ppm
433.04083
C 19 H 13 O 12 = 433.04015
1.57105 ppm
452.84344
501.10068
C 22 H 22 O 12 Na = 501.10035
0.65921 ppm
Chemical Formula: C21H20O11
Exact Mass: 448.1006
Kaempferol-3-galactoside
Relative Abundance
287.0551
85.0290
81.0341
97.0289
127.0392
153.0185
213.0541
270.0500
303.0498
349.1598
403.1548
449.2151
m/z
[M+Na]+
471.08966
C 21 H 20 O 11 Na = 471.08978
-0.25867 ppm
[M+H]+
449.10770
C 21 H 21 O 11 = 449.10784
-0.31462 ppm
451.11288
452.84369
473.09497
479.11798
C 22 H 23 O 12 = 479.11840
-0.87981 ppm
Chemical Formula: C21H20O11
Exact Mass: 448.1006
Kaempferol-3-glucoside
287.0551
85.0290
69.0342
97.0290
127.0393
153.0183
213.0912
253.0862
277.1201
303.0496
329.0678
375.1593
421.1653
449.1588

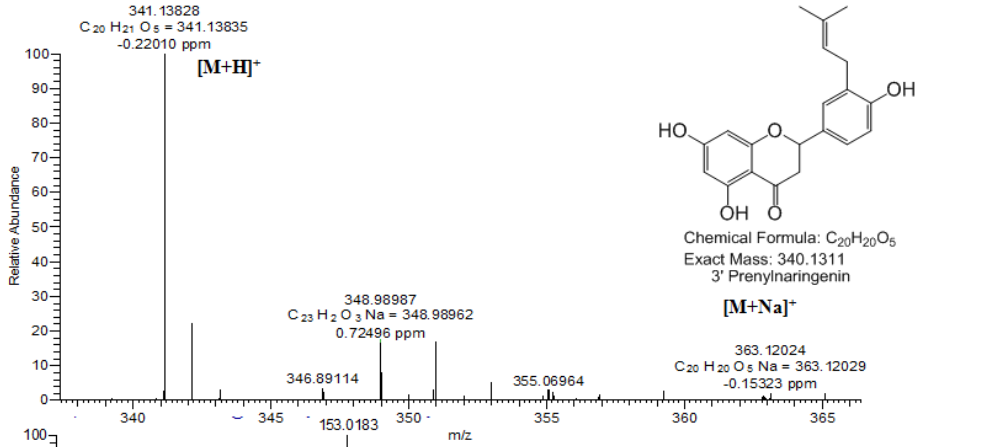
341.13828
C 20 H21 O 5 = 341.13835
-0.22010 ppm
[M+H]+
348.98987
C 23 H 2 O 3 Na = 348.98962
0.72496 ppm
346.89114
355.06964
363.12024
C 20 H 20 O 5 Na = 363.12029
-0.15323 ppm
[M+Na]+
Relative Abundance
m/z
HO
OH
OH
O
Chemical Formula: C20H20O5
Exact Mass: 340.1311
3' Prenylnaringenin

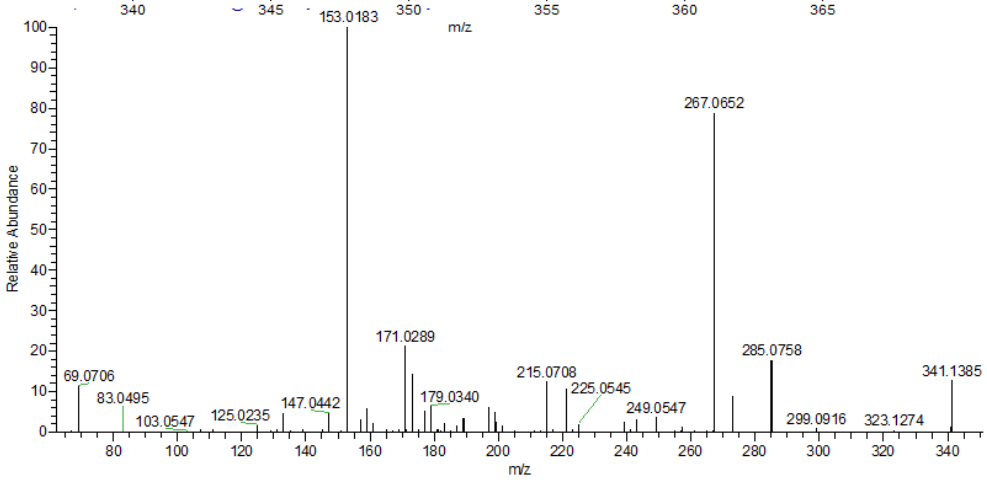
153.0183
267.0652
171.0289
285.0758
69.0706
83.0495
103.0547
125.0235
147.0442
179.0340
215.0708
225.0545
249.0547
299.0916
323.1274
341.1385
Relative Abundance
m/z

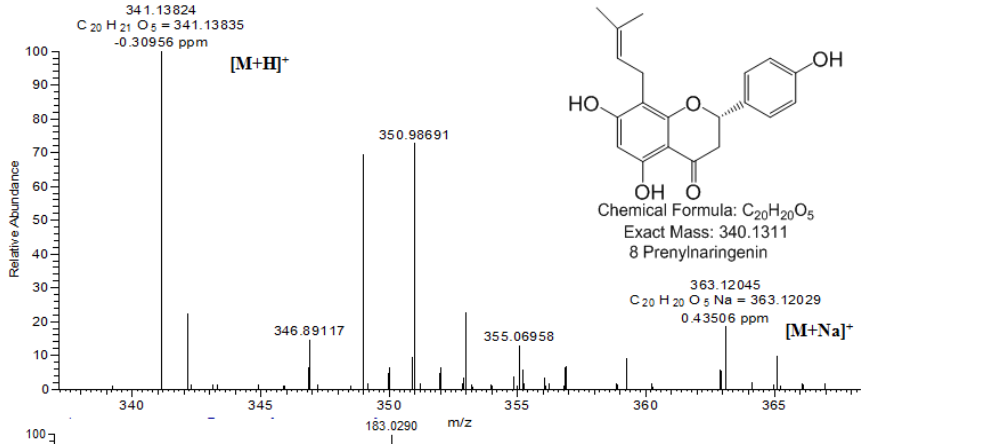
341.13824
C 20 H 21 O 5 = 341.13835
-0.30956 ppm
[M+H]+
350.98691
346.89117
355.06958
363.12045
C 20 H 20 O 5 Na = 363.12029
0.43506 ppm
[M+Na]+
Relative Abundance
m/z
HO
OH
OH
O
Chemical Formula: C20H20O5
Exact Mass: 340.1311
8 Prenylnaringenin

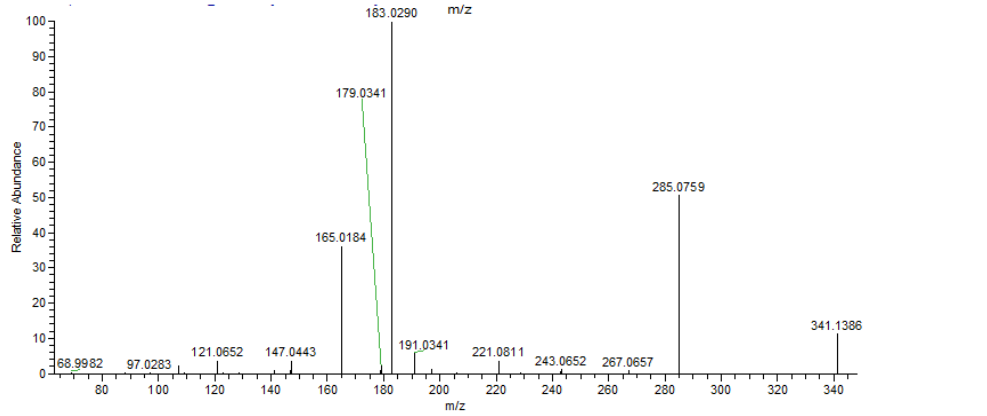
183.0290
179.0341
285.0759
165.0184
191.0341
68.9982
97.0283
121.0652
147.0443
221.0811
243.0652
267.0657
341.1386
Relative Abundance
m/z

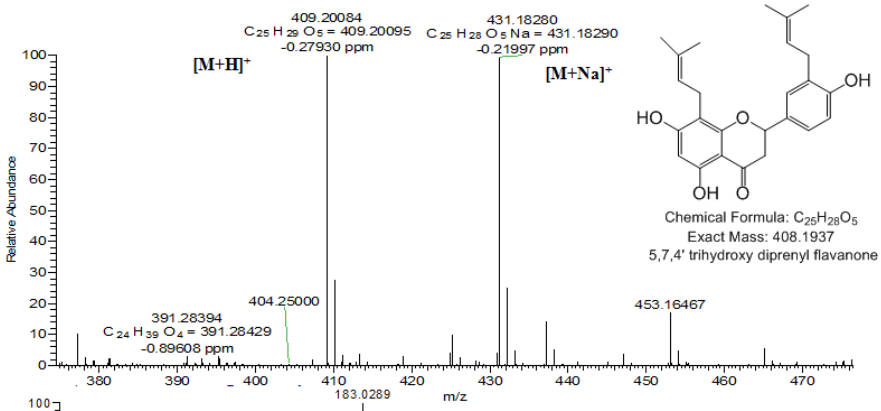
409.20084
C25 H29 O5 = 409.20095
-0.27930 ppm
[M+H]+
431.18280
C25 H28 O5 Na = 431.18290
-0.21997 ppm
[M+Na]+
OH
HO
O
OH
O
Chemical Formula: C26H28O5
Exact Mass: 408.1937
5,7,4' trihydroxy diprenyl flavanone
404.25000
391.28394
C24 H39 O4 = 391.28429
-0.89608 ppm
453.16467
Relative Abundance
m/z

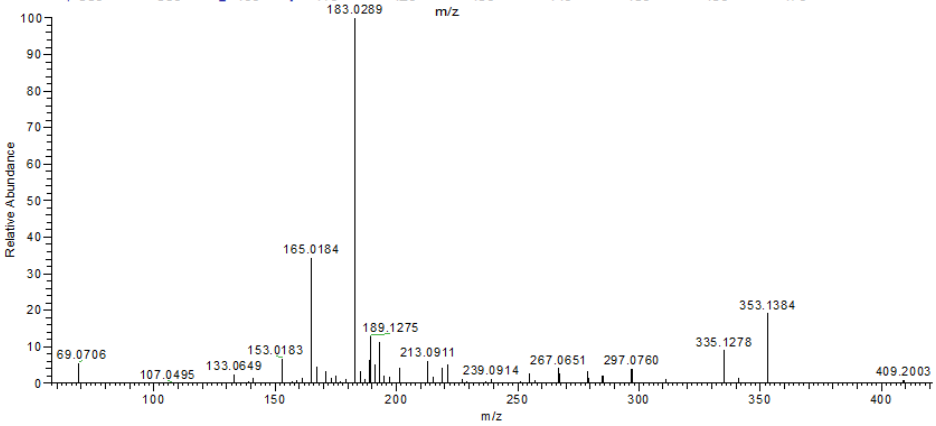
183.0289
165.0184
189.1275
353.1384
335.1278
69.0706
153.0183
133.0649
107.0495
213.0911
239.0914
267.0651
297.0760
409.2003
Relative Abundance
m/z

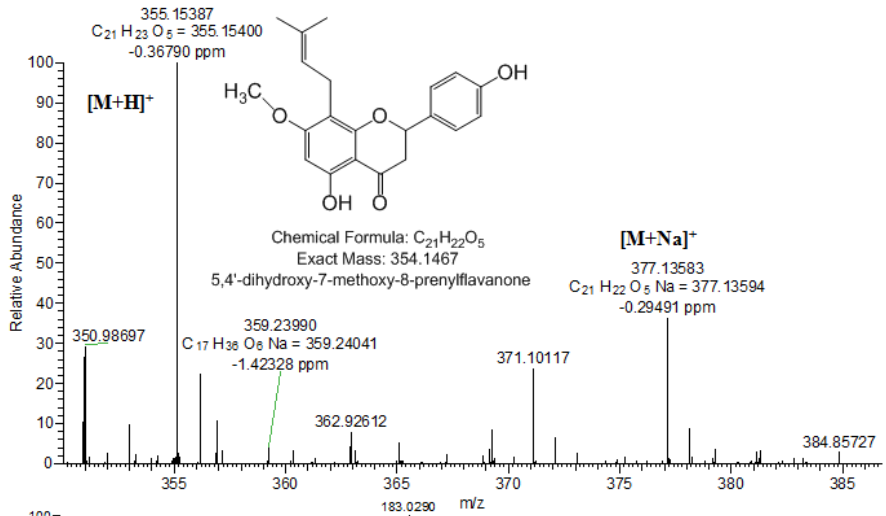
355.15387
C21 H23 O5 = 355.15400
-0.36790 ppm
[M+H]+
H3C
O
O
OH
OH
O
Chemical Formula: C21H22O5
Exact Mass: 354.1467
5,4'-dihydroxy-7-methoxy-8-prenylflavanone
[M+Na]+
377.13583
C21 H22 O5 Na = 377.13594
-0.29491 ppm
350.98697
359.23990
C17 H38 O6 Na = 359.24041
-1.42328 ppm
371.10117
362.92612
384.85727
Relative Abundance
m/z

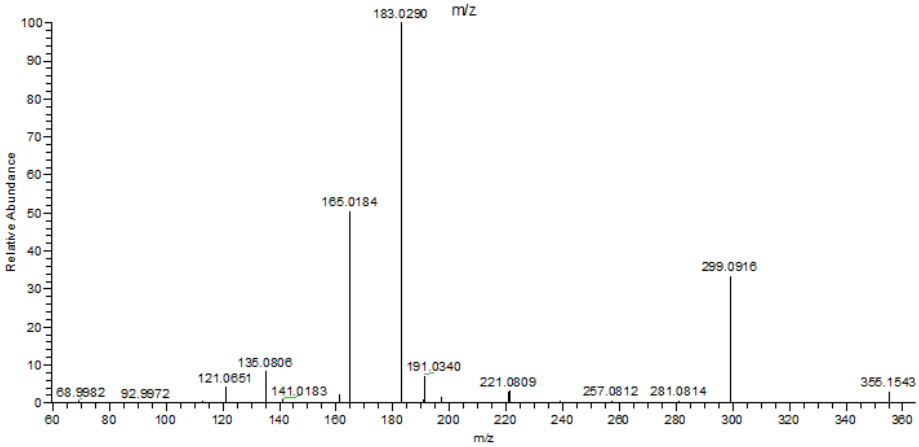
183.0290
165.0184
299.0916
135.0806
121.0651
191.0340
141.0183
221.0809
257.0812
281.0814
355.1543
68.9982
92.9972
Relative Abundance
m/z

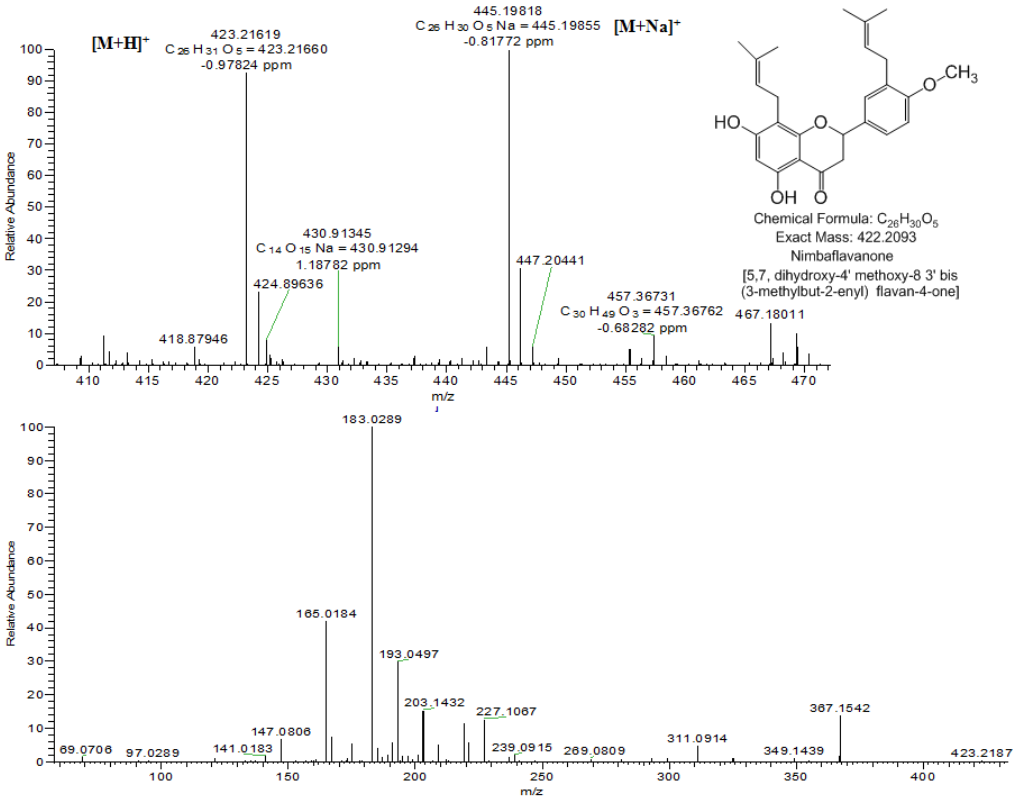

Figure 2B.5.4. Mass spectra and the corresponding MS/MS fragmentation pattern obtained at 30% NCE for the 17 identified flavonoids.

2C. References

1. K. K. Singh, Suman Phogat, R.S. Dhillon, Alka Tomar, *Neem, a Treatise*, I.K. International Publishing House, 2009.
2. A. Roy and S. Saraf, *Biol. Pharm. Bull.*, 2006, **29**, 191-201.
3. E. D. Morgan, *Bioorg. Med. Chem.*, 2009, **17**, 4096-4105.
4. A. Pandreka, D. S. Dandekar, S. Haldar, V. Uttara, S. G. Vijayshree, F. A. Mulani, T. Aarthy and H. V. Thulasiram, *BMC Plant Biol.*, 2015, **15**, 1-14.
5. J. N. Bilton, H. B. Broughton, S. V. Ley, Z. Lidert, E. D. Morgan, H. S. Rzepa and R. N. Sheppard, *J. Chem. Soc., Chem. Commun.*, 1985, 968-971.
6. K. Sanderson, *Nature*, 2007, **448**, 630-631.
7. G. E. Veitch, E. Beckmann, B. J. Burke, A. Boyer, S. L. Maslen and S. V. Ley, *Angew. Chem. Int. Ed.* , 2007, **119**, 7773-7776.
8. S. Srivastava and A. K. Srivastava, *Bioprocess. Biosyst. Eng.*, 2012, **35**, 1549-1553.
9. G. Prakash and A. K. Srivastava, *Process Biochem.*, 2007, **42**, 93-97.
10. M. Rafiq and M. U. Dahot, *Afr. J. Biotechnol.*, 2010, **9**, 449-453.
11. R. K. Satdive, D. P. Fulzele and S. Eapen, *J. Biotechnol.*, 2007, **128**, 281-289.
12. S. Sujanya, B. P. Devi and I. Sai, *J. Biosci.*, 2008, **33**, 113-120.
13. P. Srivastava and R. Chaturvedi, *Plant Signal Behav.*, 2011, **6**, 974-981.
14. G. Prakash and A. K. Srivastava, *Biochem. Eng. J.*, 2006, **29**, 62-68.
15. K. N. Raval, S. Hellwig, G. Prakash, A. Ramos-Plasencia, A. Srivastava and J. Buchs, *J. Biosci. Bioeng.*, 2003, **96**, 16-22.
16. D. Thakore and A. K. Srivastava, *Eng. Life Sci.*, 2017, **17**, 997-1005.
17. G. Prakash and A. K. Srivastava, *Appl. Biochem. Biotechnol.*, 2008, **151**, 307-318.
18. S. Chaudhary, R. K. Kanwar, A. Sehgal, D. M. Cahill, C. J. Barrow, R. Sehgal and J. R. Kanwar, *Front. Plant Sci.*, 2017, **8**, 13.
19. G. Prakash and A. K. Srivastava, *Biochem. Eng. J.*, 2008, **40**, 218-226.
20. G. Prakash and A. K. Srivastava, *Process Biochem.*, 2005, **40**, 3795-3800.
21. M. Singh and R. Chaturvedi, *Aob Plants*, 2013, **5**, 14.
22. G. Prakash, C. Emmannuel and A. K. Srivastava, *Biotechnol. Bioprocess Eng.*, 2005, **10**, 198-204.
23. N. Kaushik, B. G. Singh, U. K. Tomar, S. N. Naik, S. Vir, S. S. Bisla, K. K. Sharma, S. K. Banerjee and P. Thakkar, *Curr. Sci.*, 2007, **92**, 1400-1406.
24. A. Gairi and A. Rashid, *Biologia Plantarum*, 2005, **49**, 169-173.
25. R. Fernandez Da Silva, A. Villarroel, L. Cuamo and V. Storaci, *Acta Biol. Colomb.*, **21**, 581-592.
26. G. R. Rout, *J. Forest Res.*, 2005, **10**, 263-267.
27. B. N. S. Murthy and P. K. Saxena, *Plant Cell Rep.*, 1998, **17**, 469-475.
28. R. Chaturvedi, M. K. Razdan and S. S. Bhojwani, *Plant Sci.*, 2004, **166**, 501-506.
29. A. Quraishi, V. Koche, P. Sharma and S. K. Mishra, *Plant Cell Tissue Organ Cult.*, 2004, **78**, 281-284.
30. M. Shahin-Uz-Zaman, M. Ashrafuzzaman, M. S. Haque and L. N. Luna, *Afr. J. Biotechnol.*, 2008, **7**, 386-391.
31. G. Prakash, C. Emmannuel and A. K. Srivastava, *Biotechnol. Bioprocess Eng*, 2005, **10**, 198-204.
32. S. Srivastava and A. K. Srivastava, *Bioprocess Biosyst. Eng.*, 2012, **35**, 1549-1553.
33. J. B. Harborne, *Introduction to Ecological Biochemistry*, Elsevier Science, 2014.
34. S. V. van Breda, C. F. D. Merwe, H. Robbertse and Z. Apostolides, *Planta*, 2013, **237**, 849-858.
35. S. Haldar, F. A. Mulani, T. Aarthy, D. S. Dandekar and H. V. Thulasiram, *J. Chromatogr. A*, 2014, **1366**, 1-14.
36. S. Haldar, P. B. Phapale, S. P. Kolet and H. V. Thulasiram, *Anal. Methods*, 2013, **5**, 5386-5391.

37. E. Pichersky and R. A. C. Raguso, *New Phytol*, 2016, **220**, 692-702.
38. F. Chen, D. Tholl, J. Bohlmann and E. Pichersky, *The Plant Journal*, 2011, **66**, 212-229.
39. T. Hartmann, *Entomol. Exp. Appl.*, 1996, **80**, 177-188.
40. M. Burow and B. A. Halkier, *Curr Opin Plant Biol.*, 2017, **38**, 142-147.
41. N. R. Lersten, A. R. Czlapinski, J. D. Curtis, R. Freckmann and H. T. Horner, *Am. J. Bot*, 2006, **93**, 1731-1739.
42. B. M. Lange and G. W. Turner, *Plant Biotechnol. J.*, 2013, **11**, 2-22.
43. A. Tissier, C. Sallaud and D. Rontein, in *Isoprenoid Synthesis in Plants and Microorganisms: New Concepts and Experimental Approaches*, eds. T. J. Bach and M. Rohmer, Springer New York, New York, NY, 2012, pp. 271-283.
44. A. S. Foster, *Protoplasma*, 1956, **46**, 184-193.
45. P. G. Mahlberg, *Bot. Rev.*, 1993, **59**, 1-23.
46. D. R. Gang, J. H. Wang, N. Dudareva, K. H. Nam, J. E. Simon, E. Lewinsohn and E. Pichersky, *Plant Physiol.*, 2001, **125**, 539-555.
47. W. F. Pickard, *New Phytol.*, 2008, **177**, 877-887.
48. R. A. Dixon, *Nature*, 2001, **411**, 843.
49. P. V. Gersbach, *Ann. Bot*, 2002, **89**, 255-260.
50. S. Maiti and A. Mitra, *Plant Cell Physiol.*, 2017, **58**, 2095-2111.
51. S. Ibanez, S. Dotterl, M. C. Anstett, S. Baudino, J. C. Caissard, C. Gallet and L. Despres, *New Phytol.*, 2010, **188**, 451-463.
52. G. Heinrich, H. W. Pfeifhofer, E. Stabentheiner and T. Sawidis, *Ann. Bot.*, 2002, **89**, 459-469.
53. P. V. Gersbach, *Ann. Bot.*, 2002, **89**, 255-260.
54. C. Giuliani, R. Ascrizzi, C. Tani, M. Bottoni, L. M. Bini, G. Flamini and G. Fico, *Flora*, 2017, **233**, 12-21.
55. A. A. Lopes, E. S. Pina, D. B. Silva, A. M. S. Pereira, M. da Silva, F. B. Da Costa, N. P. Lopes and M. T. Pupo, *Chem. Commun.*, 2013, **49**, 9989-9991.
56. J. Q. D. Goodger, A. M. Heskes, M. C. Mitchell, D. J. King, E. H. Neilson and I. E. Woodrow, *Plant Methods*, 2010, **6**.
57. D. McCaskill, J. Gershenzon and R. Croteau, *Planta*, 1992, **187**, 445-454.
58. A. Tissier, *Curr. Opin. Biotechnol*, 2018, **49**, 73-79.
59. G. Guirimand, A. Guihur, O. Ginis, P. Poutrain, F. Hericourt, A. Oudin, A. Lanoue, B. St-Pierre, V. Burlat and V. Courdavault, *Febs J.*, 2011, **278**, 749-763.
60. K. M. Madyastha, J. E. Ridgway, J. G. Dwyer and C. J. Coscia, *J. Cell Biol.*, 1977, **72**, 302-313.
61. I. Carqueijeiro, A. L. Guimaraes, S. Bettencourt, T. Martinez-Cortes, J. G. Guedes, R. Gardner, T. Lopes, C. Andrade, C. Bispo, N. P. Martins, P. Andrade, P. Valentao, I. M. Valente, J. A. Rodrigues, P. Duarte and M. Sottomayor, *Plant Physiol.*, 2016, **171**, 2371-2378.
62. K. Yamamoto, K. Takahashi, H. Mizuno, A. Anegawa, K. Ishizaki, H. Fukaki, M. Ohnishi, M. Yamazaki, T. Masujima and T. Mimura, *Proc. Natl. Acad. Sci. U S A*, 2016, **113**, 3891-3896.
63. M. Weid, J. Ziegler and T. M. Kutchan, *Proc. Natl. Acad. Sci. U S A*, 2004, **101**, 13957-13962.
64. A. Onoyovwe, J. M. Hagel, X. Chen, M. F. Khan, D. C. Schriemer and P. J. Facchini, *Plant Cell*, 2013, **25**, 4110-4122.
65. S. Sirikantaramas, M. Yamazaki and K. Saito, *Phytochem Rev.*, 2007, **7**, 467.
66. L. Brisson, P. M. Charest, V. De Luca and R. K. Ibrahim, *Phytochemistry*, 1992, **31**, 465-470.
67. F. S. F. Jorge, O. D. Stephen and C. V. Kevin, *Can. J. Bot.*, 1998, **159**, 492-503.

68. W. K. Heneen, G. Karlsson, K. Brismar, P. O. Gummeson, S. Marttila, S. Leonova, A. S. Carlsson, M. Bafor, A. Banas, B. Mattsson, H. Debski and S. Stymne, *Planta*, 2008, **228**, 589-599.
69. J. T. C. Tzen and A. H. C. Huang, *J. Cell Biol.*, 1992, **117**, 327-335.
70. C. Suire, F. Bouvier, R. A. Backhaus, D. Begu, M. Bonneu and B. Camara, *Plant Physiol.*, 2000, **124**, 971-978.
71. M. Tanaka, T. Esaki, H. Kenmoku, T. Koeduka, Y. Kiyoyama, T. Masujima, Y. Asakawa and K. Matsui, *Phytochemistry*, 2016, **130**, 77-84.
72. T. L. Shimada, Y. Takano, T. Shimada, M. Fujiwara, Y. Fukao, M. Mori, Y. Okazaki, K. Saito, R. Sasaki, K. Aoki and I. Hara-Nishimura, *Plant Physiol.*, 2014, **164**, 105-118.
73. A. Tissier, C. Sallaud and D. Rontein, in *Isoprenoid Synthesis in Plants and Microorganisms: New Concepts and Experimental Approaches*, eds. T. J. Bach and M. Rohmer, Springer New York, New York, NY, 2013, pp. 271-283.
74. D. McCaskill and R. Croteau, *Trends Biotechnol.*, 1998, **16**, 349-355.
75. P. Verma, A. K. Mathur, A. Srivastava and A. Mathur, *Protoplasma*, 2012, **249**, 255-268.
76. J. A. Inamdar, R. B. Subramanian and J. S. S. Mohan, *Ann. Bot.*, 1986, **58**, 425-429.
77. C. Balasubramanian, P. S. Mohan, K. Arumugasamy and K. Udaiyan, *Phytochemistry*, 1993, **34**, 1194-1195.
78. S. Senthil-Nathan, *Front. physiol*, 2013, **4**, 359-359.
79. D. L. Ma, Y. Suzuki, H. Takeuchi, T. Watanabe and M. Ishizaki, *Phytoparasitica*, 2005, **33**, 506-514.
80. S. S. Nathan, K. Kalaivani, P. G. Chung and K. Murugan, *Chemosphere*, 2006, **62**, 1388-1393.
81. S. Raguraman and R. P. Singh, *J. Econ. Entomol.*, 1999, **92**, 1274-1280.
82. O. Koul, G. Singh, R. Singh, J. Singh, W. M. Daniewski and S. Berlozecki, *J. Biosci.*, 2004, **29**, 409-416.
83. G. Esparza-Diaz, J. Lopez-Collado, J. A. Villanueva-Jimenez, F. Osorio-Acosta, G. Otero-Colina and E. Camacho-Diaz, *Agrociencia*, 2010, **44**, 821-833.
84. O. Koul, J. S. Multani, S. Goomber, W. M. Daniewski and S. Berlozecki, *Austral. Entomol.*, 2004, **43**, 189-195.
85. O. Koul, J. S. Multani, G. Singh, W. M. Daniewski and S. Berlozecki, *J. Agric. Food Chem.*, 2003, **51**, 2937-2942.
86. J. M. Hagel, E. C. Yeung and P. J. Facchini, *Trends Plant Sci.*, 2008, **13**, 631-639.
87. U. Eilert, L. R. Nesbitt and F. Constabel, *Can. J. Bot.*, 1985, **63**, 1540-1546.
88. P. B. Dickenson and J. W. Fairbairn, *Ann. Bot.*, 1975, **39**, 707-&.
89. W. A. Southorn, *Nature*, 1960, **188**, 165-166.
90. G. Bauer, S. N. Gorb, M. C. Klein, A. Nellesen, M. von Tapavicza and T. Speck, *PLoS One*, 2014, **9**, 1-8.
91. H. Yamamoto and P. D. Gupta, *Electron microscopy in medicine and biology*, Science Publishers, Enfield, NH, 2000.
92. M. Beller, K. Thiel, P. J. Thul and H. Jackle, *FEBS Lett.*, 2010, **584**, 2176-2182.
93. I. Pateraki, J. Andersen-Ranberg, B. Hamberger, A. M. Heskes, H. J. Martens, P. Zerbe, S. S. Bach, B. L. Moller and J. Bohlmann, *Plant Physiol.*, 2014, **164**, 1222-1236.
94. D. Silvestro, T. G. Andersen, H. Schaller and P. E. Jensen, *PLoS One*, 2013, **8**.
95. E. Lewinsohn, N. Dudai, Y. Tadmor, I. Katzir, U. Ravid, E. Putievsky and D. M. Joel, *Ann. Bot.*, 1998, **81**, 35-39.
96. S. L. Geng, Z. X. Cui, B. Shu, S. Zhao and X. H. Yu, *Plant Prod. Sci.*, 2012, **15**, 1-9.
97. A. Bock, G. Wanner and M. H. Zenk, *Planta*, 2002, **216**, 57-63.
98. K. Yazaki, *Curr. Opin. Plant Biol.*, 2005, **8**, 301-307.
99. T. Hara, E. Kobayashi, K. Ohtsubo, S. Kumada, M. Kanazawa, T. Abe, R. D. Itoh and M. T. Fujiwara, *PLoS One*, 2015, **10**, 1-18.

100. G. Pasqua, B. Monacelli and A. Valletta, *Eur. J. Histochem.*, 2004, **48**, 321-327.
101. U. Eilert, B. Wolters and F. Constabel, *Can. J. Bot.*, 1986, **64**, 1089-1096.
102. K. Marinova, K. Kleinschmidt, G. Weissenbock and M. Klein, *Plant Physiol.*, 2007, **144**, 432-444.
103. F. Ferreres, R. Figueiredo, S. Bettencourt, I. Carqueijeiro, J. Oliveira, A. Gil-Izquierdo, D. M. Pereira, P. Valentao, P. B. Andrade, P. Duarte, A. R. Barcelo and M. Sottomayor, *J. Exp. Bot.*, 2011, **62**, 2841-2854.
104. I. Carqueijeiro, H. Noronha, P. Duarte, H. Geros and M. Sottomayor, *Plant Physiol.*, 2013, **162**, 1486-1496.
105. P. Talamond, J. L. Verdeil and G. Conejero, *Molecules*, 2015, **20**, 5024-5037.
106. J. H. Park, J. Seo, J. A. Jackman and N. J. Cho, *Sci. Rep.*, 2016, **6**.
107. L. P. Taylor and E. Grotewold, *Curr. Opin. Plant Biol.*, 2005, **8**, 317-323.
108. O. Ceska and E. D. Styles, *Phytochemistry*, 1984, **23**, 1822-1823.
109. K. Hsieh and A. H. C. Huang, *Plant Cell*, 2007, **19**, 582-596.
110. G. Agati, E. Azzarello, S. Pollastri and M. Tattini, *Plant Sci.*, 2012, **196**, 67-76.
111. C. Argyropoulou, A. Akoumianaki-Ioannidou, N. S. Christodoulakis and C. Fasseas, *Aust. J. Bot*, 2010, **58**, 398-409.
112. X. M. Zhang, *J. Appl. Entomol.*, 2017,**142**, 359-362.
113. M. Huang, A. M. Sanchez-Moreiras, C. Abel, R. Sohrabi, S. Lee, J. Gershenzon and D. Tholl, *New Phytol.*, 2011, **193**, 997-1008.
114. D. M. Martin, O. Toub, A. Chiang, B. C. Lo, S. Ohse, S. T. Lund and J. Bohlmann, *Proc. Natl. Acad. Sci. U S A*, 2009, **106**, 7245-7250.
115. O. Koul, J. S. Multani, S. Goomber, W. M. Daniewski and S. Berlozecki, *Aust. J. Entomol.*, 2004, **43**, 189-195.
116. Y. Zhang, J. Su, S. Duan, Y. Ao, J. Dai, J. Liu, P. Wang, Y. Li, B. Liu, D. Feng, J. Wang and H. Wang, *Plant Methods*, 2011, **7**, 1-30.

Chapter 3

Ex vivo tracer study of limonoid biosynthesis in *Azadirachta indica*

Labeling experiment

Glc [1-^{13}C]-Glc [2-^{13}C]-Glc [1,6-^{13}C]-Glc

Extraction

UPLC-ESI-Orbitrap analysis

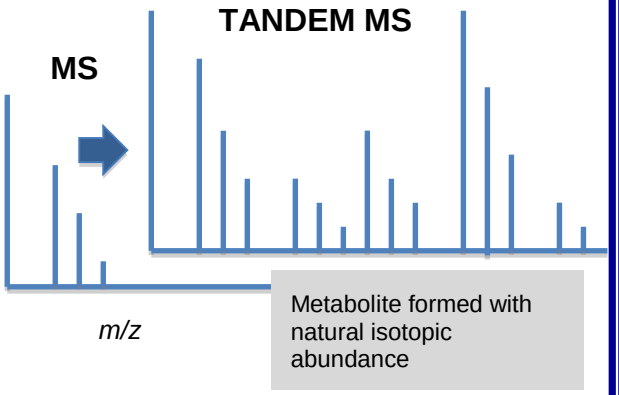

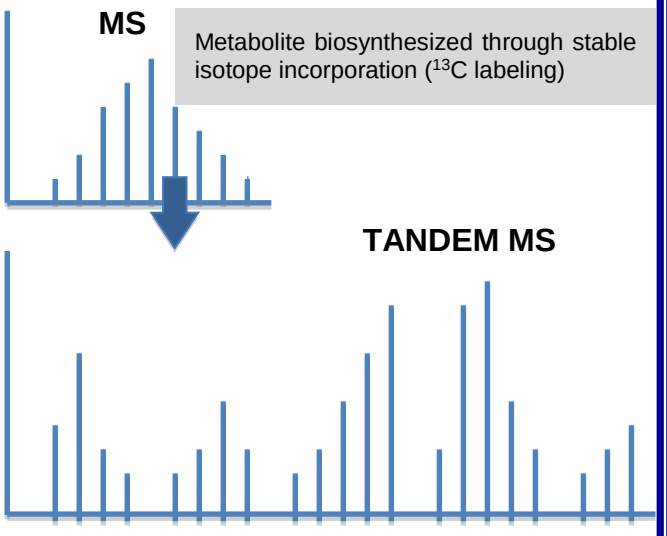

Chapter 3: Section A
Tracing biosynthetic pathways through stable isotopes - an Introduction

3A. Introduction

Many of the primary metabolic pathways in the cell have been discovered by isotope labeling which involves tracking the passage of an isotope from reactant to product or through a metabolic pathway (Figure 3A.1) in a cell in *in vivo* or *ex vivo* condition[1]. Depending upon the nuclides used for labeling, they are classified as stable and radionuclide labeling. Radioactive labeling helps in deciphering the mechanism of biochemical reactions by monitoring the radioactive label over the reactants and products. It also helps to trace the reaction products in an organism after the introduction of radioactive compound into the organism[2].

3A.1. Stable isotope labeling

Labeling studies with stable isotopic tracers such as ^{2}H, ^{13}C, ^{15}N have greatly helped in studying the various biosynthetic pathways in living systems[2]. One of famous pathway discovery made in 20^{th} century using stable isotope labeling, which is contributing for the biosynthesis of isoprene units in bacteria, algae, archaea and plants is Methyl-erythritol Phosphate pathway[3-10].

3A.2. The discovery of Methyl-erythritol Phosphate pathway

This pathway was discovered accidentally during the study of biosynthesis of bacterial triterpenes, hopanoids by Rohmer and his co-workers[9, 11-17]. Hopanoids, present in bacterial cell wall are triterpene structures with a C5 side chain. To study the origin of this side chain, labeling experiment was carried out by Rohmer *et al*[11, 12] with bacteria grown in synthetic mineral media containing acetate as a sole carbon source.

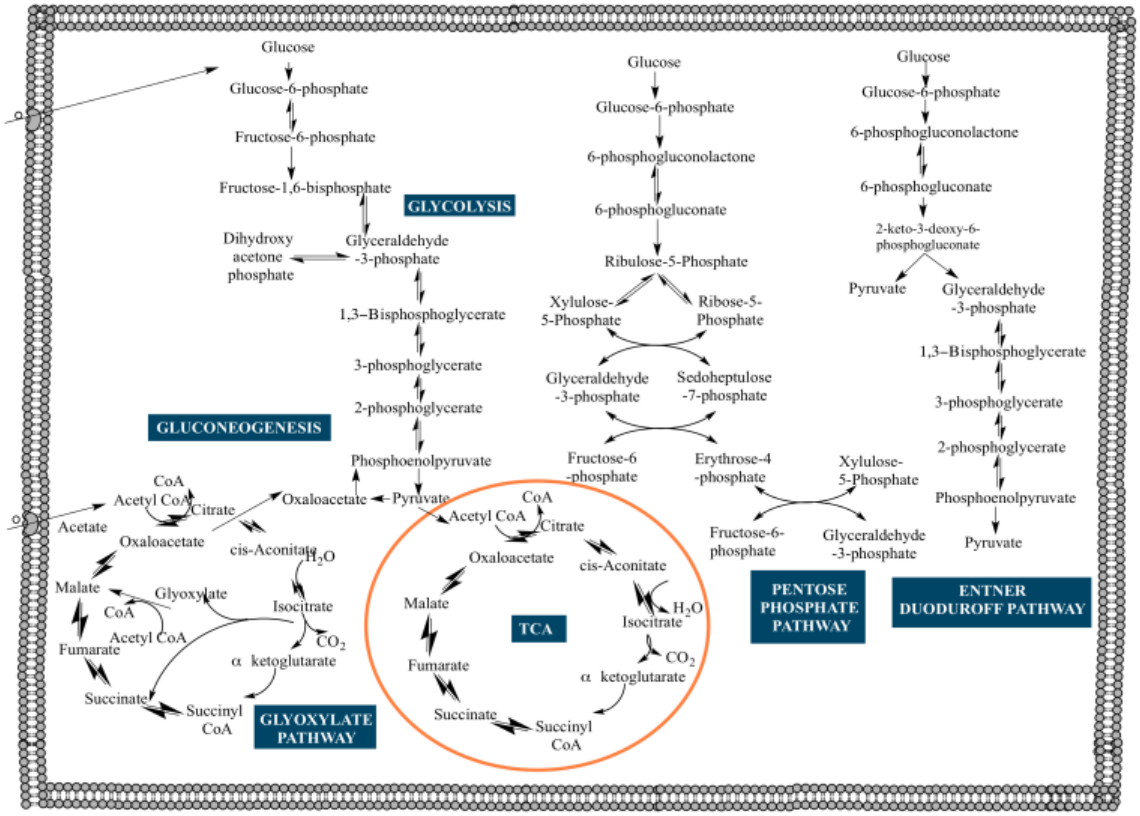

Figure 3A.1. Various pathways in bacteria for utilization of carbon sources such as acetate and glucose

Rhodopseudomonas palustris and Rhodopseudomonas acidophila, purple non-sulfur bacteria and the facultative methylotroph *Methylobacterium organophilum* respectively, uses acetate as sole carbon and energy source. They were fed with [l-^{13}C] acetate and [2-^{13}C] acetate[15]. The labeling pattern of hopanoid showed that the D-pentose derived from non-oxidative pentose phosphate pathway is linked *via* its C-5 carbon atom to the hopane isopropyl group (Figure 3A.2). The serendipity observed was that the isoprene units of the triterpenoid skeleton did not correspond to the one as expected through the MVA route (Figure 3A.3). At that time, this contradiction could not be interpreted in the frame that these isoprene units could be synthesized through completely different pathway, as the MVA pathway was strongly believed to be the universal pathway for isoprenoid biosynthesis, although the hypothesis for the existence of different pathway was not completely neglected.

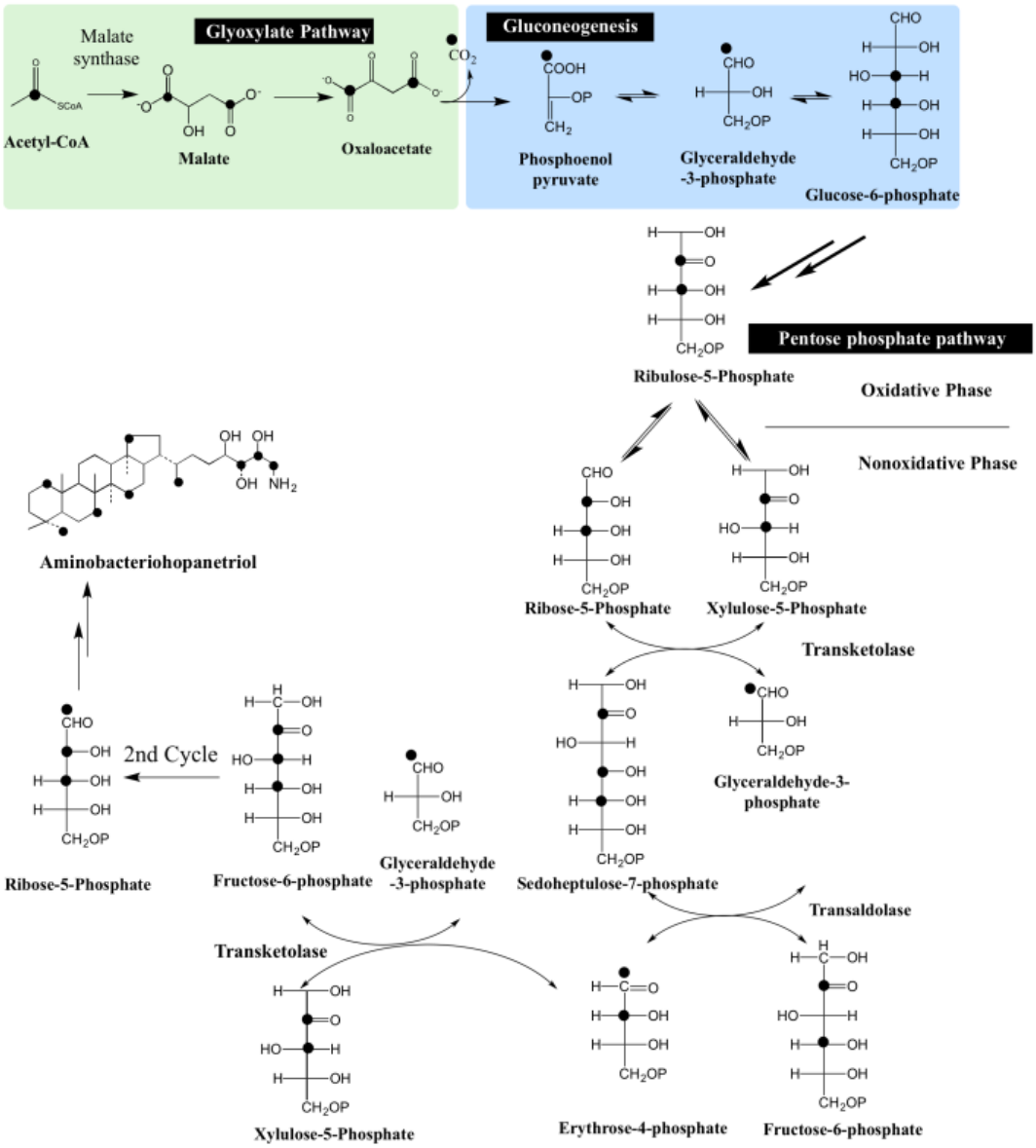

Figure 3A.2. Biosynthetic scheme for the study of formation of 5-carbon side chain of hopanoids through different biosynthetic pathways in bacteria by using labeled [1-^{13}C] acetate as carbon source.

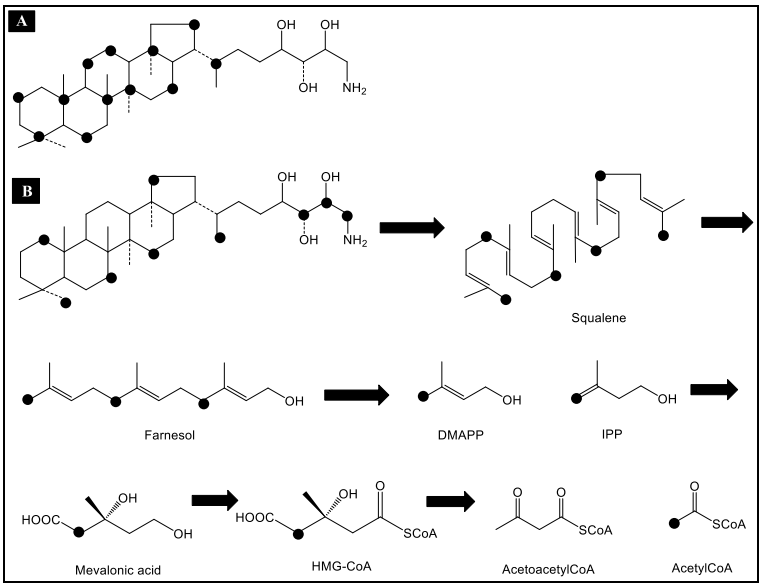

Figure 3A.3. Rohmer's labeling studies with [1-^{13}C] acetate for the study of hopanoid, aminobacteriohopanetriol from bacteria[11]. **(A)** Expected labeling pattern of the triterpene skeleton from mevalonate pathway **(B)** Observed labeling pattern of the triterpene skeleton and the deduced retro-biosynthetic scheme based on the pattern

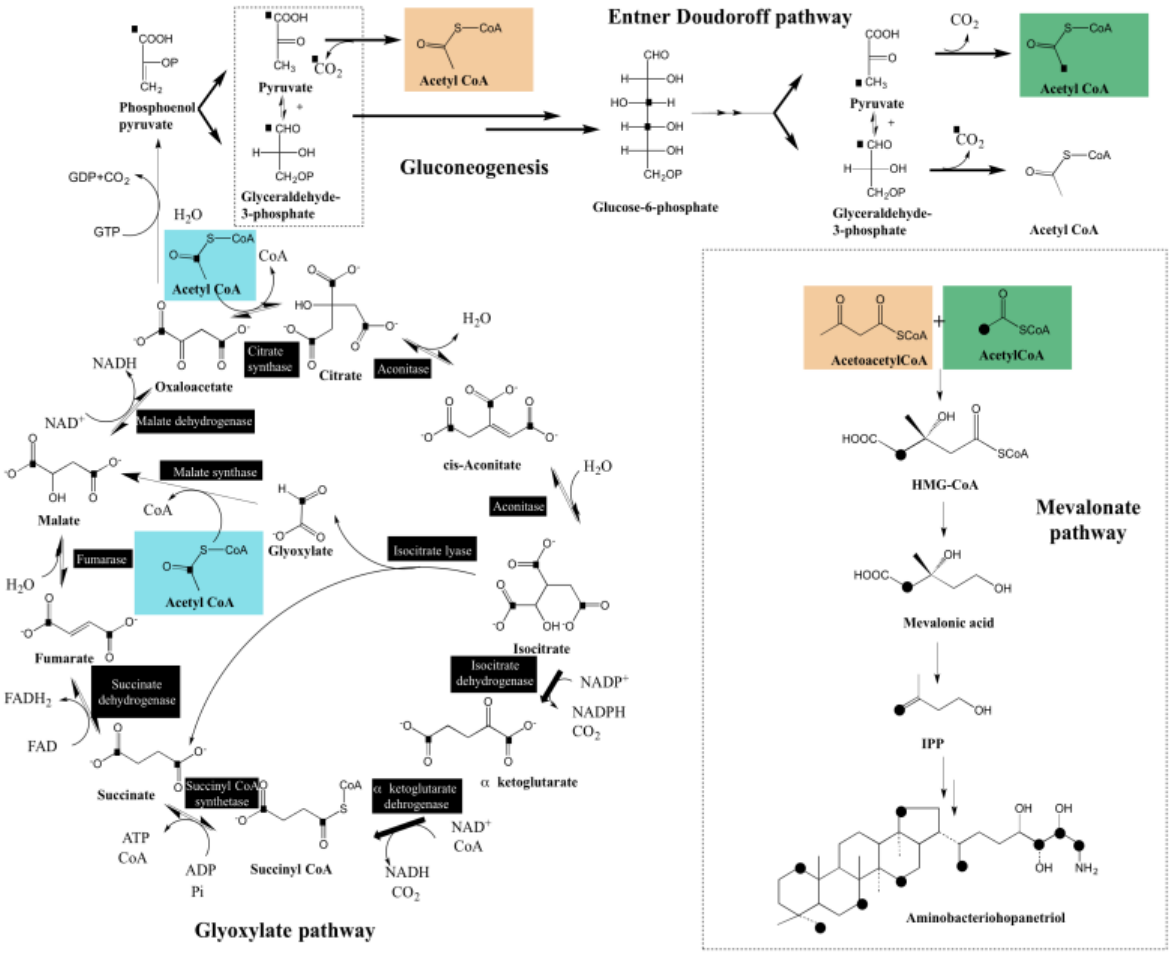

Figure 3A.4. Biosynthetic scheme for the formation of triterpenoid skeleton of hopanoids through alternate biosynthetic pathways in bacteria such as glyoxylate pathway and Entner Doudoroff pathway by utilizing labeled acetate as carbon source[11].

From the labeling pattern of hopanoids, it was concluded that MVA had to be formed from two distinct acetyl-CoA pools formed *via* the glyoxylate cycle and the Entner-Doudoroff degradation of glucose (Figure 3A.4)[11]. This labeling study raised the following problems which has to been resolved at that times: (i) exogenous acetate was not, as expected, directly incorporated into this biosynthetic pathway; (ii) no scrambling of the isotopic enrichment occurred; (iii) the observed labeling patterns differed completely from those expected from the classical isoprenoid-biosynthetic route (MVA pathway)[11].

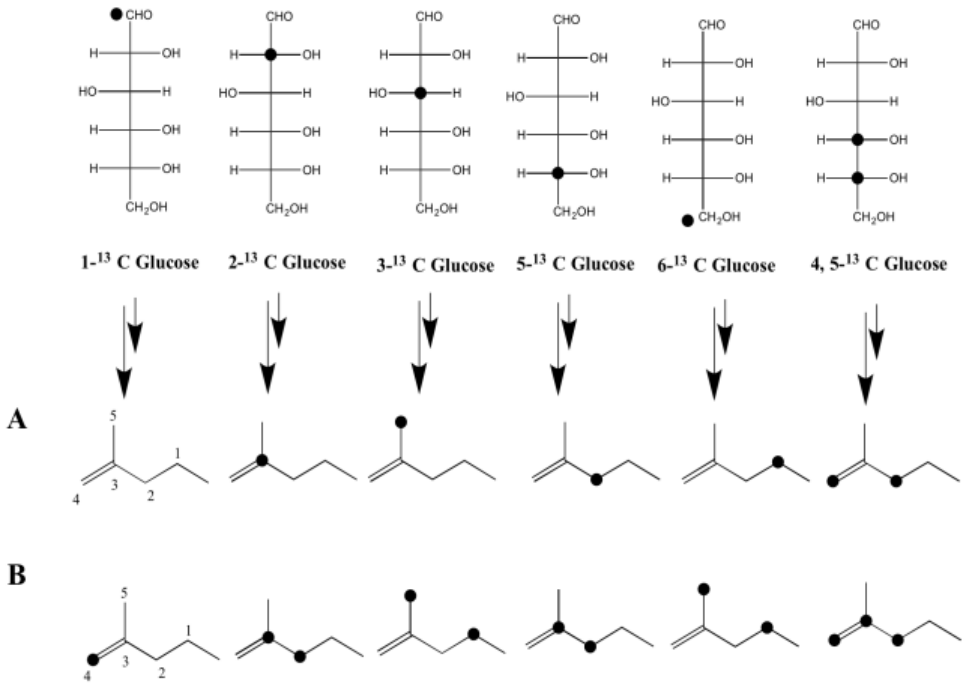

Figure 3A.5. Labeling studies with stable isotope labeled glucose isotopomers and isotopologues carried out by Rohmer *et al.* 1993[13] with two different bactererium **A.** *Zygomonas mobilis*, **B.** *Methylobacterium fujisawaense*

In his further work, Rohmer used ethanol producing bacterium *Zymomonas mobilis*, which uses hexoses as the only carbon and energy source (Figure 3A.5). *Z. mobilis* was studied for the incorporation of ^{13}C-labeled D-glucose labeled at either C-1, C-2, C-3, C-5, C-6 which confirmed that D-ribose derivative is the precursor of the side-

chain of bacteriohopanetetrol[11] (Figure 3A.2). In an effort to decipher the origin of carbon atoms in isopentenyl diphosphate biosynthesis, Rohmer[13] and his co-workers studied the hopanoid biosynthesis in different bacterial species (*Zymomonas mobilis*, *Methylobacterium fujisawaense*, and *Alicyclobacillus acidoterrestris*) which differ in their utilization of carbon source (acetate and glucose) and metabolism (glycolysis, TCA cycle, glyoxylate cycle, Entner-Doudoroff pathway) of their respective carbon source (Figure 3A.1, Figure 3A.9)[13, 15]. Since, *Escherichia coli* is a poor producer of hopanoids, the incorporation of ^{13}C carbon into Ubiquinone was studied. In *M. fujisawaense* and *E. coli*, [l-^{13}C] acetate and [2-^{13}C] acetate is incorporated into the glyoxylate and tricarboxylic acid cycles, leading to pyruvate and/or phosphoenol pyruvate. *E. coli* metabolized labeled glucose through glycolysis and oxidative pentose phosphate, whereas *M. fujisawaense* utilized glucose via the Entner-Doudoroff pathway (Figure 3A.7, 3A.8)[15]. *Z. mobilis* has incomplete TCA cycle and metabolizes glucose through Entner-Doudoroff pathway. *Alicyclobacillus acidoterrestris* utilizes only glucose as carbon source and metabolizes it through glycolysis and oxidative pentose phosphate pathway[15]. The labeling pattern in the triterpene skeleton of hopanoids in the above studied organism differed due to utilization of carbon source through different pathway and it determined the origin of carbon atoms of isoprene units[11, 15]. D-glucose isotopomers labeled at different positions gave a clear distinction in labeling pattern of isoprene units in *Z. mobilis*, which utilizes the Entner-Doudoroff pathway for catabolism of glucose (Figure 3A.9)[15]. C-1, C-2 and C-4 of IPP were derived from C-4, C-5 and C-6 of glucose, respectively. C-3 and C-5 of IPP were respectively equally derived from C-2 or C-5 and C-3 or C-6 of glucose[15]. Their study produced an opinion that a novel pathway existed for the synthesis of isoprene units. The former studies done by Rohmer *et al*. in hopane series and the one in the later for the incorporation of ^{13}C-labeled glycerol or pyruvate into the ubiquinone Q8 of *Escherichia coli* mutants lacking enzymes of the triose phosphate metabolism gave a clear idea that pyruvate as precursor of a C2 subunit and a triose phosphate derivative as precursor of a C3 subunit[14]. [1-^{13}C] and [6-^{13}C] glucose incorporation into ubiquinone in *E. coli* or into the hopanoids in *Alicyclobacillus acidoterrestris* yielded identical labeling patterns with label on all carbon atoms corresponding to C-1 and C-5 of IPP which suggested that the equivalence of carbons C-1, C-2, C-3 of glucose to C-6, C-5, C-4 due to the inter-conversion by triose phosphate isomerase of GAP and DHAP in glycolysis[11, 13, 15].

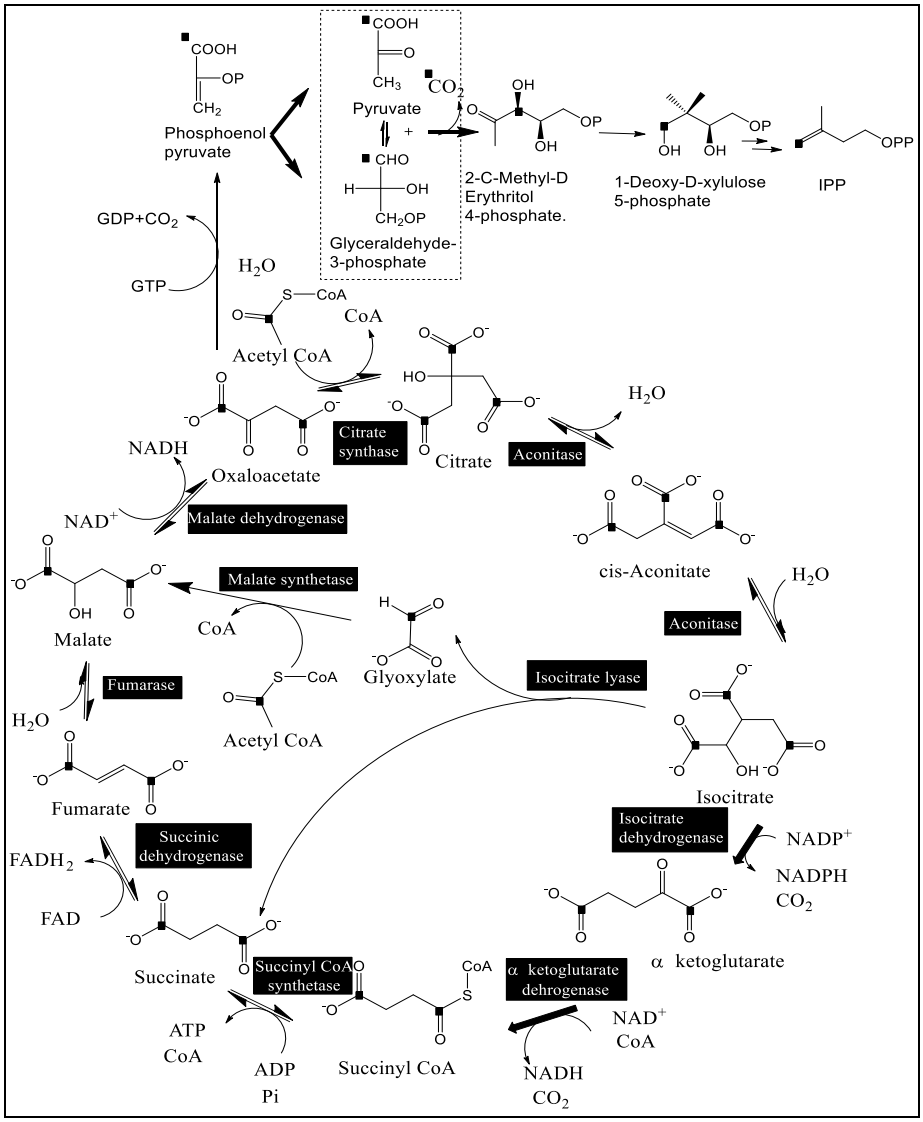

Figure 3A.6. Acetate metabolism and its incorporation into isoprene units through glyoxylate pathway shown through 1-^{13}C acetate labeling

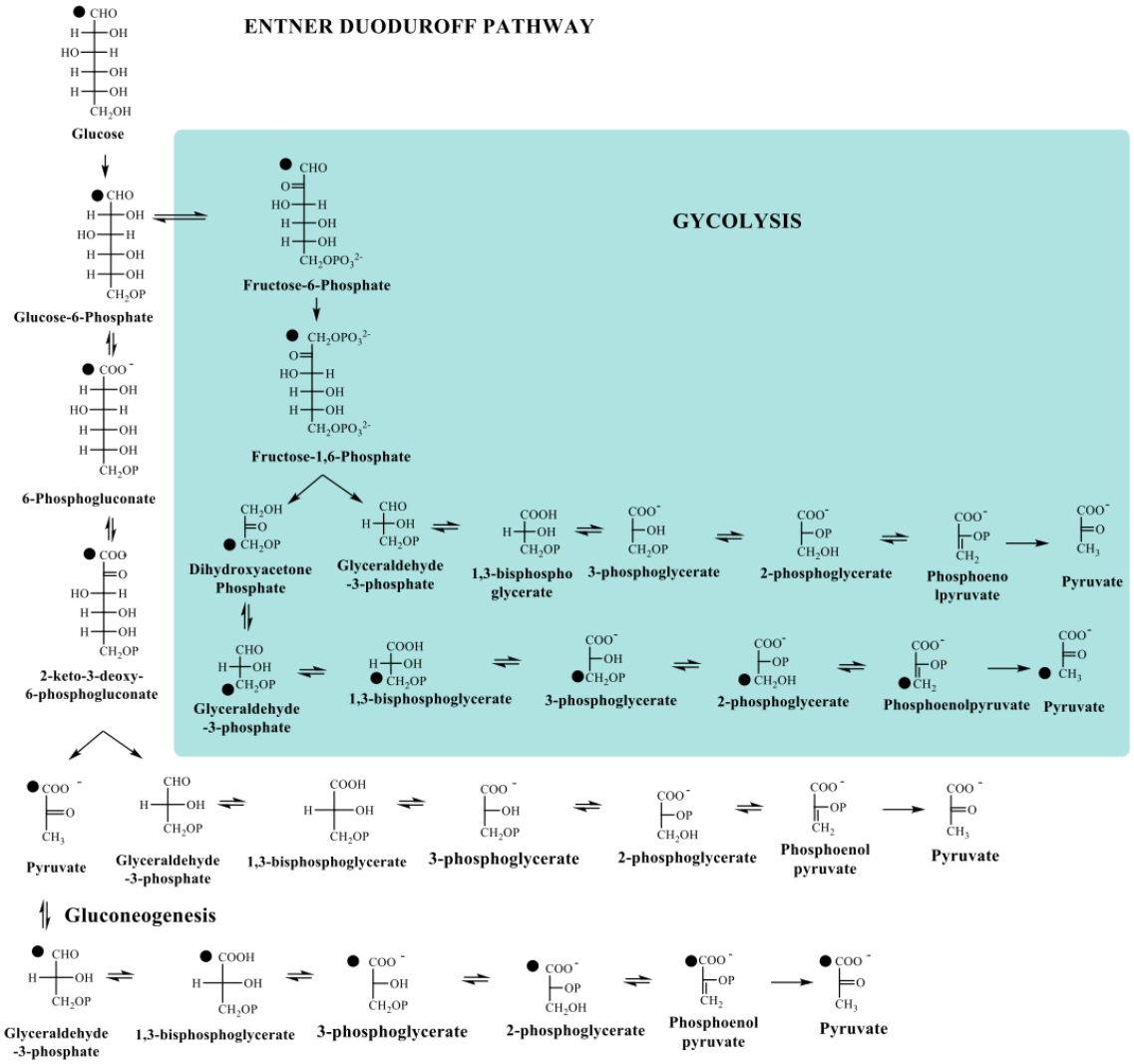

Figure 3A.7. Various pathways such as glycolysis, its alternate Entner-Duoduroff pathway and glycolysis in the cell for glucose metabolism shown through 1-^{13}C glucose labeling[12, 13].

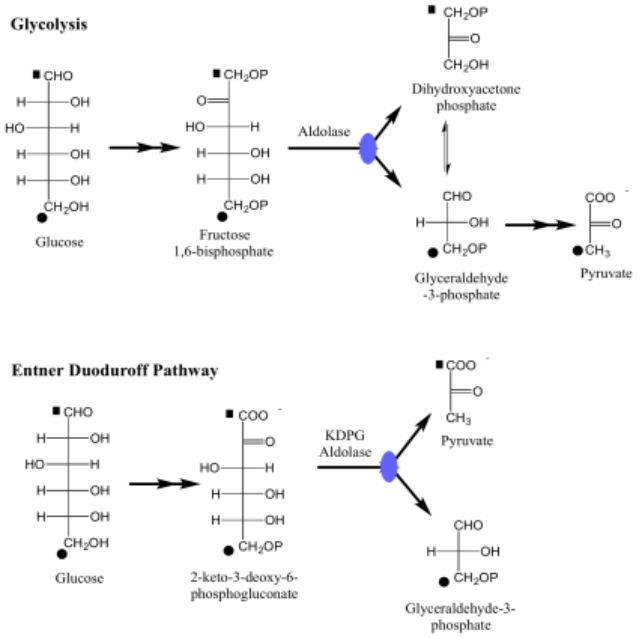

Figure 3A.8. Difference in glycolysis and Entner-Duoduroff pathway present in bacteria in metabolizing glucose into pyruvate[12, 13].

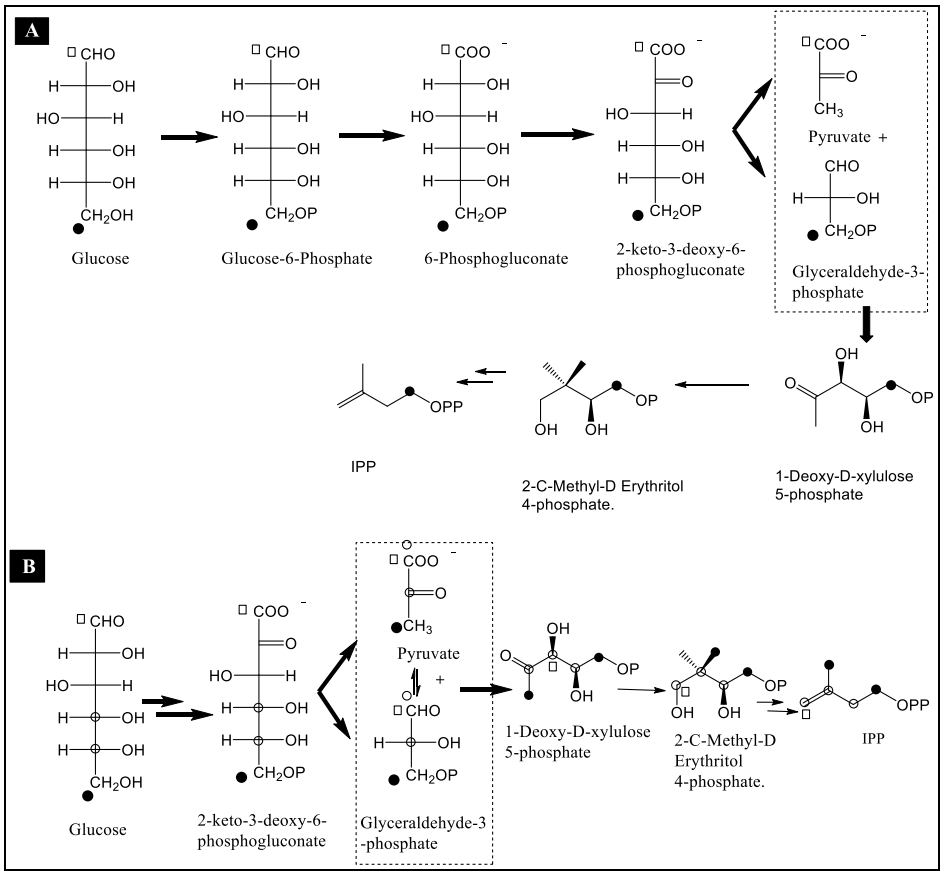

Figure 3A.9. Glucose catabolism via Entner-duoduroff pathway and incorporation of precursors via non-MVA pathway[12, 13] (A) In *Zymomonas mobiles* (B) In *Methylobacterium fujisawaense* (Filled circle denotes the ^{13}C label at 6-C position of glucose, unfilled square denotes label at 1-C whereas unfilled circles denote label at 4,5-^{13}C of glucose).

Based on these labeling patterns, mevalonate was not considered as a metabolic intermediate in the newly hypothesized pathway[12, 13]. MVA, MVA phosphate or MVA diphosphate were not at all incorporated into IPP by cell-free systems in *E. coli* and *Z. mobilis* which gave a clear idea that mevalonate pathway does not exist in most of the prokaryotes. From the identification of non-mevalonate route for isoprenoid biosynthesis through these labeling studies, the search for the existence of either of the pathways in different living systems was initiated[12, 13]. Labeling studies help in the identification of pathway intermediates, the discovery of new metabolic pathway, precursors of the pathway etc[14].

Chapter 3: Section B
Establishment of fragmentation pathway for azadirachtin A through tandem MS

3B.1. Introduction

The most useful technique available for the labeling studies of metabolite includes mass spectrometry and Nuclear Magnetic Resonance (NMR)[18, 19]. GC-QTOF, LC-HRMS, capillary electrophoresis mass spectrometry (CE-MS) and Fourier transform ion cyclotron resonance mass spectrometry (FT-ICR-MS) based metabolic profiling acts as a sensitive and reliable method to analyze the metabolite both by qualitative and quantitative means[20-30]. In particular, Isotopic Mass Spectrometry helps in the analysis of isotopologues and isotopomers of molecules[2]. The common hardware platforms available for it includes GC, LC systems[27]. GC-MS requires derivatization of the sample with reagents such as N-Methyl-N-(trimethylsilyl) trifluoroacetamide (MSTFA) and methoxyamine hydrochloride for the analysis of primary metabolites[27]. Most of the polar primary and secondary metabolites are resolved and quantified in LC-HRMS as the mass spectral data can be further analyzed using mass spectral alignment tool as it helps to divulge the unknown metabolites in the sample. Tandem mass spectrometry has evolved to be a most powerful technique that allows the cleavage of selected ions into fragment ions, the so-called product ions which helps in understanding the chemical structure of the selected ion (precursor ion)[31, 32]. Hence, this method helps in screening metabolites, drugs, contaminants in plant, human, environmental samples etc. The fragment ions formed upon cleavage serves as a signature for the identification of that particular metabolite and its derivatives in other samples[28]. Establishment of structure-fragment relationship uniquely, using different ionization technique such as ESI, APCI, EI etc.[33] helps in further studies such as labeling experiment to trace the position of stable isotopic label present in the same metabolite[18]. These techniques also helps in dereplication studies, a process of identification of molecules whose structure is already known and plays an important role in natural product discovery and metabolic pathway analysis[32, 34]. Establishment of tandem MS fingerprint of novel molecules helps in metabolic pathway discovery of same molecules and also identification of them among complex and diverse mixture of plant natural products[35-43]. Tandem MS fingerprint of ring intact limonoids[44] and nimbin, nimbinene, salannin type C seco limonoids[45] have been established earlier based on ESI-MS. Hence, section B of this chapter deals with the chromatographic separation, mass spectrometric characterization, tandem mass spectrometric characterization of 6 natural azadirachtin derivatives purified from neem tree.

3B.2. Results and discussion

3B.2.1. Mass spectrometric characterization of azadirachtin

Azadirachtin A and its derivatives such as 3-deacetylazadirachtin A, azadirachtin B, vepaol, azadirachtin H, 11-epi-azadirachtin D were subjected to UPLC-ESI(+)-quadrupole/orbitrap-MS (Figure 3B.1, 3B.2). Different azadirachtin molecules eluted at different retention times as denoted in Table 3B.1 and the mass spectra of the corresponding molecules showed Na adduct and protonated adducts generated by the loss of one or two H_2O molecules (Figure 3B.2).

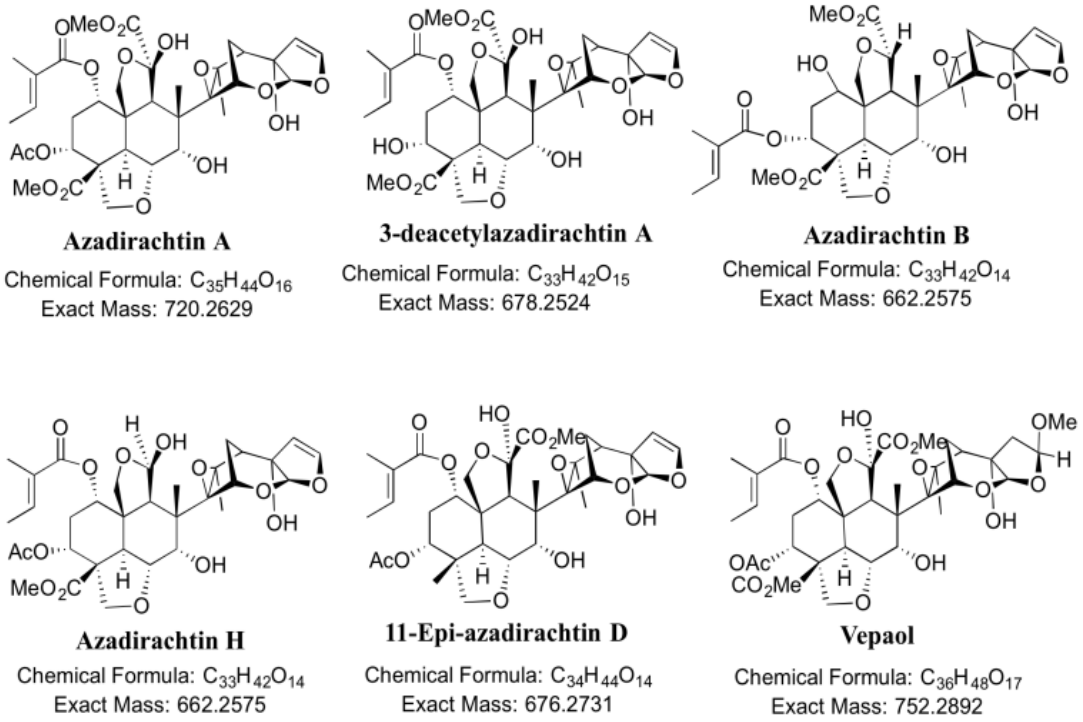

Figure 3B.1. Structures of azadirachtin A and its natural derivatives present in the tree used for comparative analysis

Molecule	**Molecular formula**	**Mass**	**Molecular ion**	***m/z* of the ion**	**Retention Time**
Azadirachtin A	$C_{35}H_{44}0_{16}$	720.2629	M-H_2O+H	703	7
Azadirachtin B	$C_{33}H_{42}0_{14}$	662.2575	M-H_2O+H	645	8
Azadirachtin H	$C_{33}H_{42}0_{14}$	662.2575	M-H_2O+H	645	6.55
Epi-azadirachtin D	$C_{34}H_{44}0_{14}$	676.2731	M-H_2O+H	659	8.2
3-deacetyazadirachtin A	$C_{33}H_{42}0_{15}$	678.2524	M-H_2O+H	661	7.16
Vepaol	$C_{36}H_{48}0_{17}$	752.2892	M-H_2O+H	735	8.23

Table 3B.1. Different azadirachtin derivatives purified from neem seed, tabulated with its formula, mass, molecular ion in ESI-MS, its *m/z* and retention time.

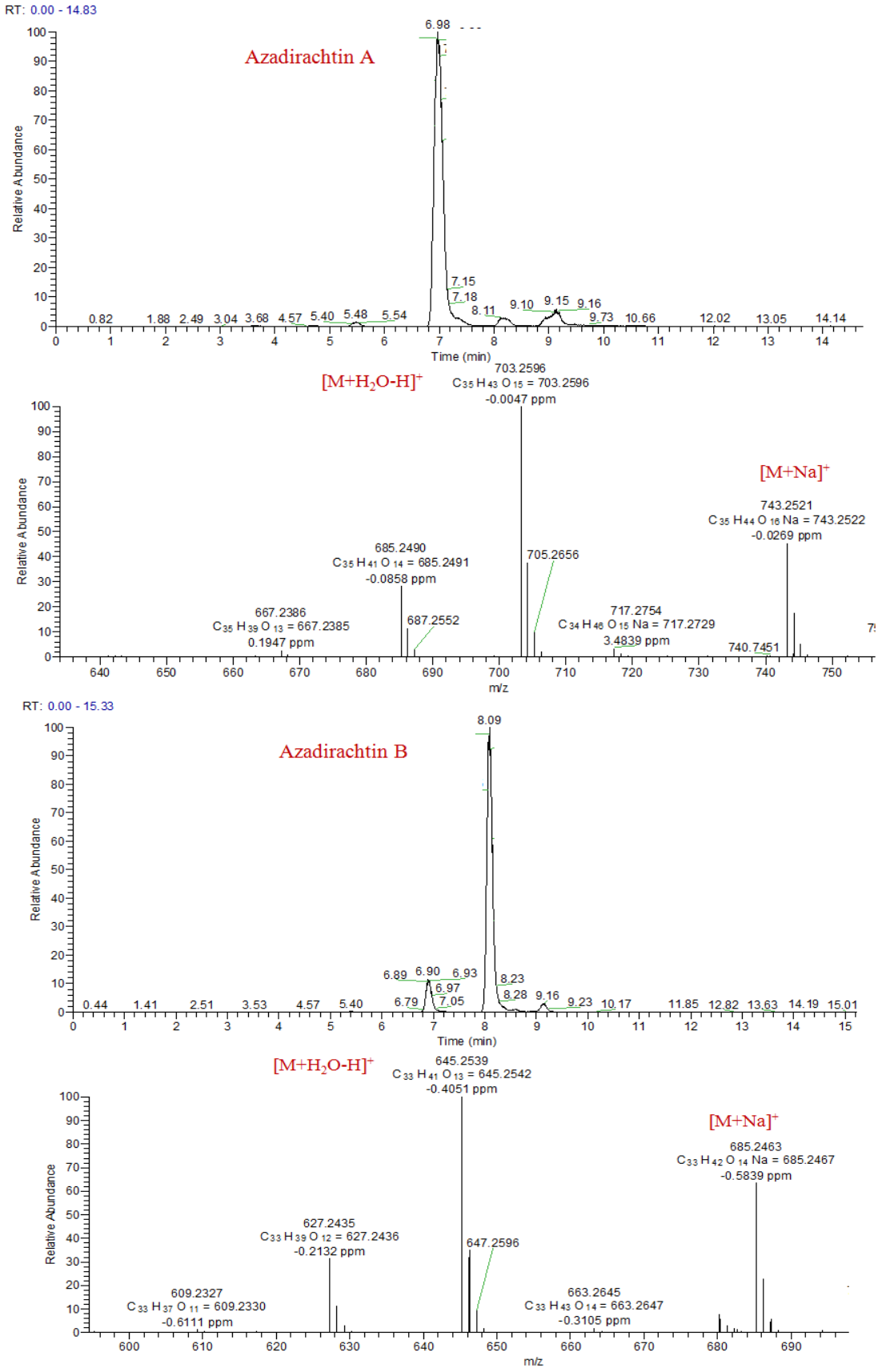
RT: 0.00 - 14.83
Azadirachtin A
6.98
Relative Abundance
Time (min)
[M+H2O-H]+
703.2596
C35 H43 O15 = 703.2596
-0.0047 ppm
[M+Na]+
743.2521
C35 H44 O16 Na = 743.2522
-0.0269 ppm
685.2490
C35 H41 O14 = 685.2491
-0.0858 ppm
705.2656
667.2386
C35 H39 O13 = 667.2385
0.1947 ppm
687.2552
717.2754
C34 H46 O15 Na = 717.2729
3.4839 ppm
740.7451
m/z
RT: 0.00 - 15.33
Azadirachtin B
8.09
Relative Abundance
Time (min)
[M+H2O-H]+
645.2539
C33 H41 O13 = 645.2542
-0.4051 ppm
[M+Na]+
685.2463
C33 H42 O14 Na = 685.2467
-0.5839 ppm
627.2435
C33 H39 O12 = 627.2436
-0.2132 ppm
647.2596
609.2327
C33 H37 O11 = 609.2330
-0.6111 ppm
663.2645
C33 H43 O14 = 663.2647
-0.3105 ppm
m/z

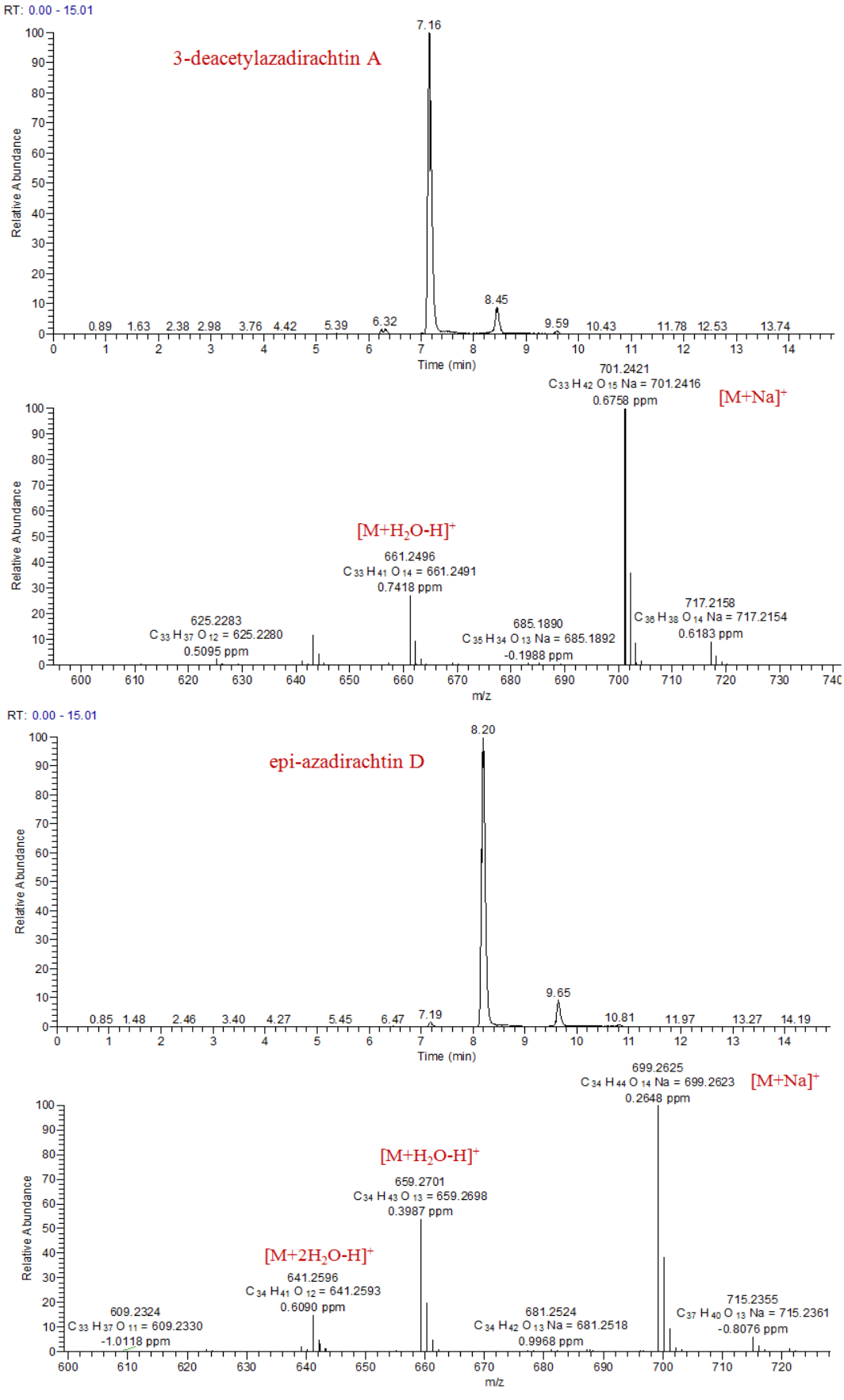
RT: 0.00 - 15.01
3-deacetylazadirachtin A
7.16
8.45
Relative Abundance
Time (min)
701.2421
C33 H42 O15 Na = 701.2416
0.6758 ppm
[M+Na]+
[M+H2O-H]+
661.2496
C33 H41 O14 = 661.2491
0.7418 ppm
625.2283
C33 H37 O12 = 625.2280
0.5095 ppm
685.1890
C35 H34 O13 Na = 685.1892
-0.1988 ppm
717.2158
C36 H38 O14 Na = 717.2154
0.6183 ppm
m/z
RT: 0.00 - 15.01
epi-azadirachtin D
8.20
9.65
7.19
Relative Abundance
Time (min)
699.2625
C34 H44 O14 Na = 699.2623
0.2648 ppm
[M+Na]+
[M+H2O-H]+
659.2701
C34 H43 O13 = 659.2698
0.3987 ppm
[M+2H2O-H]+
641.2596
C34 H41 O12 = 641.2593
0.6090 ppm
609.2324
C33 H37 O11 = 609.2330
-1.0118 ppm
681.2524
C34 H42 O13 Na = 681.2518
0.9968 ppm
715.2355
C37 H40 O13 Na = 715.2361
-0.8076 ppm
m/z

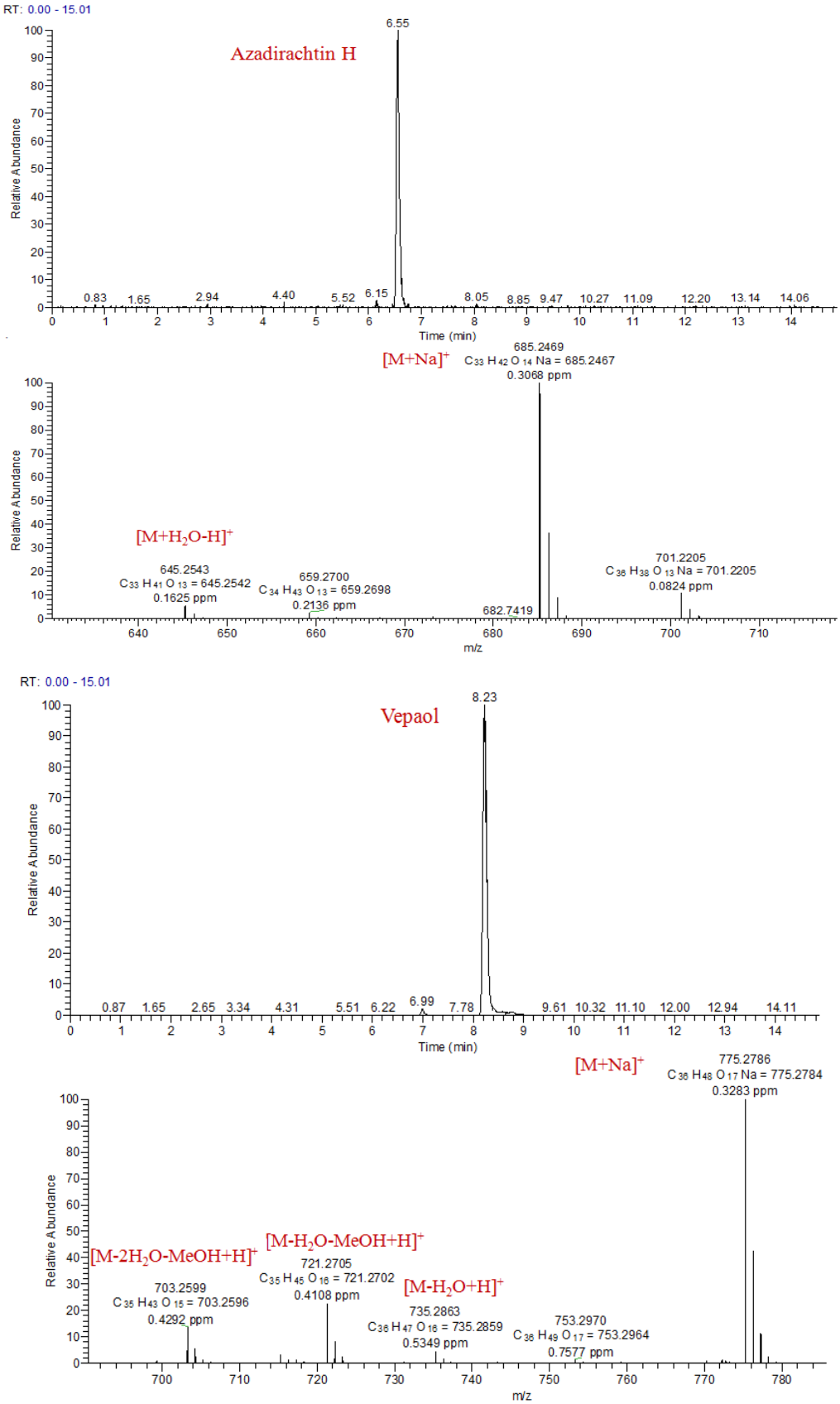

Figure 3B.2. Chromatogram and corresponding mass spectra for six limonoids (Azadirachtin A and its natural derivatives).

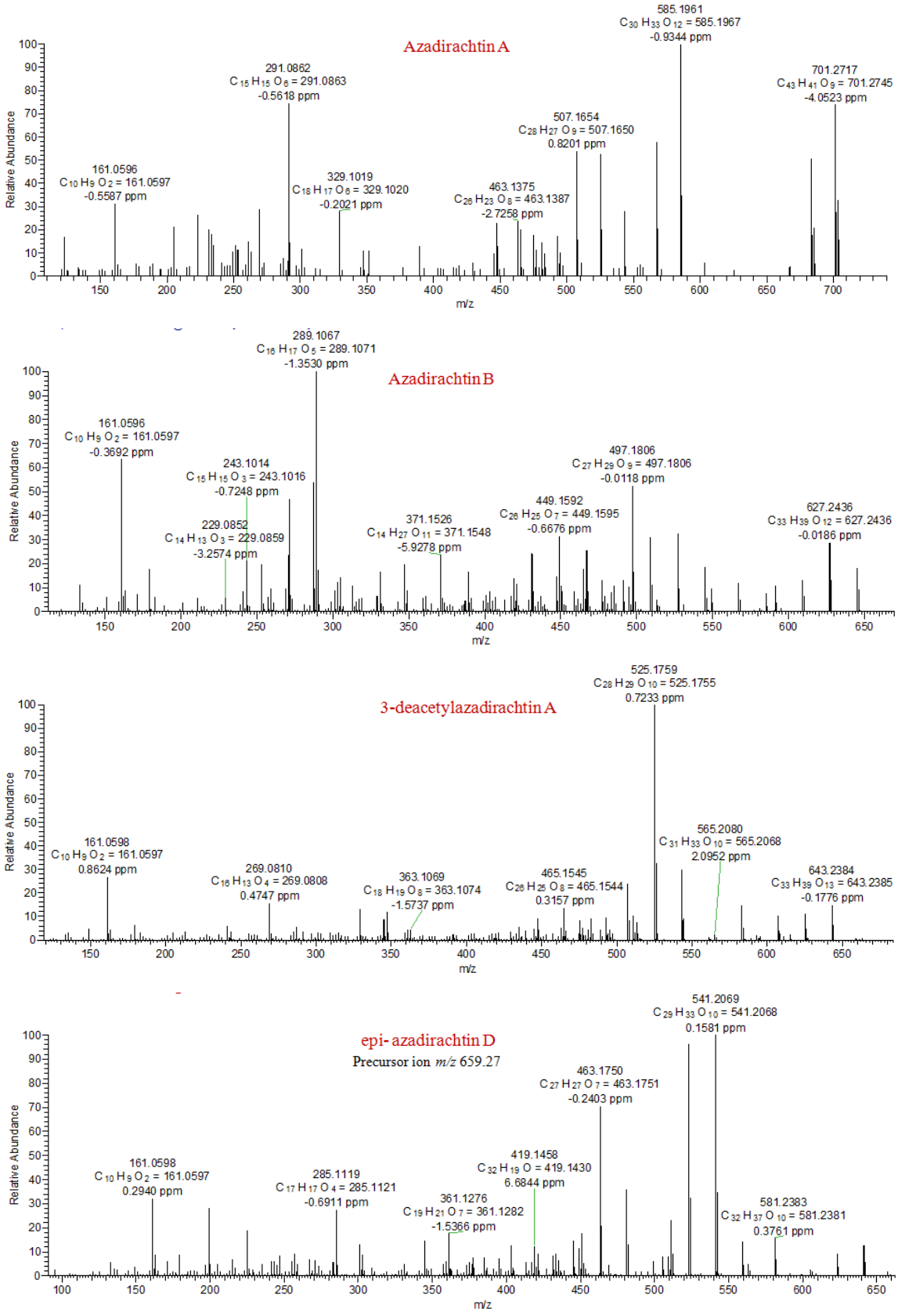
Azadirachtin A
585.1961
C30 H33 O12 = 585.1967
-0.9344 ppm
291.0862
C15 H15 O8 = 291.0863
-0.5618 ppm
701.2717
C43 H41 O9 = 701.2745
-4.0523 ppm
507.1654
C28 H27 O9 = 507.1650
0.8201 ppm
161.0596
C10 H9 O2 = 161.0597
-0.5587 ppm
329.1019
C18 H17 O6 = 329.1020
-0.2021 ppm
463.1375
C26 H23 O8 = 463.1387
-2.7258 ppm
Relative Abundance
m/z
Azadirachtin B
289.1067
C16 H17 O5 = 289.1071
-1.3530 ppm
161.0596
C10 H9 O2 = 161.0597
-0.3692 ppm
497.1806
C27 H29 O9 = 497.1806
-0.0118 ppm
243.1014
C15 H15 O3 = 243.1016
-0.7248 ppm
449.1592
C26 H25 O7 = 449.1595
-0.6676 ppm
627.2436
C33 H39 O12 = 627.2436
-0.0186 ppm
229.0852
C14 H13 O3 = 229.0859
-3.2574 ppm
371.1526
C14 H27 O11 = 371.1548
-5.9278 ppm
Relative Abundance
m/z
3-deacetylazadirachtin A
525.1759
C28 H29 O10 = 525.1755
0.7233 ppm
565.2080
C31 H33 O10 = 565.2068
2.0952 ppm
161.0598
C10 H9 O2 = 161.0597
0.8624 ppm
269.0810
C16 H13 O4 = 269.0808
0.4747 ppm
363.1069
C18 H19 O8 = 363.1074
-1.5737 ppm
465.1545
C26 H25 O8 = 465.1544
0.3157 ppm
643.2384
C33 H39 O13 = 643.2385
-0.1776 ppm
Relative Abundance
m/z
epi- azadirachtin D
Precursor ion *m/z* 659.27
541.2069
C29 H33 O10 = 541.2068
0.1581 ppm
463.1750
C27 H27 O7 = 463.1751
-0.2403 ppm
419.1458
C32 H19 O = 419.1430
6.6844 ppm
161.0598
C10 H9 O2 = 161.0597
0.2940 ppm
285.1119
C17 H17 O4 = 285.1121
-0.6911 ppm
361.1276
C19 H21 O7 = 361.1282
-1.5366 ppm
581.2383
C32 H37 O10 = 581.2381
0.3761 ppm
Relative Abundance
m/z

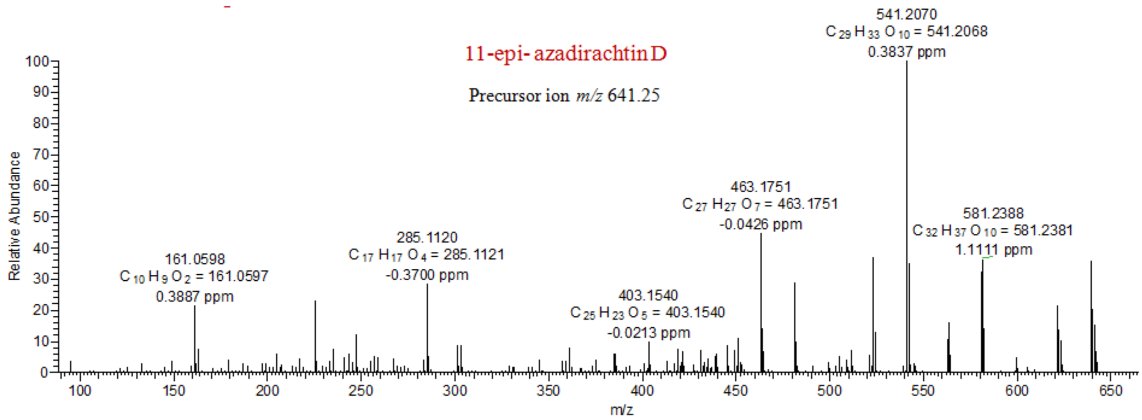
11-epi-azadirachtin D
Precursor ion m/z 641.25
541.2070
C29 H33 O10 = 541.2068
0.3837 ppm
463.1751
C27 H27 O7 = 463.1751
-0.0426 ppm
581.2388
C32 H37 O10 = 581.2381
1.1111 ppm
285.1120
C17 H17 O4 = 285.1121
-0.3700 ppm
161.0598
C10 H9 O2 = 161.0597
0.3887 ppm
403.1540
C25 H23 O5 = 403.1540
-0.0213 ppm
Relative Abundance
m/z

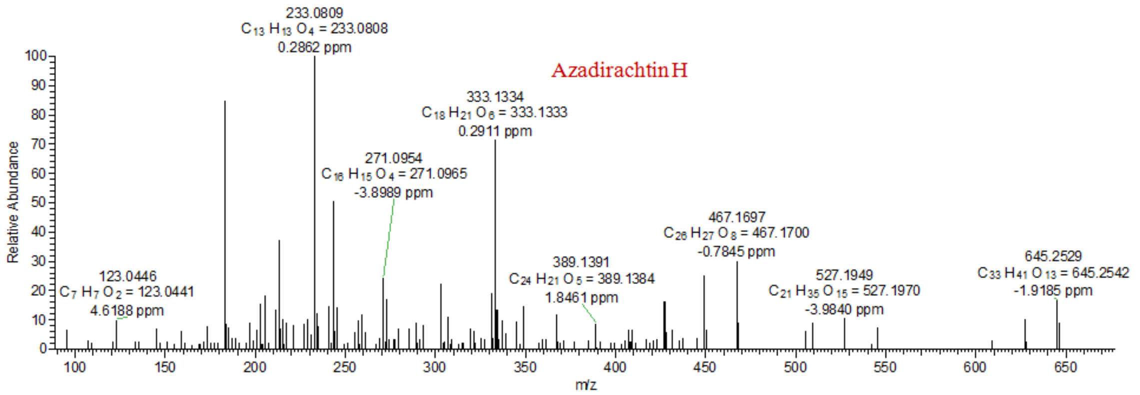
233.0809
C13 H13 O4 = 233.0808
0.2862 ppm
Azadirachtin H
333.1334
C18 H21 O6 = 333.1333
0.2911 ppm
271.0954
C16 H15 O4 = 271.0965
-3.8989 ppm
467.1697
C26 H27 O8 = 467.1700
-0.7845 ppm
389.1391
C24 H21 O5 = 389.1384
1.8461 ppm
645.2529
C33 H41 O13 = 645.2542
-1.9185 ppm
527.1949
C21 H35 O15 = 527.1970
-3.9840 ppm
123.0446
C7 H7 O2 = 123.0441
4.6188 ppm
Relative Abundance
m/z

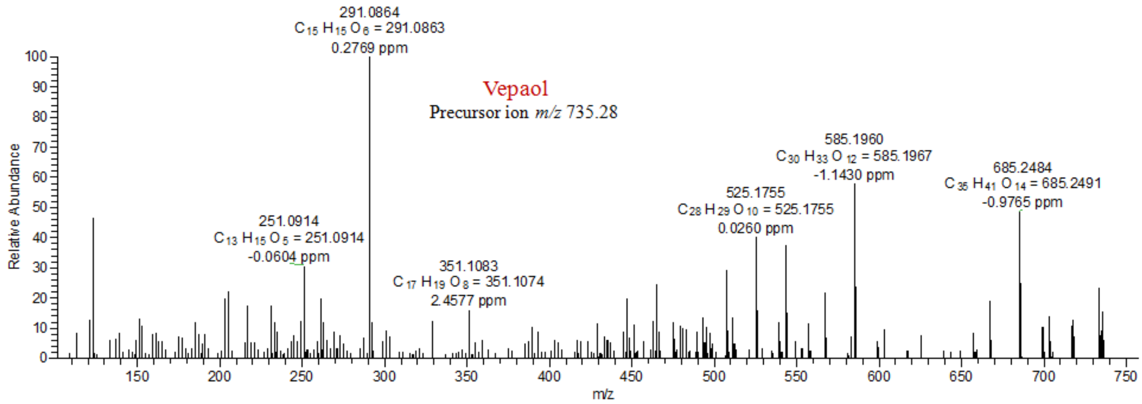
291.0864
C15 H15 O6 = 291.0863
0.2769 ppm
Vepaol
Precursor ion m/z 735.28
585.1960
C30 H33 O12 = 585.1967
-1.1430 ppm
685.2484
C35 H41 O14 = 685.2491
-0.9765 ppm
525.1755
C28 H29 O10 = 525.1755
0.0260 ppm
251.0914
C13 H15 O5 = 251.0914
-0.0604 ppm
351.1083
C17 H19 O8 = 351.1074
2.4577 ppm
Relative Abundance
m/z

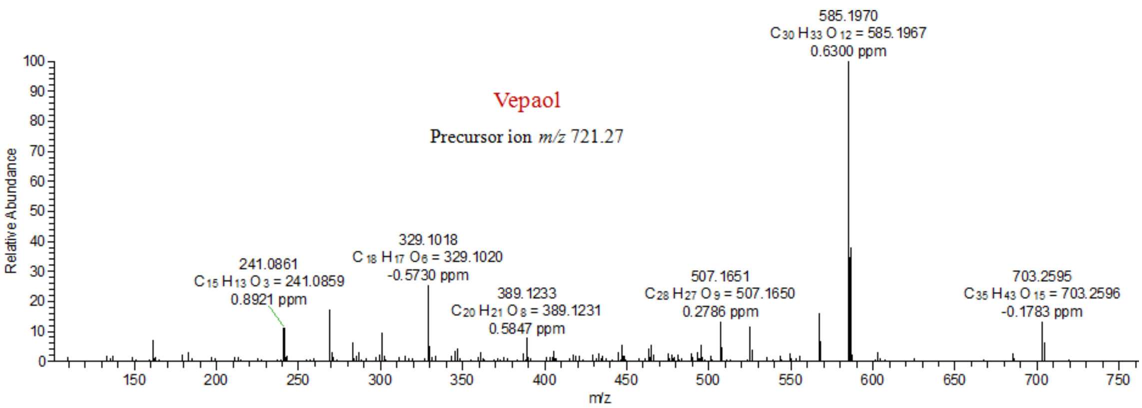
585.1970
C30 H33 O12 = 585.1967
0.6300 ppm
Vepaol
Precursor ion m/z 721.27
329.1018
C18 H17 O6 = 329.1020
-0.5730 ppm
241.0861
C15 H13 O3 = 241.0859
0.8921 ppm
389.1233
C20 H21 O8 = 389.1231
0.5847 ppm
507.1651
C28 H27 O9 = 507.1650
0.2786 ppm
703.2595
C35 H43 O15 = 703.2596
-0.1783 ppm
Relative Abundance
m/z

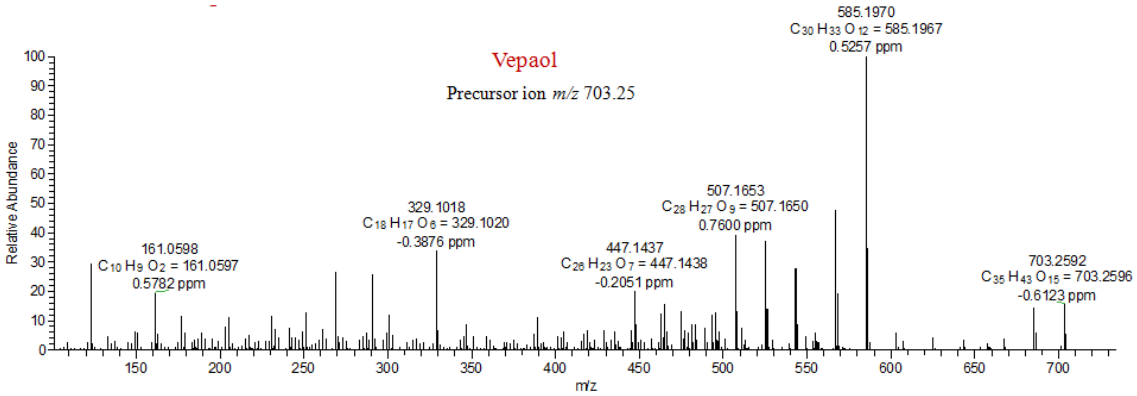

Figure 3B.3. Tandem Mass spectra at (NCE) normalized collision energy of 20% applied to precursor azadirachtin ions generated unique and common product ions among different azadirachtin molecules comparatively.

3B.2.2. Tandem mass spectrometric characterization of azadirachtin A

To understand the fragmentation pattern for azadirachtin A, we have subjected azadirachtin A and its derivatives such as 3-deacetylazadirachtin A, azadirachtin B, vepaol, azadirachtin H, 11-epi-azadirachtin D to UPLC-ESI(+)-quadrupole/orbitrap-MS/MS study. Mass spectral traces of azadirachtin A and its derivatives did not show molecular ion peak ($[M+H]^+$) however had the fragment ion with a loss of water molecule, i.e. $[M\text{-}H_2O+H]^+$ and sodium adduct $[M+Na]^+$. $[M\text{-}H_2O+H]^+$ adduct was considered as parent ion and was subjected to MS/MS fragmentation at various NCEs such as 10%, 15%, 20% and 25% (Figure 3B.4). At 20% NCE, both the high and low molecular weight fragments were equally distributed in intensity and hence used to understand the fragmentation pattern for azadirachtin. The signature spectral fragments (daughter ions) obtained after fragmentation of each azadirachtin derivative at 20% NCE and their corresponding relative intensity have been populated in the table (Table 3B.2).

Probable fragmentation pathway for the formation of daughter ions of azadirachtin A, when the parent ion, $[M\text{-}H_2O+H]^+$ *m/z* 703.2596 was subjected to MS/MS at the NCE of 20% has been schematically represented (Figure 3B.5). The mass fragmentation of parent molecular ion, *m/z* 703.2596, lead to the formation of fragment *m/z* 685.2491 $[M\text{-}2H_2O+H]^+$, due to loss of a molecule of H_2O and it was identified at the relative intensity of 2.6%. This fragment *m/z* 685.2491, undergoes several neutral losses to generate fragments in the high molecular range at *m/z* 625.2280 $[M\text{-}2H_2O\text{-}AcOH+H]^+$ (3.2%), 607.2174 $[M\text{-}3H_2O\text{-}AcOH+H]^+$ (1.2%), 585.1967 $[M\text{-}2H_2O\text{-}Tiglic\ acid+H]^+$, 567.1861 $[M\text{-}3H_2O\text{-}Tiglic\ acid+H]^+$ (62.2%), 525.1755 $[M\text{-}2H_2O\text{-}Tiglic\ acid\text{-}AcOH+H]^+$ (30.4%),

and 507.1650 [M-3H_2O-Tiglic acid-AcOH+H]$^+$ (85.6%). Hydrolysis of one of the ester group and/or removal of one or two CH_2O molecules from *m/z* 507.1650 gave rise to the fragments *m/z* 493.1493 [M-3H_2O-Tiglic acid-AcOH-CH_3+H]$^+$ (15%), 463.1387 [M-3H_2O-Tiglic acid-AcOH-CH_2O-CH_3+H] (28.9%) and 447.1438 [M-3H_2O-Tiglic acid-AcOH-2CH_2O+H]$^+$ (50%), respectively. A low relative ion intensity (13%) fragment of *m/z* 555.1861 [M-2H_2O-Tiglic acid-CH_2O+H]$^+$ was formed after removal of a H_2O, tiglic acid and a CH_2O group from the parent ion.

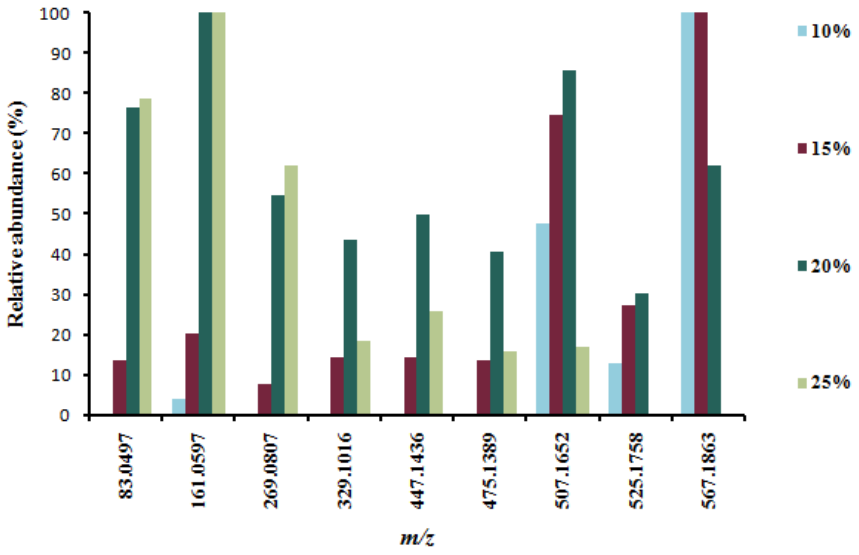

Figure 3B.4. Variation in relative abundance of MS/MS daughter ions obtained at varying normalized collision energies (NCEs) 10, 15, 20, 25% for azadirachtin A.

The lower molecular weight fragments of *m/z* 329.1020 and *m/z* 269.0808 corresponded to the decalin portion (A and B ring) of azadirachtin molecule formed after the detachment of hydrofuran acetal moiety from the fragments *m/z* 507.1650 and *m/z* 447.1438 respectively. Finally, the hydrofuran acetal moiety of azadirachtin was identified as fragment of *m/z* 161.0597 with highest intensity of 100%. The fragments of *m/z* 400 to 600 range were possibly formed through protonation-mediated cleavage of tigloyl ester bond and thereby release of tiglate daughter ion (*m/z* 83.0491) with 76.4% intensity. This was in line with the fragmentation pattern obtained with salannin and 3-deacetylsalannin molecules.

3-deacetylazadirachtin A molecule differs from azadirachtin A by the absence of acetyl group at 3-C of ring A. The parental molecular ion, *m/z* 661.2491 [M-H_2O+H]$^+$ was subjected to fragmentation at NCE of 20% and each daughter fragment obtained

were probed for its molecular formula and corresponding structure. The daughter ions, *m/z* 643.2382 $[M\text{-}2H_2O+H]^+$, 625.2281 $[M\text{-}3H_2O+H]^+$ and 607.2174 $[M\text{-}4H_2O+H]^+$ were obtained after successive removal of H_2O molecules following protonation. Fragments such as *m/z* 525.1758, 507.1655, 465.1543, 447.1436 and 329.1013 obtained were in common with azadirachtin A fragmentation pattern (Table 3B.2).

Vepaol possesses a methoxy group in the hydrofuran moiety of azadirachtin A, thereby contributing to the increase in molecular weight of 32 Da. Mass spectra of vepaol showed the presence of three protonated ion peaks with *m/z* 735.2867, 721.2705, and 703.2598 which are formed through removal of either H_2O molecule or methoxy group or both (Table 3B.2). All these three parental ions were subjected to fragmentation at NCE 20% and the resulting daughter ions for each of them were studied. Most of the daughter fragments of azadirachtin A were observed in common with vepaol, as it possess same structure of azadirachtin A after the removal of methoxy group (Table 3B.2).

Azadirachtin B is devoid of hydroxyl group at 11-C, tiglate at 1-C and 3-C acetyl functionality is replaced with tiglate group in comparison to azadirachtin A. The removal of tiglate moiety from the parent ion *m/z* 645.2542 ($[M\text{-}H_2O+H]^+$) yielded the fragment *m/z* 545.2017 $[M\text{-}H_2O\text{-Tiglic acid}+H]^+$. The fragments, *m/z* 509.1806 $[M\text{-}3H_2O\text{-Tiglic acid-AcOH}+H]^+$, 527.1912 $[M\text{-}2H_2O\text{-Tiglic acid-AcOH}+H]^+$ and 271.0965 obtained were on par with *m/z* 507.1650, *m/z* 525.1755 and *m/z* 269.0809 of azadirachtin A, respectively (Figure 3B.5, Table 3B.2) due to the absence of double bond between 9-C and 11-C.

Azadirachtin H is a decarboxymethyl derivative of azadirachtin A at 11-C position and MS/MS at NCE 20% fragmented the parent ion to greater extent such that only lower *m/z* fragments formed from decalin portion were seen (Table 3B.2). Higher mass fragments such as *m/z* 545.2017 $[M\text{-}H_2O\text{-Tiglic acid}+H]^+$, 509.1806 $[M\text{-}3H_2O\text{-Tiglic acid}+H]^+$, 467.1700 $[M\text{-}2H_2O\text{-Tiglic acid-AcOH}+H]^+$and 449.1595 $[M\text{-}3H_2O\text{-Tiglic acid-AcOH}+H]^+$ were obtained at ≤15% NCE.

11-epi-azadirachtin D lacks one of the two methylester groups of azadirachtin A and produced two types of protonated ions with *m/z* 659.2704 $[M\text{-}H_2O+H]^+$ and 641.2598 $[M\text{-}2H_2O+H]^+$. The following fragments *m/z* 285.1121 and 345.1333 were formed from the decalin portion of the molecule (Table 3B.2). The subsequent removal of the functional groups such as hydroxyl, tigloyl, acetyl groups generated fragments

such as *m/z* 541.2068 $[M\text{-}2H_2O\text{-Tiglic acid}+H]^+$, 523.1963 $[M\text{-}3H_2O\text{-Tiglic acid}+H]^+$, 481.1857 $[M\text{-}2H_2O\text{-Tiglic acid-AcOH}+H]^+$, 463.1751 $[M\text{-}3H_2O\text{-Tiglic acid-AcOH}+H]^+$, *m/z* 451.1751 $[M\text{-}2H_2O\text{-Tiglic acid-AcOH-}CH_2O+H]^+$ from both the parent ions.

The fragment *m/z* 161.0597 was identified in fragmentation pattern of most of the azadirachtin derivatives. The fragments, *m/z* 161.0597 and *m/z* 83.0491 corresponds to hydrofuran acetal moiety and tiglate group. Therefore either one acts as a signature fragment for azadirachtin class of limonoids from neem tree.

Therefore, structure-fragment relationship of azadirachtin A, thus obtained will not only help to infer the position of ^{13}C labels incorporated into it, but also serves as a sensitive method for identification of azadirachtin in environmental as well as biological samples. We have studied already, the structure-fragment relationship for C-seco limonoids such as salannin, salannolacetate, nimbin, nimbinene, 6-deacetylnimbinene and 6-deacetylnimbin, isolated and purified from neem oil[45]. These results have been used for deducing the pattern of ^{13}C incorporation into the same limonoids and their isotopologues identified in our feeding experiments.

Molecule	**Precursor ion (*m/z*)**	**Molecular formula of precursor ion**	**Adduct**	**Daughter ion *m/z* (formula, Relative intensity) at NCE 20%**
Azadirachtin A	703.2604	$C_{35}H_{43}O_{15}$	M-H_2O+H	83.0497 (C_5H_7O, 76.41), 161.0596 ($C_{10}H_9O_2$, 100), 241.0859 ($C_{15}H_{13}O_3$, 26.71), 269.0809 ($C_{16}H_{13}O_4$, 54.72), 329.1016 ($C_{18}H_{17}O_6$, 43.8), 447.1433 ($C_{26}H_{23}O_7$, 50.04), 463.1374 ($C_{26}H_{23}O_8$, 28.9), 475.1392 ($C_{27}H_{23}O_8$, 40.55), 507.1650 ($C_{28}H_{27}O_9$, 85.66) 525.1754 ($C_{28}H_{29}O_{10}$, 30.37), 567.1860 ($C_{30}H_{31}O_{11}$, 62.22), 585.1970 ($C_{30}H_{33}O_{12}$, 38.73)
Azadirachtin B	645.2548	$C_{33}H_{41}O_{13}$	M-H_2O+H	83.0497 (C_5H_7O, 100), 161.0596 ($C_{10}H_9O_2$, 40.63), 179.0701 ($C_{10}H_{11}O_3$, 12.54), 253.0857 ($C_{16}H_{13}O_3$, 5.14), 271.0962 ($C_{16}H_{15}O_4$, 13.18), 287.0910 ($C_{16}H_{15}O_5$, 10.29), 289.1066 ($C_{16}H_{17}O_5$, 79.39), 389.1372 ($C_{24}H_{21}O_5$, 6.72), 497.1801 ($C_{27}H_{29}O_9$, 12.2), 509.1799 ($C_{28}H_{29}O_9$, 7.51), 527.1910 ($C_{28}H_{31}O_{10}$, 6.38), 545.2030 ($C_{28}H_{33}O_{11}$,5.54), 643.2717 ($C_{34}H_{43}O_{12,}$)
3-deacetyl Azadirachtin A	661.2498	$C_{33}H_{41}O_{14}$	M-H_2O+H	161.0598 ($C_{10}H_9O_2$, 26.55), 269.0809 ($C_{16}H_{13}O_4$, 15.61), 329.1013 ($C_{18}H_{17}O_6$, 12.55), 347.1122 ($C_{18}H_{19}O_7$, 13.85), 447.1436 ($C_{26}H_{23}O_7$, 10.45), 465.1543 ($C_{26}H_{25}O_8$, 11.62), 507.1655 ($C_{28}H_{27}O_9$, 26.66), 511.1612 ($C_{27}H_{27}O_{10}$, 10.58), 525.1758 ($C_{28}H_{29}O_{10}$, 100), 543.1863 ($C_{28}H_{31}O_{11}$, 27.78) 583.2184 ($C_{31}H_{35}O_{11}$, 13.91), 625.2281 ($C_{33}H_{37}O_{12}$, 11.85), 643.2382 ($C_{33}H_{39}O_{13}$, 13.16)
Azadirachtin H	645.2550	$C_{33}H_{41}O_{13}$	M-H_2O+H	83.0497 (C_5H_7O, 100), 183.0807 ($C_{13}H_{11}O$, 80.84), 203.0711 ($C_{12}H_{11}O_3$, 9.09), 205.0855

				($C_{12}H_{13}O_3$, 10.83), 211.0754 ($C_{14}H_{11}O_2$, 10.35), 213.0914 ($C_{14}H_{13}O_2$, 29.61), 233.0867 ($C_{13}H_{13}O_4$, 63.36), 241.0867 ($C_{15}H_{13}O_3$, 9.05), 243.1016 ($C_{15}H_{15}O_3$, 33.8), 259.0964 ($C_{15}H_{15}O_4$, 11.76), 271.0958 ($C_{16}H_{15}O_4$, 16.76), 273.1107 ($C_{16}H_{17}O_4$, 11.94), 303.1219 ($C_{17}H_{19}O_5$, 14.07), 333.1332 ($C_{18}H_{21}O_6$, 33.68),
11-epi-azadirachtin D	659.2704	$C_{34}H_{43}O_{13}$	M-H_2O+H	83.0497 (C_5H_7O, 77.85), 161.0598 ($C_{10}H_9O_2$, 100), 199.1120 ($C_{14}H_{15}O$, 92.87), 225.0910 ($C_{15}H_{13}O_2$, 59.32), 257.1169 ($C_{16}H_{17}O_3$, 27.93), 285.1118 ($C_{17}H_{17}O_4$, 57.89), 301.1069 ($C_{17}H_{17}O_5$, 31.81), 345.1337 ($C_{19}H_{21}O_6$, 29.89), 361.1282 ($C_{19}H_{21}O_7$, 28.38), 419.1480 ($C_{25}H_{23}O_6$,), 451.1749 ($C_{26}H_{27}O_7$, 23.41), 463.1750 ($C_{27}H_{27}O_7$, 82.35), 481.1859 ($C_{27}H_{29}O_8$, 32.99), 523.1965 ($C_{29}H_{31}O_9$, 62.58), 541.2070 ($C_{29}H_33O_{10}$, 54.06)
	641.2598	$C_{34}H_{41}O_{12}$	M-$2H_2O$+H	83.0497 (C_5H_7O, 100), 161.0597 ($C_{10}H_9O_2$, 67.67), 205.0858 ($C_{12}H_{13}O_3$, 14.62), 225.0910 ($C_{15}H_{13}O_2$, 48.31), 247.0963 ($C_{14}H_{15}O_4$, 48.31), 285.1117 ($C_{17}H_{17}O_4$, 56.13), 301.1068 ($C_{17}H_{17}O_5$, 17.22), 463.1748 ($C_{27}H_{27}O_7$, 51.27), 481.1855 ($C_{27}H_{29}O_8$, 27.55), 523.1962 ($C_{29}H_{31}O_9$, 29.92), 541.2068 ($C_{29}H_{33}O_{10}$, 57.04), 581.2377 ($C_{32}H_{37}O_{10}$, 21.98),
Vepaol	735.2867	$C_{36}H_{47}O_{16}$	M-H_2O+H	83.0497 (C_5H_7O, 100), 123.0444 ($C_7H_7O_2$, 79.24), 185.0598 ($C_{12}H_9O_2$, 18.38), 203.0704 ($C_{12}H_{11}O_3$, 21.48), 205.0860 ($C_{12}H_{13}O_3$, 21.65), 217.0864 ($C_{13}H_{13}O_3$, 17.10), 231.0650 ($C_{13}H_{11}O_4$,20.49), 233.0810 ($C_{13}H_{13}O_4$, 17.55), 249.0758 ($C_{13}H_{13}O_5$, 19.52),251.0916 ($C_{13}H_{15}O_5$, 32.88), 261.0763 ($C_{14}H_{13}O_5$, 22.02), 291.0863 ($C_{15}H_{15}O_6$, 79.16), 525.1750 ($C_{28}H_{29}O_{10}$, 16.77), 543.1869 ($C_{28}H_{31}O_{11}$, 14.3),
	721.2705	$C_{35}H_{45}O_{15}$	M-H_2O-MeOH+H	83.0497 (C_5H_7O, 84.84), 161.0597 ($C_{10}H_9O_2$, 49.64), 183.0806 ($C_{13}H_{11}O$, 26.3), 241.0859 ($C_{15}H_{13}O_3$, 69.12), 269.0808 ($C_{16}H_{13}O_4$, 100), 283.0963 ($C_{17}H_{15}O_4$, 35.35), 287.0914 ($C_{16}H_{15}O_5$, 19.94), 301.1068 ($C_{17}H_{17}O_5$, 38.89), 329.1019 ($C_{18}H_{17}O_6$, 76), 347.1130 ($C_{18}H_{19}O_7$, 16.57), 389.1236 ($C_{20}H_{21}O_8$, 22.4), 507.1656 ($C_{28}H_{27}O_9$, 26.83), 525.1763 ($C_{28}H_{29}O_{10}$, 20.16), 567.1869 ($C_{30}H_{31}O_{11}$, 21.26), 585.1972 ($C_{30}H_{33}O_{12}$, 87.62).
	703.2598	$C_{35}H_{43}O_{15}$	M-MeOH-$2H_2O$+H	83.0497 (C_5H_7O, 100), 123.0444 ($C_7H_7O_2$, 46.11), 161.0599 ($C_{10}H_9O_2$, 21.81), 203.0704 ($C_{12}H_{11}O_3$, 13.94), 205.0860 ($C_{12}H_{13}O_3$, 18.84), 231.0652 ($C_{13}H_{11}O_4$, 18.34), 251.0916 ($C_{13}H_{15}O_5$, 19.28), 261.0758($C_{14}H_{13}O_5$, 17.64), 269.0809 ($C_{16}H_{13}O_4$, 26.39), 291.0865 ($C_{15}H_{15}O_6$, 45.91), 329.1020 ($C_{18}H_{17}O_6$, 17.55), 447.1444 ($C_{26}H_{23}O_7$, 12.11), 507.1656 ($C_{28}H_{27}O_9$, 18.93), 525.1758 ($C_{28}H_{29}O_{10}$, 15.57), 543.1863 ($C_{28}H_{31}O_{11}$, 12.53), 585.1972 ($C_{30}H_{33}O_{12}$, 17.47)

Table 3B.2. Azadirachtin derivatives, precursor ion, MS/MS daughter ions and intensity of fragments obtained from fragmentation of the precursor ion at 20% NCE.

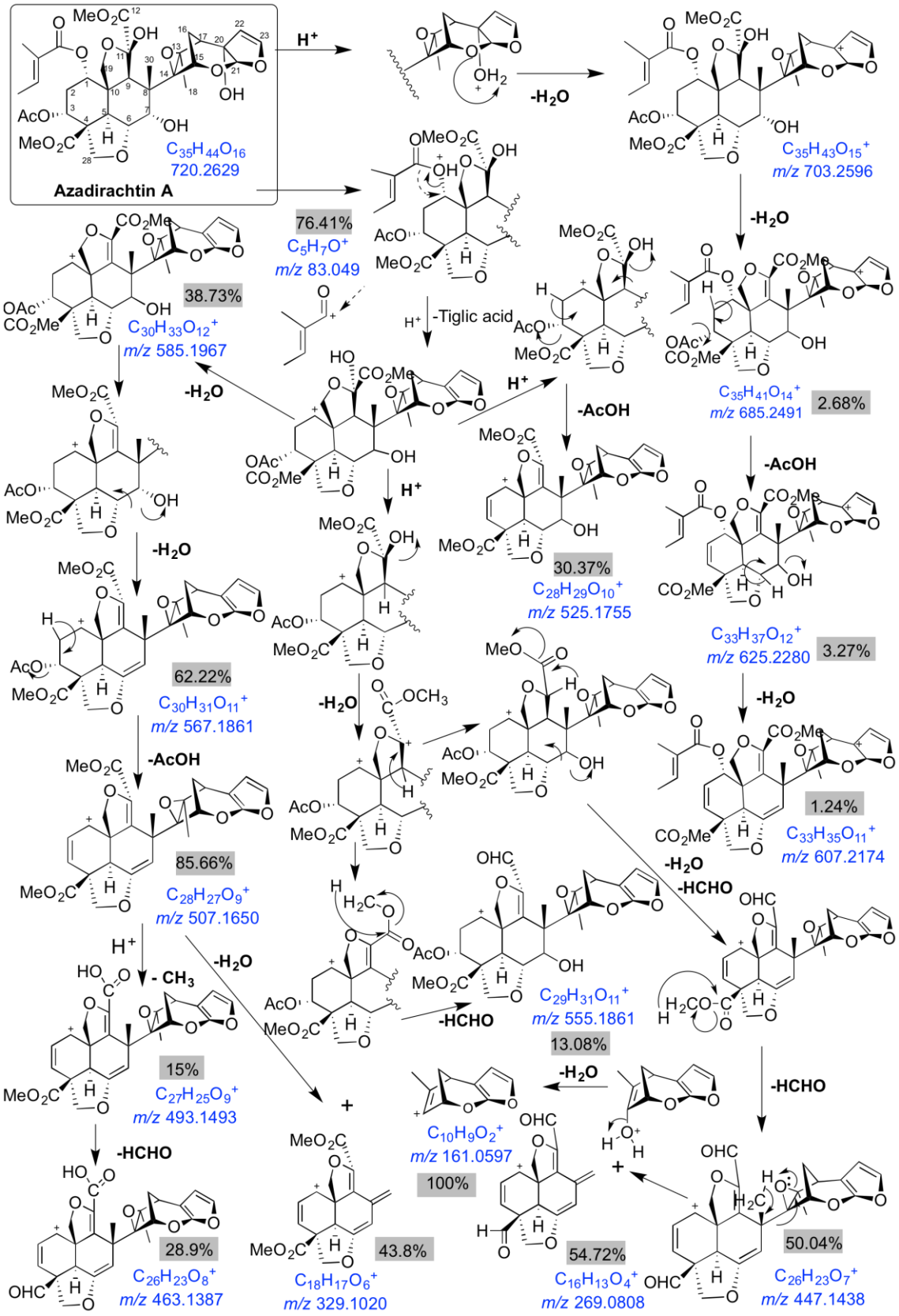

Figure 3B.5. The structure-fragment relationship of azadirachtin A was inferred from the tandem MS fragmentation studies of five azadirachtin derivatives at various NCEs based on which the putative fragmentation pathway of azadirachtin A was extrapolated.

3B.3. Conclusion

The structure fragment relationship of azadirachtin A was established based on the fragmentation pattern of azadirachtin A and its derivatives. This will help to identify and quantify azadirachtin in biomedical or environmental samples. The structure fragment relationship also helps further for the identification of the position of ^{13}C labels into the metabolite biosynthesized in *vivo* by uptake of labeled precursors in cell culture.

3B.4. Materials and methods

3B.4.1. Establishment of structure-fragment relationship for azadirachtin A

To establish the structure-fragment relationship for azadirachtin A, derivatives of azadirachtin such as azadirachtin B, 11-epi-azadirachtin D, azadirachtin H, 3-deacetylazadirachtin A, vepaol isolated and purified from neem seeds were subjected to MS/MS at various NCEs such as 10%, 15%, 20% and 25%. Based on the comparison of structure of different molecules of azadirachtin and their respective fragmentation pattern comprising of fragments from higher to lower *m/z* values, the structure of each fragment obtained after fragmentation of azadirachtin A molecule was established.

3B.4.2. LC-ESI-Mass Spectrometry conditions

Analysis of neem limonoids was performed with Thermo Scientific QExactive™ hybrid quadrupole-Orbitrap mass spectrometer associated with Accela 1250 pump and Accela open AS. The conditions of HESI source include capillary temperature of 320 °C, Heater temperature at 350 °C, s-lens RF level of 50, Spray voltage of 3.6 kV, spray current of 0.9 μA with sheath gas flow rate of 41, Auxiliary gas flow rate of 9 and sweep gas flow rate of 3. Standards, as well as the extracted samples, were analyzed in positive ionization mode, in full MS-scan with scan range of 100 to 1000 *m/z*. Following were the properties of the scan performed- resolution 70,000, AGC target 1e6, Maximum IT 200 ms. Waters Acquity UPLC BEH C18 column (particle size 1.7 μm, 2.1 X 100 mm) was used as the stationary phase while the solvent system of methanol and water containing 0.1% formic acid served as the mobile phase. The gradient started with 40% methanol (5 min isocratic), it was then increased to 50% (5 min isocratic), followed by 60% methanol for the next 15 minutes and over the next 4 minutes it was isocratic with 65% methanol. It was then increased to 90% methanol for 4 minutes. For the last 2 minutes, it was isocratic with 40% methanol. Constant flow rate of 0.3 mL min^{-1} was

maintained throughout the run time of 35 min. The chromatograms and mass spectral data were processed by Xcalibur qual browser (version 2.3; Thermo Scientific).

Chapter 3: Section C

Tracing the biosynthetic origin of limonoids and their functional groups through stable isotope labeling in neem cell suspension

3C.1. Introduction

In higher plants, biosynthesis of isoprenoids occurs through either of the two biosynthetic pathways: mevalonate pathway (MVA) or the methyl-erythritol phosphate pathway (MEP) or through a combination of both pathways[46-48]. MVA pathway is localized in the cytosol of the plant cell,[47] whereas MEP pathway occurs in the plastids[48-50]. It is found that monoterpenes, diterpenes and tetraterpenes are synthesized through the plastidic MEP pathway[51, 52] and sesquiterpenes, sterols (triterpenes) through the cytosolic MVA pathway, however it varies between plants and under different physiological conditions[53-55]. Contradictory to this prevalence of dichotomy, there are evidence based on labeling studies that suggest the differential contribution of isoprene C5 units from either of the two pathways towards the biosynthesis of different metabolites due to traversing of isoprene units across the thylakoid membrane of plastids[53, 56-59]. In neem tree, tetracyclic triterpene skeletal intermediate(s), en route to the formation of proto-limonoids through successive oxidation and rearrangement reactions[60]. The proto-limonoid further undergoes skeletal rearrangements and functionalization mediated by oxido-reductase and hydrolase enzyme systems to form higher limonoids such as basic and C-seco limonoids[60]. Depending on the skeletal modifications, limonoids can be subdivided into ring-intact (basic) and C-seco limonoids (Figure 3C.1B). Ring-intact limonoids encompass 4,4,8-trimethyl-17-furanylsteroidal skeleton such as Azadiradione and its derivatives. C-seco limonoids are generated by C-ring opening and further rearrangements thus producing nimbin, salannin and azadirachtins type of limonoids (Figure 3C.1)[61, 62]. Although intensive work has been carried out on the isolation, characterization, synthesis and bioactivity of limonoids, a very little is known about their biosynthesis and remains as a fact of speculation hitherto.

A

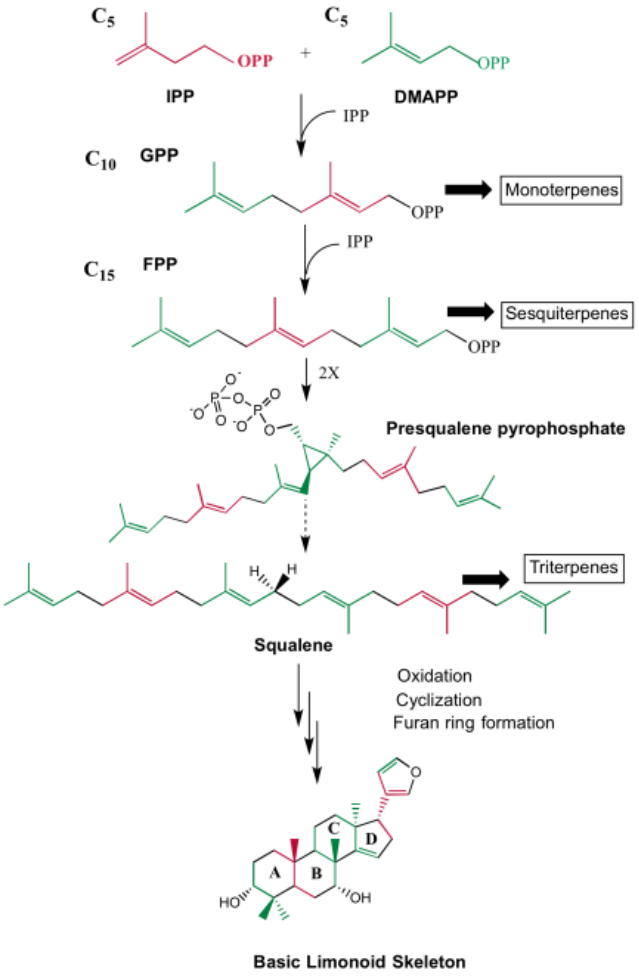

B

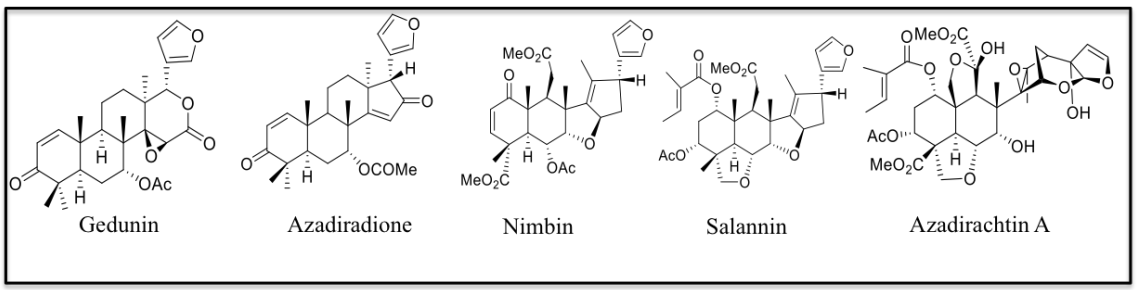

Figure 3C.1. (A) Upstream steps of limonoid biosynthesis **(B)** Structure of ring intact and C seco limonoids

3C.1.1. Isoprenoid biosynthesis in various living systems

Isoprenoid precursors are synthesized only through mevalonate pathway in archaea, fungi and animals[63]. However, in the case of bacteria, there exists plasticity in which few use only mevalonate pathway, while other pathogenic bacteria use MEP pathway, which serves as the metabolic target for most anti-infective drugs[64-66]. Some

bacteria utilize both pathways for the biosynthesis of isoprenoids, while some parasitic species lack both the pathways as they depend on the hosts for obtaining isoprenoid precursors[64-66]. Soon after the discovery of MEP pathway in bacteria, distribution of non-mevalonate pathway among different living organisms was intriguing and remained as a problem[67]. Specific inhibitors of the pathways[68] and labeled precursors were expected to be useful tools to address this unsolved issue. Experiments were performed by various research groups in different organisms to elucidate the pathway for biosynthesis of isoprene units[56-58, 69-87].

3C.1.1.1. Isoprenoid biosynthesis in bacteria

The MEP pathway is responsible for the biosynthesis of terpenoids in a number of eubacteria based on the number of labeling studies conducted by Rohmer and co-workers, whereas methanogenic archaea were found to generate terpenoids via the mevalonate pathway[67]. In addition to hopanoids of several bacteria, ubiquinone of *E. coli* was found to be synthesized through non-mevalonate pathway based on the evidence of incorporation of ^{13}C labeled deoxyxylulose into ubiquinone[88] and deuterium labeled methyl-erythritol into ubiquinone and menaquinone[89]. Contradictory to these studies, menaquinone and naphterin produced by *Streptomyces aeriouvifer* showed the simultaneous operation of mevalonate and non-mevalonate pathways for isoprene biosynthesis[90]. The green phototrophic eubacterium, *Chloroflexus aurantiacus* was also known to use mevalonate pathway for the biosynthesis of diterpene verrucosan-2β-ol[91]. The mevalonate pathway was observed only in sulfate-reducing, methanogenic, and hetero fermentative lactic acid bacteria[67].

3C.1.1.2. Isoprenoid biosynthesis in algae

The first successful experiments were performed with the green alga *Scenedesmus obliquus*[92]. From the study, the only existence of non-mevalonate pathway was obvious by investigation of biosynthesis of all plastidic isoprenoids (prenyl side chains of chlorophylls, plastoquinone-9, β-carotene and lutein) and cytoplasmic sterols through ^{13}C labeled acetate and glucose catabolism[48, 85, 92-95]. To find the involvement of either of the pathway in other species of algae, Rohmer and his co-workers conducted feeding experiments with [1-^{13}C] glucose which resulted in the evidence that only MEP pathway operates for the biosynthesis of all isoprenoids in green algae *Chlorella fusca* and

Chlamydomonas reinhardtii[93]. The red alga *Cyanidium caldarium* and the Chrysophyte, *Ochromonas danica* used the MVA route for synthesis of sterols, whereas chloroplast isoprenoids were synthesized via MEP route[48]. Euglenophyte, *Euglena gracilis* exclusively used MVA route for biosynthesis of all isoprenoids, whereas cyanobacterium *Synechocystis* PCC used MEP route[93]. Although, it was supposed that eukaryotic photosynthetic organisms possessing MVA pathway have acquired plastids as endosymbionts during the course of evolution, in algae only MEP pathway exists for the biosynthesis of all isoprenoids[63, 96, 97]. Chlorophyta encompassing classes of green algae was found to use MEP pathway for the synthesis of not only the plastidic, but also the cytosolic isoprenoids[95]. Charophyceae, which are the close relatives to the land plants and green flagellate, *Mesostigma viride* showed dichotomy as in plants: plastidic isoprenoids through MEP pathway and cytosolic through MVA pathway[95].

3C.1.1.3. Isoprenoid biosynthesis in plant system

The first evidence for the existence of MEP pathway in plant system was provided by Schwarz in an independent feeding experiment with ^{13}C labeled glucose for the study of ginkgolides and bilobalides which gave a same pattern of labeling as that found in bacteria utilizing glucose through glycolysis at the same instance of identification of this novel pathway in bacteria[15]. The labeling methods which proved successful for bacteria, were utilized for plant systems, which were grown heterotrophically with a single ^{13}C labeled carbon source under low light intensities that is not conducive for photosynthesis but allowed differentiation of chloroplasts for the study of the synthesis of pigments formed from isoprene units[98]. This condition has prevented the scrambling of the label from $^{13}CO_2$ obtained from the catabolism of the labeled carbon source as $^{13}CO_2$ could be refixed through the Calvin cycle during photosynthesis[98]. Taxol, a diterpene from *Taxus chinenesis* was demonstrated to be biosynthesized through non-mevalonate route in 1996[76]. Soon after the identification of alternative pathway for the biosynthesis of isoprenoids in bacteria and algae, Rohmer in collaboration with Lichtenthaler investigated various isoprenoids in plant system (*Daucus carota*, *Lemna gibba* and *Hordeum vulgare*) using [1-^{13}C] glucose feeding which showed the same novel labeling pattern as found in bacteria and algae, in chloroplast bound isoprenoids such as phytol, plastoquinone, carotene and lutein, whereas, labeling pattern according to MVA was obtained in sterols[48, 85, 92-95]. These results gave a reasonable interpretation that the novel

alternative pathway must be plastid bound and therefore plants possess two pathways for isoprenoid biosynthesis. To substantiate these findings, the same group conducted feeding experiments with 1-[^{2}H] deoxy-D-xylulose in various higher plants *Populus nigra*, *Chelidonium majus*, and *Salix viminalis* and algae, which produced isoprene and phytol with the deuterium incorporation[48]. Thus, studies on many other plant systems have been taken up by different groups to investigate the distribution of the pathways in plants for synthesis of different metabolites. Biosynthesis of basic isoprene units and their contribution to the final products of mono-, di-, tri-, tetraterpenoid origin were brought to light by individual research groups by examining the position and distribution of labels on the products obtained through labeled precursors, which was used to reconstruct the pathways and mechanisms[3, 86, 98-102]. Bryophytes, the primitive plants also showed a clear dichotomy as observed in plants, which was evident from various studies for biosynthesis of sesquiterpenes, diterpenes, triterpenes in liverworts[77, 80, 103]. These studies in higher plants concluded that, biosynthesis of isoprenoid precursor, isopentenyl diphosphate (IPP) occurred through both mevalonate and non-mevalonate MEP pathway, but were highly compartmentalized. This compartmentation was identified in plants in 1967 by Goodwin and his co-workers before elucidation of the plastidic Rohmer pathway, based on the impermeability of the proffered ^{14}C-mevalonate into plastids, which showed the preferential labeling of ubiquinone and sterols but not the carotenoids whereas $^{14}CO_2$ being incorporated into all isoprenoids[104]. In previous studies, Goodwin could find the incorporation of ^{14}C-mevalonate into plastidic isoprenoids in intact chloroplasts[105-107], which was later found to vary depending on plastid development stages[108].

3C.1.2. Tracing Isoprenoid biosynthesis by *in vivo* labeling

Tracer studies using potential precursors labeled with radioactive or stable isotopes are among the most important methods for elucidating the biosynthetic pathways and mechanisms leading to natural products[109, 110]. Transfer of the labeled precursors into its products is used to reconstruct the pathways and mechanisms by considering the position and distribution of the labels[109, 110]. The history of the study of isoprenoid biosynthesis right from the identification of mevalonate pathway[46] in 1950s till the discovery of MEP pathway in 1990s have deeply recorded unanimously the role played by labeled precursors in identification of the intermediates of the metabolic pathways. In

the beginning, radioactive precursors such as ^{14}C-labeled acetate and mevalonic acid have played a major role in elucidating the biochemical pathways of steroids[111], which was later replaced by stable isotope labeled precursors during the elucidation of Rohmer pathway due to its feasibility by improvement in mass spectrometry and NMR technology (review by Groeneveld and Bacher)[109, 111]. The elucidation of cholesterol biosynthesis in mammals was one of the first applications of isotope labeling in biochemistry[112, 113].

Soon, after the identification of MEP Pathway in prokaryotes, the intermediates of the pathway were identified by various isotope labeled compounds[10]. Deuterium labeling of pathway specific precursors have helped in complete elucidation of the pathway intermediates[7, 86]. Fates of the hydrogen atoms of 1-deoxyxylulose in its conversion to ubiquinone in *E. coli*[88]. Further, stable isotope-labeled (^{13}C and deuterium), pathway-specific precursors, 1-deoxy-deoxylulose and mevalolactone were used to trace the origin of isoprene units through either of the two pathways. Dual biosynthetic pathway to phytosterol was brought out by Ohyama *et al*. using deuterium and ^{13}C-labeling of the precursor mevalonate, which differentiated the phytosterol synthesized through the intermediates lanosterol and cycloartenol[86]. The essentiality of intramolecular rearrangement in pentulose for obtaining isoprene unit was proved from the quadruple-labeled isotopomers [1,2,3,4-$^{13}C_4$]-IPP obtained from the uptake of [2,3,4,5-$^{13}C_4$]-1-deoxy-D-xylulose by *Catharanthus* cells[114]. Incorporation of [1-^{13}C]-1-deoxy-D-xylulose into isoprenoids of the liverwort *Conocephalum conicum* could identify the involvement of MVA pathway for sesquiterpenes and MEP for diterpene, phytol[81]. Feeding of [5,5-$^{2}H_2$]-mevalonic acid lactone (MVL) and [5,5-$^{2}H_2$]-1-deoxy-d-xylulose (DOX) to grape leaves and berry could reveal that MEP pathway was responsible for the biosynthesis of monoterpenes[115]. Labeled precursors also helped in finding the rate of incorporation of the metabolic intermediates into pathways responsible for biosynthesis of the final metabolite[116]. Feeding experiment affords for the identification of intermediates and branching in a pathway which is evident from the [4-^{2}H]-DX uptake by cells, producing two different pools of isoprene units IPP/DMAPP in 85:15 ratio, DMAPP with the retention of deuterium labeling and IPP with loss of deuterium, which showed branching in the MEP pathway, leading separately to IPP and DMAPP from the same intermediate, allylic anion of 4-hydroxy-3-methylbut-2-enyl pyrophosphate[7, 79, 98]. These deuterium labeling have further demonstrated the fates of hydrogen atoms in

subsequent reactions in the Rohmer pathway[6]. Apart from using labeled precursor or carbon source, pulse chase experiment with $^{13}CO_2$ helped in study of plant products under normal physiological conditions[18]. Rapid development in the field of mass spectrometry provides the platform, not only for the accurate study of specific metabolites but the entire ^{13}C labeled metabolome of the organism[19].

The contribution of MVA and MEP pathway towards isoprene production for the biosynthesis of specialized metabolites in plants has been studied extensively through stable isotopic labeling followed by its characterization using NMR[9, 18, 56, 58, 69, 70, 72-74, 76, 77, 79, 82-84, 86, 87, 92, 104, 117-120]. NMR spectroscopy helped in identification of individual ^{13}C carbon atoms in the skeleton, which in turn will help in the retrobiosynthetic study of ^{13}C labeling positions of the intermediates and precursors contributed for its synthesis. Monoterpene moiety of alkaloid camptothecin originated from *Ophiorrhiza pimila* is synthesized through MEP pathway as predicted through *in silico* computer-aided metabolic analyses and confirmed through NMR[72]. The ^{13}C incorporation pattern not only helps in retrobiosynthetic study but also aids in understanding the isotopic randomization of C-5 (Z) and C-4 (E) methyl groups derived carbons from DMAPP[72].

To gain insight into the isoprenoid biosynthetic pathway(s) involved in the contribution of isoprene units into limonoid skeleton, we carried out labeling experiment with [1-^{13}C], [2-^{13}C] glucose (Glc) isotopomers and its isotopologue, [1,6-^{13}C] Glc in *Azadirachta indica* suspension cell cultures, which served as an experimental system for studying the biosynthesis of limonoids. We have utilized high resolution-tandem Mass spectrometry to study the limonoids produced in cell culture followed by the study of ^{13}C labeling pattern of limonoids obtained through feeding experiment. Dissection of chemical complexity of limonoids by rendition through isotopologues and isotopomers obtained with tandem MS was made possible because of high mass resolution and accuracy of MS. Isotopologues are molecules identical in chemical composition but different in isotopic composition, isotopomers (isotopic isomers) are isotopologues which differ from each other in the position of isotopic element in the molecule (Figure 3C.2A)[2].

A

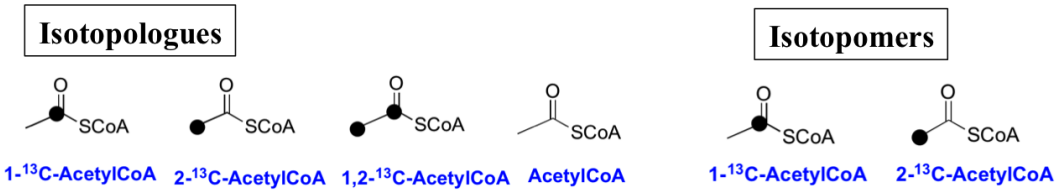

B

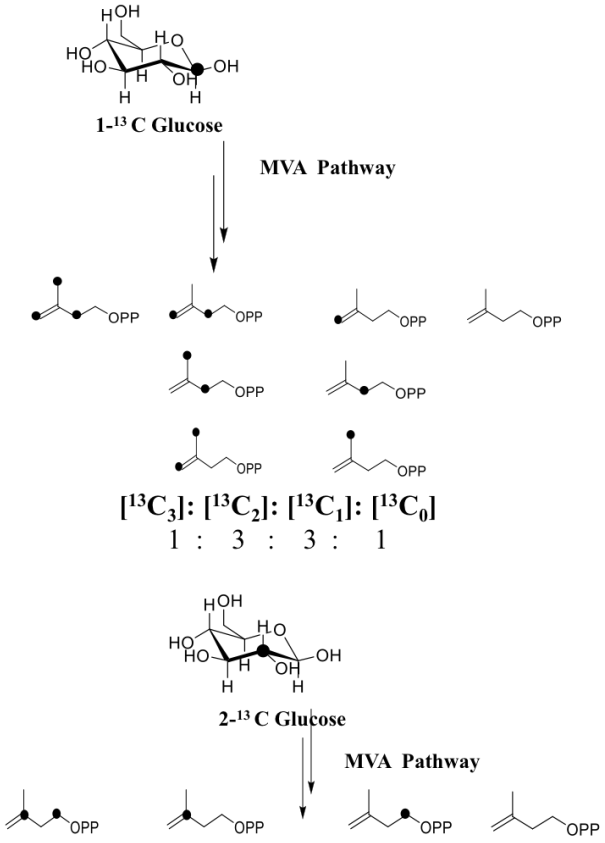

Figure 3C.2. (A) Difference between isotopologues and isotopomers represented with acetyl CoA, **(B)** Isotopologues and isotopomers of ^{13}C labeled acetyl coA forming from [1-^{13}C] Glucose and [2-^{13}C] Glucose

3C.2. Results and discussion

3C.2.1. Characterization of suspension cells for limonoid biosynthesis

UPLC-ESI-MS analysis of the suspension cells derived from callus, which has been subcultured 22 times, indicated the drastic decrease in the levels of limonoids compared to the one of third stage. This was also evidenced from the [1,6-^{13}C] Glc labeling study carried out with the suspension cells obtained at different subculturing

stage of callus. Limonoid isotopologues formed due to incorporation of ^{13}C label from [1,6-^{13}C] Glc fed cell suspension obtained from third sub-culturing stage callus was comparatively high, however no ^{13}C incorporated limonoids detected in the cell culture derived from callus which has been sub-cultured 22 times (Figure 3C.3). Feeding experiments clearly indicated that, there is a gradual drop in the biosynthesis of limonoids in due course of subculturing of callus. Labeled limonoid were not detected in the media, these results further supports that limonoids are synthesized and stored inside the suspension cells.

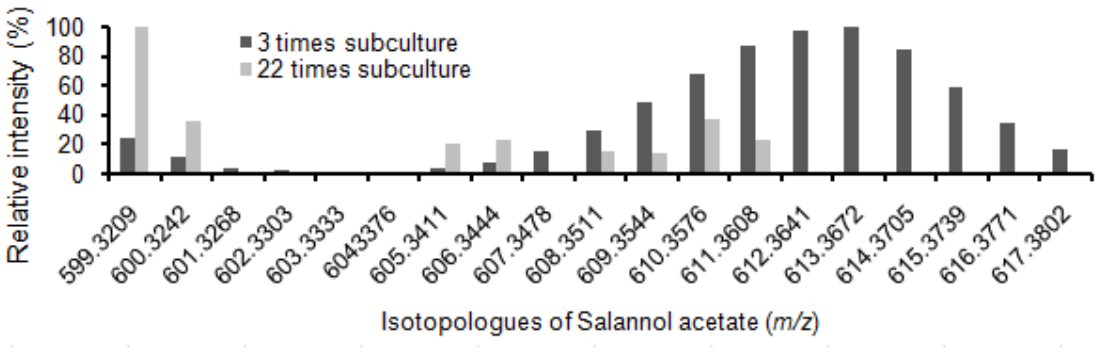

Figure 3C.3. Characterization of suspension cells for limonoid biosynthesis. Comparison of salannolacetate isotopologues formed between cell suspension obtained from callus of different subculturing stages (3 and 22) after growing the cells in the presence of D- [1,6-^{13}C] Glc.

3C.2.2. Biosynthesis of limonoids: Feeding experiment with different ^{13}C labeled D-glucose tracers.

The isoprene units synthesized through MVA and MEP pathway will have different labeling patterns when cell suspension culture is fed with ^{13}C labeled D-Glucose (Figure 3C.4). This principle is taken further to investigate the contribution of isoprene units formed through MVA and MEP pathways towards the biosynthesis of limonoids, feeding experiment was carried out with different ^{13}C labeled Glucose (Glc) tracers. 24 h old neem suspension cultures were grown in liquid MS media were re-suspended in MS media containing [1-^{13}C] Glc, [2-^{13}C] Glc or [1,6-^{13}C] Glc. The control experiment was carried out using MS media containing unlabeled glucose under similar conditions. At the end of 19 days of incubation, cell biomass were extracted for limonoids and subjected to UPLC-HRMS analysis.

Azadirachtin A, nimbin, 6-deacetylnimbin, nimbinene, 6-deacetylnimbinene, salannin, 3-deacetylsalannin, salannolacetate and nimbanal were identified in the cell

suspension generated ^{13}C isotopologues, which showed normal distribution pattern in their relative intensity. Azadirachtin A, salannin, salannolacetate, 6-deacetylnimbinene were identified in abundance with high intensity of isotopologues. The isotopologues varied in their number and intensity for each of the studied limonoid, upon labeling with different positional ^{13}C-Glc tracers. High resolution MS/MS serves as a powerful technique, and helped us for the determination of intramolecular distribution of ^{13}C in the isotopologues of the metabolite. Natural abundance of isotopologues was observed in MS for limonoids obtained from unlabeled control cell suspension (Appendix Figure 3C.5.1C, I, O, U). However, in nature, ^{13}C abundance is only 1.1% and thus the signal for lower mass fragments obtained during MS/MS spectra of limonoids are predominantly from the monoisotopic ions containing its most abundant isotope (12C). However, in ^{13}C enrichment experiments, molecular ions obtained in MS are represented by different isotopologues.

UPLC-HRMS analysis of azadirachtin A obtained from the unlabeled, control cell suspension showed a protonated parent molecular ion, *m/z* 703.2588 ($[M\text{-}H_2O+H]^+$). Neem cell suspension enriched by feeding [1-^{13}C] Glc and [1,6-^{13}C] Glc yielded with 14 and 19 isotopologues, respectively (*m/z* 703.2588 to 717.3056 and 722.3222) (Figure 8A, Appendix Figure 3C.5.1A, B, C, D, E). [2-^{13}C] Glc labeling experiment was conducted to corroborate further, the results obtained with [1-^{13}C] and [1,6-^{13}C] Glc. The ^{13}C enrichment of the suspension with [2-^{13}C] Glc gave rise to 14 mass units to the azadirachtin A parent ion (Figure 8A, Appendix Figure 3C.2.1F). Mass spectra of 6-deacetylnimbinene from the control showed parent molecular ion $[M + H]^+$ of *m/z* 441.2264 (Appendix Figure 3C.5.1 G, I). Incorporation of 11 and 14 ^{13}C atoms was reflected from the comparison of unlabeled molecular ion with that of [1-^{13}C] Glc and [1,6-^{13}C] Glc labeling experiment, respectively (*m/z* 441.2264 to 452.2632 and *m/z* 441.2264 to 455.2730). Whereas, ^{13}C enrichment with [2-^{13}C] Glc labeling culminates with 10 isotopologues (Appendix Figure 3C.5.1G, H, I, J, K, L, Figure 3C.5A). Parent molecular ion $[M + H]^+$, m/z 597.3050 was observed for salannin in the control cell culture whereas gradient increase of 14 (*m/z* 597.3050 to 611.3516) and 16 mass units (*m/z* 597.3050 to 613.3582) were generated from [1,6-^{13}C] Glc as isotopic tracer. With the use of [2-^{13}C] Glc as tracer, 12 isotopologues were observed (Appendix Figure 3C.5.1 M, N, O, P, Q, R, Figure 3C.6A).

Salannolacetate from the unlabeled culture generated parent ion $[M+H]^+$ of *m/z*

599.3209 whereas the labeled cell biomass produced 14 and 18 isotopologues upon [1-^{13}C] and [1,6-^{13}C] Glc labeling, respectively (*m/z* 599.3209 to 613.3672 and 617.3802 respectively). In case of [2-^{13}C] Glc labeling, isotopologues with 13 mass units were observed in addition to the parent ion (*m/z* 599.3209 to 612.3672) (Figure 3C.7A, Appendix Figure 3C.5.1S, T, U, V, W, X). In order to dissect the position of ^{13}C in the above limonoid skeletons, tandem MS fragmentation of the limonoid obtained from the labeled and unlabeled culture need to be compared. Structure-fragment relationship for C-seco limonoids such as salannin, salannolacetate and 6-deacetylnimbinene has been established in our previous study. However, there is no report on ESI based tandem mass spectrometric characterization of azadirachtin. Herein, we report structure-fragment relationships for azadirachtin using UPLC-ESI-quadrupole/orbitrap-MS. These data will be utilized for tracing their biosynthetic pathway for these limonoids in neem suspension culture fed with [1-^{13}C] Glc, [2-^{13}C] Glc or [1,6-^{13}C] Glc.

3C.2.3. Tracing the limonoid biosynthesis through neem cell suspension feeding experiments

After understanding the fragmentation pattern for azadirachtin A, we subjected its isotopologues obtained through incorporation of ^{13}C labels from [1-^{13}C], [1,6 -^{13}C] and [2-^{13}C] Glc feeding experiments, in order to identify the position of each ^{13}C label in the skeleton of limonoids. MS/MS traces obtained with NCE of 20% for each of the limonoid isotopologue were compared with that of unlabeled fragments to establish the number of ^{13}C labels present in that fragment (Figure. 3C.5, Figure. 3C.6, Figure. 3C.7, Figure. 3C.8, Appendix Figure. 3C.5.2). The ^{13}C-enriched fragmentation pattern thus obtained was further subjected to retro-biosynthetic label tracing approach by applying to squalene intermediated model of triterpene origami for azadirachtin biosynthesis, to probe the origin of each carbon through MVA or/and MEP pathways. According to the biosynthetic pathway of triterpene origami, tetranor- and pentanor-limonoids are formed through loss of four and five isoprenogenic carbons from the C_{30} triterpene skeleton and gain of further non-isoprenogenic carbon as functional groups.

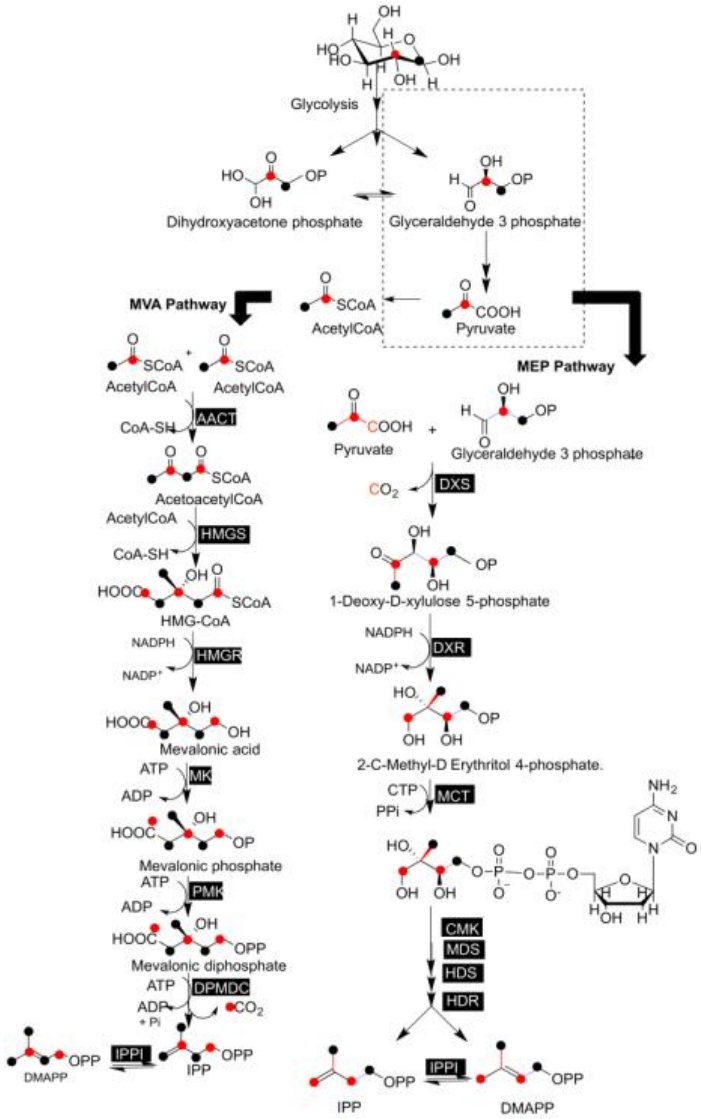

Figure 3C.4. Tracing the flow of ^{13}C from glucose through MVA and MEP pathway for the biosynthesis of isoprene unit. The black dot represents the^{13}C carbon derived from 1-^{13}C label /1,6 -^{13}C of D-glucose and the red one from 2-^{13}C label of D-glucose. AACT, acetoacetyl-CoA thiolase; HMGS, 3-hydroxy-3 methyl glutaryl coenzyme A synthase; HMGR, 3-hydroxy-3-methyl glutaryl coenzyme A reductase; MK, mevalonate kinase; PMK, 5-phosphomevalonate kinase; DPMDC, diphosphomevalonate decarboxylase; IPPI, isopentenyl diphosphate isomerase; DXS,1-deoxy-D-xylulose-5-phosphate synthase; DXR, 1-deoxy-D-xylulose-5-phosphate reductoisomerase; MCT, 2-C-methyl-D-erythritol-4 phosphate cytidyltransferase; CMK, 4-(Cytidine 5'-diphospho)-2-C-methyl-D-erythritol kinase; MDS, 2-C-methyl-D-erythritol 2,4-cyclodiphosphate synthase; HDS, 4-hydroxy-3-methylbut-2-enyl diphosphate synthase; HDR, 4-hydroxy-3-methylbut-2-enyl diphosphate reductase.

It is well established in literature[15, 47], that labeling with [1-^{13}C] Glc culminates with IPP or DMAPP labeled at C-2, C-4, C-5 when they are formed through MVA pathway whereas ^{13}C will be incorporated into isoprene units at C-1 and C-5 in case of

their biosynthesis through MEP route (Figure 3C.4). In case of [1,6-^{13}C] Glc labeling, two 2-^{13}C acetyl-CoA are generated from a Glc molecule unlike that of one unlabeled and one 2-^{13}C acetyl-CoA formed through [1-^{13}C] Glc as tracer (Figure 3C.2B). Metabolism of acetyl-CoA formed from [2-^{13}C] Glc result in labeling of isoprene units at C-1 and C-3 through MVA pathway, whereas at C-2 and C-4 in case of MEP pathway (Figure. 3C.4). Based on the above information on labeling pattern of isoprene, and considering the number of incorporated ^{13}C carbons on each of the fragments from tandem MS analysis, the pattern was fitted into the above origami model. Isotopologues generated for each of the signature fragment of labeled limonoids such as 6-deacetylnimbinene, salannin, salannolacetate and azadirachtin A are discussed in detail.

The fragment, *m/z* 147.0804 possess characteristic signature of C-seco limonoids such as salannolacetate, salannin, 3-deacetylsalannin, nimbin, 6-deacetylnimbin, nimbinene, 6-deacetylnimbinene and nimbanal corresponding to the C- and D-ring with 17-furan moiety, as per our earlier study[45]. This fragment encompasses two isoprene units and 1 carbon from third isoprene. Feeding experiment with [1-^{13}C]/ [1,6-^{13}C] Glc resulted in six isotopologues, possibly through three ^{13}C in each of the two isoprenes thereby, ignoring the participation of MEP, as only two carbons of isoprene get labeled via latter pathway. Whereas [2-^{13}C] Glc experiment did not provide any useful insight into tracing the pathway as two ^{13}C labeled isoprenes can be obtained through both pathways however at different positions resulting in increase in 4 mass units to the fragment.

Amongst the nine limonoids identified in the culture, nimbinene and 6-deacetylnimbinene constitute the class of penta-nortriterpenoids. It is important to note that the maximum number of ^{13}C incorporated into 6-deacetylnimbinene skeleton are 14 through [1,6-^{13}C] Glc labeling, corroborating to the fact that three ^{13}C may be lost during the excision of the terminal four carbons in the formation of proto-limonoid and another carbon from A ring during the formation of penta-nortriterpenoids (Figure 3C.5). The signature fragment, *m/z* 187.1119 corresponding to the decalin moiety was identified exclusively in this class of limonoids and this decalin moiety are constituted from first 3 isoprene units of squalene epoxide. Comparison of control and labeled culture, revealed the formation of 8 isotopologues in [1-^{13}C] Glc labeling. If, it had been formed through MEP route, only five ^{13}C labels would be incorporated into it. In case of [2-^{13}C] Glc labeling, five mass units were observed however, labeling through either of the

pathways may result in same number of labels into this fragment. Further, the fragment of *m/z* 409.2010, obtained after the removal of MeOH from the methylester group from the parent ion represents 6-deacetylnimbinene skeleton, composed of 4 complete isoprene units and 2 incomplete units which has lost its carbons from the triterpene skeleton, during the process of its biogenesis. It gave away fourteen isotopologues in [1-^{13}C] Glc labeling experiment and eleven in [2-^{13}C] Glc labeling, providing us with the evidence that isoprene units are derived from MVA route and also the methylgroup is of non-isoprenogenic origin (Figure 3C.5, Appendix Figure 3C.5.1)[121].

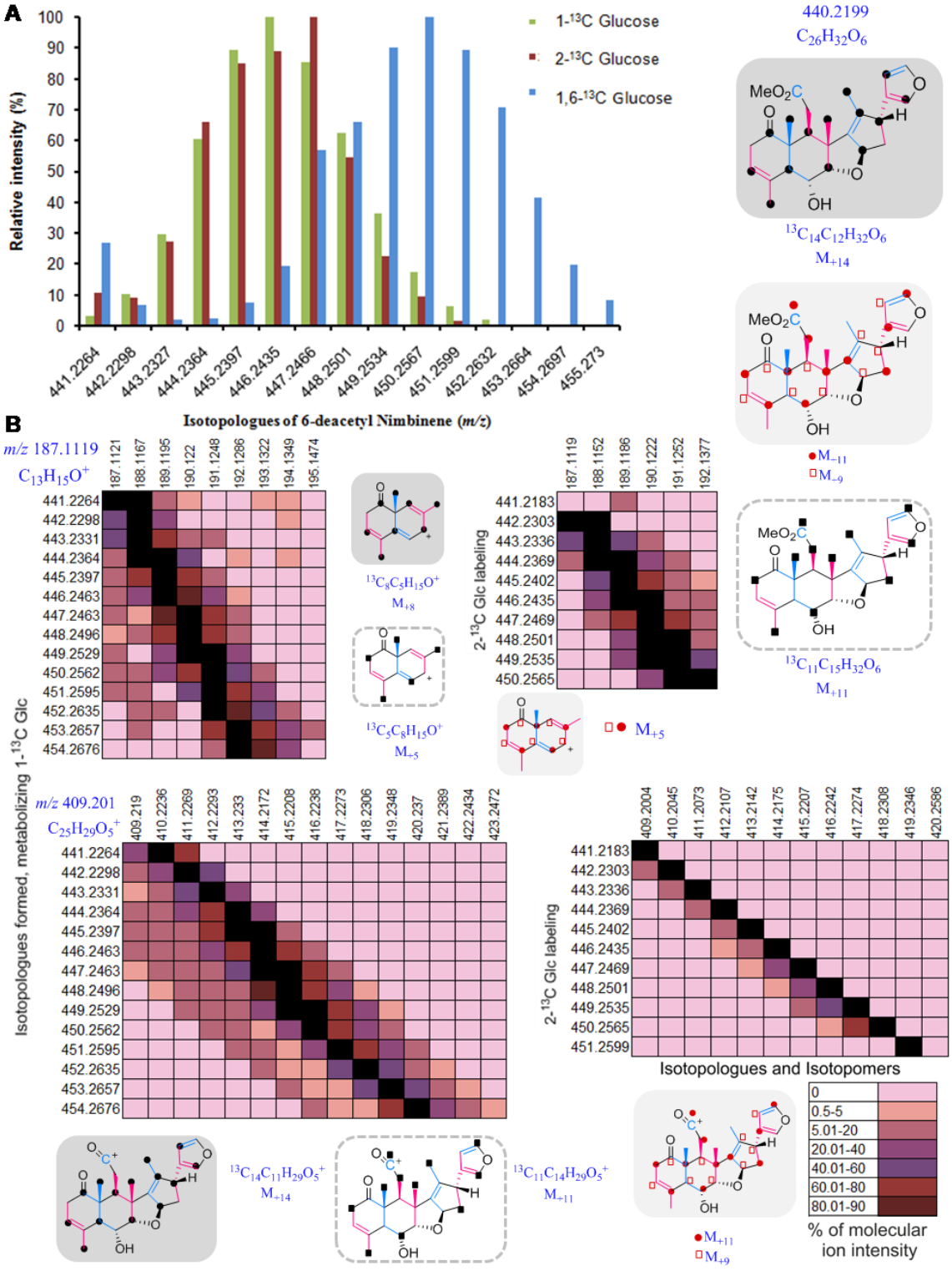

Figure 3C.5. Comparison of relative intensity of isotopologues obtained with the uptake of different ^{13}C-glucose tracers. (a) MS of 6-deacetylnimbinene isotopologues (b) Heatmap for distribution of isotopologues for specific fragments (*m/z* 187.1119, 409.2010 contributing to different part of skeleton respectively) for each 6-deacetylnimbinene isotopologues obtained from [1-^{13}C] Glc (left) and [2-^{13}C] Glc (right) labeling experiments. (M represents the *m/z* of parent ion of the molecular ion/ fragment)

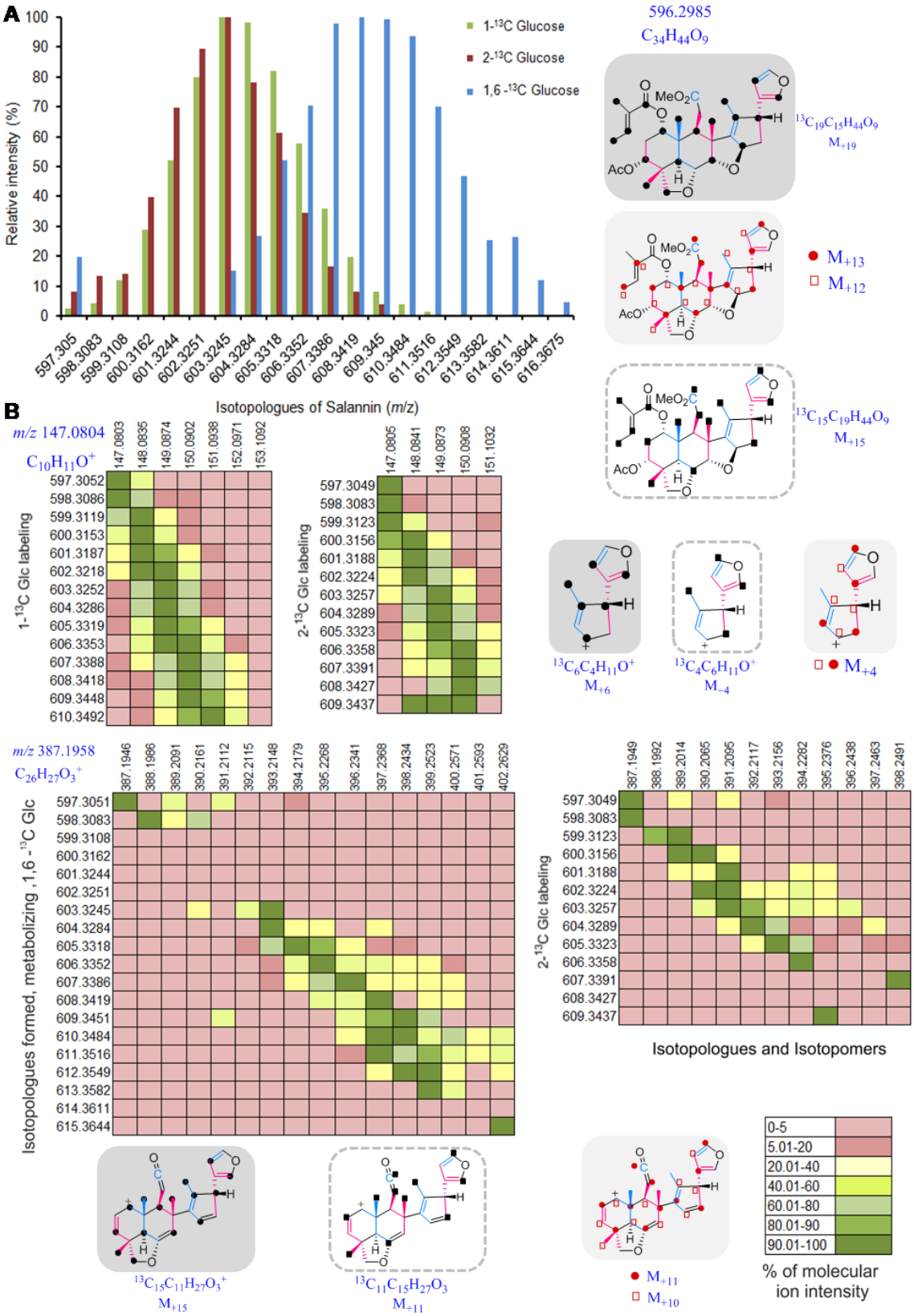

Figure 3C.6. Relative intensity of salannin isotopologues obtained from labeling study with different tracers such as [1-^{13}C], [2-^{13}C], [1,6-^{13}C] Glc. (a) MS of salannin isotopologues formed from three different Glc tracers (b) MS/MS distribution of isotopologues of the fragments

(shown here are *m/z* 147.0804 and 387.1946 representing the skeleton). (M represents the *m/z* of parent ion of the molecular ion/ fragment) (heatmap at left corresponds to isotopologues formed through [1-^{13}C]/ [1,6-^{13}C] Glc labeling and for the [2-^{13}C] Glc labeling at the right).

One of the signature fragment of salannin is *m/z* 387.1958, corresponding to its triterpene skeleton, which is without 3 functional groups *viz*, MeOH, tiglic acid and acetic acid (Appendix Figure 3C.5.2, Figure 3C.6). Similiarly, the fragment, *m/z* 419.2214, of salannolacetate gave the same skeleton but with intact methylester moiety (only devoid of isovalerate and acetate group) (Figure 3C.7, Appendix Figure 3C.5.2). These skeletal fragments comprises of 5 complete isoprene units and an incomplete isoprene unit (with only one carbon contribution from it). These fragments have been originated from 26 isoprenogenic carbons and in addition, 1 non-isoprenogenic carbon at methylester group in case of *m/z* 419.2214. [1,6 -^{13}C] Glc labeling showed addition of 15 mass units for these fragments, which might have arrived from 5 isoprenes each with three ^{13}C labels, indicating that they may have originated through MVA pathway. Eleven ^{13}C incorporations occuring in [2-^{13}C] Glc labeling further provides the evidence that isoprene units are formed through MVA as the alternative route will result in only 10 labels due to loss of one during the formation of proto-limonoids (Figure 3C.6B, Appendix Figure 3C.5.2).

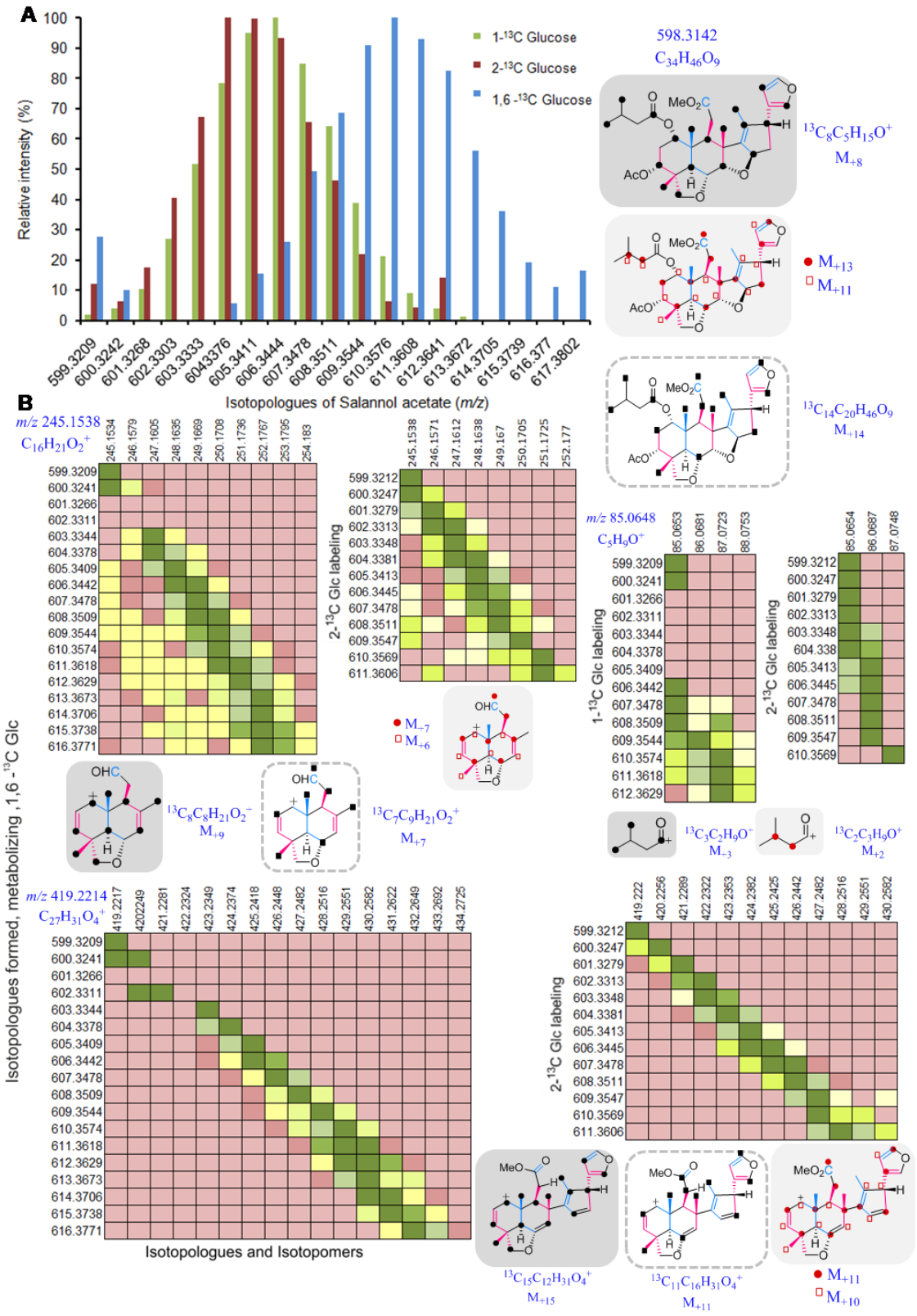

Figure 3C.7. Relative intensity of salannolacetate isotopologues formed through labeling study with different tracers of Glucose ([1-^{13}C], [2-^{13}C] and [1,6-^{13}C]) and the number of ^{13}C carbon incorporation evident from tandem MS analysis of the isotopologues. (a) MS of salannolacetate isotopologues formed through different ^{13}C Glc feeding experiments (b) MS/MS

distribution of isotopologues of the fragments (*m/z* 85.0648, 245.1538, 419.2214). Heatmap at the left corresponding to isotopologues formed through either [1-^{13}C] or [1,6-^{13}C] Glucose and the one at the right correspond to isotopologues formed through [2-^{13}C] Glc. (M represents the *m/z* of parent ion of the molecular ion/ fragment).

Further evidence was obtained after studying salannolacetate, for its fragment, *m/z* 245.1538 corresponding to decalin moiety, which is devoid of CH_2O group at methylester moiety and other functional groups. This fragment is built from 3 complete isoprene units and 1 carbon of fourth isoprene. [1,6-^{13}C] and [2-^{13}C] Glc labeling study arrived, with addition of 9 and 7 mass units for this fragment respectively, (Figure 3C.7B), thus corroborating its formation through MVA route. The same pattern of increase in mass units was obtained for another decalin fragment *m/z* 273.1414 (with intact methylester moiety) corresponding to salannin and salannolacetete (Appendix Figure 3C.5.1). MS/MS traces of unlabeled salannolacetate generated daughter ion, *m/z* 85.0653 corresponding to isovalerate moiety and the ones of labeled salannolacetate showed an increase of 3 mass units (*m/z* 86.0681, 87.0723, 88.0753) (Figure 3C.7B). Isovalerate biosynthesis was traced through primary metabolism leading to amino acid biosynthesis as it diverges from leucine biosynthesis, which corroborates with the formation of 3 mass units in our labeling experiment. Isovalerate was traced through glycolysis and amino acid leucine biosynthetic pathway, which is in agreement with previous study in *Propionibacterium*[122]. Two molecules of [3-^{13}C] pyruvate and one [2-^{13}C] acetyl-CoA formed from the glycolysis of [1,6-^{13}C] Glc contribute for the biosynthesis of leucine (Figure 3C.9B). Isovalerate originates from ketoisocaproate, a penultimate metabolite in leucine biosynthetic pathway thereby acquiring two ^{13}C from labeled pyruvate and one from acetyl-CoA. Our tandem MS data for the isotopologues of salannolacetate supports the presence of three ^{13}C labels in isovalerate as evidenced from 3 additional units generated from the fragmentation of salannolacetate isotopologues (Figure 3C.7B).

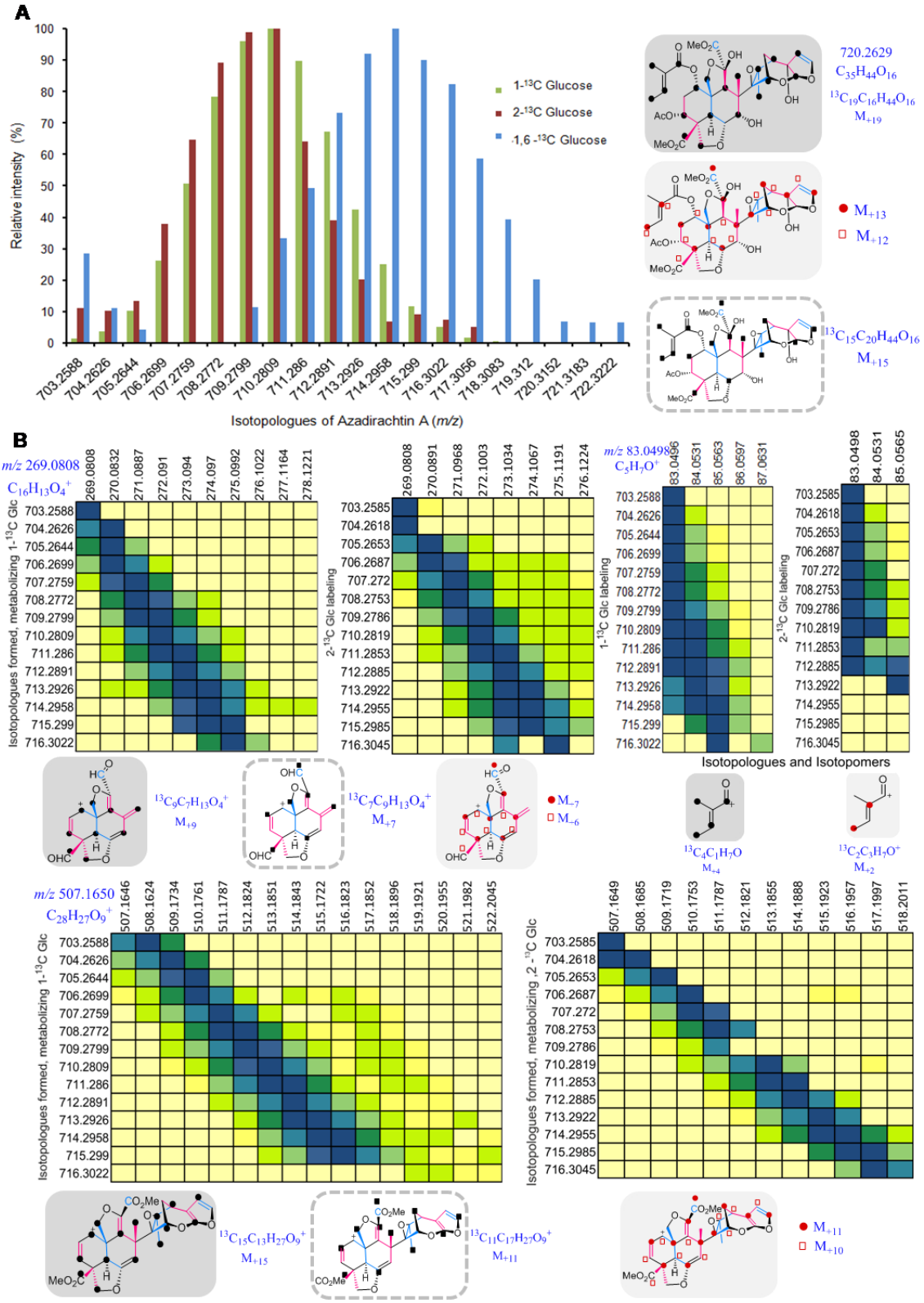
A
Relative intensity (%)
1-13C Glucose
2-13C Glucose
1,6 -13C Glucose
Isotopologues of Azadirachtin A (m/z)
720.2629
C35H44O16
13C19C16H44O16
M+19
M+13
M+12
13C15C20H44O16
M+15
B
m/z 269.0808
C16H13O4+
m/z 83.0498
C5H7O+
Isotopologues and Isotopomers
13C9C7H13O4+
M+9
13C7C9H13O4+
M+7
M-7
M-6
13C4C1H7O
M+4
13C2C3H7O+
M+2
m/z 507.1650
C28H27O9+
13C15C13H27O9+
M+15
13C11C17H27O9+
M+11
M+11
M+10

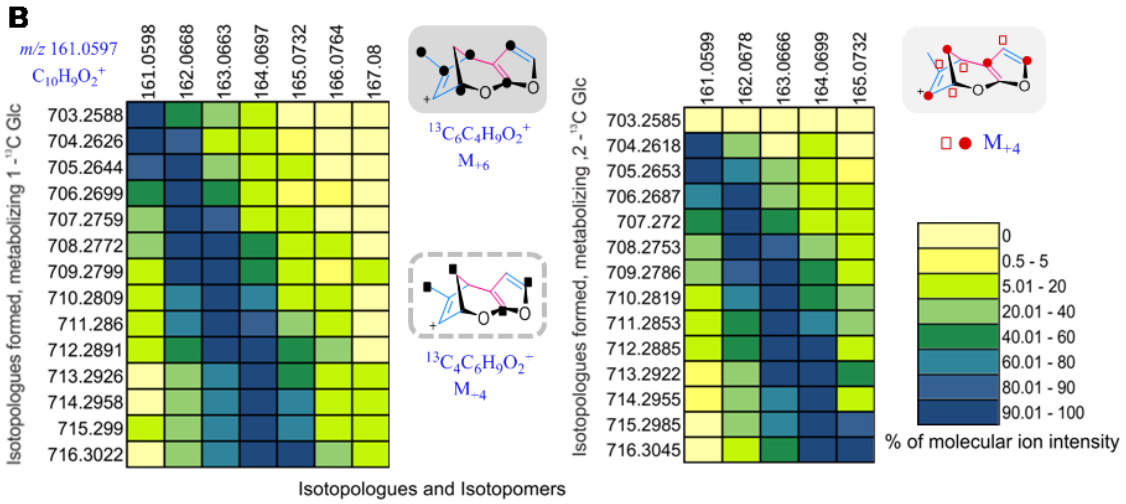

Figure 3C.8. Distribution of azadirachtin A isotopologues and isotopomers obtained from ESI-MS and MS/MS analysis. (a) Comparison of relative intensity of isotopologues of protonated ion adduct $[M\text{-}H_2O+H]^+$ of azadirachtin A obtained from independent labeling experiments with [1-^{13}C], [2-^{13}C], [1,6-^{13}C] Glc. (b) Heatmap of isotopologue of azadirachtin A in the mass spectra vs. relative intensity of each of the isotopologues for individual fragments (*m/z* 83.0498, 161.0597, 269.0808, 507.1650 derived from different part of the skeleton are represented) obtained when subjected to tandem MS at collision energy of 20%. The structure of the molecule and its fragments are given in grey boxes for the molecule denoting its ^{13}C pattern of formation through MVA pathway and dashed line boxes for its formation through MEP pathway. The black dots and squares represent the position of ^{13}C carbón in corporated from [1-^{13}C] Glc / [1,6-^{13}C] Glc whereas the red dots corresponding to those from [2-^{13}C] Glc.

When we examined the fragmentation pattern of azadirachtin A obtained from the unlabeled biomass, *m/z* 269.0808 was corresponding to the decalin moiety. Three isoprene units and a single carbon from fourth isoprene contribute to this moiety. ^{13}C enrichment through [1-^{13}C] Glc labeling showed additional 9 mass units to this fragment suggesting that each of the three ^{13}C labels may have originated from a single isoprene unit. The same experiment with [2-^{13}C] Glc labeling gave 7 additional mass units further corroborating its route of origin (Figure 3C.8B). The fragment *m/z* 507.1650 of azadirachtin A was formed devoid of all functional groups except the methylester moieties and this fragment encompasses 5 isoprenes and single carbon of terminal isoprene. This fragment showed additional 15 mass units upon [1-^{13}C] Glc labeling and generated 11 mass units upon [2-^{13}C] Glc labeling (Figure 3C.8B). The fragment *m/z* 161.0597 formed from the C, D rings and furan moiety of azadirachtin A, is originated from three isoprene units. This fragment displayed six and four additional mass units corresponding to the [1-^{13}C] Glc and [2-^{13}C] Glc labeling experiment respectively,

indicating that it is biosynthesized by utilizing IPP and DMAPP formed through MVA pathway (Figure. 3C.8B, Figure. 3C.5.2).

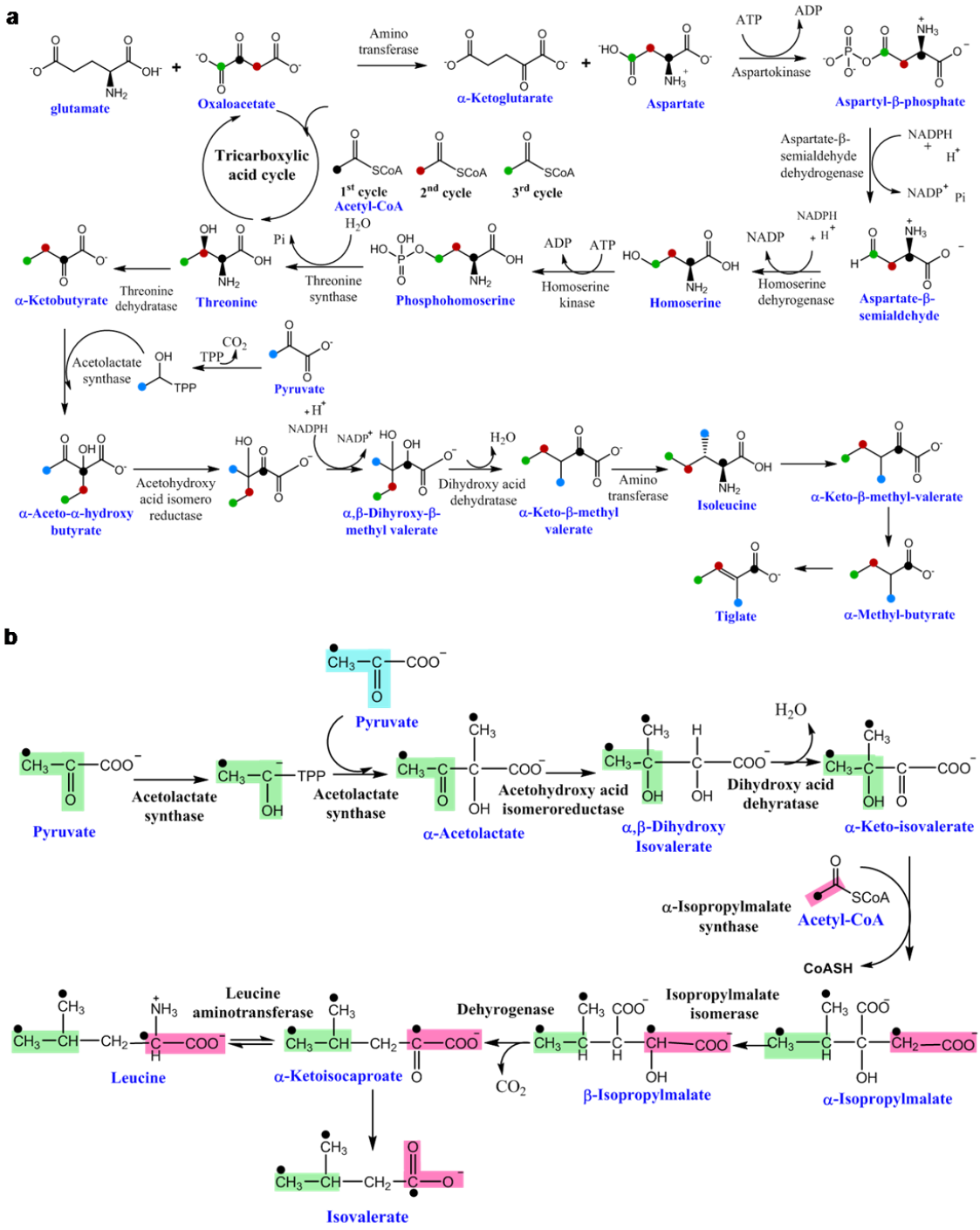

Figure 3C.9. Tracing the flow of ^{13}C carbon from [1-^{13}C] /[1,6-^{13}C] Glc through primary metabolic pathway for the formation of functional groups present in limonoids. (a) tiglate group present in azadirachtin and salannin is traced through isoleucine biosynthetic pathways. (b) isovalerate group present in salannolacetate is traced through leucine biosynthetic pathway.

The daughter ion fragment, *m/z* 83.0498, was identified as tiglate group from azadirachtin A, salannin and 3-deacetylsalannin. Four additional mass units (*m/z* 84.0531, 85.0565, 86.0597, 87.0718) were generated after fragmentation of labeled azadirachtin A from [1-^{13}C] /[1,6-^{13}C] Glc labeling whereas two mass units increase were observed through [2-^{13}C] Glc labeling experiment. The earlier report supports the formation of tiglic acid through isoleucine biosynthetic pathway, so its origami was traced through multiple primary metabolic pathways (Figure 3C.9). A plausible scheme (Figure 3C.9) is presented to determine the carbon position specific biosynthetic origin of tiglate moiety present in azadirachtin A. The [2-^{13}C] acetyl-CoA entering the TCA cycle derives its ^{13}C label from the C-1 and C-6 positions of [1,6-^{13}C] Glc thereby labeling oxaloacetate, the TCA intermediate in subsequent cycles. The resulting oxaloacetate gets ^{13}C label at three carbons producing aspartate labeled at C-2, C-3 and C-4 positions which in turn is utilized in threonine biosynthetic pathway, labeling the same positions of carbon in threonine. The amino acid, threonine by addition of another ^{13}C label from [3-^{13}C] pyruvate followed by isomerization, reduction, dehydration and group transfer reactions forms isoleucine. Isoleucine is converted in two-step reactions to tiglate containing four ^{13}C labels. This is corroborated from the four additional mass units generated from MS/MS fragmentation of isotopologues of azadirachtin and salannin (Figure 3C.8, 3C.9).

The elaborated pattern of ^{13}C distribution in the limonoid skeleton and its functional group obtained through tandem MS analysis of the *ex vivo* biosynthesized metabolite gives us the evidence that MVA pathway contributes for the biosynthesis of limonoids and the functional groups such as tiglate and isovalerate are formed through isoleucine and leucine amino acid biosynthetic pathways (Figure 3C.5, 3C.6, 3C.7, 3C.8, 3C.9, 3C.10, Appendix Figure 3C.5.1, Appendix Figure 3C.5.2).

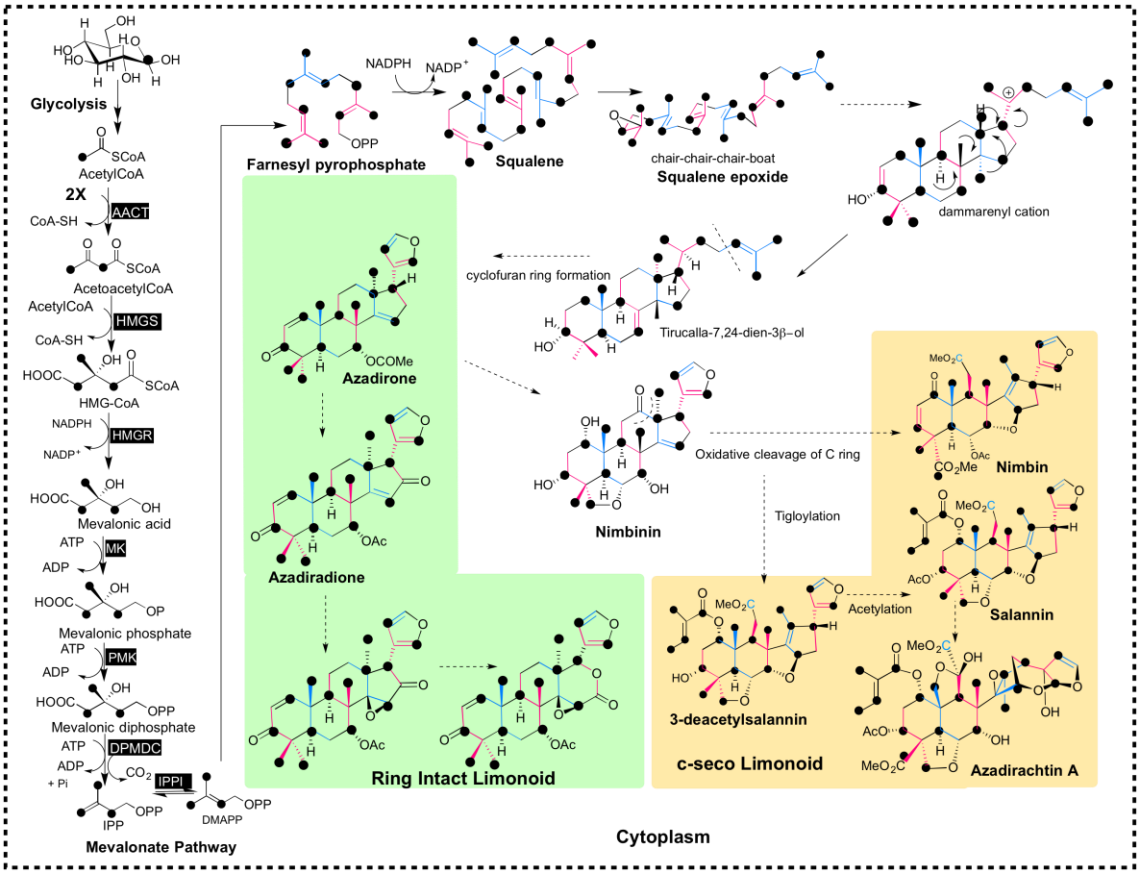

Figure 3C.10. Simplified scheme showing limonoid biosynthesis in neem being contributed by isoprene units formed through MVA pathways evident from the labeling experiment with ^{13}C glucose. C-seco and ring intact limonoid are represented in yellow and green boxes respectively. (Alternate isoprene units of the limonoid skeleton are shown in pink and blue, dotted arrow shown here are the uncharacterized steps in the pathway).

3C.3. Conclusion

Study of limonoid biosynthesis in neem tree is of potential significance as it produces agriculturally and pharmacologically important molecules. Limonoid biosynthesis of neem tree and cell lines have been unraveled through comparative quantification of limonoids with that of neem tree and through ^{13}C limonoid isotopologues analysis. Furthermore, mevalonate pathway exclusively contributes for isoprene units of limonoids as evidenced through stable isotope labeling. The work emphasizes the crucial role of MVA pathway and found to be the sole source of isoprene units for limonoid biosynthesis.

3C.4. Materials and methods

3C.4.1. Feeding Experiment with ^{13}C Glc tracers

For feeding experiments, cells from 2 days old suspension was harvested from media and sub-cultured into media with labeled carbon source. Feeding experiments with D-[1-^{13}C] Glc, D-[2-^{13}C] Glc and D-[1,6-^{13}C] Glc (99% enriched, Cambridge Isotope Lab. Inc., Andover, MA) were performed separately in 25 mL Erlenmeyer flasks containing 5 mL MS liquid with 3% of labeled Glucose in duplicates.

3C.4.2. Harvesting cells and Extraction of limonoids

The suspension culture cells were collected from media by centrifugation at 2500 × *g* for 10 min at 25 °C. The cells were homogenized in ice-cold methanol. The supernatant was collected after centrifugation at 2500 × *g* for 10 min at 25 °C. The cells were again resuspended in twice the volume of methanol and extracted twice again. The methanol extract was pooled together and evaporated to dryness. The residue was partitioned between water and ethylacetate thrice. The ethylacetate pool was then evaporated to dryness under reduced pressure and constituted with LC-MS grade methanol to the volume of 1 mL. To quantify limonoids in the media, it was partitioned with ethylacetate and extracted, as mentioned above.

3C.4.3. LC-ESI-Mass Spectrometry conditions

Analysis of neem limonoids was performed with Thermo Scientific QExactive™ hybrid quadrupole-Orbitrap mass spectrometer associated with Accela 1250 pump and Accela open AS. The conditions of HESI source include capillary temperature of 320 °C, Heater temperature at 350 °C, s-lens RF level of 50, Spray voltage of 3.6 kV, spray current of 0.9 μA with sheath gas flow rate of 41, Auxiliary gas flow rate of 9 and sweep gas flow rate of 3. Standards as well as the extracted samples were analyzed in positive ionization mode, in full MS-scan with scan range of 100 to 1000 *m/z*. Following were the properties of the scan performed- resolution 70,000, AGC target 1e6, Maximum IT 200 ms. Waters Acquity UPLC BEH C_{18} column (particle size 1.7 μm, 2.1 X 100 mm) was used as the stationary phase while the solvent system of methanol and water containing 0.1% formic acid served as the mobile phase. The gradient started with 40% methanol (5 min isocratic), it was then increased to 50% (5 min isocratic), followed by 60% methanol for the next 15 minutes and over the next 4 minutes it was isocratic with 65% methanol. It was then increased to 90% methanol for 4 minutes. For the last 2 minutes, it was isocratic with 40% methanol. Constant flow rate of 0.3 mL min^{-1} was

maintained throughout the run time of 35 min. The chromatograms and mass spectral data were processed by Xcaliburqual browser (version 2.3; Thermo Scientific).

3C.4.4. Tandem Mass Spectrometry of limonoids and its isotopologues

Tandem Mass spectrometry of limonoids and its isotopologues was done in data dependent acquisition mode (PRM) with the protonated molecular ion as a precursor for MS/MS. Isolation window was set to 1, the charge state of 1, NCE 20% and at their corresponding retention time for all the nine limonoids and its isotopologues obtained from cell suspension were set for tandem mass spectrometry. The MS/MS distribution for each isotopologue of four limonoids, azadirachtin A, salannin, salannolacetate and 6-deacetylnimbinene were evaluated individually for different ^{13}C glucose labeling. Consideration of *m/z* values accurately to fourth decimal for individual isotopologues and isotopomers eliminated the noise generated during MS and MS/MS analysis.

3C.5. Appendix

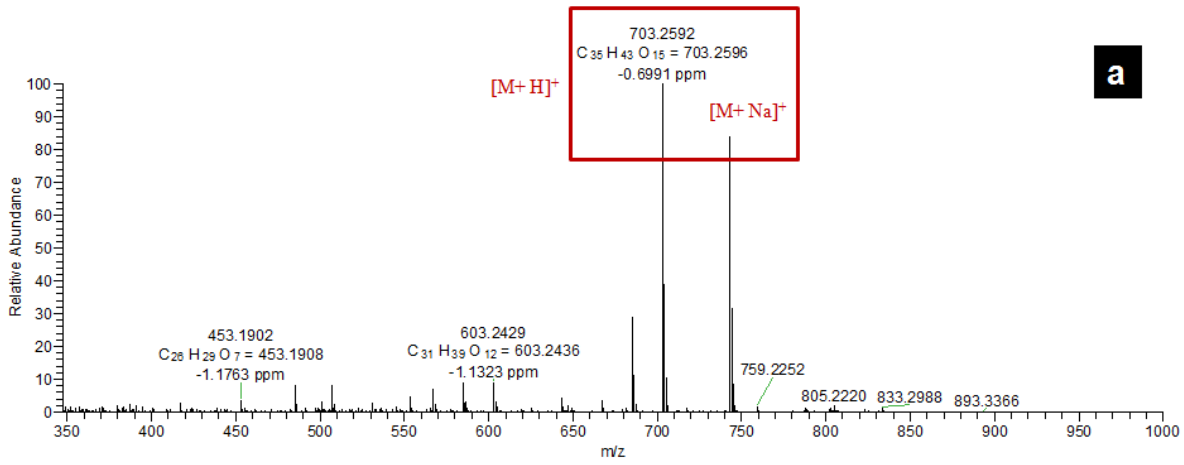

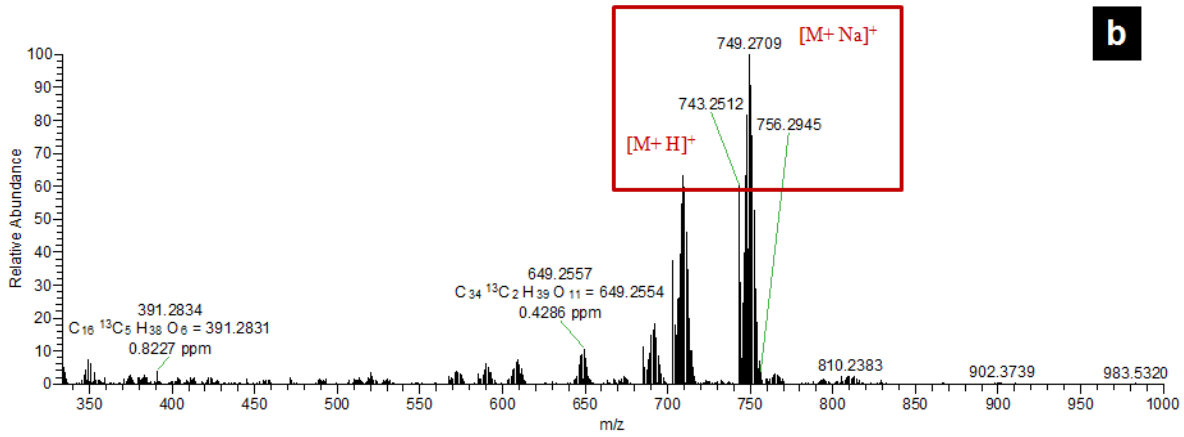
b
749.2709
[M+ Na]+
743.2512
756.2945
[M+ H]+
649.2557
C 34 13C 2 H 39 O 11 = 649.2554
0.4286 ppm
391.2834
C 16 13C 5 H 38 O 6 = 391.2831
0.8227 ppm
810.2383
902.3739
983.5320
Relative Abundance
m/z

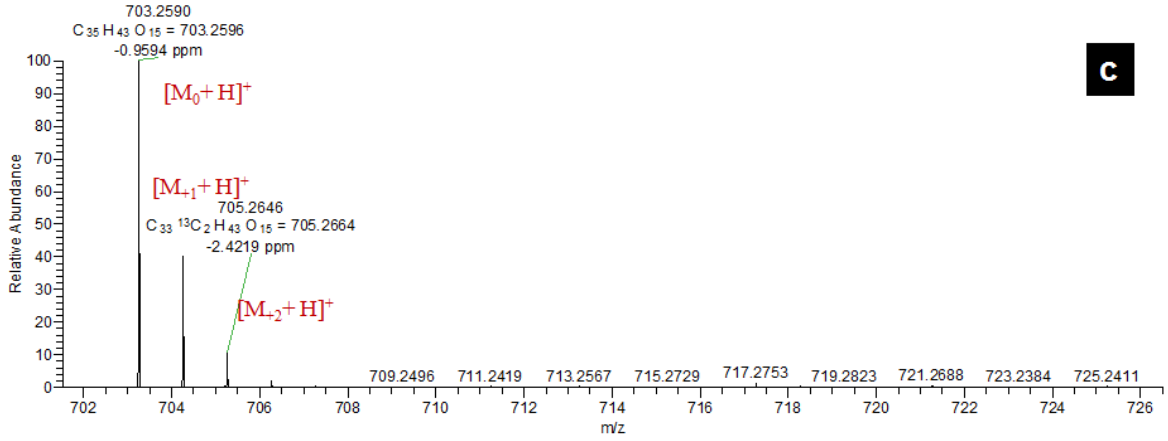
c
703.2590
C 35 H 43 O 15 = 703.2596
-0.9594 ppm
[M0+ H]+
[M+1+ H]+
705.2646
C 33 13C 2 H 43 O 15 = 705.2664
-2.4219 ppm
[M+2+ H]+
709.2496
711.2419
713.2567
715.2729
717.2753
719.2823
721.2688
723.2384
725.2411
Relative Abundance
m/z

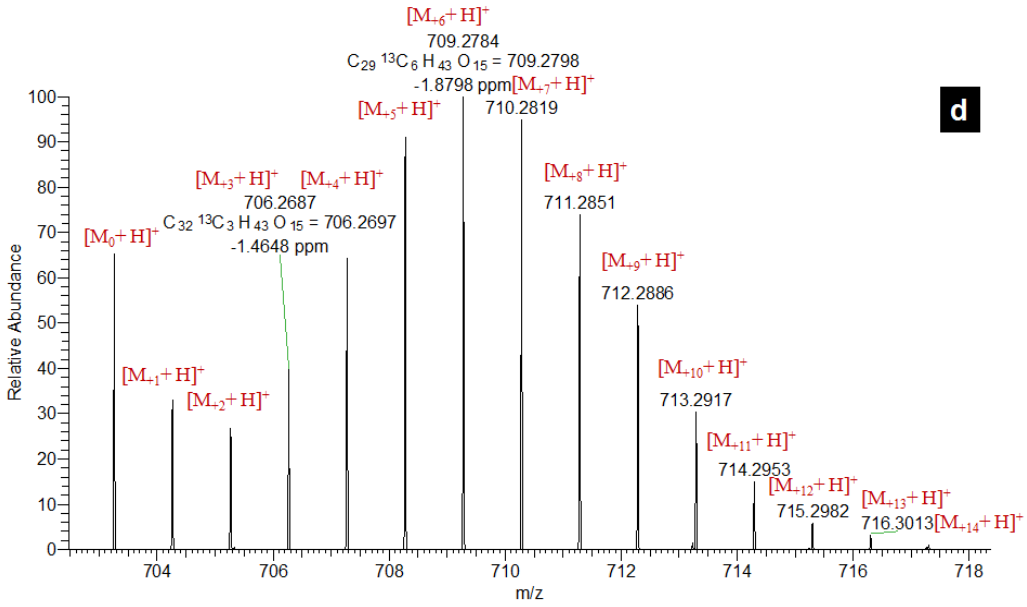
d
[M+6+ H]+
709.2784
C 29 13C 6 H 43 O 15 = 709.2798
-1.8798 ppm
[M+5+ H]+
[M+7+ H]+
710.2819
[M+3+ H]+
[M+4+ H]+
706.2687
C 32 13C 3 H 43 O 15 = 706.2697
-1.4648 ppm
[M+8+ H]+
711.2851
[M0+ H]+
[M+9+ H]+
712.2886
[M+1+ H]+
[M+2+ H]+
[M+10+ H]+
713.2917
[M+11+ H]+
714.2953
[M+12+ H]+
715.2982
[M+13+ H]+
716.3013
[M+14+ H]+
Relative Abundance
m/z

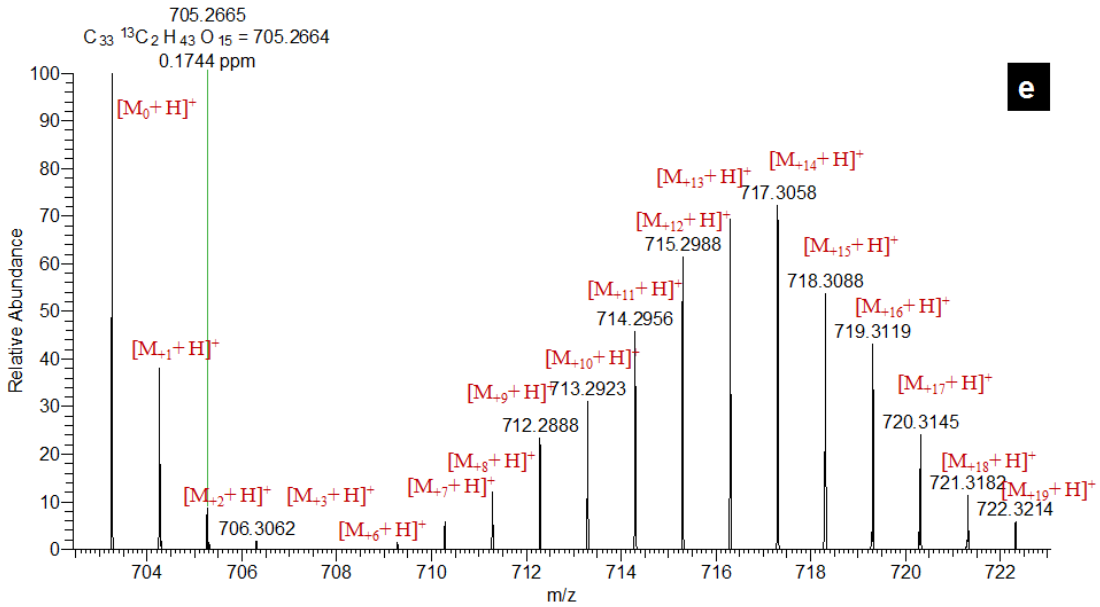
705.2665
C 33 13C 2 H 43 O 15 = 705.2664
0.1744 ppm
e
[M0+H]+
[M+1+H]+
[M+2+H]+
[M+3+H]+
706.3062
[M+6+H]+
[M+7+H]+
[M+8+H]+
712.2888
[M+9+H]+
713.2923
[M+10+H]+
714.2956
[M+11+H]+
[M+12+H]+
715.2988
[M+13+H]+
717.3058
[M+14+H]+
[M+15+H]+
718.3088
[M+16+H]+
719.3119
[M+17+H]+
720.3145
[M+18+H]+
721.3182
[M+19+H]+
722.3214
Relative Abundance
m/z

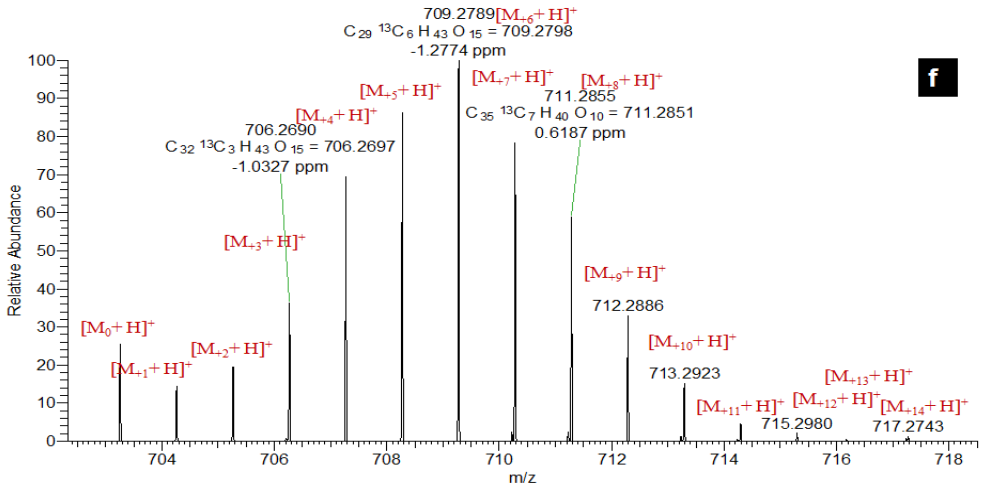
709.2789
C 29 13C 6 H 43 O 15 = 709.2798
-1.2774 ppm
[M+6+H]+
f
[M+5+H]+
[M+7+H]+
[M+8+H]+
711.2855
C 35 13C 7 H 40 O 10 = 711.2851
0.6187 ppm
[M+4+H]+
706.2690
C 32 13C 3 H 43 O 15 = 706.2697
-1.0327 ppm
[M+3+H]+
[M+9+H]+
712.2886
[M0+H]+
[M+1+H]+
[M+2+H]+
[M+10+H]+
713.2923
[M+11+H]+
715.2980
[M+12+H]+
[M+13+H]+
[M+14+H]+
717.2743
Relative Abundance
m/z

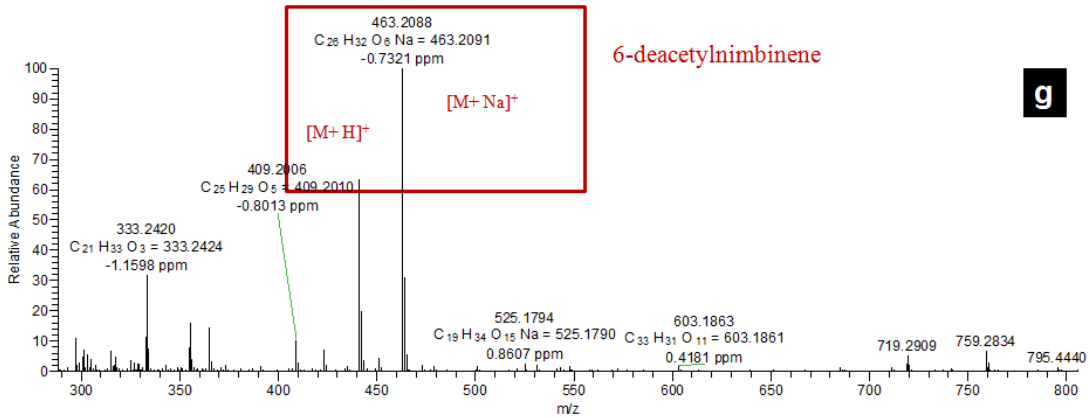
463.2088
C 28 H 32 O 6 Na = 463.2091
-0.7321 ppm
6-deacetylnimbinene
g
[M+Na]+
[M+H]+
409.2006
C 25 H 29 O 5 = 409.2010
-0.8013 ppm
333.2420
C 21 H 33 O 3 = 333.2424
-1.1598 ppm
525.1794
C 19 H 34 O 15 Na = 525.1790
0.8607 ppm
603.1863
C 33 H 31 O 11 = 603.1861
0.4181 ppm
719.2909
759.2834
795.4440
Relative Abundance
m/z

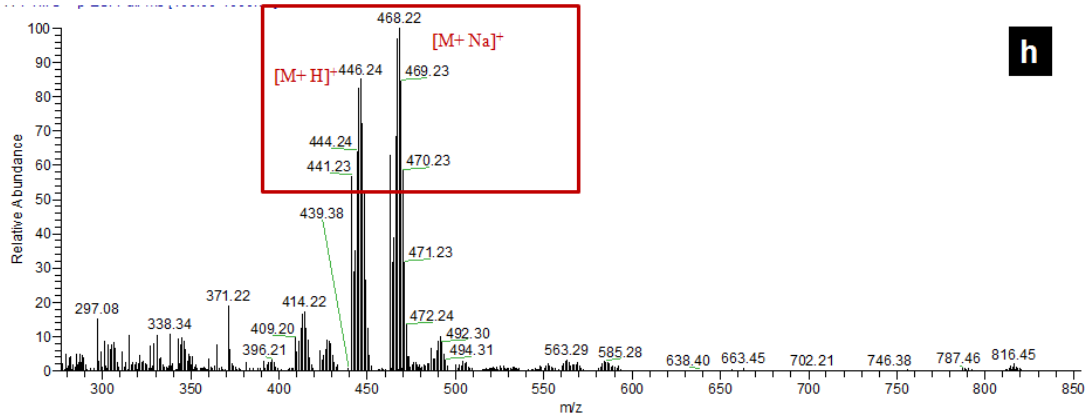
h
468.22
[M+ Na]+
[M+ H]+446.24
469.23
444.24
441.23
470.23
439.38
471.23
297.08
371.22
338.34
414.22
409.20
472.24
396.21
492.30
494.31
563.29
585.28
638.40
663.45
702.21
746.38
787.46
816.45
Relative Abundance
m/z

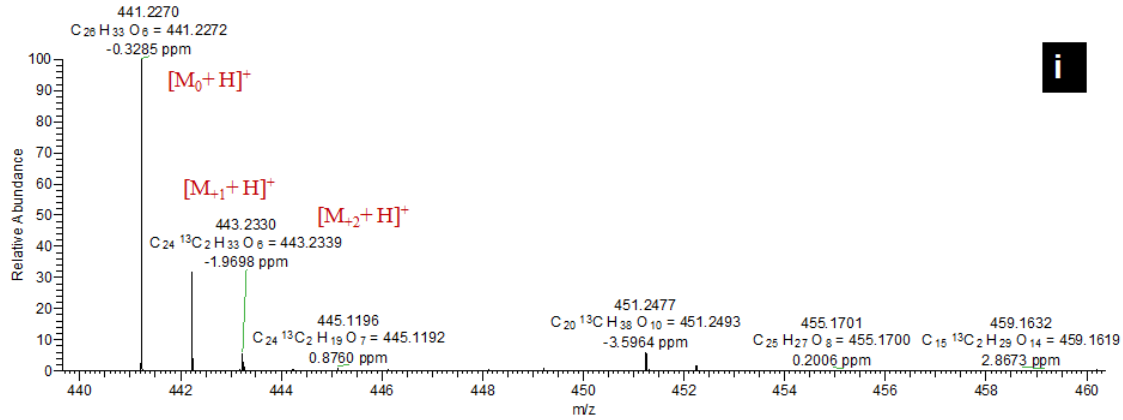
i
441.2270
C26 H33 O6 = 441.2272
-0.3285 ppm
[M0+ H]+
[M+1+ H]+
[M+2+ H]+
443.2330
C24 13C2 H33 O6 = 443.2339
-1.9698 ppm
445.1196
C24 13C2 H19 O7 = 445.1192
0.8760 ppm
451.2477
C20 13C H38 O10 = 451.2493
-3.5964 ppm
455.1701
C25 H27 O8 = 455.1700
0.2006 ppm
459.1632
C15 13C2 H29 O14 = 459.1619
2.8673 ppm
Relative Abundance
m/z

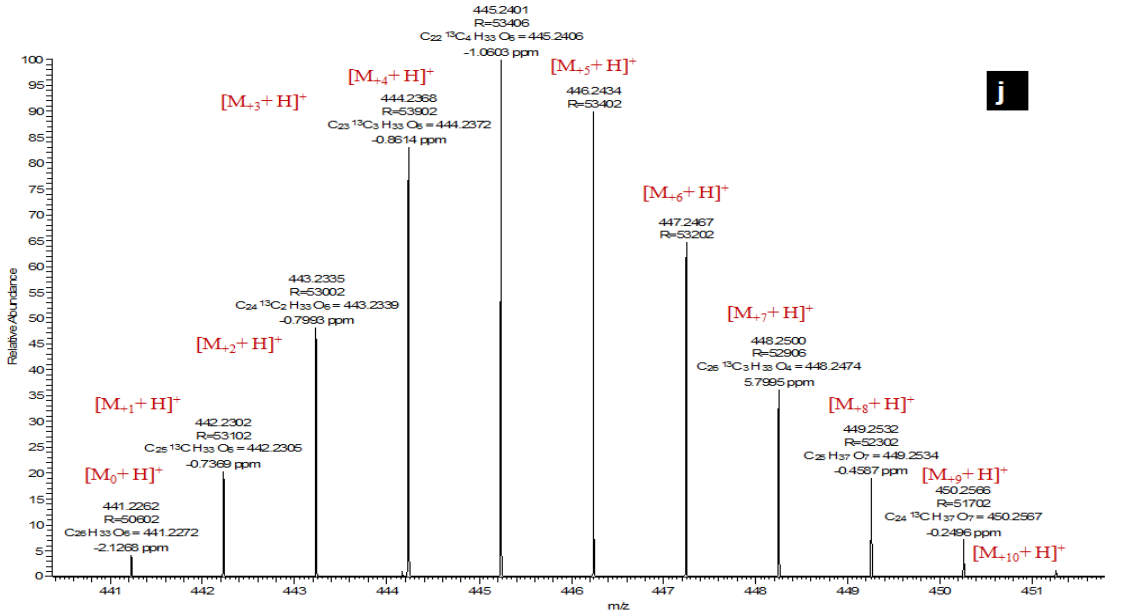
j
445.2401
R=53406
C22 13C4 H33 O8 = 445.2406
-1.0603 ppm
[M+3+ H]+
[M+4+ H]+
444.2368
R=53902
C23 13C3 H33 O8 = 444.2372
-0.8614 ppm
[M+5+ H]+
446.2434
R=53402
[M+6+ H]+
447.2467
R=53202
443.2335
R=53002
C24 13C2 H33 O6 = 443.2339
-0.7993 ppm
[M+2+ H]+
[M+7+ H]+
448.2500
R=52906
C26 13C3 H33 O4 = 448.2474
5.7995 ppm
[M+1+ H]+
442.2302
R=53102
C25 13C H33 O6 = 442.2305
-0.7369 ppm
[M+8+ H]+
449.2532
R=52302
C28 H37 O7 = 449.2534
-0.4587 ppm
[M+9+ H]+
450.2566
R=51702
C24 13C H37 O7 = 450.2567
-0.2496 ppm
[M0+ H]+
441.2262
R=50602
C26 H33 O6 = 441.2272
-2.1268 ppm
[M+10+ H]+
Relative Abundance
m/z

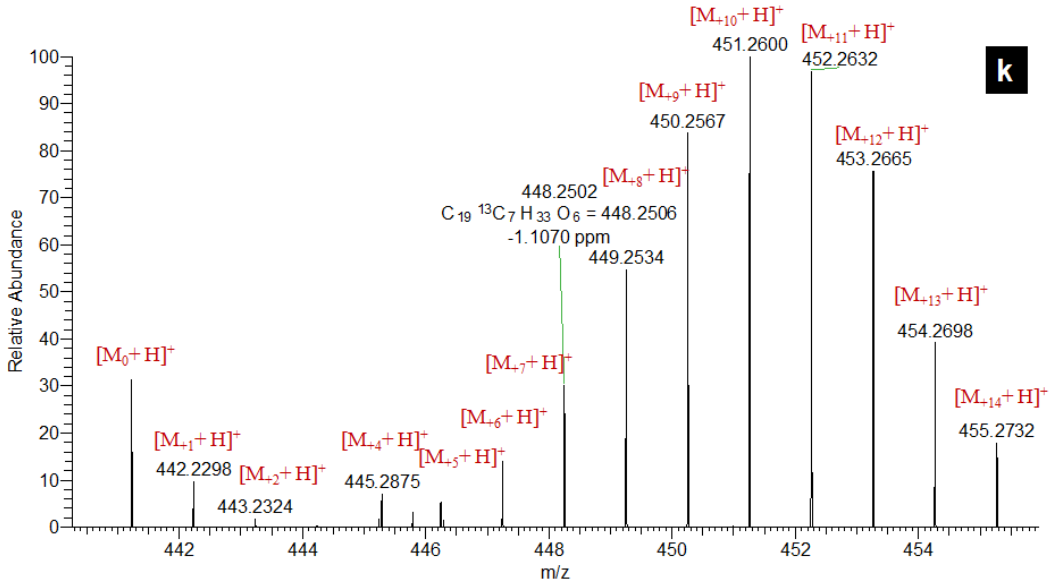
k
[M+10+H]+
451.2600
[M+11+H]+
452.2632
[M+9+H]+
450.2567
[M+12+H]+
453.2665
[M+8+H]+
448.2502
C19 13C7 H33 O6 = 448.2506
-1.1070 ppm
449.2534
[M+13+H]+
454.2698
[M+7+H]+
[M0+H]+
[M+14+H]+
455.2732
[M+6+H]+
[M+1+H]+
442.2298
[M+4+H]+
[M+5+H]+
[M+2+H]+
445.2875
443.2324
Relative Abundance
m/z

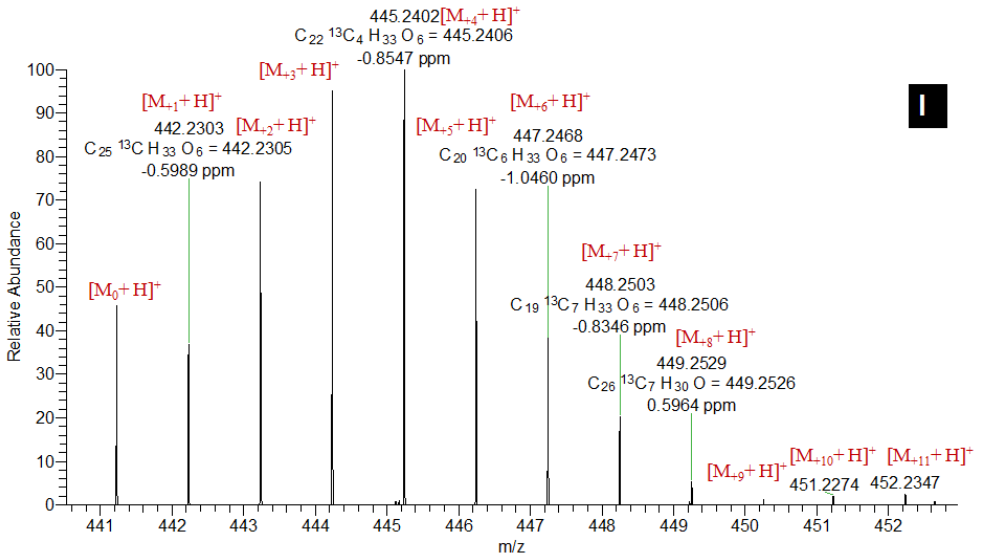
l
445.2402[M+4+H]+
C22 13C4 H33 O6 = 445.2406
-0.8547 ppm
[M+3+H]+
[M+1+H]+
442.2303
[M+2+H]+
C25 13C H33 O6 = 442.2305
-0.5989 ppm
[M+5+H]+
[M+6+H]+
447.2468
C20 13C6 H33 O6 = 447.2473
-1.0460 ppm
[M+7+H]+
[M0+H]+
448.2503
C19 13C7 H33 O6 = 448.2506
-0.8346 ppm
[M+8+H]+
449.2529
C26 13C7 H30 O = 449.2526
0.5964 ppm
[M+9+H]+
[M+10+H]+
451.2274
[M+11+H]+
452.2347
Relative Abundance
m/z

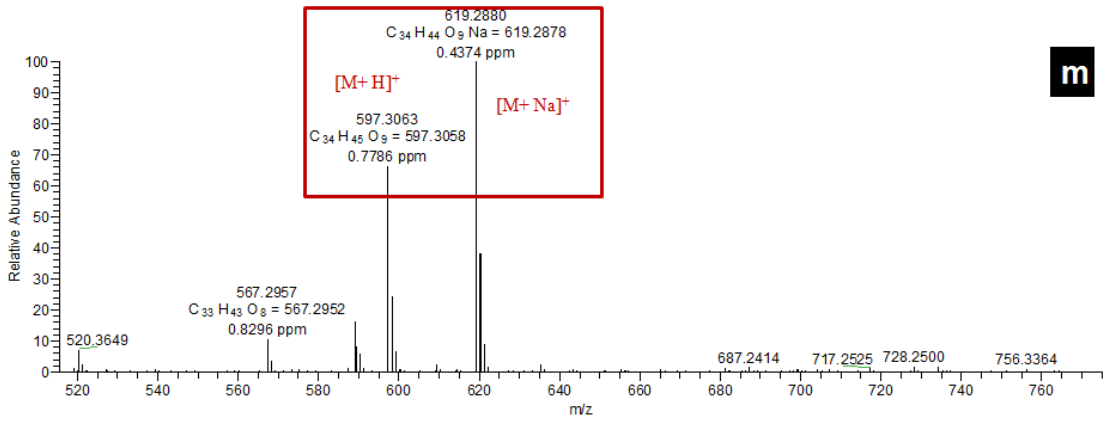
m
619.2880
C34 H44 O9 Na = 619.2878
0.4374 ppm
[M+H]+
[M+Na]+
597.3063
C34 H45 O9 = 597.3058
0.7786 ppm
567.2957
C33 H43 O8 = 567.2952
0.8296 ppm
520.3649
687.2414
717.2525
728.2500
756.3364
Relative Abundance
m/z

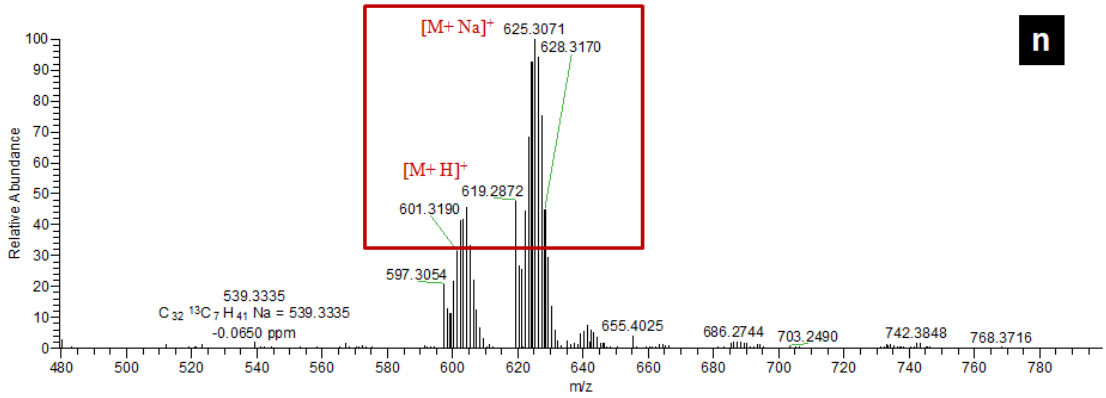
n
[M+Na]+ 625.3071
628.3170
[M+H]+
619.2872
601.3190
597.3054
539.3335
C32 13C7 H41 Na = 539.3335
-0.0650 ppm
655.4025
686.2744
703.2490
742.3848
768.3716
Relative Abundance
m/z

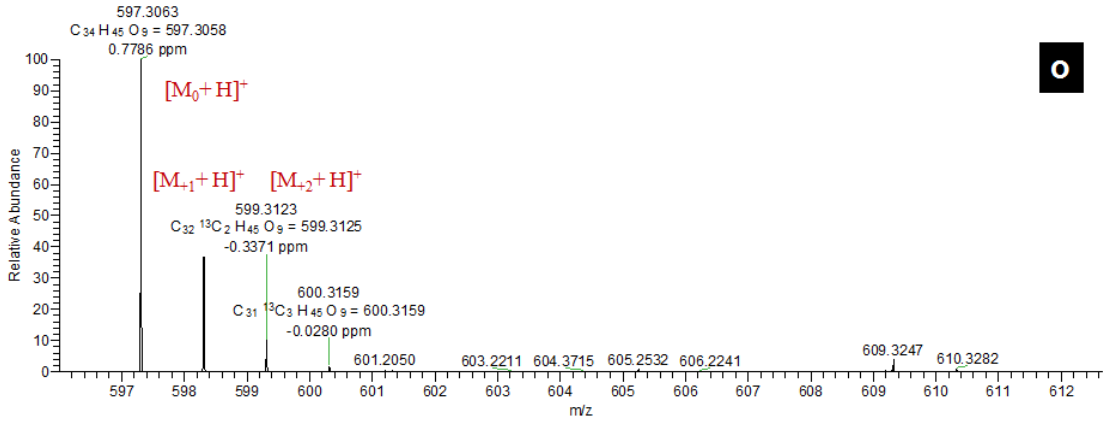
o
597.3063
C34 H45 O9 = 597.3058
0.7786 ppm
[M0+H]+
[M+1+H]+
[M+2+H]+
599.3123
C32 13C2 H45 O9 = 599.3125
-0.3371 ppm
600.3159
C31 13C3 H45 O9 = 600.3159
-0.0280 ppm
601.2050
603.2211
604.3715
605.2532
606.2241
609.3247
610.3282
Relative Abundance
m/z

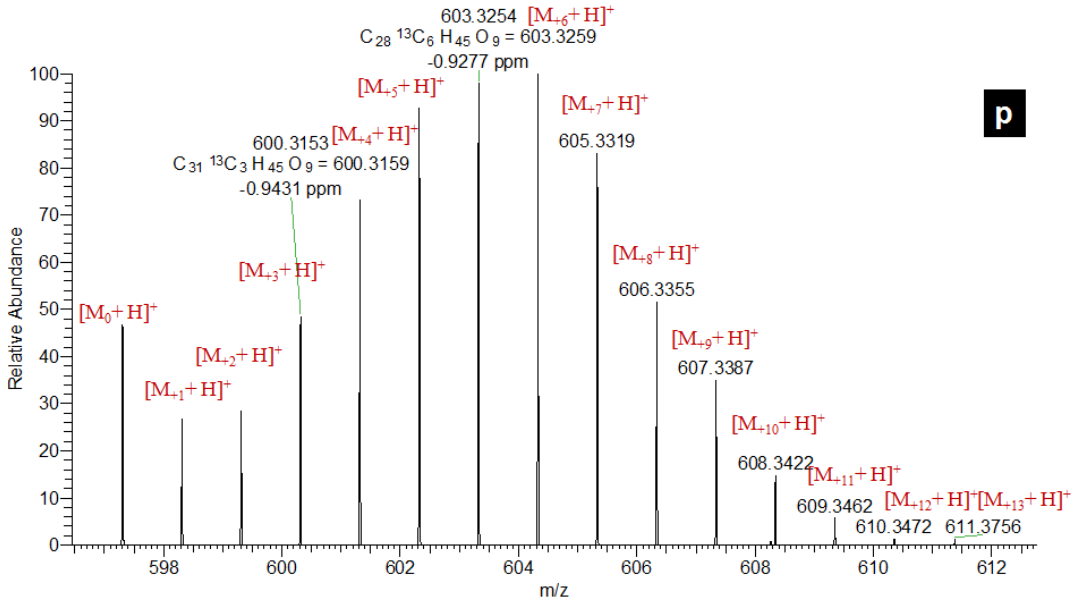
p
603.3254 [M+6+H]+
C28 13C6 H45 O9 = 603.3259
-0.9277 ppm
[M+5+H]+
[M+7+H]+
605.3319
600.3153 [M+4+H]+
C31 13C3 H45 O9 = 600.3159
-0.9431 ppm
[M+8+H]+
606.3355
[M+3+H]+
[M0+H]+
[M+9+H]+
607.3387
[M+2+H]+
[M+1+H]+
[M+10+H]+
608.3422
[M+11+H]+
609.3462
[M+12+H]+[M+13+H]+
610.3472
611.3756
Relative Abundance
m/z

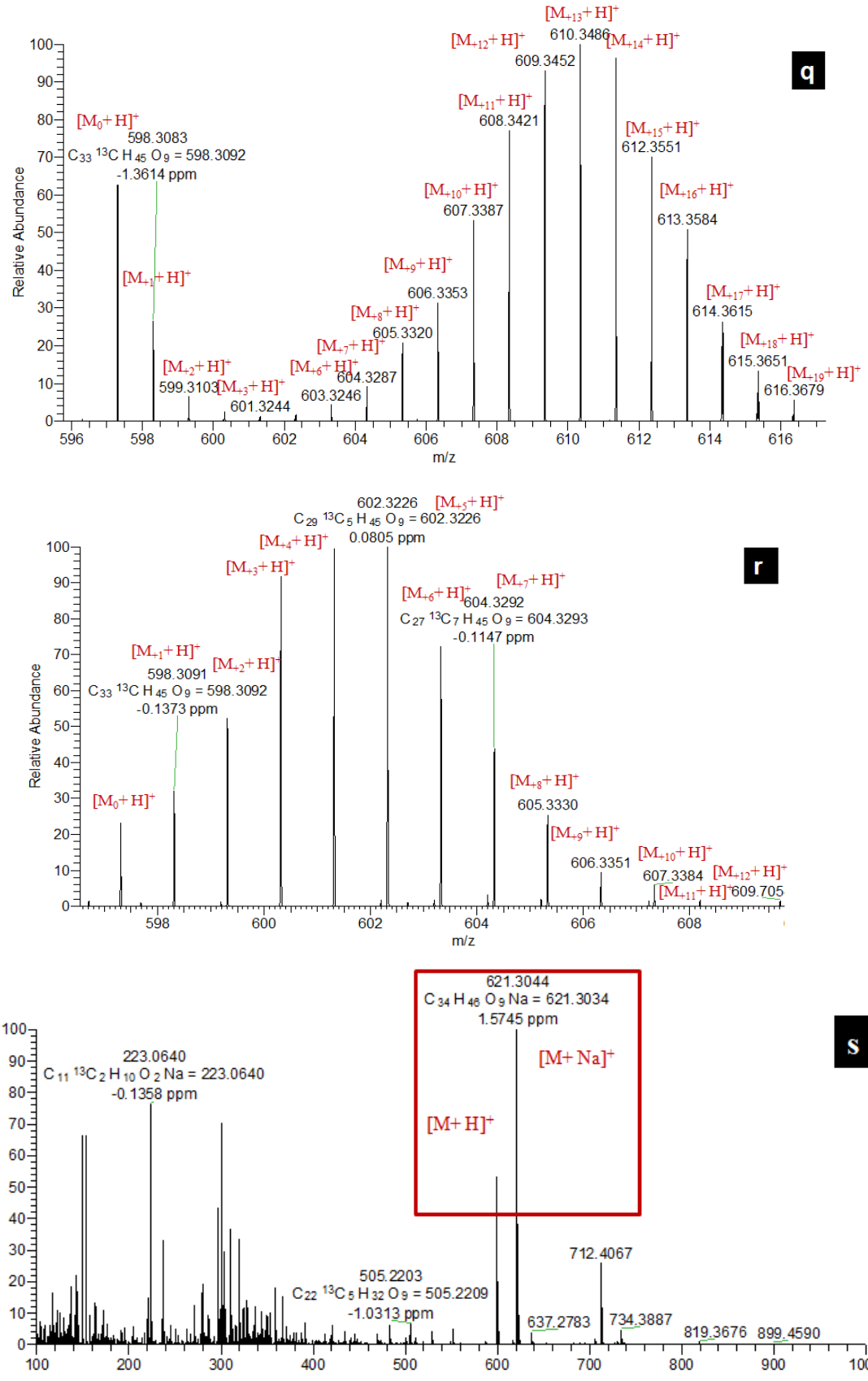
q
[M+13+H]+
610.3486
[M+12+H]+
[M+14+H]+
609.3452
[M+11+H]+
608.3421
[M+15+H]+
612.3551
[M+10+H]+
607.3387
[M+16+H]+
613.3584
[M+9+H]+
606.3353
[M+17+H]+
614.3615
[M+8+H]+
605.3320
[M+18+H]+
615.3651
[M+7+H]+
[M+6+H]+
604.3287
[M+19+H]+
616.3679
[M+2+H]+
599.3103
[M+3+H]+
601.3244
603.3246
[M0+H]+
598.3083
C33 13C H45 O9 = 598.3092
-1.3614 ppm
[M+1+H]+
Relative Abundance
m/z
r
602.3226
[M+5+H]+
C29 13C5 H45 O9 = 602.3226
0.0805 ppm
[M+4+H]+
[M+3+H]+
[M+7+H]+
[M+6+H]+
604.3292
C27 13C7 H45 O9 = 604.3293
-0.1147 ppm
[M+1+H]+
598.3091
C33 13C H45 O9 = 598.3092
-0.1373 ppm
[M+2+H]+
[M0+H]+
[M+8+H]+
605.3330
[M+9+H]+
606.3351
[M+10+H]+
607.3384
[M+12+H]+
[M+11+H]+
609.705
Relative Abundance
m/z
s
621.3044
C34 H46 O9 Na = 621.3034
1.5745 ppm
[M+ Na]+
[M+ H]+
223.0640
C11 13C2 H10 O2 Na = 223.0640
-0.1358 ppm
712.4067
505.2203
C22 13C5 H32 O9 = 505.2209
-1.0313 ppm
637.2783
734.3887
819.3676
899.4590
Relative Abundance

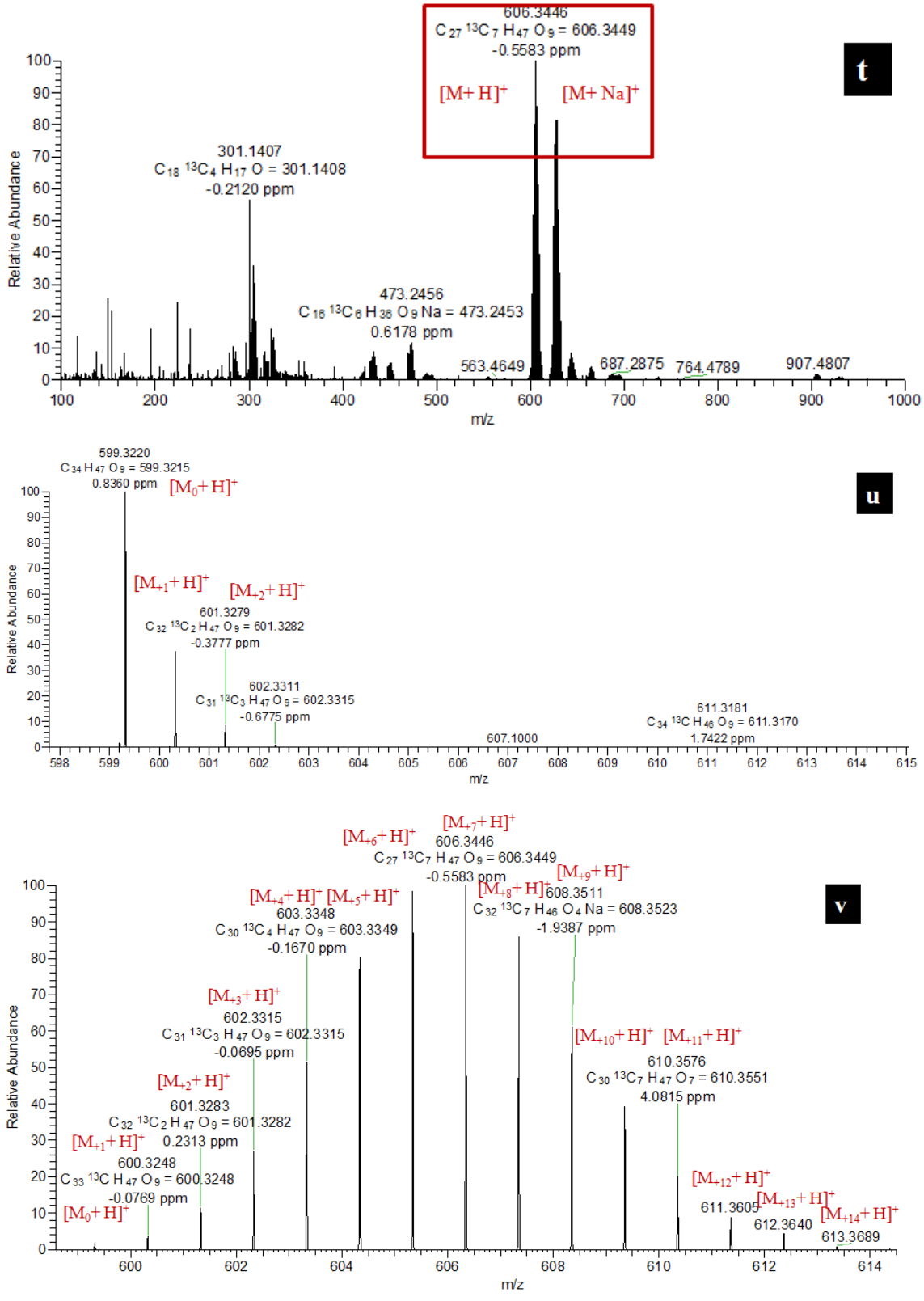
t
606.3446
C27 13C7 H47 O9 = 606.3449
-0.5583 ppm
[M+H]+
[M+Na]+
301.1407
C18 13C4 H17 O = 301.1408
-0.2120 ppm
473.2456
C16 13C6 H38 O9 Na = 473.2453
0.6178 ppm
563.4649
687.2875
764.4789
907.4807
Relative Abundance
m/z
u
599.3220
C34 H47 O9 = 599.3215
0.8360 ppm
[M0+H]+
[M+1+H]+
[M+2+H]+
601.3279
C32 13C2 H47 O9 = 601.3282
-0.3777 ppm
602.3311
C31 13C3 H47 O9 = 602.3315
-0.6775 ppm
607.1000
611.3181
C34 13C H46 O9 = 611.3170
1.7422 ppm
Relative Abundance
m/z
v
[M+7+H]+
[M+6+H]+
606.3446
C27 13C7 H47 O9 = 606.3449
-0.5583 ppm
[M+9+H]+
[M+8+H]+
608.3511
C32 13C7 H46 O4 Na = 608.3523
-1.9387 ppm
[M+4+H]+ [M+5+H]+
603.3348
C30 13C4 H47 O9 = 603.3349
-0.1670 ppm
[M+3+H]+
602.3315
C31 13C3 H47 O9 = 602.3315
-0.0695 ppm
[M+10+H]+ [M+11+H]+
610.3576
C30 13C7 H47 O7 = 610.3551
4.0815 ppm
[M+2+H]+
601.3283
C32 13C2 H47 O9 = 601.3282
0.2313 ppm
[M+1+H]+
600.3248
C33 13C H47 O9 = 600.3248
-0.0769 ppm
[M0+H]+
[M+12+H]+
611.3605
[M+13+H]+
612.3640
[M+14+H]+
613.3689
Relative Abundance
m/z

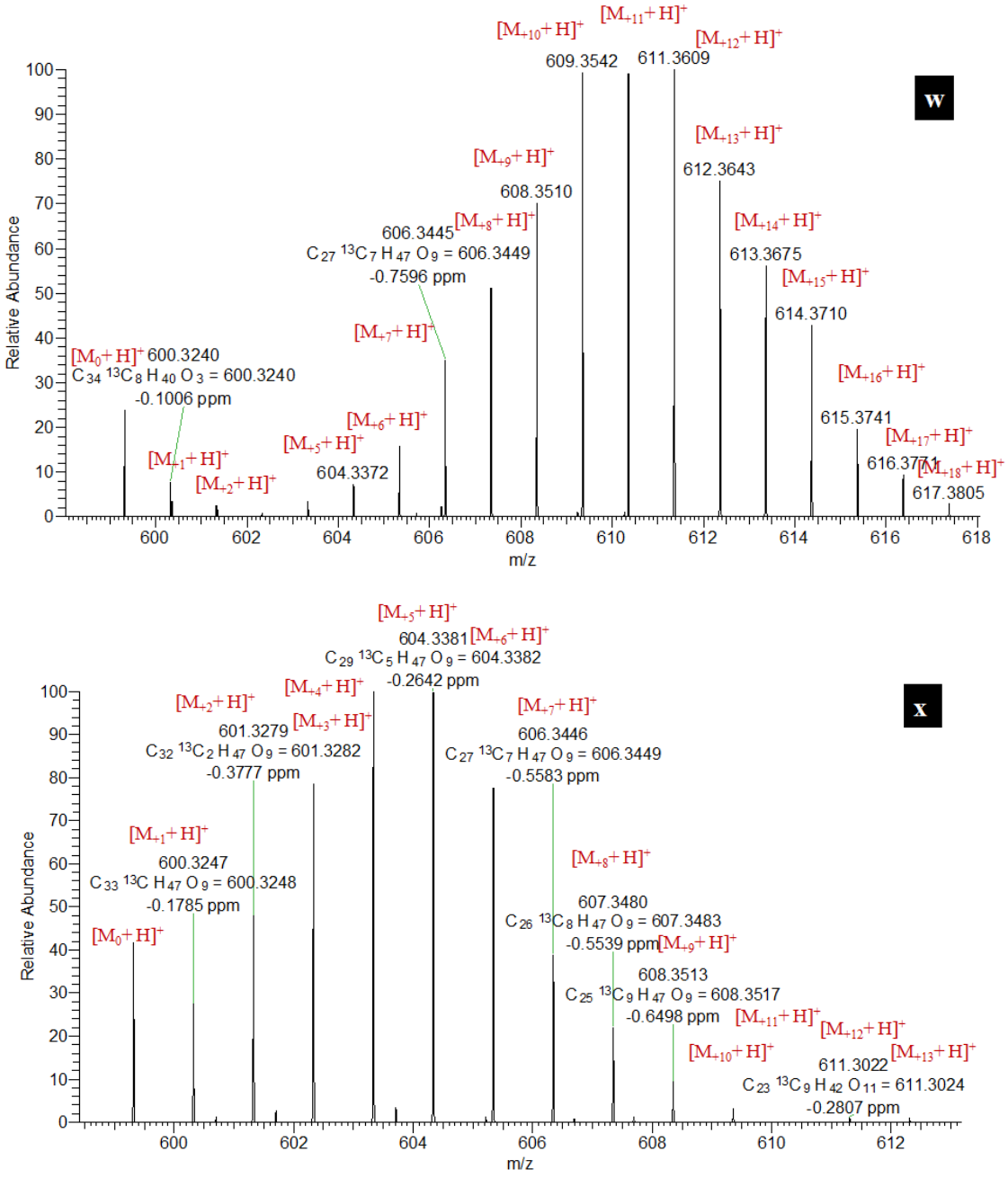

3C.5.1. Comparison of mass spectra of the unlabeled and ^{13}C limonoids from the neem cell suspension (a) azadirachtin A. (b) labeled azadirachtin A. (c) Natural abundance ^{13}C of protonated molecular ion of azadirachtin A. (d) 1-^{13}C Glc labeling of azadirachtin A. (e) 1,6-^{13}C Glc labeling of azadirachtin A. (f) 2-^{13}C Glc labeling of azadirachtin A. (g) 6-deacetylnimbinene. (h) labeled 6-deacetylnimbinene. (i) Natural abundance ^{13}C of protonated molecular ion of 6-deacetylnimbinene. (j) 1-^{13}C Glc labeling of 6-deacetylnimbinene. (k) 1,6-^{13}C Glc labeling of 6-deacetylnimbinene. (l) 2-^{13}C Glc labeling of 6-deacetylnimbinene. (m) salannin. (n) labeled salannin. (o) Natural abundance ^{13}C of protonated molecular ion of salannin. (p) 1-^{13}C Glc labeling of salannin. (q) 1,6-^{13}C Glc labeling of salannin. (r) 2-^{13}C Glc labeling of salannin. (s) salannolacetate. (t) labeled salannolacetate. (u) Natural abundance ^{13}C of protonated molecular ion of salannolacetate. (v) 1-^{13}C Glc labeling of salannolacetate. (w) 1,6-^{13}C Glc labeling of salannolacetate. (x) 2-^{13}C Glc labeling of salannolacetate.

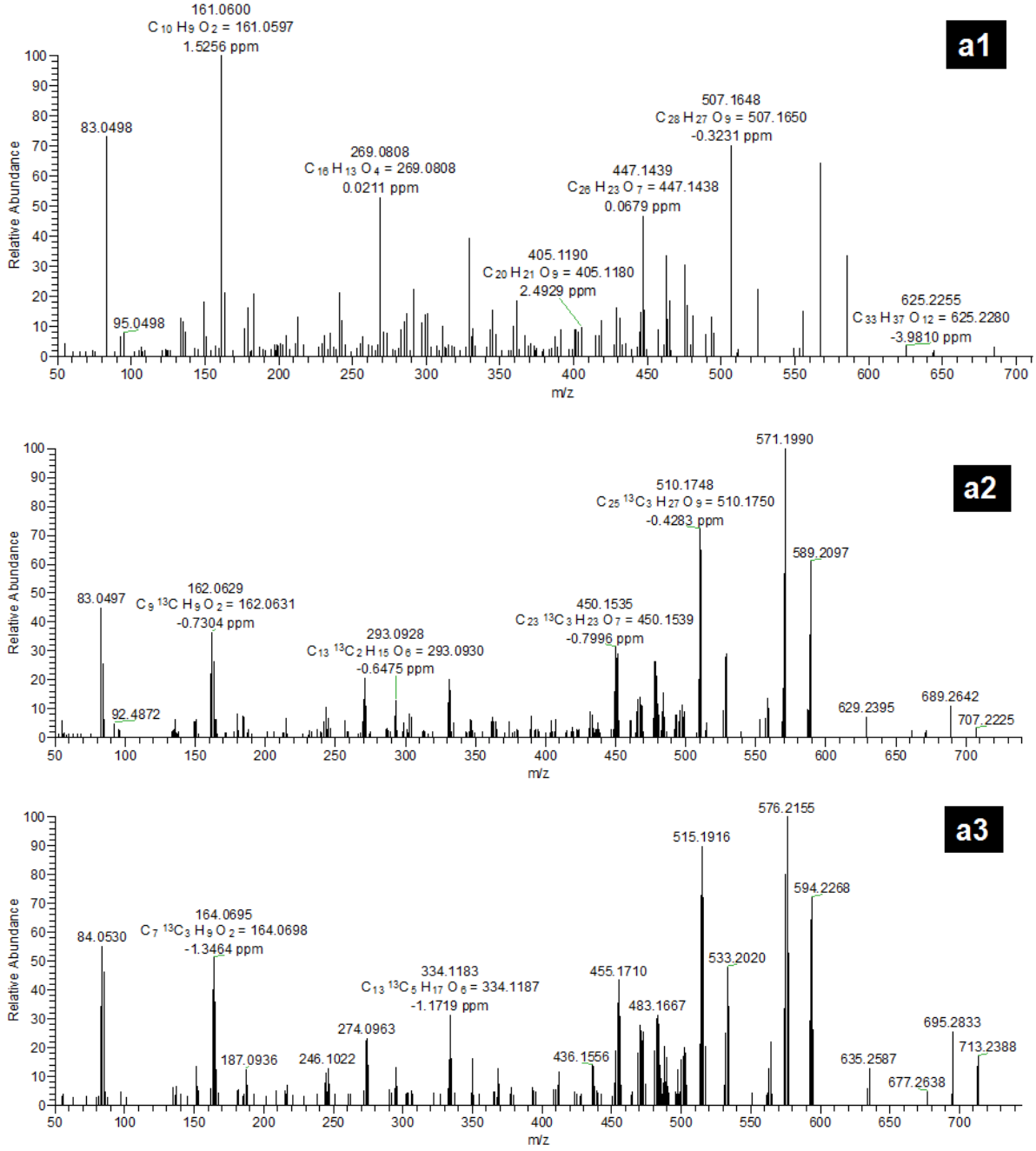
a1
161.0600
C 10 H 9 O 2 = 161.0597
1.5256 ppm
83.0498
269.0808
C 16 H 13 O 4 = 269.0808
0.0211 ppm
447.1439
C 26 H 23 O 7 = 447.1438
0.0679 ppm
507.1648
C 28 H 27 O 9 = 507.1650
-0.3231 ppm
405.1190
C 20 H 21 O 9 = 405.1180
2.4929 ppm
95.0498
625.2255
C 33 H 37 O 12 = 625.2280
-3.9810 ppm
Relative Abundance
m/z
a2
571.1990
510.1748
C 25 13C 3 H 27 O 9 = 510.1750
-0.4283 ppm
589.2097
83.0497
162.0629
C 9 13C H 9 O 2 = 162.0631
-0.7304 ppm
450.1535
C 23 13C 3 H 23 O 7 = 450.1539
-0.7996 ppm
293.0928
C 13 13C 2 H 15 O 6 = 293.0930
-0.6475 ppm
92.4872
629.2395
689.2642
707.2225
Relative Abundance
m/z
a3
576.2155
515.1916
594.2268
84.0530
164.0695
C 7 13C 3 H 9 O 2 = 164.0698
-1.3464 ppm
533.2020
455.1710
334.1183
C 13 13C 5 H 17 O 6 = 334.1187
-1.1719 ppm
483.1667
274.0963
695.2833
713.2388
187.0936
246.1022
436.1556
635.2587
677.2638
Relative Abundance
m/z

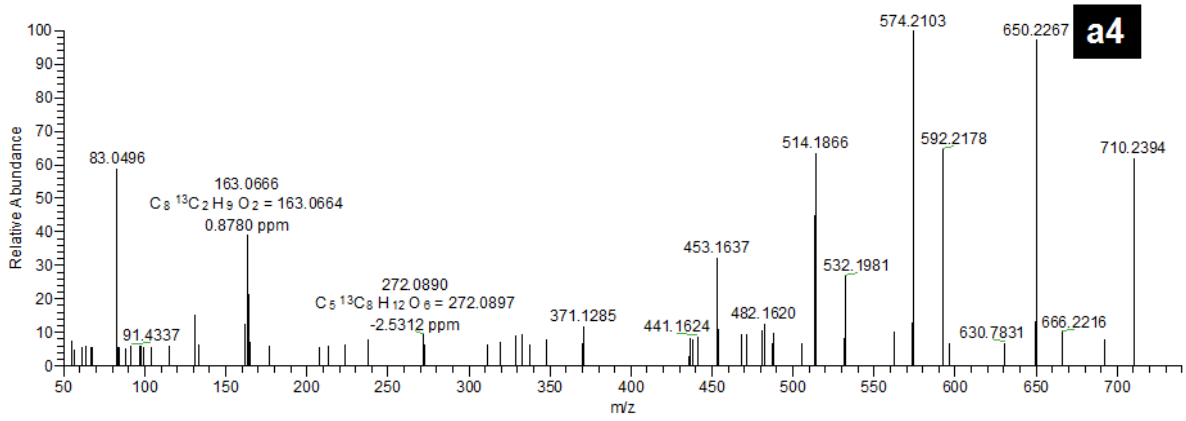
a4
Relative Abundance
m/z
574.2103
650.2267
514.1866
592.2178
710.2394
83.0496
163.0666
C 8 13C 2 H 9 O 2 = 163.0664
0.8780 ppm
453.1637
532.1981
272.0890
C 5 13C 8 H 12 O 6 = 272.0897
-2.5312 ppm
371.1285
441.1624
482.1620
91.4337
630.7831
666.2216

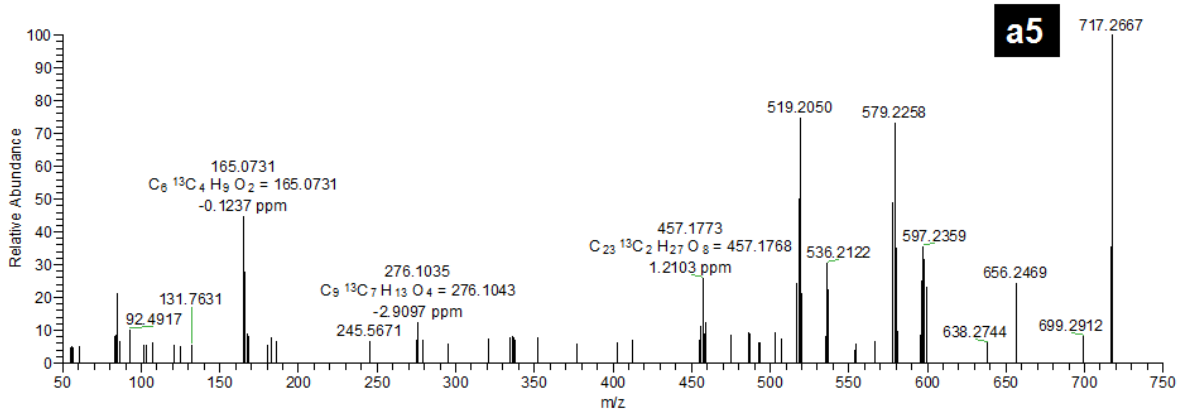
a5
Relative Abundance
m/z
717.2667
519.2050
579.2258
165.0731
C 6 13C 4 H 9 O 2 = 165.0731
-0.1237 ppm
457.1773
C 23 13C 2 H 27 O 8 = 457.1768
1.2103 ppm
536.2122
597.2359
656.2469
276.1035
C 9 13C 7 H 13 O 4 = 276.1043
-2.9097 ppm
131.7631
92.4917
245.5671
638.2744
699.2912

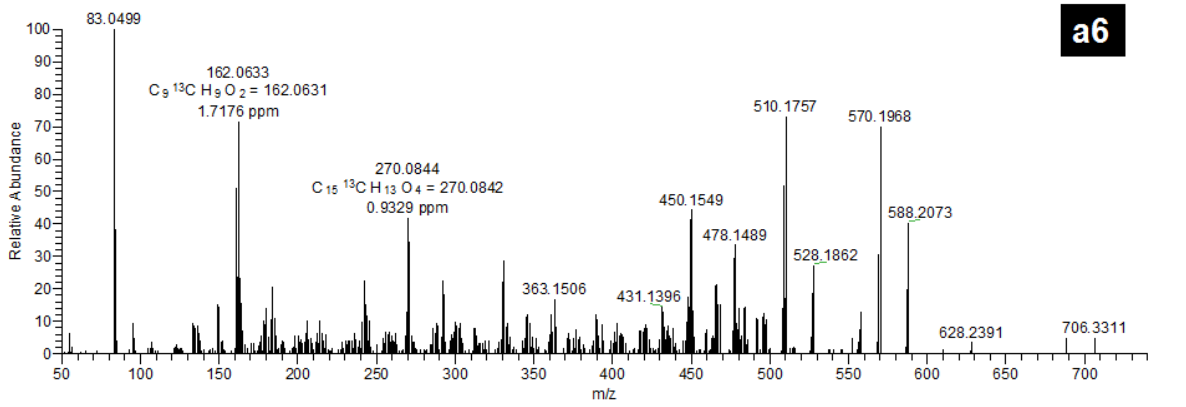
a6
Relative Abundance
m/z
83.0499
162.0633
C 9 13C H 9 O 2 = 162.0631
1.7176 ppm
510.1757
570.1968
270.0844
C 15 13C H 13 O 4 = 270.0842
0.9329 ppm
450.1549
588.2073
478.1489
528.1862
363.1506
431.1396
628.2391
706.3311

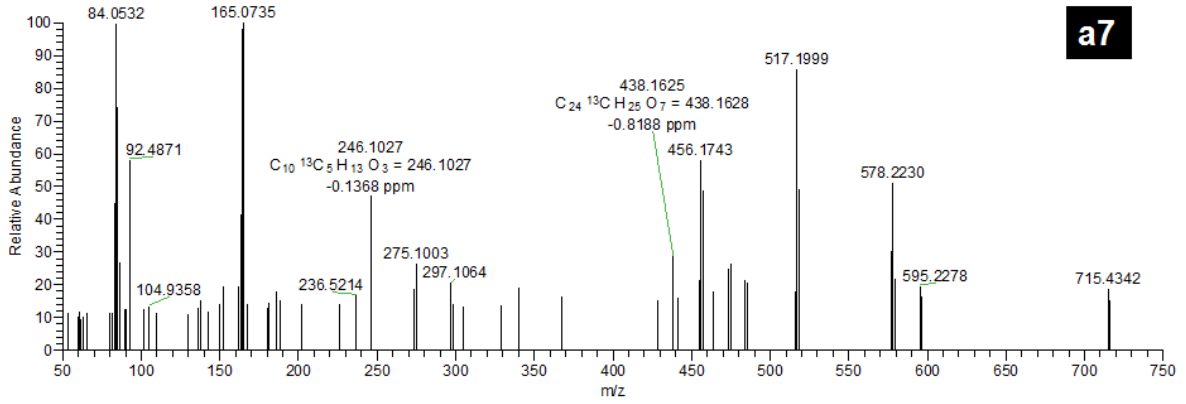
a7
Relative Abundance
m/z
84.0532
165.0735
517.1999
438.1625
C 24 13C H 25 O 7 = 438.1628
-0.8188 ppm
92.4871
246.1027
C 10 13C 5 H 13 O 3 = 246.1027
-0.1368 ppm
456.1743
578.2230
275.1003
297.1064
104.9358
236.5214
595.2278
715.4342

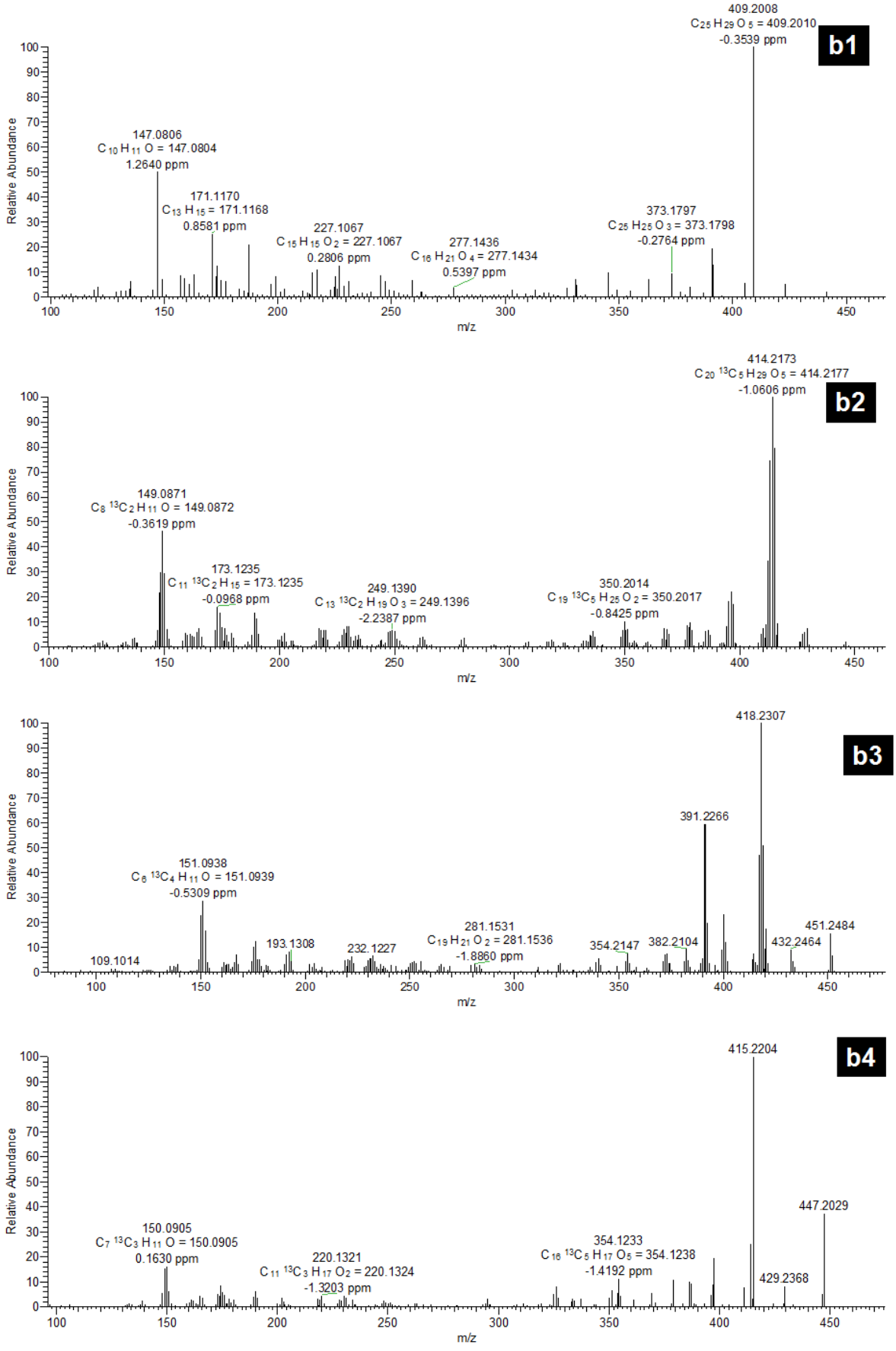
b1
409.2008
C25 H29 O5 = 409.2010
-0.3539 ppm
147.0806
C10 H11 O = 147.0804
1.2640 ppm
171.1170
C13 H15 = 171.1168
0.8581 ppm
227.1067
C15 H15 O2 = 227.1067
0.2806 ppm
277.1436
C16 H21 O4 = 277.1434
0.5397 ppm
373.1797
C25 H25 O3 = 373.1798
-0.2764 ppm
b2
414.2173
C20 13C5 H29 O5 = 414.2177
-1.0606 ppm
149.0871
C8 13C2 H11 O = 149.0872
-0.3619 ppm
173.1235
C11 13C2 H15 = 173.1235
-0.0968 ppm
249.1390
C13 13C2 H19 O3 = 249.1396
-2.2387 ppm
350.2014
C19 13C5 H25 O2 = 350.2017
-0.8425 ppm
b3
418.2307
391.2266
151.0938
C6 13C4 H11 O = 151.0939
-0.5309 ppm
281.1531
C19 H21 O2 = 281.1536
-1.8860 ppm
451.2484
193.1308
232.1227
354.2147
382.2104
432.2464
109.1014
b4
415.2204
447.2029
150.0905
C7 13C3 H11 O = 150.0905
0.1630 ppm
220.1321
C11 13C3 H17 O2 = 220.1324
-1.3203 ppm
354.1233
C16 13C5 H17 O5 = 354.1238
-1.4192 ppm
429.2368
Relative Abundance
m/z

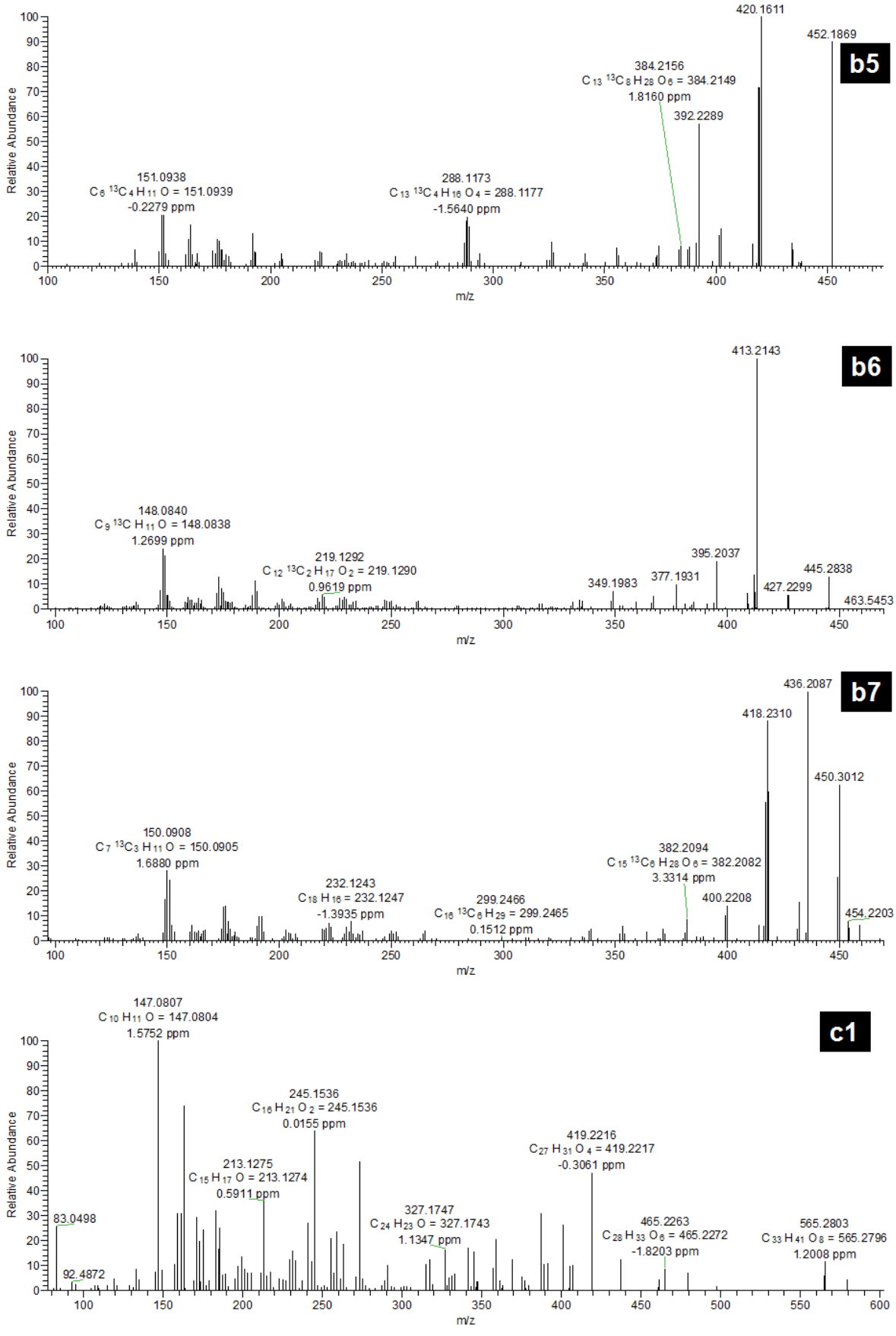
b5
Relative Abundance
m/z
420.1611
452.1869
384.2156
C13 13C8 H28 O6 = 384.2149
1.8160 ppm
392.2289
151.0938
C8 13C4 H11 O = 151.0939
-0.2279 ppm
288.1173
C13 13C4 H16 O4 = 288.1177
-1.5640 ppm
b6
413.2143
148.0840
C9 13C H11 O = 148.0838
1.2699 ppm
219.1292
C12 13C2 H17 O2 = 219.1290
0.9619 ppm
395.2037
349.1983
377.1931
445.2838
427.2299
463.5453
b7
436.2087
418.2310
450.3012
150.0908
C7 13C3 H11 O = 150.0905
1.6880 ppm
382.2094
C15 13C6 H28 O6 = 382.2082
3.3314 ppm
232.1243
C18 H16 = 232.1247
-1.3935 ppm
299.2466
C16 13C6 H29 = 299.2465
0.1512 ppm
400.2208
454.2203
c1
147.0807
C10 H11 O = 147.0804
1.5752 ppm
245.1536
C16 H21 O2 = 245.1536
0.0155 ppm
419.2216
C27 H31 O4 = 419.2217
-0.3061 ppm
213.1275
C15 H17 O = 213.1274
0.5911 ppm
327.1747
C24 H23 O = 327.1743
1.1347 ppm
83.0498
465.2263
C28 H33 O6 = 465.2272
-1.8203 ppm
565.2803
C33 H41 O8 = 565.2796
1.2008 ppm
92.4872

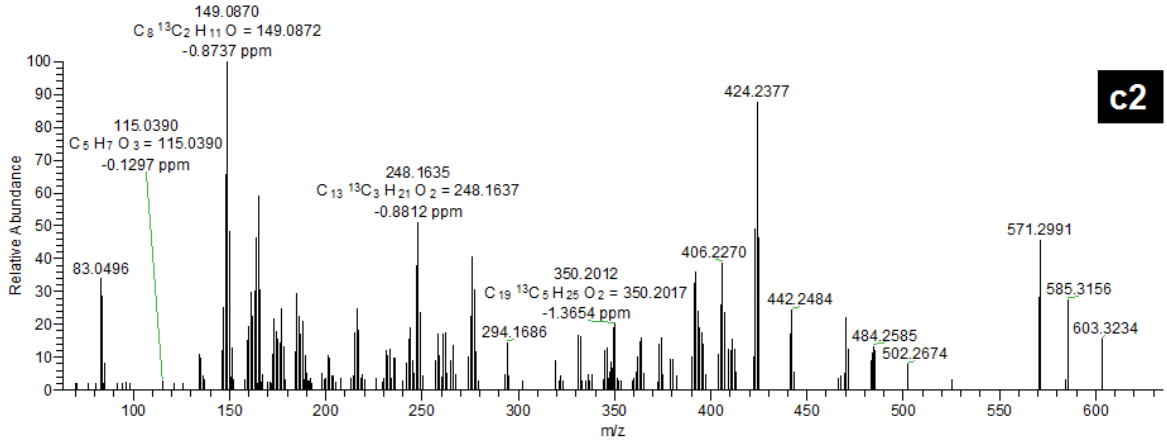
c2
149.0870
C8 13C2 H11 O = 149.0872
-0.8737 ppm
115.0390
C5 H7 O3 = 115.0390
-0.1297 ppm
248.1635
C13 13C3 H21 O2 = 248.1637
-0.8812 ppm
424.2377
406.2270
350.2012
C19 13C5 H25 O2 = 350.2017
-1.3654 ppm
571.2991
585.3156
603.3234
442.2484
484.2585
502.2674
294.1686
83.0496
Relative Abundance
m/z

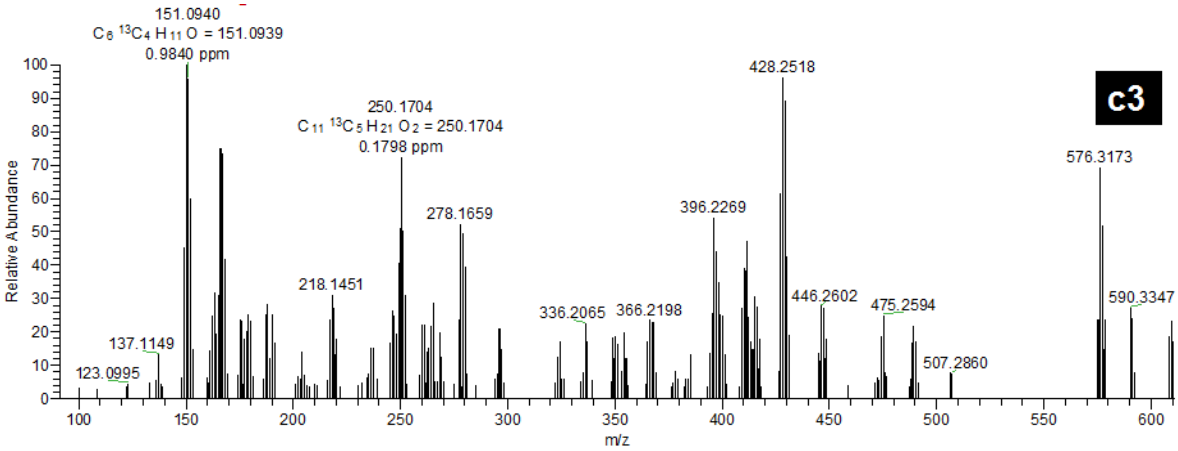
c3
151.0940
C8 13C4 H11 O = 151.0939
0.9840 ppm
250.1704
C11 13C5 H21 O2 = 250.1704
0.1798 ppm
428.2518
576.3173
396.2269
278.1659
218.1451
446.2602
475.2594
590.3347
336.2065
366.2198
137.1149
123.0995
507.2860
Relative Abundance
m/z

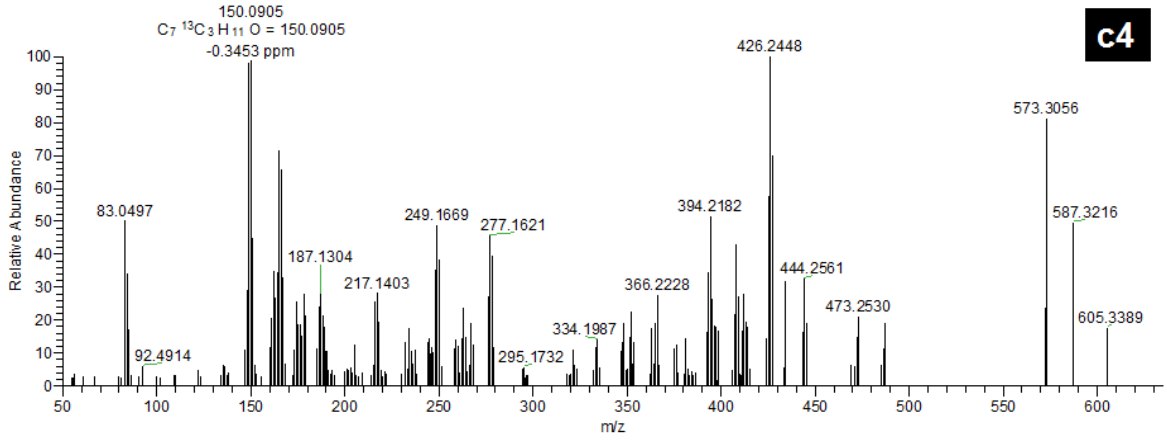
c4
150.0905
C7 13C3 H11 O = 150.0905
-0.3453 ppm
426.2448
573.3056
83.0497
249.1669
277.1621
394.2182
587.3216
187.1304
217.1403
444.2561
366.2228
473.2530
605.3389
334.1987
92.4914
295.1732
Relative Abundance
m/z

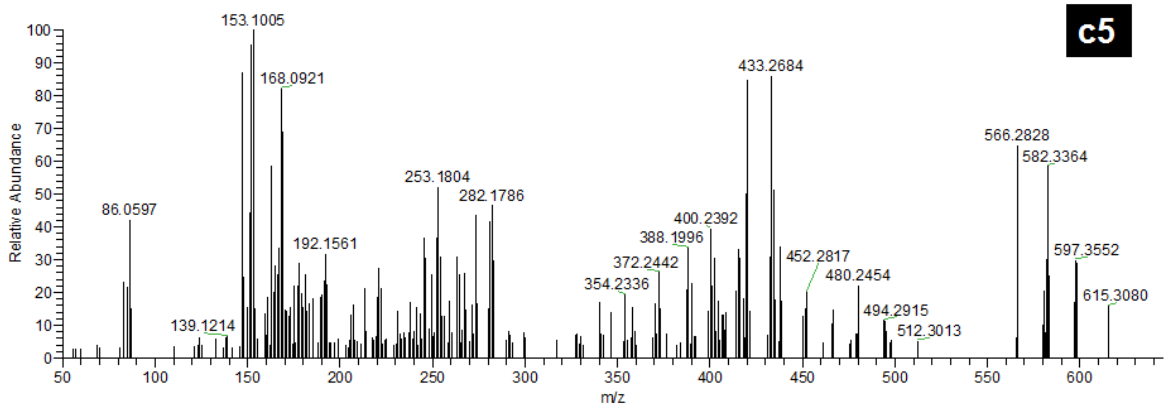
c5
153.1005
168.0921
433.2684
566.2828
582.3364
253.1804
282.1786
86.0597
400.2392
388.1996
192.1561
452.2817
597.3552
372.2442
480.2454
354.2336
615.3080
494.2915
139.1214
512.3013
Relative Abundance
m/z

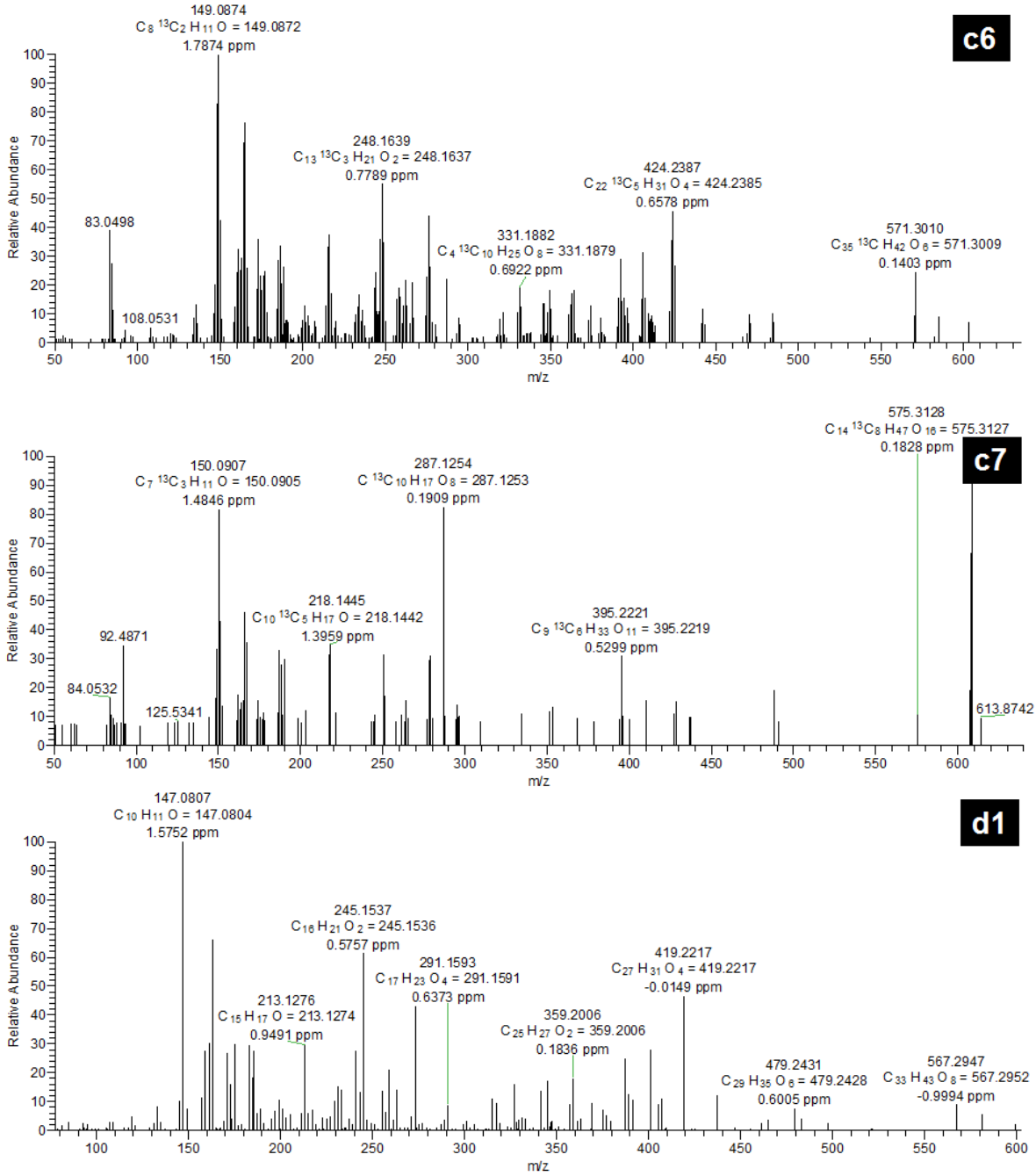
c6
149.0874
C 8 13C2 H 11 O = 149.0872
1.7874 ppm
248.1639
C13 13C3 H21 O 2 = 248.1637
0.7789 ppm
424.2387
C22 13C5 H31 O 4 = 424.2385
0.6578 ppm
83.0498
331.1882
C 4 13C 10 H25 O 8 = 331.1879
0.6922 ppm
571.3010
C35 13C H42 O 6 = 571.3009
0.1403 ppm
108.0531
Relative Abundance
m/z
c7
575.3128
C 14 13C8 H47 O 16 = 575.3127
0.1828 ppm
150.0907
C 7 13C 3 H 11 O = 150.0905
1.4846 ppm
287.1254
C 13C 10 H 17 O 8 = 287.1253
0.1909 ppm
218.1445
C 10 13C 5 H 17 O = 218.1442
1.3959 ppm
395.2221
C 9 13C 6 H 33 O 11 = 395.2219
0.5299 ppm
92.4871
84.0532
125.5341
613.8742
Relative Abundance
m/z
d1
147.0807
C 10 H 11 O = 147.0804
1.5752 ppm
245.1537
C 16 H 21 O 2 = 245.1536
0.5757 ppm
291.1593
C 17 H 23 O 4 = 291.1591
0.6373 ppm
419.2217
C 27 H 31 O 4 = 419.2217
-0.0149 ppm
213.1276
C 15 H 17 O = 213.1274
0.9491 ppm
359.2006
C 25 H 27 O 2 = 359.2006
0.1836 ppm
479.2431
C 29 H 35 O 6 = 479.2428
0.6005 ppm
567.2947
C 33 H 43 O 8 = 567.2952
-0.9994 ppm
Relative Abundance
m/z

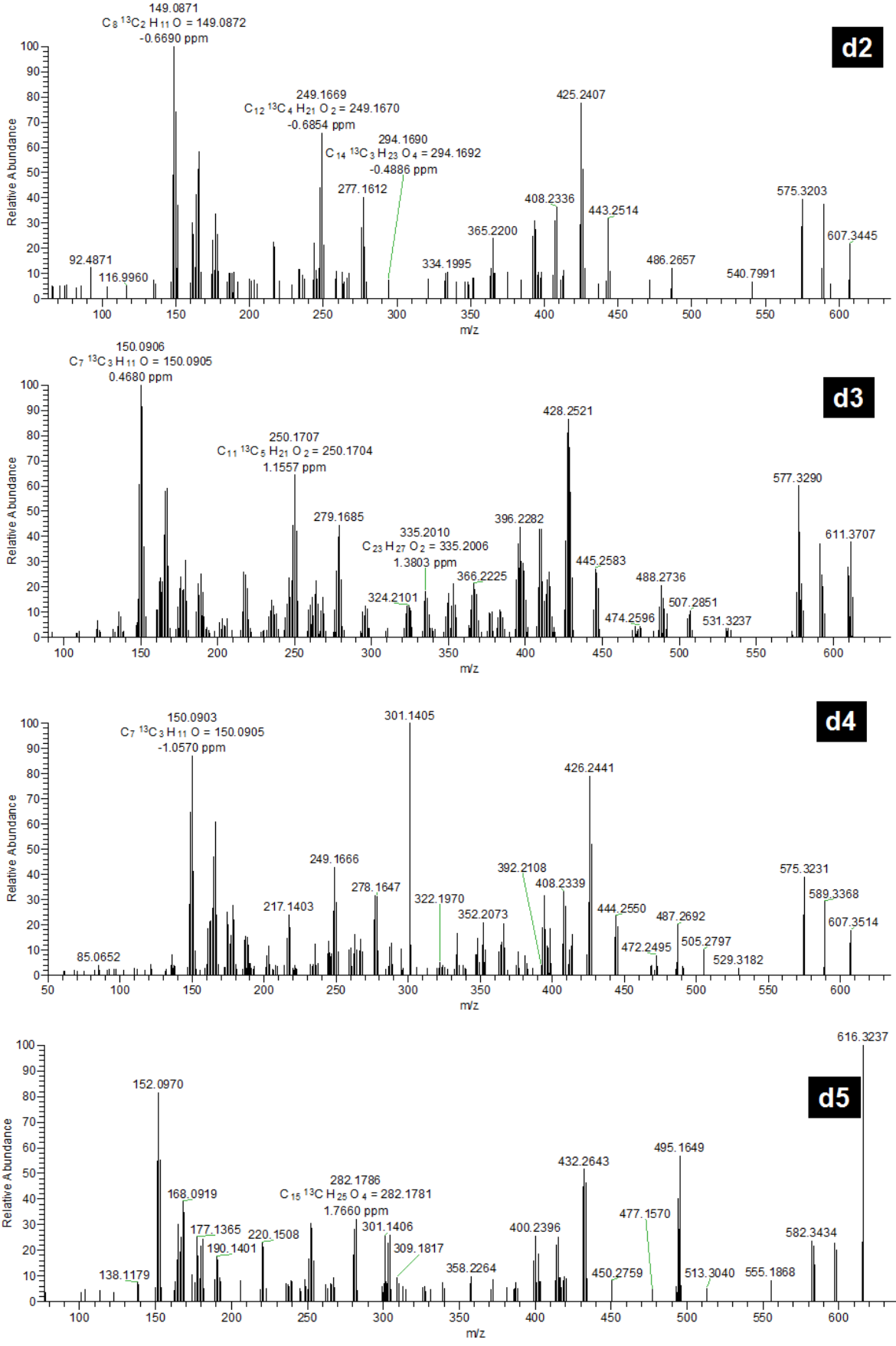
d2
149.0871
C8 13C2 H11 O = 149.0872
-0.6690 ppm
249.1669
C12 13C4 H21 O2 = 249.1670
-0.6854 ppm
294.1690
C14 13C3 H23 O4 = 294.1692
-0.4886 ppm
277.1612
425.2407
408.2336
443.2514
575.3203
607.3445
365.2200
334.1995
486.2657
540.7991
92.4871
116.9960
Relative Abundance
m/z
d3
150.0906
C7 13C3 H11 O = 150.0905
0.4680 ppm
250.1707
C11 13C5 H21 O2 = 250.1704
1.1557 ppm
428.2521
577.3290
279.1685
396.2282
335.2010
C23 H27 O2 = 335.2006
1.3803 ppm
611.3707
445.2583
366.2225
488.2736
324.2101
507.2851
474.2596
531.3237
Relative Abundance
m/z
d4
150.0903
C7 13C3 H11 O = 150.0905
-1.0570 ppm
301.1405
426.2441
249.1666
392.2108
408.2339
278.1647
575.3231
589.3368
217.1403
322.1970
352.2073
444.2550
487.2692
607.3514
505.2797
472.2495
85.0652
529.3182
Relative Abundance
m/z
d5
616.3237
152.0970
495.1649
432.2643
282.1786
C15 13C H25 O4 = 282.1781
1.7660 ppm
168.0919
477.1570
177.1365
220.1508
301.1406
400.2396
582.3434
190.1401
309.1817
138.1179
358.2264
450.2759
513.3040
555.1868
Relative Abundance
m/z

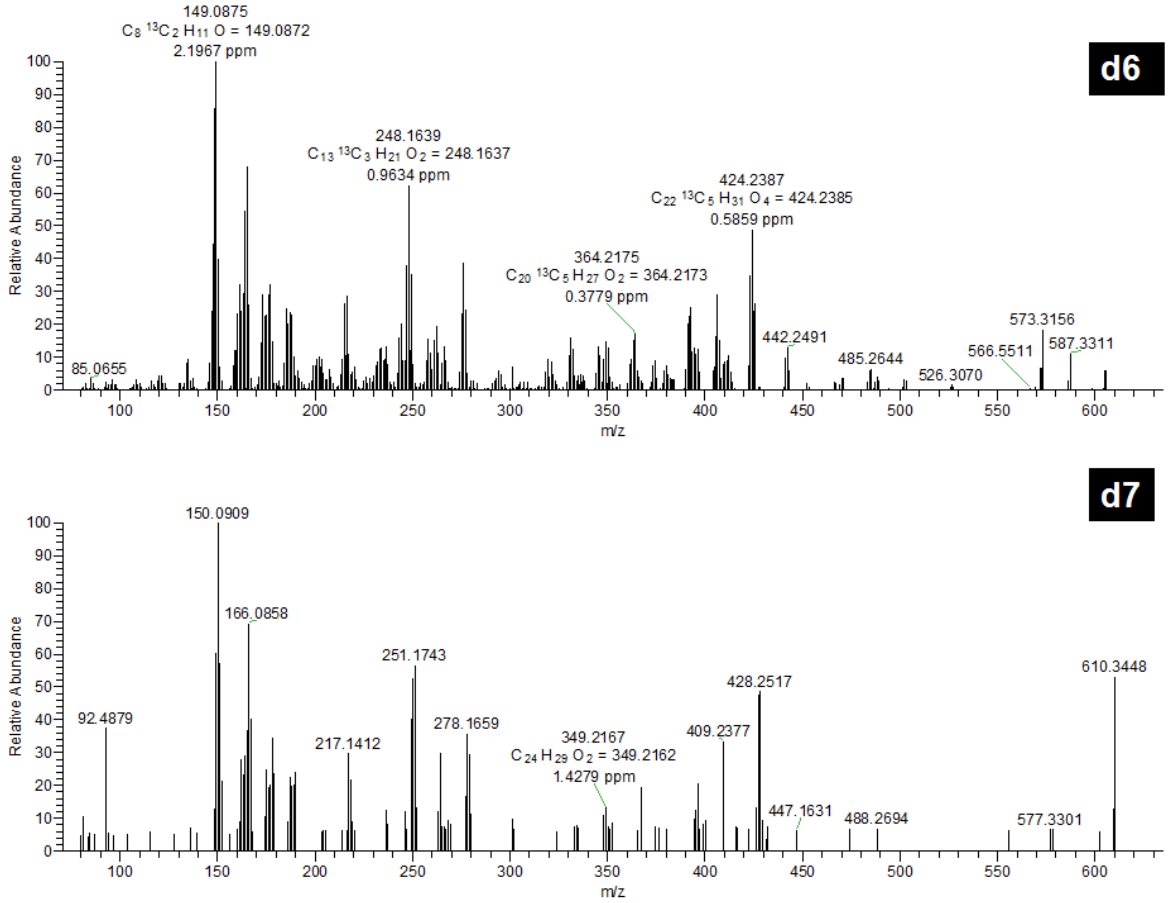

Figure 3C.5.2. Comparison of MS/MS spectra of the unlabeled and ^{13}C labeled limonoids from the neem cell suspension. (a1) azadirachtin A. azadirachtin isotopologues obtained through 1-^{13}C Glc labeling. (a2) *m/z* 707. (a3) *m/z* 713. azadirachtin isotopologues obtained through 1,6-^{13}C Glc labeling. (a4) *m/z* 710. (a5) *m/z* 717; azadirachtin isotopologues obtained through 2-^{13}C Glc labeling (a6) *m/z* 706; (a7) *m/z* 716. (b1) 6-deacetylnimbinene. 6-deacetylnimbinene isotopologues obtained through 1-^{13}C Glc labeling (b2) *m/z* 446. (b3) *m/z* 452. 6-deacetylnimbinene isotopologues obtained through 1,6-^{13}C Glc labeling. (b4) *m/z* 447. (b5) *m/z* 452. 6-deacetylnimbinene isotopologues obtained through 2-^{13}C Glc labeling. (b6) *m/z* 445. (b7) *m/z* 450. (c1) salannin. salannin isotopologues obtained through 1-^{13}C Glc labeling (c2) *m/z* 603. (c3) *m/z* 610. salannin isotopologues obtained through 1,6-^{13}C Glc labeling. (c4) *m/z* 605.(c5) *m/z* 615.salannin isotopologues obtained through 2-^{13}C Glc labeling (c6) *m/z* 603. (c7) *m/z* 608. (d1) salannolacetate. salannolacetate isotopologues obtained through 1-^{13}C Glc labeling (d2) *m/z* 607. (d3) *m/z* 611. salannolacetate isotopologues obtained through 1,6-^{13}C Glc labeling (d4) *m/z* 607. (d5) *m/z* 616. salannolacetate isotopologues obtained through 2-^{13}C Glc labeling (d6) *m/z* 605. (d7) *m/z* 610.

3D. References

1. C. Birkemeyer, A. Luedemann, C. Wagner, A. Erban and J. Kopka, *Trends Biotechnol.*, 2005, **23**, 28-33.
2. A. M. Zyakun, *J. Anal. Chem.*, 2011, **66**, 1243-1252.
3. W. Eisenreich, A. Bacher, D. Arigoni and F. Rohdich, *Cell. Mol. Life Sci.*, 2004, **61**, 1401-1426.
4. W. Eisenreich, F. Rohdich and A. Bacher, *Trends Plant Sci.*, 2001, **6**, 78-84.
5. W. Eisenreich, M. Schwarz, A. Cartayrade, D. Arigoni, M. H. Zenk and A. Bacher, *Chemistry & Biology*, 1998, **5**, R221-R233.
6. J.-L. Giner and B. Jaun, *Tet. Lett.*, 1998, **39**, 8021-8022.
7. J. F. Hoeffler, A. Hemmerlin, C. Grosdemange-Billiard, T. J. Bach and M. Rohmer, *Biochem. J.*, 2002, **366**, 573-583.
8. M. Rodriguez-Concepcion and A. Boronat, *Plant Physiol.*, 2002, **130**, 1079-1089.
9. M. Rohmer, *Pure Appl. Chem.*, 1999, **71**, 2279-2284.
10. M. Rohmer, *Pure Appl. Chem.*, 2003, **75**, 375-387.
11. G. Flesch and M. Rohmer, *Eur. J. Biochem.*, 1988, **175**, 405-411.
12. M. Rohmer, B. Sutter and H. Sahm, *J. Chem. Soc. Chem. Commun.*, 1989, 1471-1472.
13. M. Rohmer, M. Knani, P. Simonin, B. Sutter and H. Sahm, *Biochem. J.*, 1993, **295**, 517-524.
14. M. Rohmer, M. Seemann, S. Horbach, S. BringerMeyer and H. Sahm, *J. Am. Chem. Soc.*, 1996, **118**, 2564-2566.
15. M. Rohmer, *Nat. Prod. Rep.*, 1999, **16**, 565-574.
16. M. Rohmer, *Pure Appl. Chem.*, 2007, **79**, 739-751.
17. M. Rohmer, *Lipids*, 2008, **43**, 1095-1107.
18. L. M. Pena-Rodriguez, A. Yam-Puc, N. Knispel, N. Schramek, C. Huber, C. Grassberger, F. G. Ramirez-Torres, F. Escalante-Erosa, K. Garcia-Sosa, M. R. Hiebert-Giesbrecht, M. J. Chan-Bacab, G. Godoy-Hernandez, A. Bacher and W. Eisenreicht, *J. Org. Chem.*, 2014, **79**, 2864-2873.
19. P. Giavalisco, K. Kohl, J. Hummel, B. Seiwert and L. Willmitzer, *Anal. Chem.*, 2009, **81**, 6546-6551.
20. M. A. Farag, A. Porzel and L. A. Wessjohann, *Phytochemistry*, 2012, **76**, 60-72.
21. O. Potterat and M. Hamburger, *Nat. Prod. Rep.*, 2013, **30**, 546-564.
22. J. L. Wolfender, G. Marti, A. Thomas and S. Bertrand, *J. Chromatogr. A*, 2015, **1382**, 136-164.
23. A. K. Jarmusch and R. G. Cooks, *Nat. Prod. Rep.*, 2013, **31**, 730-738.
24. M. Hur, A. A. Campbell, M. Almeida-de-Macedo, L. Li, N. Ransom, A. Jose, M. Crispin, B. J. Nikolau and E. S. Wurtele, *Nat. Prod. Rep.*, 2013, **30**, 1569-1569.
25. J. W. Allwood and R. Goodacre, *Phytochem. Anal.*, 2009, **21**, 33-47.
26. P. Krishnan, N. J. Kruger and R. G. Ratcliffe, *J. Exp. Bot.*, 2005, **56**, 255-265.
27. J. Kopka, A. Fernie, W. Weckwerth, Y. Gibon and M. Stitt, *Genome Biol.*, 2004, **5**, 9.
28. L. W. Sumner, Z. Lei, B. J. Nikolau and K. Saito, *Nat. Prod. Rep.*, 2015, **32**, 212-229.
29. H. F. Wu, J. Guo, S. L. Chen, X. Liu, Y. Zhou, X. P. Zhang and X. D. Xu, *J. Pharm. Biomed. Anal.*, 2012, **72**, 267-291.
30. R. G. Ratcliffe and Y. Shachar-Hill, *Biol. Rev.*, 2005, **80**, 27-43.
31. A. Weissberg and S. Dagan, *Int. J. Mass Spectrom.*, 2011, **299**, 158-168.
32. A. Bouslimani, L. M. Sanchez, N. Garg and P. C. Dorrestein, *Nat. Prod. Rep.*, 2014, **31**, 718-729.
33. B. L. Milman, *Trac-Trends Anal. Chem.*, 2015, **69**, 24-33.
34. A. Fredenhagen, C. Derrien and E. Gassmann, *J. Nat. Prod.*, 2005, **68**, 385-391.
35. G. P. Aguiar, K. A. L. Wakabayashi, G. F. Luz, V. B. Oliveira, L. Mathias, I. J. C. Vieira, R. Braz Filho and A. E. M. Crotti, *Rapid Commun. Mass Spectrom.*, 2010, **24**, 295-308.

36. H. Awad, U. Das, J. Dimmock and A. El-Aneed, *Rapid Commun. Mass Spectrom.*, 2015, **29**, 1307-1316.
37. H. Budzikiewicz, J. M. Wilson and C. Djerassi, *J. Am. Chem. Soc.*, 1963, **85**, 3688-&.
38. B. Carey, M. J. F. Saez, B. Hamilton, J. O'Halloran, F. van Pelt and K. J. James, *Rapid Commun. Mass Spectrom.*, 2012, **26**, 1793-1802.
39. C. R. Cheng, M. Yang, Z. Y. Wu, Y. Wang, F. Zeng, W. Y. Wu, S. H. Guan and D. A. Guo, *Rapid Commun. Mass Spectrom.*, 2011, **25**, 1323-1335.
40. E. A. P. Ekanayaka, M. D. Celiz and A. D. Jones, *Plant Physiol.*, 2015, **167**, 1221-U1146.
41. C. Li, C. P. Huang, T. L. Lu, L. D. Wu, S. P. Deng, R. Y. Yang and J. Li, *Rapid Commun. Mass Spectrom.*, 2014, **28**, 2363-2370.
42. T. Madl, H. Sterk and M. Mittelbach, *J. Am. Soc. Mass Spectrom.*, 2006, **17**, 795-806.
43. L. R. Sartori, R. Vessecchi, H. U. Humpf, F. B. Da Costa and N. P. Lopes, *Rapid Commun. Mass Spectrom.*, 2014, **28**, 723-730.
44. S. Haldar, P. B. Phapale, S. P. Kolet and H. V. Thulasiram, *Anal. Methods*, 2013, **5**, 5386-5391.
45. S. Haldar, F. A. Mulani, T. Aarthy, D. S. Dandekar and H. V. Thulasiram, *J. Chromatogr. A*, 2014, **1366**, 1-14.
46. T. J. Bach, *Lipids*, 1995, **30**, 191-202.
47. H. K. Lichtenthaler, M. Rohmer and J. Schwender, *Physiol. Plant.*, 1997, **101**, 643-652.
48. J. Schwender, J. Zeidler, R. Groner, C. Muller, M. Focke, S. Braun, F. W. Lichtenthaler and H. K. Lichtenthaler, *FEBS Lett.*, 1997, **414**, 129-134.
49. H. K. Lichtenthaler, J. Schwender, A. Disch and M. Rohmer, *FEBS Lett*, 1997, **400**, 271-274.
50. H. K. Lichtenthaler, *Annu. Rev. Plant Physiol. Plant Mol. Biol.*, 1999, **50**, 47-65.
51. W. Eisenreich, B. Menhard, P. J. Hylands, M. H. Zenk and A. Bacher, *Proc. Natl. Acad. Sci. U S A*, 1996, **93**, 6431-6436.
52. Y. Yamazaki, M. Kitajima, M. Arita, H. Takayama, H. Sudo, M. Yamazaki, N. Aimi and K. Saito, *Plant Physiol.*, 2004, **134**, 161-170.
53. W. De-Eknamkul and B. Potduang, *Phytochemistry*, 2003, **62**, 389-398.
54. D. Kongduang, J. Wungsintaweekul and W. De-Eknamkul, *Tetrahedron Lett.*, 2008, **49**, 4067-4072.
55. N. Dudareva, S. Andersson, I. Orlova, N. Gatto, M. Reichelt, D. Rhodes, W. Boland and J. Gershenzon, *Proc. Natl. Acad. Sci. U S A*, 2005, **102**, 933-938.
56. D. Hampel, A. Mosandl and M. Wust, *Phytochemistry*, 2005, **66**, 305-311.
57. H. Kasahara, A. Hanada, T. Kuzuyama, M. Takagi, Y. Kamiya and S. Yamaguchi, *J. Biol. Chem.*, 2002, **277**, 45188-45194.
58. A. Hemmerlin, J. F. Hoeffler, O. Meyer, D. Tritsch, I. A. Kagan, C. Grosdemange-Billiard, M. Rohmer and T. J. Bach, *J. Biol. Chem.*, 2003, **278**, 26666-26676.
59. N. D. Chaurasiya, N. S. Sangwan, F. Sabir, L. Misra and R. S. Sangwan, *Plant Cell Rep.*, 2012, **31**, 1889-1897.
60. P. M. Dewick, in *Medicinal Natural Products*, John Wiley & Sons, Ltd, 2001, pp. 167-289.
61. Q. G. Tan and X. D. Luo, *Chem Rev.*, 2011, **112**, 2591-2591.
62. A. Pandreka, D. S. Dandekar, S. Haldar, V. Uttara, S. G. Vijayshree, F. A. Mulani, T. Aarthy and H. V. Thulasiram, *BMC Plant Biol.*, 2015, **15**, 1-14.
63. J. Lombard and D. Moreira, *Mol. Biol. Evol.*, 2011, **28**, 87-99.
64. A. R. Odom, *PLoS Pathog.*, 2011, **7**.
65. E. Vranova, D. Coman and W. Gruissem, *Mol. Plant*, 2012, **5**, 318-333.
66. J. Perez-Gil and M. Rodriguez-Concepcion, *Biochem. J.*, 2013, **452**, 19-25.
67. S. M. Trutko, L. V. Dorofeeva, V. A. Shcherbakova, N. A. Chuvil'skaya, K. S. Laurinavichus, V. I. Binyukov, D. N. Ostrovskii, M. Hintz, J. Wiesner, H. Jomaa and V. K. Akimenko, *Microbiology*, 2005, **74**, 153-158.

68. T. Kuzuyama, T. Shimizu, S. Takahashi and H. Seto, *Tet. Lett.*, 1998, **39**, 7913-7916.
69. J. C. Bede, P. E. A. Teal, W. G. Goodman and S. S. Tobe, *Plant Physiol.*, 2001, **127**, 584-593.
70. J. Zeidler and H. K. Lichtenthaler, *Planta*, 2001, **213**, 323-326.
71. O. Laule, A. Furholz, H. S. Chang, T. Zhu, X. Wang, P. B. Heifetz, W. Gruissem and B. M. Lange, *Proc. Natl. Acad. Sci. U S A*, 2003, **100**, 6866-6871.
72. Y. Yamazaki, M. Kitajima, M. Arita, H. Takayama, H. Sudo, M. Yamazaki, N. Aimi and K. Saito, *Plant Physiol.*, 2004, **134**, 161-170.
73. M. J. Towler and P. J. Weathers, *Plant Cell Rep.*, 2007, **26**, 2129-2136.
74. K. Skorupinska-Tudek, J. Poznanski, J. Wojcik, T. Bienkowski, I. Szostkiewicz, M. Zelman-Femiak, A. Bajda, T. Chojnacki, O. Olszowska, J. Grunler, O. Meyer, M. Rohmer, W. Danikiewicz and E. Swiezewska, *J. Biol. Chem.*, 2008, **283**, 21024-21035.
75. D. E. Cane, T. Rossi, A. M. Tillman and J. P. Pachlatko, *J. Am. Chem. Soc.*, 1981, **103**, 1838-1843.
76. W. Eisenreich, B. Menhard, P. J. Hylands, M. H. Zenk and A. Bacher, *Proc. Natl Acad. Sci. U S A*, 1996, **93**, 6431-6436.
77. W. Eisenreich, C. Rieder, C. Grammes, G. Hessler, K. P. Adam, H. Becker, D. Arigoni and A. Bacher, *J. Biol. Chem.*, 1999, **274**, 36312-36320.
78. M. Fellermeier, K. Kis, S. Sagner, U. Maier, A. Bacher and M. H. Zenk, *Tet. Lett.*, 1999, **40**, 2743-2746.
79. C. Rieder, B. Jaun and D. Arigoni, *Helvetica Chimica Acta*, 2000, **83**, 2504-2513.
80. D. Spiteller, A. Jux, J. Piel and W. Boland, *Phytochemistry*, 2002, **61**, 827-834.
81. R. Thiel and K. P. Adam, *Phytochemistry*, 2002, **59**, 269-274.
82. J. W. Yang and Y. Orihara, *Tetrahedron*, 2002, **58**, 1265-1270.
83. J. Wungsintaweekul and W. De-Eknamkul, *Tet. Lett.*, 2005, **46**, 2125-2128.
84. L. Kutrzeba, F. E. Dayan, J. Howell, J. Feng, J. L. Giner and J. K. Zjawlony, *Phytochemistry*, 2007, **68**, 1872-1881.
85. H. K. Lichtenthaler, *Photosynthesis Research*, 2007, **92**, 163-179.
86. K. Ohyama, M. Suzuki, J. Kikuchi, K. Saito and T. Muranaka, *Proc. Natl. Acad. Sci. U S A*, 2009, **106**, 725-730.
87. N. Srivastava and A. Akhila, *Phytochemistry*, 2010, **71**, 1298-1304.
88. S. R. Putra, L. M. Lois, N. Campos, A. Boronat and M. Rohmer, *Tet. Lett.*, 1998, **39**, 23-26.
89. T. Duvold, P. Calí, J.-M. Bravo and M. Rohmer, *Tet. Lett.*, 1997, **38**, 6181-6184.
90. H. Seto, H. Watanabe and K. Furihata, *Tet. Lett.*, 1996, **37**, 7979-7982.
91. C. Rieder, G. Strauss, G. Fuchs, D. Arigoni, A. Bacher and W. Eisenreich, *J. Biol. Chem.*, 1998, **273**, 18099-18108.
92. J. Schwender, M. Seemann, H. K. Lichtenthaler and M. Rohmer, *Biochem. J.*, 1996, **316**, 73-80.
93. A. Disch, J. Schwender, C. Muller, H. K. Lichtenthaler and M. Rohmer, *Biochem. J.*, 1998, **333**, 381-388.
94. H. K. Lichtenthaler, J. Schwender, A. Disch and M. Rohmer, *Febs Lett.*, 1997, **400**, 271-274.
95. J. Schwender, C. Gemunden and H. K. Lichtenthaler, *Planta*, 2001, **212**, 416-423.
96. F. Bouvier, A. Rahier and B. Camara, *Prog. Lipid Res.*, 2005, **44**, 357-429.
97. B. M. Lange, T. Rujan, W. Martin and R. Croteau, *Proc. Natl. Acad. Sci. U S A*, 2000, **97**, 13172-13177.
98. D. Tritsch, A. Hemmerlin, T. J. Bach and M. Rohmer, *FEBS Lett.*, 2010, **584**, 129-134.
99. D. J. McGarvey and R. Croteau, *Plant Cell*, 1995, **7**, 1015-1026.
100. J. D. Newman and J. Chappell, *Crit. Rev. Biochem. Mol. Biol.*, 1999, **34**, 95-106.
101. V. S. Dubey, R. Bhalla and R. Luthra, *Journal of Biosciences*, 2003, **28**, 637-646.
102. P. Pulido, C. Perello and M. Rodriguez-Concepcion, *Mol. Plant*, 2012, **5**, 964-967.

103. K. P. Adam, R. Thiel, J. Zapp and H. Becker, *Arch. Biochem. Biophys.*, 1998, **354**, 181-187.
104. Threlfal.Dr, Griffith.Wt and T. W. Goodwin, *Biochem. J.*, 1967, **103**, 831-&.
105. G. D. Braithwaite and T. W. Goodwin, *Biochem. J.*, 1960, **76**, 194-197.
106. J. M. Charlton, K. J. Treharne and T. W. Goodwin, *Biochem. J.*, 1967, **105**, 205-&.
107. T. W. Goodwin, *Biochem. J.*, 1958, **70**, 612-617.
108. A. R. Wellburn and F. A. Wellburn, *Ann. Bot.*, 1973, **37**, 11-19.
109. A. Bacher, C. Rieder, D. Eichinger, D. Arigoni, G. Fuchs and W. Eisenreich, *FEMS Microbiol. Rev.*, 1998, **22**, 567-598.
110. C. Birkemeyer, A. Luedemann, C. Wagner, A. Erban and J. Kopka, *Trends in Biotechnol.*, 2005, **23**, 28-33.
111. H. W. Groeneveld, *Crit. Rev. Biochem. Mol. Biol.*, 1999, **34**, 59-69.
112. H. N. Little and K. Bloch, *J. Biol. Chem.*, 1950, **183**, 33-46.
113. R. Zetterstrom, *Acta Paediatrica*, 2009, **98**, 1223-1227.
114. D. Arigoni, S. Sagner, C. Latzel, W. Eisenreich, A. Bacher and M. H. Zenk, *Proc. Natl Acad. Sci. U S A*, 1997, **94**, 10600-10605.
115. F. Luan and M. Wust, *Phytochemistry*, 2002, **60**, 451-459.
116. S. Sagner, C. Latzel, W. Eisenreich, A. Bacher and M. H. Zenk, *Chem. Comm.*, 1998, 221-222.
117. K. P. Adam and J. Zapp, *Phytochemistry*, 1998, **48**, 953-959.
118. J. A. Bick and B. M. Lange, *Arch. Biochem. Biophys.*, 2003, **415**, 146-154.
119. W. Knoss, B. Reuter and J. Zapp, *Biochem. J.*, 1997, **326**, 449-454.
120. D. Kongduang, J. Wungsintaweekul and W. De-Eknamkul, *Tet. Lett.*, 2008, **49**, 4067-4072.
121. B. Heasley, *Eur. J. Org. Chem.*, 2011, 19-46.
122. A. Thierry, M. B. Maillard and M. Yvon, *Appl. Environ. Microbiol.*, 2002, **68**, 608-615.

Chapter 4

Study of contribution of MVA and MEP pathway for limonoid formation and cloning of putative genes

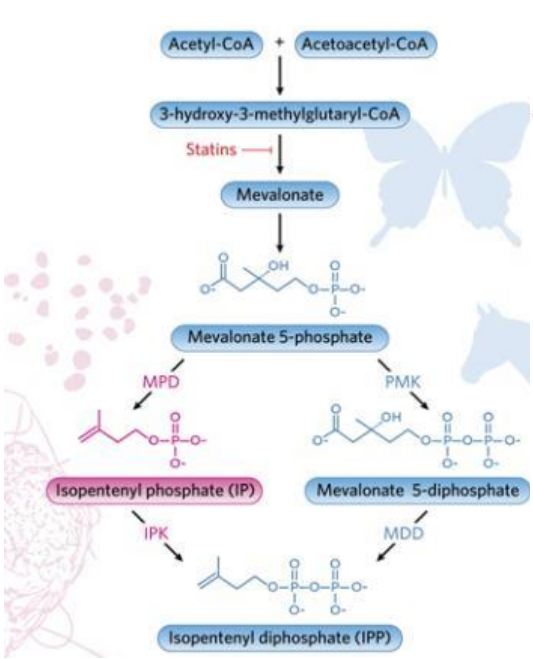

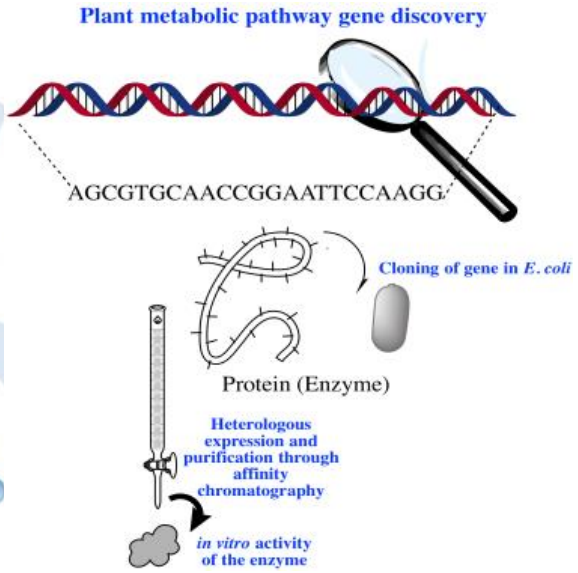

Chapter 4: Section A

Study of the contribution of MVA and MEP pathway for limonoid formation through inhibitor study and expression analysis

4A.1. Introduction

To interrogate the role of a metabolic pathway towards its contribution into another pathway, or role of an intermediate in a pathway, generation of gene mutant strains are essential. Alternatively, use of chemical inhibitors specific to a single biocatalysis step in a pathway help to study the functional contribution of a pathway. Further, use of pathway specific stable isotope intermediates, helps to study the complementation of the pathway for the biosynthesis of a metabolite[1-3]. Isoprene units of isoprenoids are biosynthesized through two different pathways; mevalonate (MVA) pathway and MEP pathway[4-11]. The contribution of one pathway towards a formation of isoprenoid natural product can be studied through chemical inhibition [1-3]and subsequent stable isotope labeling approach[12-15].

Ascomycete species in the rhizosphere, like *Aspergillus terreus*, ubiquitously produce HMGR inhibitors such as mevinolin also called as lovastatin, whose potential to inhibit MVA production was known already over decades and has been used to study isoprenoid biosynthesis[16]. It is also used as a cholesterol-lowering agent in mammalian system[16] and also shown to have effect on cell cycle[17]. Similiarly, 2-C-methyl-D-erythritol 4-phosphate, the reaction intermediate of MEP pathway is mimicked by fosmidomycin[18], hence it inhibits deoxy-xyulose phosphate reductoisomerase[19], the key enzyme involved in non-mevalonate pathway of terpenoid biosynthesis[20, 21]. Hence, use of these chemical inhibitors helps to study the role and contribution of isoprene biosynthetic pathways towards the formation of different isoprenoids[1, 3, 21-25] (Figure 4A.1). For example, azole drugs are found to target cytochrome P450 enzymes and down-stream enzymes of sterol biosynthetic pathway. Miconazole, clotrimazole, fucanazole etc. are some of the anti-fungal and chemotherapeutic agents used in medicine[26]. Miconazole is a N-substituted imidazole which is hypothesized to act by binding to the heterocyclic nitrogen of ferric protoheme of cytochrome P450 enzyme[22].
Tracing study with stable isotopes has helped in the identification of role of MVA pathway towards limonoid biosynthesis. In the section A of the chapter, the isotope labeling experiments were carried out subsequent to the inhibition of isoprenoid biosynthetic pathways to study the complementation of MVA and MEP pathways for the biosynthesis of limonoids in neem cell culture. Role of miconazole (Figure 4A.2) on the effect of limonoid biosynthetic pathway has also been studied.

Spatial expression levels of genes involved in the rate-limiting step of the MVA and MEP pathways were studied in different tissues of neem tree. Rate-limiting enzyme of MVA pathway is 3-hydroxy-3-methyl-glutaryl-coenzyme A reductase (HMGR), catalyzing the third step of the pathway for the formation of mevalonate from 3-hydroxy-3-methyl-glutaryl-coenzyme A[27]. Whereas in MEP pathway, rate limiting is the first step of the pathway, catalysed by deoxyxylulose-5-phosphate synthase (DXS)[28]. It catalyzes the formation of 1-Deoxy-D-xylulose 5-phosphate (DXP) from pyruvate and D-glyceraldehyde 3-phosphate through transketolase-type condensation reaction[28]. DXS controls the flux through the pathway and overexpression of it have proved the increase in production of isoprenoid end products[29]. To further comprehend their regulatory roles during the inhibition of MVA pathway, the expression level of the same genes were examined through quantitative polymerase chain reaction (qPCR) experiments.

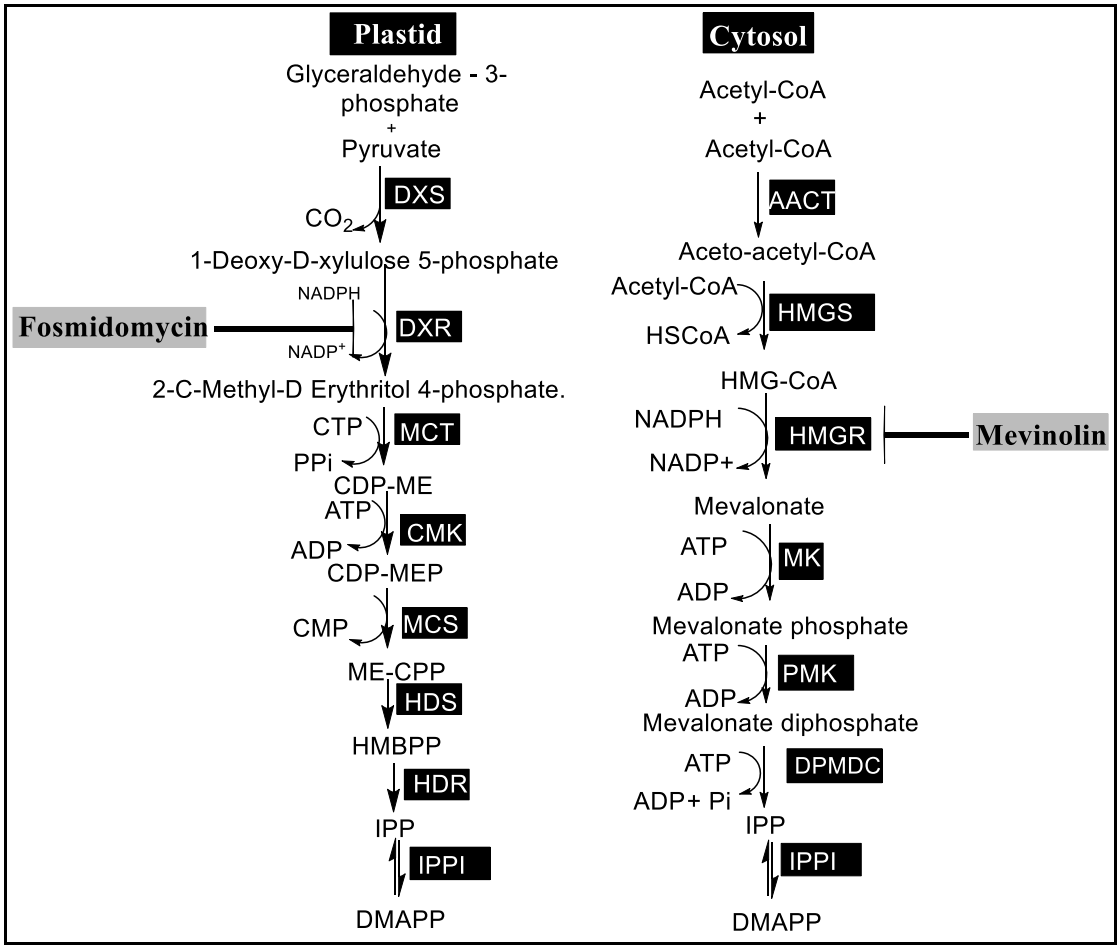

Figure 4A.1. Use of specific pathway inhibitors to study the role of MVA and MEP pathway towards the formation of isoprene unit for a metabolite.

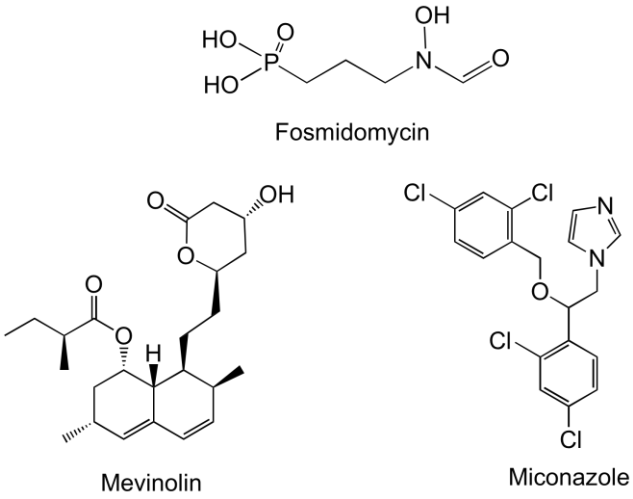

Figure 4A.2. Structure of pathway inhibitors used in this study

4A.2. Results and discussion

4A.2.1 Evaluation of contribution from MVA and MEP pathway for limonoid biosynthesis

4A.2.1.1. Inhibition of MVA pathway with mevinolin

In order to establish the role of MVA and MEP pathways in limonoid biosynthesis, pathway specific chemical inhibition studies were carried out. When suspension cultures were treated with MVA pathway specific inhibitor, mevinolin, it affected both the growth and limonoid content simultaneously in all the concentrations such as 0.05 mM, 0.1 mM, 0.5 mM, and 1 mM (Figure 4A.3 and Figure 4A.4).

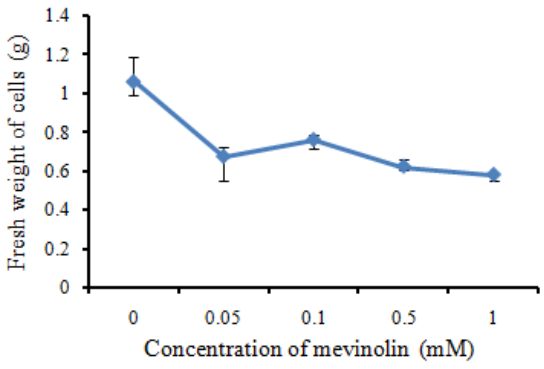

Figure 4A. 3. Effect of inhibitor, mevinolin on growth of cells at different concentrations.

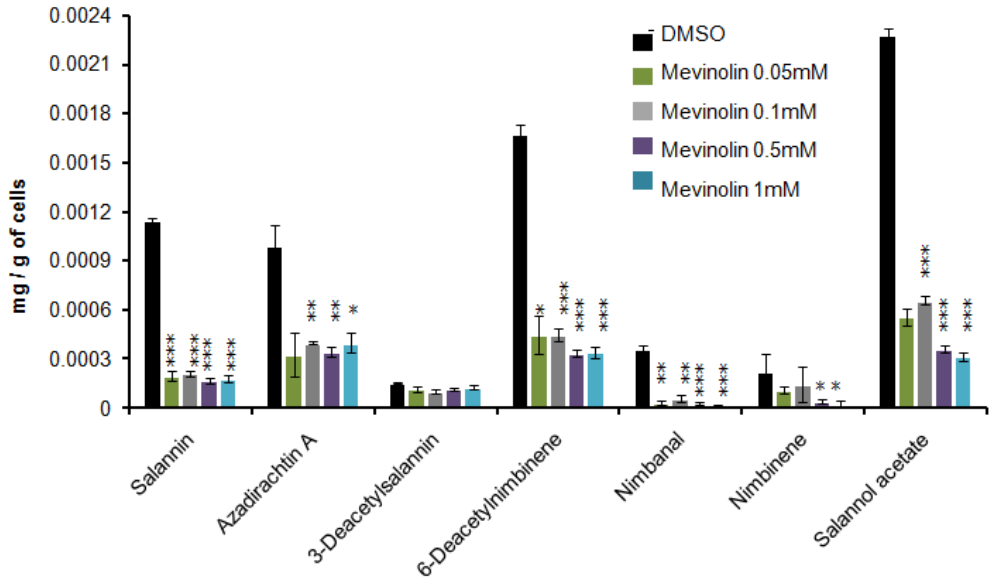

Figure 4A. 4. Effect of different concentrations of mevinolin on limonoid biosynthesis.

4A.2.1.2. Inhibition with miconozole

Miconazole, the inhibitor of cytochrome enzymes affects the growth of cells relatively higher to that of mevinolin at higher doses, 0.5 and 1 mM concentration (Figure 4A.5). The limonoid biosynthesis is also severely affected with miconazole from 0.1 mM concentration and above. The concentration of limonoids biosynthesized is comparatively less in miconazole treated cells to that of the one with mevinolin (Figure 4A.4, Figure 4A.6).

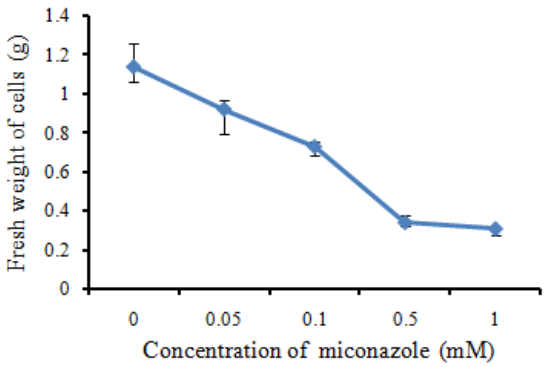

Figure 4A. 5. Effect of inhibitor, miconazole on growth of cells at different concentrations.

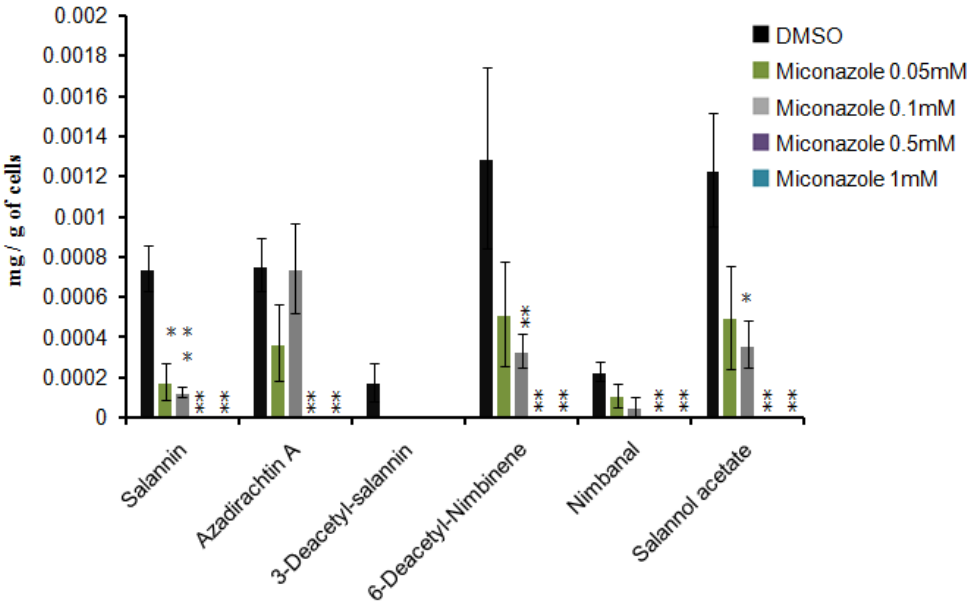

Figure 4A. 6. Effect of different concentrations of miconazole on limonoid biosynthesis

4A.2.1.3. Inhibition of MEP pathway with Fosmidomycin

Cells grown in the presence of the inhibitor fosmidomycin was analyzed for its carotenoid contents. When 0.1 mM fosmidomycin was used to inhibit MEP pathway from the formation of isoprene units, the levels of total carotenoid content was decreased by 78.8% as compared to that of control (Figure 4A.7). Further, the suspension culture showed blanching during the course of exponential growth of the cells in presence of fosmidomycin (Figure 4A.7).

The inhibition studies were also carried out using both inhibitors individually in presence of unlabeled glucose (Glc) and [1,2-^{13}C] Glc. Fosmidomycin treatment didn't interfere with the biosynthesis of limonoids as evidenced from the formation of ^{13}C limonoid isotopologues whereas in case of inhibition of MVA pathway with mevinolin, drastic decrease in the levels of ^{13}C isotopologues was observed (Figure 4A.8). *Ex vivo* labeling studies carried out with ^{13}C labeled glucose gives proof of evidence that MVA pathway contributes for the isoprene units of limonoid skeleton and further, inhibitor treatment combined with [1,2-^{13}C] Glc labeling experiment shows that blocking the MEP pathway doesn't have any impact on the limonoid biosynthesis. The blanching of

cells due to drop in carotenoids during fosmidomycin inhibition was consistent with the leaf bleaching observed in *Arabidopsis* seedling[1].

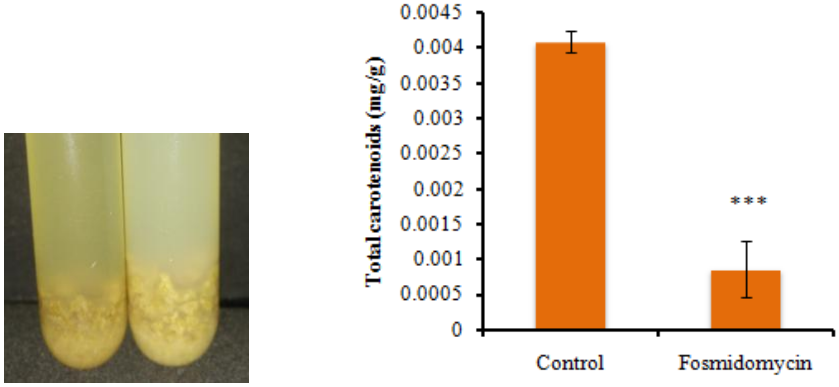

Figure 4A.7. (Left panel) control vs. fosmidomycin treatment (0.1 mM) demonstrating the blanching of color of cell suspension due to drop in carotenoid level: (Right panel) Effect of 0.1 mM fosmidomycin on MEP pathway metabolites: carotenoids

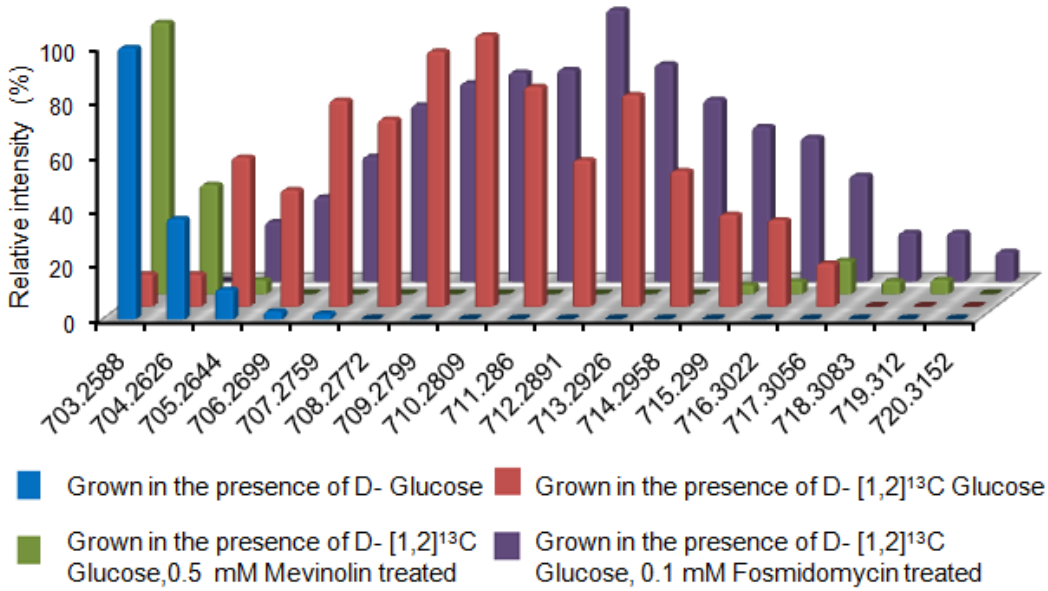

Figure 4A. 8. Chemically inhibited MVA and MEP pathway cells grown in the presence of [1,2-^{13}C] Glc to monitor the formation of isotopologues.

4A.2.2. Expression profiling of genes involved in rate limiting step of MVA and MEP pathway

The spatial expression of the genes encoding the rate-limiting enzymes involved in MVA and MEP pathway were studied in different neem tissues such as pericarp and kernel of fruit, leaf, flower, suspension and callus derived from kernel so as to correlate their transcript level to the limonoid biosynthesis. Two transcripts for HMGR and 4 for DXS from MVA and MEP pathway respectively were identified from the neem transcriptome[30] and the real-time analysis for all the 6 sequences were performed to determine their expression profile (Figure 4A.9). Even though all the isoforms of HMGR and DXS are expressed, the relative expression of HMGR2 was predominant in all the tissues studied, with the exception of flower (Figure 4A.9). In kernel and pericarp, the expression of DXS transcripts was very low when compared to the HMGR levels. This substantiates the results of ^{13}C labeling and inhibitor studies giving proof that MVA pathway plays a major role in limonoid biosynthesis. We also compared the transcript abundance of each gene in different tissues studied (Figure 4A.11). Among the DXS isoforms, DXS1 and DXS3, showed higher level of expression in the leaf tissue whereas, DXS4 level was slightly higher in suspension culture when compared to the leaf tissue. DXS2 and HMGR1 showed comparatively very high level of expression in flower among the tissues studied. The level of expression of HMGR2 was high in kernel and suspension cells relative to the other tissues (Figure 4A.11). Further, to study the effect of pharmacological block of MVA pathway by inhibitor, mevinolin on the transcript level, the real-time PCR profiling was carried out with mevinolin treated neem suspension cells. In comparison to control, the expression profile showed that the relative expression levels of all the seven studied genes of inhibitor-treated cells were comparatively reduced (Figure 4A.10).

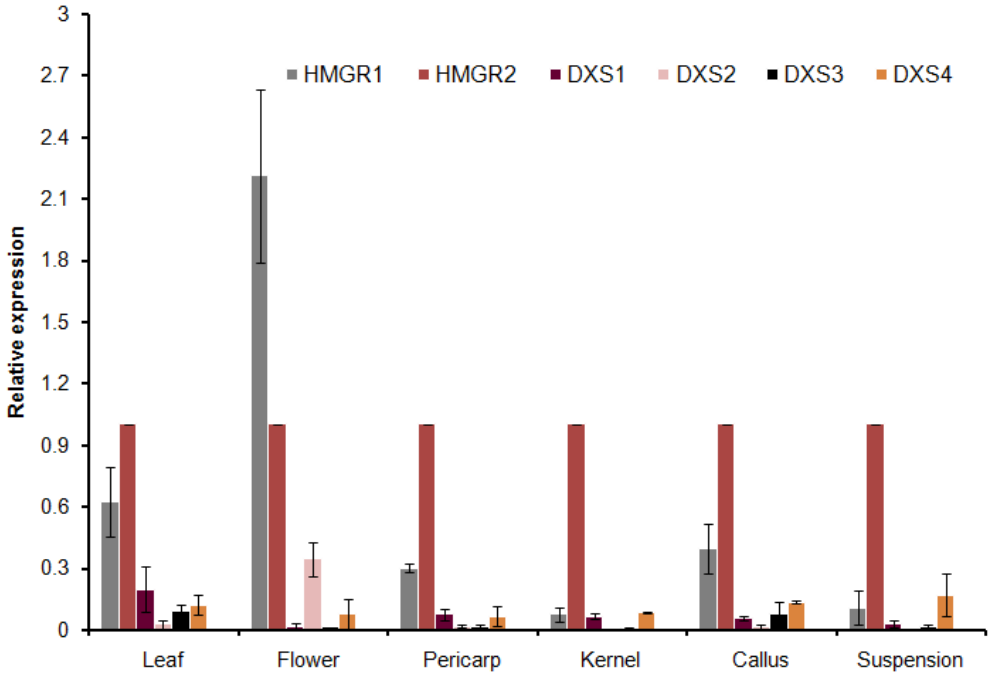

Figure 4A.9. Expression profile of HMGR and DXS genes in various tissues relative to the expression of HMGR2

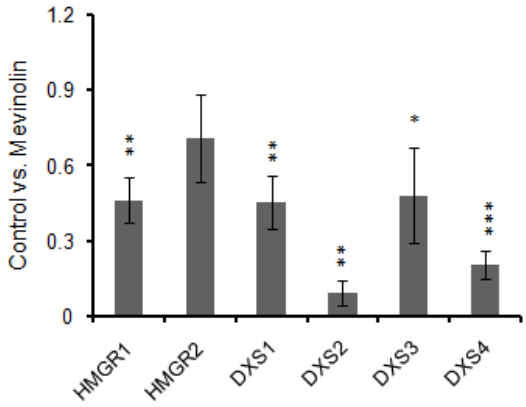

Figure 4A.10. Comparison of expression profile of the studied genes in mevinolin treated cells with respect to control.

Spatial expression profile of genes encoding for the rate-limiting step of isoprene biosynthetic pathway shows that HMGR relative expression level being the highest when compared to MEP pathway genes in all the tissues and cells studied, further bolstering the finding that mevalonate pathway contributes for the isoprene units of limonoid skeleton (Figure 4A.9). Though blocking of MVA pathway at 0.05 mM mevinolin concentration does not affect the growth significantly, the metabolic process of cell and limonoid biosynthesis were decreased, which is also evident from the

marginal reduction in transcript level of HMGR and DXS genes, the rate-limiting steps of both the pathways. Miconazole, the inhibitor of cytochrome enzymes, severely affected limonoid biosynthesis in cell suspension culture when compared to mevinolin (Figure 4A.4, Figure 4A.6), which signifies the fact that cytochrome P450 enzymes play a major role in the limonoid biosynthetic pathway, as most of the downstream steps in the pathway are subsequent oxidation and reduction reactions.

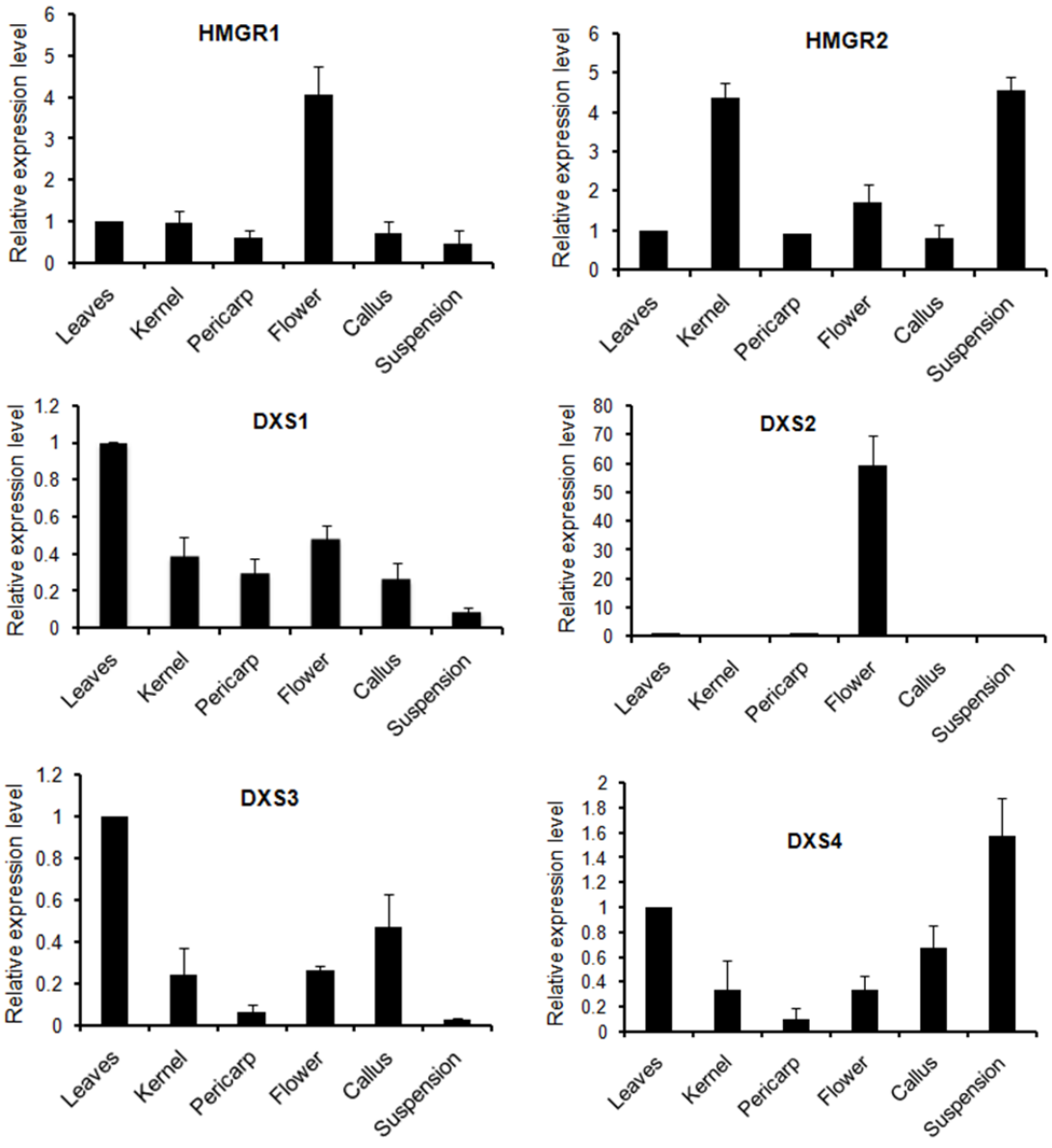

Figure 4A.11. Relative expression level of genes of MVA and MEP pathway encoding for the rate limiting enzymes in different neem tissues. HMGR, 3-hydroxy-3-methyl-glutaryl-coenzyme A reductase; DXS, 1-deoxy-D-xylulose-5-phosphate

4A.3. Conclusion

In the previous chapter, analyses of labeled limonoid extract lead to the identification of signature isoprenoid units involved in azadirachtin and other limonoid biosynthesis, which are found to be formed through mevalonate pathway. This was further confirmed by treatment of cell suspension with mevinolin, a specific inhibitor for MVA pathway, which resulted in drastic decrease in limonoid levels whereas their biosynthesis was unaffected with fosmidomycin mediated plastidial methylerythritol 4-phosphate (MEP) pathway inhibition. This was also conspicuous, as the expression level of genes encoding for the rate-limiting enzyme of MVA pathway, 3-hydroxy-3-methyl-glutaryl-coenzyme A reductase (HMGR) was comparatively higher to that of deoxyxylulose-phosphate synthase (DXS) of MEP pathway in different tissues and also in the *in vitro* grown cells.

4A.4. Materials and methods

4A.4.1. Inhibitor Studies

Mevinolin and fosmidomycin (Sigma) were solubilized in DMSO and water respectively, filter sterilized using membrane filter of 0.22 μm pore size (Millipore) and introduced into culture under aseptic conditions. The inhibitor of cytochrome, miconazole was added to the neem suspension cultures at different concentrations along with control for each treatment containing the same solvent in which inhibitors are dissolved. Suspension cultures were treated in triplicates with mevinolin and miconazole at different concentrations such as 0, 0.05, 0.1, 0.5 and 1 mM. Quantification of biomass of cells was done by determining the fresh weight of cells by centrifugation in swinging bucket at 1000 × *g* (Thermofisher Scientific).

Mevinolin (final concentration 0.05 mM) and fosmidomycin (final concentration 0.1 mM) were added to the cell suspension culture after 2 days of initiation of culture after replacing the cells with fresh media containing no sugars. 3% D-[1,2-^{13}C] Glc (99% enriched, Cambridge Isotope Lab. Inc., Andover, MA) was supplemented to the 5 mL culture after inhibitor treatment. Two independent experiments were performed each in duplicates. Limonoid extraction was carried out from the cells after ten days of fosmidomycin addition. To further analyze the total carotenoid content, the cells were

frozen in liquid nitrogen, made into fine powder and extracted with acetone in the dark. The extract was centrifuged to remove debris and concentrated to the volume of 3 mL. It was read spectrometrically at 470 nm and the total carotenoid contents were calculated using equation as follows, (described by Lichtenthaler[31]).

$$C_a = 11.24\ A_{661.6} - 2.04\ A_{644.8}$$

$$C_b = 20.13\ A_{644.8} - 4.19\ A_{661.6}$$

$$C_a+C_b = 7.05\ A_{661.6} + 18.09\ A_{644.8}$$

$$C_x+C = 1000\ A_{470} - 1.9\ C_a - 63.14\ C_b\ /\ 214$$

4A.4.2. HRMS Analysis

Analysis of neem limonoids was performed with Thermo Scientific QExactive™ hybrid quadrupole-Orbitrap mass spectrometer associated with Accela 1250 pump and Accela open AS. The conditions of HESI source include capillary temperature of 320 °C, Heater temperature at 350 °C, s-lens RF level of 50, spray voltage of 3.6 kV, spray current of 0.9 μA with sheath gas flow rate of 41, auxiliary gas flow rate of 9 and sweep gas flow rate of 3. Standards as well as the extracted samples were analyzed in positive ionization mode, in full MS-scan with scan range of 100 to 1000 *m/z*. Following were the properties of the scan performed- resolution 70,000, AGC target 1e6, Maximum IT 200 ms. Waters Acquity UPLC BEH C_{18} column (particle size 1.7 μm, 2.1 X 100 mm) was used as the stationary phase while the solvent system of methanol and water containing 0.1% formic acid served as the mobile phase. The gradient started with 40% methanol (5 min isocratic), it was then increased to 50% (5 min isocratic), followed by 60% methanol for the next 15 minutes and over the next 4 minutes it was isocratic with 65% methanol. It was then increased to 90% methanol for 4 minutes. For the last 2 minutes, it was isocratic with 40% methanol. Constant flow rate of 0.3 $mLmin^{-1}$ was maintained throughout the run time of 35 min. The chromatograms and mass spectral data were processed by Xcalibur qual browser (version 2.3; Thermo Scientific).

4A.4.3. Quantitative PCR studies

For quantitative PCR analysis, RNA isolation was carried out using Spectrum™ plant total RNA isolation kit (Sigma) from neem callus, suspension, leaf, flower, pericarp, kernel tissues and also from 0.05 mM mevinolin treated suspension cells. RNA

isolation was followed by DNase treatment by using DNase I Amplification Grade kit (Sigma). cDNA was synthesized using SuperScript® III First-Strand Synthesis System (Invitrogen) from 3 μg of total RNA. Through transcriptome analysis, we could identify two ORFs encoding for HMGCoA reductase (HMGR) and 4 for deoxyxylulose-phosphate synthase (DXS), the enzyme involved in the catalysis of rate-limiting step in MVA and MEP pathway respectively[30]. qPCR primers were designed for the above 6 transcripts along with the housekeeping genes, elongation initiation factor 4a (ELF4A) and actin (adopted from Rajakani *et al*[32]) for normalization (Table 1). Real-time PCR was carried out in AriaMx Realtime PCR system (Agilent Technologies) by using FastStart Universal SYBR Green Master (Roche). The cycling conditions comprised of initial denaturation at 95 °C for 5 min followed by 40 amplification cycles consisting of 95 °C for 15 s and 58 °C for 30 s. All reactions were performed in triplicate assays for 3 biological replicates and relative quantifications were performed using $\Delta\Delta C_T$ method. The two housekeeping genes gave same level of expression and the results were normalized with ELF4A.

Gene name	**Forward primer (5′–3′)**	**Reverse primer (5′–3′)**	**Amplicon**
Actin	AGGCATCCACGAGACCACTT	TGGCGCTAGAGCAGAAATTTC	151 bp
EF4a	AACCAGTGTTCGTGAAGACCAA	AAGCATTTCATCCGCCTCAT	151 bp
HMGR1	GGAAGCCGTCAATGATGGGA	ATTCAGGCACGCAGACTGAG	112 bp
HMGR2	TACTGCCATCTACTTAGCCACCG	CCCAACTGTGCCAACCTCAATAGA	145 bp
DXS1	ATGGTTGCCACTGCTGCCAG	CTCTACAAGAACTTTCCCTTTTCCAATCTC	135 bp
DXS2	AGAGAAATGGAGCGTGGTTCA	TAAGTCTAGGTCCTGCGGCTGG	145 bp
DXS3	TGACTGGGAGAAGAGATAAGATGC	CAGCAGAAATAGTGGTAGAACTGT	126 bp
DXS4	CAATGGGAGGTGGCACTGGTC	TGGCTTGAGACCTTCCGTAGC	128 bp

Table 4A.1. List of primers used in this study for real time PCR analysis.

4A.4.4. Statistical analysis

Asterisks on the tops of bar denotes the values that were determined by Student's t-test using Microsoft Office Excel 2007. They were found to be significantly different from their respective controls (*, **, ***, indicate $p < 0.05$, 0.01 and 0.001, respectively).

4A.5. Appendix

>Master_Control_18493_HMGR1

GATTCCGGTGGGAATTGCGGGGCCGTTATTGCTTG**ATG**GTTTTGAATATTCTGTGCC
GATGGCGACGACTGAAGGGTGTTTGGTCGCCAGTACTAATAGAGGCTGTAAGGCGA
TCTATGCGTCTGGCGGCGCCACCAGTATGTTGCTGAAAGATGGGATGACGAGAGCG
CCCGTTGTGAGGTTTTCAACTGCTAAGAGAGCTTCTGAATTGAAGTTCTTCTTGGAG
GACTCAGATAATCGCGAAACTTTGTCCGTTGTCTTTAACAGGTCGAGTAGATTTGCG
AGGCTGCAACACATTCAGTGCTCTATTGCCGGGAAGAATCTTTTCATCAGATTTAGC
TGTAGCACAGGTGATGCAATGGGAATGAACATGGTTTCCAAAGGAGTTCAGAATGT
GCTGGAATTCCTTCAAAATGATTTCCCTGACATGGAAGTTATTGGAATATCTGGAAA
CTTTTGTTCGGACAAGAAACCGGCTGCTGTGAATTGGATAGAAGGGCGTGGCAAAT
CAGTGGTGTGTGAGGCAACAATCAAAGAAGAGGTGGTAAAGAAGGTGTTGAAAAC
CAACGTGTCTACTCTGGTTGAACTCAACATGCTCAAGAACCTCACCGGCTCTGCCAT
TGCTGGTTCCCTTGGTGGATTCAATGCCCATGCTGCCAACATTGTCTCTGCAATCTTC
ATTGCCACCGGCCAGGATCCAGCGCAAAATGTTGAGAGTTCTCACTGCATTACCATG
ATGGAAGCCGTCAATGATGGGAAGGATCTGCATATGTCTGTTACTATGCCATCCATA
GAGGTGGGTACAGTTGGAGGCGGGACTCAACTCGCATCTCAGTCTGCGTGCCTGAA
TTTGTTAGGTGTGAAGGGTGCAAACAAAGAGTCACCGGGATCAAATTCAAGGCACT
TGGCAACAATTGTAGCCGGTTCTGTTCTGGCAGCAGAACTCTCCCTGATGTCTGCCA
TAGCAGCTGGTCAGCTTGTCAATAGTCACATGAAATACAACAGGTCCACCAAAGAG
ATATGCACATCTGCATCA**TAG**ATGGTGAGGTGGAGCCACCAATTTAATCAAATTAG
AAATAAAAATTAAGTGAAGGATAGACATATAAATTAGGCAAAGGAAGAAAGCTAT
AAAAAGGGGGGGAAAAAAAAGTGAAAGCTGTTGGGCGCCAACATGGAATTTACTA
CTTCTTAACTTCTGAGGCCGTAAAGTTAGCGAATTTGAATCACAATGTGGCTAGCTG
TTCTGGTCCTAAGTCCTTCAGCATATCTATATCTCCAATGGCATCTTCTCGCAACAAG
GGTGTAGAAAGGGCCCCAATTTCGAATAATTAGGACTTTGCCTGGTTTGTGCTTGTG
TTTGTGTGTCCTACTTGTGAAATTTTTATCTGTCCTTTCGTCTTTTTAGTAGTTGTTAT
TACATGTTTAGTGGCTGTTATATGTTTGTAGCTGGGGACTGGAGTCTTTTGATCGGTT
CTCTGTCTTTTTATTTTGTCTTTTCTGTATACAAGATTGTGACCTTCCTCCGAATTGAT
TTGGATAGTAGTCCTAGTTTTATGGTATGTAATTAAATTATTTTCAGCTGTTTCATGT
GAGATTGTGTTCTGGCTTTTTATTTATATTTATAGTTATCGATGATAATTCTTCTGTTT
TTTTTTTGTTCATCAAGTATTACTAACTGATAATTCTTAATCACGTCGTGAGAGTGGC
TTTCTCTCAACAATGGAGAAAGCACTGCTTTTATATTTGCTACTTGATAG

>Master_Control_9263_HMGR2

CCCATCACATGCCTCCATTGAAATACACCCCCCCCACCCAAAAGAAAAAAAAAATTA
AAAAAAAATTAAAAAACAAAACCCCCTATAATACTCGAAAATTTACATTTTTCTCTC
CGCCGTCTGATCCGCCGCCGGCGAGACAACTACCACCACCAGA**ATG**GAGGCCCGTC
GGCGATCAATGGCCAAGCCTATCCATGCCAAATCCATTGATGACGAAACAAACGCC
AAAACGCAGTCAGATTCGCTGCCGCTTCCTTTGTATATAGTAAATGCTGTGTTTTTTA

CTCTCTTTTTCACCGTCGTTTACTATTTGCTTTCTCGTTGGCGTGAGAAGATTCGTAA
CTCCACGCCGTTACACGTCGTTACGCTTTCCGAAATGGGGGCGATTCTGGCGTTCGT
TGCTTCTTGTATTTATCTCTTGGGTTTCTTTGGCATCGATTTTGTTCAGTCTATTCTCC
GTCCCTCTGCTGACGTCTGGGCTTCCGAAGAAGAGGAGGACGATTCCCGCCTCATGC
TTAAGGAAGATTCCCGGAAATTACCCTGTGGTCAAGCCCTAGATTGCTCTACTGTCA
TCACTCCGTCGCCCCCGCCACTGCTACAGCCTAAAGCTGCGAAATTGATTGATCATG
ATCCCAATACGGTCTCCTTTACTACCGAAGCTGATGAAGACATTATAAAGTCTGTGG
TTGATGGTACGACGCCGTCTTATTCTCTGGAAACAAAATTGGGGGATTGCAGGCGG
GCTGCTGCGATTAGGCGGGAGGCGTTACAGAGAATGACCGGAATGTCTTTGTTGGG
CTTGCCCTTGGAGGGTTTTGATTACGAGTCAATTTTGGGACAGTGTTGCGAGATGCC
AGTTGGATATGTGCAGATTCCGGTGGGAATTGCGGGGCCTTTGTTGCTTGACGGAAG
GGAGTATTCAGTTCCGATGGCGACGACCGAAGGTTGCCTGGTGGCAAGTACTAATA
GGGGTTGTAAAGCTATTCATTTGTCCGGTGGAGCTACGAGTGTTTTGTTGAAAGATG
GAATGACCAGAGCTCCTGTCGTTAGATTTGGAACTGCTAAAAGAGCTGCTGATCTG
AAGTTATTCTTGGAGAATCCTGCAAATTTCGACACGATATCTGTGGTTTTTAACAAA
TCAAGCAGATTTGGAAGACTTCAAAGCATCAAATGTGCAATTGCTGGTAAGAATCT
CTACTTGAGATTTTGTTGCAGCACAGGTGATGCTATGGGGATGAACATGGTTTCCAA
GGGGGTCCAGAATGTTTTGGATTTCCTTCAGGATGAGTTCTCCGACATGGAAGTCAT
CGGCATTTCTGGTAATTTCTGTTCGGATAAAAAGCCTGCAGCTGTAAACTGGATTGA
AGGACGGGGCAAATCTGTGGTTAGTGAGGCCATAATTAAGGGTGATGTTGTGAGGA
AGGTATTGAAGACAAATGTGGAAGCCTTGGTGGAGCTGAACATGCTCAAGAACCTT
ACTGGTTCTGCTATGGCTGGAGCTCTTGGTGGCTTTAATGCCCATGCCAGTAACATT
GTTACTGCCATCTACTTAGCCACCGGCCAAGATCCTGCGCAAAACGTGGAGAGTTCT
CACTGTATCACAATGATGGAAGCCGTTAATGATGGCAAGGACCTTCACATTTCTGTA
ACAATGCCTTCTATTGAGGTTGGCACAGTTGGGGGCGGCACCCAGCTTGCATCTCAG
TCAGCATGTTTGAACCTTCTTGGGGTTAAAGGTGCCAGAAAAGAGTCACCTGGAGC
AAACGCAAGGCTACTTGCCACCATTGTTGCTGGTTCTGTTCTAGCTGGAGAGTTATC
TCTCATGTCTGCTCTAGCAGCTGGACAGCTTGTTAGGAGTCACA**TGA**AGTACAATAG
ATCAAGCAGGGATGTTACCAAGGCCACATGAAAAACGTTGTGGTACAGGAAGTCCA
TAAAGATGCAAAATAACTGAGTAGTTGAATTTCAATTAGGATTGGAAGAACAACGA
ATGAATACACCTTCTCTCTTTCCTTTTATTTTTATTTTTTCGGTTCTCTCTTTCCAAGT
CTAAGCCTTTGTAATCTGCAAATTCTGTATAATGGCCAAAAAGTTTAATGCATTTCT
TTTCAAAATCTCTAGACGTCAGAGCCAGTGTTGAATTTATTGTATCACTAATCAATC
AATCAATCAATCAAT

>Master_Control_80593_DXS1
ATGGCTTTGAATTTGCTATCTCCAGCTGAAATCAAGGCTATTTCCTTCTTGGATACTG
CCAGGTCCAATCACCGCCTTCCGAAGCTTTCAGGTGGCTTCTCTTTGAAGAGGAAGG
ATGGTGGAACTTCATTTGGCAGAATACTTCAATGTTCTGCTCAGGCACCTCCTTCAG
CATGGCCAGGCCGAGCTGTTCTAGAGCCAGGTCAGAAGACTTGGGATGGTCCAAAG
CCAATCTCAATTGTTGGATCAACTGGTTCCATTGGAACTCAGACATTAGACATAATT
GCAGAGCATCCAGATAGATTCAGAGTTGTGGCACTAGCAGCTGGTTCAAATGTAAC
TCTTCTTGCTGATCAGGTGAAGAGATTCAAACCTCAACTGGTTGCTGTTAGAAATGA
GTCACTACTTGATGAACTGAAGGAGGCTTTGGCAAATGTTGAACAACAGCCCGAGA
TTATTCTCGGCGAACAAGGAACTATTGAGGTTGCCCAACACCCAGATGCTGCCATTG
TGGTGACAGGGATAGTAGGCTGTGCAGGATTAAAGCCTACAGTTGCTGCAATAGAA
GCAGGGAAAGACATAGCTTTGGCCAACAAGGAAACGCTGATTGCTGGTGGTCCTTT
CGTCCTTCCTCTGGCTCACAAGCATAACATAAAAATTCTTCCAGCTGATTCAGAACA
TTCTGCTATATTCCAGTGTATTCAAGGCTTGCCAGAGGGTGCACTTCGGCGCATTAT
TTTGACTGCATCTGGTGGGGCCTTCAGGGATTGGCCAGTTGAGAAACTGAAAGAAG
TTAAAGTAGCTGATGCATTGAAGCATCCTAACTGGTCAATGGGAAAAAAGATCACT
GTTGATTCTGCTACCCTTTTCAACAAGGGTTTAGAAGTAATTGAAGCCCATTATCTA
TTTGGAGCTGAATATGACAATATTGAGATAATAATTCATCCACAATCTATCATACAT

TCAATGGTCGAAACACAGGATTCGTCTGTTATCGCACAATTGGGGTGGCCTGATATG
CGTTTACCAATCATTTATACAATGTCTTGGCCAGAAAGAATTTACTGCTCAGAAGTA
ACATGGCCTCGCCTTGATCTTGCAAAGCTTGGTTCATTAACATTTGTAACCCCTGAC
AATGCAAAATTCCCATCCATGAATCTCGCCTATGCTGCTGGAAGGACAGGAGGCAC
CATGACAGGAGTCCTTAGTGCAGCAAATGAGAAAGCAGTGGAGATGTTCATTGATG
AAAAGATTAGCTATCTGGATATATTTAAGGTTGTGGAGTTAACATGTGATAAGCACC
GGGCAGAATTGGTGGAGTCACCTTCCCTAGAAGATATATTACATTATGATTTGTGGG
CACGAGAATATGCAGCTAGTTTGCAACATTCCTCGGGTAAAAGCCCTGTTCTTGCAT
GA

>Master_Control_27753_DXS2
ATGGCTTCCTCTTCCCCCAAAGCAAGTTTTAGCTCGTTGCTCCATTGCCATTATCCTT
CAAACAAAACTGGTTTTCCCACTACTTCGTTCCCTAGCTGCGGCGACCGCAAGCTCA
AGAGTGTTAGAGCTTCTTCGGATAATATCAGTACAAGTGATGTTAAGGAATTCAGA
GTGAAGAGGACCGAGCATTTACTACCAGAACAGAATGGACAGATTATTAAAAGAAT
CCTCAATTTCTCCGGACATAAGCCATCCACGCCTATTCTTGACACCATTAACTATCC
CTTCCACATGAAGAACCTTTCCACTCAGGAACTTGAGATGTTGGCTGCGGAGCTACG
AGAAGAGATAGTGTACACGGTGTCGAAGACCGGCGGGCATCTAAGTTCAAGCCTGG
GTGTGACTGAGCTCACGGTGGCTCTCCACCATGTTTTCAACTGTCCTGACGATAAAA
TCATTTGGGATGTTGGTCATCAGGCATATATGCATAAGATTTTAACAGGAAGGAGGT
CGAGAATGCACACAATTCGACAGACCTTTGGGCTTGCTGGTTTTCCCAAGAGGGAG
GAGAGTGTATATGACGCCTTTGGCGCTGGCCACAGTTCTACTAGCATTTCTGCTGGC
TTAGGCATGGCAGTAGGAAGAGATTTGCTAAAGAAGAACAATCATGTAATCTCGGT
GATCGGCGATGGTGCCATGACGGCAGGAATGGCATACGAGGCATTGAACAATGCAG
GTTTTCTTGACACAAATCTTATCATCATCTTAAACGATAACCAGCAAGTCTCCTTGC
CCACCGCCACCGTAGACGGCCCTGCTCCTCCTACTGGCGCTCTCAGCAGAGCCTTGA
GACGACTACAGTCAAAAACAGAATTTCGCCAACTATGTCAAGCTGCTAAGGACAAG
ATGAAGCAATATGGAGGGCAAGCGGGTGAAATTGCAGCCAAAAGCAATGGGTTCTC
GAGAGAAATGGAGCGTGGTTCAGGGGCTTGTTTCTTTGAAGAACTAGGTATAAACT
ATATTGGTCCAGTAGATGGCCATAATTTGGAAGACCTTGTTTATGTTTTAAAGCAAG
TCCAGGCTATGCCAGCCGCAGGACCTAGACTTATTCATGTAATTACTGAAAAAGGA
AAAGGCTACTCTCCTGCTGAATCCGCACCAGACAAGATGCATGGTGTAGTGAAATT
CGATCCTGTGTCAGGAAAACAGTTGAAATCCAAACCGAAAACACTTTCCTACACGC
AATATTTTGCAGAATCTCTGATAGCAGAAGCTGAGAGAGATGAGAAGATTGTAGGC
GTCCATGCGGCAATGGGTGGTGGTACTGGACTTAACTTATTTCAAAAGCGATTCCCT
GATAGATGTTTCGACGTGGGCATAGCCGAACAACACGCCGTCACCTTTGCTGCAGG
CCTGGCTGCTGAAGGCCTGAAACCATTTTGTGCCATTTACTCCAGCTTTTTACAAAG
AGGCTTCGATCAGGTAGTTCACGATGTGGACCTTCAAAAGCTTCCGGTGAAATTTGC
GATGGACAGGGCAGGCCTTGTCGGGGCAGACGGTCCTACACATTGCGGCGCGTTCG
ACACCACTTTCATGGCATGTTTGCCCAACATGGTGGTCATGGCTCCTTCAGATGAGA
CTGAGCTCATGCACATGGTGGCTACAGCCGCAGCCATTAATGACCGTCCTTGTTGCT
TTAGGTATCCCAGAGGAAATGGCTTTGGTTCAGTGATCCCGCCGAATAACAAAGGA
ACGCCTTTAGAGGTTGGCAAAGGAAGAATTTTAAGAAAGGGAAGTGATGTGGCTAT
TTTGGGTTACGGGACAATTGTTAAAAGCTGCCTGGAAGCAGCAGAGCTTCTGAAAA
TGCTTGGAATATCAGCAACTGTGGCTGATGCTCGATTCTGCAAGCCACTTGATGGAG
AACTGATAAGGCAGCTAGCACAAGAGCATGAGATCCTCATCACTGTCGAAGAAGGA
TCTATTGGAGGATTCAGTTCTCATGTTTCCAATTTCCTGGCTTTAAATGGATTATTAG
ATGGAAAGCTTAAGTGGAGGCCAATGATGCTTCCGGATAGATATATCGAGCATGGA
AGTCAGGCTGATCAGATTGAAGAAGCAGGGCTAAGTTCAAAGCACATTGCAGGAAC
TCTGTTTTCATTATTGGCAGGGGTACGCAGGGATGTGCCTCTTTACAAACTG**TAG**

>Master_Control_16457_DXS3

ATGGCTCTCTGTGCATTCTCATTTCCAGCTCATGTCAACCGACCAAGTATAGTTTCA
GATCCTCAAAAGTCTATTCCTCTTACTTCTCATGTGTTCTGGCGAGCAGATCTAGTTT
CCCATTCTTCACACAAGCTCAATCAGATTCAGGTCAGAAAAAGGTCAGGTGGGGTT
TGTGCATCACTTTCGGAGAGAGGAGAATATTATTCACAAAGACCAGCCACACCTCT
CTTGGACACCGTAAACTATCCAATTCATATGAAAAATCTATCTATCAAGGAGCTGAA
ACAACTAGCAGATGAATTGCGGTCGGACGTCATATTCAATGTTTCAAAAACTGGGG
GTCACCTAGGCTCAAGTCTTGGTGTGGTTGAGCTTACTGTGGCACTTCATTATGTTTT
CAATGCTCCTAAAGACAAGATACTATGGGATGTTGGTCATCAGTCTTACCCCCACAA
AATTTTGACTGGGAGAAGAGATAAGATGCATACCATGAGACATACAAATGGTCTTT
CGGGATTCACAAAGCGGTCTGAGAGTGAATATGATTGCTTTGGAACTGGCCACAGT
TCTACCACTATTTCTGCTGGCTTGGGTATGGCTGTCGGTAGAGATCTTAAGGGAAAC
GAGAATCATGTGGTAGCAGTTATAGGCGATGGTGCCATGACTGCAGGCCAAGCTTA
TGAAGCCATGAACAATGCTGGGTACCTGGATTCTGACATGATTGTTATTCTCAATGA
CAACAAACAAGTTTCTTTACCCACTGCTACTCTAGATGGACCCATACCCCCTGTAGG
GGCTTTGAGCAGTGCTCTCAGCAGGTTGCAATCAAACAGGCCTCTCAGAGAACTCA
GGGAGGTTGCAAAGGGAGTTACCAAGCAAATAGGTGGGCCTATGCATGAACTGGCT
GCAAAAGTTGATGAATATGCTCGTGGGATGATCAGTGGTTCTGGGTCAACTCTGTTT
GAAGAGCTTGGACTCTATTATATTGGCCCTGTTGATGGTCACAACATAGATGACCTT
ATTGCCATTCTCGAAGAAGTTAAGAATACCAAAACAACAGGTCCAGTCCTGATCCA
TGTTGTCACTGAGAAAGGCAGGGGATATCCATATGCTGAGAAGGCTGCAGACAAGT
ACCACGGAGTGGCAAAGTTTGATCCTGCAACTGGAAAGCAATTCAAACCCAGTTCT
CTCACCCAGTCTTATACAACATATTTTGCGGAAGCTTTGATTGCAGAAGCAGAGGTG
GACAAGGATATTGTTGCAATCCATGCTGCAATGGGAGGTGGAACAGGACTGAATCT
CTTCCTTCGCCGCTTCCCTAATAGATGCTTTGATGTTGGGATAGCAGAACAGCATGG
TGTTACTTTTGCTGCAGGTCTGGCCTGTGAAGGCCTTAAACCATTTTGTGCAATTTAC
TCATCTTTTATGCAGAGGGCTTATGACCAAGTGGTGCACGATGTGGATTTGCAGAAG
CTGCCTGTAAGATTTGCTATGGACAGAGCTGGATTGGTTGGAGCTGATGGTCCCACA
CATTGTGGGTCTTTTGATGTCACTTTCATGGCATGCCTTCCTAACATGGTGGTAATGG
CTCCGTCTGATGAGGCAGAGCTTTTTCACATGGTTGCCACTGCTGCTGCCATCAATG
ATCGACCCAGCTGTTTCCGATACCCAAGAGGAAATGGGATTGGTGTACAGTTGCCA
CCAGGAAACAAAGGCATTCCTCTTGAGATTGGGAAAGGCAGGATATTAATTGAAGG
GGAGAGGGTTGCACTCCTGGGCTATGGAACACCCGTTCAGAGCTGTTTAGCTGCTGC
TTCTTTATTAGAAACCCATGGATTACGGCTGACGGTAGCAGATGCTCGATTCTGTAA
ACCACTGGATCATGCCCTCATTCGTAGTCTGGCAAAATCGCATGAAGTTCTGATTAC
TGTGGAGGAAGGATCAATTGGGGGCTTTGGGTCTCATGTCGCACACTTCCTGGCTCT
CAATGGTCTTCTTGATGGCACAGTCAAGTGGAGACCACTCGTACTCCCTGATCAGTA
CATCGACCACGGATCACCTGCTGACCAGTTGGCTCGAGCTGGTCTTACTCCATCTCA
CATTGCAGCAACAGTGTTTAACATACTTGGACAAACAAGGGAGGCGCTCGAGATTA
TGTCATTCAAAAAG**TAA**

>Master_Control_122176_DXS4
ATGGCTCTTTCTTCTGGATTTTCCATTGGAACAAACCAATCTCTTTCTCCATTTTTTA
CACCTTCAAGGCCAAAACTTAGTTGCAGAAAACAGTTCTGTTTGAGAGCCGCAGCT
GATAACTCAGTCTCTGATGGGGACGAATGGAAGAAGGTGATTATGAGGAAAGAAA
AGGATGGCAAGAAATTTGATTTTTCTGGGGAAAATCCAGTCACACCATTGTTGGAC
ACAATAAATTACCCAGTTCATATGAAGAATCTATCTAAACAGGATCTTGAACAACT
GGCAGCGGAGCTCAGAGAAGATATTGTGCACAGTGTATCTAAGACAGGTGGGCATC
TTGGTTCAAGCTTAGGGGTGGTGGAGCTAGCAGTTGCATTGCATCATGTTTTCAACA
CACCCGAAGATAAAATTATATGGGACGTGGGCCATCAGGCGTACGTTCATAAAATT
CTTACCGGAAGAAGATCCAGGATGCACACCATAAGGAAAACTTCTGGGCTTGCAGG
ATTTCCCAAAAGAGATGAGAGCGTTCATGATGCTTTTGGCGCAGGACATAGTTCAA
CAAGCATCTCCGCTGGTCTTGGTATGGCGGTTGCAAGGGATCTTCTAGGGAAGAAC
AATAATGTAATTTCTGTGATTGGAGATGGAGCCATGACTGCAGGACAAGCATATGA

GGCCATGAACAATGCAGGATTTCTTGACACTAATCTAATTGTTGTTCTGAATGACAA
CAAACAAGTCTCTCTACCCACTGCTACTCTTGATGGTCCTGCATCTCCAGTTGGAGC
ACTCAGCAGTGCCTTAAGCAAGCTTCAAGCTAGTACTCAGTTCCGCAAACTTCGTGA
AGCGGCAAAAAGCCTCACCAAGCAAATTGGTGGACAAACACATCAAGTTGCCGCAA
AAGTGGATGAGTATGCAAGAGGAATGATTGGTGCTTCTGGGTCAATTCTCTTTGAGG
AGCTAGGGTTATACTACATTGGTCCAGTAGACGGACATAATGTTGAAGATCTAGTA
ACCATCTTTGAAAAGGTGAAAGCAATGCCTGCCCCAGGGCCAGTTCTGATCCATGTT
GTAACAGAAAAAGGGAAGGGTTATTCCCCAGCAGAAGCAGCAGCGGATAAAATGC
ATGGAGTTGTCAAGTTTGATCCAAAAACCGGCAAGCAATTTAAGTCCAAATCGCCT
ACACTTTCATATACAAAGTACTTTGTTGATTCTCTGATAAAAGAAGCCGAGGTGGAT
GATAAGATTATTGCCATCCATGCTGCAATGGGAGGTGGCACTGGTCTCAATTATTTC
CAGAAAAGGTTTCCAGATCGCTGCTTTGATGTGGGGATCGCTGAGCAACATGCTGTT
ACTTTTGCAGCTGGTTTAGCTACGGAAGGTCTCAAGCCATTTTGTGCCATCTACTCA
TCATTTCTGCAAAGAGGATATGATCAGGTGGTACATGATGTAGATCTTCAAAAATTA
CCAGTCCGCTTTGCAATGGATCGAGCTGGTTTGGTTGGTGCAGATGGACCTACTCAT
TGTGGAGCATTTGATGTCACATATATGTCTTGCTTGCCCAATATGGTGGTCATGGCT
CCATCGGATGAAGCTGAGCTTATGCACATGGTTGCCACAGCAGCAGCTATAGATGA
CAGACCCAGCTGCTTTAGATTTCCAAGGGGCAATGGAATTGGAGCAGTTCTTCCACC
TGACAACAAAGGAACCCCACTCGAGATCGGGAAGGGAAGAGTACTAACAGAAGGC
AATAGAGTCGCTATTTTGGGGTATGGTTCTATAGTTCAACAATGTATGGAAGCTGCA
AGCCTGCTCAGGAGCCGAGACATTTATGTAACAGTAGCTGATGCAAGATTTTGCAA
ACCTTTGGATACAGAGCTCATTAGACAGTTGGCCAATGAGCATGAAATCCTAATTAC
TGTGGAAGAGGGTGCTATTGGAGGCTTTGGCTCCCATGTATGCCACTTCCTAAGCTT
AACTGGCATTCTGGATGGACCTCTCAAGTTGAGATCAATGGTGCTTCCTGATAGATA
CATTGACCATGGATCACCAGTAGATCAGATTGAAGAAGCAGGGCTTTCCTCAAAGC
ATATCTCTGCAACAGTCTTATCTCTCTTAGGGAGGCAAAAAGAAGCTCTTCTGTTTA
AA**TAA**

Chapter 4: Section B

Cloning and characterization of putative acyltransferases in *Azadirachta indica*

4B.1. Introduction

Azadirachta indica A. Juss (Meliaceae) is an indigenous tree of India grown in tropical and sub-tropical regions. Most of the biological properties of neem have been contributed by limonoids, which are highly oxygenated, modified triterpenoids. Limonoids are triterpenes present abundantly in Rutaceae and Meliaceae plant family[33]. They are responsible for the bitter principle in citrus and neem, which belongs to Rutaceae and Meliaceae families respectively. Limonoids were named after limonin, the first tetranortriterpenoid isolated from citrus. Limonoids in Meliaceae family are called meliacin-type limonoids[33, 34].

Azadirachtin and related compounds are the highly complex limonoids among the numerous limonoids isolated and characterized from neem. In addition to the complex azadirachtin A skeleton, it is highly decorated with different functional groups[35]. It has two methyl esters, one acetate, a tiglate ester, two tertiary and one secondary hydroxyl groups, along with its dihydrofuran ring linked to another ether ring[35, 36].

The information available on limonoid biosynthetic pathway is very limited. Though the upstream steps involved in the formation of the triterpene skeleton has been characterized recently[37], different class of enzymes are found and predicted to be involved in the catalyzing this multistep pathway. Some of them include, prenyltransferases[37], triterpene cyclases, cytochrome P450 oxido-reductases, and the decoration of the skeleton in the downstream step with functional groups will perhaps be carried out by tigloyltransferases, acetyltransferases etc. These tigloyl and acetyl functional groups are present not only on azadirachtin, but also on the other limonoids, which were hypothesized to be the intermediates in the azadirachtin biosynthetic pathway. Azadirachtin A, salannin, nimbin, nimbinene are the major c-seco limonoids, which exist in, deacetylated form as deacetylazadirachtin A, deacetyl salannin, deacetyl nimbin, deacetyl nimbinene too in the neem tree. Among the major ring intact limonoids of neem, azadiradione and gedunin exist in deacetylated form as nimbocinol and 7-deacetyl gedunin whereas, second major limonoid epoxyazadiradione, the epoxide form of azadiradione has not been found to be exist in its deacetyl form as 7-deacetylepoxyazadiradione (Figure 4B.1). In the present work, screening and identification of different acetyl transferase from neem will be carried out to identify the

acetyltransferase involved in the acetylation of c-seco and ring intact limonoids. This investigation will aid in understanding the functionalization of limonoid skeleton.

The large diversity of secondary metabolites is achieved by elaboration of the basic skeletons, modifying enzymes that catalyze decarboxylation, oxidation/reduction, hydroxylation, glycosylation, methylation, and acylation reactions. One of the common forms of modification of secondary metabolite is the acylation of oxygen-containing substrates to produce esters[38]. Either acyl-sugars, acylated acylcarrier proteins or acyl-activated coenzyme A thioesters serve as active acyl donors and the enzymes that catalyze these acylations on diverse group of plant metabolites belong to large protein family named as BAHD which utilize CoA thioesters as acyl donor[38]. The BAHD acyltransferase family was named according to the first letter of each of the first four biochemically characterized enzymes of this family as follows, benzylalcohol O-acetyltransferase, anthocyanin O-hydroxycinnamoyltransferase, anthranilate N-hydroxycinnamoyl/benzoyltransferase from *Dianthus caryophyllus* and deacetylvindoline 4-O-acetyltransferase from *Catharanthus roseus,* (BEAT, AHCT, HCBT and DAT respectively)[38-44]. Acetylation has been found to serve as a protective group in the multistep biosynthetic reactions of noscapine pathway in opium poppy [45]. Acyltransferases, highly specific for each subsequent step of taxol biosynthetic pathway have been discovered in yew tree (*Taxus sp.*). Taxa-4(20),11(12)-dien-5α-ol O-acetyltransferase (TAT)[46-48] catalyzes the first acylation step of taxol biosynthetic pathway followed by taxane 2α-O-benzoyltransferase (TBT)[49] that act on 2-debenzoyl taxoid-type intermediate to form 10-deacetylbaccatin III which in turn is converted to baccatin III regiospecifically, by 10 β-acetyltransferase (DBAT)[50]. Further, 3-amino-3-phenylpropanoyltransferase (BAPT) was instrumental in 13-O-acylation of baccatin III with β-phenylalanoyl CoA as the acyl donor to form N-debenzoyl-2'-deoxytaxol[51]. Next is the last and final acylation step of taxol biosynthesis and it is catalyzed by taxoid C 13-side-chain N-benzoyltransferase (DBTNBT) using benzoyl-CoA as acyl donor[52]. Taxusin, a prominent side-route metabolite of taxol pathway of *Taxus* has also been found to be formed due to the catalytic activity of two taxoid-O-acetyl transferases[53]. Acetyl-CoA-dependent acyltransferases have been found to catalyze crucial steps in several alkaloid pathways such as salutaridinol acetyltransferase in morphine biosynthetic pathway in *Papaver somniferum*[54, 55], vinorine synthase in ajmaline

biosynthetic pathway of medicinal plant *Rauvolfia serpentina*[56, 57] and in *Catharanthus roseus*, the biosynthesis of vindoline, a biogenetic precursor of the dimeric alkaloids vinblastine and vincristine is catalyzed by DAT[44] whereas a different enzyme minovincinine-19-Oacetyltransferase (MAT) catalyzes the formation of minovincinine [58].

On the other hand, acyltransferases such as monoterpene acetyltransferases of *Lavandula x intermedia* is capable of acting on different monoterpenes (lavandulol, geraniol, nerol) as substrate to form its corresponding acetates [59]. These acetyltransferases act on fragrance and flavor metabolites in flower and fruit respectively. The geraniol/citronellol acetyltransferase in rose flower catalyzes the formation of geraniol and citronellol[60]. Range of alcohol substrates from short to medium straight chain (C3–C10), branched chain, aromatic and terpene alcohols are acylated by apple alcohol acyl transferases[61]. Similarly, a BAHD acyltransferases of petunia have been characterized for its catalytic ability to act efficiently on phenylpropanoid substrates coniferyl alcohol but can also catalyze different alcohol substrate[62]. In plants, phospholipid:sterol acyltransferase (PSAT) is capable of transferring acyl donors to both phospholipids and sterols[63], whereas in *Arabidopsis*, saturated fatty acyl-coenyzme A are transferred to sterols by sterol O-acyltransferase[64]. Thus diverse acyl coA donars such as acetyl-CoA, β-phenylalanine-CoA, malonyl-CoA, tiglyl-CoA, anthraniloyl-CoA, benzoyl-CoA[65] and (hydroxy) cinnamoyl-CoA are utilized by plant BAHD acyltransferases[66].

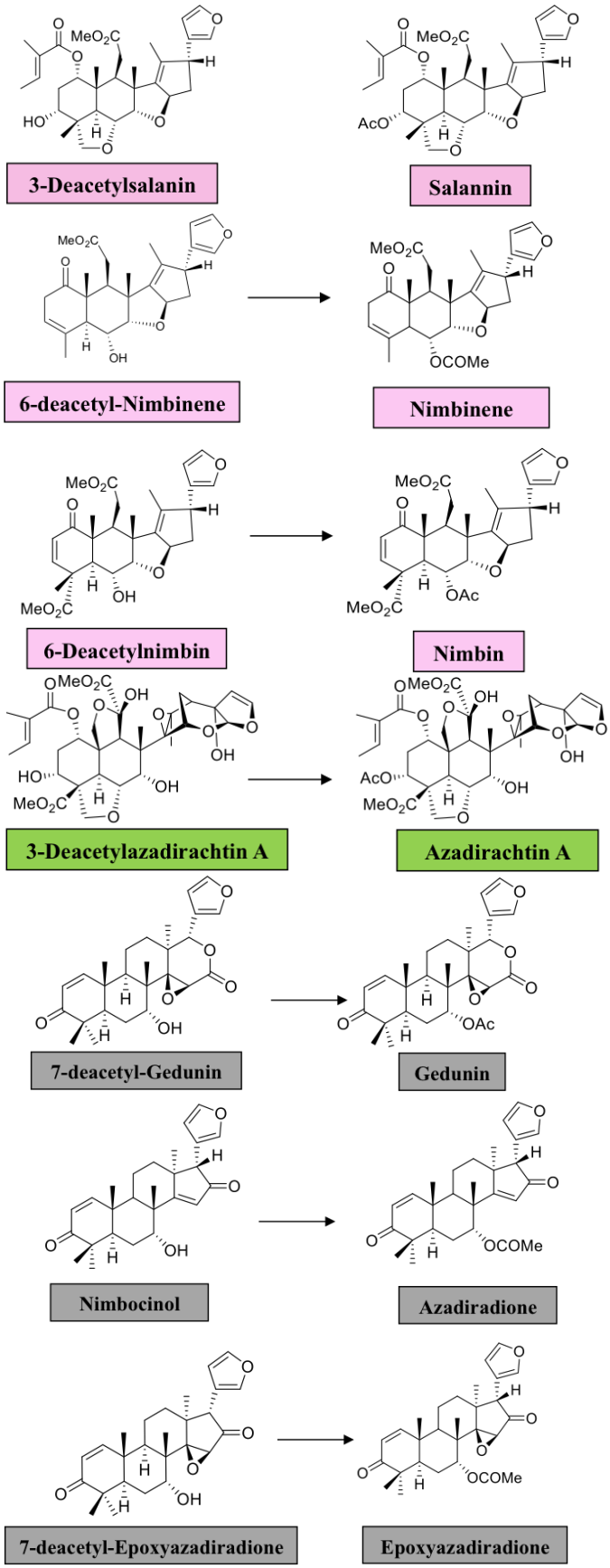

Figure 4B.1. Possible acetylation sites in some of the most abundant limonoids in neem

4B.2. Results and discussion

4B.2.1. Phylogenetic analysis

The predicted neem acyltransferases grouped with hypothetical acyltransferases of citrus, which belongs to Rutaceae family, which is another source of limonoid group of natural products. The clade of comprising of acyltransferases of neem and citrus are close to the clade of the enzymes involved in acetyl transfer reactions in taxol biosynthetic pathway of *Taxus* (Figure 4B.2).

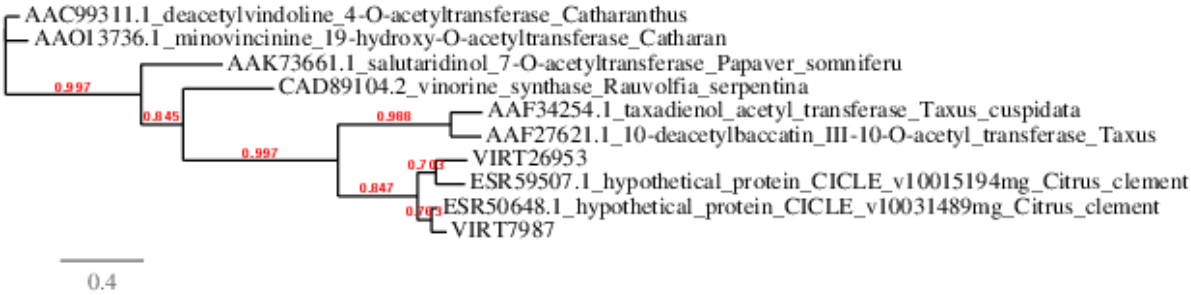

Figure 4B.2. Phylogenetic analysis of acetyltransferases of plant BAHD family

4B.2.2. RNA isolation

The RNA isolated from pericarp and leaves were checked for its concentration and quality spectrometrically by verifying its 260/280 and 260/230 ratios. RNA analyzed through electrophoresis evidenced clear 28S rRNA, 18S rRNA and 5S rRNA as three bands along with mRNA (Figure 4B.3).

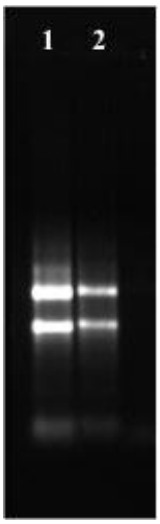

Figure 4B.3. Total RNA isolation, **Lane 1:** Neem fruit pericarp, **Lane 2:** Neem leaf, (RNA electrophoresed in 1% agarose gel)

4B.2.3. Cloning of acyltransferase 1 (AiACT1)

AiACT1 transcript sequence (Master control_17413) information was used for designing full-length primers. The Open Reading Frame (ORF) was found to be 1353 bp, which may encode a polypeptide of 450 amino acids. It showed 72% identity with annotated citrus acyltransferase sequence, which belongs to the BAHD family of plant acyltransferase. Deduced protein was calculated to have a theoretical molecular weight of 51.19 kDa and pI of 8.1. The deduced sequence was found to have HTICD catalytic domain and DFGWG conserved motif as of plant BAHD acyltransferases, which has HXXXD, a catalytic domain and DFGWG conserved motif respectively.

Amplicon of 1.6 Kbp obtained was amplified from cDNA obtained from neem fruit pericarp RNA (Figure 4B.4). The AiACT1 ORF was cloned into pET32a vector frame with N-terminal His-6 tag for affinity purification *E.coli* Rosetta Gammi 2 (DE3) cells. Positive clones were screened using T7 Forward and reverse primers by colony PCR (Figure 4B.5) and the presence of insert was confirmed by subjecting the plasmid to restriction digestion. The cloned insert was confirmed for its sequence and orientation using DNA sequencing using T7 Forward and reverse primers, which confirmed the size of ORF as 1353 bp.

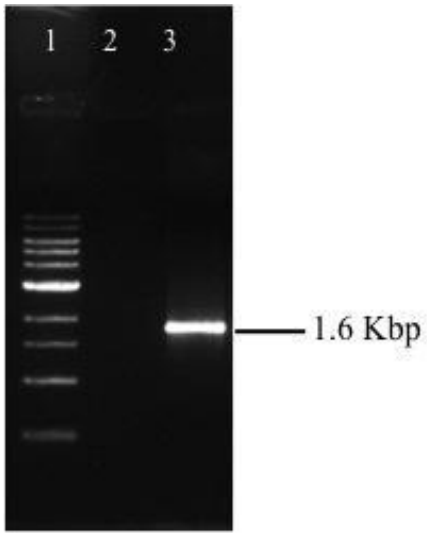

Figure 4B.4. AiACT1 full-length ORF amplification, **Lane 1:** 1 Kb DNA ladder, **Lane 2:** No template control (NTC), **Lane 3:** PCR of AiACT1 full-length primers with pericarp cDNA as template (DNA electrophoresed in 1% agarose gel)

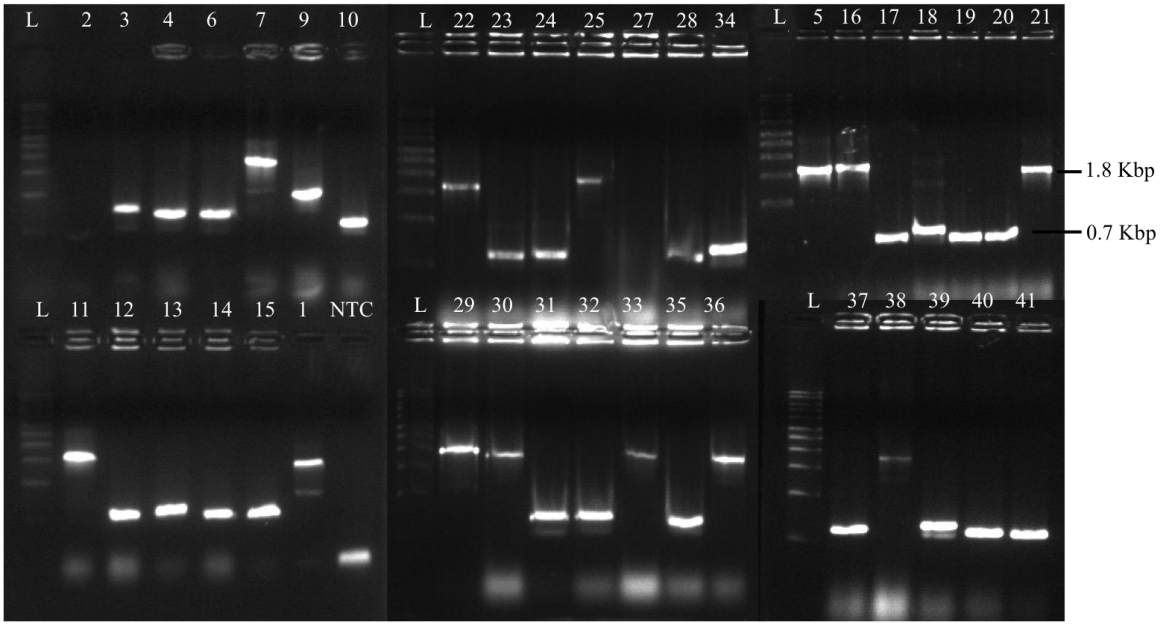

Figure 4B.5. Colony PCR screening of full-length ORF of AiACT1 in pET32a, PCR performed with T7 promoter and T7 reverse primer **Lane L:** 1 Kb DNA ladder, **NTC:** No template control (negative control), **positive colonies 1, 5, 7, 11, 16, 21, 22, 25, 29, 30, 33, 36, 38:** Showed amplicon of ~ 1.8 Kbp, others colonies showed ~ 0.7 Kbp amplicon- self-ligated colonies. (DNA electrophoresed in 1% agarose gel)

4B.2.4. Cloning of Acyltransferase 2 (AiACT2)

AiACT2 transcript sequence (Master control_99887) information was used for designing full-length primers. The Open Reading Frame (ORF) was found to be 1395 bp, which may encode a polypeptide of 464 amino acids. It showed 83% identity with annotated citrus acyltransferase sequence, which belongs to BAHD family of plant acyltransferase. Deduced protein was calculated to have a theoretical molecular weight of 51.35 kDa and pI of 7.9. The deduced sequence was found to have HTMSD catalytic domain and DFGWG conserved motif as of other BAHD acyltransferases, which has HXXXD, a catalytic domain and DFGWG conserved motif respectively.

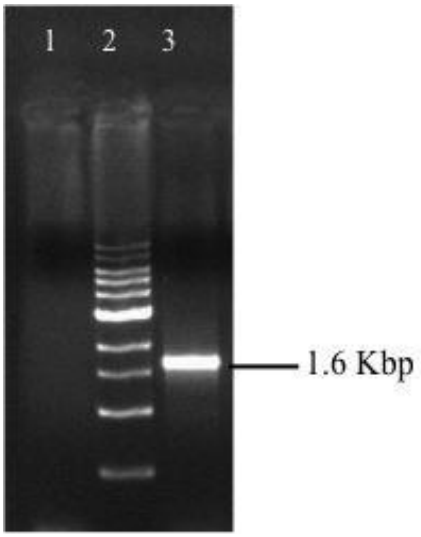

Figure 4B.6. AiACT2 full length ORF amplification, **Lane 1:** 1 Kb DNA ladder, **Lane 2:** No template control (NTC), **Lane 3:** PCR of AiACT2 full-length primers with leaf cDNA as template (DNA electrophoresed in 1% agarose gel).

Amplicon of 1.6 Kbp obtained was amplified from cDNA obtained from neem leaf RNA (Figure 4B.6). The AiACT2 ORF was cloned into pET32a vector frame with N-terminal His6 tag for affinity purification in *E.coli* Rosetta 2 (DE3) cells. Positive clones were screened using T7 Forward and reverse primers by colony PCR (Figure 4B.7) and the presence of insert was confirmed by subjecting the plasmid to restriction digestion. The cloned insert was confirmed for its sequence and orientation using DNA sequencing using T7 Forward and reverse primers, which confirmed the size of ORF as 1395 bp.

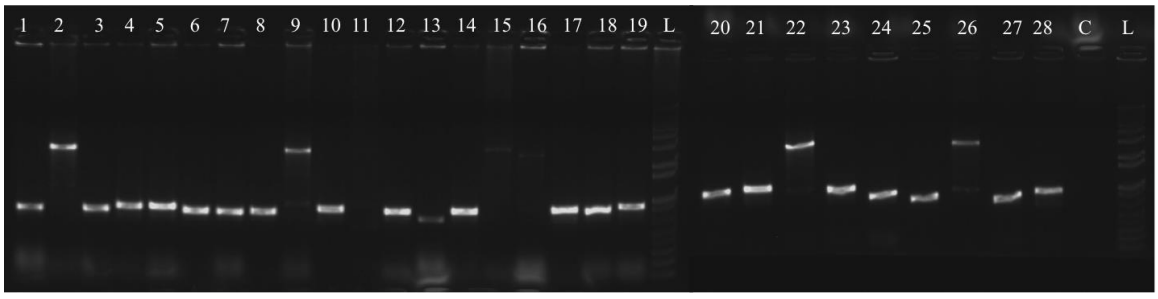

Figure 4B.7. Colony PCR screening of full-length ORF of AiACT2 in pET32a, PCR performed with T7 promoter and T7 reverse primer **Lane L:** 1 Kb DNA ladder, **C:** No template control (negative control), **colony 2, 9, 15, 16, 22, 26:** Showed amplicon of ~ 1.8 Kbp, others colonies showed ~ 0.7 Kbp amplicon- self-ligated colonies. (DNA electrophoresed in 1% agarose gel)

4B.2.5. Codon analysis of AiACT1 and AiACT2

Codon analysis of AiACT1 showed that 2 rare codons of bacteria such as CCC and GGA were present in the sequence. In AiACT2, eight rare codons of bacterial system were present. Hence, Rosetta 2 (DE3) and Rosetta Gammi 2 (DE3), which contains 7 bacterial rare codons have been used as a host system for expression of the recombinant AiACT proteins.

>AiACT1
ATG TCG TTA AAG TTC CCA CAG GTC TTT TCC GTA ACG CGC CAG GCG CCA GAA TTG
ATT GCG CCA GCT CGC CCG ACG CCA CGC GAG GTT AAA CAG CTG AGC GAC ATT GAT
GAC CAA GAG AGC TTT CGT TTC CAG GTT CCA GTC ATC TTC TTT TAC AAA AAT AAT
CCC AGC CCC AGC ATG AAG GGT AAA GAT CCA GTC GGG GTT ATC CGC GAA GCT ATC
TCC AAA GCG CTG GTG TTC TAC TAC CCG TTG GCG GGT CGT CTT AAA GAA GGG GAT
AAC CGC AAA CTT ATG GTC GAT TGC AAT GGA GAA GGG TTA TTG TTT ATC GAA GCT
GAC GCT AAT TTC ACC CTT GAG CAA TTA CGC GAC GAC GAC CAA TCT CCT TCC TCA
TAC CTG GAT GAG CTT CTG TAT AAC GTC CCG GGC AGT GAT GGA ATT CTG GGG TGC
CCG CTG TTA TTA ATT CAG GTT ACC CGC CTT ATC TGC GGC GGG TTC ATC TTA GCC TTG
CGC CTT AAT CAC ACT ATT TGT GAC GCA CAA GGT TTA GTT CAA TTC CTG AAG ACC
ATT GAG GAA ATG GGG CGC GGT GAG AAC GCT CCG TCC ATC TTT CCG GTC TGG CAG
CGT GAG TTG CTG AAC GCC CGT AAC CCC TTA CAG GTT ACG TGT ATC CAC CAT GAG
TAT GGA GAA GAA AAA TAT AAC CCC GAT ACT AAC GAG AAC GAC ATG CAC AAT AAA
TTA TTT TTT TTC GCA TTA AAA GAG ATT CGT GCC TTA CGT AAC CAG TTC CCG CTG CAT
CTG CGC AAG TGT AGT ACC TTC GAT CTT CTG ACG GCC CTT GCG TGG AAA TGC CGC
ACG CGC GCA CTG AAA TAC GAC CCT GAG GAG ATT GTA CGT TTC TCT TGT ATT GTA
TCC GCG CGT GGG AAG CGC TAC AAT ATG CAG TTG CCT AGC GGC TAC TAC GGG AAC
GCC TTT GCT TTC CCT GCC GTG TGC TCG AAT GCG GAG GAC TTA TGT CGT AAC CCC
CTG GGA TAT GCA GTT GAG CTG GTT CAA AAG GCA AAG GCT AAA ATG AAT GAA GAA
TAT ATT CGT AGT GTA GCA GAT TTG ATG GTA ATC TCG GGA CGC CAA ATC AAA CAT
CCC GTA CGT GGT AAC TTT ATC GTT AGT AAC GTA ACA CAA GTA GGC TTT GGG GAG
GTG GAC TTC GGA TGG GGG AAG CCG ATC TAT GCG GGT ACA CCG TGT GCA GTA TCA
CTT ATC TCT TTC GTG ATG AAA AAT CAA AAT AAG AAT GGC GAA CCT CGC TAC GTC
TTA CCT ATG TGT TTA CCT ATG CTG GCC ATG AAA CGT TTC GAA GAA GAG GTT AAA
CGT GTT ATG CAG CAG GAG TTT GAA CAG ACC CAG ATC TTC TGT AAA CTG TAG

>AiACT2
ATG CCA CCA TCA CAA CCA CCA CGC CCC GCC TCC CTT GTC TTT ACC GTC CGG AGG
AGC ACC CCG GAA CTA ATC TCT CCG GCC AAA CAG ACA CCT CGC GAG CTC AAA TCC
TTG TCC GAT ATC GAT GAT CAA GAG GGT CTC CGG TTC CAA ATT CCG GTC ATA CAA
TTC TAC AAG TAC CAC CCT TCC ATG AAA GGG AGG GAC CCG GTT AAG GTG ATC AGA
GAA GCC TTA GCG GAA ACG CTT GTC TTT TAC TAC CCG TTT GCC GGT AGG CTC CGG
GAG GGG GCT AAC CGG AAA CTT ATG GTG GAT TGT AAC GGC GAA GGT GTG ATG TTC
ATT GAA GCT GAT GCT GAT GTT ACA CTT GAA CAA TTT GGT GAT GAT CTT CAA CCT
CCA TTT CCA TGC TTG GAA GAG CTG CTT TTT GAT CTT CCA GGA TCT GCT GGA GTA ATC
AAC TGC CCT TTG TTG CTC ATT CAG GTG ACA CGT TTG AAG TGC GGC GGT TTC ACT TTC
GCC CTC CGT CTC AAC CAC ACC ATG AGC GAC GCA GCT GGT ATC GTC CAG TTC ATG
GCC GCC GTA GCT GAA ATC GCA CGC GGC GCG GCT GGC CCC ACC ATT CTT CCT GTC
TGG GAA AGA CAC GTA CTC AAC GCC CGG GAC CCA CCT CGC GTA ACA TGC ACG CAC
CAT GAA TAC GAT GAA GTC GCC GAC ACC AAG GGG ACG ATC ATC CCG CTC GAT GAT
ATG GTT CAT CGT TCT TTC TTC TTC GGC CCT CAA GAA ATC AAC GCC ATT CGC CGA TTT
CTT CCA CAG CAT CTA CGC TGC AGC TCC AGT TTC GAA ATT CTC ACC GCC TGC CTC
TGG CGC TGT CGC ACC ATC GCA CTG CGG CCG GAC CCG AGC GAA GAA ATG CGC GTG
ATT TGC ATC GTC AAC TCG CGT TGC AAG TTT AAT CCA CCC TTA CCT AGA GGA TTC
TAC GGC AAC GGG TTC GCT TTC CCG GTT GCA TTG TCG ACG GCG GAG AAA GTG TGT
CAA AAT CCA ATA GGT TAT GCT TTG GAG CTA GTG AGG AAA GCC AAG AAT GAC GTG

AAC GAA GAG TAT ATG AAA TCA GTG GCG GAT TTA ATG GTG ATA AAA GGC CGA CCC CAT TTC ACC GTC GTC CGA TCC TAC CTT GTT TCG GAT GTG ACT CGA GCC GGG TTC GGG GAT GTG GAC TTT GGG TGG GGA AAA CCG GCT TAT GGG GGG CCT GCC AAG GGT GGG GTT GGC GCC ATT CCA GGA GTT GCA AGC TTT TAT ATT CCT TTC AGG AAT AAG AAA GGA GAG GAG GGT ATT GTA GTG CCG GTG TGC TTG CCG GCT CCG GCA ATG GTG AGA TTC GTG GAG GAA TTG GAC AAG ATG TTG AAG GAG AAG CCA GTT GCT GCT GGC GAG AAT AAA TCT ACT TTC ATA GCA TCT GCT CTG TAA

Figure 4B.8. Codon analysis for AiACT1 and AiACT2 sequences

4B.2.6. Expression and purification of AiACT1

Expression was carried out in Rosetta gammi 2 (DE3). Initially different imidazole gradients were tried, washing the unbound protein fractions were carried out starting with 5 mM, and 10 mM imidazole containing buffer. Later at 20 mM imidazole, the unbound protein eluted. Recombinant AiACT1 protein was eluted in 50 mM imidazole containing buffer. Further, 100 mM, 150 mM, 200 mM, 250 mM imidazole containing buffer were used, in which no more elutions were seen. The protein fractions show a band at 72 kDa for AiACT1on a 12% SDS-PAGE (Figure 4B.9). Desalted proteins were flash-frozen and stored at -80 °C until use. Enzyme assay with studied limonoid substrates did not showed any product formation.

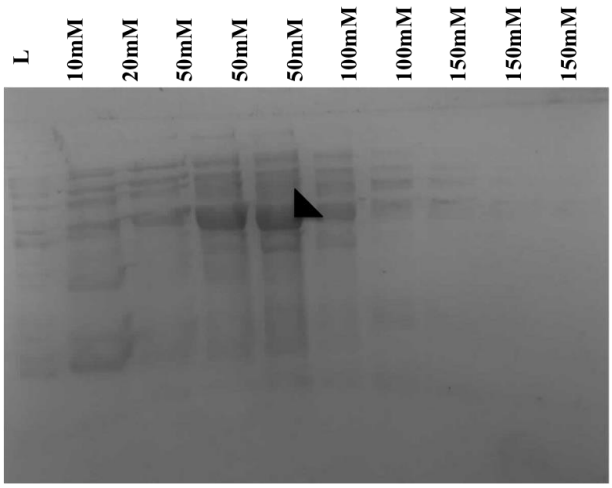

Figure 4B.9. SDS-PAGE analysis of eluted AiACT1 protein fractions from Ni-NTA agarose column. The **arrow** shows **72 kDa protein** corresponding to **AiACT1**

4B.2.7. Expression and purification of AiACT2

Expression was carried out in Rosetta 2 (DE3). The protein eluted in 50 mM imidazole containing buffer. The protein fractions show a band at 72 kDa for AiACT1on a 12% SDS-PAGE (Figure 4B.10). 20 L of culture gave final yield of 0.5 mg of protein

of 50% purity as seen in Figure 4B.10. This low level of expression may be due to several rare codons present in AiACT2 sequence (Figure 4B.8). Desalted proteins were flash-frozen and stored at -80 °C until use. Enzyme assay with studied limonoid substrates did not showed any product formation.

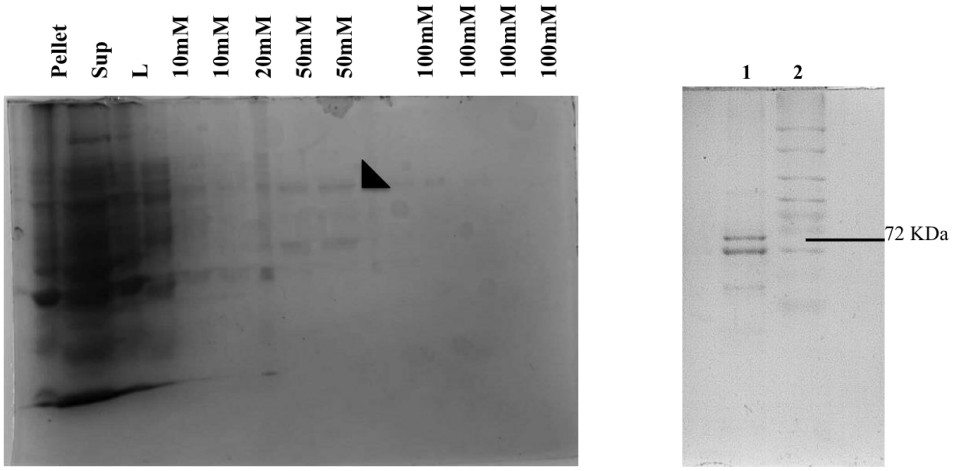

Figure 4B.10. SDS-PAGE analysis of eluted AiACT2 protein fractions from Ni-NTA agarose column (*Left*), **Lane 1,** The purified protein obtained with 50% purity seen at 72 KDa, **Lane 2**, Protein Ladder (*Right*). The **arrow** shows **72 KDa protein** corresponding to AiACT2.

Since the expression level of AiACT2 was very less in Rosetta 2 (DE3) cells, the plasmid was transformed into other expression cells such as Rosetta gammi 2 (DE3), B834 (DE3) LysS and Arctic express cells expressed. Faint band was observed with Rosetta gammi 2 (DE3), B834 (DE3) expression cells upon induction, whereas no desired protein was observed with Arctic express cells which indicates that the expression of ACT2 is facilitated by rare codons encoded in these bacterial strains.

4B.2.8. Cloning, expression of AiACT1 in *Saccharomyces cerevisiae* and identification of its function

The ORF of AiACT1 was amplified using accuprime DNA polymerase (Figure 4B.11) and cloned into pYES2/CT vector for expression of active protein under the control of T7-RNA polymerase promoter in INVSc yeast cell. Positive clones were screened by colony PCR using T7 Forward and CYC reverse primers (Figure 4B.12). The protein was expressed by inducing with 2% galactose in CSM-Ura dropout media and grown for 24 hrs (as mentioned in methods section). To check the activity of enzymes the substrates were added to the media and incubated for 8 hrs. Due to the

activity of ATF gene[67] (alcohol acetyltransferase) in yeast, substrates such as benzyl alcohol, hexanol, heptanol, farnesol, nerol gave very little conversion of < 0.5 conversion into its acetylated forms such as benzyl acetate, hexyl acetate, heptyl acetate, farnesyl acetate, neryl acetate (Figure 4B. 15C) respectively and more activity was observed towards geraniol comparatively[68]. In case of geraniol, it was reduced into citronellol (Figure 4B.15B), due to the activity of old yellow enzyme (OYE) gene of *Saccharomyces cereviseae*[67, 69, 70] whereas interconversion into different terpenes such as linalool, nerol, terpeniol, geraniol, citronellol has be identified variably in different yeast strains as evident from the literature[69, 71]. Hence, conversion of geraniol to citronellol, citronellol acetate and geraniol acetate was observed in control yeast cells. Farnesyl acetate peak was 1.5 fold higher than the control, uninduced cells (Figure 4B.15A). To further check the activity of the gene on sterol triterpenes, saponified yeast cells were extracted for triterpenes with n-hexane and no activity was observed on the yeast triterpene alcohols.

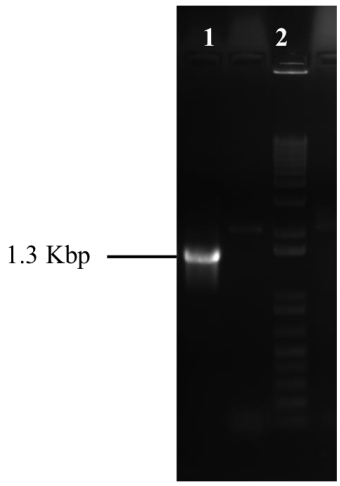

Figure 4B.11. AiACT1 full-length ORF amplification, **Lane 1:** PCR using AiACT1 full-length primers for cloning into pYES2/CT, **Lane 2:** 1 Kb +DNA ladder

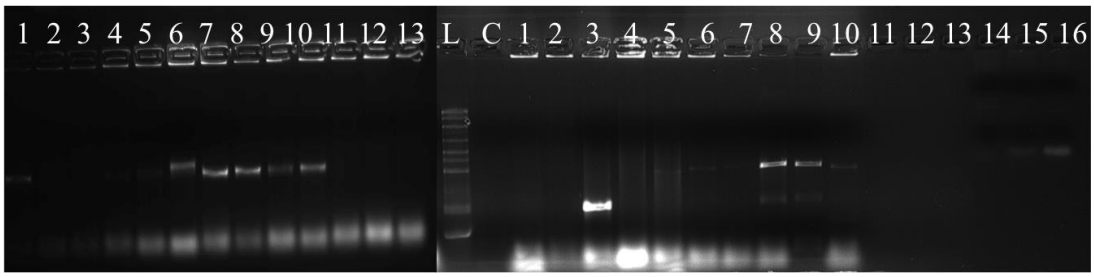

Figure 4B.12. Colony PCR screening of full-length ORF of AiACT1 in pYES2/CT in 2 transformation experiments (13 colonies and 16 colonies screened from 2 transformation

reactions), PCR performed with T7 forward and CYC reverse primer **Lane L:** 1 Kb DNA ladder. **Lane C:** No template control. Positive colonies are seen as 1.3 Kbp. Positive colonies are 6A, 7A, 8A, 9A, 10A, 8B, 9B, 10B.

4B.2.9. Cloning and expression of AiACT2 in *Saccharomyces cerevisiae* and identification of its function

The ORF of AiACT2 was amplified using accuprime DNA polymerase (Figure 4B.13) and cloned into pYES2/CT vector for expression of active protein under the control of T7-RNA polymerase promoter in INVSc yeast cell. Positive clones were screened by colony PCR using T7 Forward and CYC reverse primers (Figure 4B.14). The protein was expressed by inducing with 2% galactose in CSM-Ura dropout media as mentioned in methods section and grown for 24 hrs. To check the activity of enzymes the substrates were added to the media and incubated for 8 hrs. Farnesyl acetate peak was 1.5 fold higher than the control, uninduced cells (Figure 4B.15A). No activity was seen for any of the other screened substrates.

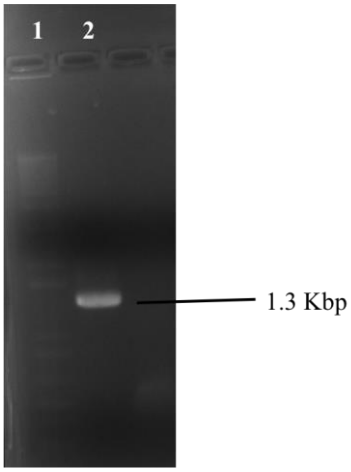

Figure 4B.13. AiACT2 full-length ORF amplification, **Lane 1:** 1 Kb +DNA ladder, **Lane 2:** PCR using AiACT2 full-length primers for cloning into pYES2/CT

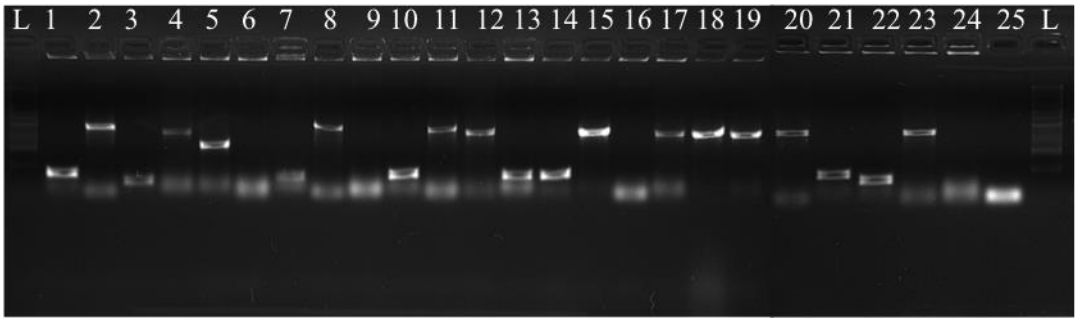

Figure 4B.14. Colony PCR screening of full-length ORF of AiACT2 in pYES2/CT, PCR performed with T7 forward and CYC reverse primer **Lane L:** 1 Kb DNA ladder. Positive colonies are seen as 1.3 Kbp and self-ligated at 0.3 Kbp.

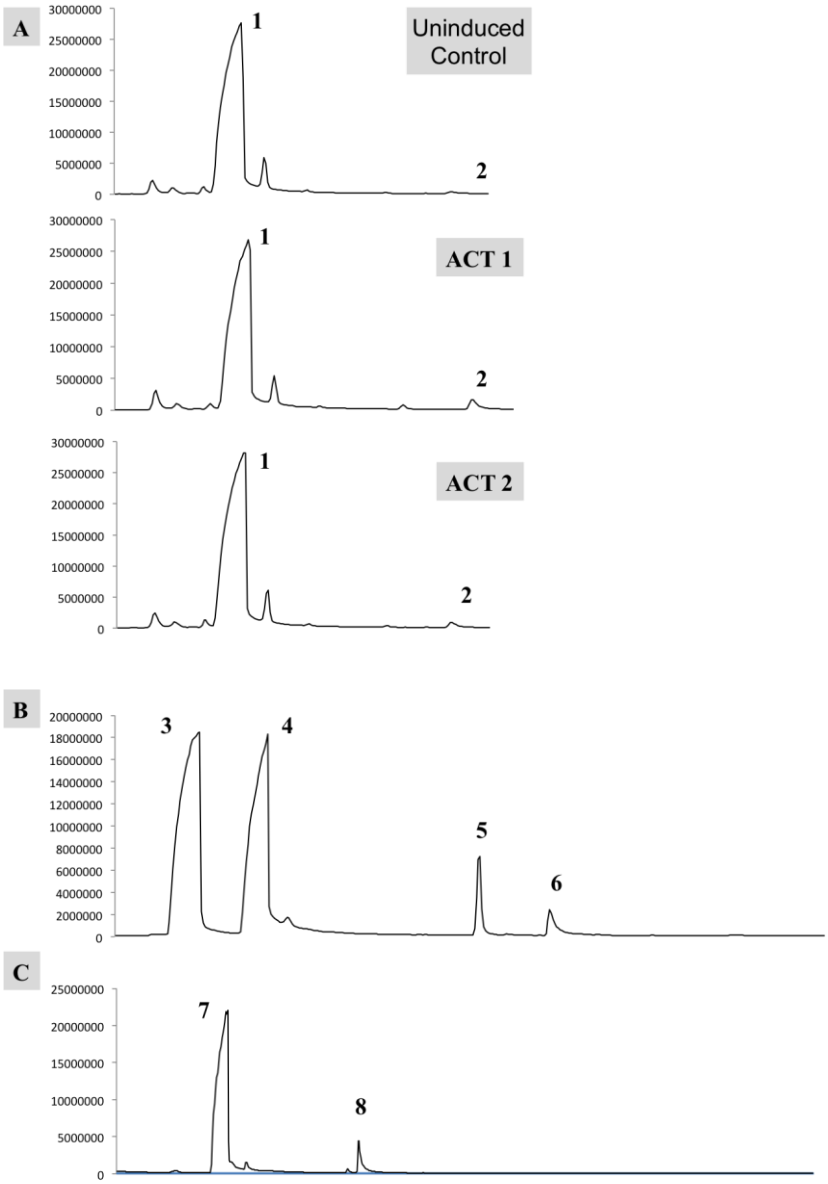

Figure 4B.15. GC-MS chromatogram showing the conversion of various alcohol substrates into acetyl group by in yeast system. 1. Farnesol, 2. Farnesyl acetate, 3. Citronellol, 4. Geraniol, 5. Citronellol acetate, 6. Geraniol acetate, 7. Nerol, 8. Neryl acetate, B and C represents control, uninduced yeast cells.

4B.3. Conclusion

The neem acyltransferases AiACT1 and AiACT2 were cloned and expressed in bacterial and yeast expression system. They didn't show activity on ring intact and c-

seco limonoids. Its activity on aliphatic and terpene alcohols were not significant. Hence, the result shows that these enzymes may act on the low abundance or labile pathway intermediates of limonoid biosynthetic pathway. This is also evident from the transcriptome analysis that their expression was high in pericarp and leaf tissues, which are enriched with triterpenoid intermediates of less complex structure. These tissues are high in the biosynthesis of ring intact limonoids, hence their activity may exists on the conversion of protolimonoids into the intermediate limonoids.

4B.4. Materials and methods

4B.4.1. Bacterial Strains and Plasmids used in the Study

Escherichia coli Mach1™ $T1^R$ (ThermoFisher Scientific, USA)

Escherichia coli Rosetta 2 (DE3) (Novagen)

Escherichia coli Rosetta Gammi 2 (DE3) (Novagen)

INVSc1, *S. cerevisiae* Yeast Strain (ThermoFisher Scientific, USA)

pET-32a expression vector (Novagen)

pYES2/CT Yeast Expression Vector (ThermoFisher Scientific, USA)

4B.4.2. Kits and reagents used in the study

SuperScript® III Reverse Transcriptase (ThermoFisher Scientific, USA)

JumpStart™ Taq DNA Polymerase (Sigma-Aldrich, USA)

Platinum® PCR SuperMix (Invitrogen)

AccuPrime™ Pfx DNA Polymerase (ThermoFisher Scientific, USA)

PureLink™ Quick Gel Extraction and PCR Purification Combo Kit (ThermoFisher Scientific, USA)

GenElute™ PCR Clean-Up Kit (Sigma-Aldrich)

GenElute™ Plasmid Miniprep Kit (Sigma-Aldrich)

GelRed™ (Biotium Inc., USA)

Restriction enzymes (New England Biolabs, USA)

T4 DNA ligase (Invitrogen/ Life Technologies, USA)

T4 DNA ligase (New England Biolabs, USA)

S.c. EasyComp™ Transformation Kit (ThermoFisher Scientific, USA)

FastStart Universal SYBR Green Master (Rox) (Roche, Switzerland)

DNase I Amplification Grade Kit (Sigma-Aldrich, USA)

4B.4.3. Phylogenetic analysis of acyltransferase of neem

A phylogenetic tree was constructed for the two genes from neem, in comparison with acyltransferases from closely related species. Multiple sequence alignments were performed using software Clustal Omega and phylogenetic tree was generated using the nearest neighbour joining method through Phylogeny.fr.

4B.4.4. RNA isolation and cDNA synthesis

Neem leaves and fruits collected from the neem tree in NCL campus during the month of April-May and were frozen in liquid nitrogen and stored at -80 °C. 100 mg of finely ground-powdered tissue was used for RNA isolation. The materials were treated with 0.1% Diethyl pyrocarbonate (DEPC) (Sigma). RNA isolation was carried out using Spectrum™ plant total RNA isolation kit (Sigma) from neem leaves and fruit pericarp. Three µg of total RNA was used for first strand cDNA synthesis using SuperScript® III Reverse Transcription Kit (ThermoFisher Scientific) and the synthesized cDNA, was stored at -20 °C till further use.

4B.4.5. Sequence analysis

After identification of the genes involved in triterpene biosynthesis, sequences were analyzed by NCBI GenBank database. Sense strand ORFs were selected using online ORF finder tool, and based on the ORFs, primers were designed, which contained sites for restriction enzyme at both the ends, for cloning full-length ORF in expression vector using OligoAnalyzer tool.

Name	5'-3' Primer sequence	Size in bp
AiACT1-FP	AGCTGCGATATCATGTCATTAAAATTTCCTCAAGT	35
AiACT1-RP	AGCCGTCTCGAGCTAAAGCTTGCAAAATAT	30
AiACT2-FP	AATTGAGGATCCATGCCACCATCACAACCACCA	33
AiACT2-RP	TTACTTGCGGCCGCTTACAGAGCAGATGCTATGA	34

Table 4B.1. Primer sequence for isolation of full length ORF of the genes acyltransferases involved in limonoid biosynthesis. (The underlined sequence represents the recognition site for restriction enzyme).

4B.4.6. Isolation and cloning of ORF of Acyltransferase 1 (AiACT1)

Synthesized cDNA was used for PCR reaction using Platinum® PCR SuperMix (Invitrogen) using the PCR program: Initial denaturation at 94 °C for 3 min, followed by 35 cycles at 94 °C for 30 sec, 54 °C for 30 sec, 72 °C for 1 min 30 sec followed by final extension at 72 °C for 3 min. PCR product of 1.6 Kbp was cloned into pET32a expression vector after digesting both with EcorV and XhoI restriction sites. Restriction digested vector and insert were subjected to ligation using T4 DNA ligase (NEB) at 16 °C incubation overnight. The ligation mixture was transformed into Mach1 chemical competent cells by applying heat shock at 42 °C, then plated on Luria Bertani agar with 50 µg/mL of ampicillin and incubated at 37 °C overnight. From 7 positive clones of colony PCR, plasmid isolation was carried out. To check for the sequence in the correct vector frame of the vector, it was sequenced with T7 forward and T7 terminator reverse primers.

4B.4.7. Isolation and cloning of ORF of Acyltransferase 2 (AiACT2)

Synthesized cDNA was used for PCR reaction using Platinum® PCR SuperMix (Invitrogen) using the PCR program: Initial denaturation at 94 °C for 3 min, followed by 35 cycles at 94 °C for 30 sec, 57 °C for 30 sec, 72 °C for 1 min 30 sec followed by final extension at 72 °C for 3 min. PCR product of 1.6 Kbp was cloned into pET32a expression vector after digesting both with BamHI and NotI restriction sites. Restriction digested vector was subjected to alkaline phosphatase, calf intestinal (CIP) (NEB) treatment to remove the phosphate at the 5´- and 3´ terminal, in order to prevent the self-ligation of vector during ligation reaction. Insert and above said treated vector were subjected to ligation using T4 DNA ligase (Invitrogen) at 16 °C incubation overnight. The ligation mixture was transformed into Mach1 chemical competent cells by applying heat shock at 42 °C, then plated on Luria Bertani agar with 50 µg/mL of ampicillin and incubated at 37 °C overnight. Positive clones were screened by colony PCR with T7 promoter and T7 terminator primers.

4B.4.8. Expression and purification of AiACT1

Expression was carried out in Rosetta gammi 2 DE3, cells were grown in Terrific Broth at 37 °C and induced with IPTG at a final concentration of 1mM and incubated for

12 hours at 16 °C. The culture was then centrifuged at 4000 × g for 20 minutes and the cell pellet (5 g/L) was re-suspended in 10 mL/g of cell pellet of Lysis buffer (25 mM MOPSO, 100 mM NaCl, 0.5% CHAPS, 0.1% Triton x-100, pH 7.4, 10% v/v Glycerol) with 1 mg/mL concentration of lysozyme, 1mM PMSF incubated on ice for 30 minutes. After the incubation period, the cells were sonicated with a pulse of 30 sec ON and 30 sec OFF for 10 cycles. The crude lysate obtained upon centrifugation at 5,000 × g for 10 minutes at 4 °C was subjected to Ni-NTA column (2 mL resin /g cell pellet). The unbound proteins were eliminated by using wash buffer (25 mM MOPSO, 100 mM NaCl, pH 7.4, 20 mM Imidazole, 10% v/v Glycerol). The protein was finally eluted out in the elution buffer (25 mM MOPSO, 100 mM NaCl, pH 7.4, 50 mM Imidazole, 10% v/v Glycerol) each. Protein fractions (after checking on 12% SDS gel) were pooled together, desalted and purified using Amicon centrifugal filter units with desalting buffer (25 mM MOPSO, pH 7.4, 10% v/v Glycerol). The desalted proteins were estimated using Bradford reagent (Bio-Rad) and a Bovine Serum Albumin standard.

4B.4.9. Expression and purification of AiACT2

Expression was carried out in Rosetta 2 DE3, cells were grown in Terrific Broth at 37 °C and induced with IPTG at a final concentration of 1 mM and incubated for 12 hours at 16 °C. The culture was then centrifuged at 4000 × g for 20 minutes and the cell pellet (5 g/L) was re-suspended in 10 mL/g of cell pellet of Lysis buffer (25 mM MOPSO, 100 mM NaCl, 0.5% CHAPS, 0.1% Triton x-100, pH 7.4, 10% v/v Glycerol) with 1 mg/mL concentration of lysozyme, 0.5 mM PMSF incubated on ice for 30 minutes. After the incubation period, the cells were sonicated with a pulse of 30 sec ON and 30 sec OFF for 10 cycles. The crude lysate obtained upon centrifugation at 5,000 × g for 10 minutes at 4 °C was subjected to Ni-NTA column (2 mL resin / g cell pellet). The unbound proteins were eliminated by using wash buffer (25 mM MOPSO, 100 mM NaCl, pH 7.4, 20 mM Imidazole, 10% v/v Glycerol). The protein was finally eluted out in the elution buffer (25 mM MOPSO, 100 mM NaCl, pH 7.4, 50 mM Imidazole, 10% v/v Glycerol) each. Protein fractions (after checking on 12 % SDS gel) were pooled together and desalted, purified using Amicon centrifugal filter units with desalting buffer (25 mM MOPSO, pH 7.4, 10% v/v Glycerol). The desalted proteins were estimated using Bradford reagent (Bio-Rad) and a Bovine Serum Albumin standard.

4B.4.10. Enzyme assays

Reaction buffer used for the assay was 25 mM MOPSO, 300 mM NaCl, pH 7.4, 10% v/v Glycerol, 3 mM DTT. 400 μM of substrates (3-deacetylsalannin, 3-deacetylazadirachtin, 7-deaceetylgedunin, 7-deacetylepoxyazadiradione, nimbocinol, 6-deacetylnimbin, 6-deacetylnimbinene), 400μM of acetyl-CoA and the purified protein were incubated at 25 °C for 3 hrs and extracted thrice with n-hexane.

4B.4.11. Characterization of assay products

Analysis of neem limonoids was performed with HRMS, Thermo Scientific QExactive^{TM} hybrid quadrupole-Orbitrap mass spectrometer associated with Accela 1250 pump and Accela open (as mentioned earlier). The conditions of HESI source include capillary temperature of 320 °C, Heater temperature at 350 °C, s-lens RF level of 50, Spray voltage of 3.6 kV, spray current of 0.9 μA with sheath gas flow rate of 41, Auxiliary gas flow rate of 9 and sweep gas flow rate of 3. Standards as well as the extracted samples were analyzed in positive ionization mode, in full MS-scan with scan range of 100 to 1000 *m/z*. Following were the properties of the scan performed-resolution 70,000, AGC target 1e6, Maximum IT 200 ms. Waters Acquity UPLC BEH C_{18} column (particle size 1.7 μm, 2.1 X 100 mm) was used as the stationary phase while the solvent system of methanol and water containing 0.1% formic acid served as the mobile phase. The method used was 90% methanol and 10% water. Constant flow rate of 0.3 mL min^{-1} was maintained throughout the run time of 10 min. The chromatograms and mass spectral data were processed by Xcalibur qual browser (version 2.3; Thermo Scientific).

4B.4.12. Cloning into yeast system

The following primer sequences were designed for cloning the genes into yeast pYES2/CT.

Name	5'-3' Primer sequence	Size in bp
AiACT1 YRS -FP	AGCTGCGGATCC*AAAACAATGTCT*ATGTCATTAA AATTTCCTCAAGT	47
AiACT1 YRS -RP	AGCCGTCTCGAGCTAAAGCTTGCAAAATAT	33

AiACT2 YRS -FP	AATTGAGGATCC*AAAACAATGTCT*ATGCCACCAT CACAACCACCA	45
AiACT2 YRS -RP	TTACTTGCGGCCGCTTCAGAGCAGATGCTATGA	33

Table 4B.2. Primer sequence for isolation of full length ORF of the acyltransferases genes involved in limonoid biosynthesis. (The underlined sequence represents the recognition site for restriction enzyme, and Kozak sequence shown in italics).

4B.4.13. AiACT1 Cloning and expression in yeast system

PCR reaction was performed using Accuprime® Pfx DNA Polymerase (ThermoFisher Scientific, USA) in the following PCR program: Initial denaturation at 94 °C for 3 min, followed by 35 cycles at 94 °C for 30 sec, 54 °C for 30 sec, 68 °C for 1 min 30 sec followed by final extension at 68 °C for 3 min. PCR product of 1.3 Kbp was cloned into pYES2/CT expression vector (Invitrogen^{TM}) after digesting both with BamHI and XhoI restriction sites. Restriction digested vector was subjected to alkaline phosphatase, calf intestinal (CIP) (NEB) treatment to remove the phosphate at the 5´- and 3´ terminal, in order to prevent the self-ligation of vector during ligation reaction. Then, the vector and insert were subjected to ligation using T4 DNA ligase (NEB) at 16 °C incubation overnight. The ligation mixture was transformed into Mach1 competent cells and plated on LB agar and incubated overnight at 37 °C. Positive clones were screened by colony PCR with T7 forward and CYC reverse primers. From 6 positive clones of colony PCR, plasmid isolation was carried out. To check for the sequence in the correct vector frame of the vector, it was sequenced with T7 forward and CYC reverse primers. The plasmid was again transformed into Invsc1 competent cells *S. c*. EasyComp^{TM} Transformation Kit and, plated on 2% glucose containing complete supplement mixture (CSM) agar without Uracil (as selection marker) and incubated for 24 hours at 30 °C.

The transformed colony was inoculated into 10 mL liquid CSM-URA media with 2% glucose and incubated for 24 hours at 30 °C. It was further transferred into 100 mL CSM-URA dropout media with 2% glucose by maintaining OD_{600} of 0.4 in the freshly initiated culture. Further, the cells were inoculated into 1 L CSM-URA dropout induction media with 2% galactose followed by centrifugation at 1500 × g for 10 min for pelleting the cells. It was incubated at 180 rpm at 30 °C in rotary shaker for 24 hrs. The cells were incubated with 1 mg of different substrates such as hexanol, geraniol,

farnesol, nerol, linalool, dihydromyrcenol, benzyl alcohol for 8 hrs at the pH 6. The incubated cells were extracted with n-Hexane twice and reduced to final volume of 0.5 mL and analyzed using GC-MS.

4B.4.14. AiACT2 Cloning and expression in yeast system

PCR reaction was performed using Accuprime® Pfx DNA Polymerase (ThermoFisher Scientific, USA) in the following PCR program: Initial denaturation at 94 °C for 3 min, followed by 35 cycles at 94 °C for 30 sec, 54 °C for 30 sec, 68 °C for 1 min 30 sec followed by final extension at 68 °C for 3 min. PCR product of 1.3 Kbp was cloned into pYES2/CT expression vector after digesting both with BamHI and NotI restriction sites. Restriction digested vector was subjected to alkaline phosphatase, calf intestinal (CIP) (NEB) treatment to remove the phosphate at the 5´- and 3´ terminal, in order to prevent the self-ligation of vector during ligation reaction. Then, the vector and insert were subjected to ligation using T4 DNA ligase (NEB) at 16 °C incubation overnight. The ligation mixture was transformed into Mach1 competent cells and plated on LB agar and incubated overnight at 37 °C. Positive clones were screened by colony PCR with T7 forward and CYC reverse primers. From 6 positive clones of colony PCR, plasmid isolation was carried out. To check for the sequence in the correct vector frame of the vector, it was sequenced with T7 forward and CYC reverse primers. The plasmid was again transformed into Invsc1 competent cells using *S. c*. EasyComp™ Transformation Kit and, plated on CSM-URA dropout agar and incubated overnight at 30 °C.

The transformed colony was inoculated into 10 mL liquid CSM-URA dropout media with 2% glucose and incubated for 24 hours at 30 °C. It was further transferred into 100 mL CSM-URA media with 2% glucose by maintaining OD_{600} of 0.4 in the freshly initiated culture. Further, the cells were inoculated into 1 L CSM-URA dropout induction media with 2% galactose followed by centrifugation at 1500 × g for 10 min for pelleting the cells. It was incubated at 180 rpm at 30 °C in rotary shaker for 24 hrs. The cells were incubated with 1 mg of different substrates such as hexanol, heptanol, geraniol, farnesol, nerol, linalool, dihydromyrcenol for 8 hrs at the pH 6. The incubated cells were extracted with n-Hexane twice and reduced to final volume of 0.5 mL and analyzed using GC-MS as mentioned below.

For the isolation of triterpenes, saponification was done with 10 % KOH in 80 % ethanol at 70ºC for 2 h, and then extracted thrice with equal volumes of n-hexane. Hexane extract was concentrated to dryness and reconstituted in 0.5 mL hexane.

4B.4.15. GC-MS analysis

It was analyzed by a 7890A Gas Chromatography system coupled to MS 5975C (Agilent Technologies). Separation of monoterpenes, sesquiterpenes and other alcohol, their acetates was performed by using Restek Rtx-5 (30 m × 0.25 mm × 0.25 µm) capillary column with helium as a carrier gas at a flow rate of 1 mL min^{-1}. The extract of 1 µL was injected in splitless mode. The temperature program was set at 50 °C for 2 min, followed by a temperature gradient from 50 °C to 250 °C at a ramping rate of 10 °C/min, and held at 250 °C for 10 min. The molecules were identified by matching the acquired mass spectra with the reference library (National Institute of Standards and Technology). For the separation of triterpenes of yeast, the following method was used, 80 °C for 2 min, followed by a temperature gradient from 80 °C to 290 °C at a ramping rate of 20 °C/min, and held at 290 °C for 20 min.

4B.5. Appendix

Master_Control_17413_ACT1

ATGTCATTAAAATTTCCTCAAGTTTTCTCAGTCACCCGTCAGGCCCCGGAACTAATT
GCTCCGGCAAGACCTACACCGCGAGAAGTGAAGCAACTCTCAGACATAGATGACCA
AGAAAGCTTCAGGTTTCAGGTTCCTGTAATATTCTTTTACAAGAATAATCCTTCACC
TTCAATGAAAGGGAAAGATCCAGTTGGGGTTATTAGAGAAGCCATAAGTAAAGCTC
TCGTGTTTTATTATCCTCTAGCCGGTAGGCTTAAAGAAGGTGACAATCGCAAGCTTA
TGGTGGACTGCAATGGGGAAGGACTATTGTTTATTGAGGCTGATGCTAACTTTACAC
TTGAGCAGCTTAGAGATGATGATCAGTCTCCTTCTTCTTATTTGGATGAATTACTTTA
TAATGTTCCAGGCTCCGACGGCATTCTTGGTTGCCCATTATTGTTAATTCAAGTGACT
CGTTTGATTTGTGGAGGATTCATTCTTGCCTTACGTTTGAACCACACAATATGTGAT
GCACAGGGATTGGTACAATTCTTGAAAACGATAGAAGAGATGGGAAGAGGAGAAA
ATGCACCATCCATATTCCCTGTTTGGCAACGAGAACTCTTAAACGCTAGAAATCCAC
TGCAAGTAACATGCATCCACCATGAATACGGGGAAGAAAAATACAATCCAGACACA
AACGAAAATGACATGCACAACAAGTTATTCTTCTTTGCTCTCAAGGAGATAAGAGC
TCTGAGAAATCAGTTTCCTCTTCACCTCAGAAAATGTTCGACATTTGATTTGTTGACT
GCTCTTGCATGGAAATGTCGAACAAGAGCACTTAAATATGATCCTGAAGAGATTGT
TCGATTTTCATGTATAGTTAGCGCACGAGGGAAACGTTATAACATGCAACTACCATC
TGGGTATTATGGCAATGCATTTGCATTCCCAGCTGTGTGTTCAAATGCTGAAGATTT
GTGTAGAAATCCGTTGGGATATGCTGTGGAATTGGTGCAGAAGGCGAAGGCTAAAA
TGAACGAAGAATATATAAGATCAGTGGCGGATCTTATGGTAATCAGTGGACGCCAA
ATCAAGCACCCAGTTAGGGGGAATTTCATTGTTTCTAATGTAACTCAAGTTGGTTTT
GGAGAGGTTGATTTTGGGTGGGGAAAACCAATTTATGCTGGAACTCCTTGTGCTGTC
TCATTGATTAGCTTCGTTATGAAGAACCAAAACAAGAATGGAGAGCCTAGATATGT

TTTGCCAATGTGCTTGCCAATGTTGGCTATGAAGAGGTTTGAAGAAGAGGTAAAGA
GGGTGATGCAGCAGGAATTTGAGCAGACTCAGATATTTTGCAAGCTT**TAG**

>ACT1_Protein
MSLKFPQVFSVTRQAPELIAPARPTPREVKQLSDIDDQESFRFQVPVIFFYKNNPSPSMKG
KDPVGVIREAISKALVFYYPLAGRLKEGDNRKLMVDCNGEGLLFIEADANFTLEQLRDD
DQSPSSYLDELLYNVPGSDGILGCPLLLIQVTRLICGGFILALRLNHTICDAQGLVQFLKTI
EEMGRGENAPSIFPVWQRELLNARNPLQVTCIHHEYGEEKYNPDTNENDMHNKLFFFA
LKEIRALRNQFPLHLRKCSTFDLLTALAWKCRTRALKYDPEEIVRFSCIVSARGKRYNM
QLPSGYYGNAFAFPAVCSNAEDLCRNPLGYAVELVQKAKAKMNEEYIRSVADLMVISG
RQIKHPVRGNFIVSNVTQVGFGEVDFGWGKPIYAGTPCAVSLISFVMKNQNKNGEPRYV
LPMCLPMLAMKRFEEEVKRVMQQEFEQTQIFCKL

Master_Control_99887_ACT2
ATGCCACCATCACAACCACCACGCCCCGCCTCCCTTGTCTTTACCGTCCGGAGGAGC
ACCCCGGAACTAATCTCTCCGGCCAAACAGACACCTCGCGAGCTCAAATCCTTGTCC
GATATCGATGATCAAGAGGGTCTCCGGTTCCAAATTCCGGTCATACAATTCTACAAG
TACCACCCTTCCATGAAAGGGAGGGACCCGGTTAAGGTGATCAGAGAAGCCTTAGC
GGAAACGCTTGTCTTTTACTACCCGTTTGCCGGTAGGCTCCGGGAGGGGGCTAACCG
GAAACTTATGGTGGATTGTAACGGCGAAGGTGTGATGTTCATTGAAGCTGATGCTG
ATGTTACACTTGAACAATTTGGTGATGATCTTCAACCTCCATTTCCATGCTTGGAAG
AGCTGCTTTTTGATCTTCCAGGATCTGCTGGAGTAATCAACTGCCCTTTGTTGCTCAT
TCAGGTGACACGTTTGAAGTGCGGCGGTTTCACTTTCGCCCTCCGTCTCAACCACAC
CATGAGCGACGCAGCTGGTATCGTCCAGTTCATGGCCGCCGTAGCTGAAATCGCAC
GCGGCGCGGCTGGCCCCACCATTCTTCCTGTCTGGGAAAGACACGTACTCAACGCCC
GGGACCCACCTCGCGTAACATGCACGCACCATGAATACGATGAAGTCGCCGACACC
AAGGGGACGATCATCCCGCTCGATGATATGGTTCATCGTTCTTTCTTCTTCGGCCCTC
AAGAAATCAACGCCATTCGCCGATTTCTTCCACAGCATCTACGCTGCAGCTCCAGTT
TCGAAATTCTCACCGCCTGCCTCTGGCGCTGTCGCACCATCGCACTGCGGCCGGACC
CGAGCGAAGAAATGCGCGTGATTTGCATCGTCAACTCGCGTTGCAAGTTTAATCCAC
CCTTACCTAGAGGATTCTACGGCAACGGGTTCGCTTTCCCGGTTGCATTGTCGACGG
CGGAGAAAGTGTGTCAAAATCCAATAGGTTATGCTTTGGAGCTAGTGAGGAAAGCC
AAGAATGACGTGAACGAAGAGTATATGAAATCAGTGGCGGATTTAATGGTGATAAA
AGGCCGACCCCATTTCACCGTCGTCCGATCCTACCTTGTTTCGGATGTGACTCGAGC
CGGGTTCGGGGATGTGGACTTTGGGTGGGGAAAACCGGCTTATGGGGGGCCTGCCA
AGGGTGGGGTTGGCGCCATTCCAGGAGTTGCAAGCTTTTATATTCCTTTCAGGAATA
AGAAAGGAGAGGAGGGTATTGTAGTGCCGGTGTGCTTGCCGGCTCCGGCAATGGTG
AGATTCGTGGAGGAATTGGACAAGATGTTGAAGGAGAAGCCAGTTGCTGCTGGCGA
GAATAAATCTACTTTCATAGCATCTGCTCTG**TAA**

>ACT2_Protein

MPPSQPPRPASLVFTVRRSTPELISPAKQTPRELKSLSDIDDQEGLRFQIPVIQFYKYHPSM
KGRDPVKVIREALAETLVFYYPFAGRLREGANRKLMVDCNGEGVMFIEADADVTLEQF
GDDLQPPFPCLEELLFDLPGSAGVINCPLLLIQVTRLKCGGFTFALRLNHTMSDAAGIVQ
FMAAVAEIARGAAGPTILPVWERHVLNARDPPRVTCTHHEYDEVADTKGTIIPLDDMV
HRSFFFGPQEINAIRRFLPQHLRCSSSFEILTACLWRCRTIALRPDPSEEMRVICIVNSRCK
FNPPLPRGFYGNGFAFPVALSTAEKVCQNPIGYALELVRKAKNDVNEEYMKSVADLMV
IKGRPHFTVVRSYLVSDVTRAGFGDVDFGWGKPAYGGPAKGGVGAIPGVASFYIPFRN
KKGEEGIVVPVCLPAPAMVRFVEELDKMLKEKPVAAGENKSTFIASAL

4C. References

1. O. Laule, A. Furholz, H. S. Chang, T. Zhu, X. Wang, P. B. Heifetz, W. Gruissem and B. M. Lange, *Proc. Natl. Acad. Sci. U S A*, 2003, **100**, 6866-6871.
2. H. Kasahara, A. Hanada, T. Kuzuyama, M. Takagi, Y. Kamiya and S. Yamaguchi, *J. Biol. Chem.*, 2002, **277**, 45188-45194.
3. A. Hemmerlin, J. F. Hoeffler, O. Meyer, D. Tritsch, I. A. Kagan, C. Grosdemange-Billiard, M. Rohmer and T. J. Bach, *J. Biol. Chem.*, 2003, **278**, 26666-26676.
4. H. K. Lichtenthaler, M. Rohmer and J. Schwender, *Physiol. Plant.*, 1997, **101**, 643-652.
5. T. J. Bach, *Lipids*, 1995, **30**, 191-202.
6. A. Frank and M. Groll, *Chem. Rev.*, 2016, **117**, 5675-5703.
7. W. Eisenreich, A. Bacher, D. Arigoni and F. Rohdich, *Cell. Mol. Life Sci.*, 2004, **61**, 1401-1426.
8. T. W. Goodwin, *Annu. Rev. Plant Physiol.*, 1979, **30**, 369-404.
9. J. Lombard and D. Moreira, *Mol. Biol. Evol.*, 2011, **28**, 87-99.
10. M. Sapir-Mir, A. Mett, E. Belausov, S. Tal-Meshulam, A. Frydman, D. Gidoni and Y. Eyal, *Plant Physiol.*, 2008, **148**, 1219-1228.
11. H. K. Lichtenthaler, *Fett-Lipid*, 1998, **100**, 128-138.
12. L. Kutrzeba, F. E. Dayan, J. Howell, J. Feng, J. L. Giner and J. K. Zjawlony, *Phytochemistry*, 2007, **68**, 1872-1881.
13. K. P. Adam and J. Zapp, *Phytochemistry*, 1998, **48**, 953-959.
14. W. Knoss, B. Reuter and J. Zapp, *Biochem. J.*, 1997, **326**, 449-454.
15. H. W. Groeneveld, *Crit. Rev. Biochem. Mol. Biol.*, 1999, **34**, 59-69.
16. A. W. Alberts, J. Chen, G. Kuron, V. Hunt, J. Huff, C. Hoffman, J. Rothrock, M. Lopez, H. Joshua, E. Harris, A. Patchett, R. Monaghan, S. Currie, E. Stapley, G. Albersschonberg, O. Hensens, J. Hirshfield, K. Hoogsteen, J. Liesch and J. Springer, *Proc. Natl. Acad. Sci. U. S. A.*, 1980, **77**, 3957-3961.
17. A. Hemmerlin and T. J. Bach, *Plant J.*, 1998, **14**, 65-74.
18. T. Umeda, N. Tanaka, Y. Kusakabe, M. Nakanishi, Y. Kitade and K. T. Nakamura, *Sci. rep.*, 2011, **1**, 9.
19. B. Lell, R. Ruangweerayut, J. Wiesner, M. A. Missinou, A. Schindler, T. Baranek, M. Hintz, D. Hutchinson, H. Jomaa and P. G. Kremsner, *Antimicrob. Agents and Chemother.*, 2003, **47**, 735-738.
20. T. Kuzuyama, T. Shimizu, S. Takahashi and H. Seto, *Tetrahedron Lett.*, 1998, **39**, 7913-7916.
21. M. Fellermeier, K. Kis, S. Sagner, U. Maier, A. Bacher and M. H. Zenk, *Tetrahedron Lett.*, 1999, **40**, 2743-2746.
22. J. C. Bede, P. E. A. Teal, W. G. Goodman and S. S. Tobe, *Plant Physiol.*, 2001, **127**, 584-593.
23. K. Skorupinska-Tudek, J. Poznanski, J. Wojcik, T. Bienkowski, I. Szostkiewicz, M. Zelman-Femiak, A. Bajda, T. Chojnacki, O. Olszowska, J. Grunler, O. Meyer, M. Rohmer, W. Danikiewicz and E. Swiezewska, *J.Biol. Chem.*, 2008, **283**, 21024-21035.
24. H. Kasahara, A. Hanada, T. Kuzuyama, M. Takagi, Y. Kamiya and S. Yamaguchi, *J.Biol. Chem.*, 2002, **277**, 45188-45194.
25. K. Ohyama, M. Suzuki, J. Kikuchi, K. Saito and T. Muranaka, *Proc. Natl. Acad. Sci. U. S. A.*, 2009, **106**, 725-730.
26. J. L. Song, C. N. Lyons, S. Holleman, B. G. Oliver and T. C. White, *Med. Mycol.*, 2003, **41**, 417-425.
27. J. Chappell, F. Wolf, J. Proulx, R. Cuellar and C. Saunders, *Plant Physiol.*, 1995, **109**, 1337-1343.
28. J. M. Estevez, A. Cantero, A. Reindl, S. Reichler and P. Leon, *J. Biol. Chem.*, 2001, **276**, 22901-22909.

29. L. P. Wright, J. M. Rohwer, A. Ghirardo, A. Hammerbacher, M. Ortiz-Alcaide, B. Raguschke, J. P. Schnitzler, J. Gershenzon and M. A. Phillips, *Plant Physiol.*, 2014, **165**, 1488-1504.
30. A. Pandreka, D. S. Dandekar, S. Haldar, V. Uttara, S. G. Vijayshree, F. A. Mulani, T. Aarthy and H. V. Thulasiram, *BMC Plant Biol.*, 2015, **15**, 1-14.
31. H. K. Lichtenthaler, *Methods Enzymol.*, 1987, **148**, 350-382.
32. R. Rajakani, L. Narnoliya, N. S. Sangwan, R. S. Sangwan and V. Gupta, *Tree Genet. Genomes.* , 2014, **10**, 1331-1351.
33. A. Roy and S. Saraf, *Biol. Pharm. Bull*, 2006, **29**, 191-201.
34. Q. G. Tan and X. D. Luo, *Chem. Rev.*, 2011, **112**, 2591-2591.
35. K. K. Singh, *Neem, a Treatise*, I.K. International Publishing House, 2009.
36. S. V. Ley, A. A. Denholm and A. Wood, *Nat. Prod. Rep.*, 1993, **10**, 109-157.
37. A. Pandreka, D. S. Dandekar, S. Haldar, V. Uttara, S. G. Vijayshree, F. A. Mulani, T. Aarthy and H. V. Thulasiram, *BMC Plant Biol*, 2015, **15**, 1-14.
38. J. C. D'Auria, *Curr. Opin. Plant Biol.*, 2006, **9**, 331-340.
39. K. H. Nam, N. Dudareva and E. Pichersky, *Plant Cell Physiol.*, 1999, **40**, 916-923.
40. N. Dudareva, J. C. D'Auria, K. H. Nam, R. A. Raguso and E. Pichersky, *Plant J.*, 1998, **14**, 297-304.
41. H. Fujiwara, Y. Tanaka, Y. Fukui, M. Nakao, T. Ashikari and T. Kusumi, *Eur. J. Biochem.*, 1997, **249**, 45-51.
42. K. Yonekura-Sakakibara, Y. Tanaka, M. Fukuchi-Mizutani, H. Fujiwara, Y. Fukui, T. Ashikari, Y. Murakami, M. Yamaguchi and T. Kusumi, *Plant Cell Physiol.*, 2000, **41**, 495-502.
43. Q. Yang, K. Reinhard, E. Schiltz and U. Matern, *Plant Mol.Biol.*, 1997, **35**, 777-789.
44. B. St-Pierre, P. Laflamme, A. M. Alarco and V. De Luca, *Plant J.*, 1998, **14**, 703-713.
45. T. T. T. Dang, X. Chen and P. J. Facchini, *Nat. Chem. Biol.*, 2014, **11**, 104-U122.
46. K. Walker, R. E. B. Ketchum, M. Hezari, D. Gatfield, M. Goleniowski, A. Barthol and R. Croteau, *Arch. Biochem. Biophys.*, 1999, **364**, 273-279.
47. K. Walker, A. Schoendorf and R. Croteau, *Arch. Biochem. Biophys.*, 2000, **374**, 371-380.
48. G. Y. Kai, Z. Q. Miao, C. X. Qiu, L. Zhang, L. X. Zhao, Z. G. Li, T. F. Xu, L. D. Zhang, Y. F. Gong, D. L. Zhao, D. H. Liu, X. F. Sun and K. X. Tang, *Plant Sci.*, 2004, **167**, 759-764.
49. K. Walker and R. Croteau, *Proc. Natl. Acad. Sci. U. S. A.*, 2000, **97**, 13591-13596.
50. C. Loncaric, E. Merriweather and K. D. Walker, *Chem. Biol.*, 2006, **13**, 309-317.
51. K. Walker, S. Fujisaki, R. Long and R. Croteau, *Proc. Natl. Acad. Sci. U. S. A.*, 2002, **99**, 12715-12720.
52. K. Walker, R. Long and R. Croteau, *Proc. Natl. Acad. Sci. U. S. A.*, 2002, **99**, 9166-9171.
53. D. Hampel, C. J. D. Mau and R. B. Croteau, *Arch. Biochem. Biophys.*, 2009, **487**, 91-97.
54. T. Grothe, R. Lenz and T. M. Kutchan, *J. Biol. Chem.*, 2001, **276**, 30717-30723.
55. R. Lenz and M. H. Zenk, *J. Biol. Chem.*, 1995, **270**, 31091-31096.
56. A. Bayer, X. Y. Ma and J. Stockigt, *Bioorg. Med. Chem.*, 2004, **12**, 2787-2795.
57. I. Gerasimenko, X. Y. Ma, Y. Sheludko, R. Mentele, F. Lottspeich and J. Stockigt, *Bioorg. Med. Chem.*, 2004, **12**, 2781-2786.
58. P. Laflamme, B. St-Pierre and V. De Luca, *Plant Physiol.*, 2001, **125**, 189-198.
59. L. S. Sarker and S. S. Mahmoud, *Planta*, 2015, **242**, 709-719.
60. M. Shalit, I. Guterman, H. Volpin, E. Bar, T. Tamari, N. Menda, Z. Adam, D. Zamir, A. Vainstein, D. Weiss, E. Pichersky and E. Lewinsohn, *Plant Physiol.*, 2003, **131**, 1868-1876.
61. E. J. F. Souleyre, D. R. Greenwood, E. N. Friel, S. Karunairetnam and R. D. Newcomb, *FEBS J.*, 2005, **272**, 3132-3144.

62. R. Dexter, A. Qualley, C. M. Kish, C. J. Ma, T. Koeduka, D. A. Nagegowda, N. Dudareva, E. Pichersky and D. Clark, *Plant J.*, 2007, **49**, 265-275.
63. A. Banas, A. S. Carlsson, B. Huang, M. Lenman, W. Banas, M. Lee, A. Noiriel, P. Benveniste, H. Schaller, P. Bouvier-Nave and S. Stymne, *J. Biol. Chem.*, 2005, **280**, 34626-34634.
64. Q. Chen, L. Steinhauer, J. Hammerlindl, W. Keller and J. Zou, *Plant Physiol.*, 2007, **145**, 974-984.
65. J. C. D'Auria, F. Chen and E. Pichersky, *Plant Physiol.*, 2002, **130**, 466-476.
66. A. Eudes, M. Mouille, D. S. Robinson, V. T. Benites, G. Wang, L. Roux, Y. L. Tsai, E. E. K. Baidoo, T. Y. Chiu, J. L. Heazlewood, H. V. Scheller, A. Mukhopadhyay, J. D. Keasling, S. Deutsch and D. Loque, *Microb. Cell. Fact.*, 2016, **15**, 16.
67. E. Pardo, J. Rico, J. V. Gil and M. Orejas, *Microb.Cell Fact.*, 2015, **14**.
68. W. Liu, X. Xu, R. B. Zhang, T. Cheng, Y. J. Cao, X. X. Li, J. T. Guo, H. Z. Liu and M. Xian, *Biotechnol. Biofuels*, 2016, **9**.
69. A. s. Herrero, D. Raman and M. Orejas, *Metab. Eng.*, 2008, **10**, 78-86.
70. A. King and J. Richard Dickinson, *Yeast*, 2000, **16**, 499-506.
71. A. J. King and J. R. Dickinson, *FEMS Yeast Res.*, 2003, **3**, 53-62

Thesis summary

Neem tree, is one of the well-known Indian medicinal plants, used for its healing property from ancient past. Its remarkable insecticidal and various pharmacological activities are contributed by terpenoids called limonoids. Over 250 compounds have been isolated and characterized from neem seeds, around 150 of these being limonoids. They belong to triterpene class of natural product. Terpenes are composed of isoprene units (C5), isopentenyl diphosphate (IPP) and its isomer dimethylallyl pyrophosphate (DMAPP), the repetitive motives in the terpenoids. The isoprene building blocks are biosynthesized through MVA and MEP pathway localized in cytosol and plastid respectively in plant cell. Though mono-, di-, tetra-terpenes are biosynthesized through MEP pathway, and sesqui- and tri-terpenes through MVA pathway, exchange of isoprene units occur either uni- or bi-directionally between the compartments under certain conditions in plants. And also, for the immense biosynthesis of specialized metabolites and their sequestration, plants have evolved specialized anatomical appendages and cell types such as trichomes, idioblast cells, laticifers, resin cells, secretory cells, gland or cavities. These structures help plants for the efficient utilization of secondary metabolites for defense or pollinator attraction and also to protect the adverse and detrimental effect for the producing plant. Apart from the specialized cells, vacuoles and vesicles are important intracellular organelles, which are known to accumulate secondary metabolites, thereby aiding in prevention of self-toxicity for the host cells. Synthesis of a complex secondary metabolite requires multiple organelles such as chloroplast, cytosol, endoplasmic reticulum, vesicles, vacuoles and nucleus. Hence, the biosynthetic machinery that plant cell employs for terpene production and thereby its storage remains unexplored for this wonder tree, which is examined through this study.

In the present study, histochemical analysis of different tissues has been carried out, to study the limonoid localization in cellular and subcellular compartments. Metabolite profiling of the isolated organelle was performed which showed the individual localization of different class of metabolites across different tissues of neem. It suggested that laticifers are rich in basic limonoids and oil bodies are found to be the major source of C-seco limonoids in pericarp and kernel of neem fruit respectively, whereas limonoids exist in abundance in idioblast vacuoles in pericarp and leaf tissues. Average number of idioblasts per mm^2 of tissue was comparatively high in pericarp to that of leaf, which matched with the abundance of limonoids in these tissues

respectively. In addition, flower was found to contain flavonoids in pollen, and sesquiterpenes in secretory vesicles.

Neem callus and suspension culture capable of limonoid biosynthesis was established from surface sterilized fresh neem cotyledons. Limonoid profiling of callus and suspension culture showed the stable biosynthesis of nine C-seco limonoids. Limonoid biosynthesis in the cell suspension at different stages of subculturing were characterized by using [1,6-^{13}C] Glc label as carbon source for the cells, which showed that limonoids biosynthesis was decreased in cells obtained from callus subcultured 22 times as compared to callus subcultured 3 times.

^{13}C labeled isotopologues of glucose were used to study limonoid biosynthetic pathway in neem cell suspension. In order to identify the signature fragment of azadirachtin A generated through ESI-MS, fragments generated from MS/MS of azadirachtin derivatives such as azadirachtin B, H, 3-deacetylazadirachtin A, epi-azadirachtin D, vepaol were studied comparatively at different normalized collision energies. The plausible fragmentation pathway for azadirachtin A has been proposed showing the structure-fragment relationship. This helped in tandem mass spectrometry (MS/MS) analyses of labeled limonoid extract, which lead to the identification of signature isoprenoid units involved in azadirachtin and other limonoid biosynthesis. Therefore, the isoprene units contributed for limonoid skeleton biosynthesis are found to be formed through mevalonate (MVA) pathway from this study.

Chemical inhibition of the pathways along with concomitant ^{13}C Glc labeling was carried out to study the complementation of both the pathways. Treatment of cell suspension with mevinolin, a specific inhibitor for MVA pathway, resulted in drastic decrease in limonoid levels whereas their biosynthesis was unaffected with fosmidomycin mediated plastidial methylerythritol 4-phosphate (MEP) pathway inhibition. This was also conspicuous, as the expression level of genes encoding for the rate-limiting enzyme of MVA pathway, 3-hydroxy-3-methyl-glutaryl-coenzyme A reductase (HMGR) was comparatively higher to that of deoxyxylulose-phosphate synthase (DXS) of MEP pathway in different tissues and also in the *in vitro* grown cells as evident from real time PCR analysis. The genes encoding for the enzymes mediating the downstream steps of limonoid biosynthesis need to be studied. In order to understand limonoid diversity in neem, putative acyltransferase ORFs were selected from neem transcriptome for cloning. The selected acyltransferases matched with BAHD family of

plant acetyltransferases, which transfers acyl group from CoA to natural products. The two full length ORFs were cloned and expressed in bacterial system and due to low level of expression in bacteria, it was further cloned into yeast system. Different limonoid substrates, mono-, sesquiterpene alcohols were used as substrate, but the activity for acylation of the studied natural products was not seen. Hence, the result shows that these enzymes may act on the low abundance or labile pathway intermediates of limonoid biosynthetic pathway, which needs to be studied further.

List of Publications from thesis

1. Haldar S, Mulani FA, **Aarthy T.**, Dandekar DS, Thulasiram HV., Expedient preparative isolation and tandem mass spectrometric characterization of C-seco triterpenoids from Neem oil, ***J. Chromatogr. A*., 2014,** 1366, 1 – 14.

2. Haldar S, Mulani FA, **Aarthy T.**, Thulasiram HV, 11β-Hydroxylation on the Basic Limonoid Skeleton by Fungal Biocatalyst, *Cunninghamella echinulata*, ***J. Org. Chem*., 2015**, 80, 6490 - 6495.

3. Pandreka A, Dandekar DS, Haldar S, Uttara V, Vijayshree S, Mulani FA, **Aarthy T.**, H. V. Thulasiram, Triterpenoid profiling and functional characterization of the initial genes involved in isoprenoid biosynthesis in neem (*Azadirachta indica*), ***BMC Plant Biol*., 2015**, 15:214, 1 - 14

4. B Deshmukh, S.a Bai, **T. Aarthy**, R. S Kazi, R. Banarjee, R. Rathore, Vijayakumar MV, Thulasiram H.V, M. Bhat, Kulkarni MJ, Methylglyoxal impairs insulin signaling, downregulates the enzymes involved in cholesterol biosynthesis and decreases glucose uptake, ***Molecular Biosyst*., 2017**, 13, 2338

5. Soujanya K N, Siva R, Mohana K. P, A. Srimany, Ravikanth G, T Pradeep, Mulani F A, **Aarthy T.**, Thulasiram H V, Santhoshkumar T R, K. N Nataraja, Camptothecin-producing endophytic bacteria from *Pyrenacantha volubilis* Hook. (Icacinaceae): A possible role of a plasmid in the production of camptothecin ***Phytomedicine*, 2017**, 36, 160-167

6. B. Natarajan, H. S. Kalsi, P. Godbole, N. Malankar, **T. Aarthy**, S. Siddappa, H. V. Thulasiram, S. K. Chakrabarti, A. K. Banerjee, MiRNA160 plays a potential role in local defense and systemic acquired resistance of potato during *Phytophthora infestans* infection ***J.Exp. Bot*., 2018**, 69, 2023- 2036

7. **T. Aarthy**, F. A. Mulani, A. Pandreka, A. Kumar, S. S Nandikol, S. Haldar, H. V. Thulasiram, Tracing the biosynthetic origin of limonoids and their functional groups through stable isotope labeling and pathway inhibition in neem tree (*Azadirachta indica*) cell suspension, ***BMC Plant Biol*., 2018**, 18:230

8. N. V. Gorantla, F. A. Mulani, T. Dubey, R. Das, **T. Aarthy**, H. V. Thulasiram, S. Chinnathambi, Inhibition and dissolution of tau filaments by limonoids ***(Manuscript communicated)***

9. **T. Aarthy**, A. Pandreka, Hirekodathakallu V. Thulasiram, Dissecting the cellular and subcellular localization terpenes, flavanoids and hydrocarbons in *Azadirachta indica* through Histochemistry and Mass spectrometry ***(Manuscript under preparation)***

10. FA. Mulani, S.K. Jagadeesh, **T. Aarthy**, S. Haldar, S. Poojadevi, P. Sharanappa, H. V. Thulasiram, Metabolic profiling of Meliaceae trees and comparative analysis of limonoids by using Ultra - performance liquid chromatography/ tandem mass spectrometry ***(Manuscript under preparation)***

11. Pandreka A., Chaya, P. S., Bhagyashree D. B., Ashish R. K., **Aarthy, T.,** Mulani, F.A., and Thulasiram, H.V. Tirucalladienol synthase is the key enzyme involved in triterpenoid biosynthesis in neem **(*Manuscript under preparation*)**

Curriculum Vitae

Ms. T. AARTHY
Senior Research Fellow,
Chemical Biology Unit,
Division of Organic Chemistry,
CSIR-National Chemical Laboratory.
Dr. Homi Bhabha Road,
Pune-411008.
Maharashtra, India.
Email: bio.arty@gmail.com
Mob: +91 9049519412

Summary

- Chemical Biologist with research experience in the study of primary and specialized metabolism in plants
- Research background in biochemistry and molecular biology; conversant with the techniques for the study of Plant Natural Product metabolic pathways.
- Interested in natural product biochemistry.

Current position

- **Research Fellow**, CSIR-National Chemical Laboratory, Division of Organic Chemistry, Pune, India (Since July 2012)
- **Research Supervisor**: Dr. H. V. Thulasiram
- **Ph. D. Thesis Title:** Limonoid Biosynthesis in *Azadirachta indica*: Characterization of pathway genes and analysis of labeled metabolites through stable isotope feeding

Education

Bachelor of Technology (B.Tech) **Biotechnology**, 2011, Agricultural college and Research Institute, Tamil Nadu Agricultural University, Coimbatore, India
Cumulative Grade Point Average - 8.89 / 10

Class	Institution	Board/ University	Year of Completion	Marks %
X	Jaycees Matriculation Higher Secondary School, Kangayam, Tamil Nadu	Matriculation	2005	88.81
XII (Bio/Chem/ Phy/Maths)	Jaycees Matriculation Higher Secondary School, Kangayam, Tamil Nadu	State Board	2007	94.08

Thesis highlights

- Stable isotope labeling study to trace the flow of carbons en route from primary metabolic pathway to triterpenoid biosynthesis.
- Study of role and complementation of metabolic pathways through chemical inhibition and mRNA expression levels.

- Localization of different classes of natural product in specialized cells and organelles in different plant tissues.
- Cloning and characterization of genes involved in secondary metabolite biosynthesis.

Projects / training before PhD programme

- Biotechnology Industrial Training Programme 2011-12 at Indo-American Hybrid Seeds Private Limited, Bengaluru, India in the project entitled 'Induced mutagenesis and detection of somoclonal variants in *Philodendron xanadu* plants regenerated through direct and indirect shoot organogenesis' organized by Biotechnology Consortium India Limited (BCIL), New Delhi, India
- As part a of B.Tech degree, worked on 'Screening of high β□carotene in pearl millet genotypes and its segregating generation through RP-HPLC for developing mapping population for enhanced β□carotene' at Centre for Plant Molecular Biology and Biotechnology, Tamil Nadu Agricultural University, Coimbatore, India
- Completed a short term project on 'Genotyping Analysis of Tomato Hybrids using DNA and Protein Finger Printing' at Indo-American Hybrid Seeds Private Limited, Bangalore, India
- Undergone summer Training at Center for Research in Medical Entomology (CRME), Madurai, India

Presentations /Workshops

- Genetically Modified Bacteria Mediated Food Preservation (Poster) National symposium on Recent Trends in Food Processing on World Food Day 2008, Tamil Nadu Agricultural University, Coimbatore, India
- "Treatment of Cancer by Gene Silencing", Poster presentation, Glimpses of future prospects in Biotechnology, Rasipuram, India
- Organised National Level technical Symposium BIOCONCORRENZA-2010, Tamil Nadu Agricultural University, Coimbatore, India
- Workshop on Molecular Biology Techniques for Detection of Infectious diseases at Thiruchirapalli, India.
- Participated in National Level technical Symposium BIOCONCORRENZA-2011, Tamil Nadu Agricultural University, Coimbatore, India.
- Fingerprinting of COH(M)5 Maize Hybrid and its Parental lines for Genetic purity Assessment (Poster) World Congress of Biotechnology, 21 - 23 March 2011, Hyderabad, India.
- Screening of high β carotene in pearl millet genotypes and its segregating generation through RP-HPLC for developing mapping population for enhanced β-carotene (Poster) World Congress of Biotechnology, 21 - 23 March 2011, Hyderabad, India.

- Participated in "Indo-Mexico workshop on Biotechnology: Beyond borders" organized by CSIR-NCL, Pune and CINVESTAV, Mexico, October, 2013.
- "*In vivo* tracer study for biosynthesis of limonoids in *Azadirachta indica* cell culture", Poster presentation, Peptide Engineering Meeting-7 (PEM7), (December 5-7, 2015) IISER Pune
- "*In vivo* tracer study for biosynthesis of limonoids in *Azadirachta indica* cell culture", Poster presentation, International Conference on Biotechnology and Bioinformatics (February 5-7, 2016), Pune
- "*In vivo* tracer study for biosynthesis of limonoids in *Azadirachta indica* cell culture", Poster presentation, National Science Day, CSIR-NCL, Pune, (February 25-26, 2016), **Best poster award in 'National Science Day Celebrations 2016'**
- Participated in workshop on "Transcriptome Data Analysis" (August 16-18, 2016), NCL Innovation Park, Pune.
- "Study of limonoid biosynthesis and cellular localization in *Azadirachta indica*", Poster presentation, EMBO conference on Micro and metabolic regulators in plants, Thiruvananthapuram, Kerala, India (February 01-04, 2017)

Educational accomplishments

- **"NCL-RF-GUPTA-PARDESHI-SAINANI award"** for "Best Published Research Paper in Biological Sciences" for the year 2018 in National chemical Laboratory.
- Secured All India Rank 17 in Category A in Biotechnology Eligibility Test for Junior Research Fellowship (BET-JRF) 2012, conducted by Department of Biotechnology (DBT), Government of India
- Secured All India Rank Graduate Aptitude Test in Engineering (GATE) 2012 in Biotechnology (BT) Percentile Score- 99.6
- Graduate Record Examination (GRE) 2011 Score-1270 (Verbal-590, Quants-680)
- Received awards for academic excellence for being a School topper in class XI and XII
- Award for securing first mark in Biology and Chemistry in class XII.

Research publications

1) Haldar S, Mulani FA, **Aarthy T.**, Dandekar DS, Thulasiram HV., , Expedient preparative isolation and tandem mass spectrometric characterization of C-seco triterpenoids from Neem oil, ***J. Chromatogr. A*., 2014,** 1366, 1 – 14.

2) Haldar S, Mulani FA, **Aarthy T.**, Thulasiram HV, 11β-Hydroxylation on the Basic Limonoid Skeleton by Fungal Biocatalyst, *Cunninghamella echinulata*, ***J. Org. Chem.*, 2015**, 80, 6490 - 6495.

3) Pandreka A, Dandekar DS, Haldar S, Uttara V, Vijayshree S, Mulani FA, **Aarthy T.**, H. V. Thulasiram, Triterpenoid profiling and functional characterization of the initial genes involved in isoprenoid biosynthesis in neem (*Azadirachta indica*), ***BMC Plant Biol.*****, 2015**, 15:214, 1 - 14

4) B Deshmukh, S.a Bai, **T.Aarthy**, R. S Kazi, R. Banarjee, R. Rathore, Vijayakumar MV, Thulasiram H.V, M. Bhat, Kulkarni MJ, Methylglyoxal impairs insulin signaling, downregulates the enzymes involved in cholesterol biosynthesis and decreases glucose uptake, ***Molecular Biosyst.*****, 2017**, 13, 2338

5) Soujanya K N, Siva R, Mohana K. P, A. Srimany, Ravikanth G, T Pradeep, Mulani F A, **Aarthy T.**, Thulasiram H V, Santhoshkumar T R, K. N Nataraja, Camptothecin-producing endophytic bacteria from *Pyrenacantha volubilis* Hook. (Icacinaceae): A possible role of a plasmid in the production of camptothecin ***Phytomedicine*****, 2017**, 36, 160-167

6) B. Natarajan, H. S. Kalsi, P. Godbole, N. Malankar, **T. Aarthy**, S. Siddappa, H. V. Thulasiram, S. K. Chakrabarti, A. K. Banerjee, MiRNA160 plays a potential role in local defense and systemic acquired resistance of potato during *Phytophthora infestans* infection ***J.Exp. Bot.*****, 2018**, 69, 2023- 2036

7) **T. Aarthy**, F. A. Mulani, A. Pandreka, A. Kumar, S. S Nandikol, S. Haldar, H. V. Thulasiram, Tracing the biosynthetic origin of limonoids and their functional groups through stable isotope labeling and pathway inhibition in neem tree (*Azadirachta indica*) cell suspension, ***BMC Plant Biol.*****, 2018**, 18:230

8) N. V. Gorantla, F. A. Mulani, T. Dubey, R. Das, **T. Aarthy**, H. V. Thulasiram, S. Chinnathambi, Inhibition and dissolution of tau filaments by limonoids ***(Manuscript communicated)***

9) **T. Aarthy**, A. Pandreka, Hirekodathakallu V. Thulasiram Dissecting the cellular and subcellular localization terpenes, flavanoids and hydrocarbons in *Azadirachta indica* through Histochemistry and Mass spectrometry, ***(Manuscript under preparation)***

10) F.A. Mulani, S.K Jagadeesh, **T. Aarthy**, S. Haldar , Poojadevi S, Sharanappa P , H. V. Thulasiram, Metabolic profiling of Meliaceae trees and comparative analysis of limonoids by using Ultra - performance liquid chromatography/ tandem mass spectrometry, ***(Manuscript under preparation)***.

11) Tirucalladienol synthase is the key enzyme involved in triterpenoid biosynthesis in neem Pandreka A., Chaya, P. S., Bhagyashree D. B., Ashish R. K., **Aarthy, T.,** Mulani, F.A., and Thulasiram, H.V. ***(Manuscript under preparation)***

Technical skills

Molecular biology:

- RNA extraction, reverse transcription, Real time (Quantitative) and endpoint PCR, DNA purification
- DNA fingerprinting studies
- Cloning in bacterial and yeast system: primers designing, restriction digestions, ligations, competent cell preparation, transformation

Biochemistry:

- Heterologous protein expression and affinity column purification
- Whole cell mediated biotransformation of natural products
- Microsomal and *in vitro* enzyme assays
- Enzyme kinetics

Analytical methods:

- Chromatography (Thin layer, HPLC, Gas chromatography),
- Mass spectrometry (LC-ESI-Orbitrap, GC-QTOF, GC-MS)
- Spectrophotometric techniques
- Sound theoretical knowledge and interpretation of most the analytical techniques

Metabolic profiling:

- Metabolite extraction from bacterial, fungal, plant and animal systems.
- Metabolic profiling, fingerprinting, metabolite quantification.

Cell biology and Histochemistry

- Bacterial and yeast cell culture
- Microscopy: Epi-fluorescence, confocal and light microscopy.
- Tissue sectioning, staining

Plant cell culture:

- Plant cell and tissue culture
- Protoplast isolation and culture

Other Skills:

- **IT:** extensive knowledge on standard office software, Chembiodraw, Coreldraw, Photoshop, Graphpad Prism, Origin Pro, Endnote, Mendeley.
- **Languages:** Tamil (mother tongue), English (fluent), Hindi (moderate).

Declaration

I hereby declare that the above mentioned details are true and accurate to the best of my Knowledge and belief.

T. Aarthy